

NO-A191 203 UNITED STATES AIR FORCE SUMNER FACULTY RESEARCH PROGRAM 1/11  
(1997) PROGRAM OF THE INTERDISCIPLINARY ENERGY CENTER FOR

1/11

(1907) PROGRAM TE. (U) UNIVERSAL ENERGY SYSTEMS INC

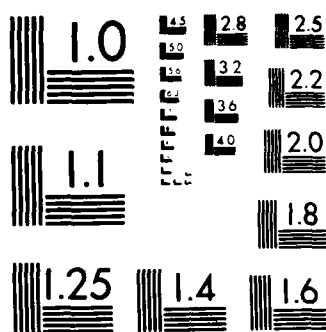
BRYTON ON R C DUNGAN ET AL. DEC 07 AFOSR-YR-88-0212  
 F49620-85-C-0013 F/G 5/1

**R-88-0212**  
**FEB 5 1989**

13

UNCLASSIFIED F49620-85-C-0013

A 6x14 grid of 84 small, dark, square images, likely representing a dataset of handwritten digits or characters. The images are arranged in 6 rows and 14 columns, showing various patterns and noise, possibly representing different classes or instances in a classification task.



MICROCOPY RESOLUTION TEST CHART  
NATIONAL BUREAU OF STANDARDS 1963-A



OTIC FILE COPY

AD-A191 283

①

UNITED STATES AIR FORCE

UNIVERSAL AIRCRAFT RESEARCH PROGRAM

1987

PROGRAM TECHNICAL REPORT

UNIVERSAL AIRCRAFT SYSTEMS, INC.

WHEELS, INC.

CHIEF OF DIRECTOR, AIR FORCE PROGRAM MANAGER, AIR FORCE

ROBERT D. DARRAGH

MAJOR RICHARD KOEKA

PROGRAM ADMINISTRATOR, USAF

HUSAIN K. BRY

Submitted to

AIR FORCE OFFICE OF SCIENTIFIC RESEARCH

DEFENSE AIR FORCE BASE

WHEELS, INC.

WHEELS, INC.

DISTRIBUTION STATEMENT 2

Approved for public release  
Distribution Unlimited

DTIC  
ELECTE  
MAR 01 1988  
S H D

AD-A191283

①

UNITED STATES AIR FORCE  
SUMMER FACULTY RESEARCH PROGRAM  
1987  
PROGRAM TECHNICAL REPORT  
UNIVERSAL ENERGY SYSTEMS, INC.  
VOLUME I of III

Program Director, UES  
Rodney C. Darrah

Program Manager, AFOSR  
Major Richard Kopka

Program Administrator, UES  
Susan K. Espy

Submitted to  
Air Force Office of Scientific Research  
Bolling Air Force Base  
Washington, DC

December 1987

DTIC  
ELEMENT  
MAR 01 1988  
S H D

**DISTRIBUTION STATEMENT A**

Approved for public release  
Distribution Unlimited



I. INTRODUCTION

Universal Energy Systems, Inc. (UES) was awarded the United States Air Force Summer Faculty Research Program on August 15, 1984. The contract is funded under the Air Force Systems Command by the Air Force Office of Scientific Research.

The program has been in existence since 1978 and has been conducted by several different contractors. The success of the program is evident from its history of expansion since 1978.

The Summer Faculty Research Program (SFRP) provides opportunities for research in the physical sciences, engineering, life sciences, business, and administrative sciences. The program has been effective in providing basic research opportunities to the faculty of universities, colleges, and technical institutions throughout the United States.

The program is available to faculty members in all academic grades: instructor, assistant professor, professor, department chairman, and research facility directors. It has proven especially beneficial to young faculty members who are starting their academic research programs and to senior faculty members who have spent time in university administration and are desirous of returning to scholarly research programs.

Beginning with the 1982 program, research opportunities were provided for 17 graduate students. The 1982 pilot student program was highly successful and was expanded in 1983 to 53 students; there were 84 graduate students in the 1984 program.

In the previous programs, the graduate students were selected along with their professors to work on the program. Starting with the 1985 program, the graduate students were selected on their own merits. They were assigned to be supervised by either a professor on the program or by an engineer at the Air Force Laboratories participating in the program. There were 92 graduate students selected for the 1985 program.

Again in the 1986 program, the graduate students were selected on their own merits, and assigned to be supervised by either a professor on the program or by an engineer at the participating Air Force Laboratory. There were 100 graduate students selected for the 1986 program.

Follow-on research opportunities have been developed for a large percentage of the participants in the Summer Faculty Research Program in 1979-1983 period through an AFOSR Minigrant Program.

On 1 September 1983, AFOSR replaced the Minigrant Program with a new Research Initiation Program. The Research Initiation Program provides follow-on research awards to home institutions of SFRP participants. Awards were made to approximately 50 researchers in 1983. The awards were for a maximum of \$12,000 and a duration of one year or less. Substantial cost sharing by the schools contributes significantly to the value of the Research Initiation Program. In 1984 there were approximately 80 Research Initiation awards.

USAF  
PREFACE

The ~~United States~~ Air Force Summer Faculty Research Program (USAF-SFRP) is a program designed to introduce university, college, and technical institute faculty members to Air Force research. This is accomplished by the faculty members being selected on a nationally advertised competitive basis for a ten-week assignment during the summer intersession period to perform research at Air Force laboratories/centers. Each assignment is in a subject area and at an Air Force facility mutually agreed upon by the faculty members and the Air Force. In addition to compensation, travel and cost of living allowances are also paid. The USAF-SFRP is sponsored by the Air Force Office of Scientific Research, Air Force Systems Command, United States Air Force, and is conducted by Universal Energy Systems, Inc..

The specific objectives of the 1987 USAF-SFRP are:

- (1) To provide a productive means for Scientists and Engineers holding Ph.D. degrees to participate in research at the Air Force Weapons Laboratory;
- (2) To stimulate continuing professional association among the Scholars and their professional peers in the Air Force;
- (3) To further the research objectives of the United States Air Force;
- (4) To enhance the research productivity and capabilities of Scientists and Engineers especially as these relate to Air Force technical interests.

During the summer of 1987, 159-faculty members participated. These researchers were assigned to 25 USAF laboratories/centers across the country. This three volume document is a compilation of the final reports written by the assigned faculty members about their summer research efforts.

LIST OF 1987 PARTICIPANTS

# LIST OF 1987 PARTICIPANTS

## NAME/ADDRESS

## DEGREE, SPECIALTY, LABORATORY ASSIGNED

Dr. Suresh K. Aggarwal  
Assistant Professor  
Dept. of Mechanical Eng.  
Univ. of Illinois at Chicago  
P O Box 4348  
Chicago, IL 60680  
(312) 996-2235/5317

Degree: Ph.D., Aerospace Eng., 1979  
Specialty: Aerospace Engineering  
Assigned: APL

Dr. Gurbux S. Alag  
Associate Professor  
Dept. of Electrical Eng.  
Western Michigan University  
1940 Howard Street, #410  
Kalamazoo, MI 49008  
(616) 383-1538

Degree: Ph.D., Systems Eng., 1976  
Specialty: Systems Engineering  
Assigned: RPL

Dr. John W. Amoss  
Associate Professor  
Dept. of Systems Science  
University of West Florida  
Pensacola, FL 32514  
(904) 474-2547

Degree: Ph.D., Electrical Eng., 1972  
Specialty: Electrical Engineering  
Assigned: AL

Dr. Victor H. Appel  
Associate Professor  
Dept. of Educational Psychology  
Univ. of Texas at Austin  
Austin, TX 78712  
(512) 471-4155

Degree: Ph.D., Psychology, 1959  
Specialty: Psychology  
Assigned: HRL/MO

Dr. Xavier J.R. Avula  
Associate Professor  
Dept. of Engineering Mechanics  
University of Missouri-Rolla  
Rolla, MO 65401  
(314) 341-4585

Degree: Ph.D., Engineering Mechanics  
1968  
Specialty: Engineering Mechanics  
Assigned: HRL/MO

Dr. Francesco L. Bacchialoni  
Associate Professor  
Dept. of Electrical Engineering  
University of Lowell  
1 University Avenue  
Lowell, MA 02173  
(617) 452-5000

Degree: Ph.D., Ingegneria, 1946  
Specialty: Engineering Mechanics  
Assigned: HRL/MO

Dr. Praphulla K. Bajpai  
Professor  
Dept. of Biology  
University of Dayton  
300 College Park  
Dayton, OH 45469  
(513) 229-3029

Degree: Ph.D., Immunophysiology,  
1965  
Specialty: Immunology  
Assigned: AAMRL

Dr. Vernon L. Bakke  
Associate Professor  
Dept. of Math. Science  
University of Arkansas  
Fayetteville, AR 72701  
(501) 575-4531

Degree: Ph.D., Mathematics, 1971  
Specialty: Mathematics  
Assigned: AL

Dr. Shankar S. Bale  
Professor  
Dept. of Science and Math  
Saint Paul's College  
Lawrenceville, VA 23868-1299  
(804) 848-3111

Degree: Ph.D., Genetics, 1971  
Specialty: Genetics  
Assigned: AAMRL

Dr. William W. Bannister  
Professor  
Dept. of Chemistry  
University of Lowell  
Lowell, MA 01824  
(617) 452-5000

Degree: Ph.D., Organic Chemistry,  
1961  
Specialty: Organic Chemistry  
Assigned: ESC

Prof. Beryl L. Barber  
Assistant Professor  
Dept. of Electronic Eng. Tech.  
Oregon Institute of Technology  
3201 Campus Drive  
Klamath Falls, OR 97601-7791  
(503) 882-6321

Degree: MS, Electronic Eng., 1961  
Specialty: Electrical Engineering  
Assigned: RADC

Dr. William M. Bass  
Professor  
Dept. of Anthropology  
The University of Tennessee  
252 South Stadium Hall  
Knoxville, TN 37996  
(615) 974-4408

Degree: Ph.D., Physical Anthropology  
1961  
Specialty: Physical Anthropology  
Assigned: ESC



Dr. Bryan R. Becker  
Associate Professor  
Dept. of Mechanical Engineering  
Rose-Hulman Institute  
5500 Wabash Avenue  
Terre Haute, IN 47803  
(812) 877-1511

Degree: Ph.D., Engineering Science,  
1979  
Specialty: Engineering Science  
Assigned: APL

Dr. Charles Bell  
Professor  
Dept. of Engineering  
Arkansas State University  
P O Drawer 1080  
State University, AR 72467-1080  
(501) 972-2088

Degree: Ph.D., Mechanical Eng.,  
1965  
Specialty: Mechanical Engineering  
Assigned: AD

Prof. Kweku K. Bentil  
Associate Professor  
School of Building Construction  
University of Florida  
Gainesville, FL 32611  
(904) 392-5965

Degree: M.S., Building Construction,  
1975  
Specialty: Building Construction  
Assigned: LMC

Dr. David E. Betounes  
Associate Professor  
Mathematics Department  
Univ. of Southern Mississippi  
S.S. Box 5045  
Hattiesburg, MS 39406-5045  
(601) 266-4293

Degree: Ph.D., Mathematics, 1978  
Specialty: Mathematics  
Assigned: AD

Prof. Phillip A. Bishop  
Assistant Professor  
Area of HPER  
University of Alabama  
Tuscaloosa, AL 35487-9909  
(205) 348-8370

Degree: Ed.D., Exercise Physiology,  
1983  
Specialty: Exercise Physiology  
Assigned: SAM

Dr. Jerome W. Blaylock  
Associate Professor  
Dept. of Computing & A.S.  
Texas Southern University  
3100 Cleburne Avenue  
Houston, TX 77004  
(713) 527-7011

Degree: Ph.D., Computer Science,  
1982  
Specialty: Computer Science  
Assigned: LMC

Dr. John W. Bopp  
Assistant Professor  
Dept. of Chemistry  
Nazareth College  
4245 East Avenue  
Rochester, NY 14610  
(716) 586-2525

Degree: Ph.D., Chemistry, 1984  
Specialty: Computer Science  
Assigned: AD

Dr. Kevin Bowyer  
Assistant Professor  
Dept. of Computer Sci. & Eng.  
University of South Florida  
4202 E. Fowler Avenue  
Tampa, FL 33620  
(813) 974-3032

Degree: Ph.D. Computer Science, 1980  
Specialty: Computer Science  
Assigned: RADC

Mr. Lee I. Britt  
Instructor  
Dept. of Physics  
Grambling State University  
Grambling, LA 71245  
(318) 274-2575

Degree: M.S., Physics, 1978  
Specialty: Physics  
Assigned: AEDC

Mr. Richard H. Brown  
Associate Professor  
Dept. of Biology  
Ouachita Baptist University  
Box 3686  
Arkadelphia, PA 71923  
(501) 246-4531

Degree: M.S., Physiology, 1963  
Specialty: Physiology  
Assigned: OEHL

Dr. Robert A. Buchl  
Assistant Professor  
Dept. of Physics & Astronomy  
Univ. of Wisconsin-Eau Claire  
Eau Claire, WI 54702-4004  
(715) 836-2272

Degree: Ph.D., Physics, 1971  
Specialty: Physics  
Assigned: AD

Dr. Charles M. Bump  
Assistant Professor  
Dept. of Chemistry  
Hampton University  
P O Box 6483  
Hampton, VA 23668  
(804) 727-5330

Degree: Ph.D., Organic Chemistry,  
1979  
Specialty: Organic Chemistry  
Assigned: FJSRL

Dr. Allan R. Burkett  
Associate Professor  
Dept. of Chemistry  
Dillard University  
2601 Gentilly Blvd.  
New Orleans, LA 70122  
(504) 283-8822

Degree: Ph.D., Inorganic Chemistry,  
1972  
Specialty: Inorganic Chemistry  
Assigned: RPL

Dr. Ronald V. Canfield  
Professor  
Dept. of Applied Science  
Utah State University  
UMC 42002601 Gentilly Blvd.  
Utah State University, UT 84233  
(801) 750-2434

Degree: Ph.D., Statistics, 1975  
Specialty: Statistics  
Assigned: RADC

Dr. Patricia A. Carlson  
Professor/Director  
Dept. of Humanities  
Rose-Hulman Inst. of Technology  
5500 Wabash Avenue  
Terre Haute, IN 47803  
(812) 877-1511

Degree: Ph.D., Literature/Language,  
1973  
Specialty: Literature/Language  
Assigned: HRL/LR

Dr. Kwo-Sun Chu  
Chairman  
Dept. of Physics & Comput. Sci.  
Talladega College  
Talladega, AL 35160  
(205) 362-0206

Degree: Ph.D., Theoretical Physics,  
1974  
Specialty: Theoretical Physics  
Assigned: ML

Dr. David Y. Chung  
Professor  
Dept. of Physics  
Howard University  
Washington, DC 20059  
(202) 636-7903

Degree: Ph.D., Physics, 1966  
Specialty: Theoretical Physics  
Assigned: FJSRL

Dr. Robert W. Courter  
Associate Professor  
Dept. of Mechanical Engineering  
Louisiana State University  
CEBA 2513D  
Baton Rouge, LA 70803  
(504) 388-5891

Degree: Ph.D., Aerospace Eng., 1965  
Specialty: Aerospace Engineering  
Assigned: AD

Dr. Bruce A. Craver  
Associate Professor  
Dept. of Physics  
University of Dayton  
300 College Park  
Dayton, OH 45469  
(513) 229-2219

Degree: Ph.D., Physics, 1976  
Specialty: Physics  
Assigned: ML

Prof. William K. Curry  
Assistant Professor  
Dept. of Computer Science  
Rose-Hulman Inst. of Technology  
5500 Wabash Ave.  
Terre Haute, IN 47803  
(812) 877-1511

Degree: M.S., Computer Sci., 1976  
Specialty: Computer Science  
Assigned: AL

Dr. Phanindramohan Das  
Professor  
Dept. of Meteorology  
Texas A&M University  
College Station, TX 77843  
(409) 845-0633

Degree: Ph.D., Meteorology, 1963  
Specialty: Meteorology  
Assigned: ESD

Dr. Bruce A. DeVantier  
Assistant Professor  
Dept. of Civil Eng. & Mechanics  
S. Illinois University  
Carbondale, IL 62901  
(618) 536-2368

Degree: Ph.D., Civil Eng., 1983  
Specialty: Civil Engineering  
Assigned: ML

Dr. Elvis E. Deal  
Assistant Professor  
Dept. of Industrial Engineering  
University of Houston  
4800 Calhoun  
Houston, TX 77004  
(713) 749-4487

Degree: Ph.D., Industrial Eng., 1985  
Specialty: Industrial Engineering  
Assigned: OEHL

Dr. Suhrit K. Dey  
Professor  
Dept. of Mathematics  
Eastern Illinois University  
Charleston, IL 61920  
(217) 581-3217

Degree: Ph.D., Aerospace Eng., 1970  
Specialty: Aerospace Engineering  
Assigned: AEDC

Dr. Ronna E. Dillon  
Professor  
Depts. of Educational Psychology  
and Psychology  
Southern Illinois University  
Carbondale, IL 62901  
(618) 536-7763

Degree: Ph.D., Educational  
Psychology, 1978  
Specialty: Educational Psychology  
Assigned: HRL/MO

Dr. Ravinder Diwan  
Professor  
Dept. of Mechanical Engineering  
Southern University  
Baton Rouge, LA 70813  
(504) 771-4701

Degree: Ph.D., Metallurgy, 1973  
Specialty: Metallurgy  
Assigned: ML

Dr. Verlynda S. Dobbs  
Assistant Professor  
Dept. of Computer Science  
Wright State University  
414 Fawcett  
Dayton, OH 45435  
(513) 873-2491

Degree: Ph.D., Computer Sci., 1985  
Specialty: Computer Science  
Assigned: AL

Dr. F. Carroll Dougherty  
Assistant Professor  
Dept. of Aerospace Engineering  
University of Colorado  
Campus Box 429  
Boulder, CO 80309  
(303) 492-8464

Degree: Ph.D., Aeronautical/  
Astronautical Engr., 1985  
Specialty: Aerospace Engineering  
Assigned: AEDC

Dr. John M. Dunn  
Assistant Professor  
Dept. of Elec. & Compt. Eng.  
University of Colorado  
Campus Box 425  
Boulder, CO 80309  
(303) 492-5487

Degree: Ph.D., Applied Physics, 1984  
Specialty: Applied Physics  
Assigned: RADC

Dr. Thomas A.W. Dwyer  
Associate Professor  
Dept. of Aero & Astro Eng.  
University of Illinois  
104 S. Mathews Avenue  
Urbana, IL 61801  
(217) 244-0720

Degree: Ph.D., Mathematics, 1971  
Specialty: Mathematics  
Assigned: WL

Dr. Kiah Edwards  
Professor  
Dept. of Biology  
Texas Southern University  
3100 Cleburne Street  
Houston, TX 77004  
(713) 527-7829

Degree: Ph.D., Molecular Biology,  
1974  
Specialty: Molecular Biology  
Assigned: OEHL

Dr. Marco A. Egoavil  
Associate Professor  
Dept. of Mechanical Engineering  
University of Puerto Rico  
Mayaguez, PR 00709  
(809) 834-4040

Degree: Ph.D., Mechanical Eng., 1981  
Specialty: Mechanical Engineering  
Assigned: AEDC

Dr. Ira Elder  
Professor  
Dept. of Mathematical Sciences  
Eastern New Mexico University  
Portales, NM 88130  
(505) 356-6208

Degree: Ph.D., Applied Mathematics  
1979  
Specialty: Applied Mathematics  
Assigned: WL

Dr. Ramez Elmasri  
Assistant Professor  
Dept. of Computer Science  
Univ. of Houston  
Houston, TX 77036  
(713) 749-2630

Degree: Ph.D., Computer Science,  
1980  
Specialty: Computer Science  
Assigned: RADC

Dr. John E. Erdei  
Assistant Professor  
Dept. of Physics  
University of Dayton  
Dayton, OH 45469  
(513) 229-2318

Degree: Ph.D., Condensed Matter,  
1983  
Specialty: Physics  
Assigned: APL

Dr. Joseph J. Feeley  
Associate Professor  
Dept. of Electrical Engineering  
University of Idaho  
Moscow, ID 83843  
(208) 885-7482

Degree: Ph.D., Electrical Eng., 1980  
Specialty: Electrical Engineering  
Assigned: AD

Dr. Wilton Flemon  
Associate Professor  
Dept. of Chemistry  
Metropolitan State College  
Denver, CO 80204  
(303) 556-2838

Degree: Ph.D., Physical Organic  
Chemistry, 1970  
Specialty: Physical Organic Chemistry  
Assigned: RPL

Dr. Dennis R. Flentge  
Associate Professor  
Dept. of Math/Science  
Cedarville College  
Box 601  
Cedarville, OH 45314-0601  
(513) 766-2211

Degree: Ph.D., Physical Chemistry,  
1974  
Specialty: Physical Chemistry  
Assigned: APL

Dr. Luther D. Flippen, Jr.  
Assistant Professor  
Dept. of Mechanical and  
Nuclear Engineering  
Mississippi State University  
P O Drawer ME  
Mississippi State, MS 39759  
(601) 325-3412

Degree: Ph.D., Mechanical Eng., 1982  
Specialty: Mechanical Engineering  
Assigned: RPL

Dr. Lee A. Flippin  
Assistant Professor  
Dept. of Chemistry  
San Francisco State Univ.  
San Francisco, CA 94132  
(415) 469-1627

Degree: Ph.D., Organic Chemistry,  
1980  
Specialty: Organic Chemistry  
Assigned: AFGL

Dr. Lionel R. Friedman  
Professor  
Dept. of Electrical Eng.  
Worcester Polytechnic Inst.  
100 Institute Road  
Worcester, MA 01609  
(415) 469-1627

Degree: Ph.D., Physics, 1961  
Specialty: Physics  
Assigned: RAOC

Dr. John W. Gilmer  
Assistant Professor  
Polymer Science Program  
Penn State University  
University Park, PA 16802  
(814) 863-1487

Degree: Ph.D., Physical Chemistry,  
1984  
Specialty: Physical Chemistry  
Assigned: ML

Dr. Stephen J. Gold  
Associate Professor  
Dept. of Electrical Engineering  
South Dakota State University  
P O Box 2220  
Brookings, SD 57007  
(605) 688-4419

Degree: Ph.D., Electrical Eng., 1969  
Specialty: Electrical Engineering  
Assigned: FJSRL

Dr. Michael R. Gorman  
Assistant Professor  
Dept. of Engineering Mechanics  
Univ. of Lincoln-Nebraska  
216 Bancroft Hall  
Lincoln, NE 68588-0347  
(402) 472-2397

Degree: Ph.D., Physics, 1981  
Specialty: Physics  
Assigned: RPL

Dr. Benjamin Gottlieb  
Professor  
Dept. of Science  
Bishop College  
3837 Simpson Stuart Road  
Dallas, TX 75042  
(214) 372-8773

Degree: Ph.D., Physics, 1964  
Specialty: Physics  
Assigned: AFGL

Dr. Gary M. Graham  
Assistant Professor  
Dept. of Mechanical Engineering  
Ohio University  
261 Stocker  
Athens, OH 45701  
(614) 593-1556

Degree: Ph.D., Mechanical Eng., 1985  
Specialty: Mechanical Engineering  
Assigned: FDL

Mr. William M. Grissom  
Assistant Professor  
Dept. of Physics  
Morehouse College  
630 Westview Dr., S.W.  
Atlanta, GA 30314  
(404) 681-2800

Degree: M.S., Mechanical Eng., 1978  
Specialty: Mechanical Engineering  
Assigned: AEDC

Dr. Timothy A. Grogan  
Assistant Professor  
Dept. of Electrical and  
Computer Engineering  
University of Cincinnati  
ML#30 898 Rhodes Hall  
Cincinnati, OH 45245  
(513) 475-2349

Degree: Ph.D., Electrical Eng., 1983  
Specialty: Electrical Engineering  
Assigned: RADC



Dr. Vijay K. Gupta  
Professor  
Dept. of Chemistry  
Central State University  
Wilberforce, OH 45384  
(513) 376-6423

Degree: Ph.D., Chemistry, 1969  
Specialty: Chemistry  
Assigned: ML

Dr. Narayan C. Halder  
Professor  
Dept. of Physics  
University of South Florida  
Tampa, FL 33620  
(813) 974-2781

Degree: Ph.D., Physics, 1963  
Specialty: Physics  
Assigned: AL

Dr. Kenneth R. Halliday  
Associate Professor  
Dept. of Mechanical Engineering  
Ohio University  
259 Stocker Center  
Athens, OH 45701  
(614) 593-1557

Degree: Ph.D., Mechanical Eng., 1977  
Specialty: Mechanical Engineering  
Assigned: ML

Dr. Elmer C. Hansen  
Assistant Professor  
Dept. of Mechanical Engineering  
University of Florida  
222 MEB  
Gainesville, FL 32611  
(904) 392-0827

Degree: Ph.D., Mechanical Eng., 1978  
Specialty: Mechanical Engineering  
Assigned: AD

Dr. David Hart  
Assistant Professor  
Dept. of Mathematics  
University of Cincinnati  
Cincinnati, OH 45221  
(513) 475-4851

Degree: Ph.D., Mathematics, 1980  
Specialty: Mathematics  
Assigned: FDL

Dr. Terence Hines  
Assistant Professor  
Dept. of Psychology  
Pace University  
Pleasantville, NY 10570  
(914) 741-3791

Degree: Ph.D., Psychology, 1978  
Specialty: Psychology  
Assigned: HRL/OT

Dr. Albert Hirschberg  
Professor  
Dept. of Chemistry  
Long Island University  
Brooklyn, NY 11201  
(516) 536-5719

Degree: Ph.D., Organic Chemistry,  
1960  
Specialty: Organic Chemistry  
Assigned: FJSRL

Dr. Robert Hoffman  
Associate Professor  
Dept. of Psychology  
Adelphi Univ.  
Garden City, NY 11530  
(516) 663-1055

Degree: Ph.D., Psychology, 1978  
Specialty: Psychology  
Assigned: AFGL

Dr. James Hoffmaster  
Chairman  
Dept. of Physics  
Gonzaga University  
Spokane, WA 99205  
(509) 328-2416

Degree: Ph.D., Physics, 1970  
Specialty: Physics  
Assigned: AD

Dr. Gwendolyn Howze  
Associate Professor  
Dept. of Biology  
Texas Southern University  
Houston, TX 77054  
(713) 795-0280

Degree: Ph.D., Molecular Biology,  
1974  
Specialty: Physics  
Assigned: AD

Dr. Mayer Humi  
Associate Professor  
Dept. of Math  
WPI  
Worcester, MA 01609  
(617) 755-3777

Degree: Ph.D., Applied Math, 1970  
Specialty: Applied Mathematics  
Assigned: AFGL

Dr. Peter Jeffers  
Professor  
Dept. of Chemistry  
S.U.N.Y.  
Cortland, NY 13045  
(607) 753-2903

Degree: Ph.D., Chemistry, 1964  
Specialty: Chemistry  
Assigned: ESC

Dr. Gordon Johnson  
Professor  
Dept. of Physics  
Walla Walla College  
College Place, WA 99324  
(509) 527-2881

Degree: Ph.D., Electrical Eng., 1972  
Specialty: Electrical Engineering  
Assigned: ML

Dr. Louis Johnson  
Associate Professor  
Dept. of Electrical Engineering  
Oklahoma State Univ.  
Tryon, OK 74875  
(918) 375-2374

Degree: Ph.D., Electrical Eng., 1973  
Specialty: Electrical Engineering  
Assigned: RADC

Dr. William Jordon  
Assistant Professor  
Dept. of Engineering  
Louisiana Tech. Univ.  
Ruston, LA 71272  
(318) 257-4304

Degree: Ph.D., Interdis. Eng., 1985  
Specialty: Engineering  
Assigned: ML

Dr. William Kauder  
Assistant Professor  
Dept. of Accounting  
North Carolina A&T State Univ.  
Greensboro, NC 27411  
(919) 294-4539

Degree: Ph.D., Accounting, 1982  
Specialty: Business Administration  
Assigned: LMC

Dr. John Kenney  
Assistant Professor  
Dept. of Physical Sciences  
Eastern New Mexico University  
Portales, NM 88130  
(505) 562-2152

Degree: Ph.D., Physical Chemistry,  
1979  
Specialty: Physical Chemistry  
Assigned: RPL

Dr. Yong Kim  
Assistant Professor  
Dept. of Civil Engineering  
Catholic University of America  
Washington, D.C. 20904  
(301) 635-5164

Degree: Ph.D., Civil Eng., 1984  
Specialty: Civil Engineering  
Assigned: ESC

Dr. Charles Kimble  
Associate Professor  
Dept. of Psychology  
University of Dayton  
Dayton, OH 45469  
(513) 229-2168

Degree: Ph.D., Psychology, 1972  
Specialty: Psychology  
Assigned: AAMRL

Dr. Jerome Knopp  
Associate Professor  
Dept. of Engineering  
University of Missouri  
Independence, MO 64050-1799  
(913) 276-1278

Degree: Ph.D., Electrical Eng., 1976  
Specialty: Electrical Engineering  
Assigned: WL

Dr. Lawrence Koons  
Professor  
Dept. of Chemistry  
Tuskegee University  
Tuskegee, AL 36088  
(205) 727-8835

Degree: Ph.D., Chemistry, 1956  
Specialty: Chemistry  
Assigned: FJSRL

Dr. Henry Kurtz  
Assistant Professor  
Dept. of Chemistry  
Memphis State Univ.  
Memphis, TN 38107  
(901) 454-2630

Degree: Ph.D., Chemistry, 1977  
Specialty: Chemistry  
Assigned: FJSRL

Dr. Thomas Lalk  
Assistant Professor  
Dept. of Mechanical Eng.  
Texas A&M Univ.  
College Station, TX 77840  
(409) 693-9495

Degree: Ph.D., Mechanical Eng., 1972  
Specialty: Mechanical Engineering  
Assigned: APL

Dr. Dan Landis  
Professor  
Dept. of Psychology  
Univ. of Mississippi  
University, MS 38677  
(601) 236-2441

Degree: Ph.D., Psychology, 1963  
Specialty: Psychology  
Assigned: DEOMI

Dr. Steven Leon  
Professor  
Dept. of Mathematics  
Southeastern Massachusettes  
North Dartmouth, MA 02747  
(617) 999-8320

Degree: Ph.D., Mathematics, 1971  
Specialty: Mathematics  
Assigned: AFGL

Dr. David Ludwig  
Assistant Professor  
Dept. of Mathematics  
Univ. of North Carolina  
Greensboro, NC 27412-5001  
(919) 334-5749

Degree: Ph.D., Mathematics, 1971  
Specialty: Mathematics  
Assigned: SAM

Dr. Mohammed Maleque  
Associate Professor  
Dept. of Pharmacology  
Meharry Medical College  
Nashville, TN 37208  
(615) 327-6510

Degree: Ph.D., Pharmacology, 1976  
Specialty: Pharmacology  
Assigned: SAM

Dr. Robert Masingale  
Professor  
Dept. of Sciences and Math  
Jarvis Christian College  
Hawkins, TX 75765  
(214) 769-2174

Degree: Ph.D., Chemistry, 1966  
Specialty: Chemistry  
Assigned: FJSRL

Dr. Michael Matthews  
Assistant Professor  
Dept. of Behavioral Sciences  
Drury College  
Springfield, MO 65802  
(417) 865-8731

Degree: Ph.D., Psychology, 1984  
Specialty: Psychology  
Assigned: HRL/MO

Dr. Alastair McAulay  
Professor  
Dept. of Electrical Engineering  
Wright State University  
Dayton, OH 45440  
(513) 873-2167

Degree: Ph.D., Electrical Eng., 1974  
Specialty: Electrical Engineering  
Assigned: AL

Dr. Barry McConnell  
Assistant Professor  
Dept. of Computer & Info Sci.  
Florida A&M University  
Tallahassee, FL 32307  
(904) 599-3022

Degree: Ph.D., Computer Sci., 1984  
Specialty: Computer Science  
Assigned: WL

Mr. Oliver McGee  
Sr. Research Associate  
Dept. of Civil Engineering  
Ohio State University  
Gahanna, OH 43230  
(614) 476-5035

Degree: M.S., Eng. Mechanics, 1983  
Specialty: Engineering Mechanics  
Assigned: FDL

Dr. Daniel Mihalko  
Associate Professor  
Dept. of Math & Statistics  
Western Michigan University  
Kalamazoo, MI 49008  
(616) 383-6165

Degree: Ph.D., Math Statistics, 1977  
Specialty: Math Statistics  
Assigned: SAM

Mr. Augustus Morris  
Mathematics Instructor  
Dept. of Natural Sciences  
Wilberforce University  
Wilberforce, OH 45426  
(513) 376-2911

Degree: B.S., Biomedical Eng., 1981  
Specialty: Biomedical Engineering  
Assigned: AAMRL

Dr. Mary Morton-Gibson  
Associate Professor  
Dept. of Chemistry/Physics  
Lock Haven University  
Lock Haven, PA 17745  
(717) 893-2054

Degree: Ph.D., Physiology, 1970  
Specialty: Physiology/Biophysics  
Assigned: SAM

Dr. Lena Myers  
Professor  
Dept. of Sociology/Social Psych.  
Jackson State University  
Jackson, MS 39217  
(601) 968-2591

Degree: Ph.D., Sociology, 1973  
Specialty: Sociology  
Assigned: DEOMI

Dr. James Nail  
Associate Professor  
Dept. of Engineering  
Mississippi State Univ.  
Mississippi State, MS 39762  
(601) 325-3665

Degree: Ph.D., Electrical Eng., 1976  
Specialty: Electrical Engineering  
Assigned: AD

Dr. Henry Nebel  
Associate Professor  
Dept. of Physics  
Alfred University  
Alfred, NY 14802  
(607) 871-2208

Degree: Ph.D., Physics, 1967  
Specialty: Physics  
Assigned: AFGL

Dr. Maurice Neveu  
Associate Professor  
Dept. of Chemistry  
State University College  
Fredonia, NY 14063  
(716) 673-3285

Degree: Ph.D., Chemistry, 1959  
Specialty: Physical/Organic Chemistry  
Assigned: FJSRL

Dr. James Noyes  
Associate Professor  
Dept. of Math & C.S.  
Wittenberg University  
Springfield, OH 45501  
(716) 673-3285

Degree: Ph.D., Computer Sci., 1977  
Specialty: Computer Science  
Assigned: AL

Dr. Noel Nussbaum  
Associate Professor  
Dept. of Biology  
Wright State University  
Dayton, OH 45401-0927  
(513) 426-8935

Degree: Ph.D., Biology, 1964  
Specialty: Biology  
Assigned: AAMRL

Dr. Thomas Nygren  
Associate Professor  
Dept. of Psychology  
Ohio State University  
Columbus, OH 43221  
(614) 486-7931

Degree: Ph.D., Psychology, 1975  
Specialty: Psychology  
Assigned: AAMRL

Dr. Kurt Oughstun  
Assistant Professor  
Dept. of Electrical/Computer  
Engineering  
University of Wisconsin  
Madison, WI 53705  
(608) 231-3126

Degree: Ph.D., Optics, 1979  
Specialty: Optical Sciences  
Assigned: SAM

Dr. Surgounda Patil  
Professor  
Dept. of Math  
Tennessee Technical University  
Cookeville, TN 38501  
(615) 528-6924

Degree: Ph.D., Math Stat., 1966  
Specialty: Math Statistics  
Assigned: AEDC

Dr. Martin Patt  
Associate Professor  
Dept. of Electrical Engineering  
University of Lowell  
Lowell, MA 01854  
(617) 452-5000

Degree: M.S., Electrical Eng., 1964  
Specialty: Electrical Engineering  
Assigned: AFGL

Dr. William Patten  
Assistant Professor  
Dept. of Mechanical Eng.  
University of Iowa  
Iowa City, IA 52242  
(319) 335-5675

Degree: Ph.D., Mechanical Eng., 1986  
Specialty: Mechanical Engineering  
Assigned: FDL

Dr. Ralph Peters  
Associate Professor  
Dept. of Biology  
Wichita State University  
Wichita, KS 67217  
(316) 943-8762

Degree: Ph.D., Zoophysiology, 1975  
Specialty: Zoology  
Assigned: SAM

Dr. Randall Peters  
Associate Professor  
Dept. of Physics  
Texas Tech University  
Lubbock, TX 79409  
(806) 742-3757

Degree: Ph.D., Physics, 1968  
Specialty: Physics  
Assigned: WL

Dr. Gerald Pollack  
Professor  
Dept. of Physics/Astronomy  
Michigan State University  
East Lansing, MI 48823  
(517) 353-9590

Degree: Ph.D., Physics, 1968  
Specialty: Physics  
Assigned: SAM

Dr. Spencer Porter  
Professor  
Dept. of Chemistry  
Capital Univeristy  
Columbus, OH 43209  
(614) 236-6107

Degree: Ph.D., Phys. Chemistry, 1968  
Specialty: Physcial Chemistry  
Assigned: ML

Dr. Leonard Price  
Chairman  
Dept. of Chemistry  
Xavier Univ. of Louisiana  
New Orleans, LA 77012  
(504) 486-7411

Degree: Ph.D., Org. Chemistry, 1962  
Specialty: Organic Chemistry  
Assigned: SAM

Dr. Stephen Pruett  
Assistant Professor  
Dept. of Biological Sciences  
Mississippi State University  
Mississippi, MS 39762  
(601) 325-3120

Degree: Ph.D., Immunology, 1980  
Specialty: Immunology  
Assigned: SAM

Dr. Panapkkam Ramamoorthy  
Associate Professor  
Dept. of Electrical/Computer Eng.  
University of Cincinnati  
Cincinnati, OH 45221  
(513) 475-4247

Degree: Ph.D., Digital Signal  
Process, 1977  
Specialty: Electrical Engineering  
Assigned: RADC



Dr. Gandikota Rao  
Professor  
Dept. of Meterology  
St. Louis University  
St. Louis, MO 63156  
(314) 658-3115

Degree: Ph.D., Meteorology, 1965  
Specialty: Meteorology  
Assigned: AFGL

Dr. Donald Robertson  
Associate Professor  
Dept. of Psychology  
Indiana University of PA  
Indiana, PA 15705  
(412) 357-4522

Degree: Ph.D., Psychology, 1981  
Specialty: Psychology  
Assigned: AAMRL

Dr. Kenneth Roenker  
Associate Professor  
Dept. of Electrical/Computer Eng.  
University of Cincinnati  
Cincinnati, OH 45221  
(513) 475-4461

Degree: Ph.D., Solid State Physics,  
1973  
Specialty: Solid State Physics  
Assigned: AL

Dr. Ramendra Roy  
Professor  
Dept. of Nuclear Engineering  
Arizona State University  
Mesa, AZ 85202  
(602) 838-0551

Degree: Ph.D., Nuclear Engr., 1975  
Specialty: Nuclear Engineering  
Assigned: APL

Dr. Paul Rybski  
Assistant Professor  
Dept. of Physics  
University of Wisconsin  
Whitewater, WI 53190-1790  
(414) 472-5766

Degree: Ph.D., Astronomy, 1972  
Specialty: Astronomy  
Assigned: AFGL

Dr. Joseph Saliba  
Assistant Professor  
Dept. of Civil Engineering  
University of Dayton  
Dayton, OH 45469  
(513) 229-3847

Degree: Ph.D., Solid Mechanics, 1983  
Specialty: Solid Mechanics  
Assigned: FDL

Dr. Richard Schori  
Professor  
Dept. of Mathematics  
Oregon State University  
Corvallis, OR 97333  
(503) 754-4686

Degree: Ph.D., Mathematics, 1964  
Specialty: Mathematics  
Assigned: SAM

Dr. Lawrence Schovanec  
Assistant Professor  
Dept. of Mathematics  
Texas Tech University  
Lubbock, TX 79409  
(806) 742-1424

Degree: Ph.D., Mathematics, 1964  
Specialty: Mathematics  
Assigned: RPL

Dr. William Schulz  
Associate Professor  
Dept. of Chemistry  
Eastern Kentucky University  
Richmond, KY 40475  
(606) 622-1463

Degree: Ph.D., Chemistry, 1975  
Specialty: Chemistry  
Assigned: ESC

Dr. Nisar Shaikh  
Assistant Professor  
Dept. of Engr. Mechanics  
Univ. of Nebraska  
Lincoln, NE 68588-1347  
(402) 472-2384

Degree: Ph.D., Mechanics, 1983  
Specialty: Mechanics  
Assigned: ML

Dr. Shiva Singh  
Professor  
Dept. of Mech. Engineering  
Univ. of Kentucky  
Lexington, KY 40506  
(606) 257-3825

Degree: Ph.D., Mathematics, 1959  
Specialty: Mathematics  
Assigned: FDL

Dr. Gary Slater  
Professor  
Dept. of Aerospace Engineering  
University of Cincinnati  
Cincinnati, OH 45221  
(513) 475-6287

Degree: Ph.D., Aerospace Engr., 1971  
Specialty: Aerospace Engineering  
Assigned: FDL

Dr. Timothy Su  
Professor  
Dept. of Physical Chemistry  
Southeastern Massachusetts Univ.  
North Dartmouth, MA 02790  
(617) 999-8235

Degree: Ph.D., Physical Chem., 1971  
Specialty: Physical Chemistry  
Assigned: AFGL

Dr. David Sumberg  
Associate Professor  
Dept. of Electrical Engr.  
Rochester Institute of Tech.  
Rochester, NY 14618  
(716) 475-6067

Degree: Ph.D., Physics, 1972  
Specialty: Physics  
Assigned: RADC

Dr. Wesley Tanaka  
Associate Professor  
Dept. of Chemistry  
University of Wisconsin  
Eau Claire, WI 54701  
(715) 836-5388

Degree: Ph.D., Biochemistry, 1974  
Specialty: Biochemistry  
Assigned: SAM

Dr. Richard Tankin  
Professor  
Dept. of Mechanical Engr.  
Northwestern University  
Evanston, IL 60201  
(312) 491-3532

Degree Ph.D., Mechanical Eng., 1960  
Specialty: Mechanical Engineering  
Assigned: APL

Dr. Joseph Tedesco  
Assistant Professor  
Dept. of Civil Engineering  
Auburn University  
Auburn, AL 36849  
(205) 826-4320

Degree Ph.D., Civil Engr., 1982  
Specialty: Civil Engineering  
Assigned: ESC

Dr. Forrest Thomas  
Professor  
Dept. of Chemistry  
University of Montana  
Missoula, MT 59812  
(406) 549-8205

Degree Ph.D., Chemistry, 1959  
Specialty: Chemistry  
Assigned: FDL

Dr. Howard Thompson  
Professor  
Dept. of Mechanical Engineering  
Purdue University  
W. Lafayette, IN 47907  
(317) 494-5624

Degree Ph.D., Mech. Engr., 1965  
Specialty: Mechanical Engineering  
Assigned: FJSRL

Dr. David Townsend  
Associate Professor  
Dept. of Psychology  
Montclair State College  
Upper Montclair, NJ 07043  
(201) 783-9407

Degree Ph.D., Cog. Psychology, 1972  
Specialty: Cognitive Psychology  
Assigned: HRL/LR

Dr. Michele Trankina  
Assistant Professor  
Dept. of Biology  
St. Mary's University  
San Antonio, TX 78284  
(512) 436-3241

Degree Ph.D., Nutrit. Physiology  
1982  
Specialty: Nutritional Physiology  
Assigned: SAM

Dr. Robert Trenary  
Assistant Professor  
Dept. of Computer Sci. & Math  
Western Michigan University  
Kalamazoo, MI 49008  
(616) 383-6151

Degree Ph.D., Computer Science/Math  
1987  
Specialty: Computer Science  
Assigned: AL

Dr. Dennis Truax  
Assistant Professor  
Civil Engineering  
Dept. of Civil Engineering  
Mississippi State Univeristy  
Mississippi State, MS 39762  
(601) 325-3050

Degree Ph.D., Civil Eng., 1986  
Specialty: Civil Engineering  
Assigned: ESC

Dr. John Uhlarik  
Professor  
Dept. of Psychology  
Kansas State University  
Manhattan, KS 66506  
(913) 532-6850

Degree Ph.D., Psychology, 1970  
Specialty: Psychology  
Assigned: HRL/OT

Dr. P. Vaidya  
Associate Professor  
Dept. of Mechanical Engineering  
Washington State Univ.  
Pullman, WA 99164  
(509) 335-7436

Degree Ph.D., Acoustics, 1969  
Specialty: Acoustics  
Assigned: ESC

Dr. Joseph Verducci  
Assistant Professor  
Dept. of Statistics  
Ohio State University  
Columbus, OH 43210  
(614) 292-3886

Degree: Ph.D., Statistics, 1982  
Specialty: Statistics  
Assigned: OEHL

Dr. Robert Voigt  
Associate Professor  
Metallurgy  
Dept. of Mechanical Engr.  
University of Kansas  
Lawrence, KS 66045  
(913) 864-3181

Degree: Ph.D., Metallurgical Engr.,  
1981  
Specialty: Metallurgical Engineering  
Assigned: ML

Dr. Keith Walker  
Professor  
Dept. of Physics  
Point Loma College  
San Diego, CA 92106  
(619) 221-2374

Degree: Ph.D., Physics, 1971  
Specialty: Physics  
Assigned: AFGL

Dr. Richard Walker  
Assistant Professor  
Dept. of Mathematics  
Fort Lewis College  
Durango, CO 81302  
(303) 247-7147

Degree: Ph.D., Math/Geophysics, 1979  
Specialty: Mathematics  
Assigned: AFGL

Dr. Jacob Weinberg  
Professor  
Dept. of Mathematics  
University of Lowell  
Lowell, MA 01854  
(617) 727-9820

Degree: Ph.D., Mathematics, 1961  
Specialty: Mathematics  
Assigned: RADC

Dr. Howard Weiss  
Associate Professor  
Dept. of Management  
Temple University  
Philadelphia, PA 19122  
(215) 787-6829

Degree: Ph.D., Industrial Eng., 1975  
Specialty: Industrial Engineering  
Assigned: LC

Dr. Charles Wells  
Associate Professor  
Dept. of Decision Sciences  
University of Dayton  
Dayton, OH 45469  
(513) 229-3332

Degree: Ph.D., Management Sci., 1982  
Specialty: Management Science  
Assigned: HRL/LR

Dr. Ward Wells  
Assistant Professor  
Human Performance  
Dept. of Physical Education  
University of Alaska  
Fairbanks, AL 99775-0240  
(907) 479-5115

Degree: Ph.D., Human Performance,  
1981  
Specialty: Human Performance  
Assigned: SAM

Dr. John Westerkamp  
Assistant Professor  
Dept. of Electrical Engr.  
University of Dayton  
Dayton, OH 45469  
(513) 229-3611

Degree: Ph.D., Electrical Eng., 1985  
Specialty: Electrical Engineering  
Assigned: AAMRL

Dr. Robert Wetherhold  
Assistant Professor  
Mechanical & Aerospace Eng.  
State University of New York  
Buffalo, NY 14260  
(716) 636-2593

Degree: Ph.D., Applied Science, 1983  
Specialty: High Temperature Composite  
Materials  
Assigned: ML

Dr. William Wheless  
Assistant Professor  
Dept. of ECE  
New Mexico State University  
Las Cruces, NM 88003  
(505) 646-3214

Degree: Ph.D., Electrical Eng., 1985  
Specialty: Electrical Engineering  
Assigned: WL

Dr. Stanley Whidden  
Researcher  
Hyperbaric Medicine  
Dept. of Hyperbaric Medicine  
JESM Baromedical Research Inst.  
New Orleans, LA 70115  
(504) 363-7656

Degree: M.D., Hyperbaric Medicine,  
1984  
Specialty: Hyperbaric Medicine  
Assigned: SAM

Dr. Andrew Whipple  
Associate Professor  
Dept. of Biology  
Taylor University  
Upland, IN 46989  
(317) 998-5333

Degree: Ph.D., Cell Biology, 1979  
Specialty: Cell Biology  
Assigned: AAMRL

Dr. Sharon Williams  
Instructor  
Dept. of Chemistry  
Southern University  
Baton Rouge, LA 70813-0572  
(504) 771-3990

Degree: M.S., Cell Biology, 1979  
Specialty: Biochemistry  
Assigned: SAM

Dr. Frank Witzmann  
Assistant Professor  
Dept. of Biology  
IUPUI Columbus  
Columbus, OH 47203  
(614) 372-8266

Degree: Ph.D., Biology, 1981  
Specialty: Biology  
Assigned: AAMRL

Dr. William Wolfe  
Associate Professor  
Dept. of Civil Engineering  
Ohio State University  
Columbus, OH 43210  
(614) 292-0790

Degree: Ph.D., Engineering, 1979  
Specialty: Engineering  
Assigned: FDL

Dr. Lawrence Wolpert  
Associate Professor  
Dept. of Psychology  
Ohio State University  
Columbus, OH 43210  
(614) 267-9328

Degree: M.S., Psychology, 1983  
Specialty: Psychology  
Assigned: AAMRL

Dr. Cheng-Hsiao Wu  
Associate Professor  
Solid State Physics  
Dept. of Electrical Engineering  
Univ. of Missouri  
Rolla, MO 65401  
(314) 341-4677

Degree: Ph.D., Solid State Physics,  
1972  
Specialty: Solid State Physics  
Assigned: APL

Dr. Joan Wyzkoski  
Associate Professor  
Dept. of Math & Computer Sci.  
Fairfield University  
Fairfield, CT 06430-7524  
(203) 254-4000

Degree: Ph.D., Mathematics, 1979  
Specialty: Mathematics  
Assigned: WL

Dr. Melvin Zandler  
Associate Professor  
Physical Chemistry  
Dept. of Chemistry  
Wichita State Univ.  
Wichita, KS 67204  
(316) 689-3120

Degree: Ph.D., Physical Chemistry,  
1966  
Specialty: Physical Chemistry  
Assigned: FJSRL

Dr. George Zobrist  
Professor  
Dept. of Computer Science  
University of Missouri  
Rolla, MO 65401  
(314) 341-4492

Degree: Ph.D., Electrical Eng., 1965  
Specialty: Electrical Engineering  
Assigned: ESMC

PARTICIPANT LABORATORY ASSIGNMENT



C. PARTICIPANT LABORATORY ASSIGNMENT (Page 1)

1987 USAF/UES SUMMER FACULTY RESEARCH PROGRAM

AERO PROPULSION LABORATORY (AFWAL/APL)  
(Wright-Patterson Air Force Base)

- |                    |                   |
|--------------------|-------------------|
| 1. Suresh Aggarwal | 5. Thomas Lalk    |
| 2. Bryan Becker    | 6. Ramendra Roy   |
| 3. John Erdei      | 7. Richard Tankin |
| 4. Dennis Flentge  | 8. Cheng-Hsiao Wu |

ARMAMENT LABORATORY (AD)  
(Eglin Air Force Base)

- |                   |                     |
|-------------------|---------------------|
| 1. Charles Bell   | 6. Joseph Feeley    |
| 2. David Betounes | 7. Elmer Hansen     |
| 3. John Bopp, Jr. | 8. James Hoffmaster |
| 4. Robert Buchl   | 9. James Nail       |
| 5. Robert Courter |                     |

ARMSTRONG AEROSPACE MEDICAL RESEARCH LABORATORY (AAMRL)  
(Wright-Patterson Air Force Base)

- |                     |                      |
|---------------------|----------------------|
| 1. Xavier Avula     | 8. Thomas Nygren     |
| 2. Praphulla Bajpai | 9. Donald Robertson  |
| 3. Shankar Bale     | 10. John Westerkamp  |
| 4. Gwendolyn Howze  | 11. Andrew Whipple   |
| 5. Charles Kimble   | 12. Frank Witzmann   |
| 6. Augustus Morris  | 13. Lawrence Wolpert |
| 7. Noel Nussbaum    |                      |

ARNOLD ENGINEERING DEVELOPMENT CENTER (AEDC)  
(Arnold Air Force Station)

- |                      |                    |
|----------------------|--------------------|
| 1. Lee Britt         | 4. Marco Egoavil   |
| 2. Suhrit Dey        | 5. William Grissom |
| 3. Carroll Dougherty | 6. Surgounda Patil |

AVIONICS LABORATORY (AFWAL/AL)  
(Wright-Patterson Air Force Base)

- |                   |                     |
|-------------------|---------------------|
| 1. John Amoss     | 6. Alastair McAulay |
| 2. Vernon Bakke   | 7. James Noyes      |
| 3. William Curry  | 8. Kenneth Roenker  |
| 4. Verlynda Dobbs | 9. Robert Trenary   |
| 5. Narayan Halder |                     |

DEFENSE EQUAL OPPORTUNITY MANAGEMENT INSTITUTE (DEOMI)  
(Patrick Air Force Base)

1. Dan Landis
2. Lena Myers

EASTERN SPACE AND MISSILE CENTER (ESMC)  
(Patrick Air Force Base)

1. George Zobrist

C. PARTICIPANT LABORATORY ASSIGNMENT (Page 2)

ELECTRONICS SYSTEMS DIVISION (ESD)

(Hanscom Air Force Base)

1. Phanindramoha Das

ENGINEERING AND SERVICES CENTER (ESC)

(Tyndall Air Force Base)

- |                      |                   |
|----------------------|-------------------|
| 1. William Bannister | 5. William Schulz |
| 2. William Bass      | 6. Joseph Tedesco |
| 3. Peter Jeffers     | 7. Dennis Truax   |
| 4. Yong Kim          | 8. P. G. Vaidya   |

FLIGHT DYNAMICS LABORATORY (AFWAL/FDL)

(Wright-Patterson Air Force Base)

- |                   |                   |
|-------------------|-------------------|
| 1. Gary Graham    | 6. Shiva Singh    |
| 2. David Hart     | 7. Gary Slater    |
| 3. Oliver McGee   | 8. Forrest Thomas |
| 4. William Patten | 9. William Wolfe  |
| 5. Joseph Saliba  |                   |

FRANK J. SEILER RESEARCH LABORATORY (FJSRL)

(USAF Academy)

- |                      |                    |
|----------------------|--------------------|
| 1. Charles Bump      | 6. Henry Kurtz     |
| 2. David Chung       | 7. Maurice Neveu   |
| 3. Stephen Gold      | 8. Howard Thompson |
| 4. Albert Hirschberg | 9. Melvin Zandler  |
| 5. Lawrence Koons    |                    |

GEOPHYSICS LABORATORY (AFGL)

(Hanscom Air Force Base)

- |                          |                    |
|--------------------------|--------------------|
| 1. Francesco Bacchialoni | 8. Martin Patt     |
| 2. Lee Flippin           | 9. Gandikota Rao   |
| 3. Benjamin Gottlieb     | 10. Paul Rybski    |
| 4. Robert Hoffman        | 11. Timothy Su     |
| 5. Mayer Humi            | 12. Keith Walker   |
| 6. Steven Leon           | 13. Richard Walker |
| 7. Henry Nebel           |                    |

HUMAN RESOURCES LABORATORY/LR (HRL/LR)

(Wright-Patterson Air Force Base)

1. Patricia Carlson
2. David Townsend
3. Charles Wells

C. PARTICIPANT LABORATORY ASSIGNMENT (Page 3)

HUMAN RESOURCES LABORATORY/MO (HRL/MO)  
(Brooks Air Force Base)

1. Victor Appel
2. Ronna Dillon
3. Michael Matthews

HUMAN RESOURCES LABORATORY/OT (HRL/OT)  
(Williams Air Force Base)

1. Terence Hines
2. John Uhlarik

LOGISTICS COMMAND (LC)  
(Wright-Patterson Air Force Base)

1. Howard Weiss

LOGISTICS MANAGEMENT CENTER (LMC)  
(Gunter Air Force Base)

1. Kweku Bentil
2. Jerome Blaylock
3. William Kauder

MATERIALS LABORATORY (AFWAL/ML)  
(Wright-Patterson Air Force Base)

- |                     |                       |
|---------------------|-----------------------|
| 1. Kwo-Sun Chu      | 8. Gordon Johnson     |
| 2. Bruce Craver     | 9. William Jordan     |
| 3. Bruce DeVantier  | 10. Spencer Porter    |
| 4. Ravinder Diwan   | 11. Nisar Shaikh      |
| 5. John Gilmer      | 12. Robert Voigt      |
| 6. Vijay Gupta      | 13. Robert Wetherhold |
| 7. Kenneth Halliday |                       |

OCCUPATIONAL AND ENVIRONMENTAL HEALTH LABORATORY (OEHL)  
(Brooks Air Force Base)

- |                  |                     |
|------------------|---------------------|
| 1. Richard Brown | 4. Robert Masingale |
| 2. Elvis Deal    | 5. Joseph Verducci  |
| 3. Kiah Edwards  |                     |

ROCKET PROPULSION LABORATORY (RPL)  
(Edwards Air Force Base)

- |                   |                       |
|-------------------|-----------------------|
| 1. Gurbux Alag    | 5. Michael Gorman     |
| 2. Allan Burkett  | 6. John Kenney        |
| 3. Wilton Flemon  | 7. Lawrence Schovanec |
| 4. Luther Flippen |                       |

C. PARTICIPANT LABORATORY ASSIGNMENT (Page 4)

ROME AIR DEVELOPMENT CENTER (RADC)  
(Griffiss Air Force Base)

- |                    |                           |
|--------------------|---------------------------|
| 1. Beryl Barber    | 7. Timothy Grogan         |
| 2. Kevin Bowyer    | 8. Louis Johnson          |
| 3. Ronald Canfield | 9. Panapakkam Ramamoorthy |
| 4. John Dunn       | 10. David Sumberg         |
| 5. Ramez Elmasri   | 11. Jacob Weinberg        |
| 6. Lionel Friedman |                           |

SCHOOL OF AEROSPACE MEDICINE (SAM)  
(Brooks Air Force Base)

- |                       |                      |
|-----------------------|----------------------|
| 1. Phillip Bishop     | 9. Leonard Price     |
| 2. David Ludwig       | 10. Stephen Pruett   |
| 3. Mohammed Maleque   | 11. Richard Schori   |
| 4. Daniel Mihalko     | 12. Wesley Tanaka    |
| 5. Mary Morton-Gibson | 13. Michele Trankina |
| 6. Kurt Oughstun      | 14. Ward Wells       |
| 7. Ralph Peters       | 15. Stanley Whidden  |
| 8. Gerald Pollack     | 16. Sharon Williams  |

WEAPONS LABORATORY (WL)  
(Kirtland Air Force Base)

- |                    |                    |
|--------------------|--------------------|
| 1. Thomas Dwyer    | 5. Randall Peters  |
| 2. Ira Elder       | 6. William Wheless |
| 3. Jerome Knopp    | 7. Joan Wyzkoski   |
| 4. Barry McConnell |                    |

RESEARCH REPORTS

RESEARCH REPORTS  
1987 SUMMER FACULTY RESEARCH PROGRAM

<u>Technical Report Number</u>	<u>Title</u>	<u>Professor</u>
Volume I		
1	Vaporization Behavior of Multicomponent Fuel Droplets in a Hot Air Stream	Dr. Suresh K. Aggerwal
2	Large Space Structure Parameter Estimation	Dr. Gurbux S. Alag
3	Correlation and Simulation Studies of GaAs Microwave MESFET Power Devices	Dr. John W. Amoss
4	Air Force Officer Selection Revisited: Entertaining The Possibilities for Improvement	Dr. Victor H. Appel
5	Evaluation of Three-Dimensional Kinetics Analysis Methods of Robotics for the Study of Human Articulated Motion	Dr. Xavier J.R. Avula
6	Pointing Control Systems for Balloon-Flown Instruments	Dr. Franceso Bacchialoni
7	Sustained Delivery of Volatile Chemicals by Means of Ceramics	Dr. Praphulla K. Bajpai
8	Frequency Estimation in the Analysis of Radar Signals	Dr. Vernon L. Bakke
9	Invitro Cytotoxic Effects of Perflurodecanoic Acid on L5178Y Mouse Lymphoma Cells	Dr. Shankar S. Bale
10	Fire Technology of Jet Fuels (JP-8 vs. JP-4)	Dr. William W. Bannister
11	Microwave Measurements	Prof. Beryl L. Barber
12	Identification Techniques Using Fragmentary Human Bone	Dr. William M. Bass
13	A Numerical Simulation of the Flow Field and Heat Transfer in a Rectangular Passage with a Turbulence Promoter	Dr. Bryan R. Becker
14	Synergistic Effects of Bomb Cratering	Dr. Charles Bell

15	Construction Contract Administrator's Technical Handbook	Prof. Kweku K. Bentil
16	Least Squares Estimation Theory and Geometrical Smoothers	Dr. David E. Betounes
17	Increasing Work Capacity of Personnel Wearing Protective Clothing in Hot Environments	Prof. Phillip A. Bishop
18	User-System Interface Standards	Dr. Jerome W. Blaylock
19	Fourier Transform Infrared Studies of Ethylenediammonium Dinitrate and 1,4-Butanediammonium Dinitrate	Dr. John M. Bopp, Jr.
20	A "Form and Function" Knowledge Representation for Reasoning about Classes and Instances of Objects	Dr. Kevin W. Bowyer
21	An Analysis of Infrared Light Propagation in Hollow Metallic Light Pipes	Mr. Lee I. Britt
22	Phytotoxicity of Soil Residues of JP-4 Aviation Fuel	Mr. Richard. H. Brown
23	Dynamics of a Metallic Jet	Dr. Robert A. Buchl
24	Reactions of Nitryl Chloride with Aromatic Substrates in Chloraluminat Melts	Dr. Charles M. Bump
25	Chemistry for the Space Program	Dr. Allan R. Burkett
26	Bayesian Testability Demonstration	Dr. Ronald V. Canfield
27	Hypertext and the Integrated Maintenance Information System (IMIS)	Dr. Patricia Carlson
28	Dopant Diffusion in NIPI Semiconductor Superlattices	Dr. Kwo-Sun Chu
29	Nonlinear Optical Effects in Fibers and Small Crystals	Dr. David Y. Chung
30	The Effect of Model Flexibility on the Accuracy of Aerodynamic Coefficients Determined from Free-Flight Ballistic Tests	Dr. Robert W. Courter
31	Tunable Absorption in Superlattices	Dr. Bruce A. Craver

- |    |  |                          |
|----|--|--------------------------|
| 32 | Computer Simulation of Adaptive Resource Management in Real-Time   | Prof. William K. Curry   |
| 33 | Effect of Wind and Turbulence on an Artificially Generated Strato-Mesospheric Plasma   | Dr. Phanindramoha Das    |
| 34 | Analysis and Modeling of the Thermal Response of an Autoclave for Expert System Control of Carbon-Epoxy Composite Fabrication  | Dr. Bruce A. DeVantier   |
| 35 | A Study of Service Demand Distribution and Task Organization for the Analysis of Environmental Samples and Associated Support Services at the USAF Occupational and Environmental Health Laboratory-Brooks AFB, San Antonio, Texas | Dr. Elvis Deal           |
| 36 | Vectorized Perturbed Functional Iterative Scheme (VPFIS) for Numerical Solution of Nonlinear Partial Differential Equations  | Dr. Suhrit K. Dey        |
| 37 | An Eight-Domain Framework for Understanding Intelligence and Predicting Intelligent Performance  | Dr. Ronna F. Dillon      |
| 38 | Microstructural Developments in Titanium Aluminides: A Study of Dynamic Material Modeling Behavior   | Dr. Ravinder Diwan       |
| 39 | Ada and Artificial Intelligence Applications for Electronic Warfare  | Dr. Verlynda S. Dobbs    |
| 40 | Computational Simulation of Transonic Store Separation   | Dr. F. Carroll Dougherty |
| 41 | Guided Waves in Millimeter Wave Circuit Design   | Dr. John M. Dunn         |
| 42 | Slew-Coupled Structural Dynamics Identification and Control  | Dr. Thomas A.W. Dwyer    |
| 43 | The Effects of Metal Mutagens on the Synthesis and Accumulation of Macromolecules  | Dr. Kiah Edwards         |
| 44 | Project 1 - Scaling Laws of Two-Dimension Nozzle Plumes; Project 2 - Design of a Mechanism to Control Turbulence Levels in Wind Tunnels  | Dr. Marco A. Egoavil     |



45	Computation of Rutherford Scattering Cross Sections	Dr. Ira T. Elder
46	Database Processing in Real-Time Systems	Dr. Ramez A. Elmasri
47	Non-Uniform Spatial Systems and the Transition to Turbulence	Dr. John E. Erdei
48	Bank-To-Turn Control of Air-To-Air Missiles	Dr. Joseph J. Feeley
49	Borazine Reactions	Dr. Wilton Flemon
50	Chemical and Spectroscopic Evaluation of Antimony Sulfides	Dr. Dennis R. Flentge
51	The Evaluation of a Thermal-Hydraulic Design of a Fixed Particle Bed Reactor and Suggested Model Revisions	Dr. Luther D. Flippen
52	Sift Studies of Gas Phase Ion-Molecule Reactions	Dr. Lee A. Flippin
53	Silicon Junction-Difet Electrooptic Modulator	Dr. Lionel R. Friedman
Volume II		
54	Phase Behavior of Poly(p-phenylene benzobisthiazole) Molecular Composites	Dr. John W. Gilmer
55	Design of an Omnidirectional Torquer	Dr. Stephen J. Gold
56	Acoustic Emission and the Fracture Behavior of 2-D Carbon Carbon	Dr. Michael R. Gorman
57	No Report Submitted	Dr. Benjamin Gottlieb
58	High Amplitude Airfoil Motion Using Point Vortices	Dr. Gary M. Graham
59	Liquid Film Cooling of Rocket Engines	Mr. William M. Grissom
60	Cellular Logic Image Processor Evaluationn	Dr. Timothy A. Grogan
61	Thermal Decomposition Investigations of Candidate High Temperature Base Fluids II. Silahydrocarbons	Dr. Vijay K. Gupta
62	Effect of Surface States on the Electronic Transport Properties in Semi-Insulating GaAs	Dr. Narayan C. Halder

63	The Surface Primitive Method of Feature Based Computer Aided Design for Manufacture	Dr. Kenneth R. Halliday
64	Gun Gas Diversion	Dr. Elmer C. Hansen
65	Multi-Block Grid Optimization	Dr. David Hart
66	Encoding in Less than 100 Milliseconds Demonstrated Using a Reaction Time Task	Dr. Terence M. Hines
67	Nitrated Heterocyclic Compounds: A Synthetic Study	Dr. Albert I. Hirschberg
68	A Human Factors Approach to the Process of Developing the Advanced Meteorological Processing System	Dr. Robert R. Hoffman
69	Pressure Attenuation in Solids: A Computer Model	Dr. James S. Hoffmaster
70	In Situ Detection of Osteoprogenitor Cells in an Actively Growing Bone System	Dr. Gwendolyn B. Howze
71	Non-local Turbulance Theories	Dr. Mayer Huml
72	Leaching and Hydrolysis of some Chlorinated Solvents	Dr. Peter M. Jeffers
73	Cholesteric Liquid Crystals of Bio-molecules for Use as Optical Filters	Dr. Gordon O. Johnson
74	Contribution of the Value Assignment Problem to the Complexity of Test Generation in Combinational Logic Circuits and Power Line Testing of CMOS Digital Logic Circuits	Dr. Louis G. Johnson
75	Effect of Stacking Sequence Upon Deamination Fracture Toughness	Dr. William M. Jordan
76	"Generic" Credit Card Feasibility Study	Dr. William F. Kauder
77	High Energy Metastable Species in Cryogenic Matrices: Preparation, Photophysics, and Photochemistry	Dr. John W. Kenney
78	Development of a Geotechnical Centrifuge Facility at Tyndall Air Force Base	Dr. Yong S. Kim

79	Emergent Leadership and Team Effectiveness on a Team Resource Allocation Task	Dr. Charles E. Kimble
80	Experimental Testing of Imaging Correlography	Dr. Jerome Knopp
81	A Study of the Electrochemical Behavior of Trihalide Ions Containing Bromine and Chlorine in Melts Composed of Aluminum Chloride and 1-Methyl-3-Ethylimidazolium Chloride	Dr. Lawrence F. Koons
82	Semiempirical Calculation of Non-Linear Optical Properties	Dr. Henry A. Kurtz
83	Mathematical Removal of Low Frequency Fluctuations From Experimental LDV Data	Dr. Thomas R. Lalk
84	Construction of a Preliminary Validation of an Equal Opportunity Climate Assessment Instrument	Dr. Dan Landis
85	A Hyperbolic Interpolation Algorithm for Modelling Radiance Data and Exponential Inversion	Dr. Steven J. Leon
86	Experimental Protocols for Investigating the Physiology of Orthostatic Intolerance in Humans	Dr. David A. Ludwig
87	Effect of Repeated Low Dose Soman On Acetylcholinesterase Activity	Dr. Mohammad A. Maleque
88	Disposal of Chemotherapeutic Wastes	Dr. Robert E. Masingale
89	Assessing Costs and Benefits of Personnel Research: Application of Utility Concepts to Military Programs	Dr. Michael D. Matthews
90	Investigation of New Luminescent Rebroadcasting Devices for Optical Information Processing	Dr. Alastair D. McAulay
91	Automated Extraction of Knowledge-Based Object Tuples from Domain Documents	Dr. Barry A. McConnell
92	Automated Design of Large-Scaled Frame Structures with Multiple Frequency Constraints	Mr. Oliver G. McGee

93	Statistical Methodology for Assessing Group Health Differences	Dr. Daniel Mihalko
94	A Comparison of Tracking with Active Stick Controllers with an Optimal Control Model	Mr. Augustus Morris
95	Examination of the Point Spread Function in the Retinal Thermal Model	Dr. Mary L. Morton-Gibson
96	Developing Models for Empirical Research on Women in the Military	Dr. Lena W. Myers
97	Multi-Mode Sensing in Air-to-Air Missiles	Dr. James B. Nail
98	Night-Time CO <sub>2</sub> (001) Vibrational Temperatures and Limb-View Integrated Radiances in the 50 to 150 KM Altitude Range	Dr. Henry Nebel
99	A Kinetic Study of Thermal Decomposition by TNT By High Performance Liquid Chromatography	Dr. Maurice C. Neveu
100	Evaluating Expert Systems	Dr. James L. Noyes
101	Isolation of Osteoprogenitor Cells from the Trauma-Activated Periosteum	Dr. Noel S. Nussbaum
102	Assessing the Attributes of Expert Judgment: Measuring Bias in Subjective Uncertainty Estimates	Dr. Thomas E. Nygren
103	On the General Existence of Precursor Fields in a Casually Dispersive Medium	Dr. Kurt E. Oughstun
104	Estimation of Spectral Density by Random Samples	Dr. Surgounda A. Patil
105	Computer Skeleton Program Generator	Prof. Martin A. Patt
106	A Suboptimal Feedback Control for Wing Rock	Dr. William N. Patten
Volume III		
107	Release of Dynorphin B From Mossy Fiber Synaptosomes	Dr. Ralph I. Peters
108	Momentum Transfer and Mass Loss for a C.W. Laser Irradiated Target	Dr. Randall D. Peters

109	Raman Spectrum of Acetanilide	Dr. Gerald L. Pollack
110	X-Ray Diffraction by Superconducting Oxides	Dr. Spencer K. Porter
111	A New Sensitive Fluorometric Method for the Analysis of Submicrogram Quantities of Cholesterol	Dr. Leonard Price
112	A Model System for Examining Macrophage-Lymphocyte Interactions	Dr. Stephen B. Pruett
113	Digital Optical Computing Potentials and Problems	Dr. Panapakkam A. Ramamoorthy
114	A Critical Review of Some Recent Remotely Sensed Studies of Typhoons in the North West Pacific	Dr. Gandikota V. Rao
115	Ambiguity and Probabilistic Inference in a Missile Warning Officer Task	Dr. Donald U. Robertson
116	A Test Chip for Evaluation of MBE Epitaxial Layers for Novel Device Applications	Dr. Kenneth P. Roenker
117	Heat Removal from High Heat Flux/Large Area Surfaces by Single-Phase and Two-Phase Flow of Water	Dr. Ramendra P. Roy
118	Late Appointment No Report Submitted at this time	Dr. Paul M. Rybski
119	Three-Dimensional Finite Element Program Elastic Viscoplastic	Dr. Joseph E. Saliba
120	A Case for Neural Networks	Dr. Richard M. Schori
121	Fracture in Damaged Media: An Inhomogeneous Material Approach	Dr. Lawrence E. Schovanec
122	Characterization of Fire Training Facility Wastewater	Dr. William D. Schulz
123	Leaky Rayleigh Waves on Surfaces With Laminar Microstructures	Dr. Nisar Shaikh
124	Radiation Hypersonic Aerodynamics	Dr. Shiva N. Singh
125	Robustness and Control/Structure Design Integration for Flexible Dynamic Systems	Dr. Gary L. Slater

126	Theoretical and Experimental Investigations of Ion-Polar Molecule Interactions	Dr. Timothy C. Su
127	A Balanced Fiber Optic Distribution Network for Phased Array Antennas	Dr. David A. Sumberg
128	Use of High Performance Molecular Exclusion Chromatopography to Separate Lippoproteins	Dr. Wesley K. Tanaka
129	Visualization, Velocity and Frequency Measurements of a Two-Dimensional Jet	Dr. Richard S. Tankin
130	Pressure Waves in Foam and Foam-Sand Samples	Dr. Joseph W. Tedesco
131	High Velocity Projectiles	Dr. Forrest D. Thomas
132	The Effect of Transient Shock Waves in a Mach 3 Flow	Dr. Howard D. Thompson
133	A Computational Model of Resource Allocation in Experts and Novices	Dr. David J. Townsend
134	Development of an Animal Model for G-Induced Loss of Consciousness	Dr. Michele L. Trankina
135	An Advanced Vision System Testbed	Prof. Robert G. Trenary
136	Ozonation of Firefighter Training Facility Wastewater and its Effect on Biodegradation	Dr. Dennis D. Truax
137	Effects of Adaptation to Fourier Descriptor Stimuli on Discrimination Thresholds for Visual Form	Dr. John J. Uhlarik
138	Prediction of Structural Response to Sonic Booms: An Assessment of Technological Gaps	Dr. P. G. Vaidya
139	Model-free Statistical Analyses of Contaminated Ground Water	Dr. Joseph S. Verducci
140	Microstructure and Mechanical Properties of Titanium Aluminides	Dr. Robert C. Voigt
141	Excitation Cross Sections of Atomic Oxygen by Electron-Impact Dissociative Excitation of O <sub>2</sub>	Dr. Keith G. Walker
142	Fifth Force Studies for a Layered Earth	Dr. Richard C. Walker
143	Magnetostatic Waves Studies	Dr. Jacob Weinberg

144	Lateral Resupply of Spare Parts	Dr. Howard J. Weiss
145	Design Optimization of Complex Systems by Goal Decomposition	Dr. Charles E. Wells
146	Thermal Physiology: Selected Field Study Problems and Methodology	Dr. Ward T. Wells
147	Adaptive Filtering of Evoked Brain Potentials	Dr. John J. Westerkamp
148	Thermal Fatigue of Ceramic Matrix Composite (CMC) Materials	Dr. Robert C. Wetherhold
149	Mode Extraction from an Electromagnetic Slow Wave System	Dr. William P. Wheless
150	Hyperbaric (3ATA) Oxygen 100% Therapy as an Adjuvant in the Treatment of Resuscitated (Lactated Ringer's and Dextrose 5%) Guinea Pigs' Burn (3°, 50 BSA) Shock	Dr. Stanley J. Whidden
151	Perfluorodecanoic Acid Interactions with Mouse Lymphoma Cells and Primary Rat Hepatocytes	Dr. Andrew P. Whipple
152	Polyunsaturated Omega-3 Fatty Acids As A Risk Predictor of Coronary Artery Disease	Ms. Sharon Williams
153	In Vitro Cytotoxicity Assessment Via Two-Dimensional Polyacrylamide Gel Electrophoresis	Dr. Frank A. Witzmann
154	Low Velocity Impact of Graphite/Epoxy Plates	Dr. William E. Wolfe
155	The Active Control of Altitude Over Differing Texture	Mr. Lawrence Wolpert
156	The Interface Contribution to GaAs/Ge Heterojunction Solar Cell Efficiency	Dr. Cheng-Hsiao Wu
157	Parallel Processing and Numerical Linear Algebra	Dr. Joan P. Wyzkoski
158	Semi-Empirical Molecular Orbital (MOPAC) Studies of Energetic Materials: Nitrogen Heterocyclics and Nitroenamine	Dr. Melvin E. Zandler
159	Specification of a Computer Aided Design System	Dr. George W. Zobrist

1987 USAF-UES SUMMER FACULTY RESEARCH PROGRAM/

GRADUATE STUDENT SUMMER SUPPORT PROGRAM

Sponsored by the

AIR FORCE OFFICE OF SCIENTIFIC RESEARCH

Conducted by the

Universal Energy Systems, Inc.

FINAL REPORT

VAPORIZATION BEHAVIOR OF MULTICOMPONENT FUEL DROPLETS  
IN A HOT AIR STREAM

Prepared by: Suresh K. Aggarwal and Khan Nguyen  
Academic Rank: Assistant Professor  
Department and University: Department of Mechanical Engineering  
University of Illinois at Chicago  
Research Location: Fuels Division, Aero-Propulsion Laboratory  
USAF Researcher: Dr. T.A. Jackson and Dr. M. Roquemore  
Date: September 21, 1987  
Contract No.: F49620-85-C-0013



# VAPORIZATION BEHAVIOR OF MULTICOMPONENT FUEL DROPLETS IN A HOT AIR STREAM

by

Suresh K. Aggarwal\* and K. Nguyen\*\*

## Abstract

An experimental-theoretical investigation of the behavior of evaporating fuel droplets in an hot air flow was initiated. In the theoretical part, a computer code was developed to calculate the droplet size, velocity, and surface properties along its trajectories. The major features of the code are (i) three different liquid-phase models, namely the diffusion-limit, infinite-diffusion, and vortex, can be employed, (ii) Two gas-phase models used for the external convection effect on the transport rates are the Ranz-Marshall and the axisymmetric models, (iii) vaporization of pure as well as multicomponent fuel droplets can be predicted, and (iv) variable property effects are considered. A parametric study was completed, where the predictions of the three liquid-phase models were compared, and the variable-property effects were evaluated. From these results, the operating conditions for the experimental study were identified.

In the experimental part, the facility to inject a single stream of droplets in well-characterized hot air flow was set up. A LDV system and a thermocouple measure the local air properties. The droplet properties were measured by the Phase-Doppler particle analyzer and photography. Several tests were completed to fully characterize the experimental conditions. In future, the focus will be to compare the experimental and theoretical data for laminar flow conditions. The study would be then extended to turbulent flows. The future work is described in the Research Initiation Proposal.

\* Assistant Professor

\*\* Graduate Student

### Acknowledgements

I wish to thank the Fuels Division of the APL for a very rewarding and enriching summer. My almost daily interaction with Dr. T. Jackson and Dr. M. Roquemore provided an excellent working atmosphere. Their constant help, interest, and commitment in my research work was a great source of inspiration and stimulation. The commitment and hardwork of Gary Switzer in making the experiment work was truly remarkable. Jeff Stutrud was always available to tackle any computer problem my student and I encountered. My thanks are also due to Cindy O'Bringer, Curtiss Reeves, and Dr. Charles Martin of the Fuels Division. I also wish to acknowledge the AFOSR for sponsoring this research, and the Universal Energy Systems for an efficient administration of this program.

## Introduction

In spite of many significant advances reported in spray combustion research, as reviewed by Law [1], Faeth [2], Sirignano [3], and Mann and Tishkoff [4], we have a long way to go before the current spray models become reliable predictive and/or design tools. New advances must be made in physical modeling, numerics, and diagnostic capabilities. One critical area, where further fundamental understanding is required, is the vaporization behavior of a droplet in a hot flow field. Clearly, an accurate prediction of droplet vaporization rate and trajectory would provide the fundamental input in any realistic spray model.

The Aero-Propulsion Laboratory at WPAFB has great interest in advancing the fundamental understanding of complex spray processes. The laboratory has the most modern experimental facility for combustion and fluid-dynamic research. It has played a leading role in developing flow visualization techniques and providing laser-based data base for modeling, and for further insight into the complex combustion phenomena. I have worked extensively in the area of spray ignition, droplet ignition, development of advanced vaporization models, and numerical methods for spray computations. My research interests have much in common with those of Dr. T. Jackson and Dr. M. Roquemore of APL. This led to my summer assignment at APL. One graduate student, Mr. K. Nguyen, worked with us on the project.

## II. OBJECTIVES OF THE RESEARCH

The literature search indicates that the behavior of an evaporating/burning droplet has been extensively studied [1]. Starting with the early work of Godsave [5], which led to the classical  $d^2$ -law model, many experimental and theoretical investigations have been reported. Major outcome of these investigations has been the development of several improved vaporization models [1,3] to represent the effects of transient liquid-phase processes and of external convection on the gasification behavior of pure as well as multicomponent fuel droplets. However, there is no information available as yet on the behavior of evaporating droplets under relatively cold but convective environments. When the ambient temperature is (say) about 500 K, the possibility of an envelope flame around a droplet is precluded, the

gasification rate is relatively low, and the droplet heat-up time may not be small as compared to its lifetime, which means that the liquid-phase transient processes would be important. A need therefore existed to generate data base and to assess the advanced vaporization models for low temperature environment. Studying the vaporization behavior under low temperature conditions is also particularly relevant for the multicomponent case. Most of the theoretical developments have been based on the assumption that the liquid mass diffusion is much slower than the surface regression rate. At lower environment temperature, however, the mass diffusion rate may be comparable to the regression rate. The validation of the theoretical models under such conditions will be thus of great practical and fundamental value. The overall objective of this research is to develop an experimental facility and comprehensive theoretical models to investigate the behavior of evaporating sprays. The specific tasks to be completed are:

- (i) To develop a computer code which employs the advanced vaporization models to predict the behavior of multicomponent fuel droplets in an hot air flow.
- (ii) To set up an experimental facility for generating a single stream of droplets in an hot air flow, and to make measurements of local gas-phase and droplet properties along a droplet trajectory.
- (iii) To generate experimental data for evaluating the various vaporization models for pure and multicomponent fuel droplets.
- (iv) To extend the work to study the droplet dispersion and vaporization behavior in hot well-characterized turbulent flows.

The first two tasks were completed during the summer program and are described in the next two sections. Tasks #3 and #4 would be pursued under the Research Initiation Program.

### III. THEORETICAL WORK

A computer code was developed to predict the transient behavior of a droplet along its trajectory. The major features of the code are (i) Three different liquid-phase models, namely the diffusion-limit, infinite-diffusion, and vortex models, can be employed, (ii) Two different models can be used to

account for the effect of external convection on the transport rates, (iii) heat-up and vaporization behavior of pure as well as multicomponent fuel droplets can be obtained, and (iv) variable-property effects are considered. The various liquid- and gas-phase models, as well as the other aspects of the theoretical work are now discussed. Some representative numerical results are also presented.

### IIIa. Droplet Equations

The equations governing the variation of droplet position, velocity, and size are:

$$\frac{dX_p}{dt} = V_p \quad (1)$$

$$\frac{dV_p}{dt} = \frac{3 C_D \mu R_e (V_p - V)}{16 \rho_p r_p^2} \quad (2)$$

$$\frac{d r_p^{*2}}{dt^*} = - \frac{2 \lambda \bar{m}}{c_{pg} \rho_p \alpha_p} \quad (3)$$

where the drag coefficient is assumed to be given by

$$C_D = \frac{24}{R_e} \left( 1 + \frac{R_e^{2/3}}{6} \right) \quad (4)$$

$$R_e = \frac{2 \rho r_p |V_p - V|}{\mu} \quad (5)$$

here  $V$  is the gas velocity, and  $\rho$  the gas density.  $\mu$ ,  $\lambda$ , and  $c_{pg}$  are respectively the average viscosity, thermal conductivity, and specific heat of gas layer surrounding the droplet. As discussed by Faeth [2], their variations with local gas temperature and composition should be considered in order to accurately predict the droplet vaporization history.  $\rho_p$  and  $\alpha_p$  are the liquid density and thermal diffusivity. Further, the drop radius in Eq. (3) is normalized by its initial value ( $r_{p0}$ ), and the temporal variable is normalized by  $r_{p0}$  and  $\alpha_p$ . Expression for  $\bar{m}$  depends on the gas-phase model used to represent the effect of external convection, and is given as:

$$\bar{m} = (1 + 0.3 \text{ Re}^{1/2}) \ln(1 + B_Y)$$

for Ranz-Marshall correlation (6)

$$= \frac{4}{\sqrt{\pi}} \text{Re}^{1/2} f(B_Y)$$

for simplified axisymmetric model

where  $f$  is the Blasius function [6] of the mass transfer  $B_Y$ , which is defined as

$$B_Y = \frac{Y_{fs} - Y_{f\infty}}{1 - Y_{fs}} \quad (7)$$

with  $Y_{fs} = \sum Y_{is}$

(8)

$$Y_{f\infty} = \sum Y_{fi}$$

Here the subscripts  $s$  and  $\infty$  represent respectively the properties at droplet surface and in the gas environment outside the gas layer. The summation is over all species in the gas phase. The above set of equations is complete except for  $Y_{fs}$  (or  $Y_{is}$ ) which is a function of liquid composition and temperature at the droplet surface. The Clausius-Clapeyron relation for phase equilibrium and the Raoult's law for ideal mixtures [6] are used to determine  $Y_{is}$ . This leaves the liquid composition ( $Y_{lis}$ ) and temperature at the droplet surface as the unknowns. Different liquid-phase models, employed in the study, differ essentially in the determination of these unknowns. These are briefly described next.

### IIIb. The Diffusion-Limit Model

In this model, the transient heat and mass transport processes in the liquid are assumed to be diffusion-controlled, and are represented by the unsteady heat and mass diffusion equations. Since the droplet is vaporizing, a transformation is used to cast the moving boundary problem into a fixed one. The transformed equations are:

$$\frac{\partial T_l^*}{\partial \bar{t}} = \frac{\partial^2 T_l^*}{\partial \bar{r}^2} + \frac{\partial T_l^*}{\partial \bar{r}} \left( \frac{2}{\bar{r}} - \bar{r} \bar{m} K \right) \quad (9)$$

$$\frac{\partial Y_{li}}{\partial \bar{t}} = \frac{1}{Le} \frac{\partial^2 Y_{li}}{\partial \bar{r}^2} + \frac{\partial Y_{li}}{\partial \bar{r}} \left( \frac{1}{Le} \frac{2}{\bar{r}} - \bar{r} \bar{m} K \right) \quad (10)$$

Here  $T_l^*$  is the normalized liquid temperature inside the droplet,  $Y_{li}$  the mass fraction of liquid species  $i$ ,  $Le$  the liquid Lewis number,  $\bar{r}$  the normalized radial location inside the droplet, and  $\bar{t}$  the normalized temporal variable. The initial conditions, the boundary conditions, and other details of these equations can be found in earlier publications [1,6]. The numerical solution of Eqs. (9)-(10) yield the transient distribution of liquid temperature and composition inside the droplet, and thus at the surface.

### IIIc. The Infinite-Diffusion Model

The diffusion-limit model does not consider the effect of internal circulation, which would be induced due to the relative gas motion, on the transport processes. The infinite-diffusion model, on the other hand, considers the other limiting situation. It assumes that the liquid temperature and composition remain uniform as the droplet vaporizes. The relative rate of vaporization of each component is then controlled by its volatility. The model may be relevant when the droplet lifetime is small as compared to the liquid-mass-diffusion time, an highly unlikely situation. The temporal variations of temperature and composition are determined from the overall energy and mass conservation.

$$\frac{dT_p^*}{d\bar{t}} = \frac{3 C_k \bar{m} (H - \bar{u})}{c_{pg} (T_B - T_o)} \quad (11)$$

$$\frac{dm_i}{d\bar{t}} = 3 \epsilon_i \bar{m} K r_p^{*3} \quad (12)$$

Here  $m_i$  is the non-dimensional mass of liquid species  $i$  in the droplet. Then

the ratio of  $m_i$  and the total remaining mass gives the liquid mass fraction of species  $i$ . Again, the reader is referred to an earlier publication [6] for more details.

#### IIIId. The Vortex Model

The condition of complete mixing, as assumed in the infinite-diffusion model, is never realized in combustor situations [3]. Even with large internal circulation, the liquid temperature and composition become uniform along the streamlines but not across them. To represent the effect of internal circulation realistically and still maintain one-dimensionality a simplified model has been developed by Sirignano and coworkers [3,7]. After certain simplifications [7], the equations for the liquid temperature and composition inside the droplet are

$$\frac{1}{b_1} \frac{\partial T_l^*}{\partial \tau_1} = \phi \frac{\partial^2 T_l^*}{\partial \phi^2} + [1 + c(\bar{\tau}) \phi] \frac{\partial T_l^*}{\partial \phi} \quad (13)$$

$$\frac{1}{b_1} \frac{\partial Y_{li}}{\partial \tau_1} = \frac{\phi}{Le} \frac{\partial^2 Y_{li}}{\partial \phi^2} + \left[ \frac{1}{Le} + c(\bar{\tau}) \phi \right] \frac{\partial Y_{li}}{\partial \phi} \quad (14)$$

where  $\phi$  is the dimensionless stream function. For further details of the vortex model, the reader is referred to Tong and Sirignano [7], and Aggarwal [6]. The initial and boundary conditions are also discussed in the cited references.

#### IIIe. Numerical Results

Equations (1)-(3), (11) and (12) were solved by using a second-order Runge-Kutte scheme. The local gas-phase properties were assumed; when the results are compared with experiments, the measured flow properties would be employed. The Eqs. (9)-(10) for the diffusion-limit, and (13)-(14) for the vortex models were solved by an implicit Crank-Nicolson scheme. Due to the large liquid Lewis number, a thin diffusion layer exists near the droplet surface, i.e. the Eqs. (9)-(10) and (13)-(14) are stiff. A variable-size mesh is employed to resolve the stiffness.



Some representative results from the numerical study are now discussed. A bicomponent hexane-decane fuel droplet at initial temperature of 300 K is assumed to be injected at a velocity of 3 m/s in an hot air flowing at 1 m/s. Initial mass fraction of liquid hexane is assumed to be 0.5 and the initial droplet diameter is 60 microns. These values correspond to the expected experimental conditions.

Figures 1 and 2 show the droplet surface temperature, liquid mass fraction of hexane at the surface, and square of the droplet radius normalized by its initial value, as predicted by the three liquid-phase models. All the properties are all plotted along the droplet trajectory. The air temperature is 400 K and 800 K for Figs. 1 and 2 respectively. The differences between the predictions of infinite-diffusion model and other two are greater for the latter case. This can be expected since increasing the air temperature enhances the surface regression rate, as evident in the reduction of axial distance traversed by the droplet during its lifetime. This reduces the liquid mass diffusion rate relative to the regression rate. Perhaps, a more interesting observation is that the differences between the diffusion-limit and infinite-diffusion models are quite significant even at relatively low air temperature (400 K). Thus, an experimental study of the vaporization behavior of multicomponent fuel droplets in low temperature conditions would provide some information.

The vaporization behavior of a pure fuel droplet is portrayed in Fig. 3. These results are given because we plan to obtain the corresponding experimental results. The air temperature is 400 K. Note that the droplet surface temperature decreases for the hexane fuel since its wet-bulb temperature is below its initial temperature. The differences between the diffusion-limit and infinite diffusion models are again non-negligible. Also the heating time is not negligibly small as compared to its lifetime, indicating that the transient liquid-phase processes are important even when the air temperature is low.

More detailed results from a systematic parametric study would be given when the predicted values are compared with experiments. The purpose of presenting a few numerical results was to indicate some of the capabilities of the code and to demonstrate the importance of an experimental study.

### III.f. Variable-Property Effects

There are three aspects of the variable-property effects. First, the temperature and composition in the gas layer surrounding a droplet can vary significantly from their values at the droplet surface to those in the far field. This aspect is considered by defining a reference state for calculating the thermo-physical properties. Following Faeth [2], the reference state is defined as

$$\phi_r = \alpha \phi_s + (1 - \alpha) \phi_\infty \quad (15)$$

where  $\phi$  is a generic quantity,  $\alpha$  is the weighting factor, and subscripts  $s$  and  $\infty$  represent values at the droplet surface and in the far field.

The second aspect is that  $\phi_r$  can change significantly during the droplet lifetime because  $\phi_s$  varies due to droplet heating and vaporization, and  $\phi_\infty$  varies as the droplet traverses through different gas regions. The third aspect is that the liquid thermophysical properties would vary due to the changes in liquid temperature and composition. All three aspects were considered in the study.

The variations in the specific heat, density, thermal conductivity, heat of vaporization, and mass diffusivity of liquid were evaluated over the temperature range of interest. It was found that the effects of liquid-phase variable properties can be effectively considered by using the properties at an average liquid temperature. Further details would be given in a separate report. To evaluate the effects of gas-phase variable properties, a mixture of hexane, decane,  $O_2$  and  $N_2$  was considered. Following Faeth [2], the value of  $\alpha$  was assumed to be 0.7. Note that the comparison of experimental and numerical results would be used to get a better value. Then, using the composition and temperature at the drop surface and in the ambience, the reference state can be obtained. The thermophysical properties of the mixture were calculated by following the procedure used by Shuen et al. [8], where several sources were employed to obtain the properties of each species. More details would be provided in a separate report. Here, the effect of considering variable properties in the gas phase is presented. As shown in Fig. 4, the droplet surface temperature is higher which results in greater

vaporization rate for the variable-property case. This is because the gas conductivity increases due to the increase in the reference temperature for this case. Consequently, the rate of heat transfer to the droplet is enhanced. Also notable is the fact that the variable-property effect is stronger for the lower air temperature case. Note that in the present study, the ambient conditions are held fixed during the droplet lifetime. As a result, the effect is entirely due to the changes in surface properties. In a combustor, the ambient conditions would change along the droplet trajectory, and the variable-property effects would be more significant.

#### IV. THE EXPERIMENTAL FACILITY

The schematic of the experimental set-up used to generate a single stream of droplets in an hot air flow, and of the diagnostic facility is shown in Fig 5. The hot air flow system consists of a settling chamber, which contains the screens, electric heater, and honeycomb. The chamber is connected to the test section, which is a 18" long square duct (3.5" x 3.5"), through a contraction elbow. The droplet generation system consists of a fuel supply line, a 0.75" piezoelectric system for applying the pulse to a liquid fuel column, and a glass nozzle with a tip diameter of 50 microns. An air cooling system in an annulus around the fuel tube is used to keep the temperature of liquid fuel at room conditions. The whole experimental set-up is mounted on an adjustable frame to provide movement in all three directions. The major diagnostic facility consists of a Phase-Doppler Particle Analyzer (PDPA) for measuring the local gas velocity as well as the droplet size and velocity, a thermocouple to measure the local gas temperature, and a photographic system to record the droplet size variation along the trajectory directly. A thermocouple is also used to measure the initial droplet temperature. Also, the laser sheet lighting along with a Bragg cell is used for droplet visualization.

During the summer program, the experimental facility was set-up. The preliminary tests conducted to characterize the droplet and hot-air flow necessitated many modifications in the air flow and droplet-generation systems. Several changes were made in the air flow system to enhance the transverse mixing in the settling chamber and to have a uniform air flow with very low turbulence level. Some modifications were also made in the liquid

flow system. The present measurements indicate that the air flow has fairly uniform velocity and temperature distributions in the central part of the duct. In addition, the flow visualization indicates that it is possible to generate and maintain a single stream of droplets along the duct axis. The experimental set-up is now fully operational and ready for measurement of droplet size and velocity along its trajectory. The local air properties needed for numerical calculations will also be measured. Further details of the experimental work are provided in the next section and in the RIP.

## V. RECOMMENDATIONS

a. First set of experiments will focus on the vaporization behavior of pure fuel (n-decane) droplets in the hot air flow. The droplet size and velocity history will be measured by the PDPA and photographically. The experimental values will be compared with the corresponding numerical results, as shown in Figs. 1-4. The measured values of the local flow and initial droplet properties will be employed in numerical predictions. The initial comparison will help us in validating the computational results as well as in refining the diagnostics.

b. The vaporization behavior of multicomponent fuel droplets will then be studied by using a mixture of hexane and decane fuels. Following an initial comparison, a systematic parametric study will be conducted. The important parameters would be initial liquid composition, droplet size, air temperature, and relative air velocity. From the comparison, the various liquid- and gas-phase models will be evaluated. Other aspects, such as variable-property effects will also be examined.

c. A key variable for comparison is the droplet surface temperature. A technique based on the fluorescence method [9] will be developed to measure this temperature. The experimental data will be compared with the numerical values of surface temperature as predicted by different models. This would be a significant development since the surface temperature history is much more sensitive to the liquid-phase models as compared to the droplet size history. The experimental technique will also be potentially useful in spray applications.

d. The experimental-theoretical study will then be extended to the evaporating droplets in hot well-characterized turbulent flow. In the

experiment, the vaporization and dispersion of droplets will be measured in grid-generated turbulent flow field. The theoretical model will consider the discrete as well as stochastic models to predict the dispersion behavior of vaporizing droplets. Again, a parametric investigation will be conducted. The additional parameters here will be the turbulent scales.

e. Turbulent sprays will also be studied experimentally and theoretically in the future.

## REFERENCES

1. Law, C.K., Recent Advances in Droplet Vaporization and Combustion. Prog. Energy Comb. Sci., 1982, Vol. 8, pp. 171-201.
2. Faeth, G.M., Evaporation and Combustion of Sprays. Prog. Energy Comb. Sci., 1983, Vol. 3, pp. 1-76.
3. Sirignano, W.A., Fuel Droplet Vaporization and Spray Combustion Theory, Prog. Energy Comb. Sci., 1983, Vol. 9, pp. 291-322.
4. Mann, D.M., and Tishkoff, J.M., Specialists Meeting on Atomization and Non Dilute Sprays, AFOSR-TR-85-0640.
5. Godsave, G.A.E., Studies of the Combustion of Drops in a Fuel Spray: The Burning of Single Drops of Fuel. Fourth Symposium (International) on Combustion, Williams and Wilkins, Baltimore, 1953, pp. 818-830.
6. Aggarwal, S.K., Tong, A., and Sirignano, W.A., A Comparison of Vaporization Models for Spray Calculations. AIAA Journal, 1984, Vol. 22, pp. 1448-1457.
7. Tong, A.Y., and Sirignano, W.A., Multicomponent Droplet Vaporization in a High Temperature Gas. ASME Winter Annual Meeting, 84-WA/HT-17, 1984.
8. Shuen, J.S., Solomon, A.S.P., and Faeth, G.M., The Structure of Dilute Combusting Sprays. NASA-CR (74838), 1985.
9. Murray, A.M., and Melton, L.A., Fluorescence Methods for Determination of Temperature in Fuel Sprays. Applied Optics, 1985, Vol. 24, pp. 2783-2787.

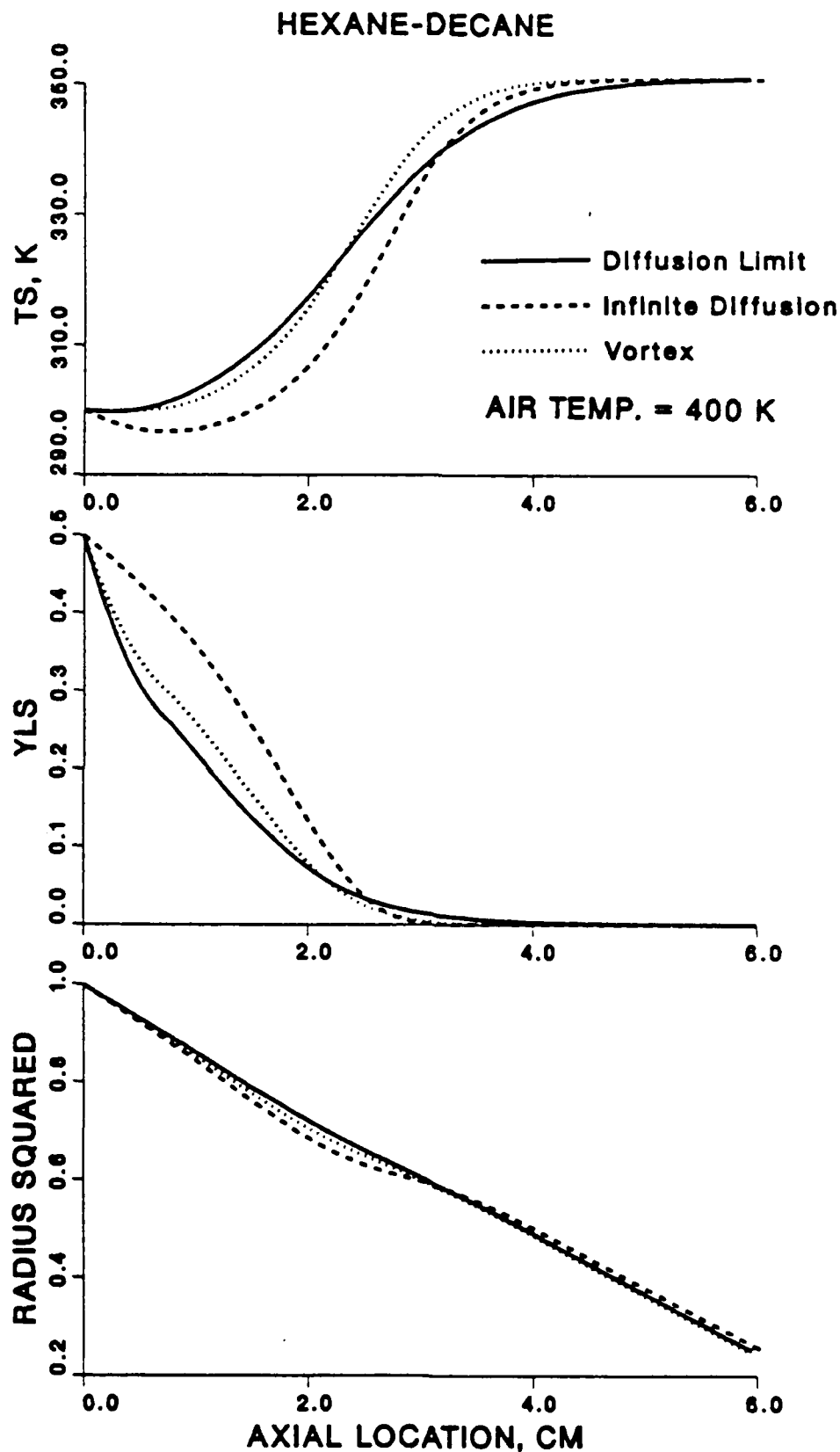


Figure 1 Variation of droplet surface temperature, mass fraction of liquid hexane at the surface, and square of the normalized radius along the trajectory.

# HEXANE-DECANE

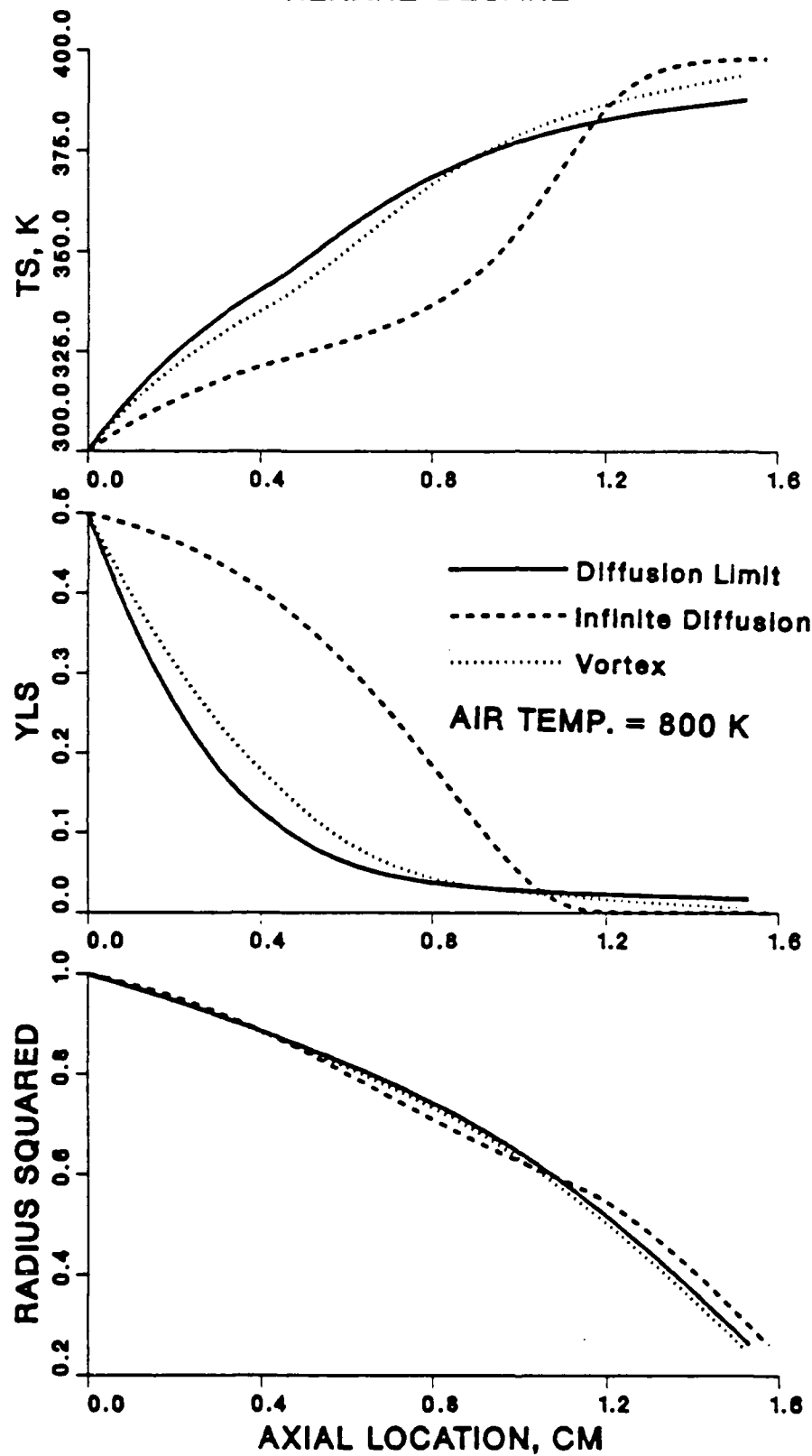


Figure 2 Variation of droplet surface temperature, mass fraction of liquid hexane at the surface, and square of the normalized radius along the trajectory.



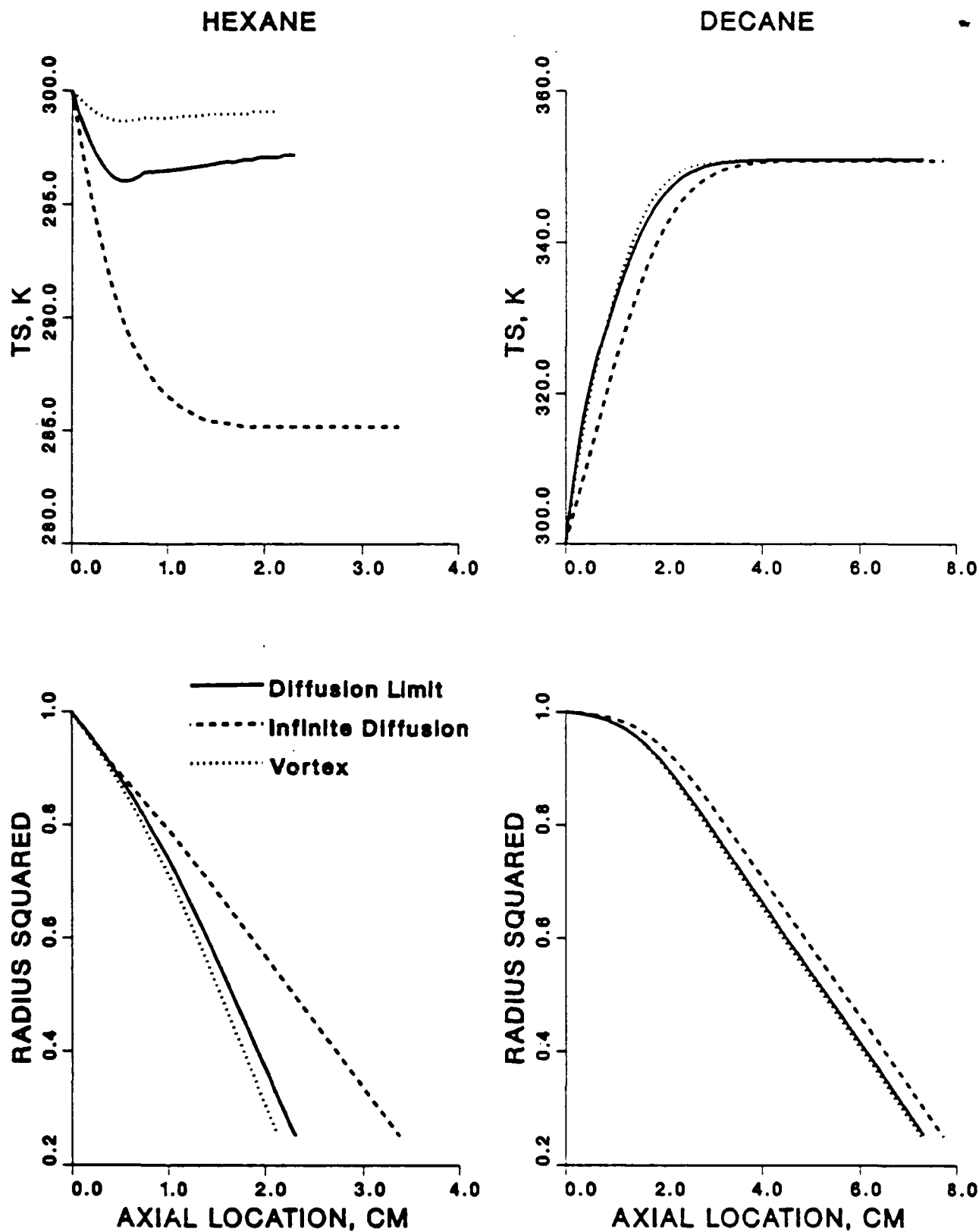


Figure 3 Comparison of three liquid-phase models for the pure hexane and decane droplets. Air temperature = 400 K.

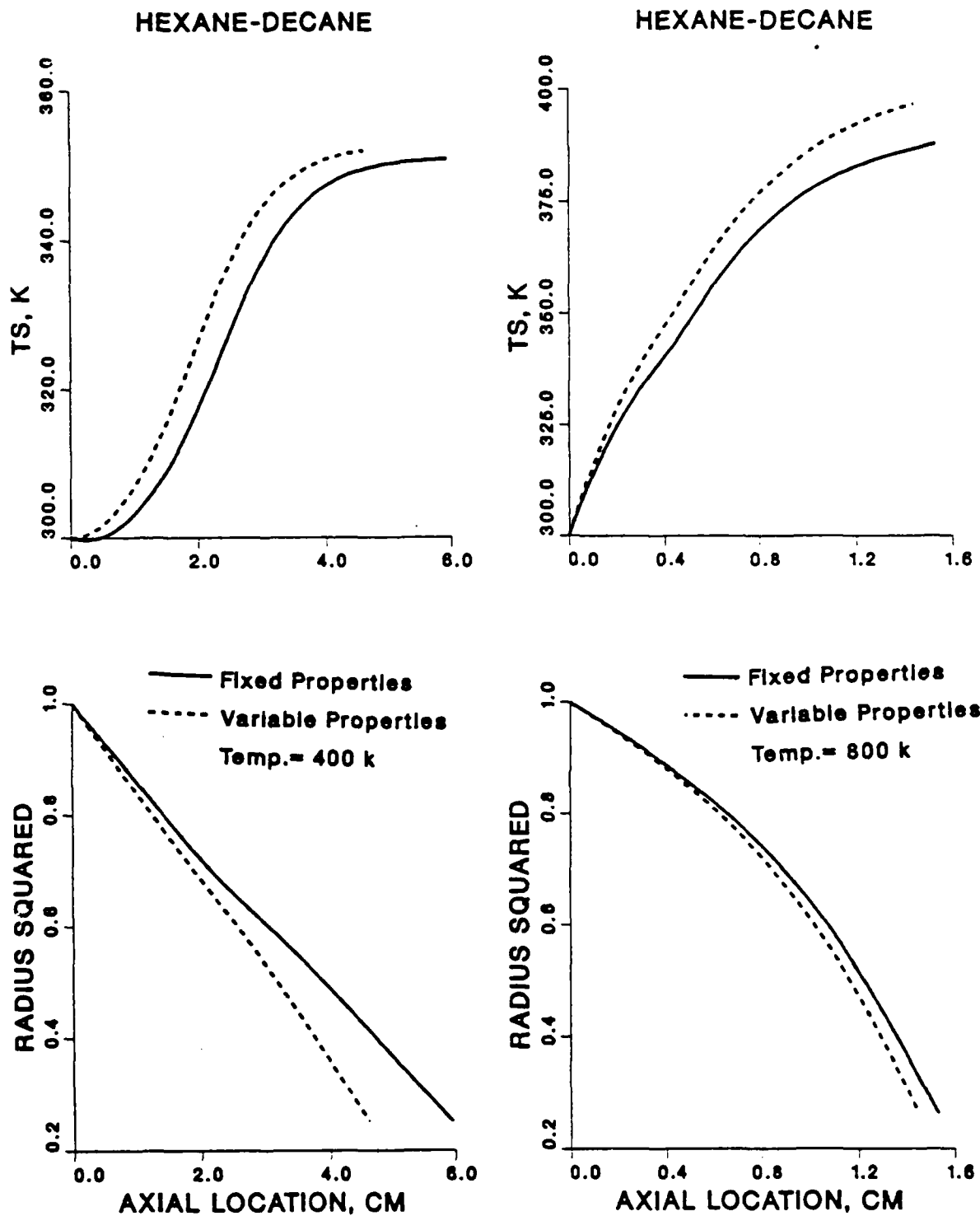


Figure 4 Comparison of droplet properties for the fixed and variable-property cases.

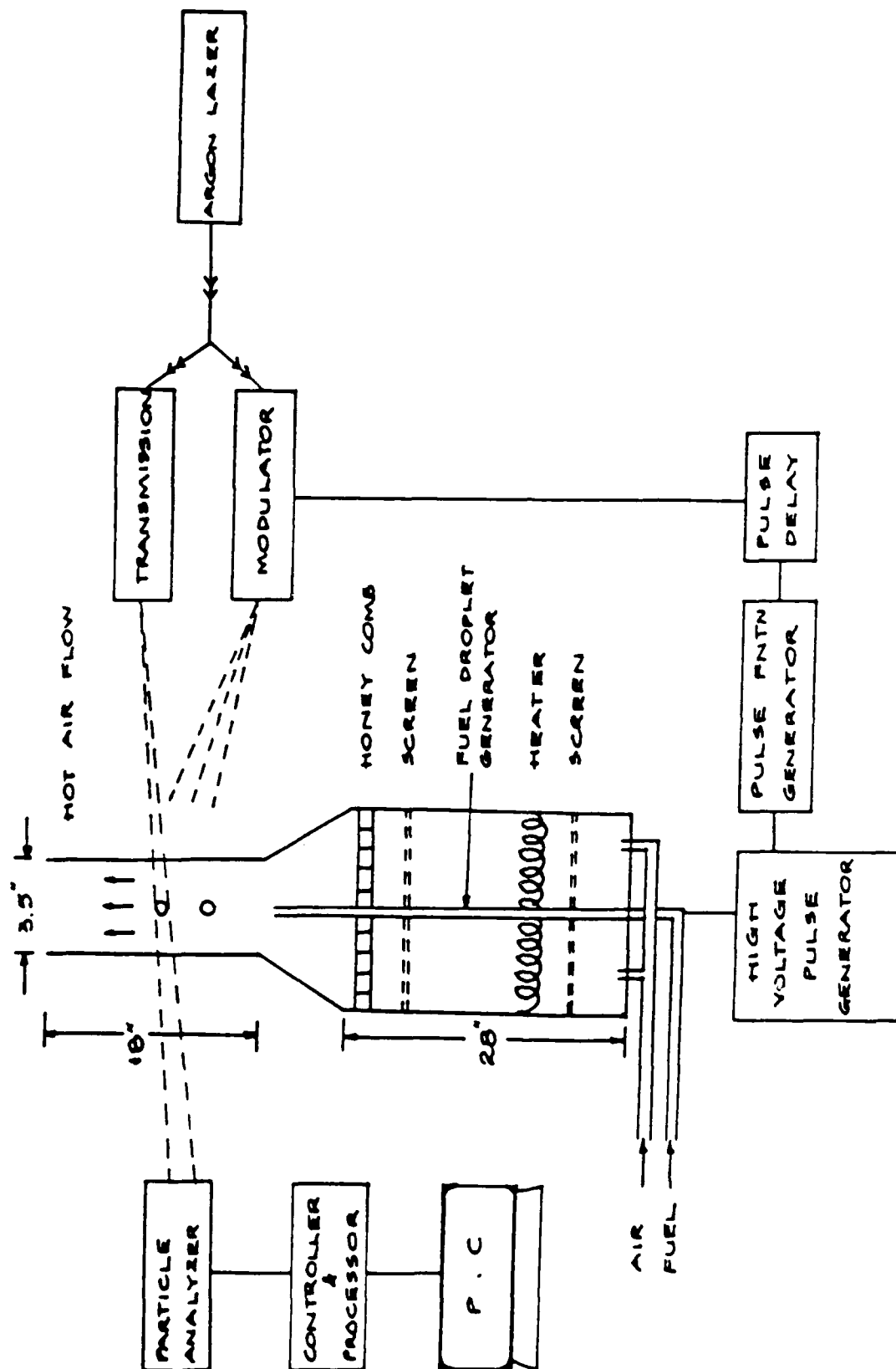


Figure 5 Schematic of the droplet evaporation experiment.

1987 USAF-UES SUMMER FACULTY RESEARCH PROGRAM  
GRADUATE STUDENT SUMMER SUPPORT PROGRAM

Sponsored by the

AIR FORCE OFFICE OF SCIENTIFIC RESEARCH

Conducted by the

Universal Energy Systems, Inc.

FINAL REPORT

Prepared by:	Gurbux S. Alag D. ENG.
Academic Rank:	Professor
Department and	Electrical Engineering Department
University:	Western Michigan University
Research Location:	AFAL/DYSS Edwards AFB CA 93523-5000
USAF Researcher:	Dr Alok Das
Date:	28 Aug 87
Contract No:	F49620-85-C-0013

## Large Space Structure Parameter Estimation

by

Gurbux S. Alag

### ABSTRACT

There has been a great deal of interest in experimental modal analysis as a part of an integrated computer aided engineering approach to the solution of structural dynamics problems. Experimental modal analysis refers to the process of determining the modal parameters (frequencies, damping factors, and modal vectors) of a linear, time-invariant system by way of an experimental approach. One common reason for the experimental approach is the verification of the results of the analytical approach, such as finite element analysis.

The determination of modal parameters from experimentally measured data involves the use of parameter estimation techniques. The estimation methods are changing due to the transfer of existing technology from the other fields where estimation techniques have been more commonly used over the past several decades. It is proposed to investigate the practical implementation and use of various parameter estimation techniques to determine modal parameters from experimentally measured data.

### ACKNOWLEDGEMENTS

I wish to thank the Air Force Systems Command, the Air Force Office of Scientific Research, and the Air Force Astronautics Laboratory for sponsorship of this research.

A special word of thanks is due to all the staff of AFAL/DYSS for making my experience rewarding and enriching. In particular, Alok Das provided me with support, an enjoyable working atmosphere, and all the help I needed to carry out the research. Lt Waid Schlaegel also needs special mention for day to day assistance showing great deal of patience and selflessness.

## I. INTRODUCTION:

Several planned USAF Space Systems will pose serious vibration control problems when very precise vibration control of large flexible structures in presence of on board noise is performed. The accuracy of vibration control is dependant on the accuracy of the mathematical structural model. A popular approach for determination of structural model is to perform system identification. There is a proliferation of identification techniques currently being advocated. It is, therefore, essential that various system identification schemes be evaluated in their application to large flexible space structures.

The Air Force Astronautics Laboratory, Edwards Air Force Base, is currently developing an in-house capability for experimentally evaluating new techniques in system identification and vibration control for large flexible space structures. Towards this end a cantilevered two dimensional flexible grid structure has been constructed. Suitable equipment which will enable on-line and off-line identification experiments to be performed, has also been acquired.

My research interest has been in the area of digital adaptive control specially where explicit identification of the system is also involved. I have also worked at NASA on development of flight control systems for aircraft using MATRIX<sub>x</sub> software. My background, thus, enabled me to work on the comparative analysis of various identification schemes using the experimental setup at AFAL and the control system design software MATRIX<sub>x</sub>.

## II. OBJECTIVES:

The Air Force Astronautics Laboratory at Edwards Air Force Base is currently involved in the evaluation of various modal parameter estimation schemes in the first phase of its long term research effort in the area of large space structures control. An experimental facility has been built to conduct system identification studies on a flexible two-dimensional grid structure.

Results obtained by using parameter estimation techniques will be used to verify results obtained by analytical methods like NASTRAN.

It is proposed to determine the modal parameters experimentally for the grid structure in the region up to 10hz.

The following is the details of the proposed work undertaken as a part of this research.

- 1) Frequency response functions are obtained using impact testing
- 2) Use different parameter estimation methods to determine the modal parameters from the frequency response function. The methods considered are:
  - i) Single degree of freedom approximation
  - ii) Ibrahim time-domain method
  - iii) Linearized least squares multiple degree of freedom method

### III. MODAL PARAMETER ESTIMATION:

Modal parameter estimation is the estimation of frequency, damping, and modal coefficients from the measured data. The measured data may be either in raw form or in processed form such as frequency response. Regardless of the form of the measured data, the modal parameter techniques have been divided into two categories: (1) Single degree-of-freedom (SDOF) approximations, and (2) multiple degree-of-freedom (MDOF) approximation.

Over the last twenty years, many modal parameter estimation methods have been developed. Often, it seems that these methods are very different and unique. In reality, all methods are derived from the same equation and are concerned with the decomposition of a composite function into its constituent parts. The decomposition may occur in the time domain in terms of damped complex exponentials, in the frequency domain in terms of SDOF functions, or in the modal domain in terms of modal vectors. The various modal estimation methods are enumerated in the following:



- Forced Normal Mode Method
- Quadrature Amplitude
- Kennedy-Pancu Circle Fit
- SDOF Polynomials
- Non-linear Frequency Domain
- Least Squares Complex Exponential
- Ibrahim Time Domain
- Eigensystem Realization Algorithms
- Orthogonal Polynomial
  
- Global Orthogonal Polynomial
- Polyreference : Time Domain  
: Frequency Domain
- Direct Parameter Identification: Time Domain  
: Frequency Domain
- Autoregressive Moving Average (ARMA)

The following parameter estimation schemes were considered:

- Single degree of freedom approximation: In most modal parameter estimation schemes, the typical procedure is to first estimate the eigenvalues (natural frequencies and damping factors) and then to estimate the eigenvectors (modal coefficients). The simplest modal estimation procedure is to measure the magnitude of frequency response at one of the natural frequencies. The natural frequency for this simple case can be determined by choosing the frequencies where the magnitude of the frequency response reaches a maximum. The damping factor and modal coefficients can be estimated with known techniques.

- The second method a MDOF approximation is the Ibrahim time domain method developed to extract the modal parameters from damped complex exponential response information.

- The third method involves the development of a linearized least squares algorithms. The parameter estimation is done in two steps. In the first

step, the frequencies and damping factors are calculated. Using this information, the modal vectors are obtained in the next step.

#### IV. RESULTS:

With the advent of small, dedicated mini-computer systems it is possible to measure frequency response information and computationally determine the modal parameters. As a result of this improved computational capability a large number of computational algorithms have been developed in recent years for computing modal information. A few of this algorithms were evaluated to compare each technique in respect of its implementation, advantages, and disadvantages.

The SDOF is the simplest to use but its main disadvantage is that the technique does a very poor job of separating modes. The Ibrahim Time Domain approach based on the damped complex exponential response method is rather straight forward in application. It does require the use of an oversized mathematical modal to improve the accuracy of the identified parameters. The linear least square algorithm while implementable is computational intensive.

Dus to the time limitation, most of the recent popular methods could not be investigated. It is proposed to continue to investigate the other techniques before a recommendation of the most suitable method/methods is made.

#### V. RECOMMENDATIONS:

Experimental modal analysis is playing an increasingly important role in structural dynamics efforts which are in need of analytical model verification. The determination of modal parameters from experimentally measured data involved the use of parameter estimation techniques. Numerous parameter estimation methods are available and each has its advantages and disadvantages, and as such, have their own ardent devotees. The objective of the present study is to evaluate the ease or difficulty in implementing these techniques and compare the qualities of their results.

A very limited study was carried out under this research because of limited duration of the effort. It is proposed that the study be continued to embrace all the techniques mentioned in Section III before a final recommendation can be made for suitable method/methods that can be used for parameter estimation.

A mini-grant proposal will be submitted to Universal Energy System to continue this research and to study the implementation feasibility, advantages, and disadvantages of all the parameter estimation methods.

## REFERENCES

1. Brown, D. L., Allenmang, R. J., Zimmerman, R., and Mergeay, M., "Parameter Estimation Techniques for Modal Analysis," SAE Paper Number 790221, SAE Transactions, Volume 88, pp 828-846, 1979.
2. Ibrahim, S. R., Mikulcik, E. C., "A Method for Direct Identification of Vibration Parameters from the Free Response," Shock and Vibration Nov 1976.
3. Ramsey, K., "Effective Measurements fro Structural Dynamics Testing: Part I." Sound and Vibration Nov. 1976.
4. Richardson, M., and Potter, R., "Identification of Modal Properties of an Elastic Structure from Measured Transfer Function Data," ISA ASI 74250, 1974, pp. 239-246.
5. Class notes on intensive course on Modal Analysis - Theory and Measurement Techniques at AFWL/ARBH, Kirtland AFB, NM, May 4-6 1987, by Dept of Mechanical & Industrial Engineering, University of Cincinnati in conjunction with Anotrol West Corporation.

1987 USAF-UES SUMMER FACULTY RESEARCH PROGRAM/  
GRADUATE STUDENT SUMMER SUPPORT PROGRAM

Sponsored by the  
AIR FORCE OFFICE OF SCIENTIFIC RESEARCH  
Conducted by the  
Universal Energy Systems, Inc.

FINAL REPORT

Correlation and Simulation Studies of  
of  
GaAs Microwave MESFET Power Devices

Prepared by:	John W. Amoss, Ph.D., P.E.
Academic Rank:	Associate Professor
Department and	Systems Science Department
University:	University of West Florida
Research Location:	Avionics Laboratory/AADM Wright-Patterson Air Force Base Dayton, OH
WPAFB Researcher:	Robert T. Kemerley
Date:	3 Aug 1987
Contract Number:	F4921-85-C-0013

Correlation and Simulation Studies  
of  
Microwave MESFET Power Devices

by

John W. Amoss

ABSTRACT

Correlation plots of dc data for microwave power MESFETs are presented. These data were measured on devices processed on substrates grown by low-pressure and high-pressure Czochralski techniques. The purpose of the correlation was to assess the merits of GaAs materials grown by the two methods and to establish the uniformity of ion implantation, annealing, and processing of full 3 inch diameter substrates. Since the characteristics of the devices seemed to be process and device related, correlation plots of measured data were compared with correlation plots of Monte-Carlo simulations to help identify what process or device parameters were causing the observed variations in dc characteristics.

### Acknowledgements

I wish to thank the Air Force Office of Scientific Research for sponsorship of this research. I also wish to thank those personnel of Universal Energy Systems who provided logistical and administrative support during all phases of this program.

I am especially indebted to Mr. John Sizelove and Mr. John King for their support and cooperation in supplying numerous histograms and scatter plots and to Capt. Scott Dudley and Lt. Stu Labovitz for providing indispensable computer support throughout the program. Special thanks is due Mr. Robert Kemerley and Mr. Gary McCoy for providing leadership, support, and a stimulating work environment so evident throughout my tenure at the Avionics Laboratory, Wright-Patterson Air Force Base, Dayton, Ohio.

### Introduction

The Avionics Laboratory, Wright-Patterson Air Force Base, has ongoing programs with several companies that process semiconductor materials into devices for use in microwave and high-speed logic circuits. The primary tasks of each program are (1) to process, using established procedures, GaAs substrates grown by low-pressure and high-pressure liquid encapsulated Czochralski techniques; (2) to obtain data describing the material, process, and device parameters before, during and after the processing of the substrates; and (3) to provide such data for material and device correlation studies. The companies involved in the programs and the devices they are processing are:

#### Material Growth

Texas Instruments	- Low-pressure Boule
Rockwell International	- High-pressure Boule

#### Device Processing

Texas Instruments	- Low-noise MESFET
Raytheon Semiconductor	- High-power MESFET
Raytheon Research	- MMIC
Hughes Microwave Products	- Logic Devices

The overall objectives of the programs are to assess the relative merits of GaAs material grown by the two methods and to establish the uniformity and repeatability of ion implantation, annealing, and processing of full 3 inch diameter GaAs substrates.



### Goals and Objectives

My general tasks were to help correlate some of the data provided by the companies under item (3) listed above. I feel I was chosen to participate in the program because of my previous experience in the area of microwave solid-state device research. Because of the vast amount of data and the number of devices involved, I was afforded the opportunity to review the available data and company reports before setting specific goals and objectives.

Specific goals and objectives decided upon are:

1. To conduct a detailed analysis of the Raytheon data taken during the processing of the High-power MESFETs, and
2. To obtain correlation plots of that data and to compare them with simulated plots obtained from appropriate theoretical models of the devices, hoping, thereby,
3. To extract information pertaining to material, process, and device parameters.

### Background Information

Throughout the programs, each company received five wafers from a sequence of four low-pressure and four high-pressure boules. To distinguish between wafers, the following code was used. A first letter, L or H, followed by a digit was used to distinguish between the low and high-pressure boules within the sequence of four sets. Next, two digits were used

to distinguish the location of a wafer within a boule with the numbers running consecutively from seed to tail. Thus wafer H232 means wafer 32 from high-pressure boule 2 with the next three digits denoting a measured characteristic of some material, process, or device parameter.

During the processing of high-pressure and low-pressure boule 2, Raytheon divided the wafers into lots as shown in Table 1.

Table I Processing Arrangement	
<u>Process Lot</u>	<u>Wafers</u>
1	L235, L236 H229, H232
2	L233, L237 H228, H231
Destructive Tests	L234, H230

Although RF measurements were made on selected devices, they required that each device be mounted in separate test fixtures. Unfortunately, the mounting procedure and the RF measurements were costly and time consuming and only a limited number of devices from each wafer (16/wafer) were RF tested. On the other hand, large amounts of data (> 2000 values) were measured on the active-layer and dc characteristics and, consequently, most of the correlation studies concentrated on those categories since it was felt that any conclusions reached would be more meaningful.

### Analysis Method

Ideally, one would prefer to compare the various characteristics of each wafer with those of a "standard". One could then evaluate the various wafers based on how their measured characteristics deviated from those of the standard. Unfortunately, no such standard exists and the next approach would be to compare the wafers among themselves. A cursory examination of the data, however, showed considerable variation between boules, and, in fact, among near adjacent wafers of a particular boule, even those processed in the same lot. The data taken over a given wafer even showed considerable variations in the dc characteristics. These variations made it difficult to establish a criteria by which to evaluate the wafers. Comparing correlation plots of measured data to simulation plots of simulated data adds a new dimension and insight into the interpretation of the distributions observed in the histograms.

The dc characteristics of the MESFET used in the simulations are based, in part, on limiting cases of small-signal models developed by Pucel, Haus, and Statz<sup>1</sup>, Fukyi<sup>2</sup>, and Treetman<sup>3</sup>. In discussing the limiting cases, reference will be made to certain equations of Pucel et al. by number rather than by repeating the equations here.

Insofar as possible, their nomenclature will also be used here. The paper by Pucel et al. contains an excellent discussion of previous work by others which led to the more complete models, and should be reviewed by those unfamiliar with MESFET modeling.

The model is based on a uniformly doped channel of effective thickness,  $a$ , which is analyzed by dividing the MESFET longitudinally into two sections as first proposed by Grebene and Ghandhi<sup>4</sup>. One section, that nearest the source and denoted section I of length  $L_1$ , is taken to have constant carrier mobility and the other, that nearest the drain and denoted section II of length  $L_2$ , is taken to have saturated carrier velocity. The boundary between the two regions is a function of the electric field and depends upon the operating conditions. The equations which describe this model are highly nonlinear and the boundary between the two regions, the length of section I, is determined by use of a computer. Since the model is a complicated model, the results are presented graphically, rather than analytically, which makes it more difficult to compare the characteristics with those of the more simple analysis.

and [3] were used in Monte-Carlo type simulations to generate "theoretical" scatter plots with which the measured scatter plots were compared. The main purpose of the simulations were to help identify some of the material, process, or device parameters that might be contributing to the large differences in the scatter plots of the measured data. The general approach used here was to determine certain average material and device parameters from the similarities of the plots based on the Monte-Carlo model and to determine what deviations in those parameters would lead to the observed deviations in the scatter plots.

### Results

Figure 1 shows scatter plots for the measured source-to-drain resistance  $R_{SD}$  and for the measured saturated current  $I_{SAT}$ . The difference between the scatter plots for  $R_{SD}$  and  $I_{SAT}$  is the difference between the

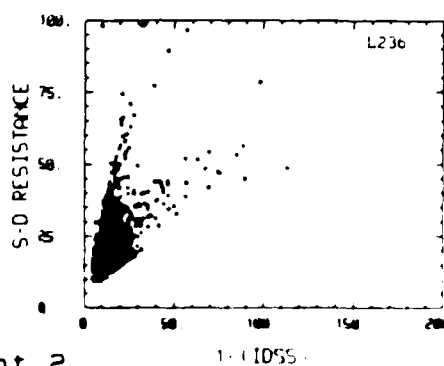
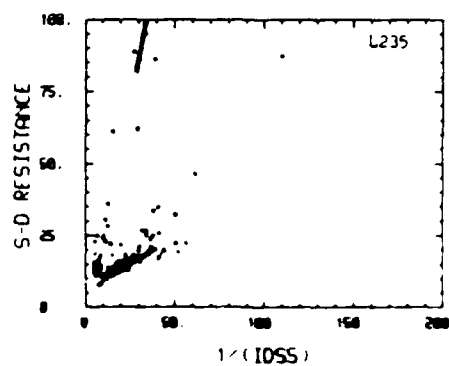
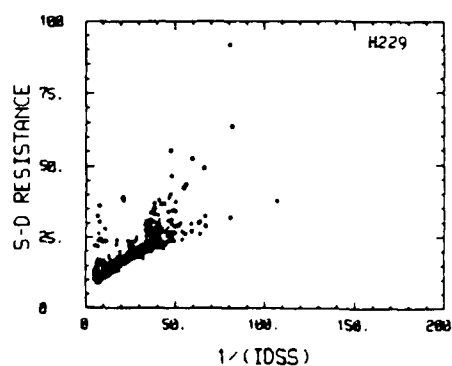
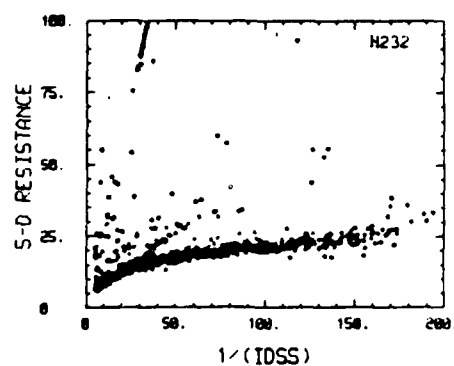
measured and simulated values of  $R_{SD}$  and  $I_{SAT}$ . The difference between the measured and simulated values of  $R_{SD}$  and  $I_{SAT}$  is the difference between the

measured and simulated values of  $R_{SD}$  and  $I_{SAT}$ . The difference between the measured and simulated values of  $R_{SD}$  and  $I_{SAT}$  is the difference between the

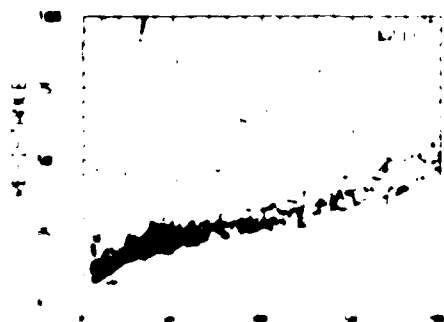
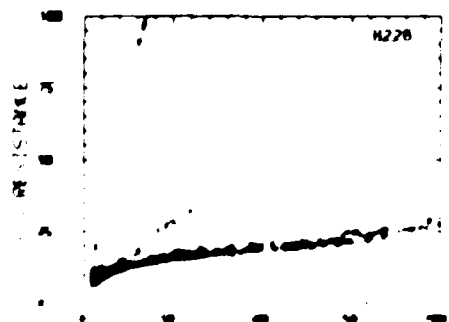
measured and simulated values of  $R_{SD}$  and  $I_{SAT}$ . The difference between the measured and simulated values of  $R_{SD}$  and  $I_{SAT}$  is the difference between the

measured and simulated values of  $R_{SD}$  and  $I_{SAT}$ . The difference between the measured and simulated values of  $R_{SD}$  and  $I_{SAT}$  is the difference between the

# Lot 1



# Lot 2



Using the equations of Pucel et al. it can be shown that, for  $p \approx s$  (the large current condition for a given device), the scatter plot should have an average slope equal to  $v_s L / \mu_0 = E_s L = 0.3$  for  $E_s = 0.3E_4$  volts/cm and  $L = 1E-4$  cm for fully saturated devices. The slope should be greater than this value since the effective gate length (the depleted length under the gate) will be larger than the actual gate length. The experimental points for  $1/I_D \approx 20$  (corresponding to  $I_D > .050$  A) indicates a slope of about 0.50 for six of the seven plots. For  $N = 1.2E+17$ ,  $a = .17E17$ ,  $Z = .025$ , and  $v_s = 1.4E7$  (this value for  $v_s$  and the above value for  $E_s$  implies a constant low field mobility of 4666), the calculated ungated value of  $I_D$  would be equal to .115 A for an  $I_D/I_{D0}$  ratio of greater than .44. Figure 8 of Pucel et al. shows that we expect the ratio  $I_D/I_{D0}$  to be less than .44 for  $I_D/I_{D0}$  ratios greater than .44. The experimental data also shows that for  $I_D/I_{D0}$  ratios greater than .44, the ratio  $I_D/I_{D0}$  is less than .44.

Figure 8 of Pucel et al. shows that we expect the ratio  $I_D/I_{D0}$  to be less than .44 for  $I_D/I_{D0}$  ratios greater than .44.

Figure 8 of Pucel et al. shows that we expect the ratio  $I_D/I_{D0}$  to be less than .44 for  $I_D/I_{D0}$  ratios greater than .44.

Figure 8 of Pucel et al. shows that we expect the ratio  $I_D/I_{D0}$  to be less than .44 for  $I_D/I_{D0}$  ratios greater than .44.

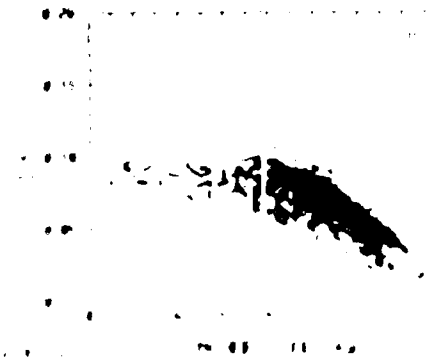
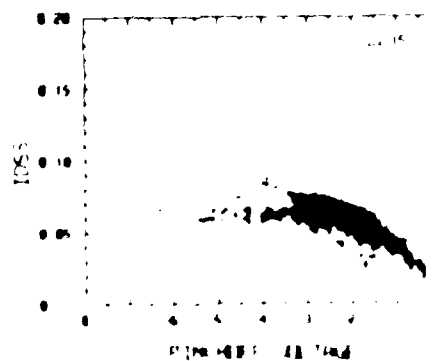
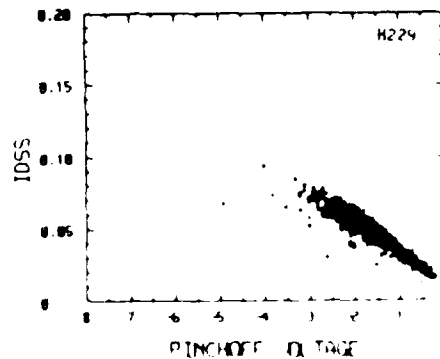
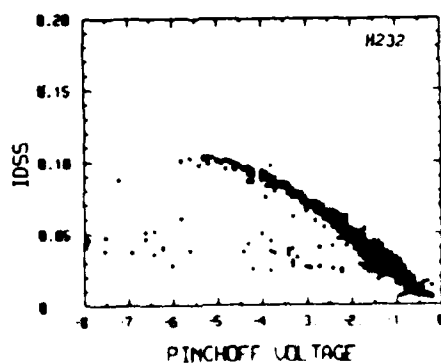
Figure 8 of Pucel et al. shows that we expect the ratio  $I_D/I_{D0}$  to be less than .44 for  $I_D/I_{D0}$  ratios greater than .44.

Figure 8 of Pucel et al. shows that we expect the ratio  $I_D/I_{D0}$  to be less than .44 for  $I_D/I_{D0}$  ratios greater than .44.

This indicates that the device resistance at 3.0 volts for those devices is essentially equal to the unsaturated value or, conversely, that those devices are barely saturated at 3.0 volts. One should compare the scatter plots for wafer H229 (different lots) that show a relatively well defined scatter plot with the scatter plot for wafer L236 that shows a broad scatter plot between a line of slope 0.5 and 3.0. The average external pinchoff voltage for these wafers are 1.4 and 2.7 (using the positive pinchoff voltage convention making the total pinchoff voltages,  $W_{00}$ , equal to about 2.2 and 3.5, respectively. Since MESFETs start saturating at drain voltages close to  $W_{00}$ , the knee voltage range of the devices on wafer L236 are not in the saturation region at a drain voltage of 3.0 volts. The measured gate voltages for these devices pinchoff voltages are shown in Figure 1. The pinchoff voltages for these devices are generally in the range 1.0 to 2.0 volts. The pinchoff voltages are shown in Figure 1. The pinchoff voltages are shown in Figure 1.

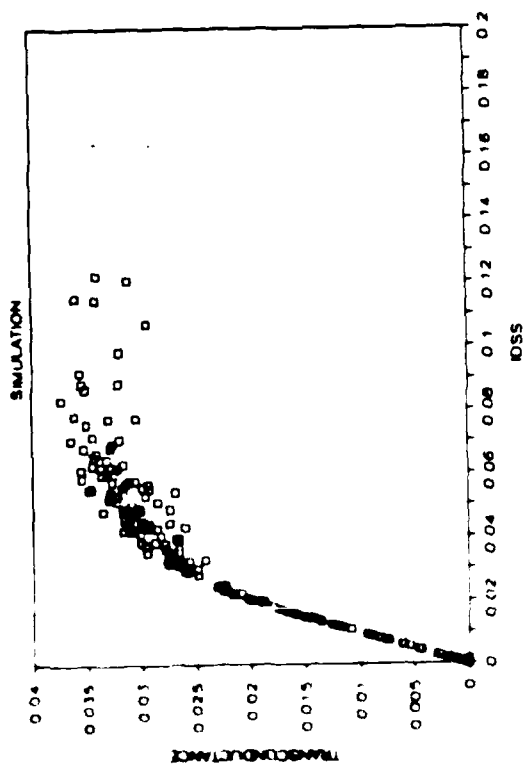
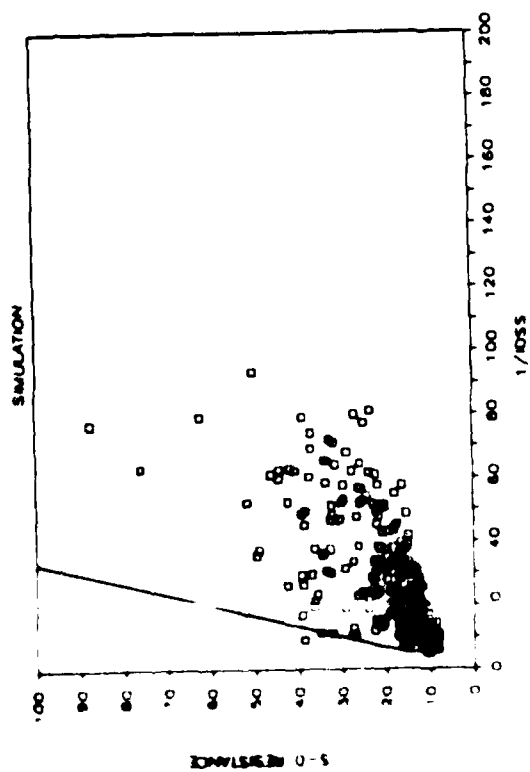


Lot 1



simulation assumed  $a$  to have a mean value of .17 microns with a standard deviation of .04 and  $N$  to have a mean value of  $1.2E17/cm^3$  with a mean value of  $.2E17$ . The average values of  $a$  and  $N$  were chosen so that the average external pinchoff voltage,  $W_{00} - \phi$ , is less than 3.0 volts and the device was assumed to operate in the saturation region with a saturation factor of 0.5. The saturated velocity was assumed to be  $1.4E7$  cm/sec and the low field mobility to have a mean value of 4000 with a standard deviation of 500. These values were chosen to simulate devices such as those in water walls where most of the devices operate in the saturation region.

The simulation was run for 1000 iterations. The results are shown in Figure 1. The average values of the parameters are shown in Table I. The standard deviation of the parameters is shown in Table II. The average values of the parameters are shown in Table III. The standard deviation of the parameters is shown in Table IV. The average values of the parameters are shown in Table V. The standard deviation of the parameters is shown in Table VI.



Simulated scatter plots.

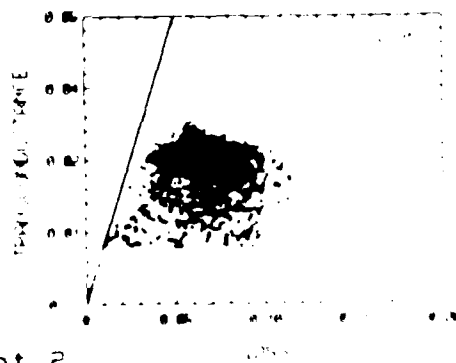
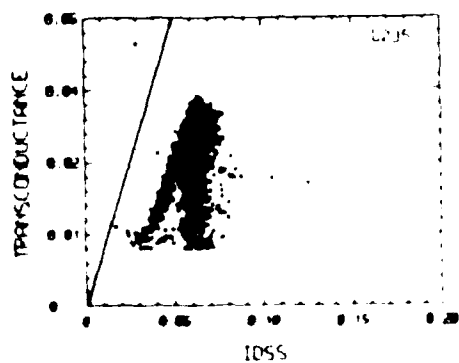
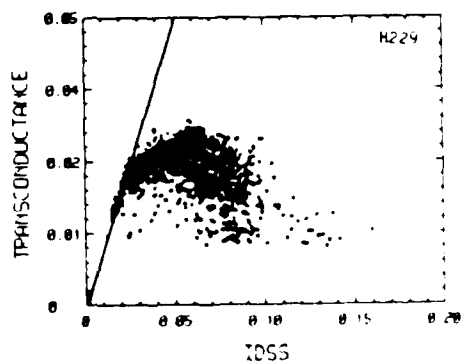
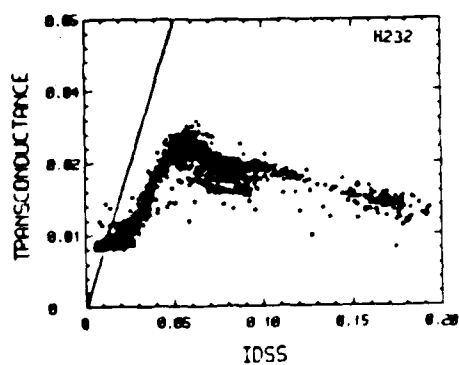
a condition where the velocity saturation region is relatively short ( $L_1 \approx L$ ,  $L_2 \approx 0$ , where  $p \approx d$ ) and the other scatter plot for the condition where the velocity saturation region is relatively long ( $L_1 \approx 0$ ,  $L_2 \approx L$  where  $p \approx s$ ). In general there is fair agreement between the simulated scatter plots for  $I_{DSS}$  vs pinchoff voltage and the actual scatter plots of Figure 4 in that the actual scatter plots tend to fall between the limiting cases. The differences between the simulated scatter plots and the actual scatter plots for transconductance vs  $I_{DSS}$  raises some interesting questions. The transconductance was defined by Raytheon to be

$$g_m = I_D(V_G=0) - I_D(V_G=-1)$$

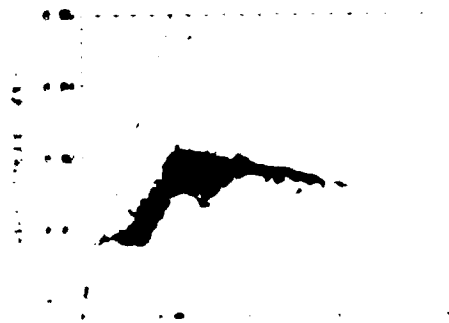
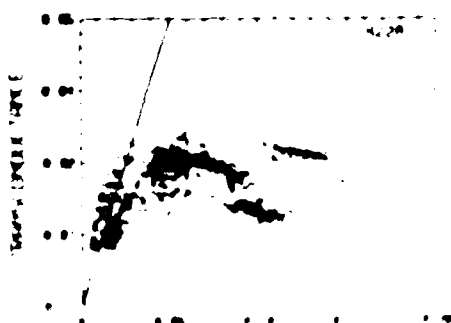
which is the same expression used in the simulations. Plots for those devices having pinchoff voltages less than 10V lie along the linear portion of the simulated scatter plot with slope = 1, since for these devices the gate voltage bias is small compared to the pinchoff voltage. The data for devices having pinchoff voltages greater than 10V lie along the curved portion of the simulated scatter plot.

1. The simulated scatter plot for  $I_{DSS}$  vs  $V_{PO}$  is in good agreement with the actual scatter plot.
2. The simulated scatter plot for  $I_{DSS}$  vs  $V_{PO}$  is in good agreement with the actual scatter plot.
3. The simulated scatter plot for  $I_{DSS}$  vs  $V_{PO}$  is in good agreement with the actual scatter plot.
4. The simulated scatter plot for  $I_{DSS}$  vs  $V_{PO}$  is in good agreement with the actual scatter plot.

Lot 1



Lot 2



scatter plots of Figure 4 clearly show most wafers have an abundance of points representing devices with pinchoff voltages less than 1.0 volts with the possible exception of wafer L236. Its transconductance scatter plot does not show a scatter of points about a linear region which is what one would expect if all devices had pinchoff voltages greater than 1.0 volts. The transconductance curves of the actual plots seems to have been clamped to values greater than 0.010 and displaced to higher  $V_{DS}$  values. The general trend in transconductance past the peak seems to be widely scattered about a line which decreases with increasing current. The simulations of wafers show a strong correlation past the peak of the transconductance curve with the approximate decrease of the peak transconductance and the  $V_{DS}$  value at which the peak occurs. These results suggest that the pinchoff voltages less than 1.0 volts are not a significant factor in the  $I_D$  vs  $V_{DS}$  characteristics of the devices. The peak  $I_D$  values are not a function of the pinchoff voltage. The  $V_{DS}$  value at which the peak occurs is a function of the pinchoff voltage.

to material parameters. This conclusion was largely based on the deviations in average values and the histograms of the dc data relating to the various waters.

The results of this study, taken together with the results of the previous program, indicate that the use of the computer in the laboratory is a valuable tool for the study of the effects of the environment on the behavior of the organism. The use of the computer in the laboratory is a valuable tool for the study of the effects of the environment on the behavior of the organism.

THEORY

The first part of the paper is devoted to a discussion of the general principles of the theory of the structure of the atom. It is shown that the structure of the atom is determined by the laws of quantum mechanics, which are based on the principle of the uncertainty of the position and momentum of the particles.

The second part of the paper is devoted to a discussion of the structure of the atom in the case of a central potential.

The third part of the paper is devoted to a discussion of the structure of the atom in the case of a non-central potential.

The fourth part of the paper is devoted to a discussion of the structure of the atom in the case of a non-central potential.

The fifth part of the paper is devoted to a discussion of the structure of the atom in the case of a non-central potential.

The sixth part of the paper is devoted to a discussion of the structure of the atom in the case of a non-central potential.

The seventh part of the paper is devoted to a discussion of the structure of the atom in the case of a non-central potential.

The eighth part of the paper is devoted to a discussion of the structure of the atom in the case of a non-central potential.

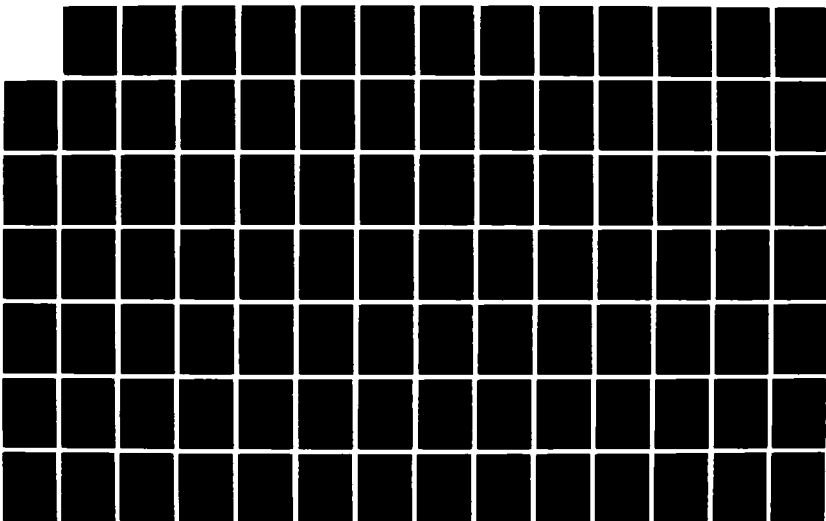
The ninth part of the paper is devoted to a discussion of the structure of the atom in the case of a non-central potential.

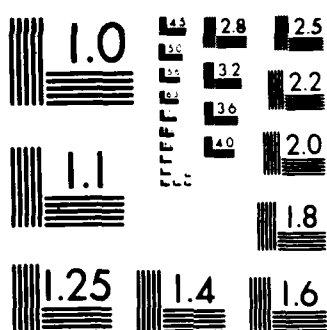
The tenth part of the paper is devoted to a discussion of the structure of the atom in the case of a non-central potential.

The eleventh part of the paper is devoted to a discussion of the structure of the atom in the case of a non-central potential.



NO-A191 203 UNITED STATES AIR FORCE SUMMER FACULTY RESEARCH PROGRAM 2/11  
(1987) PROGRAM TE.. (U) UNIVERSAL ENERGY SYSTEMS INC  
DAYTON OH R C DARRAH ET AL. DEC 87 AFOSR-TR-88-0212  
UNCLASSIFIED F49620-85-C-0013 F/O 5/1 NL





MICROCOPY RESOLUTION TEST CHART  
NATIONAL BUREAU OF STANDARDS-1963-A

1987 USAF-UES SUMMER FACULTY RESEARCH PROGRAM/  
GRADUATE STUDENT SUMMER SUPPORT PROGRAM

Sponsored by the  
AIR FORCE OFFICE OF SCIENTIFIC RESEARCH

Conducted by the  
Universal Energy Systems, Inc.

Final Report

AIR FORCE OFFICER SELECTION REVISITED: ENTERTAINING  
THE POSSIBILITIES FOR IMPROVEMENT

Prepared by:	Victor H. Appel, Ph.D.
Academic Rank:	Associate Professor
Assisted by:	Andrew D. Carson, M.A.
Academic Rank:	Doctoral Student
Department and	Educational Psychology
University	The University of Texas at Austin
Research Location:	Air Force Human Resources Laboratory Air Force Systems Command Brooks AFB, Texas 78235-5601
USAF Researcher:	Thomas W. Watson, Ph.D.
Date:	September 20, 1987
Contract No:	F49620-85-C-0013

Air Force Officer Selection Revisited: Entertaining  
The Possibilities for Improvement

by

Victor H. Appel

and

Andrew D. Carson

ABSTRACT

Research literature was examined to identify selection devices or methodological/conceptual developments appearing promising as a means for enhancing the system of officer selection for Officer Training School and Air Force ROTC candidates. In that the current system is focused almost exclusively on cognitive/intellective predictors, the investigators sought to broaden the scope by incorporating predictors of other likely sources of variance, particularly leadership/managerial and commitment variables. Recommendations are offered how such constructs might be tapped by incorporating an appropriate biodata form within the existing selection device, the AFOQT. Experimentation over the long run with an assessment center methodology is also proposed.

### ACKNOWLEDGEMENTS

We wish to express our thanks to the Air Force Systems Command and to the Air Force Office of Scientific Research for the sponsorship of this research. Thanks are also due to the Universal Energy Systems for their help in the administrative oversight of this effort.

Most of all, however, we owe a great debt of gratitude to the personnel at AFHRL. Our deepest appreciation goes to Dr. Tom Watson, our liaison at the lab, who worked unstintingly to facilitate our task and to Dr. Bill Alley, Effort Focal Point, who allowed us the autonomy our wide-ranging project required. Linda Elliott and Teri Mercatante gave invaluable help as part-time members of our research team. Lt. Col. Brown provided unparalleled administrative and personal support for the project. Drs. Lonnie Valentine and Malcolm Ree lent the benefit of their long term experience at the lab. Gene Ligon was generous in obtaining resources for us and in making arrangements. All contributed to a rich and memorable research experience.

## I. INTRODUCTION

For the past 34 years the means employed for the selection of the bulk of Air Force officers has remained relatively unchanged. These officers are those whose source of commissioning is Officer Training School (OTS) or Air Force ROTC (AFROTC). They represent approximately 74% of the active duty force (Gandi, 1987). As Rogers, Roach and Short (1986) have observed, the basic sequential selection strategy for these applicants is a four step process. Once a vacancy occurs, candidates are evaluated successively to see if they qualify with regard to 1) Education 2) Physical Fitness 3) Moral Character and 4) Mental Competence.

Though any applicant may be eliminated at any of the four selection points, the fourth step, determination of mental competence, serves as the principal selection hurdle. This hurdle is satisfied or not based on the score attained on a measure of general ability, the Air Force Officer Qualifying Test (AFOQT). Since its introduction in 1953 as a means for predicting success in OCS and as a means for screening for aircrew training, the AFOQT has undergone 16 revisions (Rogers, Roach and Short, 1986). Still, the AFOQT remains a measure of general ability. When validated against OTS or other early training criteria, the AFOQT yields validity coefficients ranging from .10 to .40, but most commonly validities are between .20 and .30.

During the more than three decades in which the AFOQT has been used, there have been multiple advances in the field of personnel selection (Dunnette, 1976). It is only logical that the Officer Selection and Classification Function of AFHRL should expand its efforts beyond those related to the AFOQT. The Officer Selection group hoped that by commissioning outside assistance to review selection literature, recommendations for improving the selection process might be obtained.

The senior investigator is a vocational and organizational psychologist. For more than 20 years he has been concerned with the goodness of fit between persons and positions. Personnel psychologists at AFHRL felt his background would be helpful in taking a fresh look at means for enhancing officer selection. This seemed particularly appropriate in light of his collaboration with some AFHRL personnel in isolating factors influencing turnover propensity among Air Force personnel.

The second author of this report, with background experience and training as a Developmental and Counseling Psychologist, brings useful experience in the areas of career development and career planning.

## II. OBJECTIVES OF THE RESEARCH EFFORT

The objectives of the research effort were two fold:

1. To carry out a literature review in the area of occupational success prediction for officers/executives.

2. To conduct follow-up telephone interviews with investigators engaged in personnel selection research deemed promising and relevant to us.

### III. APPROACHES TAKEN IN REALIZING OBJECTIVE 1

- 1a. Approach 1a: As a precursor to conducting a literature review, the investigators sought to find job analyses carried out on various of the officer AFSC's. The investigators reasoned that if officer job analyses were available, they would illumine the major components of the positions, and thereby suggest the types of competencies for which predictors needed to be sought. With that information in hand, it was hoped that the scope of the literature review would be reduced.
- 1b. Results Achieved When Approach 1a Pursued: This initial effort did not prove worthwhile. Although the investigators were able to locate a substantial body of officer AFSC's which had been subjected to Job Analysis, the tasks identified were at such a micro level, there were literally hundreds of job components. It was decided to forego further attempts. The effort did demonstrate that there are substantial differences across officer AFSC's. It raises the question whether the many, non-rated AFSC's re-



quire differentiation of selection composites in the same fashion as rated officer positions now do.

2a. Approach 2a: In an effort to cull fresh possibilities for selection enhancement from the research literature, the investigators conducted a computer search of the civilian and military literature on the prediction of occupational success among officers/executives. The literature surveyed covered a twenty year span from 1967 through 1987 as listed in the PSYCINFO data base of the American Psychological Association. This resulted in a data file of 458 entries.

2b. Results Achieved When Approach 2a Pursued: Having surfaced many more relevant studies than anticipated the investigators devised a three dimensional, cube model into which the various studies could be sub-divided. The model allowed each study to be classified with regard to 1) Type of Selection Measure (e.g. paper and pencil--aptitude) 2) Type of Variable (e.g. Flexibility) 3) Measured Against Which Criteria (e.g. Performance Rating by Supervisor). The investigators devised a form by which each study could be quickly classified. This was in an effort to facilitate generalizing about the results found.

When the results were tallied it became apparent that there were many more studies involving

the use of paper and pencil measures than there were performance based or naturalistic studies. Further, of the paper and pencil measures used, general ability measures were most effective, along with biodata forms. Personality and interest measures were least effective along with unstructured interviews. When peer ratings were conducted they often were quite predictive. Most striking was the impressive validity coefficients achieved by assessment centers. Whereas validity coefficients of .20 or .30 or less were typically found for paper and pencil measures, assessment centers consistently produced validity coefficients in the .40's (Hakel, 1986, Tenopyr and Oeltjen, 1982; Thornton and Byham, 1982).

- 3a. Approach 3a While not originally planned, literature review efforts unearthed related work on Utility Analysis. Utility analysis is a means for estimating the dollar savings achieved when a selection device's predictive efficiency is improved. Recent improvements by Hunter and Hunter (1984) in the means for estimating the dispersion component of the utility formula have simplified computation and thereby stimulated the conduct of Utility analyses. These analyses are impressive in that they demonstrate the substantial dollar savings which even a modest increment in predict-

ive validity can bring about.

3b. The investigators decided to apply Hunter and Hunter's (1984) Utility formula to the problem of AF officer selection enhancement. Using figures from meta-analyses performed by Schmidt et al (1984) for cognitive ability tests, the researchers chose .22 as a representative validity. Similarly, they chose .43 as a realistic validity coefficient value if assessment center methodologies were added. To carry out the necessary computations, using Hunter and Hunter's adaptation of the original formula developed by Cronbach and Gleser (1965), the investigators required certain demographic information about AF officers. This was readily available from Gandi (1987) at the Air Force Military Personnel Center, Randolph AFB. When the requisite values were substituted in the equation, the results were startling. Current selection based on a validity of .22 can be demonstrated to save the USAF \$153,243,890 over what it would cost if random selection were used. If the validity of officer selection procedures could be raised to .43, the USAF would save an additional annual amount of \$146,278,130.

#### IV. APPROACHES TAKEN IN REALIZING OBJECTIVE 2

- 1a. Approach 1a: These investigators simply made use of AUTOVON resources at AFHRL to contact both mili-

tary and civilian colleagues throughout the country. These investigators were particularly interested in contacting counterpart scientists in the other branches of service.

- 1b. The telephone contacts proved to be highly valuable. These investigators were able to find that there was appreciably more interest in selection enhancement procedures for officers than other sources had indicated. Further, these investigators were able to find out that parallel research was being funded by other branches of service, with possible overlap. Some research materials were exchanged.

#### V. RECOMMENDATIONS

- 1a. Since the two objectives of this research are both related to enhancing officer selection within the Air Force, recommendations with regard to that issue will be combined, and presented here.

1. There is strong reason to support continuing efforts at improving the psychometric properties of the AFOQT, as now available in Forms P. In addition to continuing the new types of cognitive subtests being developed, additional work on establishing the extent to which differential validities exist on the AFOQT for various sub-groups.
2. The current officer selection system is virtually a unidimensional one, with the AFOQT, the

requirement of college completion and the Patton rating of colleges all appear to be "soaking up" the cognitive sources of variance. Selection devices aimed at tapping factors orthogonal to the cognitive ones would appear to offer good prospect for significantly increasing the validity if added.

3. The major lack visible to these investigators with regard to the current officer selection system deals with leadership/managerial ability. While there is some relationship between intellectual abilities and leadership/managerial abilities, that relationship is a modest one. Selection devices which can differentiate among those high and low in these regards are badly needed. While ambiguity remains in the constructs, efforts at paper and pencil measures of leadership/managerial ability could begin. Bass et al(1987) have provided a conceptual foundation in their paradigm of transactional versus transformational leadership which seems promising. In the near term, these investigators propose the use of biodata forms, which might be developed, to differentiate applicants. In the far term, these investigators propose moving to an assessment center methodology. Initially, experimental efforts, using the assessment center in San Antonio, would be

required.

4. Since selection devices are no better than the criteria against which they are validated, it is requisite that efforts at criterion development be expanded.
- b. The investigators propose that a biodata form appraising leadership/managerial abilities be developed in a follow on effort. Such a measure could be incorporated within the AFOQT. Content of the form would primarily be demographic. The biodata form might also be used to tap commitment to the Air Force, a variable closely linked to turnover propensity.
- c. In the view of these investigators, there is insufficient collaboration among AFHRL and the other personnel and training commands (ATC and MPC) in the San Antonio area. Each of these elements could contribute to selection enhancement in significant ways, were they to have their mission expanded to include selection issues. Similarly, AFHRL could contribute to classification and training functions. Similarly, there does not seem to be adequate collaboration across the branches of service among those concerned with selection issues. Much more should be done on a voluntary basis to keep other branches

of service apprised of developments.

## REFERENCES

Bass, B.M., Avolio, B.J. and Goodheim, L. Biography and the Assessment of Transformational Leadership at the World-Class Level. J. of Management. 1987, Vol. 13, 7-19.

Cronbach, L.J. and Gleser, G.C. Psychological Tests and Personnel Decisions. Urbana, Il.: University of Illinois Press, 1965.

Dunnette, M.D. (Ed.). Handbook of Industrial and Organizational Psychology. Chicago: Rand McNally, 1976.

Gandi, D., Personal Communication, August 4, 1987.

Hakel, M.D. Personnel Selection and Placement. Ann. Rev. Psychol. 1986, Vol. 37, 351-380.

Hunter, J.E. and Hunter, R. F. Validity and Utility of Alternative Predictors of Job Performance. Psychol. Bull. 1984, Vol. 96, 72-98.

Rogers, D. L., Roach, B.W., and Short, L.D. Mental Ability Testing in the Selection of Air Force Officers: A Brief Historical Review. AFHRL-TP-86-23, October, 1986.



Tenopyr, M. L. and Oeltjen, P.D. Personnel Selection and Classification. Ann. Rev. Psychol. 1982, Vol. 33, 581-618.

Thornton, G.C. and Byham, W.C. Assessment Centers and Managerial Performance. Orlando, Fl.: Academic Press, Inc., 1982.

1987 USAF-UES SUMMER FACULTY RESEARCH PROGRAM/

GRADUATE STUDENT SUMMER SUPPORT PROGRAM

Sponsored by the

AIR FORCE OFFICE OF SCIENTIFIC RESEARCH

Conducted by the

Universal Energy Systems, Inc.

FINAL REPORT

EVALUATION OF THREE-DIMENSIONAL KINEMATICS ANALYSIS METHODS OF  
ROBOTICS FOR THE STUDY OF HUMAN ARTICULATED MOTION

Prepared by:	Xavier J.R. Avula, Ph.D.
Academic Rank:	Professor
Department and	Department of Engineering Mechanics
University:	University of Missouri-Rolla
Research Location:	AAMRL/BBM Wright Patterson Air Force Base, Ohio 45433
USAF Researcher:	Ints Kaleps, Ph.D.
Date:	30 September 1987
Contract No.:	F49620-85-C-0013

EVALUATION OF THREE-DIMENSIONAL KINEMATICS ANALYSIS METHODS OF  
ROBOTICS FOR THE STUDY OF HUMAN ARTICULATED MOTION

by

Xavier J. R. Avula

ABSTRACT

The three-dimensional kinematic analysis methods of robotics were considered for the study of human articulated motion. Literature on the direct and indirect kinematics analysis was reviewed for the purpose of evaluating the Articulated Total Body (ATB) Model at the Armstrong Aerospace Medical Research Laboratory as a simulation tool in the development of robotics telepresence technology. The behavior of the ATB right arm was simulated on the computer with a force applied to the center of the hand. The arm positions at various times, and the workspace were determined. Recommendations were made to develop software based on the three-dimensional kinematics methods for the ATB Model, and to perform reach analysis for determining workspace boundaries.

#### ACKNOWLEDGMENTS

I wish to thank the Air Force Systems Command and the Air Force Office of Scientific Research for sponsorship of this research under the Summer Faculty Research Program. Sincere appreciation is due Universal Energy Systems, Inc., administrators of the above program, for their help throughout my tenure as a researcher at the Armstrong Aerospace Medical Research Laboratory.

This work was performed under the guidance of Dr. Ints Kaleps, Chief, Modeling and Analysis Branch. I wish to express my thanks and deep gratitude to Dr. Kaleps for his support, encouragement and intellectual stimulation. Thanks are due Ms. Louise Obergefell for her invaluable technical advice and help with ATB simulations.

## I. INTRODUCTION

Some technological advancements, in addition to being beneficial to humans, expose them to risks that threaten their personal safety. Several defense and industrial operations are performed in hazardous environments contaminated by nuclear materials and toxic chemicals, and in extreme temperatures. For operations in such hazardous environments, the employment of mobile robots, which are remotely controlled by humans, is a natural alternative. Also, some operations in modern air- and spacecraft place such great demands on the senses that it is humanly impossible to perform optimally without the aid of some electronic and mechanical manipulators. The technology of utilizing and controlling robots by a human in the control loop is called Robotic Telepresence, and lately much attention is being directed towards its development. It is believed that better manipulation of remotely located robots can be achieved with a human in the control loop.

The technology of robotic telepresence will provide the understanding necessary to link a human's hands, arms, eyes, and ears to a robot's sensors and manipulators through exoskeletal devices. In the development of the overall robotic telepresence technology, three-dimensional kinematics and dynamics analysis of robots is important. In the Robotic Telepresence Program of the Harry G. Armstrong Aerospace Medical Research Laboratory (AAMRL), Wright-Patterson Air Force Base, the Articulated Total Body (ATB) Model will be used as a dynamics and feedback control simulation tool. The ATB Model is a computer model developed under the sponsorship of the AAMRL to aid in the study of crew member dynamics during ejection from high-speed aircraft.

This model is based on the rigid body dynamics which uses Euler's equations of motion with constraint relations of the type employed in the Lagrange method. The model has been successfully used to study the articulated human body motion under various types of body segment and joint loads. The present study is limited to the evaluation of the kinematics methods of robotics for understanding the human articulated motion as simulated by the ATB Model.

My research task as a participant in the 1987 Summer Faculty Research Program (SFRP) was to determine what three-dimensional kinematics analysis methods are most applicable to study the human articulated motion utilizing the ATB Model as a simulation tool. My experience in teaching advanced dynamics at University of Missouri-Rolla, and my previous work on the calculation of maximum aerodynamic loads on the body segments and joints of the Advanced Dynamic Anthropomorphic Manikins (ADAM), and my involvement in research on various aerospace medical problems have led to my placement as an SFRP participant in the Laboratory. These experiences have been found to be compatible with and desirable for the technical needs of the Robotics Telepresence Program at the AAMRL.

## II. OBJECTIVE

The technology of Robotics Telepresence involves the investigation of methods to provide remote, closed-loop, human control of mobile robots. The effectiveness of a remotely located robot, or any robot for that matter, is based on the trajectory and reach of its end-effector which are analysed using three-dimensional kinematics and dynamics methods. Here we confine ourselves to the evaluation of the kinematic analysis methods. There are several types

of analyses: The direct kinematic analysis uses a straight forward geometric solution in which the position, velocity and trajectory of the end-effector are expressed in terms of the joint angles and link lengths, and their derivatives. This method is suitable for description in time of structural elements but does not take into account the forces acting within or on the system nor does it include inertial effects. To handle consecutive coordinate transformations associated with multiple degrees of freedom, a more general method based on homogeneous transformation matrices is used. This method can also be utilized for inverse kinematic problems in which axis motions that produce desired end-effector motions are calculated. Yet another general method is the one based on rotation matrices involving quaternions which is usually preferred for the solution of inverse kinematic problems.

The objective of the present study is to review the above methods of kinematic analysis for the purpose of using them to understand human articulated motion. In consideration of similarities between the robotic arm and the human arm, and in view of human-in-the-loop control of remotely located robots through exoskeletal devices, such a study will be beneficial. In this study the ATB Model will be used as the simulation tool because of its proven success in earlier studies.

### III. THREE-DIMENSIONAL KINEMATICS ANALYSIS IN ROBOTICS

Kinematics is a fundamental tool in the study of geometry of the end-effector arm motions of a robot. A robotic arm is a system of rigid bodies connected in series to form a kinematic structure. Most robotic arms are open kinematic chains. The problem of finding the end-effector position and orientation for given joint displacements is referred to as the direct kinematics problem.

In direct kinematics the end-effector position is determined uniquely. The problem of finding the joint displacements that lead the end-effector to the specified position and orientation is the inverse kinematics problem. Inverse kinematics is more complex in the sense that multiple solutions may exist for the same end-effector location and arm structure (Asada and Slotine, 1986). In the inverse kinematics problems it is not always possible to derive a closed-form solution since the kinematic equations are comprised of non-linear - simultaneous equations with many trigonometric functions. When the kinematic equations cannot be solved analytically, numerical methods are used to derive the desired joint displacements.

The direct kinematics problem of defining the position of the end-effector as a function of the joint angle values can be solved using straightforward geometry (Koren, 1985). Only simple kinematic structures can be handled by this method. The relationship between a pair of adjacent links in a kinematic chain coupled by a revolute joint can be described by the Denavit-Hartenberg (1955) notation which employs a minimum number of parameters. This notation is based on the  $4 \times 4$  matrix representation of rigid body position and orientation. The forerunner of this notation is the method of representing the kinematic relationships by homogeneous coordinate transformation matrices. The coordinate transformation matrices represent the relative translation and rotation between the coordinate systems of adjacent links  $i$  and  $i-1$  (Richard et al., 1984) as shown in Fig. 1. Considering each link with respect to a suitably chosen local coordinate system the relative translation and rotation between the links are represented by a  $4 \times 4$  matrix called 'A' matrix. In a kinematic structure of  $n+1$  consecutive links we will have  $n$  consecutive coordinate transformations along the serial linkage



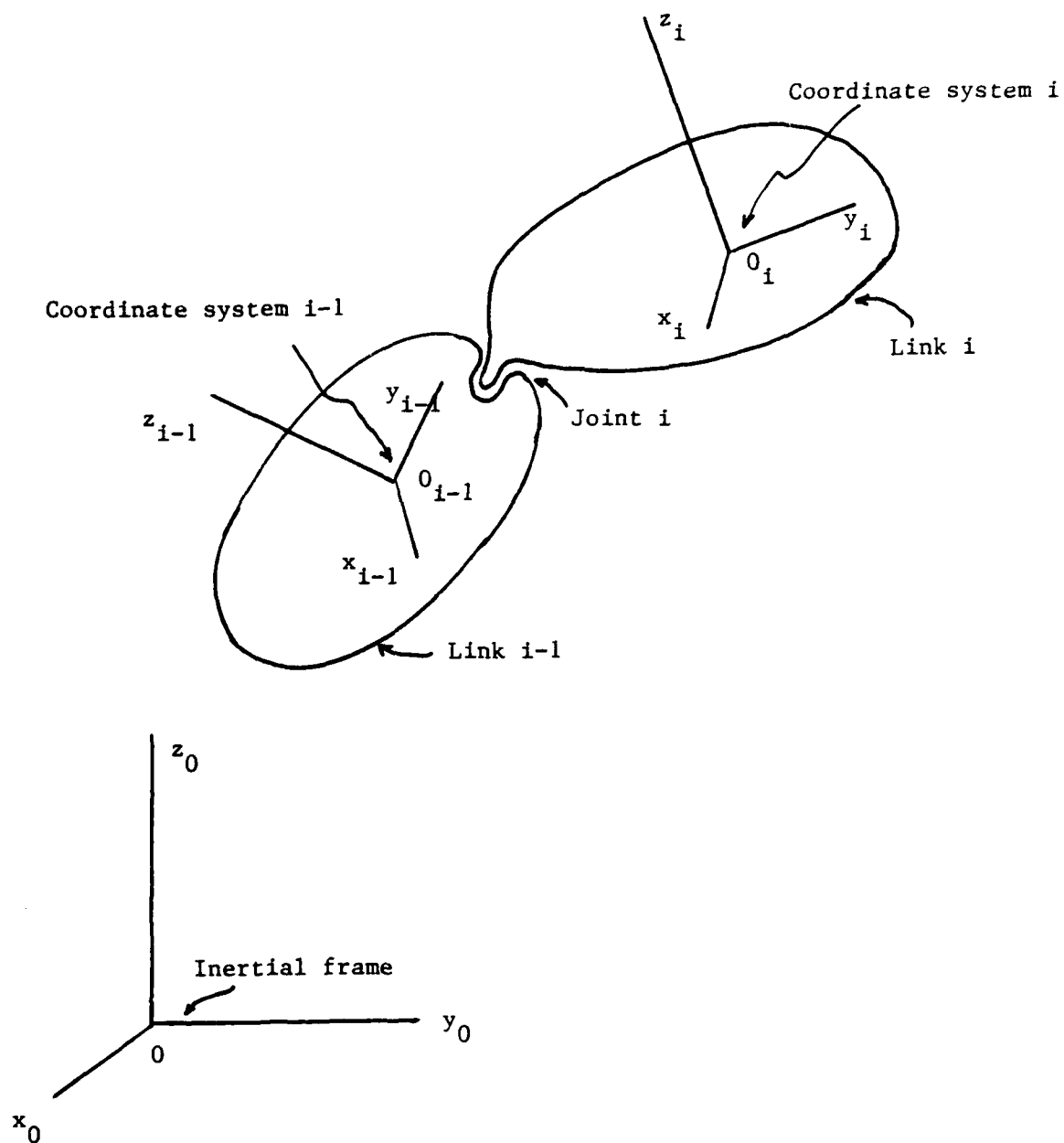


Fig. 1 Coordinate systems attached to a pair of adjacent links in an open kinematic chain.

that can be compactly described by a single equation

$$\bar{X}^0 = [A_1^0][A_2^1][A_3^2] \dots [A_i^{i-1}] \dots [A_n^{n-1}] \bar{X}^n \quad (1)$$

by which the position vector  $\bar{X}^n$  in frame n is transformed to  $\bar{X}^0$  in frame 0.

The 4 x 4 'A' matrix  $[A_i^{i-1}]$ , for example, represents the position and orientation of frame i relative to frame i-1. Equation (1) can further be written as

$$\bar{X}^0 = [T] \bar{X}^n \quad (2)$$

in which

$$[T] = [A_1^0][A_2^1][A_3^2] \dots [A_i^{i-1}] \dots [A_n^{n-1}] \quad (3)$$

The matrix [T] in Equation (3) represents the end-effector position and orientation in terms of joint displacements, angle  $\theta_i$  or distance  $d_i$  depending on the type of joint. This equation provides the functional relationship between the last link position and orientation and the displacements of all the joints involved in the open kinematic chain. Equation (3) is thus referred to as the kinematic equation of the end-effector which governs its fundamental kinematic behavior.

By substituting the values of a given set of joint displacements into the right hand side of the kinematic equation, Equation (1), one can readily find the corresponding end-effector position and orientation. This is the direct kinematic problem we have referred to earlier.

The problem of solving for  $\theta_i$  and  $d_i$  in [T] when the end-effector is moved to a specified position and orientation is the inverse kinematic problem.

Only a few simple kinematic structures yield closed-form solutions for the inverse problem. If the closed-form solution cannot be obtained numerical

methods based on iterative algorithms such as the Newton-Raphson method can be employed. The iterative methods are computationally complex and time consuming. A kinematic structure which yields a closed-form solution is called a solvable structure. What makes a kinematic structure solvable is an important issue in robotics. Pieper (1968) addressed this issue at length and listed all the possible kinematic structures having six degrees of freedom that are solvable. Pieper's analytical method was extended by Featherstone (1983) and Hollerbach (1983).

There are numerous alternative kinematic modeling methods to homogeneous coordinate transformations. The problem of determining the position and orientation of a rigid body in space is studied by using the method of screw axes and line geometry. Yuan and Freudenstein (1971) described the kinematic analysis of spatial mechanisms using screw coordinates. Roth (1967), Sugimoto and Duffy (1982), and Woo and Freudenstein (1970) investigated various aspects of rigid body motions in the light of screw theory and line geometry which were found to be more efficient in numerical kinematic analysis.

The design of arm linkages and the determination of workspace volume are important objectives in robotics technology. Roth (1975) was the first to address the design problem of finding appropriate kinematic structures and link dimensions to allow the arm to cover a specified workspace. Kumar and Waldron (1981), Gupta and Roth (1982), and Tsai and Soni (1981) also have dealt with work space volume and shape determinations by a variety of analytical and numerical methods. Further discussion of kinematics analysis methods in robotics is beyond the scope of this report. Let us now turn our attention to the Articulated Total Body Model which we wish to consider as a tool for understanding human articulated motion from robotics point of view.

#### IV. THE ARTICULATED TOTAL BODY (ATB) MODEL

The Articulated Total Body (ATB) Model is a computer model developed under the sponsorship of the Harry G. Armstrong Aerospace Medical Research Laboratory to aid in the study of crew member dynamics during ejection from high speed aircraft. The forerunner of this model was the Crash Victim Simulator (CVS) developed by Calspan Corporation under the joint sponsorship of the Motor Vehicle Manufacturers Association and the National Highway Traffic Safety Administration to simulate the three-dimensional dynamic response of motor vehicle crash victims. The ATB Model is based on the rigid body dynamics which uses Euler's equations of motion with constraint relations of the type employed in the Lagrange method. The model has been successfully used to study the articulated human body motion under various types of body segment and joint loads. (See Fleck and Butler, 1975)

The dynamic behavior of the ATB Model is determined by classical methods of analysis. The body segments are coupled to form an open chain of interconnected rigid bodies. For an arbitrary segment  $n$ , the translational dynamic equation is

$$M_n \ddot{X}_n = \sum F_{nk} + \sum f_{nj} \quad (4)$$

in which

$M_n$  = mass of segment  $n$

$X_n$  = position of the center of gravity of the  $n$ th segment

$f_{nj}$  = constraint force at joint  $j$  acting on segment  $n$

$F_{nk}$  =  $k$ th external force acting on the  $n$ th segment

The angular dynamic equation in the inertial system is

$$\dot{D}_n^{-1} \phi_n \dot{\omega}_n + D_n^{-1} \dot{\phi}_n \omega_n + D_n^{-1} \phi_n \dot{\omega}_n = D_n^{-1} \sum \text{Torques} \quad (5)$$

where,

$\omega_n$  = angular velocity vector of segment n

$\phi_n$  = inertia matrix about the center of gravity of segment n

$D_n$  = the direction cosine matrix associated with segment n

A vector exponential integrator is used to solve Equations (4) and (5) with appropriate constraint equations. The constraints considered in the ATB program are:

- (i) linear position constraint
- (ii) angular joint constraint (locked joint, pinned joint)
- (iii) distance constraints (zero distance, fixed distance, rolling and sliding constraints)
- (iv) force constraints, and
- (v) torque constraints

The integration of Equations (4) and (5) yields the position vector components of body segments. These quantities are displayed graphically by VIEW and PLOT computer programs.

In the ATB Model the kinematic variables are determined by the integration of dynamical equations of motion. The direct and inverse kinematic methods of robotics have not been applied. However, a recent modification in the ATB program utilizes a direct kinematic method to automatically position a crew member (seated occupant in the CVS) before the dynamic loads are applied. With this modification the model computes the position of each body segment in the inertial reference frame provided that the location of the first segment and the angular orientation of each segment are known. This is similar to the direct kinematics method in robotics involving straight forward computations. A computer subroutine called CHAIN based on

the relationship

$$z_i + D_i^T r_{j,i} = z_{j+1} + D_{j+1}^T r_{j,j+1} \quad (6)$$

in which

$z_k$  = vector from the origin of the inertial coordinate system to the center of gravity of segment k

$D_k$  = direction cosine matrix for segment k (the superscript T stands for the transpose)

$r_{j,k}$  = vector from the center of gravity of segment k to joint j whose components are expressed in the local reference coordinate system of segment k, and

i = joint (j)

Equation (6) can be used to solve for the location of each successive segment from that of the previously defined segments. Note that the program CHAIN is used only to automatically position a seated occupant in equilibrium. The program specifies the axes about which the segments are rotated, and the sequence of rotations to achieve the desired orientation.

## V. AN EXAMPLE

In this example the behavior of the right arm of a crew member to which a five-pound force is applied in the vertically upward direction is simulated. The force remains constant throughout the simulation. For each segment of the arm, the x-y coordinate system is parallel to the cross-section, and the z-axis is oriented along the longitudinal axis of the segment. The following are the segment properties:

Right Upper Arm

Principal Moments of Inertia:

$$I_{xx} = 0.102 \text{ lb-sec}^2\text{-in}$$

$$I_{yy} = 0.099 \text{ lb-sec}^2\text{-in}$$

$$I_{zz} = 0.011 \text{ lb-sec}^2\text{-in}$$

Major and Minor Axes:

$$a = 1.9 \text{ in}$$

$$b = 1.8 \text{ in}$$

$$c = 6.0 \text{ in}$$

Right Lower Arm (Weight = 3.82 lb)

Principal Moments of Inertia:

$$I_{xx} = 0.12 \text{ lb-sec}^2\text{-in}$$

$$I_{yy} = 0.12 \text{ lb-sec}^2\text{-in}$$

$$I_{zz} = 0.007 \text{ lb-sec}^2\text{-in}$$

Major and Minor Axes:

$$a = 1.775 \text{ in}$$

$$b = 1.775 \text{ in}$$

$$c = 5.8 \text{ in}$$

The seated crew member at time  $t = 0$  sec is shown in Fig. 2. A force  $F = 5$  lb is applied at the center of gravity of the hand, and the subsequent motion of the arm is simulated. The arm positions which are calculated by the ATB Model software are displayed in Fig. 2 (b-f) for times  $t = 60, 120, 180, 240,$  and 300 milliseconds. Figure 3 is constructed by superposition of arm motion sequences to indicate the workspace generated under the prescribed conditions. It must be emphasized once again that the segment positions have been calculated by solving the dynamical equations of motion, Equations (4) and (5), and not the kinematic equations.

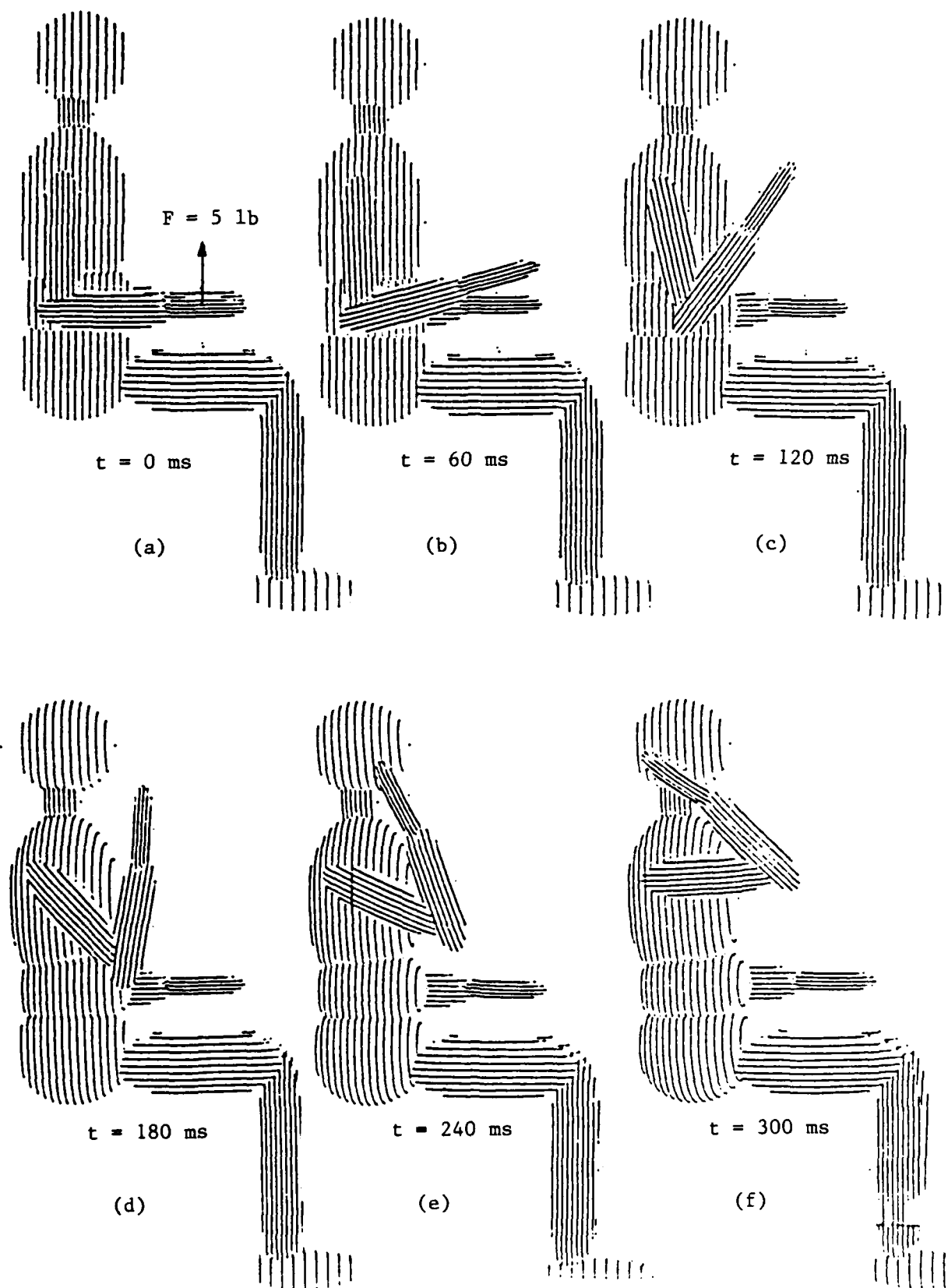


Fig. 2 ATB simulation of the right arm.



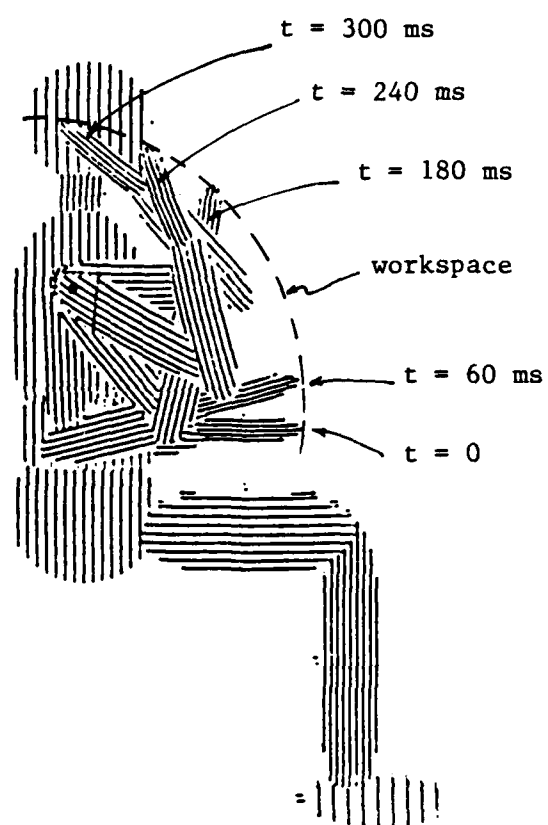


Fig. 3 Workspace of the ATB right arm with  $F = 5$  lb( $\uparrow$ )  
(Arm positions are superposed)

## V. DISCUSSION AND RECOMMENDATIONS

There exists a vast body of knowledge on the three-dimensional kinematic analysis methods addressing the behavior of robot manipulators. Numerous methods of analysis have been developed in attempting to reduce the computational complexities associated with kinematic structures representing robotic arms. Using rotation vectors and quaternion algebra, the number of arithmetic operations required for kinematic solutions can be reduced to only three or four parameters to define the relative spatial orientation of a rigid body, whereas in the coordinate transformation matrix methods we have to deal with  $3 \times 3$  matrices. Regardless of the method chosen, as we increase the number of links and joints in a kinematic chain the analysis becomes more complex and leads to huge mathematical expressions. This has motivated researchers to seek a unified theory of notations for simplification. In reference to the Robotic Telepresence Program at AAMRL and the role of the dextrous hand (DH) in this program, the kinematics of the robotic arm should be analyzed using such a unified theory of notations because the DH has numerous linkages in comparison with a common industrial manipulator.

The computation of workspace of the end-effector is important in determining the effectiveness of a robot. In view of using the ATB Model as a simulation tool in the Robotic Telepresence Program, software based on the three-dimensional kinematics methods of robotics should be developed to study the ATB Model behavior. At present the ATB Model analysis is based on the integration of equations of motion.

The ATB Model does not have a joint at the wrist. In the recommended analysis a spherical joint should be introduced at the wrist, and the reach analysis should be performed for the ATB arm to determine the workspace and its boundaries. Such an analysis will be useful in trajectory planning of the end-effector (the ATB hand).

The methods of neuromuscular control should be investigated to determine appropriate mechanisms for controlling the ATB hand. The knowledge of these mechanisms can be carried over to understand the dextrous hand behavior and to specify exoskeletal devices for control.

## REFERENCES

- Asada, H. and J.-J. E. Slotine, Robot Analysis and Control, John Wiley and Sons, New York, 1986
- Denavit, J. and R. S. Hartenberg, "A Kinematic Notation for Lower Pair Mechanisms Based on Matrices", Journal of Applied Mechanics, Vol. 22, 1985
- Fleck, J. J. and F. E. Butler, "Development of an Improved Computer Model of the Human Body and Extremity Dynamics", Report No. AMRL-TR-75-14, July 1975
- Featherstone, R. "Position and Velocity Transformations Between Robot End-Effector Coordinates and Joint Angles", Int. J. of Robotics Research, Vol. 2, No. 1, 1983
- Gupta, K. C. and B. Roth, "Design Considerations for Manipulator Work Space", ASME Journal of Mechanical Design, Vol. 104, No. 4, 1982
- Hollerbach, J. M., "Wrist-Partitioned Inverse Kinematics, Accelerations and Manipulator Dynamics", Int. J. of Robotics Research, Vol. 2, No. 4, 1983
- Koren, Yoram, Robotics for Engineers, McGraw-Hill Book Company, New York, 1986
- Kumar, A. K. and K. J. Waldron, "The Workspace of a Mechanical Manipulator", ASME Journal of Mechanical Design, Vol. 103, No. 3, 1981
- Pieper, D. L., "The Kinematics of Manipulators Under Computer Control"  
Doctoral Thesis, Stanford University, Stanford, California, 1968

Richard, P., M. Renaud, and N. Stevenson, " A Systematic Approach for Obtaining the Kinematics of Recursive Manipulators Based on Homogeneous Transformations", Robotics research, The First International Symposium, M. Brady and R. Paul, Editors, The M.I.T. Press, Cambridge, Massachusetts, 1984

Roth, B., "On the Screw Axes and Other Special Lines Associated with Spatial Displacements of a Rigid Body", J. of Engineering for Industry, February, 1967

Roth, B., "Performance Evaluation of Manipulators from Kinematics Viewpoint", National Bureau of Standards Special Publication: Performance Evaluation of Programmable Robots and Manipulators, 1975

Sugimoto, K. and J. Duffy, "Application of Linear Algebra to Screw Systems" Mechanism and Machine Theory, Vol. 17, 1982

Tsai, Y. C. and A. H. Soni, "Accessible Region and Synthesis of Robot Arms", ASME Journal of Mechanical Design, Vol. 103, No. 4, 1981

U. S. Department of Transportation - National Highway Safety Administration, "Validation of the Crash Victim Simulator, Vols. 1, 2 and 3, Final Report 1983

Woo, L. and F. Freudenstein, "Application of Line Geometry to Theoretical Kinematics and Kinematic Analysis of Mechanical Systems", Journal of Mechanisms, Vol. 5, pp. 417-460, 1970

Yuan, M. S. C. and F. Freudenstein, "Kinematic Analysis of Spatial Mechanisms by Means of Screw Coordinates, Parts 1 and 2", ASME Transactions, Series B, Vol. 93, No. 1, pp. 61-66 and pp. 67-73, 1971

1987 USAF-UES SUMMER FACULTY RESEARCH PROGRAM

GRADUATE STUDENT SUMMER SUPPORT PROGRAM

Sponsored by the

AIR FORCE OFFICE OF SCIENTIFIC RESEARCH

Conducted by the

Universal Energy Systems, Inc.

FINAL REPORT

POINTING CONTROL SYSTEMS FOR BALLOON-FLOWN INSTRUMENTS

Prepared by:	Francesco L. Bacchialoni
Academic Rank:	Associate Professor
Department and	Electrical Engineering
University	University of Lowell, Lowell, Massachusetts
Research Location:	Air Force Geophysics Laboratory, Hanscom Air Force Base, Bedford, MA 01731-5000 Aerospace Systems Division Systems Development & Verification Branch
USAF Researcher:	Russell G. Steeves
Date:	September 4, 1987
Contract No:	F49620-85-C-0013

# POINTING CONTROL SYSTEMS FOR BALLOON-FLOWN INSTRUMENTS

by

Francesco L. Bacchialoni

## ABSTRACT

This report considers the motions of a balloon-borne payload and examines in a qualitative fashion the overall requirements of pointing systems for balloon-borne scientific experiments.

General purpose support platforms are considered, and two general configurations are recommended. One is simple, of moderate accuracy and cost, the other is more complex, more accurate and considerably more expensive.

### ACKNOWLEDGMENT

The author would like to thank the Air Force Office of Scientific Research and Universal Energy Systems, Inc. for providing him with the opportunity to spend a worthwhile and interesting summer at the Air Force Geophysics Laboratory, Hanscom AFB, Massachusetts. He would like to acknowledge the Laboratory, in particular the Development and Verification Branch of the Aerospace Engineering Division for its hospitality and excellent working conditions. Finally, he would like to thank Russell G. Steeves for suggesting this area of investigation and for his guidance and collaboration.



## I. INTRODUCTION

Some of the missions that the Air Force Geophysics Lab has supported in past years, and will continue to support in coming years consist in balloon flights of scientific instruments. These flights are considerably less expensive and generally last longer than rocket flights, therefore offer unique advantages in the support of some scientific experiments. The next observation is that it appears possible to design and build some general purpose platforms, each capable of supporting different scientific experiments, in separate flights. Power, balloon controls, and telemetry are necessary on all flights, therefore they form a core of common elements present on a general purpose platform. In addition, many experiments require controlled pointing of an instrument in various directions in space. This suggests to make angular references and pointing control systems part of the support platform, and this is the subject of the present investigation.

I have been involved in control systems for many years, both in professional practice and in teaching the theory. I have worked on airborne servos for optical instruments and on the pointing system of a ground based 48" optical telescope. This background makes the present assignment a natural continuation of my previous experience.

## II. OBJECTIVES OF THE RESEARCH EFFORT

Several balloon-borne platforms have been used in the past to support scientific experiments. Some were very elaborate and expensive, others very limited in capability. The objective of this research effort consists in exploring the possibility of utilizing one or more general purpose platforms to support balloon-borne scientific experiments, and obtaining recommendations for the design of instrument pointing systems for these platforms.

## III. APPROACH

A tentative approach has been established as follows:

1. Considerations on experiments and support platforms.
2. Summary of suitable state of the art position and direction references, including cost estimates.
3. Considerations on pointing control system design, including angular references and command signals.
4. Recommendations on verification procedures.

#### IV. EXPERIMENTS AND SUPPORT PLATFORMS

From a logical point of view, the scientific experiment to be performed has to be considered first, and the support platform specifications are derived from the desired experiment. In practice it is very difficult to identify in abstract all the support needed by future experiments, but in order to consider general purpose platforms, it is necessary to find the requirements common to a vast class of experiments. As indicated earlier, power, balloon controls and telemetry are necessary in all flights, but since the related technologies are well established they have been excluded from this investigation. An additional item common to many balloon-borne experiments consists in pointing controls for the scientific instruments used on board, and this is the subject on which the present investigation is concentrated.

Pointing a scientific instrument in a certain direction requires a mechanical structure capable of rotations about some axes, and this implies different possible geometric configurations. Command angles, usually variable with time, are applied to servo systems driving the axes of rotation, so obtaining the pointing angles. Errors appear in this process: acceptable pointing errors versus time depend on the individual experiment, and it is clear that reduction of these errors means increase of system cost. It is

difficult to relate error reduction to cost increase in a precise fashion, since the cost of subsystems may change rather rapidly with the development of new technology, therefore overall engineering judgment remains the dominant criterion for setting the specifications of a general purpose support platform.

A balloon-borne payload is subject to various motions caused by the flight. Typical motions are [5]:

- Pendulum-type oscillations, with amplitude from about 5 deg. during ascent to about 10 arcmin. and period 15 sec. when floating at high altitude.
- Rotation, random, with angular velocity up to 0.25 rpm.
- Vertical bounce, random, amplitude up to 1000 ft, period several minutes.

It is clear that pointing errors possibly caused by these motions must be considered. The system designer must also keep in mind these other physical conditions:

- Atmospheric pressure: almost zero.
- Ambient temperature: from -65 to +75 deg. C.
- High energy radiation (cosmic rays, etc.).

## V. POSITION AND DIRECTION REFERENCES

The position of a free flying balloon is usually important for the experiment, and in some case it must also be used to calculate in real time the instrument pointing

angles. It can be obtained using several different methods, some of which are listed here, with a summary of their characteristics.

1. Ground radar tracking:

- Accuracy is high.
- Balloon coordinates are available at the tracking facility: if needed on the balloon, they have to be telemetered.
- No need of computation on the balloon platform.
- Distance limited approximately to the visible horizon: for a balloon flying at 30 Km (100,000 ft.) and a sea level radar, max. distance is approximately 437 Km.
- Cost is variable, depending on the availability of a ground tracker near the launch site.

2. Global Positioning System (GPS):

- Position in three dimensions, fully available in 1989, with 50 m maximum error (Collins Navcore 1).
- Velocity within 0.5 m/sec.
- Time within 250 nanosec.
- Outputs updated once a second.
- Receiver on board of the platform.
- Position, velocity and time can be utilized on board, recorded if necessary and/or telemetered to ground.
- Cost: \$ 20,000 (Collins Navcore 1).

3. Inertial Navigation System (INS):

- Combined with GPS (Honeywell Special Mission Management System) gives good accuracy position, equal to that given by GPS.
- Excellent for attitude measurement: see further ahead.
- Cost: \$ 100,000 for commercial units, hardware alone.

4. Commercial Distance Measuring Equipment (DME):

- In the past, a method utilizing DME signals has been designed. It appears inferior to the GPS system.

5. LORAN:

- Less accurate and convenient than GPS.

6. Omega:

- Less accurate and convenient than GPS.

Directional reference may be obtained in several different ways. Here are a few.

1. Local vertical established by gravity:

- Subject to errors caused by pendulum motion, of the order of 5 deg. during ascent and 10 arcmin. during flight at altitude.

## 2. Azimuth by magnetometers:

- Only the horizontal component of the earth magnetic field should be measured.
- Requires a precise knowledge of the earth magnetic field in the region of the flight.
- Does not work near the magnetic poles.
- Moderately accurate: errors of about 0.35 degrees.
- Sensitive to magnetic fields produced on the platform.
- Analog or digital signal format.
- Cost: a few thousand dollars.

## 3. Gyroscopes.

In reference 3, laser gyros are analyzed and compared with mechanical gyros and fiber-optic gyros. In addition, star trackers are briefly examined. AFGL mission requirements are there divided into two general areas, differentiated as having high vs. medium level of accuracy and stability. In previous AFGL missions (SPICE, IRBS) mechanical rather than laser gyros had to be adopted since optical gyros were not sufficiently developed. The state of the art of optical gyros is much more advanced to day, and their specs continue to improve, therefore they should be carefully considered at the actual design time. Typical drift is about 0.02 deg/hr. Power absorption is still rather high, of the order of 150 W. The price of a commercial 3-axis ring laser gyro INS is about \$ 100,000,

similar to the price of a tuned-rotor mechanical gyro system. In addition, the cost of integrating the gyro into a complete pointing system must be added, and this is high and difficult to estimate.

Fiber-optic gyros are closing in on the sensitivity and low drift of good quality mechanical gyros (Dynamically-Tuned Rate Gyros). At least two moderate performance models are available on the market (Standard Elektrik Lorenz AG, West Germany, price of the smaller unit approx. \$ 18,000). Honeywell is developing its products and expects practical devices in about two years. Reliability will be high, errors comparable to those of mechanical gyros of moderate performance (drift: 0.1 deg/hr). Estimated future price is \$ 3,000 per axis.

#### 4. Sun Trackers.

- Moderately accurate: typical maximum error 5 arcmin.
- Operate only when the sun is visible.
- Require position, precise time reference and computation to obtain absolute reference.
- Cost: estimated at \$ 30,000 for hardware.

#### 5. Star Trackers.

- Very accurate: typical maximum error 2 arcsec.
- Operate only when the stars are visible.
- Require position, precise time reference and computation



to obtain absolute reference.

- Cost: estimated at \$ 200.000 for hardware.

## VI. POINTING CONTROL SYSTEMS

Several different possible geometries can be used to align a scientific instrument with a target. A typical configuration has three axes, azimuth, elevation and roll. This geometry causes cross-coupling at high values of elevation and roll, which may be a difficulty. If necessary, corrections can be applied where needed, but otherwise the three servo systems driving the instrument axes can be considered independent.

Feedback loops are necessary to obtain reliable operation in the presence of disturbances, and it is desirable for simplicity of analysis and design to have for each axis an independent loop, with at most the classical "secant correction" as a decoupling tool. Each of these loops must be analyzed in its entirety, including sensors, controller hardware and software, actuator, load inertia and friction, and any additional hardware which may affect the loop performance. Control systems theory, classical and modern, offers analysis and design methods for linear and non-linear systems.

Assuming linearity, in each axis a feedback system type 1 or type 2 (one or two open-loop time integrations) should

be used to provide zero steady-state position error to a command angle constant in time. Reduction of the effects of disturbance torques is another important point to keep in mind at the design stage: angular accelerometers may be added for this purpose. It is generally useful to introduce a "rate loop" in each axis: this allows the application of velocity limits, which prevent excessive speed and potential damage to the instruments. In addition, suitable selection of the velocity limits may be used to obtain minimum-time motion when a large angle step command is applied, with consequent saturation [2].

In the classical linear design, in each axis a controller (analog or digital) calculates the angular error (difference between command and measured angles) and from this error the signal to drive the corresponding motor. A more elaborate controller can be designed applying "state feedback".

A "limit cycle", that is a steady-state oscillation of small amplitude, may appear in some feedback loops containing digital devices, when a command angle constant in time is applied. This may be acceptable if the amplitude of the oscillation is small. Typical example: a system where the driving motor is a d.c. motor (analog) and the pointing angle is measured by means of a digital encoder. Here the limit cycling can be eliminated by using analog format for the angle measurement and the calculations to

obtain the error and the signal driving the motor amplifier. The command angle can still be telemetered to the platform in digital format but it must be locally converted to analog before the evaluation of the error.

In general, synchros or precision potentiometers may be used for angular measurements if analog format is desired, or direct drive digital angular encoders if digital format is preferred. Motors are preferably (engineering judgment) d.c. motors, which are analog devices, and the power amplifiers driving them require analog input signals.

Selection between the alternatives of analog or digital design is rather informally done by engineering judgment. For example, if the directional references supply analog signals, it is usually considered simpler to have analog position loops rather than digital ones.

## VII. COMMAND AND FEEDBACK LOOP SIGNALS

The angular command signals for an experiment usually vary with time, making up "angular trajectories". Depending on the experiment, these trajectories may be entirely precalculated, stored and later activated, or they may involve real time calculations, possibly taking into account the balloon position coordinates, which change with its motions, including vertical bounce.

Digital and analog signals are probably both present in the feedback loops, since command signals transmitted from the ground are almost always in digital format, while the angular signals on board may be analog or digital. The signals supplied by the directional reference sensors (magnetometers, gyros, sun-trackers, star trackers) derive from analog physical quantities, but as a result of the subsystem manufacturer's preference they may be available to the system designer in either analog or digital format (or both). This is not a difficulty, since digital to analog and analog to digital converters can easily be used where necessary.

Real time calculations of the command trajectories require use of a computer, which may be located on the balloon platform or on the ground. Each of these two choices has its own advantages and disadvantages.

If the computer is on the platform, the payload has increased complexity, but only a few commands are to be telemetered for control or override of the computer.

If the computer is located on the ground, the payload has no increased complexity, but more telemetry messages are needed for the real time control operations, and this may be a difficulty.

There is no way to make a general recommendation in favor of one solution or the other, therefore their trade off must be carefully considered case by case.

## VIII. MECHANICAL CONFIGURATIONS

Assume three axes: azimuth, elevation and roll.

Some possible mechanical system configurations are considered here.

1. In one configuration the platform is suspended by means of a low friction spherical bearing, located at the center of mass, with the result that the platform in flight does not rotate when the balloon rotates or is accelerated in any direction. Various disturbance torques may still be acting on the platform, therefore there is need of three axis stabilization, using inertial references. If a three axis INS package is attached to the instrument to be pointed, no additional angle measuring device is needed: the attitude signals from the INS can be sent to the controllers driving the three corresponding motors. Appropriate reaction masses must be included in this configuration. A Ring Laser Gyro Inertial Navigation System, possibly with GPS connected to it (Honeywell) is a good attitude (and position) sensor for this system. Cost of this system, including the cost of the INS plus software and integration, is high, as indicated earlier. The platform built by VISIDYNE and that described in references 4 and 6 have a similar configuration.

2. Another possible configuration consists in a mechanical frame attached to the balloon cable by means of a low friction thrust bearing, to isolate the platform from the balloon rotation. The platform, in flight without disturbances is vertically oriented by the earth gravity, within a few arcminutes. This configuration offers vertical and horizontal references naturally available, thus saving the complexity and cost of one or two control loops.

Undesirable deflections may appear, though, when disturbances are applied to the platform, therefore this possibility should be carefully evaluated. Elevation and roll angles can be measured from the vertical or horizontal reference, and related motors move the scientific instrument as needed. Possibly mechanical counterbalances can be built into the elevation and roll drives to avoid inertial disturbances. In addition to the natural vertical, only an azimuth reference subsystem is needed. The azimuth motor rotates the instrument package using an appropriate reaction mass. References 1 and 7 describe systems having configurations of this type.

3. A third configuration is like the previous one, with the same elevation and roll subsystems. The difference consists in utilizing the balloon as reaction mass for azimuth rotation. This requires a torsionally stiff

connection between the stationary part of the azimuth bearing and the balloon, technique that has been practically applied with success (unpublished references).

#### IX. VERIFICATION PROCEDURES

- A test chamber for high altitude and low temperature tests requires a major construction project, extremely expensive. Chambers of this type exist at other facilities and can be used by AFGL. Construction of another one is not recommended at this time.
- For attitude control system tests, the platform may be suspended from a low friction azimuth bearing (air, pressurized oil, magnetic or servo driven), thus approximating the free flying environment.
- If the balloon is used as a reaction mass for the azimuth rotation, a corresponding inertia must be used in the test rig, suspended from the low friction bearing. The inertia and the bearing simulate the free flying balloon.
- Commands for static pointing tests may be sent to the platform through telemetry.
- Static pointing angles may be measured (within a few mrad.) using a portable low power laser installed on the platform and acting as a pointer on a screen set at a proper distance.
- Dynamic pointing may be tested by commanding angular test

trajectories stored on board or sent through telemetry, and analyzing the resultant error trajectories (differences between commanded and measured angles).

- Static angular errors or dynamic error trajectories may be computed on the platform, recorded there or telemetered to the ground control center, where can be recorded for analysis.
- Smoothness of motion may be measured using angular accelerometers, their signals being transmitted through additional telemetry to the control center.

#### X. RECOMMENDATIONS

The following two recommendations are presented, based on engineering judgment:

1. Two different mechanical structures may be initially considered for development: platform A and platform B.

##### Platform A:

- Vertical obtained from gravity.
- Azimuth from magnetometers.
- Analog control loops.
- Cost: relatively low.
- See references 1 and 7.



Platform B:

- Inertial Navigation System.
- Digital control loops.
- Cost: relatively high.
- See references 4 and 6.

2. A study should be conducted on the relative advantages of digital versus analog subsystems, components and signal processing for balloon-borne pointing control systems.

## REFERENCES

1. Anderson, G.A., "Design for Orientation of Balloon-Borne Equipment", School of Physics and Astronomy, University of Minnesota, June 1967, Defense Documentation Center Report AD 658 529.
2. Bacchialoni, F.L., "Optimum Synchronization of Some Saturated Control Systems", IEEE Trans. on Automatic Control, Vol 14, #2, April 1969, pp. 198-199.
3. Cassell, C.R., "Laser Gyro Attitude Control Systems Feasibility Study", AFGL/LCE Report, 1986.
4. Haser, L.N., "Dynamics and Attitude Control of the 1-meter IR Telescope Balloon Gondola", Proceedings, Ninth AFGL Scientific Balloon Symposium, 1976, AFGL-TR-76-0306, pp. 263-274.
5. Rice, C.L., "Summary of Payload Motions", AFGL table to be published.
6. Stoecker, J.E., "A Three Axes Stabilized Balloon-Borne 1-meter Telescope for High Resolution Infrared Spectroscopy", Proceedings, Ninth AFGL Scientific Balloon Symposium, 1976, AFGL-TR-76-0306, pp. 275-284.
7. Watts, A.C., "Instrumentation for a Balloon-Borne Gamma Ray Astronomy Experiment", Proceedings, Ninth AFGL Scientific Balloon Symposium, 1976, AFGL-TR-76-0306, pp. 215-234.

**1987 USAF-UES Summer Faculty Research Program**  
**Graduate Student Summer Support Program**

Sponsored by the  
Air Force Office of Scientific Research  
Conducted by the  
Universal Energy Systems, Inc.

**FINAL REPORT**

**Sustained Delivery of Volatile Chemicals By Means of Ceramics**

Prepared by:	<b>P.K. Bajpai, Ph.D and Deborah E. Hollenbach</b>
Academic Rank:	Professor and M.S. Graduate Student
Department and	Biology Department
University:	University of Dayton
Research Location:	AAMRL/TH Wright Patterson AFB Dayton, OH 45433
USAF Researcher:	<b>Dr. M.E. Andersen</b>
Date:	September 30, 1987
Contract No.:	F49620-85-C-0013

Sustained Delivery of Volatile Chemicals  
By Means of Ceramics

by

Praphulla K. Bajpai and Deborah E. Hollenbach

Abstract

A simple ceramic delivery system was developed for studying the toxicity of chemicals such as 1,1,1-trichloroethane (TCE) in animals. 1,1,1-trichloroethane was determined by gas chromatography. Use of glass tube inserts and Silicone<sup>®</sup> adhesive sealant for sealing the ceramic cavity provided the best results. Storing of TCE (45 mg) in glass tubes within the ceramic cavity allowed retention and delivery rate of TCE at 3595 ug/hr for eight hours in vitro. Reservoir modification of the glass tube-ceramic device to store 259 mg TCE, resulted in a sustained delivery rate of TCE (624 ug/hr) for 11 days in vitro. Analysis of hexane extracts of blood obtained from rats implanted with the glass tube-ceramic device containing 45 mg TCE, indicated that blood TCE was constant for 20 hours. Analysis of the chamber air housing a rat implanted with a similar device indicated that the level of TCE remained sustained at 1344 ug/hr for two hours. The data obtained in this investigation suggests that the ceramic system can be modified to deliver volatile chemicals in a sustained manner for studying the pharmacokinetics and toxicity of these solvents.

### Acknowledgements

We wish to thank the Air Force Toxic Hazards Division of the Armstrong Aerospace Medical Research Laboratory at Wright Patterson Air Force Base for the sponsorship of this research. We also wish to thank the Universal energy Systems for the sponsorship of this program.

Acknowledgements are also due to the Department of Biology and Glass Blowing Laboratory of University of Dayton, for providing the ceramics, glass tubes and reservoirs needed for this investigation.

Specifically we wish to thank SSgt. Greg Cason for teaching us how to use the various gas chromatographs and technical assistance throughout these investigations. We sincerely appreciate the time, technical support, and expertise provided by Mr. Michael Gargas. We are indebted to Dr. R. Drawbaugh for providing moral support, encouragement and constructive suggestions, and to Dr. David R. Mattie for bringing to Dr. Andersen's attention the expertise available at The University of Dayton in Drug Delivery Systems. Finally we want to thank Dr. M. E. Andersen for suggesting the problem, giving us the opportunity to work at the Toxic Hazards Laboratory under UES Program, directing us in our endeavours, and providing the facilities and personnel to successfully carry out the proposed studies.

## I. INTRODUCTION:

1,1,1-Trichloroethane (TCE) is commonly used as a dry-cleaning agent and as a cleansing solvent for electrical machinery and plastics. It is also present as a contaminant in drinking water. Toxicity studies of volatile hydrocarbons at present are performed by exposing laboratory animals to the compound by either oral dosage or inhalation. Oral dosages utilize either gavage (in mineral or vegetable oil) or microencapsulation using geletin-sorbitol (Melnick, 1987). Inhalation exposures are carried out in inhalation chambers by bubbling the chemical into the airflow lines going to the chamber (Gargas, 1986). The latter procedure is currently being used at the Toxic Hazards Laboratory of WPAFB.

The principal investigator (P. K. Bajpai, B.V.Sc., M.V.Sc., M.Sc., Ph.D) developed a ceramic delivery system in 1979 (Bajpai, 1979), and since then he and his graduate students have used the sustained release ceramic delivery systems to deliver enzymes, dyes, phenolics, polypeptides, proteins (Bajpai, 1985), and steroids in vitro and in vivo (Benghuzzi, 1986). In the 1987 Summer Faculty Research Program (SFRP) and Graduate Student Summer Support Program (GSSSP), we attempted to develop an implantable device that would deliver a volatile, chlorinated hydrocarbon (1,1,1-trichloroethane) in a sustained manner for four to eight hour durations. Such a delivery system could simplify studies of the kinetics and toxicity of these solvents.

## II. OBJECTIVES OF THE RESEARCH EFFORT:

- a. To develop a sustained delivery device for delivering 1,1,1-trichloroethane (TCE) for durations of four to eight hours either in vitro or directly in experimental animals.
- b. By the end of ten week duration we were also requested to develop a system for delivering volatile chemicals for two to three month durations in animals for studying the effects of these chemicals on neurological behavior.

## III. MATERIALS AND METHODS:

The development of a sustained delivery system for volatile chemicals was conducted in two phases to minimize the use of experimental animals. In phase I the loss of chemical from ceramic experimental devices was examined in an in vitro free air flowing environment. In phase II the ceramic system which appeared to fulfill the desired objectives in the in vitro environments was investigated in animals.

### a. Chemical.

High purity 1,1,1-trichloroethane (99.9% pure) was obtained from the Aldrich Chemical Company (Milwaukee, WI). All experiments in this study were conducted with TCE blended with 3% mineral oil.

### b. Fabrication of Non-Impregnated and PLA-Impregnated ALCAP Ceramic Delivery Devices.

Aluminum-calcium-phosphorus oxide (ALCAP) ceramic capsules (O.D.=0.75, I.D.=0.45, L=1.20 cm, Wt=0.92 g and density of 2.10 g/cm<sup>3</sup>) were fabricated by thorough mixing of 50 g aluminum oxide, 34 g calcium

oxide and 16 g phosphorus pentoxide powders, and calcining the mixture at 1315<sup>0</sup> C for 12 hours. The calcined powders were crushed to the appropriate particle size (<38 um) and molded into a cylindrical shape by means of pressure applied to a die. The ceramic cylinders were sintered at 1350-1450<sup>0</sup> C for 30-36 hours to increase the density and mechanical strength of the ceramic. Some ceramics were also impregnated with polylactic acid (PLA) in chloroform (1:50) by the procedure of Benghuzzi (1986). Typically, PLA has been used to impregnate the ALCAP in order to slow down the release of peptides and steroids. The PLA works by decreasing the size of the pores in the ceramic (Benghuzzi 1986).

For the preliminary work and the majority of the in vitro experiments conducted during this study, the ends of the ALCAP were sealed with a 2:1 cement mixture made from ALCAP powder and alpha-ketoglutaric acid (Bajpai, 1987). The acid-ceramic powder (ACP) sealed ends were then coated with Silastic<sup>®</sup> Medical Adhesive (Dow Corning, Midland, MI).

#### c. Glass Tube Inserts and Reservoirs.

One cm by four mm glass tubes with one end having an opening of two mm as well as modifications of the glass tube to include reservoirs were fabricated by the glass blowing laboratory of the University of Dayton.

#### d. In Vitro Studies .

##### I. Standardization of the Gas Chromatograph.

A Hewlett Packard 5890 Gas Chromatograph (GC) containing a flame ionization detector (FID) and a 10 ft. 10% SE-30, 80/100 Supelcoport<sup>®</sup> column was standardized in the 10-100 parts per million (PPM) range using 20 liter Mylar<sup>®</sup> bags. The oven temperature was maintained at



100° C, the injector temperature at 125° C, the detector temperature at 300° C, and the nitrogen carrier gas was maintained at a flow rate of 25 ml/min. A Hewlett Packard 3393A Integrator and a Hewlett Packard 19405A Sampler/ Event Control Module were used in conjunction with the gas chromatograph for analysis of the one ml samples injected into the GC at each sampling time.

## II. Analysis of 1, 1, 1-TCE.

For conducting the in vitro experiments, each ALCAP ceramic capsule was suspended inside a 108 ml glass gas injection chamber on a cotton string. The chamber was connected to a reciprocating electromagnetic piston air pump which was connected to the gas chromatograph. A constant air flow of 120 ml/min was maintained through the glass chamber by the air pump. The HP Sampler/Event Control Module was utilized to provide automatic sampling of the glass chamber. In order to determine the concentration of TCE released by the delivery system in the gas chamber the control module was programmed to automatically sample the contents of the gas chamber by the GC.

### e. Animal Studies.

The amount of TCE present in the blood and exhaled breath were monitored in rats implanted with ceramics containing 45 mg of TCE in 3% mineral oil.

#### I. Catheterization.

For monitoring TCE release in rat blood, anesthetized Fisher 344 male rats (Charles River, MA) weighing 350 g were catheterized with 22 G, 8 inch Deseret Radiopaque cutdown catheters (Deseret Co., Sandy Utah).

The catheter tip was passed through the left jugular vein to the right

atrium and the sampling end was passed under the skin to the back of the neck. A velcro vest was used to protect the sampling port. Ketamine-xylazine (0.1ml/kg body weight) prepared in the laboratory was used for anesthesia.

## II. Implantation of Capsules.

Thirty-five ml of Penthrane<sup>®</sup> (methoxyflurane, Abbott Laboratory, Chicago, IL) was used to saturate 10 guaze squares in a nine liter glass chamber. The rat was placed in the chamber for 15 minutes and removed for implantation of the capsule. The exposure to Penthrane<sup>®</sup> allowed the rat to remain under anesthesia for six minutes. The capsule to be implanted was prepared while the rat was being exposed to Penthrane<sup>®</sup>. A two cm incision was made in the abdomen of the anesthetized rat with scissors and the capsule inserted into the peritoneal cavity. The incision was closed with two to three stainless steel wound clips.

## III. Blood Analysis Studies.

Rats catheterized for 24 hours were implanted with an ALCAP capsule containing 45 mg TCE. Following implantation blood samples were taken at 15, 30, 45, 60, 90, 120 minutes and then at one hour intervals for a total of six hours. Additional blood samples were taken at 24, 25, 27, 29, and 48 hours. A sample of 100 ul of blood from each collection was placed in one ml of hexane and allowed to equilibrate for one hour. The amount of TCE extracted in the hexane was determined by GC using an electron capture detector (ECD). Standards of TCE (0.01 to 1 PPM) in blood were prepared for constructing the standard curve. The GC with ECD contained a 10 ft 10% SE-30, 80/100 Supelcoport<sup>®</sup> column and the

operating conditions were: oven temperature of 70<sup>0</sup> C, injector temperature of 125<sup>0</sup> C, detector temperature of 300<sup>0</sup> C, and an argon : methane (95 :5) gas flow rate of 25 ml/min. One ul of the hexane layer was analyzed by GC to detect TCE.

#### IV. Exhaled Breath Studies.

Three 230 g Fisher 344 male rats (Charles River, MA) were used for the exhaled breath experiments. The chemical concentration in the exhaled breath was analysed by GC, in one case using ECD, and in the other two cases, using FID. For ECD use the GC was standardized over a range of 0.001 to 1 PPM while it was standardized over a 0.01 to 10 PPM range for FID. The TCE standards were made up in twenty liter Mylar<sup>®</sup> bags. A 10 ft 10% SE-30, 80/100 Supelcoport<sup>®</sup> column was used with the following operating conditions: oven temperature 100<sup>0</sup> C, injector temperature 125<sup>0</sup> C, detector temperature 300<sup>0</sup> C, argon:methane (95:5) gas flow rate of 25 ml/min for ECD and nitrogen flow rate of 25 ml/min for FID.

Following implantation of a TCE containing ALCAP, the rat was placed in a 2.5 liter glass chamber modified to provide an air flow of 120 ml/min. A sampling port was inserted in the air outflow line in order to obtain air samples for analysis. Air samples of 100 ul were taken at appropriate intervals for a duration of 24 hours.

#### IV. RESULTS AND DISCUSSION:

##### a. In vitro Studies

- I. Delivery by Non-Impregnated and  
PLA-Impregnated Ceramics.

Preliminary experimental work showed that the TCE was lost from porous ALCAP ceramics in about two hours. Neither the PLA impregnation or a coating of Silastic® were able to slow the diffusion of TCE from the ceramic capsules. It was obvious that inclusion of a nonporous container within the ceramic was necessary to contain the liquid chemical.

## II. Delivery by Glass Tube Modified Ceramics.

The glass tubes were filled with 45 mg of TCE in 3% mineral oil, and the opening of the glass tube was sealed with ACP cement and the glass tube inserted into the ALCAP ceramic. The ceramic was then sealed with ACP cement and Silastic®. This particular modification resulted in a sustained delivery of TCE for 90 minutes. In subsequent experiments removal of ACP cement plug from the glass tube resulted in a six hour sustained release of TCE with a subsequent air borne delivery rate of 7200 ug/hr.

Since the removal of ACP cement from the glass tube resulted in a sustained delivery of TCE, the ACP cement was removed completely from the ceramic delivery systems. Silastic® was used to cover both ends of the ALCAP and allowed to dry overnight. TCE (45 mg) in 3% mineral oil was injected through the silastic seal into the glass tube within the ceramic with a Hamilton syringe. The latter modification resulted in a sustained release to give an air borne delivery rate of 3595 ug/hr of TCE for eight hours (Figure 1).

## III. Delivery by Glass Tube and Reservior Modified Ceramics.

Further modification of the glass tube-ceramic to accomodate 259 mg of

TCE by attaching a reservoir to the glass tube resulted in the sustained delivery rate of 624 ug/hr TCE for 11 days (Figure 2).

b. Blood Analysis Studies in Animals.

For these studies catheterized rats were implanted with TCE (45 mg) containing glass tube-ceramic capsules sealed with ACP cement and Silastic®. The blood profile of these rats showed a progressively increasing content of TCE in the blood for the first four hours. The amount of TCE in the blood remained relatively steady for the next two hours and ranged between 0.7 and 1 ug/ml. A similar pattern of TCE release was observed at 24 hours and the concentration again ranged between 0.7 and 1 ug/ml (Figure. 3). However, after 48 hours the concentration of TCE in the blood had decreased significantly to 0.009 ug/ml. It was concluded that the ALCAP ceramic delivery system did maintain a constant release rate in the body.

c. Exhaled Breath Studies in Animals.

The first exhaled breath trial was conducted using a GC with ECD to analyze the concentration of TCE. The delivery rate of TCE in the exhaled breath in chamber air increased with time and then leveled off at slightly above 1431 ug/hr. Thereafter the amounts of TCE in exhaled breath continued to increase at a slow rate for the entire duration (six hours) of the monitoring period on that day. On resumption of monitoring on the next morning the amount of TCE in exhaled breath decreased gradually. Since the ECD standard curve was not linear beyond 1 PPM TCE, the values obtained could not be considered absolute. Hence further trials were conducted using FID and the standards were prepared over a larger range (0.01 to 10 PPM) of TCE. During the first

FID trial, a sustained delivery rate was not reached during the first day of monitoring. On resumption of monitoring after 22 hours, the delivery rate of TCE had started to decline. In the final exhaled breath trial the delivery rate of TCE exhaled by the rat was monitored continuously for 18 hours. The data obtained showed that the release rate of TCE in the exhaled breath increased for eight hours after which a sustained release for two hours was observed. Thereafter the amount of TCE in the exhaled breath decreased progressively for the remainder of the monitoring period (Figure 4).

The in vivo exhaled breath trials did not give the sustained concentration levels that had been observed in the in vitro and blood studies. Since the inner cavity accomodating the glass tube was enlarged by reaming the ceramic with a file, several factors may have been responsible for the discrepancy in the results. The ALCAP ceramic may have cracked or it may have not had the same density, porosity, or thickness as the previous ones. It is also possible that the diameter of the openings of the hand made glass tubes were not the same. These factors should be further examined to determine if they are significant. If the latter were responsible for the above variations, elimination of these variables should give reproducible results.

#### V. CONCLUSION:

A major goal of this summer's work at WPAFB was to develop a delivery system that was capable of delivering volatile hydrocarbons in a sustained manner for a period of four to eight hours. The delivery device was to be of an easily implantable nature. Even though there was not enough time to repeat the experiments for obtaining a statistically analyzable data the basic goal of fabricating such a

device was accomplished. The final in vitro modified ALCAP ceramic model (Figure 1) shows that a sustained delivery rate of 3595 ug/hr TCE can be achieved in the glass chamber. With the latter system a blood concentration of over 1 ug/ml was achieved on implantation in rats and an in vivo gas outflow of 1344 ug/hr.

The small size of the ALCAP ceramic delivery system is advantageous, since it can be implanted easily in an animal, either intraperitoneally or subcutaneously. The present model containing 45 mg TCE is sufficient for short term exposures of up to 18 hours. The reservoir modification which was only one cm longer, was capable of holding 259 mg of TCE, and delivering TCE in a sustained manner at the rate of 624 ug/hr for 11 days in vitro. Further modifications of the reservoir system resulted in the development of a refillable device capable of holding 2 g and 2.7 g of TCE. The latter modification provides a mechanism for delivering volatile chemicals in a sustained manner and the opportunity for studying the toxicity and behavior of the animal for much longer periods of time.

#### VI. RECOMMENDATIONS:

Although the basic ideas and principles of fabricating a usable device for delivering volatile hydrocarbons were established, several factors have to be examined and the device modified accordingly. With the aid of mathematical modelling, the exact size of the opening of the one cm long glass tube has to be established as well as the exact dimensions, and density of the ALCAP ceramics have to be established.

Modifications of the ceramic delivery system consisting of small and large refillable glass reservoirs may fulfill the need for long term

delivery in animals and studying the toxic effect of TCE and similar substances.

## VII. REFERENCES:

1. Bajpai, P.K. ALCAP Ceramics in Drug Delivery. Amer. Chem. Soc., Polymer Preprints. 1985, Vol. 26(2), p. 203.
2. Bajpai, P.K. Surgical Cements. 1987, Patent Δ 4668295. USA.
3. Bajpai, P.K. and G.A. Graves, Jr. Porous Ceramic Carriers for Controlled Release of Proteins, Polypeptide Hormones and Other Substances Within Human and/or Mammalian Species. 1979, Patent Δ 4218255. USA.
4. Benghuzzi, H.A. and P.K. Bajpai. "Effect of Polylactic acid impregnation and variation of aqueous ethanol concentration on the in vitro delivery of testosterone by ALCAP ceramics", Biomedical Engineering V Recent Developments. Proceedings of the Fifth Southern Biomedical Engineering Conference. Shreveport, Louisiana. October 24-25, 1986. S. Saha (editor) Pergamon Press, New York, NY., 1986, pp. 482-485.
5. Gargas, M.L., M.E. Andersen and H.J. Clewell III. Physiologically Based Simulation Approach for Determining Metabolic Constants from Gas Uptake Data. Toxicology and Applied Pharmacology. 1986, Vol. 86, pp. 341-352.
6. Melnick, R.L., et. al., Application of Microencapsulation for Toxicology studies. II. Toxicity of Microencapsulated Trichloroethylene in Fischer 344 rats. Fund. & Applied Toxicol. 1986. Vol. 8, pp. 432-442.



# GLASS TUBE INSERT DELIVERY PROFILE SILASTIC ONLY

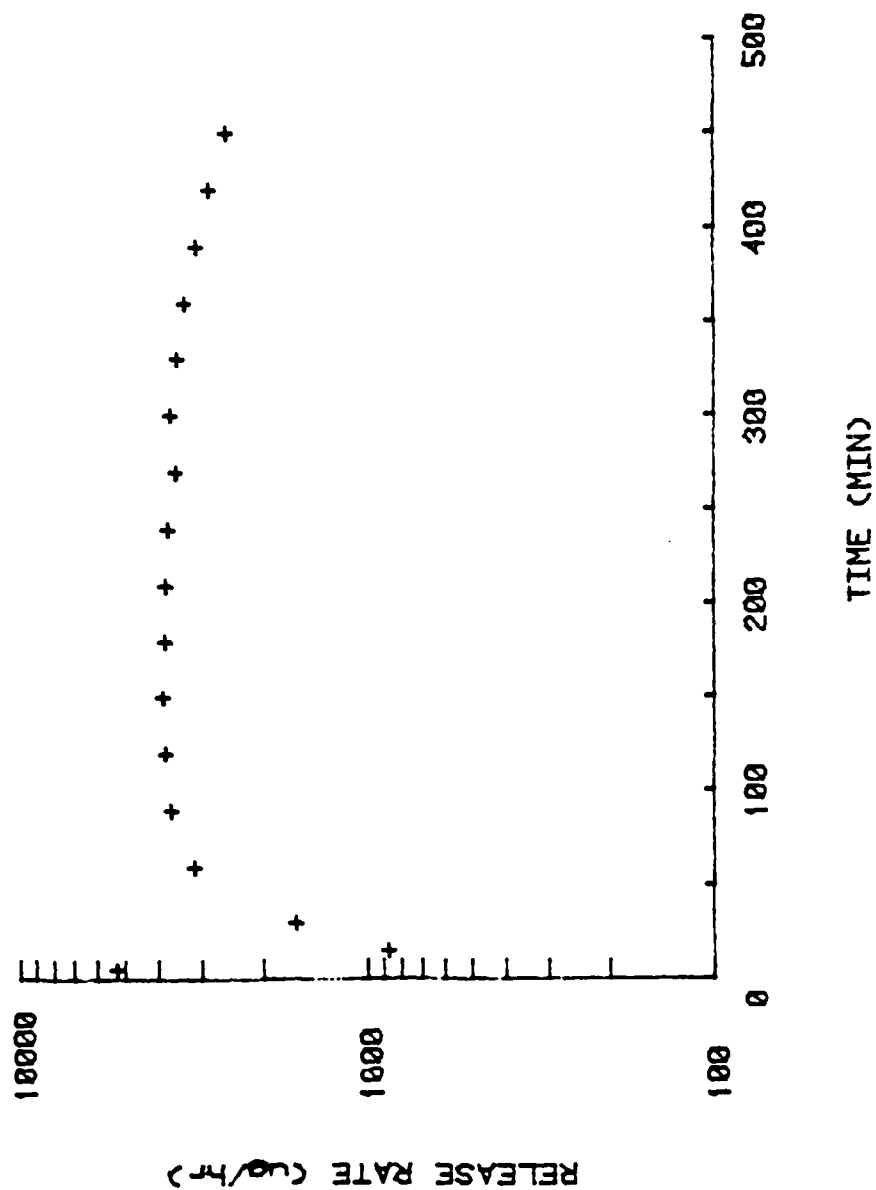


Figure 1. Effect of modifying the ALCAP ceramic delivery system (sealed with Silastic) with a non sealed non-porous glass tube insert on the delivery of 45 mg of 1,1,1-Trichloroethane (TCE), in an in vitro environment for eight hours. Release rates are approximations for non-linear regions.

# GLASS RESERVIOR CERAMIC DELIVERY PROFILE

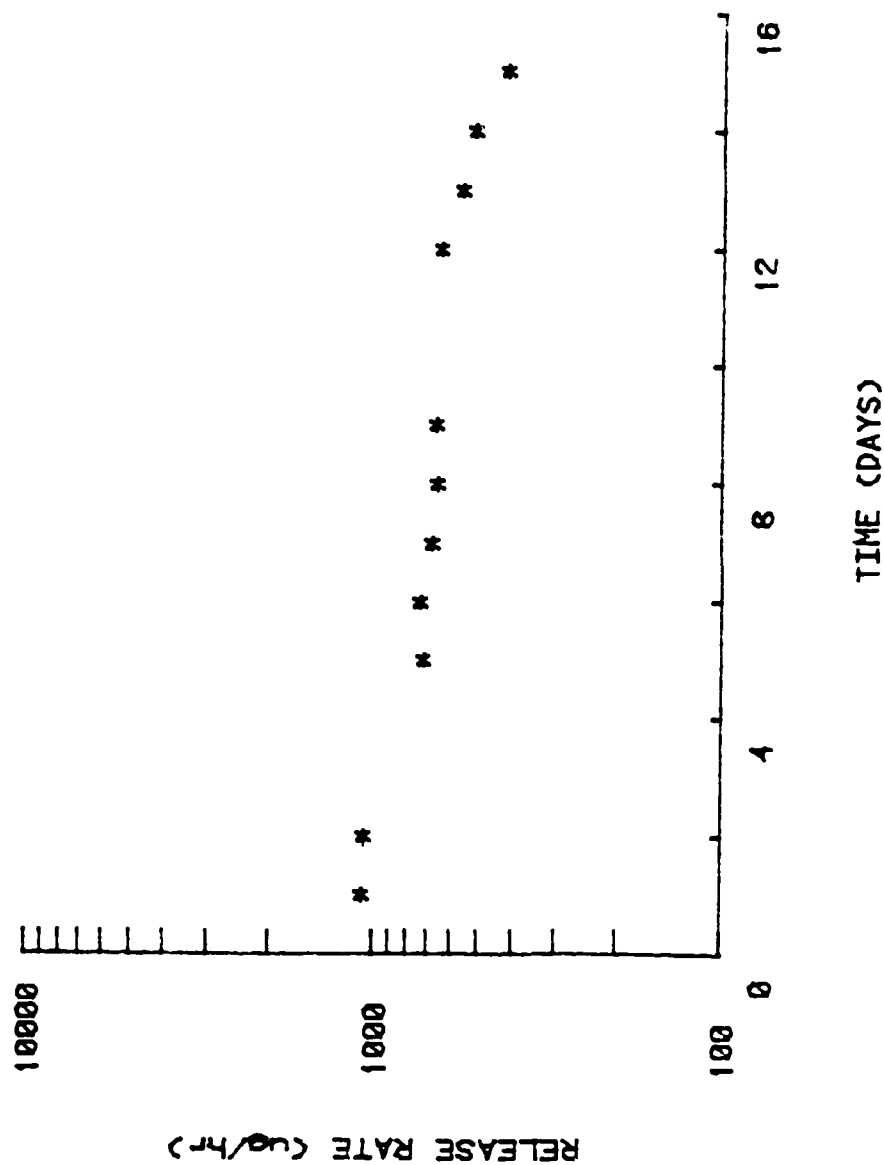


Figure 2. Effect of modifying the ALCAP ceramic delivery system (sealed with Silastic®) with a non sealed non-porous glass tube insert (having a reservoir at the blind end) on the delivery of 259 mg of 1,1,1-Trichloroethane (TCE), in an in vitro environment for 11 days.

# 1,1,1-TRICHLOROETHANE CONCENTRATION IN BLOOD

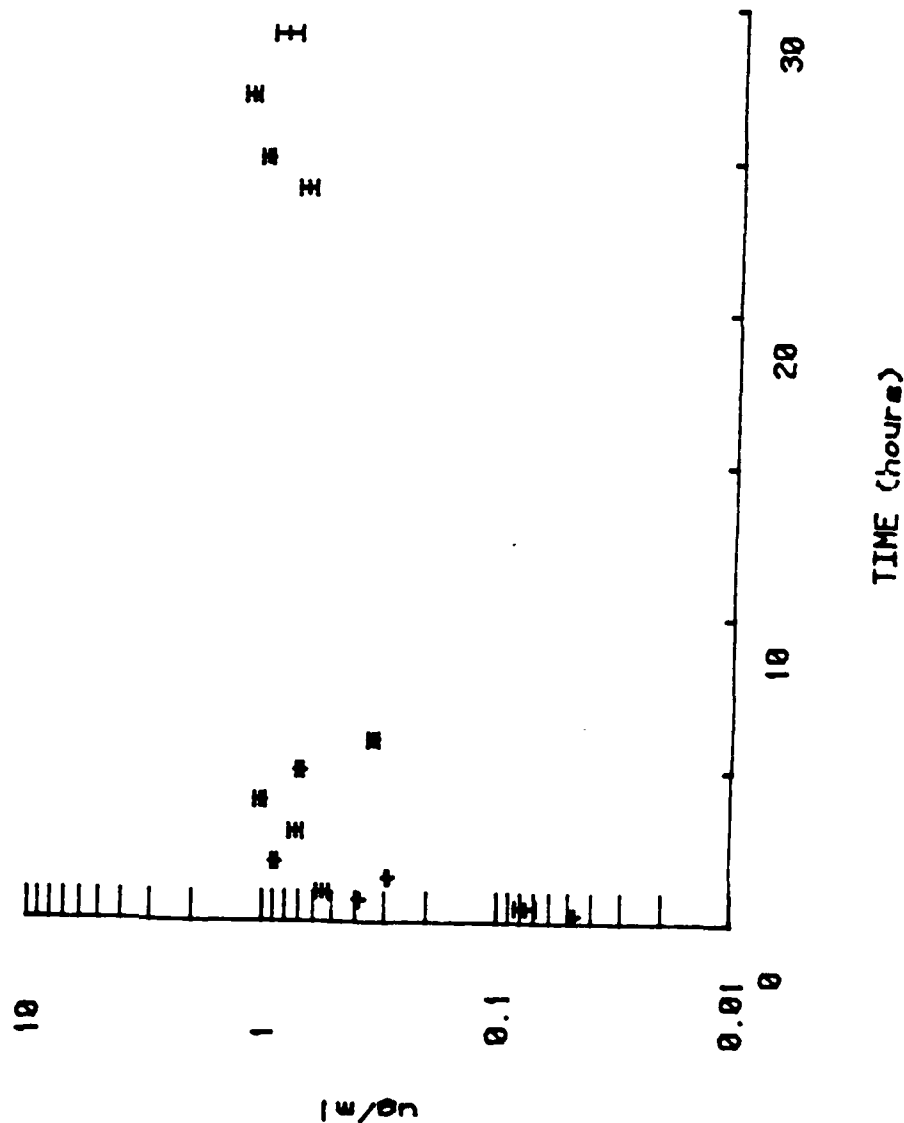


Figure 3. Effect of 1,1,1-Trichloroethane (TCE) in the venous blood of a 350 g catheterized Fisher 344 rat implanted with a glass tube ALCAP ceramic delivery system (sealed with Silastic®) containing 45 mg of TCE, in an in vivo environment. (The glass tube was sealed with ketoglutaric acid-ceramic cement).

# 1,1,1-TRICHLOROETHANE IN CHAMBER AIR

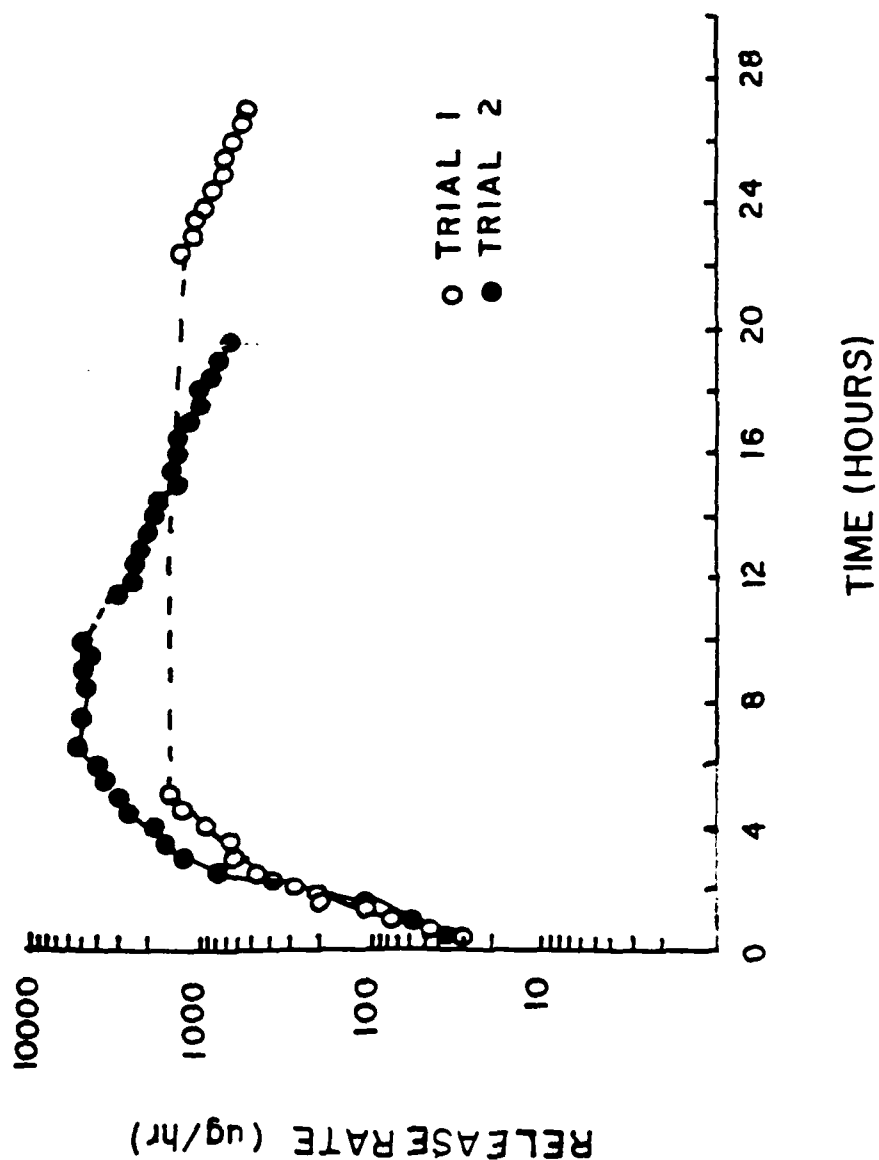


Figure 4. Effect of 1,1,1-Trichloroethane (TCE) on the chamber air containing the exhaled breath of a 230 g Fisher 344 rat that has been implanted with an glass tube ALCAP ceramic delivery system (sealed with Silastic®) containing 45 mg TCE.

# 1,1,1-TRICHLOROETHANE IN CHAMBER AIR

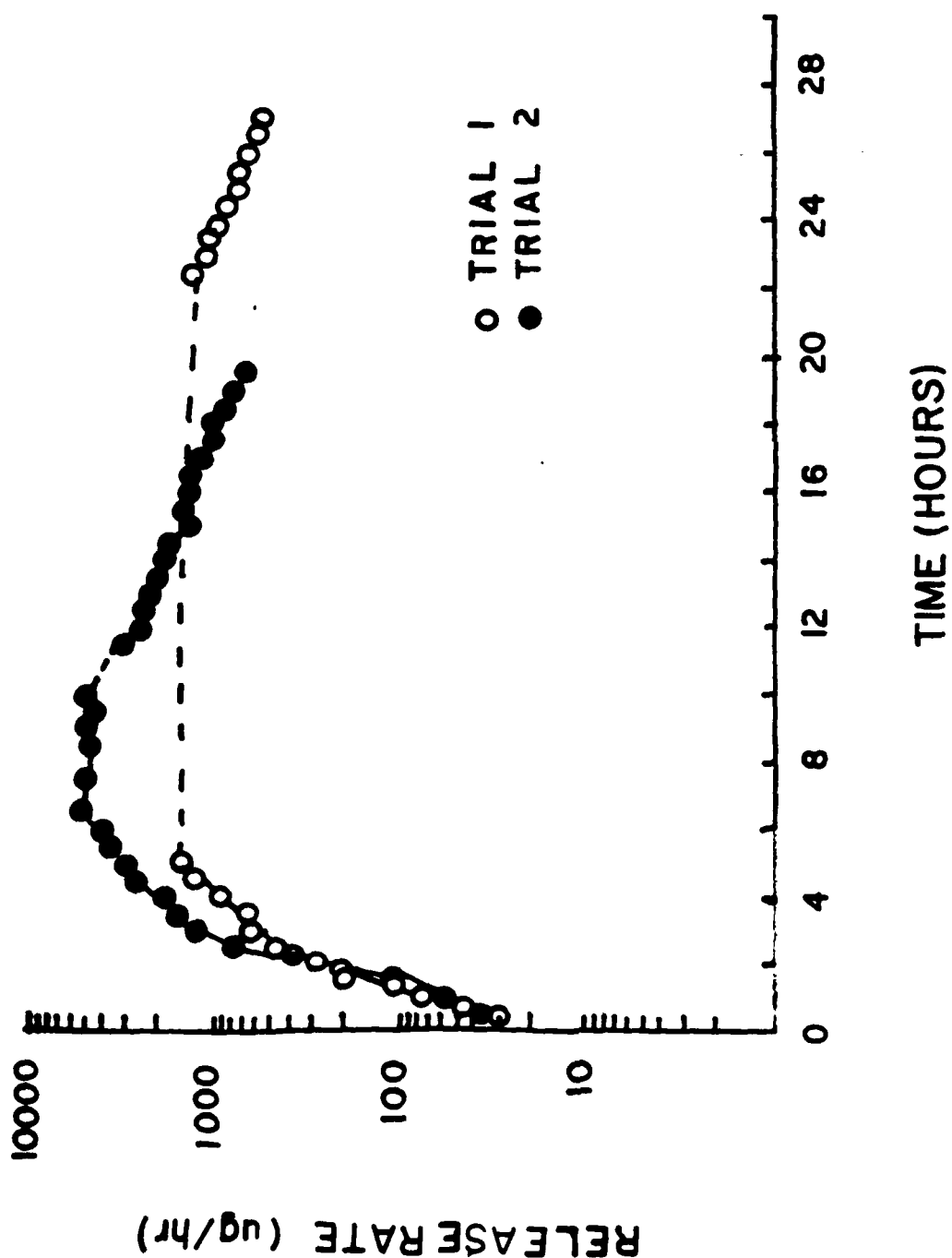


Figure 4. Effect of 1,1,1-Trichloroethane (TCE) on the chamber air containing the exhaled breath of a 230 g Fisher 344 rat that has been implanted with an glass tube ALCAP ceramic delivery system (sealed with Silastic®) containing 45 mg TCE.

1987 USAF-UES SUMMER FACULTY RESEARCH PROGRAM/  
GRADUATE STUDENT SUMMER SUPPORT PROGRAM

Sponsored by the  
AIR FORCE OFFICE OF SCIENTIFIC RESEARCH

Conducted by the  
Universal Energy Systems, Inc.

FINAL REPORT

FREQUENCY ESTIMATION IN THE ANALYSIS OF RADAR SIGNALS

Prepared by:	Dr. Vernon L. Bakke
Academic Rank:	Professor
Department and	Department of Mathematical Sciences
University:	University of Arkansas
Research Location:	Air Force Avionics Laboratory, Electronic Support Measure Group
USAF Researcher:	Dr. James Tsui
Date:	July 16, 1987
Contract Number:	F49620-85-C-0013

# FREQUENCY ESTIMATION IN THE ANALYSIS OF RADAR SIGNALS

by

Vernon L. Bakke

## ABSTRACT

A numerical algorithm for the estimation of frequencies in radar signals is presented. The algorithm is based on the autoregressive method and the Yule-Walker equations. The problem of determining the correct frequency modulus, which is associated with longer delay times is encountered, and an algorithm to resolve this ambiguity is presented. When multiple frequencies are present, the above problem complicates the algorithm and a scheme is developed to correctly pair the frequencies with their associated modulus.

### ACKNOWLEDGMENTS

The author would like to thank the Air Force Wright Aeronautical Laboratories and the Air Force Office of Scientific Research for sponsoring this program. I also wish to thank Universal Energy Systems, Inc. for their competent assistance regarding administrative and other details.

The Electronics Support Measure Group associated with the Avionics Laboratory at WPAFB, Dayton, Ohio provided me with excellent working conditions as well as ready access to computing facilities. In particular, I would like to thank Dr. James Tsui who provided me with encouragement, support and guidance throughout the work on the project. In addition, I was able to benefit from the insight and assistance of Dr. William McCormick, a former summer research fellow associated with this group.



## I. INTRODUCTION:

The problem of frequency estimation in signal analysis is a very important aspect of the detection of radar signals and sources. Once the signal has been digitized, there are a number of numerical schemes which can be used to derive certain parameters from the collected data. The most widely used methods are related to the Fourier transform, and in fact the Fast Fourier Transform has been rather popular. Autoregressive methods are also related to the Fourier transform, but the actual transform of the data is not performed, rather a difference equation is constructed, the solution of which contains the signal frequencies. The system of equations generated to find the coefficients of the linear difference equation is called the Yule-Walker equations (see [6]). An equivalent scheme in which a polynomial is constructed directly from the sampled data and whose zeros correspond to the associated frequencies is called the Prony method (see [1]).

The problems encountered in the Electronics Support Measurement Group include that of accurately estimating the frequencies present in radar signals, where the frequencies are very high. The accuracy of the collected data will affect the calculated values in the sense that a rather small perturbation in the initial data, possibly due to noise or to quantization, can cause a significant magnification in the error of the calculated frequencies. It is therefore necessary to develop an

analysis of the associated error, and possibly to construct an appropriate algorithm for these calculations.

My research interests include the study of integral equations, differential equations, optimal control theory, and numerical analysis. Thus, my work in these areas could possibly lead to a development of some helpful analysis, and a scheme for the improvement of accuracy.

## II. OBJECTIVES:

The preliminary goals associated with this project included the study of various numerical schemes for estimation of parameters related to radar signals. The suitability of certain methods will be determined by the method of acquiring the data, and the associated errors. During the course of this research, the goal came to that of forming a basis for the analysis of the error due to quantization or noise, and the possible implementation of algorithms which would be effective within the bounds of that error.

## III. ANALYTICAL DISCUSSION:

A fundamental approach to frequency estimation for a given signal is the Prony method. For this method, suppose we have a signal given by

$$S(t) = \sum_{n=1}^p P_n \exp[i(\omega_n t + \theta_n)],$$

where  $t \in [T_0, T_1]$ , the  $\omega_n$  are the angular frequencies,  $\theta_n$  are the phase angles and  $P_n$  are the amplitudes. For a fixed sample interval  $\tau$ , samples of this signal may be obtained, and assuming we have no error, then we have, for  $t_j = T_0 + j\tau$ ,

$$\begin{aligned} S(t_j) &= \sum_{n=1}^p P_n \exp[i(\omega_n t_j + \theta_n)] \\ &= \sum_{n=1}^p P_n \exp[i(\omega_n (T_0 + j\tau) + \theta_n)] \\ &= \sum_{n=1}^p P_n \exp[i(\omega_n T_0 + \theta_n)] \exp(i\omega_n j\tau) \end{aligned}$$

$j=0, 1, \dots, r$ . If we redefine the complex coefficients as

$$q_n = P_n \exp[i(\omega_n T_0 + \theta_n)],$$

$n=1, 2, \dots, p$ , then we have the following system of equations

$$S(t_j) = \sum_{n=1}^p q_n \exp(i\omega_n j\tau) \quad (1)$$

Now, if we put  $\mu_n = \exp(i\tau\omega_n)$ , the fundamental idea of Prony's method (see [1],[2]) is to find coefficients  $a_i$ ,  $i=1, 2, \dots, p$  such that the polynomial

$$P(z) = z^p + a_1 z^{p-1} + \dots + a_p$$

has roots  $\mu_1, \mu_2, \dots, \mu_p$ . Thus, assuming we have such coeffic-

ients, then for any  $k$ ,

$$a_p S(t_k) = a_p \sum_{n=1}^p q_n \exp(i w_n k \tau)$$

$$a_{p-1} S(t_{k+1}) = a_{p-1} \sum_{n=1}^p q_n \exp(i (k+1) w_n \tau)$$

.

$$a_1 S(t_{k+p-1}) = a_1 \sum_{n=1}^p q_n \exp(i (k+p-1) w_n \tau)$$

hence we have the relation

$$S(t_{k+p}) + a_1 S(t_{k+p-1}) + \dots + a_p S(t_k) = 0$$

$k=0,1,2,\dots$ . The right hand side is zero since the  $\exp(i \tau w_n)$  are zeros of the polynomial  $P(z)$ . The values for the  $a_n$  can be determined from the system

$$\sum_{n=1}^p a_n S(t_{k+p-n}) = -S(t_{k+p}) \quad (2)$$

for  $k=r, r+1, \dots, r+p-1$ , as long as the coefficient matrix

$$M = (S(t_{k+p-n})), \quad r \leq k \leq r+p-1, \quad 1 \leq n \leq p$$

is nonsingular. If we look at the matrix  $M$ , we have the general form

$$EP = M \quad (3)$$

where

$$E = (e_{j,k}), \quad P = (p_{j,k}), \quad 1 \leq j,k \leq p,$$

and

$$e_{j,k} = \exp[i(j-1)\tau w_k]$$

$$p_{j,k} = q_j \exp[i(r+p-k)\tau w_k].$$

Note also that the right hand side of (2) can be given as  $-ET$ , where (using superscript  $t$  to denote transpose)

$$T = (q_1 \exp[i(r+p)\tau w_1], q_2 \exp[i(r+p)\tau w_2], \dots, q_p \exp[i(r+p)\tau w_p])^t.$$

Now, one observes that if the matrix  $E$  is nonsingular, then we can rewrite the system (2) as

$$PA = -T \tag{4}$$

and from (4) and the definition of  $P$  we see that the solution  $A$  is independent of the values  $q_1, q_2, \dots, q_p$ . Hence we only need to look at the system

$$\sum_{n=1}^p a_n \exp[i(r+p-n)\tau w_1] = \exp[i(r+p)\tau w_1]$$

$$\sum_{n=1}^p a_n \exp[i(r+p-n)\tau w_2] = \exp[i(r+p)\tau w_2]$$

.

.

.

$$\sum_{n=1}^p a_n \exp[i(r+p-n)\tau w_p] = \exp[i(r+p)\tau w_p]$$

or simplified to

$$\sum_{n=1}^p a_n \exp(-in\tau w_m) = 1 \quad (5)$$

$m=1,2,\dots,p$ . Note that the coefficient matrix in this case is the Vandermonde matrix, and it is well-known that if the  $\exp(-in\tau w_m)$  are all distinct, then the system (5) has a unique solution. Note also that  $E$  is of this form, and as a result, will also be nonsingular.

The essential point concerning the above analysis is that we can obtain the unique values for  $a_j$  provided the rank of the system (2) is  $p$ . This will be true if all the frequencies are distinct and  $\tau$  is sufficiently small.

The principal method used in connection with instantaneous frequency measurement (IFM) receivers is based on the autoregressive spectral estimator. The main idea of this method is that the signal satisfies a  $p$ th order linear difference equation of the form

$$S(n) = - \sum_{k=1}^p a_k S(n-k) + \mu_n$$

where  $\mu_n$  represents the error due to noise and the  $a_k$  are coefficients to be determined. The  $S(n)$  represent the signal  $S$  at a time  $t_n$ , and since  $\mu_n$  has zero mean, the autocorrelation coefficients  $R_{xx}(n)$  are computed from the relation  $R_{xx}(n) = E(S(k+n)S(k))$ , where  $E$  is the expectation. From this the Yule-Walker equations are derived

$$R_{xx}(n) = - \sum_{k=1}^p a_k R_{xx}(n-k),$$

$n=1,2,\dots$  from which the coefficients  $a_k$  are calculated. As indicated in [2], this method is equivalent to the Prony method.

In problems related to signal analysis where the setting is that of interpretation of radar signals, it may be assumed that  $p$  frequencies are present, while in fact fewer than  $p$  frequencies are present. In this case, the system has rank  $r$ , where  $r < p$ , and a solution may be obtained by selecting a certain  $p-r$  of the coefficients and solving the remaining system. In this case, the polynomial  $P(z)$  will have  $r$  roots on the unit circle. Some variation of this idea is presented in [3].

Once the coefficients  $a_n$  are obtained the zeros of the polynomial  $P(z)$  are then calculated, and the results are of the form

$$\exp(i\tau w_1), \exp(i\tau w_2), \dots, \exp(i\tau w_p)$$

hence we can then find the frequencies  $\tau w_n$ , as long as  $\tau w_n \leq 2\pi$ . In the analysis of radar signals, the frequencies may be quite large, so that unless  $\tau$  is chosen to be very small,  $w_n$  will only be known modulo  $2\pi$ .

As expressed in [4], the method of formulation of the autocorrelation matrix contains errors of a magnitude such that for small enough  $\tau$ , the accuracy of the  $w_i$  is not sufficiently reliable. Thus, there exist suitable reasons for using values

of  $\tau$  which are too large for the  $w_n$  to be completely determined.

#### IV. THE PROBLEM OF AMBIGUITY.

In [4] this problem of ambiguous frequencies was encountered, and a reasonable approach to the solution was presented. The sensitivity to inherent error is high, and in this section we study the basic problem. As a basis for this study, the ideal case is considered first.

Thus, suppose we have a signal with  $p$  distinct frequencies  $w_n \in [A, B]$ ,  $n=1, 2, \dots, p$ . In this case we can write  $w_n = A + z_n$ , where  $z_n \in [0, B-A]$ . If we put this in equation (1), then we have

$$S(t_j) = \sum_{n=1}^p q_n \exp(ij\tau(A+z_n)) = \sum_{n=1}^p q_n \exp(ij\tau A) \exp(ij\tau z_n)$$

and if we put

$$s(k) = \sum_{r=1}^p q_r \exp(ik\tau z_r),$$

the system (2) then has the form

$$\sum_{n=1}^p \exp[i(k+p-n)\tau A] a_n s(k+p-n) = -\exp[i(k+p)\tau A] s(k+p)$$

or



$$\sum_{n=1}^p \exp[-in\tau A] a_n s(k+p-n) = -s(k+p)$$

so if we solve the system

$$\sum_{n=1}^p b_n s(k+p-n) = -s(k+p)$$

for the  $b_n$  and then define  $a_n = \exp(in\tau A)b_n$ , we have an equivalent solution.

In view of the above discussion, we may assume that  $w_n \in [0, B-A]$ . If  $\tau$  is such that  $\tau/(B-A) \geq 2\pi$ , then the values of  $w_n$  satisfy the relation

$$2\pi(\theta_n + N_n) = \tau w_n,$$

for some integers  $N_n$ ,  $n=1, 2, \dots, p$ . The values of  $\theta_n$  can be obtained via the Prony method, where

$$\exp(2\pi i \theta_n) = \exp(i\tau w_n).$$

Note that in general, the values of  $N_n$  are not known. Suppose, however that we apply Prony's method twice, using  $\tau_1 = 2\pi k_1/(B-A)$  and  $\tau_2 = 2\pi k_2/(B-A)$ . In this case, we have the two sets of relations

$$\theta_n + N_n = k_1 w_n / (B-A), \quad \phi_n + M_n = k_2 w_n / (B-A),$$

$n=1, 2, \dots, p$ , where  $k_1$  and  $k_2$  are given integers. We assume the system (2) has rank  $p$ , so that the  $\theta_n$  are all distinct and the  $\phi_n$  are all distinct.

If  $\theta_n$  and  $\phi_n$  represent the same frequency  $w_n$ , then we must have  $k_2(\theta_n + N_n) = k_1(\phi_n + M_n)$  from which we see that

$$k_2\theta_n - k_1\phi_n = k_1M_n - k_2N_n \quad (6)$$

We have the following useful lemma.

Lemma 1. If  $\theta_n$  and  $\phi_n$  represent the same frequency  $w_n$  and the system (2) is nonsingular for  $\tau_1$  and  $\tau_2$  where the integers  $k_1$  and  $k_2$  are relatively prime, then there exists a unique pair of integers  $M_n$  and  $N_n$  satisfying (6).

Proof: First note that since  $\theta_n, \phi_n$  are properly paired, then  $k_2\theta_n - k_1\phi_n = I$ , some integer. Now, we have the Diophantine equation

$$k_1M_n - k_2N_n = I \quad (7)$$

where, since  $0 < \theta_n, \phi_n < 1$ , then  $0 \leq N_n < k_1$  and  $0 \leq M_n < k_2$ . We also have that  $-k_1 < I < k_2$ . Equation (7) can be restated in modular form as

$$k_1M_n \equiv I \pmod{k_2} \quad (8)$$

By a corollary to Fermat's theorem (see, e.g. [5]), the solution of (8) is given by

$$M_n = Ik_1^{R-1} \pm jk_2 \quad (9)$$

where  $R = \phi(k_2)$  is Euler's  $\phi$ -function. Thus, for some  $j$ , we can find an  $M_n$  which satisfies  $0 \leq M_n < k_2$ , and by a similar argument, there is an  $N_n$  satisfying  $0 \leq N_n < k_1$  and equation (6). From expression (9) there is only one such value if  $k_1$

and  $k_2$  are relatively prime. The above lemma is useful in the event we are able to show that  $\theta_n$  and  $\phi_n$  are associated with the same frequency  $w_n$ . In this case, we say that  $\theta_n$  and  $\phi_n$  are properly paired. Now if we note that it is necessary that the value  $I$  is an integer, we can see that this is also a sufficient condition for pairing.

Lemma 2. If the system (2) is nonsingular for  $\tau_1$ , let  $\theta$  and  $\phi$  be two values obtained via the above algorithm. If  $k_2\theta - k_1\phi = I$ , an integer, then  $\theta$  and  $\phi$  are associated with the same frequency.

Proof. Suppose they are not associated with the same frequency. Then we have that  $\theta + N = k_1w/(B-A)$ , and  $\phi + M = k_2w^*/(B-A)$ , where  $w$  and  $w^*$  are distinct. Let  $P$  be such that  $I + k_2N = k_1P$ . Then  $k_2(\theta + N) = k_2\theta + k_2N = k_1\phi + I + k_2N = k_1(\phi + P)$ , hence  $(\theta + N)/k_1 = (\phi + P)/k_2$ . from which it follows that  $\phi$  also represents  $w$ , which is a contradiction.

The above two lemmas provide the theoretical solution to the ambiguity problem. Unfortunately, the introduction of error into the system can perturb the values of  $\theta$  and  $\phi$  to the point that it will not be possible to make a reliable decision regarding the pairing based on lemma 2.

#### V. ALGORITHM FOR PAIRING.

In the presence of any perturbation, the decision that two

values  $\theta$  and  $\phi$  are properly paired breaks down when the calculations don't produce integers. Thus we consider the following scheme, again assuming that (2) is nonsingular.

In this case, we have three values of  $\tau$  :

$$\tau_1 = 2\pi k/(B-A), \quad \tau_2 = 2\pi(2k+1)/(B-A), \quad \tau_3 = 2\pi(3k+1)/(B-A).$$

Using these delay times, with the application of Prony's method, we have the relations

$$\theta_n + N_n = kw_n/(B-A), \quad \phi_n + M_n = (2k+1)w_n/(B-A)$$

$$\emptyset_n + P_n = (3k+1)w_n/(B-A),$$

$n=1,2,\dots,p$ . We first observe that if  $\theta$  and  $\phi$  are properly paired, then  $\phi + M - 2(\theta + N) = w/(B-A)$ , hence the inequality  $0 < \phi - 2\theta + M - 2N < 1$ . Since  $-2 < \phi - 2\theta < 1$ , then we have the following conditions relating  $M$  and  $N$ :

$$\begin{aligned} \text{if } 0 \leq \phi - 2\theta < 1, & \quad \text{then } M = 2N; \\ -1 \leq \phi - 2\theta < 0, & \quad \text{then } M = 2N+1; \\ -2 < \phi - 2\theta < -1, & \quad \text{then } M = 2N+2. \end{aligned} \quad (10)$$

It is also necessary that if  $\theta$  and  $\phi$  are properly paired, then  $(2k+1)\theta - k\phi = kM - (2k+1)N$ . Similarly, if  $\theta$  and  $\emptyset$  are properly paired, then we get that  $\emptyset + P - 3(\theta + N) = w/(B-A)$ , and as above, we have the conditions relating  $P$  and  $N$ :

$$\begin{aligned} \text{if } 0 \leq \emptyset - 3\theta < 1, & \quad \text{then } P = 3N; \\ -1 \leq \emptyset - 3\theta < 0, & \quad \text{then } P = 3N+1; \\ -2 \leq \emptyset - 3\theta < -1, & \quad \text{then } P = 3N+2; \\ -3 < \emptyset - 3\theta < -2, & \quad \text{then } P = 3N+3, \end{aligned} \quad (11)$$

as well as the condition  $(3k+1)\theta - k\emptyset = kP - (3k+1)N$ .

Define the intervals  $U_I = [-I, -I+1)$ ,  $I = 0, 1, 2, 3$  and the functions

$$f(x, y) = kx - (2k+1)y + kI, \text{ for } x-2y \in U_I$$

$$g(x, y) = kx - (3k+1)y + kJ, \text{ for } x-3y \in U_J.$$

Lemma 3. The values  $\theta$ ,  $\phi$ , and  $\emptyset$  are associated with the same frequency  $w$  if and only if  $f(\phi, \theta) = g(\emptyset, \theta)$ .

Proof. We prove the lemma for the case  $p = 2$  (i.e., assuming there are two frequencies present). Necessity is clear, hence suppose that they are not properly paired. If this is so, we have with  $\theta = \theta_1$ ,

$$\text{case 1: } \phi = \phi_1, \emptyset = \emptyset_2$$

$$\text{case 2: } \phi = \phi_2, \emptyset = \emptyset_1$$

$$\text{case 3: } \phi = \phi_2, \emptyset = \emptyset_2.$$

Cases 1 and 2 are similar, so we will examine case 1. In this event,  $f(\phi_1, \theta_1) = g(\emptyset_1, \theta_1)$ , so we have that

$$\begin{aligned} f(\phi_1, \theta_1) - g(\emptyset_2, \theta_1) &= g(\emptyset_1, \theta_1) - g(\emptyset_2, \theta_1) \\ &= k(\emptyset_1 - \emptyset_2) + k(J_1 - J_2) \end{aligned}$$

which is non-zero. In case 3, we have, using a similar argument as above,

$$f(\phi_2, \theta_1) - g(\emptyset_2, \theta_1) = k(\theta_2 - \theta_1) + kI$$

which is also non-zero.

The algorithm for  $p = 2$  can be described as follows:  
first calculate the three pairs

$$(\theta_1, \theta_2), (\phi_1, \phi_2), (\emptyset_1, \emptyset_2)$$

Then for the pairing, calculate the four values

$$\begin{aligned}
N_1 &= k\phi_1 - (2k+1)\theta_1 + kI_1 \\
N_2 &= k\phi_2 - (2k+1)\theta_1 + kI_2 \\
N_3 &= k\phi_1 - (3k+1)\theta_1 + kJ_1 \\
N_4 &= k\phi_2 - (3k+1)\theta_1 + kJ_2
\end{aligned} \tag{12}$$

where, if from (10) we have that  $M = 2N + I_i$  then  $k\phi_i - (2k+1)\theta_1 = kM - (2k+1)N = k(2N + I_i) - (2k+1)N = kI_i - N$ , so that we denote  $N_i$  as in (12). A similar calculation is done for  $N_j$  using (11). Then find the pair of values  $(N_1, N_3)$ ,  $(N_1, N_4)$ ,  $(N_2, N_3)$  and  $(N_2, N_4)$  for which the magnitude of the difference is a minimum. The value of the  $N_i$  in this case corresponds to the integer associated with  $\theta_1$  and we can write  $\theta_1 + N = kw_1/(B-A)$ .

For this algorithm to work in practice, it is necessary that the accepted value for  $N$ , say  $N^C$  satisfies  $|N - N^C| < .5$ . Thus, let  $\delta(x)$  represent the error in calculation. Then, since  $\theta = \theta_1 + \delta(\theta_1)$  and  $\phi = \phi_1 + \delta(\phi_1)$ , it follows that

$$N^C = N + k\delta(\phi_1) - (2k+1)\delta(\theta_1).$$

If  $|\delta(x)| \leq \delta$ , we must require that  $(3k+1)\delta < .5$ , or that  $\delta < 1/(6k+2)$ . If this condition is satisfied and if  $v_1$  denotes the calculated value for  $w_1$ , then using  $\theta$  and  $P_1$  we have  $v_1 = w_1 + (B-A)\delta(\theta_1)/(3k+1)$ , hence the error in calculating the frequency  $w_1$  is bounded by  $(B-A)/2(3k+1)^2$ .

The algorithm discussed above was coded in Fortran, and the following table illustrates these results, assuming no external noise. These values were taken from approximately 40,000 such examples and are representative of the results.

TABLE 1.

$$\tau = 2\pi(21)/2039$$

$w_1$	$w_2$	$v_1$	$v_2$
2000	2001	2000.000	2001.000
2500	3000	2499.999	2999.999
3001	3000	3000.999	2999.999
4000	3000	3999.998	2999.999
3999	4000	3998.998	3999.998

All calculations were performed on the VAX 11/780 at WPAFB, Dayton. OH.

#### VI. RECOMMENDATIONS.

A complete analysis should be done with respect to the error incurred by noise or any other source, such as measurement. In some instances, even with a relatively low signal to noise ratio, the accuracy could still be quite good, but clearly the reliability of the estimation will be rather low. In addition to this, the error introduced by measurement can be sufficient to reduce the accuracy severely. It is possible that a smoothing technique such as least squares could be employed to reduce the disastrous effects of these errors.

The author feels that the scheme discussed above for the pairing and calculating frequencies could be extended to the general case. Moreover, it is recommended that an investigation be undertaken regarding the possibility of using this algorithm with that discussed in [4].

## REFERENCES

1. Hildebrand, F. B., Introduction to Numerical Analysis, 2nd Ed., McGraw-Hill, New York, 1956.
2. Kay, Steven M. and Stanley Lawrence Marple, 'Spectrum Analysis - A Modern Perspective,' Proceedings of the IEEE, Vol. 69, No. 11, November, 1981.
3. Kumaresan, Ramdas, 'Accurate frequency estimation using an all-pole filter with mostly zero coefficients,' Proceedings of the IEEE, Vol. 70, No. 8, August, 1982.
4. McCormick, William S., 'Design of a Digital EW Passive Receiver,' Final report, AFOSR-85-045 minigrant, 1985.
5. Niven, Ivan and H.S. Zuckerman, An Introduction to the Theory of Numbers, John Wiley and Sons, New York, 4th Ed., 1980.
6. Robinson, Enders A., 'A historical perspective of Spectrum Estimation,' Proceedings of the IEEE, Vol. 70, No. 9, September, 1982.



1987 USAF-UES SUMMER FACULTY RESEARCH PROGRAM  
GRADUATE STUDENT SUMMER SUPPORT PROGRAM

Sponsored by the  
Air Force Office of Scientific Research  
Conducted by the  
Universal Energy Svstems, Inc.

FINAL REPORT

Invitro Cytotoxic Effects of Perfluorodecanoic Acid  
on L5178Y Mouse Lymphoma Cells

Prepared By :	Shankar S. Bale
Academic Rank :	Professor
Department and University :	Natural Science and Mathematics Saint Paul's College
Research Location :	AFAAMRL/THB
USAF Researcher :	Dr. Shelly A. London
Date :	Sept. 20, 1987
Contract Number :	F49620-85-c-0013

In Vitro Cytotoxic Effects of Perfluorodecanoic acid on  
L5178Y Mouse Lymphoma Cells

by

Shankar S. Pale

ABSTRACT

Cytotoxic effects of perfluorodecanoic acid on L5178Y cells were studied. Cells were exposed to 0.1  $\mu$ g, 1  $\mu$ g, 2  $\mu$ g, 8  $\mu$ g, 16  $\mu$ g, and 32  $\mu$ g/ml of perfluorodecanoic acid (PFDA) for 8, 24, 48, and 72 hours. PFDA induced cytotoxicity in all the concentrations used. Time and level response was observed in all the treatments. Cell lysis was significant at higher concentrations used. 80 to 100 percent cell death occurred within twelve hours of treatment at higher levels of treatment.

NO-A191 203

UNITED STATES AIR FORCE SUMMER FACULTY RESEARCH PROGRAM

3/11

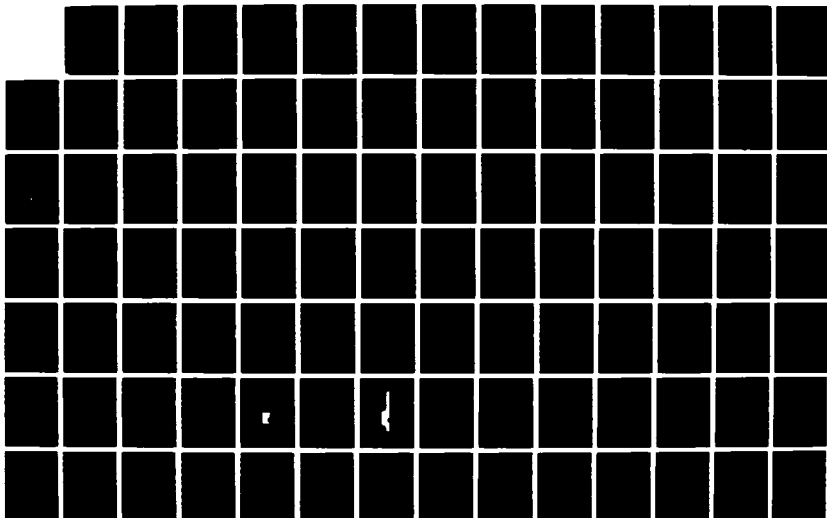
(1967) PROGRAM TE. (U) UNIVERSAL ENERGY SYSTEMS INC

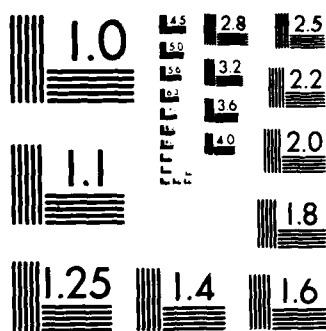
DAYTON OH R C DARRAH ET AL. DEC 07 AFOSR-TR-68-0212

UNCLASSIFIED F49620-05-C-0013

F/B 5/1

NL





MICROCOPY RESOLUTION TEST CHART  
NATIONAL BUREAU OF STANDARDS 1963 A

## A C K N O W L E D G E M E N T

I wish to express my sincere appreciation and thanks to Dr. Shelly A. London for providing me an opportunity to participate in the Summer Research Program and also for his encouragement and support.

Appreciation is also extended to Dr. Frank A. Witzmann, another SFRP fellow in our laboratory for his help, encouragement and also educating me in the use and application of Two Dimensional Electrophoresis.

Finally, I wish to express thanks to the United States Air Force Systems Command, the Air Force Office of Scientific Research, and the Toxic Hazard Division, Cell Biology Lab and Biochemistry Branch, of the Air Force Medical Research Laboratory for sponsorship of this research.

## Introduction

Perfluorodecanoic acid is a perfluorocarboxylic acid that is readily obtainable in crystalline form. Perfluorocarboxylic acids have found wide use as lubricants, surfactants, and aqueous film forming foam fire extinguishants (Guenther and Vietor 1962, Shinoda and Nomura 1980).

Perfluorodecanoic acid (PFDA) causes acute toxicity in a variety of rodent species (Anderson et al., 1981). Many perfluorinated compounds are chemically inert (Clarke et al., 1973) and some perfluorinated compounds were retained in experimental animals for significant time periods following exposure (Clarke et al., 1970). Perfluorinated compounds have been found in the serum of fluorochemical workers (Ubel et al., 1980).

Perfluorinated fatty acids caused toxicity in both *in vivo* and *in vitro* conditions (Olson and Anderson 1983, Roger et al., 1982). The acute toxicity of PFDA includes hypophagia, thymic atrophy, delayed lethality, disruption of liver and testicular degeneration (Olson and Anderson, Van Rafelghem et al., 1982). PFDA had no effect on L5178Y cells below 50ug/ml, and dose above caused cell lysis (Roger et al., 1982). Flowcytometric analysis of L5178Y cells treated with PFDA showed an increase in the number of tetraploid cells with the increase in the concentration of PFDA (Wigler and Shah 1986).

Numerous reports have appeared with respect to the effects of PFDA, but assessment of its potential cytotoxicity appears to be incomplete. The present study was made to elucidate the cytotoxic effects of PFDA on L5178Y cells.

#### APPROACH

L5178Y mouse lymphoma cells were available at the Cell Biology and Biochemistry Section of the Toxic Hazard Division. The cells were maintained in McCoy's 5A medium supplemented with sodium pyruvate, glutamine, and Nutridoma-SP(1x).

For the cytotoxicity test, cells were cultured at  $2-3 \times 10^5$  cells/ml in McCoy's 5A medium using 24 well tissue culture plates. The cells were treated with 0ug, 1ug, 2ug, 4ug, 8ug, 16ug and 32ug/ml of PFDA for 24 hours. DMSO control cultures were prepared in a similar manner to the treated cultures. The cells were examined at 1, 2, 4, 8 and 24 hours for toxic effects following the method of Palmer et al., (1972).

#### Colorimetric MTT Assay

400 microliters of cell suspension was removed from each well of the 24 well plate. 100 microliters of cell suspension was placed in each microwell and 10 ul of MTT (3-(4,5 dimethyl thiazol-2-yl)-2,5-diphenyl tetrazolium bromide) stock solution (5mg/mlPBS) was added to each well. The microplates were

incubated at 37 C in a carbondioxide incubator for 4 hours. After 4 hours 150 ul of acid isopropanol (100ul of 0.04N HCl in propanol) was added to each well to dissolve the dark blue crystals. After one hour at 37 C to ensure that all the crystals were dissolved, the microplates were read on a Titertek plate reader set at a wavelength of 540nm.

#### Cell Count and Cell Viability

Cell counts were made using Coulter counter. Viability was assessed by exclusion of 0.4% Trypan blue dye dissolved in phosphate buffered saline.

#### Results and Discussion

Cytotoxic effects of PFDA on L 5178Y cells is presented in Table 1. The results are recorded on a scale of - to 4+ in which - indicates normal growth and 4+ indicates complete cell degeneration. Cells treated with 16ug/ml and 32ug/ml showed maximum toxicity compared to other concentrations used. The toxic effect increased with the increase in the levels of PFDA. Time and level response reactions to PFDA were observed. 100 percent cell degeneration were observed in cells treated with 16ug and 32ug/ml of PFDA.

Invitro assay of cells treated with PFDA is shown in Table 2. Cells treated with 16ug and 32ug/ml produced less amount of



formazan compared to other concentrations. An increase formazan production was observed in PFDA treated cells (2ug-8ug/ml) and control groups with the increase in incubation time. The amount of formazan generated at each period decreased with the increase in level of PFDA. The level of MTT cleavage by viable cells was found to be directly proportional to the number of cells.

Viability and growth of L5178Y cells grown in different concentrations of PFDA are shown in Table 3. Viability of the cells decreased with the increase in the level of PFDA. Cell lysis and death occurred at a significant level at 16 and 32ug/ml. Time and dose response was evident in all the levels used. Similar results were observed for growth. There was decline in cell number in all the treatments compared to control.

It is evident from the results that PFDA causes toxicity. Toxic effects increased with the increase in levels of PFDA. Time and dose response were observed in all treatments. Rogers et al. (1982) have indicated that PFDA failed to induce cytotoxicity at concentration lower than 100ug/ml. However, in our study we observed cytotoxicity at concentration as low as 16ug/ml. Wigler and Shah (1986) observed an increase of tetraploid cells in PFDA treated cultures indicating that PFDA may block the G<sub>2</sub> stage of the cell cycle.

It has been suggested that PFDA alters membrane function by changing both oxidative status and fattyacid composition (Olson and Anderson 1983). The toxic effects of perfluorinated

compounds could be diminished by lowering temperature and adding serum to cell cultures. Serum albumin has been suggested to provide greater protection against perfluorinated toxicity (Levitt and Liss 1986). The mechanism by which albumin diminished toxicity of perfluorinated acids is unclear.

The effect of PFDA can be rapid in serum free medium. Cell swelling and lysis were observed in concentrations of 16 and 32ug/ml. Such observations suggests that PFDA disrupts the cell membrane, supporting the earlier findings of Olson and Anderson(1983). Perfluorinated acids do not cause mutation and long term viability in cultured cells below their lethal dose (Roger et al., 1982, Levitt and Liss 1986).

The cytotoxic effects of PFDA described in this study clearly indicate a need for further investigation to determine the potential effect of PFDA on chromosomes, protein and DNA content in mammalian cells.

#### RECOMMENDATION

Invitro cytotoxic tests have been refined over the years to provide techniques to determine the cytotoxicity of various chemical pollutants within a minimum time frame and also economical. Mosmann technique which was refined at the Toxic Hazard Division by Dr. S. A. London will provide quick results in terms of toxicity. The test is very simple, not time consuming and also economical. It can be extrapolated to the invivo system including humans.

Invitro cytotoxic test developed at the Toxic Hazard Division coupled with biochemical parameters (Electrophoresis of Proteins) will provide most of the answers. These tests can be further refined and utilised as a test to determine the toxicity of chemicals that contaminate the natural environment,

Table 1. Cytotoxicity observed in L5178Y cells after treatment with various concentrations of perfluorodecanoic acid.

Hours	Concentrations					
	oug	1ug	2ug	4ug	8ug	16ug 32ug
1	-	-	-	-	-	+
2	-	-	-	-	-	+++
4	-	-	-	-	-	+++
8	-	-	-	-	+	++++
24	-	-	-	*	+	++++

- = Normal growth  
 \* = less than 5% cell death  
 + = 25% cell death  
 ++ = 50% cell death  
 +++ = 75% cell death  
 ++++ = 100% cell death

Table 2. MTT assay of cells treated with various concentrations of PFDA.

Concentration(ug/ml)	Time(Hours)			
	8	28	52	76 <sup>+</sup>
0ug	0.275	0.438	0.738	0.613
1ug	0.213	0.434	0.639	0.553
2ug	0.158	0.265	0.526	0.529
4ug	0.152	0.177	0.200	0.203
8ug	0.101	0.107	0.122	0.113
16ug	0.103	0.022	0.006	0.005
32ug	0.051	0.016	0.001	0.001

+ = Absorbancy values

Table 3. Effect of PFDA on growth and viability of L5178Y cells.

Concentration	Hours					
	8		28		52	
	cell count	viability %	cell count	viability %	cell count	viability %
0ug	$4.4 \times 10^5$	100	$9.8 \times 10^5$	100	$1.5 \times 10^6$	100
1ug	$3.0 \times 10^5$	98	$8.7 \times 10^5$	96	$1.7 \times 10^6$	92
2ug	$2.2 \times 10^5$	97	$4.4 \times 10^5$	94	$0.9 \times 10^6$	87
4ug	$2.6 \times 10^5$	93	$3.6 \times 10^5$	74	$0.4 \times 10^6$	75
8ug	$3.0 \times 10^5$	90	$3.57 \times 10^5$	73	$0.35 \times 10^6$	71
16ug	$1.8 \times 10^5$	26	$2.5 \times 10^5$	0	$0.1 \times 10^6$	0
32ug	$1.7 \times 10^5$	6	$0.8 \times 10^5$	0	$0.8 \times 10^5$	0

# REFERENCES

- Anderson, M.E., Baskin, G., and Rogers, A.M. 1981. "The acute toxicity of perfluoro-n-decanoic acid: similarities with 2,3,7,8-tetrachlorodibenzodioxin". *The Toxicologist* 1:16.
- Clarke, L.C., Jr., Becattini, F., Kaplan, S., Obrock, V., Cohen, D., and Becker, C. 1973. Perfluorocarbons having a short dwell time in the liver. *Science* 181:680-682.
- Clarke, L.C., Kaplan, S., Becattini, F., and Benzing, G. 1970. Perfusion of whole animals with perfluorinated emulsion using a Clarke bubble de-foam heart-lung machine. *Fed. Proc.* 29: 1764-1770.
- Guenther, R. A., and Vietor, M. L. 1962. Surface active material from perfluorocarboxylic and perfluorosulfonic acids. *I&EC Prod., Res. Dev.* 1 : 165-169.
- Levitt, D., and Liss, A. 1986. Toxicity of perfluorinated acids for human and murine B cell lines. *Toxicol. Appl. Pharmacol.* 86 : 1-11.
- Olson, C.T., and Anderson, M. E. 1983. The acute toxicity of perfluoro-decanoic acid in male rats and effects on tissue fatty acids. *Toxicol. Appl. Pharmacol.* 70 : 362-372.
- Palmer, K. A., Green, A., and Legator, M.S. 1972. Cytogenetic effects of DDT and derivatives of DDA in cultured mammalian cell line. *Toxicol. Appl. Pharmacol.* 22 : 355-364.
- Rogers, A.M., Anderson, M. E., and Back, K. C. 1982. Mutagenicity of 2,3,7,8, tetrachlorodibenzo-p-dioxin and perfluoro-n-decanoic acid on L5178Y mouse lymphoma cells. *Mutation Res.* 105 : 445-449.
- Shinoda, K., and Nomura, T. 1980. Miscibility of fluorocarbon and hydrocarbon surfactants in micelles and liquid mixtures: Basic studies of oil repellent and fire extinguishing agents. *J. Phys. Chem.* 84 : 365-369.
- Ubel, F. A., Sorenson, S. D., and Roach, D. E. 1980. Health status of plant workers exposed to fluorochemical-A preliminary report. *Amer. Ind. Hyg. J.* 41 : 584-589.
- Van Ranfelgham, M., Anderson, M. E., Bruner, R., and Mattie, D. 1982. Comparative toxicity of perfluoro-n-decanoic acid (PFDA) in hamsters. *Toxicologist* 2: 148.
- Wigler, P. W., and Shah, Y. B. 1986. Perfluorodecanoic acid inactivation of a channel for 2-Aminopurine in L5178Y cell membrane and recovery of the channel. *Toxicol. Appl. Pharmacol.* 85 : 456-463.

1987 USAF-UES SUMMER FACULTY RESEARCH PROGRAM  
GRADUATE STUDENT SUMMER SUPPORT PROGRAM

Sponsored by the  
AIR FORCE OFFICE OF SCIENTIFIC RESEARCH

Conducted by the  
Universal Energy System, Inc.

FINAL REPORT

FIRE TECHNOLOGY OF JET FUELS (JP-8 VS. JP-4)

Prepared by:	William W. Bannister, PhD
Academic Rank:	Professor
Department and	Chemistry
University:	University of Lowell Lowell, MA 01854
Research Location:	AFESC/RDCF Tyndall AFB, FL
USAF Researcher:	Joseph Walker
Date:	25 September 1987
Contract No.:	F49620-85-C-0013



## FIRE TECHNOLOGY OF JET FUELS (JP-8 VS. JP-4)

William W. Bannister

### Abstract

JP-4 and JP-8 are compared, regarding recently developed fire fighting techniques, and safety hazards in terms of refuelling, spills and leakages, controlled crash landings, in-flight gunfire effects, and running fuel fires. An anomalous relationship between fuel ignitability and volatility was discovered. Thus, flash points are well known to be inversely proportional to volatility, and high volatility (low flash point) fuels are thus regarded more flammable. In this work, however, high volatility fuels were shown to be less easily ignited by contact with hot metal surfaces. This may be important in fuel selection: high volatility JP-4 may actually be safer than low volatility JP-8 (previously regarded less flammable) in terms of fires caused by gun-fire, crash landings, leakages of fuel onto hot engine surfaces, and similar situations in which fires may result from contact of fuel with hot metal surfaces rather than by ignition by flames.

### Acknowledgments

I am very grateful to the Air Force Systems Command and the Air Force Office of Scientific Research for sponsorship of this project, and to Universal Energy Systems, Inc. for administration and supervision of this work. I am also indebted for the ongoing help and friendship extended to me by military and civilian staff members at Tyndall Air Force Base: COL Lawrence Hokanson, LTCOL Robert Costigan, CAPT Larry Bramlitt, Dr. Paul Thompson, John R. Hayes, Jr., and Andrew Poulis; and the staff members of the RDCF team of which I was a happy member: Joseph Walker (Head), CWO4 Bob Barrow, Wade Grimm, Denise Maloney, Bryce Mason, James McKay, CAPT Tom Morehouse, and Jim Sartain. I received valuable advice, incorporated into this report, from Dr. Joe Leonard and Dr. Homer Carhart of Naval Research Labs, Washington, DC; Dr. Bob Tapscott and Billy Dees of the New Mexico Engineering Research Institute at Albuquerque; William Westfield, Eugene Kluegg, and Dr. George Geyer at the FAA Engine/Fuel Safety Branch, Atlantic City, NJ; Assistant Fire Chief Lopez and other fire fighting members at Lakenheath RAF Base, England; and Dr. Sukant Tripathy of the University of Lowell. I express my great appreciation to all of these experts who have contributed so greatly to these efforts.

## I. INTRODUCTION

In 1958 Jet A-1 was introduced as the principal commercial jet fuel, in the belief that this provided a balance of safety, cost, availability, and performance. JP-8 is a military version, differing in having anti-static, anti-freeze and anti-corrosion additives. JP-8 is used in the UK (there designated as AVTUR) and other NATO countries (F-34); it has not been adopted by the US Air Force in CONUS; instead, the the more volatile JP-4 has been used since the early 1950's. The Navy replaced JP-4 with the low volatility JP-5 due to fire-fighting constraints peculiar to Navy carrier operations. A problem arising from in-flight refuelling of Navy aircraft from Air Force tankers occasioned a Navy request for Air Force consideration of replacement of JP-4 by less volatile JP-8. Although the Air Force has an excellent safety record in use of the cheaper and more available JP-4, possibilities that JP-8 may become cheaper and more available had also formed a basis for examination of this for conversion from JP-4. It was deemed particularly desirable to study safety and fire fighting technology parameters for JP-8.

My previous research interests in this area have been in investigations of anti-misting fuel technology for mitigation of aircraft fires resulting from controlled crash landings, including use of gelling agents in anti-misting formulations.

## II. OBJECTIVES

The objectives of this report will be to:

1. Compile information on jet fuel characteristics and properties, as these pertain to fire fighting technology.
2. Examine development of new fire fighting technologies.
3. Correlate fuel composition effects with flammability.

## III. CURRENTLY BACKGROUND INFORMATION ON JP-4 AND JP-8 FUELS

### A. Military and commercial jet fuels (see Table I).

TABLE I. JET FUEL DEVELOPMENT<sup>1-3</sup>

JP-1,JP-2 (1944); obsolete, due to industrial difficulty in attaining military specifications

JP-3 (1947); wide-cut mixture of gasoline and kerosene; high volatility resulted in excessive fuel losses in high altitude flights (boil-off)

JP-4 (1951); lower vapor pressure version of JP-3; standard USAF and Army aviation fuel

JP-5 (1952); standard USN lower vapor pressure version of JP-4; USAF uses for Air Force 1

JP-6,JP-7 (1956); USAF ultra-low vapor pressure test fuels

### ASTM JET FUELS (1958)

Jet A Relatively high freezing point; not useful for high altitude flights. Lower vapor pressure, higher flash point than Jet B.

Jet A-1 Lower freezing point; essentially same as JP-8. JP-8 has anti-static, anti-freeze, corrosion inhibiting, similar additives

Jet B Essentially same as JP-4, with additives as described above for JP-8.

### B. Correlations of Compositions and Physical Properties of

JP-4, JP-5 and JP-8. (See Tables II and III.)

TABLE II. FUEL CHARACTERISTICS <sup>1-7</sup>

US	JP-4	JP-5	JP-8	Jet A-1
UK	AVTAG		AVTUR	
NATO	F-40	F-44	F-34	F-35
Specification, Mil-T	5624H		83133	ASTM1655
Specific gravity	0.77	0.83		.80
Vapor pressure, psi (RT)	3.0		LESS THAN 0.1 PSI	
Flash point (Fahrenheit)	- 20	+ 150		+ 125
BTU/gallon	119000	126000		124500

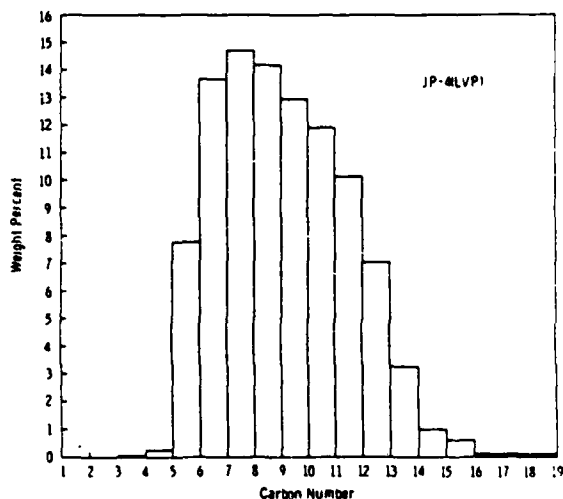
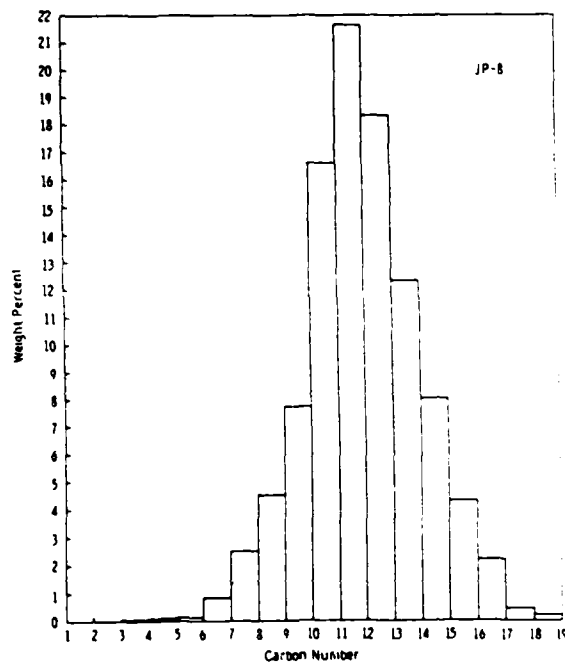
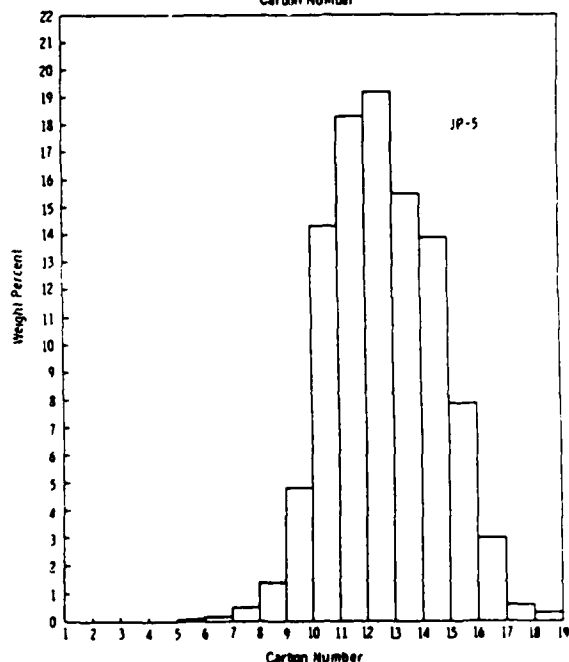


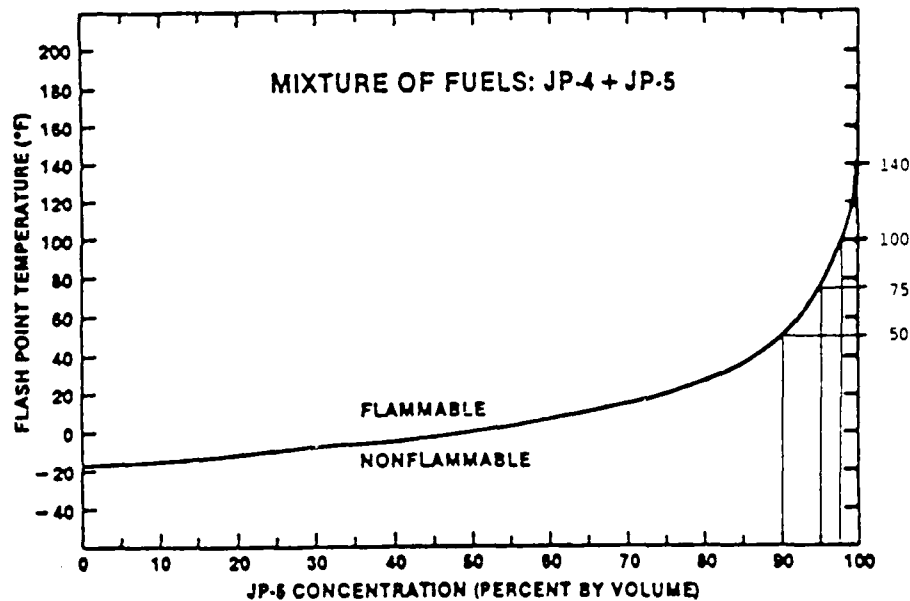
TABLE III. DISTRIBUTION OF HYDROCARBONS IN JP-4, JP-5 AND JP-8, DETERMINED BY SIMULATED DISTILLATIONS. <sup>5</sup>



1. For fire technology, the most important property cited in Table II is the flash point, defined as the temperature above which liquid fuels are prone to break into flame when exposed to a flame source.
2. Based on the increased flash point of JP-8, a preliminary assessment of JP-8 stated that "for conditions encountered during the major portions of normal aircraft operations, JP-8 offers significant fire safety advantage over JP-4. This is contingent on continued rigorous adherence to established safety procedures".<sup>2</sup> (Emphasis added.)
3. Even in "normal" conditions JP fuel compositions vary significantly.<sup>9</sup> Carhart and Leonard<sup>8</sup> have shown that very small amounts of volatile components drastically lower the flash point of a fuel (see Table IV). As shown in Table III, the content of C<sub>1</sub> - C<sub>7</sub> (with flash points below 25° F) in JP-4, JP-5 and JP-8 is typically about 36%, 0.8% and 4%, respectively. Such a JP-8 composition roughly corresponds to a 5%/95% mixture of JP-4/JP-5 in Table IV -- with a flash point of about 75° F, not 125° F as cited in Table II for JP-8. Although most JP-8 stocks might have the higher flash point, it is emphasized: very small amounts of low boiling hydrocarbons drastically lower the flash point. In abnormal situations (e.g., in war, with curtailed fuel stocks), increased probabilities for fuel variations would be anticipated: it may not be prudent to minimize concomitantly increased fire hazards.

TABLE IV. JP-4 in JP-5

Amount (%)	Flash Pt.	Δ Fl. Pt.
0	140	0
2.5	100	-40
5	75	-65
10	50	-90



4. Although running liquid fuel is important in terms of fire propagation, misted fuel can be most important in fire initiation. "In flammability of mists volatility plays a less significant role. Minute fuel droplets in air act like flammable vapor except that a larger and more intense source of ignition may be required."<sup>10</sup> Factors influencing fuel ignition temperatures will be discussed in detail subsequently in this report.

#### C. Cost, Availability, Performance.<sup>1-16</sup>

1. JP-8 costs are decreasing, relative to JP-4, and availability increasing, due to petrochemical demand for low molecular weight JP-4 components.
2. JP-8 would result in some loss of low temperature

start-up and altitude relight capability. Decreased hydrocarbon emissions result in some cost savings; smoke/particulate emission increases can be expected.

#### D. Fire Safety Hazards.

1. Refuelling. For refuelling (in the field, in aircraft shelters, or on Navy carriers), JP-8's decreased volatility provides obvious safety advantages.<sup>16-17</sup> JP-5 has entirely replaced JP-4 in Navy operations at sea; and the Navy has requested conversion by the Air Force to JP-8 to obviate problems of serious increases in fuel volatility aboard carriers, from refueling of Navy aircraft by Air Force tankers laden with JP-4.<sup>18</sup>
2. Spills and leakage. "Low volatility fuels (e.g., JP-8) are more prone to dripping, particularly at lower temperatures."<sup>5</sup> Also, low volatility fuels evaporate more slowly and tend to accumulate. Thus, JP-8 can be a greater hazard than JP-4, by accumulating in ullage or engine spaces and then enflaming on contact with static electricity or hot engine surfaces.
3. In-flight gunfire effects. Table V shows results of horizontal gunfire through small fuel tanks containing JP fuels, observing incidence of fires in tank ullages. Surprisingly, JP-4 flashed rarely; but when it did sustained fires resulted (due to the high volatility). Even more surprisingly, sprays of low volatility JP-5 and JP-8, ejected into the ullage as the round passed through the tank, flashed a great majority of the time.<sup>19</sup>



TABLE V. LIQUID FUEL .50 CAL HORIZONTAL GUNFIRE TESTS

Fuel	Total tests	% No reaction	% Flash fires	% Fires sustained
JP-4	86	30.2	1.2	68.6
JP-8	65	23.1	73.8	3.1
JP-5	51	23.5	76.5	0

Other (vertical and horizontal) gunfire tests were also performed.<sup>20-23</sup> With larger tanks, no significant differences between JP-4 and JP-8 were observed in terms of sustained fires -- these predominated for both fuel types. When JP-4 fires occurred, peak overpressures were greater than with JP-8, due to higher JP-4 volatility. High altitude (low temperature/low pressure) tests were not attempted.

A major result of this research project (discussed below) has been an explanation for this apparently anomalous inverse relationship of ignition temperature with fuel volatility. This will be discussed below.

#### E. Fire Safety and Fire Fighting Techniques

The NIMITZ (CVA-68) Fire. On 26 May 1981 an EA-6B crashed into several F-14's while attempting to land on the NIMITZ. In the ensuing fire 14 men were killed and 42 injured, with \$60 million damages (\$53 million in destroyed or damaged aircraft). In a definitive study of this fire the following observations were made:<sup>24</sup>

- a. Fire fighting efforts began immediately after the crash.
- b. Countermeasures AFFF washdown system on flight deck were not initiated until some time after the crash.
- c. Upward zone of washdown system produced only seawater with no AFFF, due to equipment malfunction.
- d. A running fuel fire resulted from at least one fully fueled F-14.
- e. Aircraft were equipped with Sidewinder, Sparrow and Phoenix missiles, and considerable 20 mm ammunition. Handlines were used to project sea water on munitions in an effort to prevent cook-off; but when fire was declared out 19 minutes later, one Sparrow missile detonated, killing two and injuring 29.
- f. There was possible involvement of JP-4 mixture with JP-5 as a result of refuelling from AF tanker.

NRL investigation of the NIMITZ fire included studies of:

- a. JP-4, JP-5 and JP-8 fuels, and mixtures of these.
- b. Wind effects (at 0, 15 and 20 knots).
- c. Ignition and flame spread tests on pools of fuel.
- d. Debris pile fires to study running fuel fires in confined and cluttered situations.
- e. AFFF, Halon 1211 and PKP extinguishing agents.
- f. Application methods and fire fighting tactics.

Conclusions from the NIMITZ investigation. Mixtures of JP-4 with JP-5 or JP-8 result in flash points similar to that of JP-4 alone. Thus, such mixtures have all the hazards of JP-4

in fire fighting situations. Flash point data were deemed to be excellent criteria in correlating fire fighting results with various fuels. In running fuel debris pile fires, AFFF was successful in extinguishing JP-8 and JP-5 fires, but not JP-4 or fuels mixed with JP-4. In wind conditions Halon does not extinguish JP-4, but will extinguish JP-5 and JP-8 fires. With AFFF, Halon will extinguish all such fires in closed conditions, but in open debris conditions AFFF/Halon is good for JP-5 and JP-8, but not JP-4 fires. Wind considerably exacerbates fire fighting problems for all fuels. AFFF is required to prevent flashback in all fires. Particularly for JP-4 fires, use of two fire fighting teams approaching at right angles to each other (with each approaching 45 degrees to the fire front) provides best fire fighting results.

Other Techniques to Mitigate Aircraft Fires. These include use of anti-misting kerosene (AMK) or gelants to prevent fuel mist formation arising from controlled crash landings or gunfire penetration of fuel tanks;<sup>29</sup> and use of halon flood or on-board inert gas generator systems (OBIGGS) to purge fuel compartments of air in such situations.<sup>30</sup>

Although AMK development had not progressed sufficiently to warrant consideration for adoption for military applications, work conducted under FAA auspices indicated that promise existed for ultimate development of a feasible, fail-safe system. A Controlled Impact Demonstration (CID) test was conducted in late 1984 in an attempt to mitigate fuel fires

resulting from the controlled crashing of a Boeing 720 aircraft. Unfortunately, the CID test resulted in a fully developed fire. Despite the facts that it was later established that the full-scale nature of the test was premature; that there was strong evidence that fire effects were indeed mitigated by the use of AMK agent; and that there were extensive research efforts underway in development of more efficient agent systems, the effect of the apparent CID failure test was to terminate this research program.

#### IV. ANOMALOUS INVERSE RELATIONSHIP BETWEEN FUEL IGNITION TEMPERATURE AND VOLATILITY

In the literature search, several anomalies were found which had been reported by other workers, but never correlated.

Gunfire tests.<sup>19-23</sup> The surprising results, that highly volatile JP-4, ejected as spray into ullage as gunfire passed through fuel, flashed rarely; and that JP-5 and JP-8 flashed usually, indicate an inverse relationship between volatility and ignition tendency arising from contact of fuel with hot metal surfaces or by means other than direct flame sources.

Detonation tendencies.<sup>26</sup> Other workers have shown high molecular weight hydrocarbon fuels to be more easily detonated in air than are low molecular weight fuels.

#### Additional experimental evidence:

1. Data pertaining to Flash Point (FP; the temperature at which a liquid fuel has sufficient volatility to ignite

when a flame is passed over it), and Ignition Temperature (IT; the temperature of a metal surface which will ignite fuel vapors in contact with it) data are presented in Table VI for a number of low molecular weight hydrocarbons.

TABLE VI. ALKANE FLASH POINT AND IGNITION TEMPERATURES<sup>25</sup>

Alkane	FP(°F)	IT(°F)	Alkane	FP(°F)	IT(°F)
CH <sub>4</sub>	--	999	C <sub>5</sub> H <sub>12</sub>	-40	588
C <sub>2</sub> H <sub>6</sub>	--	950	C <sub>6</sub> H <sub>14</sub>	- 7	477
C <sub>3</sub> H <sub>8</sub>	--	871	C <sub>7</sub> H <sub>16</sub>	25	452
C <sub>4</sub> H <sub>10</sub>	-76	806	C <sub>8</sub> H <sub>18</sub>	56	450

- In another study,<sup>27</sup> the ignition temperature for a liquid fuel mist was reported to be about the same as for the vaporized fuel. Here, vaporized octane had an ignition temperature 90 °F lower than the corresponding value for hexane. (This is inconsistent with Table V; but these tests were run at different conditions, with different equipment. The trends are consistent.)

It is likely that a viable AMK agent could prevent mist droplet formation and considerably mitigate both flash point and ignition temperature effects for jet fuels.

- In another study<sup>28</sup> it was noted (without further comment) that a more volatile fluid applied to a hot metal surface required a higher temperature to ignite than a much less volatile combustible liquid.

## B. Molecular Structure/Ignition Temperature Correlations.

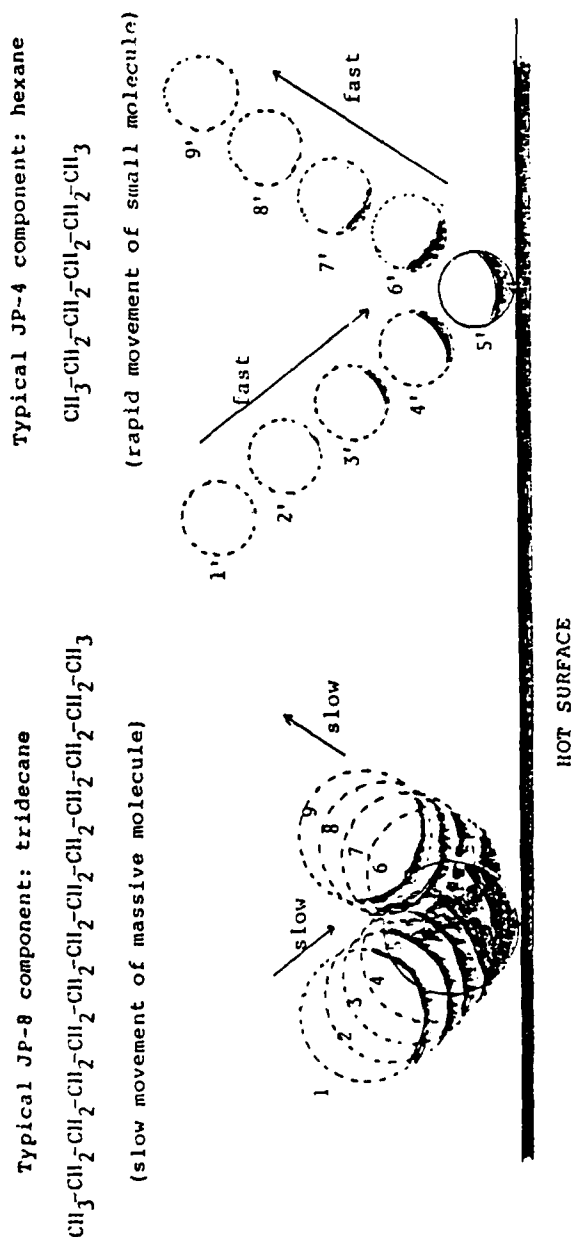
Fuel flammability has largely been predicated on flash points, resulting from exposure of fuel to flame. Low molecular weight (high volatility) fuels have lower flash points and thus are judged more flammable than high molecular weight low volatility fuels. It is now suggested there is sufficient evidence to postulate a routine inverse relationship for any given chemical family, between molecular weight and fuel ignition temperature (occasioned by contact with hot metal surfaces). Thus, less volatile high molecular weight fuels (if of the same family) will have lower ignition temperatures and will be more easily ignited when exposed to hot surfaces. This may be important in fuel selection: if fires are anticipated largely to result from contact with hot metal surfaces, instead of by contact with flame, then low flash point fuels (e.g., JP-4) may actually be safer than less volatile fuels (e.g., JP-8). (However, once a fire has occurred, less volatile fuels would be easier to extinguish.)

Molecular structure effects are illustrated and discussed in Figure 1, to explain the heretofore anomalous lower ignition temperatures for less volatile high molecular weight fuels.

## V. JP-4/JP-8 PROJECT CONCLUSIONS

JP-8 (or analogous Jet A-1) may actually be the worst fuel in some situations as described in this report (i.e., gunfire tests in Table V; and the recent FAA CID test), in view of its

Figure 1. EXPLANATIONS REGARDING LOWER IGNITION TEMPERATURES FOR HIGHER MOLECULAR WEIGHT FUELS



In the above illustration (1), (2), (3), (4) ..... (7), (8), (9) indicate positions of molecules A and B at same time intervals, relative to hot surface area.

The velocity of a molecule at a temperature (T) is inversely proportional to the square root of its molecular weight (M):

$$\text{average velocity} = 14,600 \left( \frac{T}{M} \right)^{\frac{1}{2}} \text{ cm/sec}$$

Thus, the smaller the molecule, the greater its speed at a given temperature.

In the above illustration, the slow moving heavy molecule A is therefore near the hot surface longer than the fast moving light weight molecule B, and therefore A has longer time available to it to absorb energy from the hot radiating surface.

The larger molecule A has more mobile C-C and C-H bonds and therefore more rotational degrees of freedom than the smaller molecule B. Therefore, A will tend to be "mushier" and have less elastic recoil on approach to or impact with the hot surface than does the smaller, more rigid B, which accordingly will "bounce" away more readily and more rapidly. Again, therefore, A will have more time to energize than does B.

Moreover, the massive molecule (B) has greater surface area to present toward the heat radiating surface, and will therefore absorb more heat energy than the low molecular weight molecule A with smaller surface area.

Finally, the larger molecule A has more C-H bonds than does the lower molecular weight molecule B. Statistically, therefore, there are more opportunities for free radical C-H cleavages (necessary for flame initiation and propagation) when energized by the hot surface for the heavier molecule A.

blend of prominent amounts of high and low molecular weight components (see Table III). The higher molecular weight components in JP-8 (or Jet A-1) would ignite more easily than lower molecular weight species, on contact of fuel with hot metal surfaces (hot metal sparks for the gunfire tests, and hot sparks and hot engine surfaces in the CID test). Once the fuel has ignited from this effect, the low molecular weight components would impart low flash point character to the mixture (as shown in Table IV), to sustain the fire.

JP-5 seems to have the best safety characteristics. Although its high molecular weight components will ignite most easily on contact with hot metal surfaces, its low volatility would discourage flame propagation (as evidenced in the gun fire data of Table V, and in results of the NIMITZ fire fighting studies. JP-4 might, controversially, be better than JP-8, for situations in which fires might result from contact with hot metal surfaces (e.g., gunfire or controlled crash landing situations) rather than from contact with flames.

#### VI. JP-4/JP-8 PROJECT RECOMMENDATIONS.

1. There appear to be variations in methods previously reported for fuel ignition temperature determinations. A standardized technique should be investigated.
2. The possible importance of vapor ignition temperature as a criterion for fuel selection should be studied.
3. The effects of low ambient temperatures and pressures on



ignition temperatures (as would be encountered in high altitude operations) should be investigated.

4. Possible catalytic effects various metals may have on surface temperature ignitions should be studied.
5. Other effects (e.g., from aromatic, olefinic or other substituents) on ignition temperatures of hydrocarbon fuels should be investigated, with experiments performed to determine such effects on a quantitative basis.
6. Structure/property correlations, with particular regard to relationships of ignition temperatures with molecular structure and substituent effects, should be investigated on a theoretical basis. Computer assisted molecular modelling and design techniques can be utilized for this.
7. A leaner cut of JP-8 could be achieved by removing the lower boiling 5% (principally comprised of C - C alkanes, with flash points of 56 F or lower) of the overall distillation fraction. Negative aspects include the obvious fact that fuel stocks would be reduced to 95% of levels otherwise available, and costs of additional fractional distillation would be significant. On a positive basis, offsetting savings would result since lower boiling fractions are valuable for petrochemical applications. Most importantly, the safety afforded by extra low volatility fuel would be very appreciable.
8. Support should be extended to further AMK R&D effort.

VII. REFERENCES (All references are unclassified.)

- (1) Richardson, S.A. "JP-8, A Potential Replacement For JP-4 Jet Fuel"; Air Univ., Maxwell AFB, AL (May 1973).
- (2) Beery, G.T. et al. "Assessment of JP8 as a Replacement for the Air Force Standard Jet Fuel JP4". AFAPL-TR-74-71, Part I; Aero Propulsion Lab, W-P AFB, OH (1975).
- (3) Botteri, B.P. "Flammability Properties of Jet Fuels and Techniques for Fire and Explosion Suppression", AGARD Conferences Proceedings, NATO, pp. 13-1 to 13-11.
- (4) Kuchta, J.M.; Clodfelter, R.G. "Aircraft Mishap Fire Pattern Investigations"; AFWAL-TR-85-2057, Aero Propulsion Laboratory, Wright-Patterson AFB, OH (1985).
- (5) Parts, L.; Bucher, T. J.; Botteri, P.; Cretcher, E. "Integral Aircraft Fuel Tank Leak Classification"; AFAPL-TR-79-2092, Aero Propuls. Lab, W-P AFB OH (1979).
- (6) Frame, E.A. "Behavior of Fuels at Low Temperatures"; Interim Report AFLRL 138; US Army Fuels and Lubricants Res. Lab., Southwest Res. Inst. San Antonio, TX (1980).
- (7) Gardner, L.; Whyte, R. "Jet Fuel Specifications". AGARD Conference Proceedings No. 84 on Aircraft Fuels, Lubricants and Fire Safety", NATO (1984).
- (8) Leonard, J. T.; Carhart, H.W. Nav. Res. Lab. Washington, DC. (Private communication.)
- (9) Ricciardelli, J. "Physical and Chemical Properties of JP-55, 1980-1983"; NAPC-PE-105, Naval Air Propulsion Center, Trenton, NJ (1984).
- (10) Geyer, G. FAA Technical Center, Atlantic City, NJ. (Private communication.)
- (11) Stambovsky, R. "JP-8 Fuel Conversion Evaluation"; Proc., 11th Ann. Symp., Soc. Flight Test Eng., 6.1-6.32 (1980).
- (12) Stambovsky, R.A. "JP-8 Fuel Conversion Tests"; AFFTC-TR-79-28, AF Flight Test Ctr, Edwards AFB, CA (1979).
- (13) Pittman, S.; Smith, J. "Some Civil Engineering Aspects of Conversion from JP4 to JP8 Fuel by the USAF; MS Thesis, Air Force Inst. of Technology, WPAFB, OH (1980).
- (14) Webb, A.T.; Enomoto, N.Y. "F-106A JP-8 Fuel Cold Weather Evaluation"; AFFTC-TR-80-15, San Antonio Air Logistics Center, Kelly AFB TX, 1980.

- (15) Webb, A. "F-5E JP-8 Fuel Climatic Evaluation"; AFFTC-TR-79-23, San Antonio Air Logist. Ctr, Kelly AFB TX (1979).
- (16) Thorne, P.F. "Estimation of the Hazard of Fuelling Combat Aircraft"; Fire International (Dec./Jan.) 1986.
- (17) "JP-4 Flashpoint Danger", Weekly Summary of Aircraft Mishaps (No. 20-83, 15-21 May 1983); NAVAIR.
- (18) NAVSEA ltr ser CHENG/156 of 21 July 1986 to CNO (OP-05).
- (19) Clodfelter, R. "Evaluation of JP8 vs JP4 for Enhancement of Aircraft Combat Survivability"; Proc., 10th Symp., Survival & Flight Equip. Assoc., 1972, p. 85-92.
- (20) Botteri, B.P. et al. "Evaluation of JP-8 vs JP-4 Fuel for Enhancement of Aircraft Combat Survivability"; APFH-TM-70-34, Aero Prop. Lab, W-P AFB OH (1970).
- (21) O'Neill, J. et al. "Aerospace Vehicle Hazard Protection Test Program"; FAA Report AFAPL-TR-73-87 (1974).
- (22) Sommers, D.; O'Neill, J. "AFAPL Aircraft Fire Test Program with FAA 1967-1970"; FAA Report AFAPL-TR-70-93 1971.
- (23) Manheim, J. R. "Vulnerability Assessment of JP-4 and JP-8 Vertical Gunfire Impact Conditions"; AD/A-001 628; Aero Propulsion Lab, W-P AFB OH (1973).
- (24) Carhart, H.W., et al. "Aircraft Carrier Flight Deck Fire Fighting Tactics and Equipment Evaluation Tests"; NRL Memorandum Report 5952, Feb. 1987.
- (25) Lange, N.A. "Handbook of Chemistry", 9th ed. (Handbook Publishers, Inc., Sandusky, OH); pp. 33-49 (1956).
- (26) Matsui, Combust. Inst. Proc. 17th Symp., 1269-80 (1978).
- (27) Demetri, E.P.; White, B.F. "Development of a Model for Hot-Surface Ignition of Combustible Liquids"; AFWAL-TR-85-2090; WP-AFB, OH (1985).
- (28) Myronuk, D. "Dynamic, Hot Surface Ignition of Aircraft Fuels & Hydraulic Fluids"; AFAPL-TR-79-2095, WPAFB 1980.
- (29) Proc. of Fuel Safety Workshop, 1985; FAA, Washington DC.
- (30) Vannice, V.L.; Grenich, A.F. "Fighter Aircraft OBIGGS Study"; AFWAL-TR-87-2024, WP-AFB 1987.

1987 USAF-UES SUMMER FACULTY RESEARCH PROGRAM

Sponsored by the  
AIR FORCE OFFICE OF SCIENTIFIC RESEARCH

Conducted by  
Universal Energy Systems, Inc.

FINAL REPORT

Prepared by: Beryl L. Barber  
Academic Rank: Assistant Professor  
Department: Electronic Engineering Technology  
University: Oregon Institute of Technology  
Research Location: AFRADC/OCTP  
Griffiss AFB NY 13440-5700  
USAF Researcher: Frank E. Welker  
Date: 20 August 1987  
Contract No: F49620-85-C-0013

## MICROWAVE MEASUREMENTS

by

Beryl L. Barber

### ABSTRACT

The testing of MMICs becomes the major cost/time factor in the production/cost of MMICs when the large quantity required is considered.

The theory developed to test a device (MMIC) is considered and a proposed technique is given. Test measurements are based upon the minimum number of set-up changes required, and a maximum yield of information. Qualitative rather than quantitative data is considered.

### ACKNOWLEDGEMENTS

I wish to thank the Air Force Systems Command and the Air Force Office of Scientific Research for sponsorship of this research. Universal Energy Systems must be mentioned for their concern and help in all administrative and directional aspects of this program.

The group under the direction of Mr Frank Welker has been exceptionally helpful in this project which I've undertaken. Mr Ed Jones has supplied me with specifications for various MMIC modules. Mr Mike Little has been exceptionally helpful in acquiring lab equipment and doing a set up in the lab to acquire information necessary to back up these conclusions. Mr Jim Van Damme has supplied me with data and set up required for the MMIC modules. I would like to especially thank Mr Tom McEwen for questioning my methods and in reading reports as well as in supplying computer data to back up lab work. I would like to thank Mr Bobby Gray, also, for his assistance in pulsing techniques. I believe these people have contributed greatly to the success of this project. Mr Frank Welker, in addition to being manager of the group, has also been very helpful in various peripheral items concerned with the project. I must also give a lot of credit to Beverly Sargent for her help and patience in typing of this report.

## MICROWAVE TESTING

### Test Procedures and Techniques for Large Quantity Testing of Integrated MMIC Transceiver Modules

I. INTRODUCTION. The development of MMICs provides the basis for large active phased arrays. These may be categorized into two general categories:

- a. Phased Arrays using a steerable mounting, and
- b. Electronically steerable arrays.

The mechanically steered phased array has been in existence for some time. These are usually small arrays and require only phase adjustments in their original installation. The transmitters are usually a power divided thermionic device.

Electronically steered phased arrays offer many new options in the radar field. These are arrays in which there is no mechanical movement and the field is scanned using electronically controlled phase shifters. Among other things, they offer very rapid searching. These arrays may be very large (such as PAVE-PAWS) and offer new options and overall reliability not seen before.

The MMIC offers an additional advantage over other arrays in that the transmitter is included in each module or in as many modules as desired. This provides an all solid state radar.

The major cost factor in the production of large arrays is in the testing and/or acceptance of each module. This is even more difficult when taking into consideration the pulse operation of a radar.



## II. OBJECT OF THE RESEARCH EFFORT

A phased array may be made up of hundreds or thousands of individual MMIC modules. Individual testing may take several man days to test each module. There is not enough time, if we disregard cost and other factors, to test an array of say 64 by 32 elements. Therefore, new testing techniques have been devised. This effort covers the complete testing of a transmit/receive module to determine acceptance-rejection data in a minimum timeframe.

Testing would be divided into three or four categories. The first would involve the complete testing of a first article(s) which would include at least two items to obtain reference points. This would then be performed on .1 to 1 percent of the total. The second category would involve limited testing of gain vs frequency, phase linearity, insertion phase, phase shifter operation, saturation of transmitter module, and noise figure. The third category would involve testing techniques described in this paper. A possible fourth category would be the retesting under category one or two of those items failing the category three test.

### III. TESTING

The testing of a transmit/receive module becomes very lengthy due to different set-ups required and the many points of data for each module. This, coupled with the large quantity of modules represents man years of testing. It is, therefore; desirable to reduce testing to a go-no-go situation or at least a selection level of testing.

To better understand the problem let us consider three specifications of interest. First, a gain vs frequency plot for both the transmit and receive sections are required. Secondly, a phase vs frequency plot for both transmit and receive sections are needed. The third item is receiver noise figure. Other additional tests are desired, but let us first consider the above.

Given any sine or cosine wave, we may express it as:

$$e = E_m \cos(\omega t + \phi) \quad (3-1)$$

where "e" represents the instantaneous voltage with respect to time and " $E_m$ " is the peak voltage in the cycle. Then, of course,  $\omega$  is the frequency in radians and  $\phi$  represents the phase angle. We can also express this as:

$$e = E_m e^{j\omega t} e^{j\phi}$$

and rearranging

$$\frac{e}{E_m} = e^{j\omega t} e^{j\phi} \quad (3-2)$$

We can now evaluate at  $t=0$  and  $\omega = n\pi$ . Therefore,

$$\frac{e}{E_m} = e^{j\phi} \quad \text{and if } e = E_m \text{ then}$$

$$j\phi = 0$$

We can also take the natural logarithm of both sides and find that:

$$\ln \frac{e}{E_m} = j\phi \quad \text{where } j \text{ represents a } \frac{\pi}{2} \text{ phase shift.}$$

$$\text{Again if } e = E_m \text{ then } \phi = 0$$

If we now take the derivative of

$$\ln \frac{e}{E_m} = j\phi \quad \text{then } d\left(\ln \frac{e}{E_m}\right) = d(j\phi) \quad (\text{note } j)$$

and  $\frac{E_m}{e} = d\phi$  remembering that we are evaluating the cosine function at 0 and  $n\pi$ , which tells us that if the amplitude response of the unit is flat then  $\Delta\phi$  will be zero.

Looking now at the system bandwidth necessary for evaluation of a  $1\mu\text{sec}$  pulse, we should have at least a 2 MHz bandwidth. We are making measurements at the peak voltage (whether peak or rms) and are ignoring harmonic content. In comparing the complete system - receiver

bandwidth and transmitter bandwidth - this should be a valid assumption.

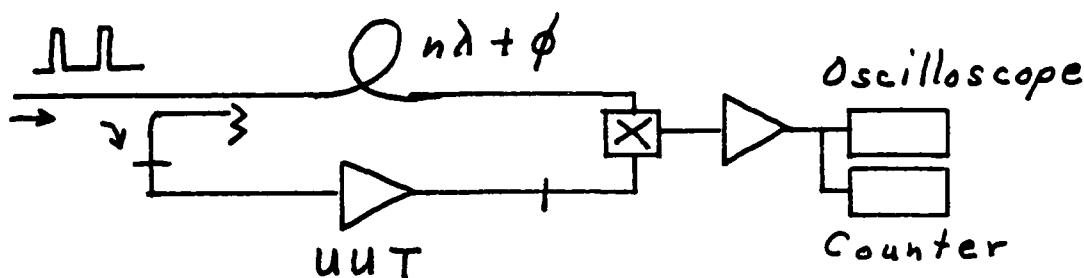
The equation  $\frac{E_m}{e} = d\phi$  also tells us that  $d\phi$  is not dependent upon the input signal level, but only upon the ratio  $E_m/e$ . This, of course, will be a function of the threshold sensitivity of the test set-up.

Preliminary results of the phase measuring system confirm the above. In the lab we were able to obtain a deflection on the oscilloscope of 1 cm/degree in phase using a  $1\mu\text{sec}$  pulse and a 10 KHz rep rate. Changing the input power by 20 db did not give a detectable change in our results.

Several things should be noted from the above. In using this technique we are evaluating our phase at 0 and  $\pi$  radians. Therefore, our values are a sine function and will be very accurate at values close to zero degrees. Accuracy will decrease as the sine function approaches 90°: This will make it necessary to switch phase in our reference arm to measure other phase angles, (i.e., 22½°, 45°, 90°, etc.).

We should also know the total length of both channels as this will effect our CM/° sensitivity. In actuality it will be somewhat sensitive to harmonics, but this can be easily noted by the  $\pm$  phase readings.

This circuit gives us a microwave, pulsed phase discriminator.



Relating the above to the overall frequency response, we find that the phase characteristics are proportional to the first derivative of the gain response. Further, the group delay of an amplifier is proportional to the derivative of the phase response and can, therefore, be concluded to be proportional to the second derivative of the gain response.

We may now look at the overall problem of production testing.

Many techniques are used to measure gain and by definition they all compare the output power or voltage to the input power or voltage. The easiest being that of using a leveled and calibrated input and then measuring the output. In order to obtain a high degree of accuracy the HP8410/HP8510 uses a ratio meter technique with enhanced accuracy. The major problem with the use of this system is that

processing is done at the IF frequency (100 KHz for the 8510 and 278 KHz for the 8410) and bandwidth is insufficient for short (less than 200  $\mu$ sec) pulse testing.

Receiver testing is such that it can be done in a C.W. mode, but the transmitter works on a saturated, duty cycle basis and must be tested using a short pulse say  $\mu$ sec or less.

A system can be made using a high IF frequency with wide bandwidth and two channels that would incorporate the ratio meter technique. (If we further use a image suppression technique with wide band video we could use dual pulse cancellation measurements). As this is the system similar to which we measure phase changes, we can design a single test set-up to measure both phase and gain.

Looking further at the overall testing/specification problem:

It does not appear necessary that we even measure input or output VSWRs to the module. The module will be specified operating into a three or four to one VSWR and by incorporating this into the test setup we may check the frequency response curve with that VSWR and if the module operates correctly it should be unnecessary to even specify VSWR. The VSWR should have a definite effect upon the gain vs frequency response curve and also upon our noise figure for the module. Gain vs frequency measurements must be made in two sections; one in the transmitter section and the other in the receiver section. The transmitter section should be measured in a saturation situation

(that is in approximately 1 db saturation). Testing has shown that the phase characteristics will closely follow the overall gain vs frequency response even in the saturated mode of the transmitter. It should be noted that in all measurements it will be necessary to have the same number of wave lengths in the reference arm as in the test arm; therefore, some type of phase shift must be incorporated in this arm. The above should be incorporated in the module test fixture.

## SUMMARY OF TEST PROCEDURE

A sample unit should be both vibration and temperature tested. A set (however many you choose) should be checked for form, fit, and function. These checks should not be necessary on production items.

Production testing can be done in four steps. The first two steps will be that of a gain vs frequency curve of the transmitter and receiver. The third measurement will be that of phase shifter test and the last test will be a noise figure test.

## GAIN VS FREQUENCY MEASUREMENT

The module is installed in the test fixture, with suitable input and output impedances, and the system set up for a sweep of the entire band. The first sweep will drive the transmitter into compression and the gain vs frequency response noted. This will be done in the pulse mode.

The module will then be switched to the receive condition and the input power reduced to provide a linear output. The system will again be swept and the gain vs frequency response noted.

Insertion phase can now be inserted, but in order to use a gain-phase technique it is necessary to balance the RF bridge phase-wise so it is necessary to add or extract an equal amount of phase length. This



should be done for each phase shift bit.

(Note: Due to the high VSWR a large reflection coefficient will be found).

#### NOISE FIGURE MEASUREMENT

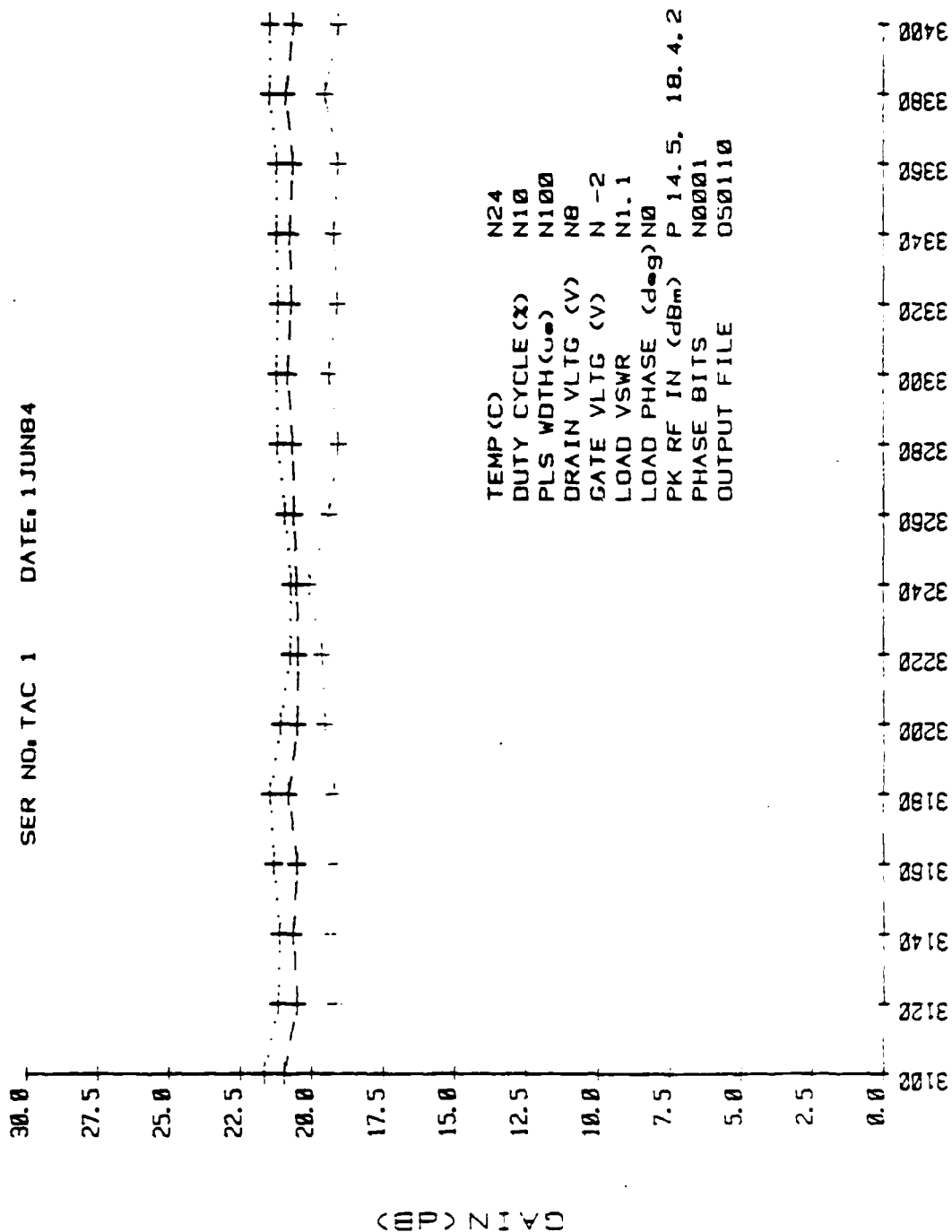
Noise figure measurements are always difficult to make even under the most favorable conditions. Even NBS will only certify approximately 10 percent. Therefore, the most accurate noise measurements should be done on a small number of modules. These will then be inserted in a receiver system and a minimum detectable signal measurement taken. This will then be used as a reference and the remaining modules measured by simply measuring MDS. Those failing an MDS can be rechecked by measuring noise figure. Using this technique it would be expected to have less than .1 percent failures.

#### PHASE ACCEPTANCE

First article test will show the relationship between amplitude and phase variation. Fundamentally, if the gain vs frequency response is flat the phase response will be linear. The amplitude response should be monotonic. (For an amplifier, 0.2 db amplitude ripple results in approximately  $8^\circ$  phase deviation.). We can now relate phase variation to gain ripple and it is unnecessary to measure phase directly.

# T/R MODULE

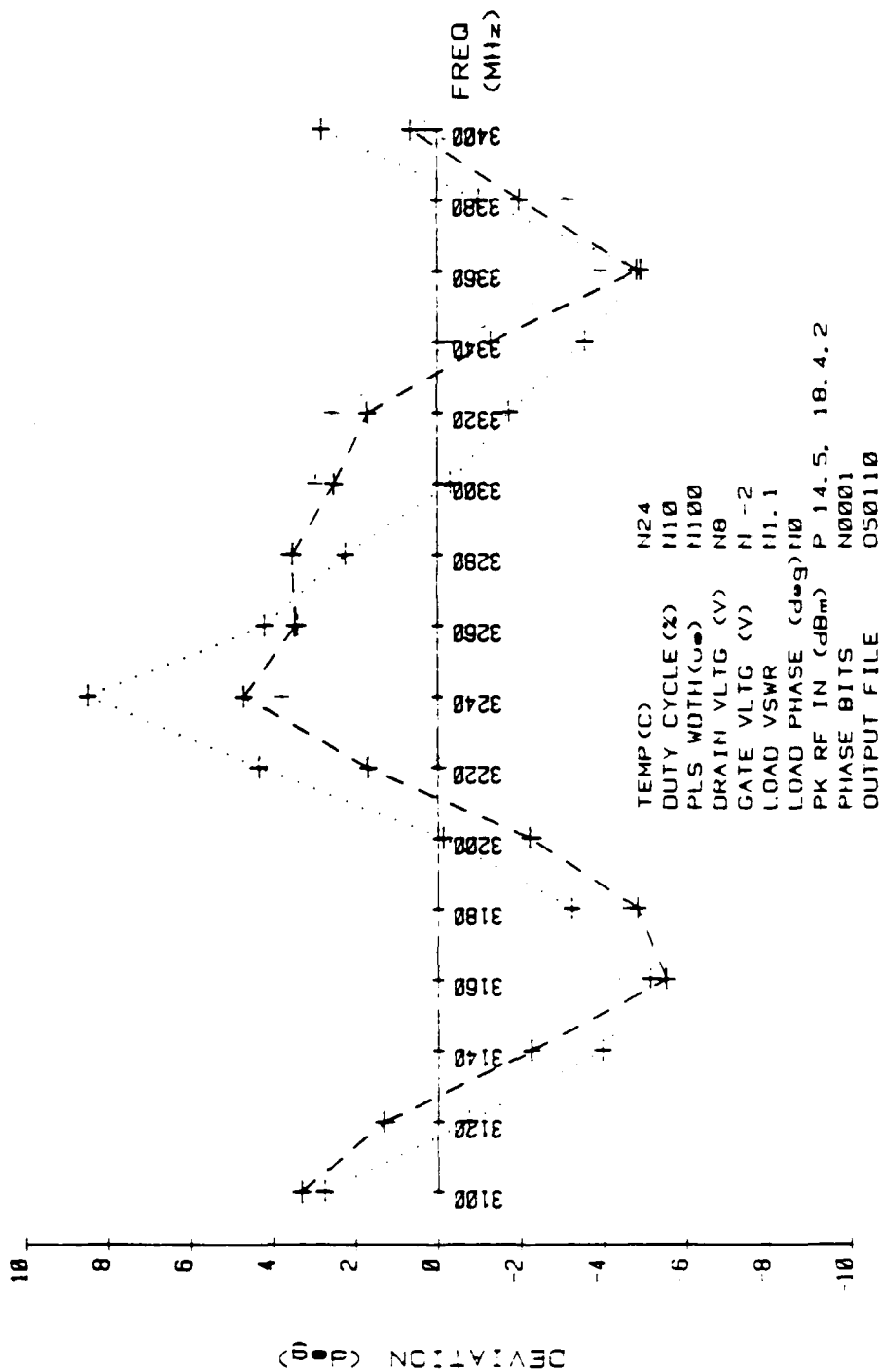
SER NO. TAC 1 DATE: 1 JUN 84



KEY: 14.5, 16.4, 18.4  
PARAMETER: PK RF INPUT +/- 0.9 (dBm)

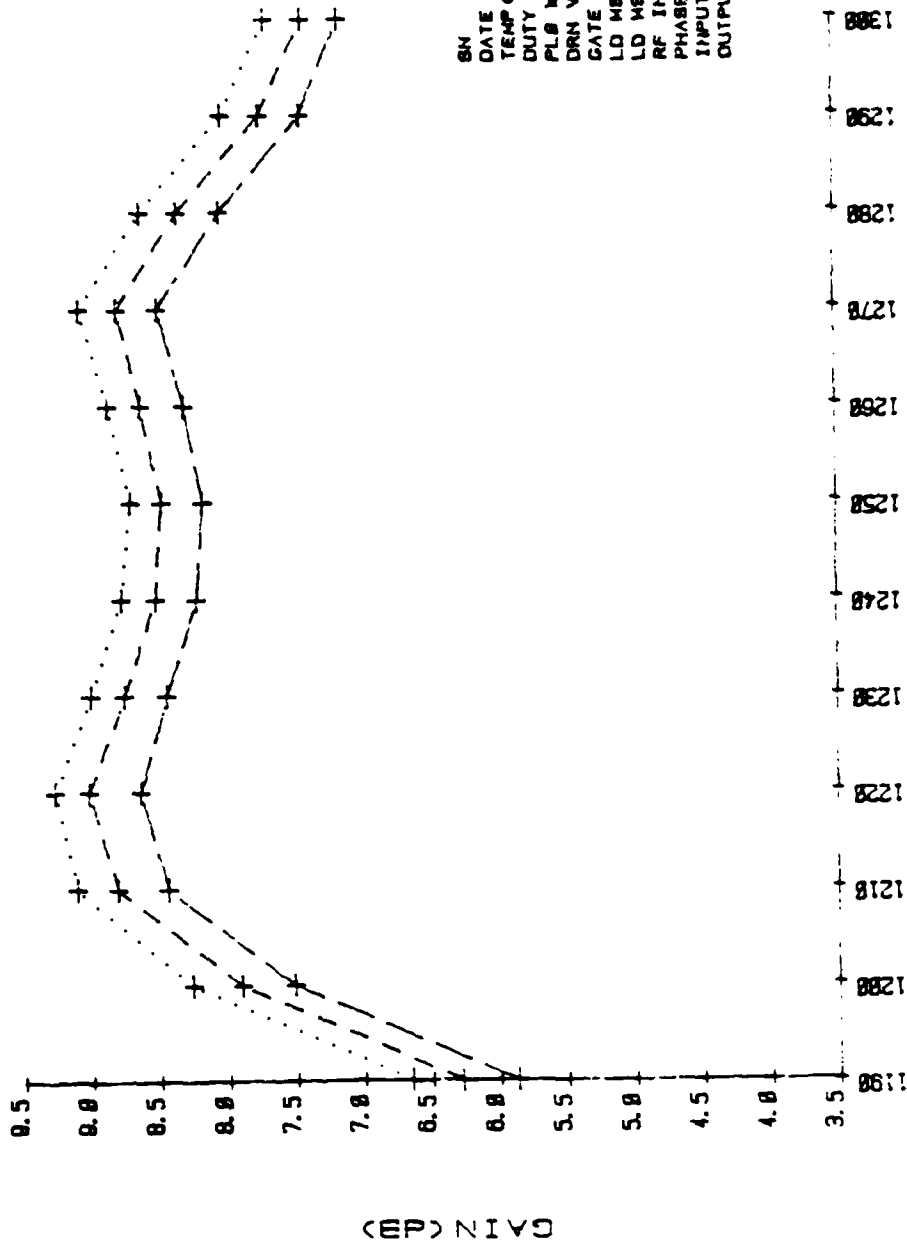
# T/R MODULE PHASE LINEARITY

SER NO. TAC 1 DATE, 1JUN84



KEY: 14.5 16.4 18.4  
 PARAMETER: PK RF INPUT 14.5 16.4 18.4 (dBm)

# T/R MODULE

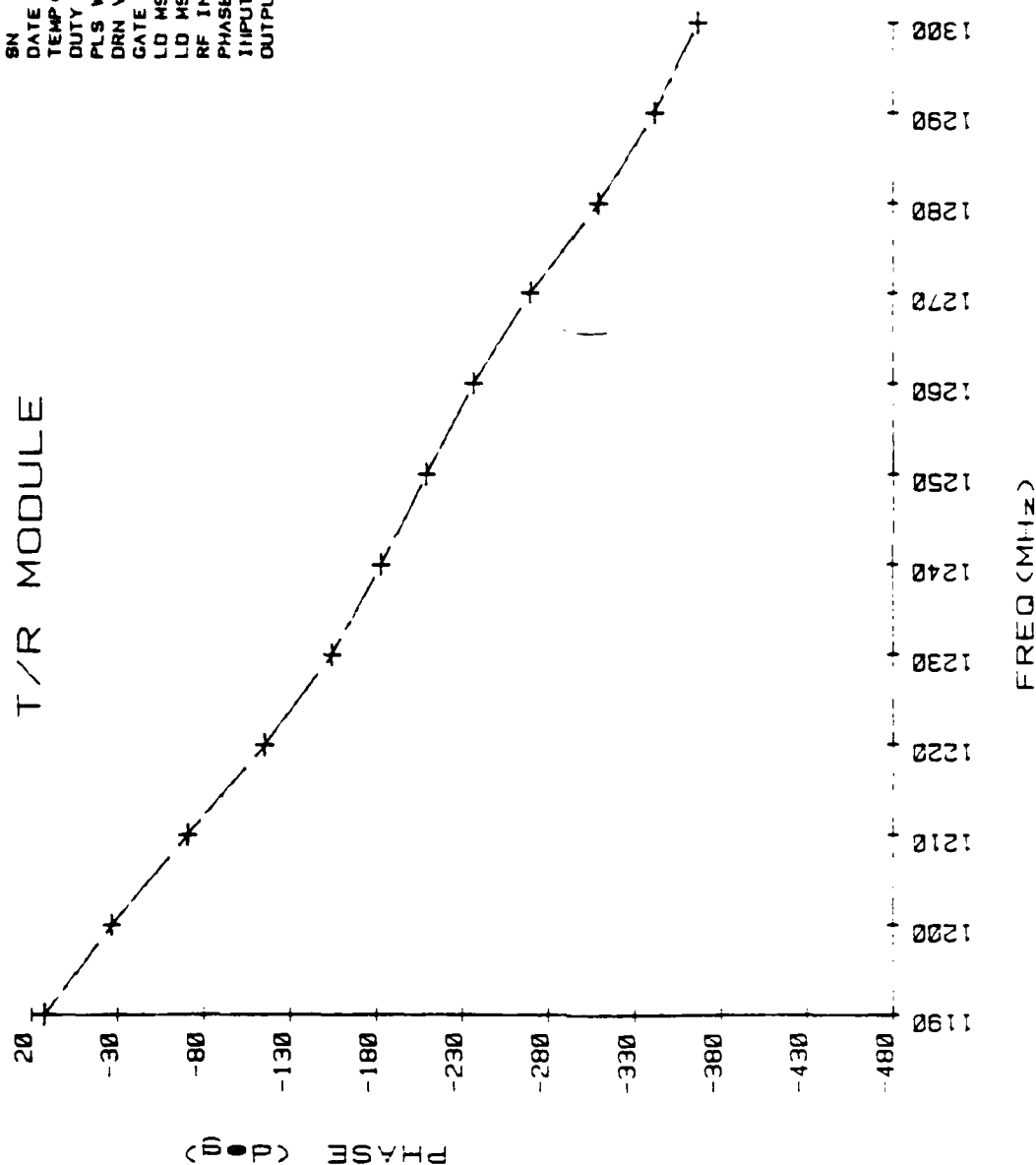


SN 10AUC93  
 DATE N24  
 TEMP (C) P10, 20, SN20  
 DUTY CYCLE (C) N100.0  
 PL0 WIDTH (u) N0.0  
 DRN VLTGE (V) N15.0  
 GATE VLTGE (V) N0.0  
 LD M0MTCN (dB) N0.0  
 LD M0MTCN (dB) N0.0  
 RF INPUT (dBm) N10.0  
 PHASE BITS N0  
 INPUT FILE 100004  
 OUTPUT FILE F00012

KEY, 10.0 FREQ (MHz) UNCLASSIFIED  
 PARAMETER, 15.0 DUTY CYCLE (%) 20.0

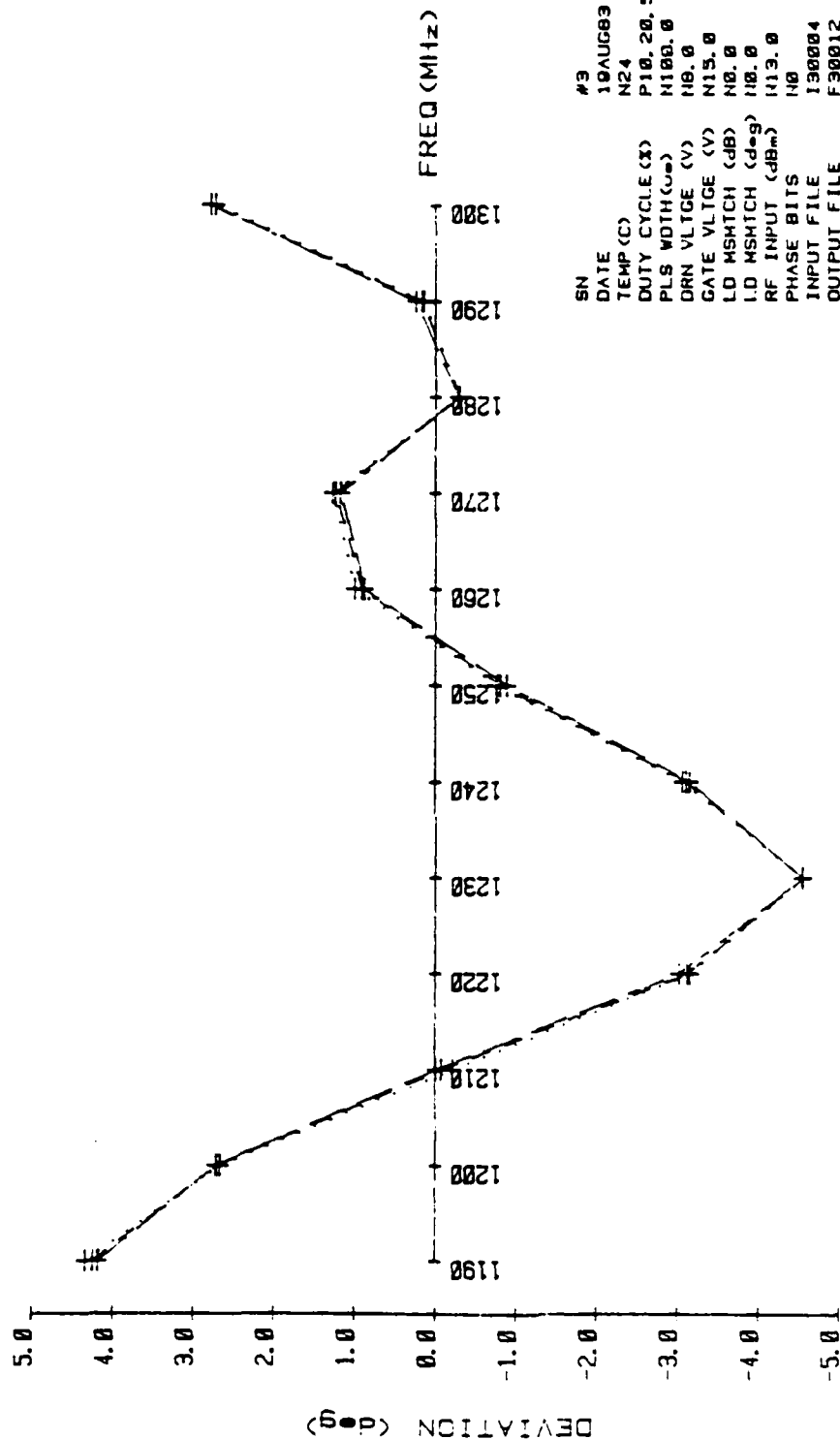
# T/R MODULE

SN 43  
 DATE 19AUG83  
 TEMP (C) N24  
 DUTY CYCLE (%) P10.28, 5K28  
 PLS WIDTH (us) N100.0  
 DRN VLTGE (V) N8.0  
 GATE VLTGE (V) N15.0  
 LD MSWITCH (dB) N0.0  
 LD MSWITCH (deg) N0.0  
 RF INPUT (dBm) N13.0  
 PHASE BITS N0  
 INPUT FILE 130004  
 OUTPUT FILE F30012



KEY: 10.0 15.0 20.0

# T/R MODULE PHASE LINEARITY



SN #3  
 DATE 19AUG83  
 TEMP (C) N24  
 DUTY CYCLE (%) P10.20, 5N20  
 PLS WDTN (ms) N100.0  
 DRN VLTGE (V) N0.0  
 GATE VLTGE (V) N15.0  
 LD MSMTCH (dB) N0.0  
 LD MSMTCH (deg) N0.0  
 RF INPUT (dBm) N13.0  
 PHASE BITS N0  
 INPUT FILE 130004  
 OUTPUT FILE F30012

KEY: 10.0 15.0 20.0

1987 USAF-UES SUMMER FACULTY RESEARCH PROGRAM/  
GRADUATE STUDENT SUMMER SUPPORT PROGRAM

Sponsored by the  
AIR FORCE OFFICE OF SCIENTIFIC RESEARCH

Conducted by the  
Universal Energy Systems, Inc.

FINAL REPORT

IDENTIFICATION TECHNIQUES USING FRAGMENTARY

HUMAN BONE

Prepared by: William M. Bass, Ph.D.  
Academic Rank: Professor and Head  
Department and Anthropology Department  
University: University of Tennessee, Knoxville  
Research Location: Mortuary Services  
Tyndall Air Force Base  
Panama City, FL. 32403-6001  
USAF Researcher: Mr L. H. Nester  
Date: August 7, 1987  
Contract No: F49620-85-C-0013

IDENTIFICATION TECHNIQUES USING FRAGMENTARY

HUMAN BONE

by

William M. Bass, Ph.D. D.A.B.F.A.

ABSTRACT

Air Force crash investigators are frequently required to identify crash victims from fragmentary remains. Research, training and development of techniques using all available scientific methods in human osteology, especially bone fragments, are essential to the proper performance of the investigators duties. Current techniques in Forensic Anthropology, and specific areas of research needs of human identification experts were explored.



### Acknowledgements

I wish to thank the Air Force Systems Command and the Air Force Office of Scientific Research for sponsorship of this research. Universal Energy Systems is gratefully acknowledged for their concern and help to me in all administrative and directional aspects of this program. The Engineering and Services Center at Tyndall Air Force Base, FL. was a pleasant place to work and Major Larry Bramlitt and Major Pat Eagan, my Effort Focal Point officers were efficient, courteous and extremely helpful in making my stay at Tyndall a productive experience.

My experience was rewarding and enriching because of many different influences. Mr L. H. Nester, Chief of Mortuary Services, and his staff of Mortuary Specialists, Brad Bates, Cam Beauchemin, Donn Durham, Gary Huey, Pete Kay and Jeannette Laningham taught me much about every day problems facing the mortuary personnel. Special appreciation is extended to Pete Kay, Brad Bates and Gary Huey, the identification specialists, who oriented me to their specific needs. The demand on their time and the variety of knowledge and expertise they must have is staggering. Linda White and Pamela Yohn were especially patient in answering my many questions. The Mortuary Services Office has an atmosphere conducive to promoting efficiency.

## I. INTRODUCTION:

Air crashes and the frequently mutilated and fragmented conditions of victims offer special problems in human identification to the investigators and mortuary specialists. Training in techniques of determining age at death, sex, race, stature and other identification criteria are required for positive identifications to be made. Personnel involved in identification of fragmentary remains must stay current in their training and need to know the latest developments being published in the literature and be able to communicate their special needs to researchers in this area. While this is only one of many areas in which they work, it is an extremely sensitive one. They must be able to make some basic identifications and be able to critique work of others to some degree.

My training and expertise is in Forensic Anthropology. Past experiences at training human identification specialists in a two-week course in human osteology for the Air Force preceded my summer research appointment. I needed the total involvement with the program in order to assess needs and better direct future research toward solving real problems faced by the Air Force identification specialists.

## II. OBJECTIVES OF THE RESEARCH EFFORT:

The focus of this summer's effort can be grouped into four (4) major areas: A. Research, B. Training, C. Identification, and D. Forensic Laboratory.

### A. Research:

The objective was to identify areas of need and to formulate plans for accomplishing the research. Research in human identification techniques is difficult to do in the Air Force since the military has no large documented skeletal collection. Research projects are therefore much easier performed by association with faculty in universities or museums that contain large well documented skeletal collections. We have one of the largest skeletal collections at the University of Tennessee, outside of the Smithsonian Institution, and we make use of all skeletal collections in our research.

There is an urgent need for research in two major areas not, as yet, approached by other researchers; commingling and stature estimations from fragmentary long bones. Commingling occurs when the skeletal remains of two or more individuals are mixed together. Some techniques have been proposed for separating the mixed remains of multiple individuals into separate persons but none of the techniques have been proven to be as accurate as they should be. A considerable amount of basic research, using new and different approaches needs to be applied here before meaningful results can be expected.

The estimation of stature from whole, long bone has been a subject researched by a number of people and fairly accurate formula exist for all of the major racial groups. Plane crashes, however, result in extensive fragmentation. The previous attempts to predict stature from fragmentary bones (Steele and McKern 1969) have not been successful, mainly because of the inability to locate the necessary landmarks. I discussed with Mr Nester and the identification specialists the possibility of developing a research project to predict stature from fragmentary long bones based on a proportional measurement of the bone which I plan to submit for continued work this year.

#### B. Training:

The objective was to identify areas where further training was needed and to provide training as it would fit with our other objectives.

The Air Force Mortuary Services Office is divided into a disposition section and an identification section. Two of the three mortuary specialists in the identification section, Bates and Kay, had taken my course in fragmentary human osteology and techniques in determining age, sex, race and stature of skeletal remains. Mr Gary Huey transferred from the disposition to the identification section and some time was spent training Mr Huey in forensic techniques. In addition, I answered specific questions raised by Bates and Kay and informed all three of research reported in the literature that will help in the performance of their duties. I critiqued methods of choosing those techniques most viable in the performance of their duties. At the same time, I was reviewing for development of methodology for use in the research project.

A sample of the type of articles covered are as follows (please see references at the end for complete citations.):

#### Animal vs Human

Owsley, D. W. et al

1985 Case involving differentiation of deer and human bone fragments.

#### Aging

Iskan, M. Y., S. R. Loth and R. K. Wright

1984 Age estimation from the rib by phase analysis: white males

1985 Age estimation from the rib by phase analysis: white females

Iskan, M. Y. and S. R. Loth

1986 Determination of age from the sternal rib in white males: a test of the phase method

1986 Determination of age from the sternal rib in white females: a test of the phase method

Katz, D. and J. Suchey

1986 Age determination of the male os pubis

Mann, R. W. and W. M. Bass

1987 Maxillary suture obliteration: aging of the human skeleton based on intact or fragmentary maxilla

Webb, P.A.O. and J. Suchey

1985 Epiphyseal union of the anterior iliac crest and medial clavicles in multiracial sample of U.S. males and females

#### Burning

Bradtmilller, B. and J. E. Buikstra

1984 Effect of burning on human bone microstructure: a preliminary study

Carr, R. F., R. E. Barsley and W. D. Davenport

1986 Postmortem examination of incinerated teeth with the Scanning Electron Microscope

#### Handedness

Glassman, D. M. and W. M. Bass

1986 Bilateral asymmetry of long arm bones and jugular foramen: implications for handedness

#### "Harris Lines"

Garn, S. M., et al

1968 Lines and bands of increased density

Symes, S. A.

1983 Harris Lines as indicators of stress: an analysis of Tibia from the Crow Creek Massacre victims

### Identification

Iten, Peter X.

1987 Identification of skulls by video superimposition

### Race

Iskan, M. Y., S. R. Loth and R. K. Wright

1987 Racial variation in the sternal extremity of the rib and its effect on age determination

### Sex

Dittrick, J. and J. Suckey

1986 Sex determination of prehistoric Central California skeletal remains using discriminate analysis of the femur and humerus

Holland, T. D.

1986 Sex determination of fragmentary crania by analysis of the cranial base

Iskan, M. Y.

1985 Osteometric analysis of sexual dimorphism in the sternal end of the rib

Iskan, M. Y. and P. Miller-Chaivitz

1984 Discriminant function sexing of the Tibia

The listed references are only a sample of literature surveyed but are ones that will aid the Air Force identification specialist to better perform his jobs. Time was spent reviewing x-ray identification and in

covering basic techniques of age, sex, race and stature determination from human skeletal remains.

#### C. Identification:

Occasionally, an identification case is encountered in which all standard techniques either do not work or, because of lost or missing material, cannot be used. We have worked on such a case this summer.

In August 1976, an airman stationed in Greenland drowned in a boating accident. Attempts to locate the body were unsuccessful and the search was terminated. In October 1986, a partially clothed skeleton was found frozen in the ice further down stream from where the airman disappeared ten years earlier. Attempts to positively identify the individual met with failure because no dental records could be located. The only before death x-ray that could be located was a chest x-ray that had been reduced to microfilm form. I have computer enhanced this early x-ray and am in the process of comparing x-rays of the separate bones from the vertebral column with the computer enhanced before death chest x-ray. We have been able to make a positive identification. This is yet a third area where future research is needed. I plan to explore the use of computer enhancement in identification this year.

I spent two days aiding the mortuary identification specialists on a F-4 crash at Eglin AFB in Ft Walton Beach, FL. This experience exposed me to the many problems faced by the Air Force crash investigators.



#### D. Forensic Laboratory

When I arrived on June 1, 1987, the Mortuary Services Division was in the process of moving into a new and larger Forensic Laboratory. I aided the two identification team members in setting up the equipment in the new lab. I took the opportunity to repair the human skeletal material used for teaching and as comparative material and to obtain a better understanding of the problems and methods used by the identification team.

### III. RECOMMENDATIONS:

#### A. Research:

Upon my return to the University of Tennessee, where a large, well documented skeletal collection is housed, I will process through the University of Tennessee a proposal for determining stature from fragmentary long bones. I shall be submitting a proposal for this project within the next few weeks.

#### B. Training:

Identification specialists dealing with air crashes are constantly faced with problems of identifying fragmentary remains, especially skeletal remains. A course on fragmentary human osteology should be offered every few years so that the investigators can keep this skill at a functional level. I will continue to keep the mortuary affairs personnel apprised of new forensic techniques and of new publications that relate to their areas.

## REFERENCES

- Bradt Miller, B. and J. E. Buikstra, "Effect of Burning on Human Bone Microstructure: a Preliminary Study," Jour. of Forensic Studies, 1984, 29:535-540.
- Carr, R. F., R. E. Barsley and W. D. Davenport, "Postmortem Examination of Incinerated Teeth with the Scanning Electron Microscope," Jour. of Forensic Sciences 1986, 31:307-311.
- Dittrick, J. and J. Suchey, "Sex Determination of Prehistoric Central California Skeletal Remains Using Discriminate Analysis of the Femur and Humerus," Amer. Jour. of Physical Anthro. 1986, 70:3-9.
- Garn, S. M., F. G. Silverman, K. P. Hertzog and C. G. Rohmann, "Lines and Bands of Increase Density." Medical Radiography and Photography, 1968, 44:58-89.
- Glassman, D. M. and W. M. Bass, "Bilateral Assymetry of Long Arm Bones and Jugular Foramen: Implications for Handedness," Jour. of Forensic Sciences 1986, 31:589-595.
- Holland, T. D., "Sex Determination of Fragmentary Crania by Analysis of the Cranial Base," Amer. Jour. of Physical Anthro. 1986, 70:203-208.
- Iskan, M. Y., "Osteometric Analysis of Sexual Dimorphism in the Sternal End of the Rib," Jour. of Forensic Sciences 1985, 30:1090-1099.

Iskan, M. Y. and P. Miller-Chaivitz, "Discriminant Function Sexing of the Tibia," Jour. of Forensic Sciences 1984, 29:1087-1093.

Iskan, M. Y., S. R. Loth and R. W. Wright, "Age Estimation from the Rib by Phase Analysis: White Males," Jour. of Forensic Sciences 1984, 29:1094-1104.

Iskan, M. Y., S. R. Loth and R. W. Wright, "Age Estimation from the Rib by Phase Analysis: White Females," Jour. of Forensic Sciences 1985, 30:853-863.

Iskan, M. Y. and S. R. Loth, "Determination of Age from the Sternal Rib in White Males: a Test of the Phase Method," Jour. of Forensic Sciences 1986, 31:122-132.

Iskan, M. Y. and S. R. Loth, "Determination of Age from the Sternal Rib in White Females: a Test of the Phase Method," Jour. of Forensic Sciences 1986, 31:990-999.

Iskan, M. Y., S. R. Loth and R. K. Wright, "Racial Variation in the Sternal Extremity of the Rib and its Effect on Age Determination," Jour. of Forensic Sciences 1987, 32:452-466.

Iten, P. X., "Identification of Skulls by Video Superimposition," Jour. of Forensic Sciences 1987, 32:173-188.

Katz, D. and J. Suchey, "Age Determination of the Male Os Pubis," Amer. Jour. of Physical Anthro. 1986, 69:427-435.

Mann, R. W. and W. M. Bass, "Maxillary Suture Obliteration: Aging the Human Skeleton Based on Intact or Fragmentary Maxilla," Jour. of Forensic Sciences 1987, 32:148-157.

Owsley, D. W., A. M. Mires and M. S. Keith, "Case Involving Differentiation of Deer and Human Bone Fragments," Jour. of Forensic Sciences 1985, 30: 572-578.

Steele, D. G. and T. W. McKern, "A Method of Assessment of Maximum Long Bone Length and Living Stature from Fragmentary Long Bones," Amer. Jour. of Physical Anthro. 1969, 21:215-228.

Symes, S. A., "Harris Lines as Indicators of Stress: An Analysis of Tibia from the Crow Creek Massacre Victims," M. A. Thesis in Anthropology, Univ. of Tennessee, Knoxville.

Webb, P. A. O. and J. Suchey, "Epiphyseal Union of the Anterior Iliac Crest and Medial Clavicles in a Modern Multiracial Sample of U. S. Males and Females," Amer. Jour. of Physical Anthro. 1985, 68:457-466.

1987 USAF-UES SUMMER FACULTY RESEARCH PROGRAM/  
GRADUATE STUDENT SUMMER SUPPORT PROGRAM

Sponsored by the  
AIR FORCE OFFICE OF SCIENTIFIC RESEARCH

Conducted by the  
Universal Energy Systems, Inc.

FINAL REPORT

A NUMERICAL SIMULATION OF THE FLOW FIELD  
AND HEAT TRANSFER IN A RECTANGULAR PASSAGE  
WITH A TURBULENCE PROMOTER

Prepared by:	Bryan R. Becker, Ph.D., P.E.
Academic Rank:	Assistant Professor
Department and	Department of Mechanical and Aerospace Engineering
University:	University of Missouri-Columbia
Research Location:	USAFWAL/POTC Wright-Patterson AFB, OH 45433
USAF Researcher:	Richard B. Rivir, Ph.D.
Date:	28 September 1987
Contract No:	F49620-85-C-0013

A NUMERICAL SIMULATION OF THE FLOW FIELD  
AND HEAT TRANSFER IN A RECTANGULAR  
PASSAGE WITH A TURBULENCE PROMOTER

by

Bryan R. Becker, Ph.D, P.E.

ABSTRACT

In the design of gas turbine engines, there are numerous heat transfer and fluid flow phenomena which need to be better understood. In particular, air is extracted from the compressor and is routed through small rectangular cooling passages within the turbine blades. Accurate prediction of the local heat transfer rate within these cooling passages is necessary to achieve a design of these components which incorporates efficient cooling. In the current study, the turbulent 2-D Navier Stokes equations are solved numerically to predict the flow field and local heat transfer rate from an isothermal wall in a rectangular passage with a turbulence promoter. Plots of the flow pattern, velocity profiles and temperature profiles are given, as well as tables of skin friction and local heat transfer rate. It was found that the widely used Reynolds Analogy greatly underpredicts the heat transfer rate as given by a direct calculation using Fourier's Law.

### ACKNOWLEDGMENTS

I wish to thank the Air Force Systems Command, the Air Force Office of Scientific Research and the Air Force Wright Aeronautical Laboratories, Aero Propulsion Laboratory for their sponsorship of this research. Universal Energy Systems must be mentioned for their concern and help to me in all administrative aspects of this program.

I wish to especially thank Dr. Richard B. Rivir not only for his excellent technical guidance and insight but also for his encouragement, support, and friendship throughout my assignment. Dr. Rivir was instrumental in making this summer a rewarding, stimulating, and enriching experience.

The concern and encouragement of Mr. William A. Troha was greatly appreciated. I would also like to thank Dr. Joseph S. Shang, Dr. Donald P. Rizzetta and Mr. Jerry Trummer for their help in overcoming many technical problems. Finally, I would like to thank Lt. Col. Jack D. Mattingly for his support.

## I. INTRODUCTION

In the design of the advanced gas turbine engines which will power the Nation's future aircraft there are numerous fluid flow and heat transfer phenomena which need to be better understood. Air is extracted from the compressor and is used to cool the turbine blades, bearings, and disks. These cooling flows are extremely complex, turbulent, three dimensional and significantly influenced by rotational effects.

Accurate prediction of the distribution of the local heat transfer coefficient near these rotating components is essential to their design. Such prediction is necessary to achieve a design of these components which incorporates efficient cooling and thus avoids structural failure due to thermal stress concentrations resulting from uneven temperature distributions.

My research interests are in the area of computational fluid dynamics and heat transfer. During my more than 10 years at the Oak Ridge National Laboratory, I used both finite difference and finite element techniques to analyze numerous thermal science problems which arose as a result of the Nation's nuclear/power production effort administered by the Department of Energy (DOE).

These problems involved the modelling of the physical processes of laminar and turbulent flow, heat transfer and



thermodynamics. In particular, as part of the DOE gas centrifuge uranium enrichment program, I developed two Navier Stokes models of the rotating flow field within the gas centrifuge: one using a Newton's method; the other, an approximate factorization scheme.

This background contributed to my assignment in the Components Branch of the Aeropropulsion Laboratory, Air Force Wright Aeronautical Laboratories.

## II. OBJECTIVES OF THE RESEARCH EFFORT

Computational fluid dynamics has become increasingly important in the design and analysis of gas turbine components. There have been numerous experimental and analytical studies of the flow field and heat transfer near a rotating disk or within a rotating cavity, simulating a single turbine disk or two corotating disks, respectively [1-6]. Likewise, there has been a considerable number of experimental and analytical studies of the fluid flow and heat transfer within straight nonrotating rectangular ducts which simulate the flow within the internal cooling passages inside a turbine blade [7-11]. However, with both of these geometries, there remains work to be done in the detailed modelling of the heat transfer and fluid flow processes very near the fluid-solid interface. Also, to the author's knowledge, there has been no analytical or experimental work which incorporates the effects of rotation upon the fluid flow and heat transfer within a rectangular passage with turbulence promoters.

At the beginning of my tenure as a Summer Research Fellow in the 1987 Summer Faculty Research Program (SFRP), I made initial inroads into the modelling of the fluid flow and heat transfer near a rotating disk in an infinite quiescent environment. This numerical study was to reproduce and correlate the experimental findings of Long

and Owen [1]. However, it was determined that this problem would require a greater effort than possible during the ten week SFRP term. Therefore, work on the rotating disk problem was postponed, to be continued at my university with funding from the Research Initiation Program.

I then began modelling of the fluid flow and heat transfer in a straight rectangular passage with a turbulence promoter. The results of this numerical study were to be compared with the experimental data reported by Han, Park and Ibrahim [7], as well as that reported by Fujita, Yokosawa and Nagata [8].

This resulting numerical study of the fluid flow and heat transfer in a rectangular passage with a turbulence promoter would also serve as the initial phase of a continuing program of study in this area to be undertaken at my university with funding from the Research Initiation Program. Future work would include the testing, modification, and incorporation of existing turbulence models as well as rotational effects and multiple turbulence promoters. In this way more detail and completeness could be added to the model so that the local heat transfer distribution along the cooling passage could be more accurately predicted, resulting in a turbine airfoil design which would incorporate adequate cooling and thus avoid structural failure due to thermal stress concentrations resulting from uneven temperature distributions.

### III. THE NUMERICAL MODEL

#### A. Computational Domain

In this initial numerical study of the fluid flow and heat transfer in a rectangular passage with a turbulence promoter, the flow field was modelled as being two dimensional. The X-coordinate was oriented along the length of the passage, coincident with the bulk flow direction. The Y-coordinate was oriented in the direction of the passage height, transverse to the main flow direction. This two dimensional approximation, which greatly reduced the computational complexity and cost, was considered to be sufficient for this initial study. The accuracy of this two dimensional assumption increases as the passage aspect ratio (width/height) increases and is a very reasonable approximation to the experimental results reported by Han et al [7] for aspect ratios of 2/1 and 4/1.

An outline of the computational mesh or domain is shown in Figure 1. The main flow direction is from left to right with the left and right boundaries being the inflow and outflow boundaries, respectively. The lower boundary is a solid wall boundary while the top boundary is a symmetry boundary which simulates the centerline of the flow passage. The turbulence promoter or rib was modelled as having a flat top whose length in the streamwise direction was equal to the rib height. The upstream and downstream faces of the rib were modelled as

# GRID 24

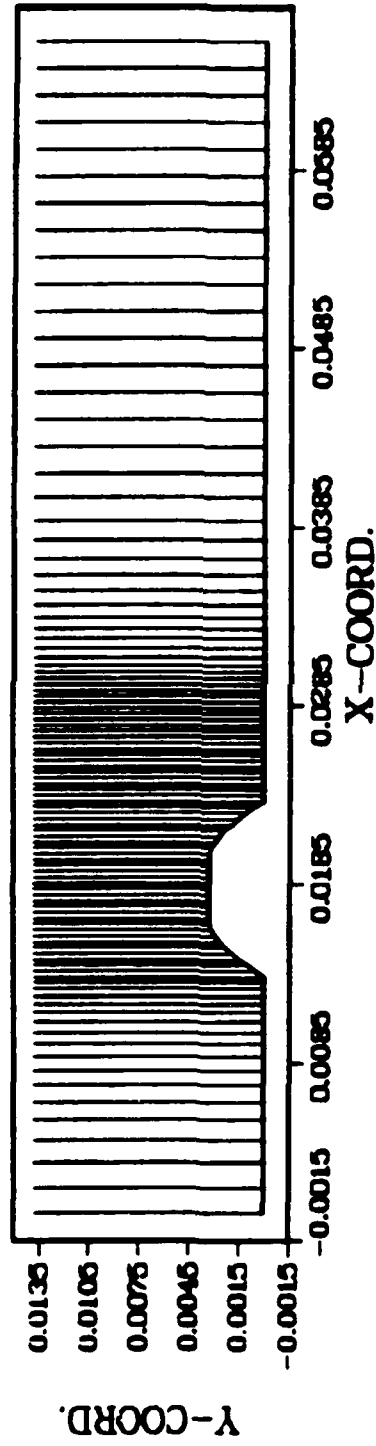


Figure 1. Outline of the computational domain.

$\sin [(x \cdot \pi) / (2) \cdot (\text{rib height})]$ , so that the total width of the rib is three rib heights, measured from the point of departure from horizontal to the point of return to horizontal.

Measured in terms of rib heights, the computational domain is 20 rib heights in the streamwise X-direction and 4.2 rib heights in the transverse, vertical Y-direction. The upstream face of the rib begins its departure from horizontal at approximately 4 rib heights from the inflow. The computational grid extends approximately 13 rib heights beyond the point where the downstream face returns to horizontal.

Measured in feet, the computation mesh is .065621 ft. long and .013827 ft. high. The rib height is .0032808 ft., well within the turbulent boundary layer. There are 60 grid lines in the Y-direction with 44 within the first .00328 ft. from the solid boundary. The mesh spacing grows as a geometric progression from an initial spacing of .000032808 ft. in the Y-direction. There are 100 grid lines in the X-direction, clustered around the turbulence promoter with the distance between grid lines growing geometrically from an initial spacing of .00032808 ft.

A plot of the complete grid is shown in Figure 2. From this figure and from the above description, it can be seen that this mesh is very fine and should reveal considerable detail of the flow field and heat transfer near the turbulence promoter.

# GRID 24

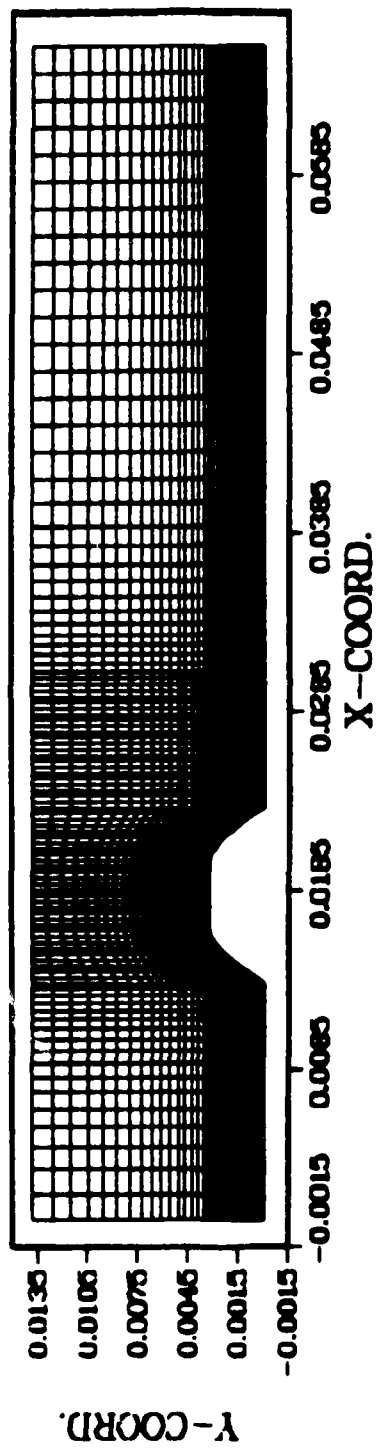


Figure 2. Complete computational grid.

## B. Governing Equations

The governing equations for the present simulation of cooling air flow through a rectangular passage with a turbulence promoter consist of the two dimensional, Reynolds averaged forms of the compressible continuity equation; the viscous, unsteady, compressible Navier Stokes equations with no body force terms; and the energy equation:

$$\frac{\partial \rho}{\partial t} + \vec{\nabla} \cdot (\rho \vec{u}) = 0 \quad (1)$$

$$\frac{\partial (\rho \vec{u})}{\partial t} + \vec{\nabla} \cdot (\rho \vec{u} \vec{u} - \vec{\tau}) = 0 \quad (2)$$

$$\frac{\partial (\rho e)}{\partial t} + \vec{\nabla} \cdot (\rho e \vec{u} - \vec{u} \cdot \vec{\tau} + \vec{q}) = 0 \quad (3)$$

The dependent variables are density, x-momentum, y-momentum and total energy:  $\rho$ ,  $\rho u$ ,  $\rho v$ , and  $\rho e = \rho [c_v T + \frac{1}{2} (u^2 + v^2)]$ .

The Reynolds averaging of the turbulent equations produces components of Reynolds stress which appear in the stress tensor,  $\vec{\tau}$ , and correlations of velocity and temperature fluctuations which appear in the heat flux vector,  $\vec{q}$ . The required turbulence closure is achieved through the use of the Baldwin-Lomax form of the Cebeci-Smith algebraic two layer eddy viscosity model [12]. The Reynolds stress components are then modelled as the product



of the eddy viscosity,  $\epsilon$ , times the velocity gradient of the mean flow while the correlations of velocity and temperature fluctuations are represented with a turbulent Prandtl number ( $Pr_t = 0.9$ ):

$$\tau_{ij} = (\mu + \epsilon) \left( \frac{\partial u_i}{\partial x_j} + \frac{\partial u_j}{\partial x_i} \right) - \left[ \frac{2}{3} (\mu + \epsilon) \left( \frac{\partial u_i}{\partial x_i} \right) + p_i \right] \delta_{ij} \quad (4)$$

$$q_i = -c_p \left( \frac{\mu}{Pr} + \frac{\epsilon}{Pr_t} \right) \frac{\partial T}{\partial x_i} \quad (5)$$

Sutherland's law is used to calculate the molecular viscosity of air,  $\mu$ , as a function of temperature. The molecular Prandtl number,  $Pr$ , is assumed to have a constant value of 0.73 while the constant volume specific heat of air,  $c_v$ , is taken to be 4290.0 ft<sup>2</sup>/s<sup>2</sup>-°R; ( $\gamma = c_p/c_v = 1.4$ ). The equation of state is assumed to be the ideal gas law with the gas constant for air equal to 1716.0 ft<sup>2</sup>/s<sup>2</sup>-°R.

As shown in Figures 1 and 2, the (X,Y) coordinate system is a body fitted coordinate system which is deformed to account for the rib on the lower boundary. This deformed coordinate system results in computational cells which are not rectangular but rather distorted quadrilaterals. In order to maintain second order calculational accuracy in the spatial domain, a coordinate transformation is made to a uniform rectangular ( $\xi, \eta$ ) grid. By means of the chain rule, the governing equations in the transformed space can be written in conservaton law form as follows:

$$\frac{\partial \vec{U}}{\partial t} + \xi_x \frac{\partial \vec{F}}{\partial \xi} + \eta_x \frac{\partial \vec{F}}{\partial \eta} + \xi_y \frac{\partial \vec{G}}{\partial \xi} + \eta_y \frac{\partial \vec{G}}{\partial \eta} = 0 \quad (6)$$

In Equation (6),  $\xi_x$ ,  $\eta_x$ ,  $\xi_y$ , and  $\eta_y$  are the first order partial derivatives of the transformed independent variables  $(\xi, \eta)$  with respect to the coordinates  $(X, Y)$ , and the vectors  $\vec{U}$ ,  $\vec{F}$  and  $\vec{G}$  are defined as follows:

$$\vec{U} = \begin{Bmatrix} \rho \\ \rho u \\ \rho v \\ \rho e \end{Bmatrix} \quad (7)$$

$$\vec{F} = \begin{Bmatrix} \rho u \\ \rho u^2 - \tau_{xx} \\ \rho uv - \tau_{xy} \\ (\rho e - \tau_{xx})u - v\tau_{xy} + q_x \end{Bmatrix} \quad (8)$$

$$\vec{G} = \begin{Bmatrix} \rho v \\ \rho uv - \tau_{xy} \\ \rho v^2 - \tau_{yy} \\ (\rho e - \tau_{yy})v - u\tau_{xy} + q_y \end{Bmatrix} \quad (9)$$

This set of equations along with the appropriate boundary and initial conditions constitutes the mathematical model of the cooling air flow through a rectangular passage with a turbulence promoter.

### C. Boundary Conditions

Specification of appropriate and consistent boundary conditions is essential to achieving a realistic and stable numerical solution for any fluid flow or heat transfer problem. In the current simulation there are four boundaries which must be considered: bottom, top, inflow and outflow. Since there are four unknowns, then at each boundary, four conditions must be specified.

The bottom boundary,  $J = 1$ , is a solid, isothermal, no slip boundary maintained at  $T_{wall} = 580^{\circ}R$ , which implies the following conditions:

$$(\rho u)_{J-1} = (\rho v)_{J-1} = 0 \quad (10)$$

$$(\rho e)_{J-1} = \rho_{wall} C_v T_{wall} \quad (11)$$

The assumption that the normal derivative of the pressure vanishes at the wall, coupled with the specification of the wall temperature, implies the following condition on the density at the wall:

$$(\rho)_{J-1} = \rho_{wall} = \frac{(\rho T)_{J-2}}{T_{wall}} \quad (12)$$

The top boundary,  $J = J_{MAX}$ , which is located at the centerline of the rectangular passage, is considered to be a symmetry boundary within the free stream. Symmetry implies that the vertical velocity vanishes:

$$(\rho v)_{J_{MAX}} = 0 \quad (13)$$

Since the top boundary is within the free stream, the horizontal velocity, pressure, temperature and density are all equal to the free stream values which are specified as follows:

$$u_{\infty} = 262.21 \text{ ft/s} \quad (14)$$

$$P_{\infty} = 2116.8 \text{ lb}_f/\text{ft}^2 \quad (15)$$

$$T_{\infty} = 540.0^\circ\text{R} \quad (16)$$

$$\rho_{\infty} = .002284 \text{ lb}_m/\text{ft}^3 \quad (17)$$

These specifications imply the following boundary conditions:

$$\rho_{JMAX} = \rho_{\infty} \quad (18)$$

$$(\rho u)_{JMAX} = \rho_{\infty} u_{\infty} \quad (19)$$

$$(\rho e)_{JMAX} = \rho_{\infty} [c_v T_{\infty} + \frac{1}{2} (u_{\infty})^2] \quad (20)$$

At the upstream inflow boundary,  $I = 1$ , it is assumed that the flow experiences reversible, adiabatic acceleration from stagnation conditions in a settling tank upstream of the inflow boundary. To determine the corresponding stagnation temperature and pressure, it is assumed that the air in the settling tank contains the total energy of the free stream. That is, the stagnation temperature and pressure are determined by applying the first law of thermodynamics and Bernoulli's equation to a reversible adiabatic total deceleration from the free stream velocity, pressure, and temperature specified above in Equations (14) through (16). The resulting stagnation temperature and pressure are thus calculated to have the following values:

$$T_0 = 545.72^\circ\text{R} \quad (21)$$

$$R_0 = 2195.33 \text{ lb}_\text{f}/\text{ft}^2 \quad (22)$$

These upstream settling tank conditions are then used to determine the inflow boundary conditions. First, it is assumed that the flow has been conditioned prior to entering the rectangular passage so that it enters as parallel flow with no vertical component which imposes the following boundary condition on vertical momentum:

$$(\rho v)_{i-1} = 0 \quad (23)$$

Second, it is assumed that the normal gradient of the temperature vanishes at the inflow which implies that the temperature is extrapolated from the interior of the flow field:

$$T_{i-1} = T_{i-2} \quad (24)$$

Thus, the horizontal velocity component can be calculated by applying the first law to the reversible adiabatic acceleration of the air from the settling tank:

$$u_{i-1} = [2C_p(T_0 - T_1)]^{1/2} \quad (25)$$

The isentropic pressure relation is then used to determine the pressure at the inflow:

$$P_{i-1} = P_0 (T_1/T_0)^{\gamma/\gamma-1} \quad (26)$$

Finally, the boundary condition on the density at the inflow is given by using the ideal gas law:

$$\rho_{i-1} = P_1 / (R_A T_1) \quad (27)$$

and,

$$(\rho u)_{i-1} = \rho_{i-1} u_1 \quad (28)$$

$$(\rho e)_{i-1} = \rho_{i-1} [C_v T_1 + \frac{1}{2} (u_1)^2] \quad (29)$$

At the downstream outflow boundary,  $I = I_{MAX}$ , the pressure is specified to be the free stream value while the normal gradients of the velocities and total energy are set to zero which implies that the values of these variables are extrapolated from the interior of the flow field:

$$P_{I_{MAX}} = P_\infty \quad (30)$$

$$U_{I_{MAX}} = U_{I_{MAX}-1} \quad (31)$$

$$V_{I_{MAX}} = V_{I_{MAX}-1} \quad (32)$$

$$e_{I_{MAX}} = e_{I_{MAX}-1} \quad (33)$$

The conditions on the velocities and the total energy at the outflow imply a specification of the temperature at the outflow which in turn implies a boundary condition on the density at the outflow via the ideal gas law:

$$\rho_{I_{MAX}} = P_{I_{MAX}} / (R_{AIR} \cdot T_{I_{MAX}}) \quad (34)$$

and,

$$(\rho u)_{I_{MAX}} = \rho_{I_{MAX}} U_{I_{MAX}} \quad (35)$$

$$(\rho v)_{I_{MAX}} = \rho_{I_{MAX}} V_{I_{MAX}} \quad (36)$$

$$(\rho e)_{I_{MAX}} = \rho_{I_{MAX}} e_{I_{MAX}} \quad (37)$$

#### D. Initial Conditions

In the current simulation, no attempt was made to produce a time accurate solution of the initial transient of the developing flow within the rectangular passage with a turbulence promoter. Therefore, the initial conditions

were only used as a starting point from which the algorithm could begin calculation of a steady state solution.

To this end, at the beginning of the calculation, it was assumed that a turbulent boundary layer, two rib heights in thickness,  $\delta$ , existed throughout the rectangular channel. Within this boundary layer, the horizontal velocity was given by the 1/7 power law:

$$u(y) = u_{\infty}(y/\delta)^{1/7} \quad (38)$$

Above the boundary layer, the horizontal velocity was set equal to the free stream velocity, Equation (14).

Throughout the flow field, the vertical component of velocity was set to zero; while the pressure, temperature and density were set equal to the free stream values, Equations (15) - (17). The initial conditions on the momentum and total energy were then calculated using the initial values of these primitive variables. Finally, the density and energy at the solid boundary were modified to account for the higher temperature of the wall.

#### E. Numerical Algorithm

The current mathematical model of the cooling air flow through a rectangular passage with a turbulence promoter is composed of the computational domain described in Section A, the set of governing equations described in Section B, and the boundary and initial conditions described in

Sections C and D. The numerical algorithm used to calculate the solution to this model is the MacCormack explicit predictor-corrector technique as implemented by Shang et al [13-16].

Although this computer code can be utilized to achieve a time accurate transient solution, it also contains an option which allows accelerated convergence to a steady state solution through the use of local time stepping. This local time stepping option was invoked in the current simulation to produce the steady state solution described in the following section.



#### IV. RESULTS

##### A. Convergence

In Shang's implementation of the MacCormack algorithm, various options exist to accelerate convergence and/or maintain numerical stability. The algorithm can be run in the local time step mode to accelerate convergence or the time accurate mode to maintain stability. The algorithm contains a numerical smoothing, which when invoked promotes stability, but can also degrade the solution. Finally, the turbulent viscosity can be omitted from the iteration which promotes stability but also produces a less realistic solution. Therefore, one must develop a strategy for the use of these various options so as to achieve a stable but realistic solution while minimizing the number of iterations required. For example, one might start the iteration with all options turned to full stability. Then, after a number of iterations, options could be switched to maximize the rate of convergence. Finally, a number of iterations should be run with the options switched to produce the most realistic solution. The strategy used in the current simulation is shown in Table 1.

In Shang's implementation, convergence is measured by the L-2 norm of the change in the normalized global solution vector between successive iterations,  $\|\delta \vec{U}_{n+1}\|$ . The global solution vector,  $\vec{U}$ , is the concatenation of all

Table 1. Iteration strategy

Iteration Count	Time Step	Smoothing	Turbulent Viscosity
0- 5,000	Time Accurate	ON	OFF
5,001-10,000	Local Time Step	ON	OFF
10,001-45,000	Local Time Step	ON	ON
45,001-99,999	Time Accurate	OFF	ON

Table 2. L-2 Norm of increments of the solution vector

Iteration Count	$\ \delta U_{n+1}\ $
0	.7137 E+1
5,000	.8197 E-2
10,000	.7993 E-2
15,000	.3739 E-2
45,000	.3735 E-2
50,000	.2662 E-2
55,000	.2415 E-2
65,000	.2560 E-2
75,000	.2353 E-2
99,999	.2414 E-2

of the nodal solution vectors as given in Equation (7). Each component of the change in the global solution vector is squared, normalized by the free stream value of the respective variable, and summed:

$$\|\delta \vec{u}_{n+1}\| = \sum_i \sum_j \left[ \left( \frac{\rho_{ij}^{n+1} - \rho_{ij}^n}{\rho_\infty} \right)^2 + \left( \frac{(\rho u)_{ij}^{n+1} - (\rho u)_{ij}^n}{(\rho u)_\infty} \right)^2 + \left( \frac{(\rho v)_{ij}^{n+1} - (\rho v)_{ij}^n}{(\rho v)_\infty} \right)^2 + \left( \frac{(\rho e)_{ij}^{n+1} - (\rho e)_{ij}^n}{(\rho e)_\infty} \right)^2 \right]^{1/2} \quad (39)$$

Typically, in the iteration to a converged steady state solution, the value of this norm will drop 3 orders of magnitude from the initial conditions and then oscillate about this reduced value, indicating that convergence has been achieved [17]. As shown in Table 2 for the current simulation, the value of this norm decreased from 7.137 at the outset to .002662 after 50,000 iterations and oscillated near that value for the remaining 49,999 iterations. This behavior is typical of convergence to the steady state solution. The current simulation required 92 minutes of execution time on the Cray-1 computer at Wright Patterson AFB, Ohio.

### B. Velocity and Temperature Profiles

As described in Section III.A., the computational grid is 20 rib heights in length with the top front corner of the rib located 5 rib heights downstream from the inflow

boundary, and the top back corner of the rib located 6 rib heights downstream from the inflow boundary. There are 100 grid lines in the streamwise x-direction, clustered around the rib. These grid lines are numbered as the K index starting at the inflow boundary. Hence,  $K = 1$  corresponds to the inflow boundary.

Profiles of  $u/u_\infty$ ,  $v/v_\infty$ , and  $T/T_\infty$  were plotted against  $Y/Y_{MAX}$  at the 16 streamwise locations listed in Table 3. In these profile plots, given in Figures 3 through 50, a rib height corresponds to  $Y/Y_{MAX} = .237$ . Hence, in the profile plots for K values of 28, 33, 38, and 47, the curve does not reach  $Y/Y_{MAX} = 0$  because the bottom of the computational mesh coincides with the top of the rib or turbulence promoter which has a  $Y/Y_{MAX}$  value greater than zero.

The profiles at  $K = 1$  represent the inflow boundary conditions where the flow has not yet properly developed which explains the wiggles in the horizontal velocity and the uniform zero vertical velocity.

At  $K = 6$ , the profiles show that the momentum and thermal boundary layers are beginning to develop. Since this flow is predominately in the horizontal direction, the vertical velocity is very small compared to the horizontal velocity. Therefore, the small variations, which are due to round off in the calculation of the vertical velocity, are nearly the same magnitude as the actual vertical

Table 3. Profile locations

K (Streamwise Index)	Distance from Inflow Boundary measured in rib heights
1	0
6	2
11	3
18 (Front bottom corner of rib)	4
28 (Front top corner of rib)	5
33 (Rib centerline)	5.5
38 (Back top corner of rib)	6
47 (Back bottom corner of rib)	7
57	8
67	9
75	10
80	11
83	12
85	13
89	15
100	20

velocity, thus producing the exaggerated wiggles exhibited in vertical velocity profiles.

At  $K = 11$  and 18, the profiles show the continued development of the momentum and thermal boundary layers and a vertical acceleration as the flow begins to move up and over the turbulence promoter. Also at  $K = 18$ , both the

FIGURES 3-50 ARE  
AVAILABLE UPON REQUEST AT  
UNIVERSAL ENERGY SYSTEMS, INC.

vertical and horizontal velocities are negative near the solid wall which testifies to the presence of a recirculation zone which will be discussed later.

The locations,  $K = 28, 33$  and  $38$ , are at the front top corner, midline and back top corner of the rib, respectively. The vertical velocity is positive indicating that the flow is moving up over the rib. The horizontal velocity has greatly accelerated near the solid wall, exhibiting a uniform profile at  $K = 38$ , typical of a fully developed turbulent flow. Both the momentum and thermal boundary layers have been destroyed due to the intense turbulent mixing which is occurring. The temperature near the wall is much lower than at previous streamwise locations and exhibits some nonphysical overshoot. This overshoot as well as the wiggles in both temperature and horizontal velocity profiles are numerical artifacts produced by over restrictive boundary conditions at the top boundary which will be corrected in future calculations.

The streamwise locations,  $K = 47$  through  $K = 83$ , start at the back bottom corner of the rib and extend to the reattachment point which marks the end of the large recirculation bubble downwind of the rib. The temperature profiles show that the turbulent mixing behind the rib has greatly diffused the energy from the hot solid wall to form a warm air region which extends almost 2 rib heights vertically from the solid wall. The horizontal velocity

profile is typical of a recirculation zone with a negative upstream flow near the wall changing to a positive downstream flow higher in the flow field. The vertical velocity profiles also show evidence of flow recirculation.

The profiles at  $K = 85, 89$  and  $100$ , demonstrate that both the momentum and thermal boundary layers are reestablished downstream of the recirculation bubble. However, comparison of these profiles to those at  $K = 6, 11$  and  $18$ , upstream of the turbulence promoter, show that the downstream boundary layers are much thicker and well mixed, testifying to the effects of the intense turbulent mixing caused by the flow over the turbulence promoter.

### C. Flow Pattern, Skin Friction, and Heat Transfer Rates

Careful analysis of the printed output at each of the  $100$  streamwise locations reveals the interesting details of the flow pattern shown in Figure 51. There are five recirculation zones or bubbles produced by the flow over the turbulence promoter. There is a clockwise rotating zone, 1 rib height in length, which begins 1 rib height upstream of the rib and is approximately .1 rib height tall. The second clockwise rotating bubble, which is about a half rib height in length and very thin, begins just downstream from the top front corner of the rib. Behind the rib there are two counterclockwise vortices which are



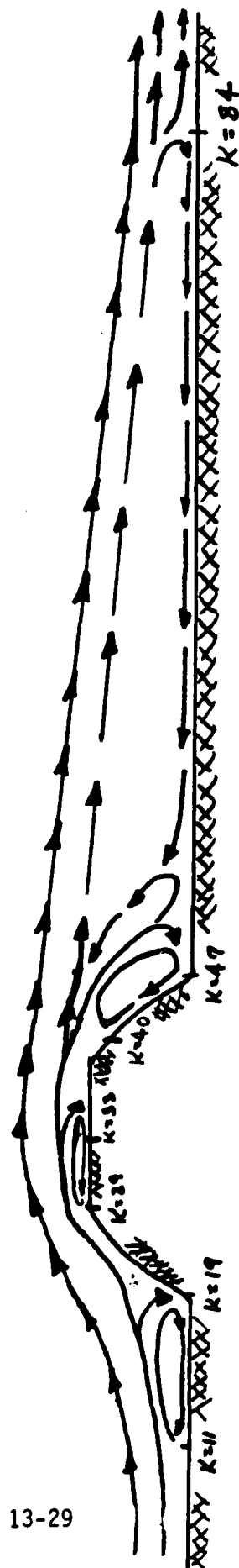


Figure 51. Schematic of flow pattern in a rectangular passage with turbulence promoter.

separated by a clockwise vortex. The first clockwise vortex, which is 1 rib height in length, begins just behind the back top corner and is .54 rib height in thickness. Adjacent to this clockwise vortex is a counterclockwise vortex of approximately the same size. Finally, there is the very large recirculation bubble which begins just downstream of the back top corner of the rib and attains a maximum thickness of .71 rib height just behind the rib. This large bubble extends to the reattachment point which is located approximately 7 rib heights from the back top corner or 6 rib heights from the back bottom corner.

The location of the reattachment point agrees very well with the wind tunnel investigations of flow over a surface mounted cube conducted by Castro and Robins [18]. They report that the wake produced by a uniform turbulent stream completely decayed within 6 cube heights downstream.

Skin friction and heat transfer rates were calculated at the 16 streamwise locations listed in Table 3. The values of local skin friction, shown in Table 4, were calculated from the following equation:

$$C_f' = \frac{T_{w-11}}{\frac{1}{2}\rho U^2} = \frac{\mu \left( \frac{\partial u}{\partial y} \right)_{y=0}}{\frac{1}{2}\rho U^2} \quad (40)$$

The normal derivative of the horizontal velocity was approximated as a central difference between the  $J = 1$  node (solid wall) and the  $J = 2$  node ( $Y \leq .3281 \text{ E-}4 \text{ ft.}$ ). The viscosity was determined by averaging the values given by Sutherland's Law evaluated at  $T_{J-1}$  and  $T_{J-2}$ .

Table 4. Local skin friction coefficient

K (Streamwise Index)	Skin Friction Coefficient ( $C_f \times 10^4$ )
1	0
6	62.28
11	7.43
18	47.62
28	77.39
33	34.11
38	12.23
47	1.34
57	15.50
67	42.67
75	52.06
80	47.80
83	55.38
85	2.24
89	20.44
100	35.57

The local heat transfer rates, given in Table 5, are expressed in terms of the nondimensional Stanton number:

$$S = \frac{Q_{wall}}{C_p \rho U_\infty (T_{wall} - T_\infty)} \quad (41)$$

Table 5. Local heat transfer rates

K (Streamwise Index)	Stanton Number $\times 10^3$	
	via Reynolds Analogy	via Fourier's Law
1	0.0	24.33
6	3.11	4.38
11	0.37	1.20
18	2.38	4.03
28	3.87	3.62
33	1.71	3.71
38	0.61	3.15
47	0.07	1.54
57	0.78	1.48
67	2.13	2.33
75	2.60	2.83
80	2.39	3.11
83	2.77	4.24
85	0.11	3.39
89	1.02	3.11
100	1.78	2.90

These heat transfer rates were calculated by two different methods. In the first method, the Reynolds Analogy was used, in which the heat transfer rate is related to the skin friction as follows:

$$\text{Stanton Number} = \frac{1}{2} C_f' \quad (42)$$

NO-A191 203

UNITED STATES AIR FORCE SUMMER FACULTY RESEARCH PROGRAM  
(1987) PROGRAM TE. (U) UNIVERSAL ENERGY SYSTEMS INC  
DAYTON OH R C DARRAH ET AL. DEC 87 AFOSR-TR-88-0212

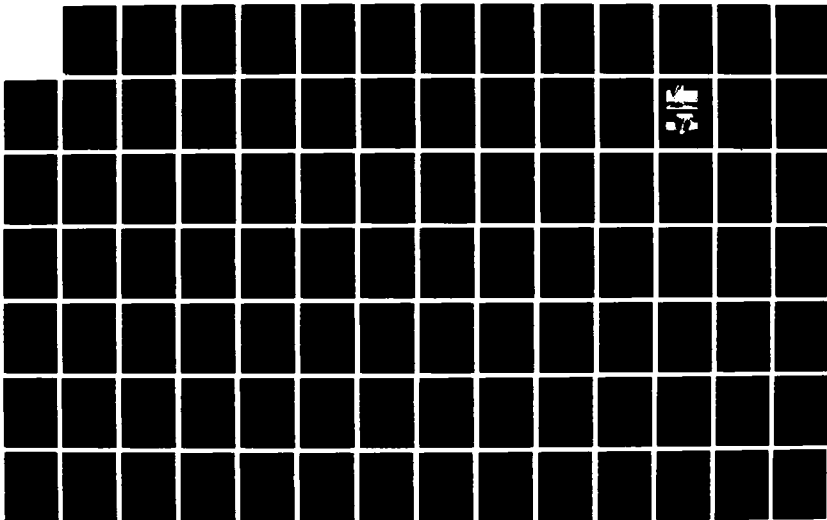
4/11

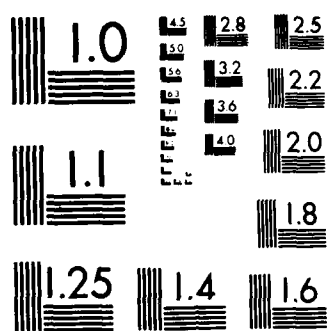
UNCLASSIFIED

F49620-85-C-0013

F/G 5/1

ML





MICROCOPY RESOLUTION TEST CHART  
NATIONAL BUREAU OF STANDARDS-1963 A

This method is widely used in turbomachinery calculations but these calculations greatly underpredict the heat transfer rates measured experimentally [19].

In the second method, Fourier's Conduction Law is used to evaluate the heat transfer rate at the wall,  $Q_{wall}$ , which appears in Equation (41):

$$Q_{wall} = -K \left( \frac{\partial T}{\partial y} \right)_{y=0} \quad (43)$$

In this calculation, the thermal conductivity was treated as a constant and the normal derivative of temperature was evaluated in a manner similar to that used for the normal derivative of the horizontal velocity discussed above.

In the convection heat transfer process, the energy is first transferred by conduction from the solid wall to the fluid particles adjacent to the wall. These fluid particles are then transported away from the solid wall by the bulk mixing of the fluid which results in the diffusion of energy from the solid wall. The basis for the Reynolds Analogy is the assumption that the same mechanism is responsible for the exchange of both heat and momentum. This assumption disregards the details of the energy transfer process at the solid wall-fluid interface. As shown in Table 5, the direct calculation of the heat transfer rate via Fourier's Law predicts heat transfer rates which can be as great as 30 times that given by the Reynolds Analogy. This great discrepancy, which exists in most turbomachinery calculations, can be explained by the

fact that the Reynolds Analogy is derived for laminar or fully turbulent flows over a flat plate with laminar and turbulent Prandtl number,  $Pr = Pr_t = 1.0$  . Thus, the Reynolds Analogy is not applicable to flows with recirculation zones and flow reversals which cause the normal gradient of velocity to differ greatly from the normal gradient of temperature.



## V. RECOMMENDATIONS

The recommendations for extensions to this work in the general area of the numerical simulation of the flow field and heat transfer in turbomachinery fall into three general categories: improvements and extensions to the current simulation, incorporation of additional computational capabilities into the Shang implementation of the MacCormack algorithm, and additional investigations.

### A. Improvements and Extensions to the Current Simulation

As mentioned in the Results section, the current simulation could be improved by first relaxing the boundary conditions at the top boundary and continuing iteration beyond the 99,999 iteration level with the purpose being to remove the wiggles in the horizontal velocity and temperature near the top boundary. If this does not correct the problem, the next step would be to refine the computational grid near the top boundary and evaluate its effects upon the solution.

As an extension to the current simulation, rotational effects could be incorporated as body force terms in the momentum and energy equations. Two different calculations should be made, one with the principal flow direction aligned inwardly along the radius of rotation, and the other with the principal flow direction aligned outwardly

along the radius of rotation. These results would then be compared with the results for the case with no rotation, allowing for an evaluation of the impact of rotational effects upon heat transfer. This evaluation would also have bearing upon the applicability of various nonrotating experimental heat transfer studies.

Another extension to the current simulation would be to modify the computational grid and algorithm to facilitate the modelling of rectangular turbulence promoters with vertical sides.

#### B. Incorporation of Additional Computational Capabilities

Various modifications could be made to the numerical algorithm. The local time stepping algorithm, convergence testing, and printed output should be improved.

Also, various post convergence calculations need to be incorporated. Values of the stream function should be evaluated at all node points. The local skin friction and local heat transfer rates should be calculated at all solid wall boundary nodes. In particular, the heat transfer rates should be calculated using two methods: Reynolds Analogy and Fourier's Law. Energy transport by convection of internal and kinetic energy through the inflow, outflow and top boundaries could be calculated. Total mass and energy transport through the boundary of the computational

mesh could be calculated, thus allowing for a verification of the conservation of mass and energy by the numerical algorithm.

Finally, the plotting capabilities need to be improved. Contour plots of temperature and pressure would be interesting and useful. Streamline plots, contours of the stream function, would exhibit the recirculation zones. Contours of the turbulent eddy diffusivity would give an indication of turbulence levels throughout the flow field.

### C. Additional Investigations

The computational mesh and boundary conditions could be modified to simulate the experimental setup used in the heat transfer studies by R. B. Rivir. One purpose of this simulation would be to compare the local heat transfer rates calculated by both the Reynolds Analogy method and Fourier's Law to the heat transfer rate measured experimentally by Rivir et al.

Another investigation could be performed to study the effects of multiple turbulence promoters. To reduce the computer resource requirements in such a calculation, the outflow conditions calculated in the current simulation could be used as the inflow conditions to the next section of the rectangular cooling passage.

Another study, which would require greater effort, would be the implementation and testing of various turbulence models. Also, other types of computational fluids algorithms, which may be more efficient for this type of simulation, could be considered.

In a different vane, a considerable amount of work still needs to be performed to complete the modelling of the fluid flow and heat transfer near a rotating disk in an infinite quiescent environment.

of Heat Transfer and Pressure Drop in Rectangular Channels with Turbulence Promoters," NASA Contractor Report 4015, 1986.

8. Fujita, H., H. Yokosawa, and C. Nagata, "The Numerical Prediction of Fully Developed Turbulent Flow and Heat Transfer in a Square Duct with Two Roughened Facing Walls," Proceedings of the Eighth International Heat Transfer Conference, San Francisco, California, 1986.
9. Linton, S. W. and J. S. Shang, "A Numerical Simulation of Jet Impingement Cooling in a Rotating Frame of Reference," AIAA-87-0609, AIAA 25th Aerospace Sciences Meeting, Reno, Nevada, 1987.
10. Launder, B. E. and W. M. Ying, "Prediction of Flow and Heat Transfer in Ducts of Square Cross-Section," Heat Fluid Flow, Vol. 3, 1973, pp. 115-121.
11. Han, J. C., J. S. Park, and C. K. Lei, "Heat Transfer and Pressure Drop in Blade Cooling Channels with Turbulence Promoters," NASA Contractor Report 3837, 1984.
12. Baldwin, B. and H. Lomax, "Thin Layer Approximation and Algebraic Model for Separated Turbulent Flows," AIAA-78-257, AIAA 16th Aerospace Sciences Meeting, Huntsville, Alabama, 1978.
13. Shang, J. S. and W. L. Hankey Jr., "Numerical Solution for Supersonic Turbulent Flow over a Compression Ramp," AIAA-75-3, AIAA 13th Aerospace Sciences Meeting,

## REFERENCES

1. Long, C. A. and J. M. Owen, "Prediction of Transient Temperatures for an Air-Cooled Rotating Disc," AGARD Conference Proceedings No. 390, Heat Transfer and Cooling in Gas Turbines Conference, Bergen, Norway, 1985.
2. Owen, J. M., "Fluid Flow and Heat Transfer in Rotating Disc Systems," XIV ICHMT Symposium on Heat and Mass Transfer in Rotating Machinery, Dubrovnik, 1982.
3. Owen, J. M., "The Reynolds Analogy Applied to Flow Between a Rotating and a Stationary Disc," International Journal of Heat Mass Transfer, 14, 1971, p. 451.
4. Morse, A. P., "Numerical Prediction of Turbulent Flow in Rotating Cavities," ASME paper 87-GT-74, Gas Turbine Conference, Anaheim, California, 1987.
5. Owen, J. M. and J. R. Pincombe, "Velocity Measurements inside a Rotating Cylindrical Cavity with a Radial Outflow of Fluid," Journal of Fluid Mechanics, 99, 1980, p. 111.
6. Chew, J. W., "Development of a Computer Program for the Prediction of Flow and Heat Transfer in a Rotating Cavity," International Journal of Numerical Methods in Fluids, 4, 1984, p. 667.
7. Han, J. C., J. S. Park, and M. Y. Ibrahim, "Measurement

Pasadena, California, 1975.

14. Shang, J. S., "Implicit-Explicit Method for Solving the Navier-Stokes Equations," AIAA-77-646, AIAA 3rd Computational Fluid Dynamics Conference, Albuquerque, New Mexico, 1977.
15. Shang, J. S., W. L. Hankey and J. S. Petty, "Three-Dimensional Supersonic Interacting Turbulent Flow along a Corner," AIAA-78-1210, AIAA 11th Fluid and Plasma Dynamics Conference, Seattle, Washington, 1978.
16. Shang, J. S., P. G. Buning, W. L. Hankey and M. C. Wirth, "Performance of a Vectorized Three-Dimensional Navier-Stokes Code on the CRAY-1 Computer," AIAA-79-1448, AIAA 4th Computational Fluid Dynamics Conference, Williamsburg, Virginia, 1979.
17. Personal communication with Dr. Donald P. Rizetta, Flight Dynamics Laboratory, Wright Patterson AFB, Ohio, 1987.
18. Castro, I. P. and A. G. Robins, "The Flow around a Surface-Mounted Cube in Uniform and Turbulent Streams," Journal of Fluid Mechanics, Vol. 79, Part 2, 1977, pp. 307-335.
19. Personal communication with Dr. Richard B. Rivir, Aero Propulsion Laboratory, Wright Patterson AFB, Ohio, 1987.

1987 USAF-UES SUMMER FACULTY RESEARCH PROGRAM/  
GRADUATE STUDENT SUMMER SUPPORT PROGRAM

Sponsored by the  
AIR FORCE OFFICE OF SCIENTIFIC RESEARCH

Conducted by the  
Universal Energy Systems, Inc.

FINAL REPORT

SYNERGISTIC EFFECTS OF BOMB CRATERING

Prepared by:	Charles J. Bell, Jr.
Academic Rank:	Professor
Department and	Department of Engineering
University:	Arkansas State University
Research Location:	Air Force Armament Test Laboratory Clusters and Warheads Branch Eglin Air Force Base, Florida
USAF Researcher:	Albert L. Weimorts, Jr.
Date:	August 14, 1987
Contract No:	F49620-85-C-0013



## SYNERGISTIC EFFECTS OF BOMB CRATERING

by

Charles J. Bell, Jr.

### ABSTRACT

Analysis of data from earlier tests of detonations beneath simulated runways was accomplished. The literature pertaining to undersurface detonations of high explosives was surveyed. Relationships between distance, time, and pressure from the literature were compared to data from earlier tests at Eglin. A modified equation was proposed for pressure waves in soils.

A failure criterion for structures was applied to the unreinforced slabs in use on the Eglin test range. This criterion was used to estimate values of parameters in the classical and proposed equations for shock wave pressure in sandy loam and in clay soils.

An equation was developed for calculating the distance between charges that results in maximum synergistic pressure on the bottom of a runway slab. Examples of application are presented.

### ACKNOWLEDGEMENTS

I wish to thank the Air Force Systems Command and the Air Force Office of Scientific Research for sponsorship of this research. Universal Energy Systems must be mentioned for their concern and help to me in all administrative and directional aspects of this program.

The Air Force Armament Test Laboratory (AFATL) provided a pleasant environment in which to work and technical support to facilitate my work. Mr Al Weimorts was quite helpful with many technical aspects of the problem. Lt Bill Foley took care of many details related to testing. Dr Sam Lambert, Chief Scientist of AFATL, saw to it that problems with housing did not complicate things and he also helped when problems arose in obtaining technical assistance in the laboratory. Mr Ronald Boulet, Chief, Clusters and Warheads Branch of AFATL, provided invaluable assistance in many ways. Mary Raymes and Donna Welle were indispensable to the preparation of this report. My thanks to all of the above for a rewarding project.

## I. INTRODUCTION

Attack of enemy airfield runways can be effectively carried out with clustered kinetic energy penetrators carrying a limited amount of high explosive (HE). Presently, available munitions of this type carry less than ten (10) pounds of HE. A number of the projectiles would be launched by each attacking aircraft.

The shape of the projectile is dictated by the dynamics of penetration of concrete, as is the choice of casing material. Two factors which affect the effectiveness of an attack are depth at which detonation occurs, and the spacing of the projectiles over the surface of the runway. There is some leeway in choice of these two factors. The present study will investigate the synergistic effect of two such projectiles as functions of depth of detonation, distance between projectiles, and time interval between detonation.

A model has been prepared which takes into account the variables noted above, as well as other factors, such as soil type and runway construction. A test plan has been proposed for the purpose of refining the model. Results of earlier single shot tests are analyzed.

## II. OBJECTIVES

The primary objective was evaluation of the synergistic effect of detonating kinetic energy penetrators spaced closely in time and distance from one another. This particular program was undertaken for the specific purpose of finding ways to enhance damage to enemy runways. The results could apply to other buried concrete structures.

## III. ANALYSIS OF EXISTING DATA

Two earlier investigations of high explosive damage to runways were completed by Wilson (1), (2), at Eglin AFB in 1979 and in 1980. The tests were conducted against concrete slabs of dimensions 20 feet by 20 feet by one foot thick. Concrete strength was 6,000 psi nominal. Both reinforced and

unreinforced slabs were tested. The reinforced slabs contained two layers of No. 4 reinforcing bar in a 12 inch by 12 inch pattern.

The high explosive charges were placed in the center of each slab with the center of gravity (c.g.) of the projectile at depths ranging from 12 inches to 48 inches below the top surface of the slab. Shaped charges were used to open a hole in the slab so that the projectile could be inserted; the shaped charge penetration simulates the kinetic energy penetration of a runway by a projectile from an aircraft. The penetration hole and the projectile were set at an angle of 60 degrees above horizontal to further simulate aircraft delivery.

The projectile was 3.50 inches in O.D., 3 inches in I.D., and 18 inches to 29 inches long depending on charge weight and type. The projectile case was either 4130 or 4340 type steel. A number of high explosives were tested including H-6, Tritonal, Octol, AFX-108, and AFX-708. The best results appear to have been achieved with AFX-708. Charge weights as low as 3 pounds to a high of 10 pounds were used. In the 1980 tests, a charge weight of 6.7 pounds nominal was used in all tests with AFX-708 explosive.

The native subsoil in the test area is a yellow sand usually described as sandy loam. Very sandy loam would appear to be more descriptive. Above the subsoil was 6 inches of compacted subsoil, 12 inches of crushed aggregate, 2 inches of sand, 6 mil polyethylene vapor barrier, and then the one foot thick concrete slabs. Of 60 total tests conducted, 56 were with the native subsoil, while four tests were above a sandy clay subgrade constructed for these tests.

High speed (about 3,500 frames/sec) photographs were taken during the tests, and still photographs of the slabs were also made to show damage. Damage was characterized by several measurements including vertical displacement of the slab, clear crater size in concrete and spall area. In order to reduce the damage characterization to a single figure, only the clear crater area of the hole is noted in this analysis. Further discussion is also be confined to those tests in which 6.7 pounds of AFX-708 was the explosive charge.

The input variables that are examined were thus reduced to depth of charge,

type of subgrade, and reinforced or unreinforced concrete. The output variable used to measure results is clear crater area. The clear crater area is the most direct indication of the volume of concrete removed by the explosion.

A tabulation of pertinent data from references (1) and (2) is shown in Table I, following.

Table I. Pertinent Data Summary from English (1) and (2).

Shot No.	Reinf. (?)	Depth (in)	Damage Area (ft <sup>2</sup> )	Subgrade Type	Report Year
28	Y	30	19.1	Sand	79
2	Y	36	7.4	Sand	80
14	Y	36	4.6	Sand	80
29	Y	36	7.3	Sand	79
30	Y	42	6.2	Sand	79
13	Y	42	8.7	Sand	80
1	Y	42	5.9	Sand	80
9	Y	36	74.4	Clay	80
7	Y	42	7.3	Clay	80
3	N	36	18.0	Sand	80
4	N	42	6.3	Sand	80
21	N	36	57.7	Clay	80
8	N	42	156.1	Clay	80

The most effective shot in sand below a reinforced slab occurred at 30 inches deep (No. 28, 1979). There was little to choose between the 36 inch and 42 inch deep tests in sand below reinforced slabs. An optimum depth for the 18 inch x 3.5 inch O.D. projectile loaded with 6.7 pounds of AFX-708 would appear to be about 30 inches for reinforced slabs above sandy loam subsoils. Until more data can be obtained, the 30 inch depth will be considered optimum for these conditions.

Comparison of the two shots in clay under a reinforced slab indicates that a

depth of 36 inches is vastly superior to a similar shot at 42 inches depth. The optimum depth for shots in clay under reinforced slabs is set at 36 inches for the present.

For unreinforced slabs, the available data does indicate that for both clay and sand subgrades the projectile should be buried more deeply than for the corresponding reinforced slab. Optimum detonation depths of 36 inches in sand and 42 inches in clay below unreinforced slabs are adopted for the 3.5 inch by 18.5 inch projectile with 6.7 lb. charge of AFX-708.

It should be noted that the trends of shallower detonation depths in sand and under reinforced slabs as compared to deeper detonation depths in clay and under unreinforced slabs is supported by data for other explosives of different weights. It should also be noted that examination of photographs and moving pictures have lent subjective support to these trends.

The fact that sand tends to dissipate the energy in elastic waves more rapidly than does clay also supports the depth trend in sand versus clay. It appears obvious that higher pressure, impulse, and energy levels would be required for damaging reinforced concrete as compared to similar unreinforced concrete.

#### IV. SURVEY OF LITERATURE

The early theoretical work on explosions within continuous media was done for underwater explosions. The book of Cole (4) on underwater explosion cites much of the early theoretical work as well as supporting experimental work. He also gives some relatively compact equations for calculating pressures and so forth. These same equations given by Cole plus one or two more of value may be found in reference (5) which was published about twenty years after the work of Cole.

The equations given for shock effects in water in references (4) and (5) are used as the starting point for analyses of underground explosives. In many cases, it is enough to simply change the values of the parameters to fit the soil (or soils) in question. In more detailed analyses, the equations have been modified to account for other differences between water and soils.

Consider a spherical charge of high explosive to be detonated at time zero within an infinite continuous medium, say, water. A sudden rise in pressure at the charge surface will be transmitted to the water. This pressure pulse (or shock wave) will propagate through the water at some velocity  $V$ . The maximum pressure ( $P_m$ ) is the pressure rise above that in the undisturbed medium to that just behind the shock front. For a given medium and explosive, the pressure ( $P_m$ ) immediately behind a spherical shock front may be taken as:

$$P_m = A \left( \frac{W^{1/3}}{R} \right)^\alpha \quad (1)$$

where  $W$  is the charge weight (in pounds).  $A$  and  $\alpha$  are parameters that depend upon charge composition and upon the medium.  $R$  is distance (in feet) from the center of explosion. For example, Cole (4) gives for TNT in seawater the values of  $A = 21,600$  and  $\alpha = 1.13$ .  $P_m$  is in psi for the values and units noted above.

Equation (1) gives only the peak pressure at the shock front. After passage of the shock front, the pressure decays exponentially from the peak value according to

$$P = P_m e^{-t/\theta} \quad (2)$$

where  $\theta$  is a time constant. The time constant may be approximated by:

$$\theta = D W^{1/3} \left( \frac{W^{1/3}}{R} \right)^\beta \quad (3)$$

where  $D$  and  $\beta$  depend upon charge type, charge weight and distance  $R$  from the charge as well as upon the medium. Note that the dependence of the parameters  $A$  and  $\alpha$  in equation (1) upon  $R$  can be ignored, while the same cannot be said of  $D$  and  $\beta$  in equation (3).

Equations for unit impulse ( $I$ ) and energy flux ( $E$ ) are also given by Cole (4) as:

$$I = B W^{1/3} \left( \frac{W^{1/3}}{R} \right)^\beta \quad (4)$$

$$E = C W^{1/3} \left( \frac{W^{1/3}}{R} \right)^{\gamma} \quad (5)$$

where I is in psi-sec and E is in in-lb/in<sup>2</sup> for W and R in the units stated previously. Values of A, B, C and  $\alpha, \beta, \gamma$  are given in Table II below for three explosives in seawater.

TABLE II. Explosive Constants for Equations (1), (4), (5)\*.

Explosive	Density (gm/cc)	Integration						
		Density	Peak Pressure	Impulse	Energy	Density	Time	
		A	$\alpha$	B	$\beta$	C	$\gamma$	T
TNT	1.52	21,600	1.13	1.46	0.89	2,410	2.05	6.7 $\theta$
Loose Tetryl	0.93	21,400	1.15	1.73	0.98	3,000	2.10	5.0 $\theta$
Pentolite	1.60	22,500	1.13	2.18	1.05	3,270	2.12	6.7 $\theta$

\*After Cole (4).

The values for I and E depend upon an integral over some time interval T; that interval is given in terms of  $\theta$  for the explosives (in seawater) shown in Table II. Evaluation of E at some radius R from the center of the spherical charge would give the energy per unit area that the shock wave delivers during T. Evaluation of I gives, for the particular explosive in seawater, the impulse per unit area evaluated from the instant of shock arrival at R and over the integration time shown in Table II.

Equations (1) through (5) are based upon an elementary analysis combined with experimental data. For explosions in water, they have proven quite useful because water is a relatively homogeneous medium whose physical characteristics are well known.

Sooner or later, shock waves must arrive at a boundary of one sort or another. In water, boundaries may be the surface, bottom, man-made structure or even a region in which the water temperature or composition changes significantly. Any boundary causes changes in the shock wave. In general, any boundary will result in a reflection of some or all of the energy, transmission of a part of



the energy as a shock wave into the bounding medium and conversion of part of the incident wave energy into other types of waves.

Explosions in soils differ from those in water in at least two important ways. Since soils can support shear stresses much more readily than water, a significant amount of energy is transported in soils by shear waves. Soils also dissipate energy at a higher rate than water. The pressure pulse therefore attenuates more rapidly in soils, but it is still possible to represent  $P_m$  by equation (1) if suitable values of  $A$  and  $\alpha$  are known. Drake and Little (6) have given values of  $\alpha$  and information required to calculate  $A$  for a variety of soils. A few values for selected soils are shown in Table III. The results given by Drake and Little are averages from data taken over many years. There is no mention in the paper of the types of explosives involved; it seems likely that TNT was the most prevalent. In any case, the type of explosive can make a significant difference in  $A$  and some difference in  $\alpha$ .

TABLE III. Soil Properties for Shock Wave Calculation.\*

Soil Description	$A^{**}$	$\alpha^{**}$
Loose, dry, poorly graded sand	1860	3.25
Dense, wet sand, poorly graded	3520	2.75
Very dense dry sand	7040	2.5
Wet sandy clay	7680	2.5
Saturated stiff clay-saturated clay shale	21600	1.5
Seawater (TNT)***	21600	1.13

\*From Drake (6). Explosive depth ( $d$ ) such that  $d/W^{1/3} > 1.4$  ( $d$  in ft.,  $W$  in pounds).

\*\*Units are such that  $P_m$  is in psi if  $R$  is in ft. and  $W$  in pounds in equations (1) - (5).

\*\*\* From Cole (4).

In the absence of more definitive data, it is suggested that values of  $A$  and  $\alpha$  be extracted from reference (6) if equations (1) - (5) are to be used.

Geometry is a major factor in damage caused by explosions. The discussion thus far has centered on spherical charges and the pressures associated with a spherical shock wave. The charges in military ordnance are most likely to be cylindrical in shape, and the target shape is certainly a slab where runways are being attacked.

Ross, et al (7), have considered the time and space variations of loads on underground structures by cylindrical explosives. Their work takes into account both radial and tangential stresses. Equation (1) is still the basic pressure attenuation equation. It is adapted to cylindrical explosions by a lumped parameter model. The paper contains procedures that should prove useful for estimating synergistic effects from two or more projectiles spaced some distance apart and detonated either simultaneously or at some time interval apart.

Runway construction is another factor that is obviously important in optimizing the effectiveness of an attack. As a rule, runways are constructed of 6000 psi concrete about one foot thick. Steel reinforcement may or may not be used. C. A. Ross, et al (8), addressed the problem of concrete breaching of reinforced concrete. A computer program is provided. T. J. Ross (9) discusses impulsive failure of buried reinforced concrete.

Cole (4) reviews some early experimental work on multiple charges. The effect upon pressure behind intersecting waves depends upon the strength of the shock. For seawater, if the shock strength is less than 10,000 psi, simple addition of the two pressures occurs. The experimental work reported by Cole appears to agree well with analytical work described in Cole's book.

## V. CONCRETE FAILURE

A dynamic failure criterion for concrete structure in terms of specific impulse was developed by Ross (8). For the case of unreinforced concrete slabs, the critical specific impulse ( $I_c$ ) leading to breaching of the slab is

$$I_c = 0.005 h [p_e f_c]^{1/2} \quad (6)$$

where

$h$  = slab thickness in feet

$\rho_c$  = concrete density in lb/ft<sup>3</sup>

$f_c$  = concrete failure strength in psi

$I_c$  = critical specific impulse in psi - sec.

For 6000 psi unreinforced concrete slabs one foot thick with a density of 150 lb/ft<sup>3</sup>, the critical specific impulse for breaching is 4.74 psi-sec.

The applied specific impulse from the shock wave of an explosion may be calculated from

$$I_{ap} = \int_0^{a\theta} p(R,t) dt \quad (7)$$

where  $p(R,t)$  is the shock wave pressure given by equation (2), and "a" is some multiplier. Breaching is assumed to occur along the locus of values of  $R$  where  $I_{ap} = I_c$ . Integration of equation (7) gives after substitution of (3),

$$I_{ap} = A \left( \frac{W^{1/3}}{R} \right)^\alpha \Theta [1 - e^{-a}] \quad (8)$$

Only the parameters  $W$  and  $R$  can be determined with certainty. The values of  $A$ ,  $\alpha$ ,  $\Theta$ , and  $a$  depend, in uncertain ways, upon explosive type and shape, medium through which the shock wave is propagated, and upon other factors known and unknown. Values of  $a$  and  $\alpha$  for TNT in seawater for one test were reported by Cole (4) as 6.7 and 0.0003 sec, respectively. For  $a$  equal 6.7, the term  $1 - e^{-a}$  is so nearly one that it may be treated as one for any reasonable purpose.

The value of the time constant can be found from pressure vs time data. The values of  $\Theta$  reported by Cole were determined from such data. In the absence of  $p$  vs  $t$  data for the materials below the test slabs at Eglin, an estimate was made of  $\Theta$  from movie film of test number 8 of reference (2). This estimate gave a  $\Theta$  value of 0.001 sec for that case in which the subsoil was sandy clay.

The value selected for  $A$  was 22,000 psi, which is a rough average of the values in table II. In order to determine a suitable value of  $\alpha$ , the high

speed film of the same shot 8 of reference (2) was again used. From the film and other data, the breach radius was estimated to be 10 inches;  $R_{cA}$  at 10 inches from 30 inches below the slab becomes 2.64 feet. Setting  $I_c = I_{ap}$  and solving for  $\alpha$  gives a value of 4.50 for the exponent. Using the values thus determined, the following equations result.

$$P_m = 22,000 \left( \frac{W^{1/3}}{R} \right)^{4.50} \quad (9)$$

$$I_{ap} = 0.001 P_m \quad (10)$$

where  $R$  is in feet,  $P_m$  in psi and  $I_{ap}$  in psi-sec. Equation (9) is simply the model proposed by Cole (4) with an experimentally determined value of the exponent  $\alpha$ . In the context of the existing data, the Cole model does not appear logical. Note that the maximum pressure depends upon the charge weight raised to the 1.5 power. Analytical results indicate the pressure should vary as the 0.333 power of the charge weight. Experimental results cited by Cole for seawater show values of  $\alpha$  of very nearly unity, in which cases the exponent of  $W$  is essentially 0.333.

As a result of the above cited facts, the following model for shock waves in soil is proposed.

$$P_m = \frac{A W^{1/3}}{R^n} \quad (11)$$

Specific impulse would still be calculated from equation (7).

Using the model consisting of equation (10) and (11) along with equation (2), values of  $n$  were found for both sandy loam and clay subsoils under the Eglin slabs. For sandy loam, a value of  $n$  (for use only in equation (11)) of 2.52 is proposed until more data can be obtained. The critical depth ( $R_{cA}$ ) recommended is 2.4 feet. The time constant recommended for sand is 1.06ms. Where the subsoil is clay, the value of  $n$  recommended for use in equation (11) becomes 2.30,  $\theta$  becomes 1.00ms and critical depth is 2.64 feet.

$R_{cA}$  is the estimated maximum distance of the explosive C.G. from the slab base

which will yield breaching of the unreinforced slab. Any shot placed further below the slab surface should result in no breaching. Cracking could result, and chunks may be taken out of unreinforced slabs, even in the absence of breaching. Figure 1 shows the status of the slab 0.385 seconds after detonation for test number 8 of reference (2). The effects of cracking and the resulting large chunks can be seen. The pressure and specific impulse required to lift the chunks are much less than those required for breaching. The status of the reinforced slab of test 2 of reference (2) is shown in Figure 2 for comparison with the unreinforced slab. The estimated time after detonation 0.152 seconds in the latter case.

## VI. SYNERGISTIC EFFECTS

The discussion thus far has been confined to a single charge exploding beneath a slab or runway. Clustered munitions may be detonated closely enough to one another to realize a synergistic effect. Furthermore, it may be possible to detonate these munitions simultaneously or at specified time intervals.

The interaction of two shock waves of moderate strength results in a pressure which is simply the sum of the two individual pressures. For the pressure levels expected at the bottom of the slabs, the summation approximation will be used. The pressure at any point at or behind the intersection of two explosive shock fronts will be taken to be the sum of the incident pressures at that point.

Pressure at a point behind a spherical shock front is given as a function of radius and time by equation (11). For two charges the total pressure at any point and time is given by

$$P_T = AW^{1/3} e^{-t/\theta} \left( \frac{1}{R_1^n} + \frac{1}{R_2^n} \right) \quad (12)$$

The above expression applies when two identical charges are detonated at the same depth in similar media, as shown below.



Figure 1. Test 8, 1980, reference (2). Time after detonation 385ms.  
Unreinforced slab.

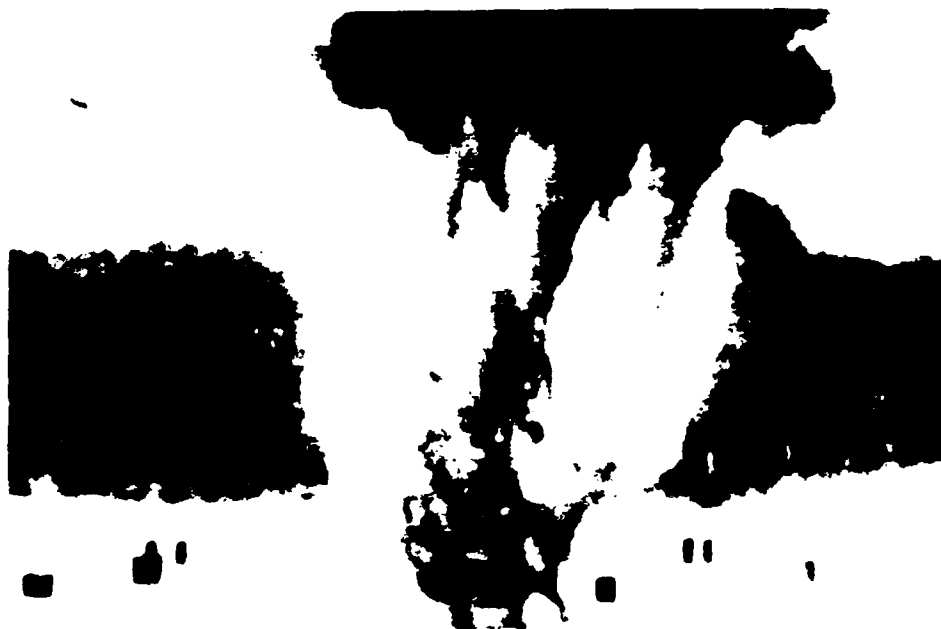
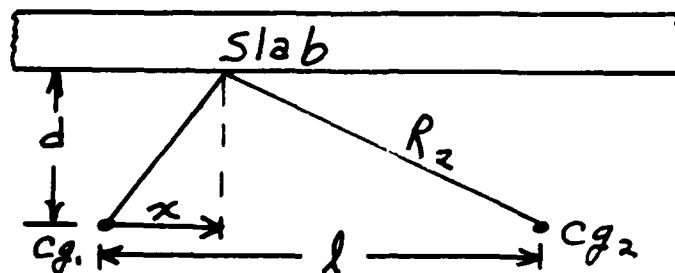


Figure 2. Test 2, 1980, reference (2). Time after detonation 385ms.  
Reinforced slab.



The pressure distribution along a line connecting the projections of the centers of gravity onto the slab is, in terms of  $x$ ,

$$P_T = AW^{1/3} \left[ \frac{e^{-t_1/\theta}}{(x^2 + d^2)^{n/2}} + \frac{e^{-t_2/\theta}}{((l-x)^2 + d^2)^{n/2}} \right] \quad (13)$$

The maximum pressure at any point  $x$  will occur when both  $t_1$  and  $t_2$  are zero.

$$P_{Tmax} = AW^{1/3} \left[ \frac{1}{(x^2 + d^2)^{n/2}} + \frac{1}{((l-x)^2 + d^2)^{n/2}} \right] \quad (14)$$

This function has either a maximum or a minimum at  $x = l/2$ . After some laborious algebra, it can be shown that  $P_T$  is a maximum at  $x = l/2$  when

$$l < \frac{2d}{\sqrt{n+1}} \quad (15)$$

For  $n = 2.3$ , as proposed here,  $P_T$  is a maximum when  $l$  is less 1.27 times  $d$ . This would indicate that if the distance between charges is set at the proper value, a useful increase in the maximum pressure acting on the slab would result. The model proposed, including values of parameters  $A, n$ , etc., is based upon analysis of the physical situation (mostly from the literature), a very small quantity of data from references (1) and (2), and a significant portion of intuition. There is little doubt that a more exact model can be derived from basic laws, but the utility of a more sophisticated model is questionable at this time. More data is needed on both single shot tests and multiple shot tests. Abundant pressure vs time data at a number of stations are needed for every test. Further mathematical exercises with equations (14) and (15), along with the assumption that reflection would increase the pressures at the slab by about 10 percent (after Cole), lead to the following results. Using the optimum depth of 2.64 for a 6.7 pound charge of AFX-708 under Eglin slabs with clay subsoil, the distance between charges from equation (15) should be 2.89 feet and the resulting maximum pressure at  $l/2$

would be 6348 psi where the breaching  $P_m$  required would be only 4310 psi assuming the reflected wave helps. Simultaneous detonation was used.

For the same subsoil, etc., the optimum values of  $d$  and  $L$  to give 4310 psi at  $L/2$  would be 44 inches deep and 48 inches apart.

A third case of distance  $L$  required to give 4310 psi at  $L/2$  when  $d$  is 2.64 feet yields a value of 57 inches between charges.

Examination of high speed films of the tests reported by Wilson (2) indicates that the numbers calculated for  $d$  and  $L$  would not necessarily produce the best results in terms of damage to runways. Significant damage radii in the two tests of most interest were of the order of two feet. The unreinforced concrete showed significant cracking to as much as 10 feet from ground zero. This significant cracking occurred to a lesser extent in reinforced slabs. Based upon the observation of photographic results and upon the calculations cited, a separation distance of up to 20 feet between simultaneously detonated rounds would appear likely to produce useful synergistic effects in unreinforced concrete.

The aforementioned movies showed that the larger chunks of unreinforced concrete moved upward for about 400 milliseconds (ms) before falling back toward ground. The plume of explosive products, soil and other debris, were still rising at 400ms. After one second, it was all over. Study of these films leads one to believe that any shock wave that is to provide a synergistic effect must arrive well before the chunks of concrete have quit rising. It is probable that detonations over 100ms apart will provide little support of one another.

It is obvious that more test data is needed to clarify this situation. A starting point for testing might be a fifteen or twenty foot separation with a time interval of zero between detonations. In testing for the effect of detonation time differences, the 100ms separation would be a reasonable starting point.

VII. TEST PROGRAM. A test program consisting of five pairs of detonations



has been proposed and specified; arrangements are virtually complete for implementation.

VIII. RECOMMENDATIONS. The proposed synergism test program should be completed. In addition, pressure measurements should be taken from future single-shot tests of similar munitions.

A data base of pressure-time-distance information for subsurface detonations should be built from all possible sources. Perhaps a central depository of P, t, R data could be set up within DOD to answer questions on instrumentation, to disseminate information and to analyze P, t, R data as it becomes available.

Data from the forthcoming synergism tests should be analyzed to improve the parameter values now being used in the model. Alternate models should be proposed and investigated for the purpose of finding an improved model for both single shot and synergistic detonation.

A computer code should be developed for mapping pressure, impulse, and energy functions onto the bases of runway slabs. This code should be capable of handling single, as well as multiple, detonations.

## REFERENCES

1. English, Wilson L., CADM Depth of Burst Test, ADTC-TR-79-7, February, 1979.
2. English, Wilson L., KEPT Depth of Burst Test, AD-TR-80-56, August, 1980.
3. Das, Braja M., Fundamentals of Soil Dynamics, Elsevier, New York, 1983.
4. Cole, Robert H., Underwater Explosions, Princeton University Press, 1948.
5. Bruno, E. J., Editor, High Velocity Forming of Metals, American Society of Tool and Manufacturing Engineers, Dearborn, Michigan, 1968.
6. Drake, James L. and Charles D. Little, Jr., Ground Shock from Penetrating Conventional Weapons, Symposium on the Interaction of Non-Nuclear Munitions with Structures, U. S. Air Force Academy, Colorado, May, 1983.
7. Ross, C. A., E. L. Jerome, and L. E. Malvern, Spatial and Time Variations of Loading on Buried Structures by Underground Cylindrical Explosives, Proceedings of the Second Symposium on the Interaction of Non-Nuclear Munitions with Structures, Panama City Beach, Florida, April, 1981.
8. Ross, C. A., et al, Concrete Breaching Analysis, AFATL-TR-81-105, Eglin AFB, Florida, 1981.
9. Ross, T. J., Characterizing Impulsive Failure in Buried Reinforced Concrete Elements, Second Symposium on the Interaction of Non-Nuclear Munitions with Structures, Panama City Beach, Florida, April, 1985.

1987 USAF-UES SUMMER FACULTY RESEARCH PROGRAM/  
GRADUATE STUDENT SUMMER SUPPORT PROGRAM

Sponsored by the  
AIR FORCE OFFICE OF SCIENTIFIC RESEARCH

Conducted by  
UNIVERSAL ENERGY SYSTEMS, INC.

FINAL REPORT

CONSTRUCTION CONTRACT ADMINISTRATOR'S TECHNICAL HANDBOOK

Prepared By:	Kweku K. Bentil, AIC
Academic Rank:	Associate Professor
Department and University:	School of Building Construction University of Florida
Research Location:	AFLMC/LGC Gunter Air Force Station Montgomery, Alabama 36114-6693
USAF Researcher:	MSgt. Herbert "Bo" Hill
Date:	July 21, 1987
Contract No.:	F49620-85-C-0013

# Construction Contract Administrator's Technical Handbook

by

Kweku K. Bentil

## ABSTRACT

Construction contracting is a complex and intricate process. Successful administration of these contracts therefore requires a combination of technical and administrative backgrounds. While there are several guides covering some of the administrative aspects, very little is provided in the technical area to assist base contracting personnel to better understand those on whom they depend for technical expertise (Civil Engineering), and those with whom they have to communicate technically throughout the duration of a contract. There is, therefore, a need for a handbook to help bridge the gap between the non-technical contracting person and their technical counterparts (Civil Engineering and Contractors). This handbook is designed to provide general information on the basic fundamentals of construction technology, construction cost estimating, construction progress scheduling, contract documents, effective contract administration and computer applications in the construction industry. It is illustrated with figures and charts and ends with quick reference appendices of tables, formulae, etc. and a bibliography of suggested reference books.

### ACKNOWLEDGEMENTS

I wish to thank the United States Air Force Office of Scientific Research, Air Force Systems Command, for the the opportunity to participate in the Summer Faculty Research program. Rodney Darrah and his staff at the Universal Energy Systems must be mentioned for their support and assistance in the administrative aspects of the program.

Contributions by many people made it possible for me to develop the "Construction Contract Administrator's Handbook" within the ten-week research period. The contributions made by various individuals at base contracting offices and the Contracting Directorates of the Air Force major commands were outstanding. The support provided by the staff of the Air University Library and the graphics section was very much appreciated.

Special gratitude is expressed to Lt Col Tom Jones and Major-select Chuck Coffin and their staff at the Contracting Directorate of the Air Force Logistics Management Center for a truly enjoyable working atmosphere. The input by Capt Dan Daley and TSgt Chuck Swartz were valuable. The administrative support by Sgt Dave Pearson was very helpful. The assistance and guidance of MSgt Herbert "Bo" Hill was invaluable in overcoming many technical roadblocks. The interest of Dr. Brisbane Brown Jr. (of the School of Building Construction, University of Florida) in every phase of this project served as a source of encouragement.

Finally I would like to thank my wife Phyllis for her loving support, trust, understanding and being there when I needed her, and my

two younger children, Sandra and Leslie for their understanding when I was not at home during most of the summer when they needed me.

## I. INTRODUCTION:

Every construction project, regardless of the size, is normally characterized by a need (usually determined by the owner), the development of the need into satisfactory plans and specifications (usually done by the architect/Engineer and/or owner), the transformation of those plans and specifications into a structure (usually by a contractor) and the administration of the project during construction by a contract administrator.

On United States Air Force construction projects, contracting officers are responsible for administering contracts to ensure:

- a) the performance of the contractor is in accordance with the terms and conditions of the contract; and
- b) the Air Force gets what it pays for.

Contracting officers and their administrators are normally not required to have formal training in construction because technical support is usually provided by base civil engineering. Unfortunately, the construction process is very technically-oriented and all the "players" with whom the contract administrator has to deal on a daily basis (such as contractors, base civil engineering, and subcontractors) are all technical types.

Therefore, this handbook was developed to enhance the technical knowledge of contract administrators. Chapter One discusses the fundamentals of the construction process and provides some of the basic terminology and abbreviations, common mathematical formulae used in

construction-related calculations, basic blueprint reading techniques, common units of measurement, types of structures, types of construction projects, and construction materials.

Chapter Two discusses the subject of construction cost estimating including its definition, types of estimates and their uses, components of an estimate and sources of pricing information.

Chapter Three discusses the topic of construction scheduling including basic scheduling terminology, types of schedules and their application.

Chapter Four discusses construction contract documents including specifications and drawings.

Chapter Five covers the subject of contract administration including communications, negotiations, modifications, claims, value engineering, site visits, contract completion and close-out procedures.

Chapter Six discusses computer applications in the construction industry.

In addition to the above chapters, quick reference information is provided in several appendices.

This handbook was developed for the construction contract administrator with little or no technical knowledge or background in construction and it is hoped its use will improve the administration of construction contracts throughout the Air Force.

My research interests are in the areas of effective construction management, cost estimating, cost control, the effective use of value



engineering as a tool for controlling costs and the avoidance of construction claims.

The School of Building Construction at the University of Florida is the oldest and America's first school of Construction Education. I currently teach the advanced course in Estimating during the normal academic year and our graduate course in Construction Management and Value Engineering during the summer. I am presently the technical editor for Walker's Estimating and Construction Journal. I have published several articles on the subjects of estimating, cost control and construction management. Prior to going into academe in 1985, I had worked in the construction industry for 15 years, the last five as the General Manager and Construction Manager for a General Contractor who performed a lot of government construction contracts. In that capacity I worked on and successfully completed several Air Force construction projects as well as other U.S. Army Corps of Engineers and Navy construction projects.

From that experience I became quite familiar with Air Force contract administration procedures from the contractor's point of view. My prior experience with Air Force projects as well as my general background in construction contributed significantly to my being assigned to the Contracting Directorate of the Air Force Logistics Management Center.

## II. OBJECTIVES OF THE RESEARCH EFFORT:

The primary objective of my assignment as a participant in the 1987 Summer Faculty Research program was to develop systems to aid Air Force base-level construction contracting personnel in order to improve the

effectiveness of the administration of Air Force contracts. The preliminary goals arrived at with my USAF Research Colleague included:

1. The development of computerized pricing models to assist construction contract administrators in determining the most advantageous prices to the Air Force.

2. The development of a construction contract administrator's handbook to enhance the technical background of non-technical base-level construction contracting personnel and contract administrators in order to achieve improved effectiveness in the administration of Air Force construction contracts.

3. The revision of Air Force Form 3052, Construction Cost Breakdown, to make it more compatible with what is used in standard construction industry practice.

4. The development of a weighted guideline type system to aid base-level contract administrators in analyzing profit on Air Force negotiated construction contracts.

Due to the fact that the installation of the Wang computer system purchased by the Air Force had not quite been completed, it was decided that goal No. 1 above should be held in abeyance for future research when all the installation had been completed. A decision was made that due to the ten-week time limitation of the SFRP goal No. 2 (the development of the handbook) be started during this period (ten-week summer period) and that goal No. 3 (The revision of AF 3052) and No. 4 (The development of the profit guidelines) be undertaken on my return to my institution with funding from the mini-grant program.

III. With the decision made to develop a construction contract administrator's technical handbook, the following approach was designed to achieve this objective:

1. Conducting a literature search.
2. Identification of selected representatives within the Air Force Major Commands and the solicitation of their input.
3. Base-level contracting personnel and solicitation of their input.
4. Identification of selected representatives of Base Civil Engineering and solicitation of their input.
5. Review of the Federal Acquisition Regulations.
6. Evaluation and analysis of inputs received.
7. Preparation of a draft handbook.
8. Distribution of the draft handbook to the appropriate personnel within the Air Force for their review and comments.
9. Evaluation and analysis of comments received.
10. Preparation of the final version of the handbook.
11. Preparation of final report.

A literature search was conducted to determine if any prior work had been done on the subject of a general technical handbook and if so if any portions can be used in the development of this handbook.

Examination of known data sources -- Defense Logistics Studies Information Exchange (DLSIE), Defense Technical Information Center (DTIC), AFLMC studies, etc. - revealed no other efforts dealing with a handbook of the nature required. There were however some studies and reports that dealt with some specific topics such as value engineering, contract administration, etc. The literature search was also used to collect technical data for the handbook.

On completion of the literature search, representatives were identified within the Air Force major commands, base contracting and civil engineering to:

- a) Ascertain if a handbook of this nature was needed.
- b) Solicit their input on the subjects to be included in the handbook.

Telephone interviews conducted confirmed the need and support for the development of the handbook. At this point a general review of the Federal Acquisition Regulations was done to avoid any conflicts.

Based on the preliminary feedback received from representatives of the Major Commands, the author's prior experience on Air Force construction projects and several authoritative sources within the construction industry, a draft of the handbook with appropriate illustrations was developed. Draft copies of the handbook were then sent to four major commands within the Air Force (ATC, MAC, SAC and TAC), one base under each of the commands and the Air Force Engineering and Services Center for their review and comments and also to ensure

that the contents of the handbook were not in conflict with Air Force regulations or policy.

#### IV. RECOMMENDATIONS FOR FUTURE RESEARCH

While there are several guides covering most of the administrative aspects of construction contracting, very little has been provided until now in the technical area to assist base contracting personnel. To complement the handbook and make it more effective in achieving the objective for which it was intended, the following recommendations should be considered:

a) Seminars should be conducted for the various base contracting personnel to supplement the handbook. The need for these seminars were also expressed by several of the bases contacted during the development of the handbook and could be done at a relatively low cost compared to the benefits. Since no formal technical training is required of contract administrators, what technical background they have has been either learned on the job or by trial and error. There is, therefore, a definite need to conduct technical seminars to complement the handbook. The School of Building Construction at the University of Florida, America's first School of construction Education is well prepared and has the staff and facilities to conduct such seminars. An alternative to the seminars may be the production of a videotape to supplement the handbook.

b) Air Force Form 3052, Construction Cost Breakdown, should be revised to make it more compatible with standard construction industry cost estimating forms. This will facilitate the comparison and

evaluation of contractors cost estimates by both contract administrators and Civil Engineering and assist them to determine the most advantageous prices to the Air Force. Particularly, with the Air Force currently installing Wang computers, it is recommended that AF 3052 be also automated after it has been revised.

c) A weighted guideline type of system should be developed to assist contract administrators in the analysis of profit on negotiated contracts and modifications. Presently, contract administrators have no established method of analyzing profit. The development of this guideline will improve the Government's chances of getting what it pays for.

d) Even though value engineering clauses are included in most Air Force contracts and a General Accounting Office report indicates an increase in savings over the last few years, the value engineering goals are still not being met. It is therefore recommended that a guide or handbook on value engineering be developed to aid the Air Force Civil Engineering division in effective application of value engineering during the design and estimating phases of construction projects.

While this handbook may not completely eliminate all the problems associated with the administration of construction contracts, it is hoped that with the implementation of above recommendations it will achieve its objective of enhancing the effectiveness in administration of construction contracts throughout the Air Force.

## REFERENCES

### A. CONFERENCE AND JOURNAL PUBLICATIONS

1. Bentil, Kweku K., "Estimating Basics", Technical Transactions of the American Association of Cost Engineers 31st Annual meeting, Atlanta, Georgia, June 1987
2. Bentil, Kweku K., "Applied Estimating-Definitive Estimates", Technical Transactions of the American Association of Cost Engineers 31st Annual Meeting, Atlanta, Georgia, June, 1987.
3. Bentil, Kweku K., "Applied Estimating-Conceptual Estimates," Technical Transactions of the American Association of Cost Engineers 31st Annual Meeting, Atlanta, Georgia, June 1987.
4. Bloomquist, Bruce N., MSgt, USAF "Construction Contract Administration", Report No. 780601-1 AFLMC, Gunter AFS, Alabama August 1979.
5. Merrill, William E., 1st Lieutenant USAF and Torchia, Linden J., Captain, USAF, "Air Force Construction Contract Disputes: An Analysis of Armed Services Board of Contract Appeals Cases to identify Dispute type and causes", Air Force Institute of Technology, Wright-Patterson AFB, Ohio, September, 1982.
6. Neil, James M., "Scheduling Basics", Technical Transactions of the American Association of cost Engineers 31st Annual meeting, Atlanta, Georgia, June, 1987.
7. Ogilvie, Raymond W, "An analysis of the Factors Influencing Performance of the Department of Defense Value Engineering Program", Masters Thesis, U.S. Army Logistics Management Center, Fort Lee, Virginia, June 1986.

## B. TEXT BOOKS

1. Allen, Edward. "Fundamentals of Building Construction Materials and Methods", John Wiley and Sons, New York 1985.
2. Crespin, V; Ziegler, D; Brown, B.H. Jr.; and Strange, L.; "Walker's Manual for Construction Cost Estimating", Frank R. Walker Company, Chicago, Illinois, 1981.
3. Dell'Isola, Alphonse J, "Value Engineering in the Construction Industry", Construction Publishing Company Co. Inc., New York, 1975.
4. Dodge, F.W., "An introduction to Building Plans and working Drawings", McGraw Hill Information Systems, New York.
5. Harris, Cyril M. "Dictionary of Architecture and Construction", McGraw Hill Company, New York, 1975
6. Horsley, William F, "Means Scheduling Manual", 2nd Edition, R. S. Means Co, Kingston, Ma., 1984.
7. Miles, Lawrence, "Techniques of value Analysis and Engineering", 2nd Edition, McGraw Hill Co., New York, 1971
8. O'brien, James J., "Value Analysis in Design and Construction", McGraw Hill Company, New York, 1976.
9. Steinberg, Joseph and Stempel, Martin, "Estimating for the Building Trades", American Technical Society, Chicago, IL., 1969.
10. Walker, Frank R. Company, "Walker's Building Estimator's Reference Book", 22nd Edition, Frank R. Walker Co., Chicago, IL., 1986.



1986 USAF-UES SUMMER FACULTY RESEARCH PROGRAM

GRADUATE STUDENT SUMMER SUPPORT PROGRAM

Sponsored by the

AIR FORCE OFFICE OF SCIENTIFIC RESEARCH

Conducted by the

Universal Energy Systems, Inc.

FINAL REPORT

Prepared by:	David Betounes, Ph.D
Academic Rank:	Professor
Department and	Mathematics Department
University:	University of Southern Mississippi
Research Location:	Armament Division, KRT Computer Sciences Directorate Eglin AFB, FL 32542
Date:	28 July 1987
Contract No.:	F49620-85-C-0013

Least Squares Estimation Theory and  
Geometrical Smoothers

By  
David Betounes

ABSTRACT

Research was conducted on possible improvements to the current algorithm for producing Time, Space, Position, Information (TSPI) from cinetheodolite tracking data. The current AD/KR program THEOD for producing TSPI employs the Davis algorithm with weights reflecting the observation errors in the tracking cameras but not reflecting the geometry of the cameras relative to one another as well as in relation to the object being tracked. These latter factors were incorporated into the Davis algorithm by means of various weighting schemes, and computer simulation studies were conducted to test the effectiveness of these schemes in producing better TSPI. Since the topic of research is a special case of non-linear (weighted) least squares estimation theory, a study of the theoretical foundations was conducted as well. Closely related to this is the use of filter/smothers to produce the TSPI, and (following the ideas of Cranford and Lindgren) a secondary focus of the research involved building a new smoother based upon the geometry of the Frenet frame and helix of curvature. This is the subject of an ensuing grant proposal.

#### ACKNOWLEDGEMENTS

I wish to thank the Air Systems Command and the Air Force Office of Scientific Research for their sponsorship of this Research. Universal Energy Systems must be mentioned for their concern and help to me in all administrative and directional aspects of this program.

Of those at Eglin AFB who contributed to a meaningful and productive research period, I should thank first Dr. Sam Lambert, Senior Scientist, especially for the interesting and informative tour of the base which he so carefully organized (This provided a broad overview of the total research effort being conducted by the Armament Division). Secondly I thank Ralph Duncan, Deputy Director of Computer Sciences, for his helpfulness in getting me settled in at AD/KR and his administrative concern with my research. Finally the technical assistance, ideas, and advice I received from Ken Cranford, John Lindegren, and George Weekly proved to be invaluable.

## I. INTRODUCTION:

The exact location of the position in time of aircraft, missiles, drones, etc. based upon measurements from various tracking devices (cinetheodolites, radars, etc.) is inherently a geometrical problem combined with mixture of probability and statistics arising from errors introduced in the measuring process. The theoretical setting for this problem is known as estimation theory. The problem of producing smoothed position, velocity, and acceleration information, either by conventional means or by recent Kalman-square root filter/smoothers has been predominantly analytical in nature. However it is clear that improvements in these techniques should incorporate the underlying geometry arising from the dynamics of the motion.

My own particular area of research interest has been differential geometry and its applications to mathematical physics (the calculus of variations, classical Lagrangian and Hamiltonian systems, elementary particle theory, and gauge theories). While the estimation theory problem of interest to Eglin AFB was not an exact match with my area of expertise, it was one to which I could contribute with both theoretical and experimental (computer) studies. The problem of building some geometry into the currently used filters is of course more directly related to my research.

## II. OBJECTIVES OF THE RESEARCH EFFORT:

The preliminary goals of my research effort (together with those added during the course of the summer) were as follows:

- (1) Improve the raw estimates of positions (for aircraft, missiles etc.) calculated from cinetheodolite tracking data. One of the current KR programs for doing this (program THEOD) uses a standard estimation scheme, first applied by Davis (1955) to this setting, of minimizing the sum of weighted squares of angular deviations: the current weights accounting only for observational errors in measurement. It was proposed to analyze alternative weighting schemes which also take into account camera geometry, camera object geometry, together with other factors that should improve the quality of the estimate.
- (2) Develop alternative models for velocity based roll angle calculation. One of the current KR models for doing this is incorporated in the Verac TDOP software package, and is based on the assumption that the aircraft acceleration is produced solely by the lifting force on the wing in conjunction with the force of gravity (namely that the aircraft maneuvers solely by use of its wings). Because of certain singularities that can develop and of certain flight paths that obviously violate the above assumption (wing coordinated flight), it was proposed to develop a more sophisticated model

for the calculation of the roll angle.

- (3) Develop alternatives to moving arc polynomial smoothing of the raw  $x, y, z$  data, with the aim of producing better TSPI (Time, Space, Position Information). Currently the polynomial (in time  $t$ ) fit treats each coordinate  $x, y, z$  separately to do the smoothing, and since this method seems to ignore the underlying physics, it was proposed (during the latter part of my research period) to devise alternative methods which could yield more accurate TSPI.

The next three sections (III-V) describe the approaches used to meet these three objectives, and the results of each approach taken.

### III. WEIGHTED DAVIS ALGORITHMS:

To explain the approach taken here it is best to first mention a few aspects of the general theory of weighted least squares (Cf. references 1,4-7 for estimation theory, filters & smoothers) Suppose (1):  $y = (y_1, \dots, y_n)$  represents the observations or measurements recorded (in our case these are the azimuths and elevations recorded by cameras at a number of different sites  $y = (az_1, el_1, \dots, az_n, el_n)$ ), and (2):  $x = (x_1, \dots, x_k)$  represents the quantities to be estimated (in our case  $x$  = the aircraft position at some time). Also assume that  $x$  and  $y$  are related by some function  $f$ , namely that  $y = f(x)$  whenever the measurements

are exact (no errors). More generally, allowing for errors in measurements, the weighted least squares estimate  $x$  (with weighting matrix  $W$ ) is chosen as the point which minimizes the function

$$S(x) = (y - f(x)) \cdot W(y - f(x)) \quad (1)$$

The extremal equations (normal equations)  $\partial S(x)/\partial x_j = 0$  for  $x$  when written in matrix form are:

$$H(x)^T W (y - f(x)) = 0 \quad (2)$$

where  $H(x) = df(x)$  is the Jacobian matrix of  $f$  at  $x$ . For non-linear estimation problems (i.e.  $f$  is non-linear) Eq.(2) is solved by an iteration scheme (Newton-Raphson):

$$x_{m+1} = x_m + [H(x_m)^T W H(x_m)]^{-1} H(x_m)^T W (y - f(x_m)) \quad (3)$$

$m = 0, 1, 2, \dots$  which yields a sequence  $\{x_m\}_{m=1}^{\infty}$  that converges to a solution  $x$  of Eq.(2) provided the initializing point  $x_0$  is properly chosen.

The probability and statistics enters the estimation theory as follows. The measurements are viewed as random fluctuations about a "true" value  $\bar{y}$ , i.e.  $y$  is a random vector with mean  $Ey = \bar{y}$ , and, say, covariance matrix  $E(y - \bar{y})(y - \bar{y})^T = P$ . Then the estimate  $x$  chosen by the above weighted least squares process is a random variable with mean  $Ex = \bar{x}$  and covariance matrix  $Q$ . For non-linear estimation problems, the connection between  $y$  and  $x$  (and thus between  $\bar{y}, P$  and  $\bar{x}, Q$ ) is very complicated; however in the linear case this connection is linear and  $\bar{x}$  minimizes  $S$ :  $H^T W (\bar{y} - f(\bar{x})) = 0$  while  $Q$  is given by:

$$Q = [H^T W H]^{-1} H^T W P W H^T [H^T W H]^{-1} \quad (5)$$

Additionally, viewing  $Q$  in Eq.(5) as a function of the weighting matrix  $W$ , the Gauss-Markov theorem says that minimum variance  $\text{var}(x) = \text{tr}(Q)$  is achieved by the choice of  $W = P^{-1}$  for the weighting matrix.

Now specializing the foregoing to the cinetheodolite tracking problem, the estimation scheme, named after Davis in this case, is non-linear and the search for an optimal weighting matrix was essentially experimental — computer simulations, since a generalization of the Gauss-Markov theorem to non-linear problems is lacking (a limited amount of effort was devoted to finding such a generalization theoretically; various 1-dimensional analogs such flag pole height estimation were investigated in this regard). The methodology for our experimental approach was as follows:

(i) The model for the measurements consisted of choosing a reference point (position)  $x_{\text{ref}}$ , computing the true az's and el's:  $Y = (AZ_1, EL_1, \dots, AZ_n, EL_n)$  of  $x$  from the various camera locations, and then perturbing these with Gaussian fluctuations to obtain random measurements:

$$az_i = AZ_i + g_i$$

$$el_i = EL_i + g_i$$

Here the  $g_i$ 's are independent Gaussian random variables with mean zero and standard deviation = sig. Consequently the measurement random variable  $y$  has mean  $\bar{y} = Ey = Y$  and covariance matrix  $P = (\text{sig})^2 I$ .



(ii) Several algorithms were selected for comparison: (a) an unweighted Davis algorithm ( $W = 1$ ), (b) two weighted Davis algorithms (one with  $W$  varying during the iteration), and (c) a generalized Bodwell algorithm. This latter algorithm chooses the estimated position  $x$  so as to minimize  $\sum_{i=1}^n D_i(x)^2$ , where  $D_i(x)$  is the distance from  $x$  to the  $i$ th line of sight. For just two cine-T's this reduces to Bodwell's (1951) algorithm. The computer simulations used as input the random measurements  $y$  described in (i) and produced as output the estimates of position (random variables)  $x_a, x_{b1}, x_{b2}, x_c$  dictated by the various algorithms. The statistics of these estimates were compared as a means of discerning the quality of the estimates.

After numerous simulation runs it was found that the difference in statistics for  $x_a, x_{b1}, x_{b2}$ , and  $x_c$ , under numerous geometries, was essentially negligible. The reason for this was finally attributed to the fact that at the estimation algorithms (a), (b), and for that matter any weighted Davis algorithm are all essentially linear at the scale under consideration. This scale was a sig = .0001 radians for the standard deviations in the cine-T's angle measurements and a cutoff of the iteration scheme Eq.(3) when  $x_m$  is within .0001 miles (approx. 6 inches of its limit). This assertion was verified directly from an analysis of the points  $x_1, x_2, x_3, \dots$  produced during the simulation runs. The first point  $x_1$  produced by the scheme in Eq.(3) is the linear estimate. The ensuing points are the improv-

ements dictated by the non-linearity. Thus it was found that in all the cases  $x_2, x_3, \dots$  were all within 6 inches of the linear estimate.

#### IV. VELOCITY BASED ROLL ANGLE CALCULATION

Only a limited amount of time during the research period was available to spend on this topic. Verac's TDOP (1987) software calculates the roll angle from velocity  $V$  and acceleration  $A$  according to the following model. Let  $G$  be the acceleration of gravity, and let  $F$  be the acceleration of the specific force defined by  $F = A - G$ . Resolving the respective vectors into tangential parts (along  $V$ ) and normal parts (in the plane normal to  $V$ ), one has  $F_n = A_n - G_n$  as the equation for the normal parts. To determine the roll angle one needs a vector  $U$  in the up direction relative to the pilot. A simple model (wing coordinated flight) assumes that  $U = F_n$ . Verac's model is slightly more sophisticated than this (allowing for the fact a diving maneuver is not executed by first rolling into an inverted position). It takes  $U = \pm F_n$ , with the  $\pm$  sign depending on whether  $F_n$  makes an acute or obtuse angle with the up position calculated at the immediately preceeding time (a  $+$  sign is used if the angle is  $90^\circ$ ). Having determined  $U$  in this fashion, let  $U_1 = (k \times V) / |k \times V|$ ,  $U_2 = (U_1 \times V) / |U_1 \times V|$ . Then  $U_1, U_2$  is a basis for the normal plane and in terms of it  $U = a U_1 + b U_2$ , with of course  $a = U \cdot U_1$  and  $b = U \cdot U_2$ . The roll angle  $R$  is then calculated as  $R = \text{ATAN2}(a, b)$ .

Several approaches were considered in an attempt to improve the above model for the roll angle determination: (1) In the determination of  $U$  the  $+$  introduces a discontinuity into the model, and of course the  $\text{ATAN2}(a,b)$  function has discontinuities at points along the ray  $a = 0, b < 0$ . Some consideration seems to indicate that there is no way to remove these discontinuities from the model. (2) Originally it was thought that the use of the Frenet frame  $T,N,B$  and the expression of the pilot's up vector  $U$  in terms of  $N$  and  $B$  might produce a somewhat better model. Some investigation indicates that there is no advantage in this directly. However it seems promising to pursue the use of the Frenet frame in the TDOP square root information filter with the aim of producing velocities  $V$  and accelerations  $A$  with less noise in them and thus in the end producing better values for the roll angle. The reasoning here is that the present filter uses a state model which does not take into account the dynamic dependence of the coordinates  $x,y,z$  on one another, and perhaps the use of the Frenet frame in the filter can model this dependence. This will be part a proposal for a Follow on Grant to this research.

#### V. MOVING FRENET FRAME & MOVING HELICAL SMOOTHERS

Only a limited amount of time was available to devote to this aspect of my summer research (the objective was just proposed during the last two weeks), which appears to be a very promis-

ing avenue for investigation. Two approaches have been briefly studied: (1) approximating the position by its third order Taylor series in  $t$  and rewriting this in terms of the Frenet frame (which is assumed known at the time under consideration), one obtains a moving arc algorithm on which a smoother can be based that models the interactive dependence of  $x, y, z$  during the motion. (2) Each space curve can be closely approximated by a helix ( the helix of curvature ) just as plane curves are approximated by their circles of curvatures. Thus it seems reasonable to base a moving arc smoother on segments of helices.

The further details of these types of smoother are contained in the proposal for a Follow on Research Grant.

#### VI. RECOMMENDATIONS:

(1) Since the data from the computer simulations indicate that the weighted Davis algorithms are essentially linear at the scale under consideration, each of these algorithms will produce (approximately) an unbiased estimate of position and the weighting matrix  $W$  which produces a minimum variance estimate is  $W = P^{-1}$ , where  $P$  is the covariance matrix for the measurement errors (Gauss-Markov). Thus unless one looks for algorithms outside the standard estimation theory (e.g. the generalized Bodwell algorithm is non-standard) or one has less precision in the measuring devices (so that effect of the non-linearities is more pronounc-

ed), no drastic improvement in the quality of the estimates produced by the present KR program THEOD can be expected by use of alternative weighting schemes. It is recommended that the present code not be modified in this regard. Another recommendation that results as a corollary to this research is that some consideration be given to whether the Newton-Raphson iterations are really needed in the code for THEOD. The present code goes through 25 iterations or cuts off when the new and old coordinate differences are less than 0.1 feet. As indicated above the first iteration produces the linear estimate, while the ensuing iterations produce refinements to this, which in theory are needed but which in practice were found to be negligible (and in some cases the refinements were oscillatory). It therefore might be worthwhile to process some actual tracking data on THEOD and keep track of how much each successive iteration improves the estimated position over the estimate produced on the first iteration.

(2) At present there is no recommendation on how to directly improve the roll angle calculation in the TDOP code. One could try to remove the singularities in the model mentioned above, and one could try to build a more sophisticated model, perhaps a so called minimum energy model, which recognises that other control mechanisms (besides the wings) can and are used during flight.

However it seems more promising to recommend that the research mentioned above be pursued: (i) incorporate the Frenet frame directly in the TDOP square root information filter , and (ii) use a moving Frenet-frame smoother or a moving helical smoother in conjunction with THEOD to produce the smoothed TSPI (conventional mode of processing). The details of this research is contained in the author's proposal for a Follow on Research Grant.

#### REFERENCES

1. Bierman, Gerald J., Factorization Methods for Discrete Sequential Estimation, New York, NY, Academic Press, 1977.
2. Bodwell, C.A., "A least squares solution for the cinetheodolite problem," Holoman AFB Report MHT-138, Alamogordon, New Mexico, 1951.
3. Davis, Thomas D., "Computation of a phototheodolite location," AD/KR Technical Report 157822 , Eglin AFB, Florida, 1955.
4. Jazwinski, A.H., Stochastic Processes and Filtering Theory, New York, NY, Academic Press, 1970.
5. Gelb, Arthur, Applied Optimal Estimation, Cambridge Massachusetts, MIT Press, 8 th Ed., 1984.
6. Linnik, Y.V., Methods of Least Squares and Principles of the Theory of Observations, Oxford, England, Pergamon Press, 1961.
7. O'Conner, C.L., et. al., "AD/KR TDOP Models and Algorithms," VERAC Reports R-053-87 & R-054-87, San Diego, CA, 1987.

1987 USAF-UES SUMMER FACULTY RESEARCH PROGRAM/  
GRADUATE STUDENT SUMMER SUPPORT PROGRAM

Sponsored by the  
AIR FORCE OFFICE OF SCIENTIFIC RESEARCH  
Conducted by the  
Universal Energy Systems, Inc.

FINAL REPORT  
Increasing Work Capacity of Personnel Wearing  
Protective Clothing in Hot Environments

Prepared by: Phillip Bishop  
Academic Rank: Assistant Professor  
Department: Department of Physical Education  
University: University of Alabama  
Research Location: School of Aerospace Medicine, Chemical  
Defense Branch, Brooks AFB  
USAF Researchers: S.H. Constable, Ph.D.; S.A. Nunneley, M.D.  
Date: July, 1987  
Contract No.: F 49620-85-C-0013



Increasing Work Capacity of Personnel Wearing  
Protective Clothing in Hot Environments

by

Phillip Bishop

ABSTRACT

It has been established that the use of protective clothing such as the Chemical Defense Ensemble (CDE) in moderate to hot environments substantially reduces work capacity. The purpose of this research was to determine the efficacy of rest and microenvironmental cooling in increasing work capacity in a hot environment. Rest proved of limited value but microenvironmental cooling increased work duration 104 percent. Final mean rectal temperature, skin temperature, heart rates, and sweat production rates were substantially lower for the cooled condition compared with the no cooling condition despite longer work times. Only working heart rate was higher in the cooled condition. The liquid cooling system removed 73% of the metabolic heat generated during the total work-rest period.

#### ACKNOWLEDGEMENTS

I appreciate this opportunity for study and research provided by the Air Force Systems Command and the Air Force Office of Scientific Research. I am grateful to the staff of the Chemical Defense Branch of the School of Aerospace Medicine for their support. Dr.'s Sally Nunneley, and Stefan Constable; and John Garza, Ann Miksch, Liz Staves and my graduate students, Carolyn Robinson and Suzanne Enlow helped make my stay especially productive. Dr. Constable's advice and assistance was particularly valuable.

## I. Introduction:

I have an undergraduate degree in oceanography from the U.S. Naval Academy, eight years commissioned service in the Navy and over 2500 hours of flight time. I received a doctorate in physical education with specialization in exercise physiology in December 1983 from the University of Georgia. I worked in the Chemical Defense Branch of USAFSAM in the Summer of 1986 and did a preliminary investigation of the impact of the CDE on work capacity.

Because of my previous involvement with this research and the work done in submitting a grant proposal in this area to the AFOSR, I was very interested in further investigating this complex problem.

## II. OBJECTIVES OF THE RESEARCH EFFORT:

The purpose of this research was to evaluate the effectiveness of a work-rest cycle coupled with microenvironmental cooling during rest in increasing work output and reducing heat storage for personnel engaged in physical labor while wearing the U.S. Armed Forces chemical defense ensemble (CDE).

## III. OVERALL APPROACH:

Work by humans in the presence or threat of a physical, chemical or radiation hazard requires the use of protective clothing. The protective clothing varies from the protective clothing of the American football player to the chemical defense ensemble of the U. S. Armed Forces. Commonly this clothing impairs the normal physiological cooling mechanisms of the body. In warm to hot environments, this compromise of the cooling ability may result in internal heat storage to

the extent that work capacity is significantly reduced relative to work in the same environment without the clothing (Joy and Goldman, 1968; Pandolf & Goldman, 1978; Yates et al, 1980; Webber et al, 1981; Frye & Flick, 1983; Carpenter & Flick, 1984). In some circumstances, the thermal burden of this protective clothing may be an inconvenience. In emergency rescue, firefighting, military operations, and other situations, the consequent heat storage may be a serious threat to both health and successful task completion (Joy & Goldman, 1968).

The simplest solution to the problem of heat storage generally is to reduce the metabolic contribution to the heat accumulation. This can be accomplished by either reducing the work rate or providing frequent rest breaks. In some situations, i.e. certain military, rescue or emergency environmental hazard scenarios, the compromise of total work output must necessarily be minimized. Also, if rest breaks occur under hot conditions, they have proven of limited value in reducing body temperature.

Another solution to the heat storage problem has been to supply some mode of external auxillary microenvironmental cooling (Nunneley, 1970; Shapiro et al, 1982; Carpenter & Flick, 1984; Flick & Frye, 1985; Cosimini et al, 1985; Epstein et al, 1986). Attempts to cool personnel during ambulatory work using portable systems have shown this approach to be currently untenable for effective large scale field use (Carpenter & Flick, 1984; Cosimini et al, 1985).

A third, previously untested solution to the heat storage problem of personnel wearing protective clothing in hot environments would be to

combine intermittent rest breaks with microenvironmental cooling during rest periods only. Such an approach reduces the requirement for cooling system portability, is more practical than attempting to cool the work environment, and could increase the total work output for a given time period by shortening the cooling (rest) time.

The purpose of this research was to evaluate the effectiveness of a work-rest cycle coupled with microenvironmental cooling during rest, in increasing work output and reducing heat storage for personnel engaged in physical labor while wearing the U.S. Armed Forces CDE.

Subjects. Subjects for these experiments were seven Air Force and two civilian volunteers. Subjects varied in age, fitness, size, and state of heat acclimation and included six males and three females. Subject characteristics are given in Table 1. Because this study was limited to volunteers, this sample may have a higher aerobic fitness level than would be representative of the Air Force.

Methods. Informed Consent was obtained and all testing was conducted in accordance with S.A.M. ACHE Protocol 86-9. Maximal oxygen uptake was determined for subjects using standard gas bag collection methods. Additionally, the metabolic cost of walking on the treadmill dressed only in shorts and tee shirts was also measured. All subjects who did not have previous experience with the protective clothing (PC) were given a practice trial which allowed them to familiarize themselves with the clothing and treadmill walking. Subjects performed treadmill walking in an environmental chamber at mean dry, wet and globe temperatures of 38.0/26.1/43.4 degrees Centigrade, respectively. Work

speed was approximately .3 m/s. Rest was conducted in the chamber without radiant load to simulate rest in the shade. Test conditions were as follows.

- 1) Treadmill walking at 3 mph and either 3% or 6% grades, (depending upon level of fitness) while wearing the PC. Subjects walked until they achieved a rectal temperature of 39.0 C. This test is referred to as "NO REST".
- 2) The same treadmill exercise except subjects walked 30 minutes followed by 30 minutes of rest. Work VO2 with the PC was normally measured during this trial. This test is designated "NO COOL".
- 3) The same treadmill exercise while wearing the PC except a personal cooling system was used during rest. This test is designated "COOLED".
- 4) The same treadmill exercise except the subject wore only military fatigue pants and cotton shirts (clo=1.40, im/clo=.476). This test is designated "NO PC".

The PC which was worn consisted of a complete chemical defense ensemble (CDE) outfit including M17 protective mask and hood. Military fatigue shirt and trousers were worn under the PC (total clo=2.55 and im/clo=.280). For safety reasons, athletic shoes were worn instead of protective rubber overboots. The personal cooling system consisted of a snug-fitting ILC Dover liquid cooling vest covering approximately .5 square meters of the upper torso. The vest contained about 48 meters of tygon tubing with quick detach, self-sealing connectors. Coolant was supplied to the vest by an electrically powered cooling system with an output of one liter per minute of coolant at 10 to 15 degrees C. Coolant was 95% water with 5% propylene glycol.

Skin temperatures, rectal temperatures, and heart rates were

monitored continuously and recorded every 30 seconds on a PDP-11 computer utilizing a custom system locally developed by John Garza (OAO Corp.). When liquid cooling was used, coolant flow rates and inlet and outlet temperatures were also recorded with the computer. Chest skin temperatures and thigh temperatures were measured with YSI 700 thermistors. Rectal temperature was measured from a probe located 10 cm beyond the sphincter. Rating of perceived exertion (Borg, 1962) was measured at the end of the work cycle. Cooling rates for the liquid system were computed from the temperature change, flow rate and specific heat of the coolant. Sweat production and sweat "losses" were computed from pre- and post-experiment nude and clothed body weights adjusted for water intake. Subjects drank water ad libitum during rest only. Body surface area was computed from a Dubois equation nomogram.

#### IV. RESULTS AND DISCUSSION;

Mean work time, mean rise in rectal temperature, peak chest and thigh temperatures, peak heartrate, and RPE for each test condition are presented in Table 2. In the NO REST and NO COOL conditions, in all cases work was terminated by the investigator due to a core temperature of 39 degrees C. Under these conditions, in some cases rectal temperatures continued to rise even during the rest cycle. In all other experimental conditions, subjects terminated work due to volitional fatigue. The use of microenvironmental cooling increased work time 104 percent and reduced the rise in working rectal temperature by 54 percent compared to the No Cool condition.

Mean Metabolic heat production, sweat production, sweat loss, and

heat loss via sweat loss are presented in Table 3. Mean heat removal by the liquid vest was 1940 kj.

Mean core temperatures and heart rates for the work rest cycles for the four conditions are shown in Figure 1.

Discussion. The purpose of this research was to evaluate the effectiveness of a work-rest cycle coupled with microenvironmental cooling during rest in increasing work output for personnel performing labor while wearing PC. Rest alone was ineffective in increasing total work output despite the fact that the time weighted rate of work was reduced 50%. In contrast, the total work output was doubled through the use of liquid cooling administered during rest periods. Work output when cooling was used was limited by physical fatigue rather than by excessive heat storage. The fatigue was most likely a consequence of the increased energy costs of wearing the suit which raised the fraction of maximal oxygen uptake of the work task. The increased heat storage may have also contributed to fatigue. The same walking task performed without the PC resulted in minimal heat storage and physical fatigue was lessened.

The sweat production rates were similar for No Rest and No Cool considering that there was no rest period for the NO REST condition. Sweat rates were substantially less for the COOL and PC conditions. The potential heat removal through sweat loss was so high as to imply that only a fraction of the sweat lost was evaporated from the skin. This is true because if all the sweat lost had evaporated, the subjects would have had a net heat loss rather than gain. There was in a number of



cases obvious sweat drippage. Estimations of sweat losses through drippage could not account for the total sweat loss. The PC and underclothing were always saturated with sweat suggesting that some sweat also evaporated from the clothing some distance from the skin providing little useful cooling. Undoubtedly, there was some evaporation from both skin and clothing which recondensed within the clothing shell, this was certainly the case when cool liquid was present in the cooling vest. Regardless of the final disposition of the sweat, more sweat was produced than could be evaporated. The effectiveness of sweating would be further compromised in more humid environments than the low relative humidity of our experiments.

The microenvironmental cooling was effective in removing approximately 70% of the metabolic heat production. In addition to the physiological benefits of the cooling, subjects benefited in terms of comfort, frequently suggesting the cooling represented welcome relief.

Although it was not the purpose of this research to test USAF Regulation 355-8 which gives guidance for use of the military (CDE), data collected allowed a cursory test of the guidance provided by this regulation. In general it was observed that for moderate and heavy work at 38 C, the work time to 120 Kcal was about double the time suggested by the regulation. Our findings did agree with the regulation regarding the futility of rest as a means of increasing work capacity at 38 C.

Recommendations:

- 1) That the AF begin research to empirically validate USAF REG. 388-5 for work in the CDE in hot environments. A research grant proposal will be submitted to evaluate some aspects of the regulation.
- 2) That the USAF explore options for individually assessing thermal status rather than attempting to predict thermal responses. There are at least 13 variables influencing physiological response and almost half of these are uncontrollable. Individual differences may render any prediction inaccurate no matter how sophisticated the model. It has been suggested previously (Pandolf and Goldman, 1978) that the convergence of core and skin temperatures marked the end point of heat tolerance in PC. It was subsequently suggested that any mean skin temperature  $> 37^{\circ}\text{C}$  marked the end point. Although we had no heat casualties, on several occasions these criteria were met. The use of convergence appears inapplicable under our test conditions. Two possibilities for monitoring individual response to thermal stress are heartrate and an externally signaled core temperature.
- 3) That additional physiological data be obtained from field tests of personnel performing their actual work tasks in PC. The constraints of the laboratory are necessary, but laboratory work must be paralleled by field test to ensure the generalizability of the results and to assist in the design of further research.

### References

- Borg, G. Physical performance and perceived exertion. Lund, Gleerup, 1962.
- Carpenter, A.J. and C.A. Flick, "Report on Liquid Cooling Development," Tech. Memo 27290404 , 4 May, 1984, VNC, SAM, Brooks AFB.
- Cosimini, H., N.A. Pimental, B.S. Cadarette, J. Cöhen, B. de Chrisofano, R. Goff, W.L. Holden, V. Iacono, M. Kupinskas, L. Levine, K. B. Pandolf, M.N. Sawka, and T. Tassinari, "A Determination of the Feasibility of Two Commercial, Portable Microclimate Cooling Systems for Military Use, Natick/TR 85/033L , March, 1985.
- Epstein, Y., Y. Shapiro and S. Brill, "Comparison Between Different Auxiliary Cooling Devices in Severe Hot/Dry Climate," Ergo. 29(1986)41-48.
- Flick, C.A. and A.J. Frye, "Chamber Evaluation of LSSI Aircrew Liquid Cooling System," ASCC Working Party 61 Final Report, TPA 787-61 , Jan. 1985, VNC, SAM, Brooks AFB.
- Frye, A.J. and C.A. Flick, "Report on Chamber Evaluation of Groundcrew Liquid Cooling System," Tech. Memo 2720009 & 27290404, 1983 , VNC, SAM, Brooks AFB.
- Joy, R.J.T., R. Goldman, "A Method of Relating Physiology and Military Performance; a Study of Some Effects of Vapor Barrier Clothing in a Hot Climate," Mil. Med. , (1968) 458-470.
- Nunneley, S.A., "Water Cooled Garments: a Review," Space Life Sci. , 2(1970)335-360.
- Pandolf, and R.F. Goldman, "Convergence of Skin and Rectal Temperatures as a Criterion for Heat Tolerance," Aviat. Space and Environ. Med., 49(1978) 1095-1101.
- Shapiro, Y., K.B. Pandolf, M.N. Sawka, M.M. Toner, F.R. Winsmann, and R.F. Goldman, "Auxiliary Cooling; Comparison of Air-Cooled vs. Water-Cooled Vests in Hot-Dry and Hot-Wet Environments," Aviat. Space and Environ. Med., 53(1982)785-789.
- Webbon, B., L. Montgomery, L. Miller and B. Williams, "A Comparison of Three Liquid-Ventilation Garments during Treadmill Exercise," Aviat. Space and Environ. Med. , 52(1981)400-415.
- Yates, R.E., C.R. Replogle, J.H. Veghte, " Thermal and Acceleration Effects on Aircrew Members in Chemical Defense Gear," AMRL-Tech. Report 79-71 , (1980)01-36.

Table 1. Mean ( $\pm$  s.d.) Physical Characteristics of Subjects.

Age (yrs)	Ht. (cm)	Wt. (kg)	SFC (m <sup>2</sup> )
36 $\pm$ 8.5	174 $\pm$ 8.5	71.7 $\pm$ 10.7	1.85 $\pm$ .19

Max. V02 (l/min)	Work V02 (l/min)	PC V02 (l/min)	Max HR (bt/min)
3.59 $\pm$ .86	1.09 $\pm$ 0.26	1.46 $\pm$ 0.23	184 $\pm$ 13

\* PC V02 is the work V02 with PC.

Table 2. Mean (+s.d.) work time, and Physiological responses.

	Work Time (mins.)	Rectal Temp. (C)	Peak Chest Temp. (C)	Peak Thigh Temp. (C)	HR (bt/min)	RPE
NO REST						
work	59 $\pm$ 9	39.1 $\pm$ .1	38.5 $\pm$ 0.4	37.8 $\pm$ 0.5	163 $\pm$ 12	14 $\pm$ 4
NO COOL						
work	70 $\pm$ 14	39.0 $\pm$ 0.2	38.3 $\pm$ 0.5	37.7 $\pm$ 0.7	145 $\pm$ 50	15 $\pm$ 3
rest	62 $\pm$ 17	38.8	37.9 $\pm$ 0.2	37.7 $\pm$ 1.0	115 $\pm$ 18	
COOL						
work	143 $\pm$ 29	38.3 $\pm$ 0.4	37.4 $\pm$ 0.8	37.2 $\pm$ 1.0	164 $\pm$ 16	14 $\pm$ 3
rest	143 $\pm$ 20	37.7 $\pm$ 0.3	28.4 $\pm$ 3.1	37.0 $\pm$ 1.1	87 $\pm$ 15	
NO PC						
work	115 $\pm$ 12	37.6 $\pm$ 0.1	35.6 $\pm$ 0.2	35.5 $\pm$ 0.8	113 $\pm$ 9	11 $\pm$ 4
rest	115 $\pm$ 12	37.3 $\pm$ 0.2	35.0 $\pm$ 0.9	35.6 $\pm$ 0.4	69 $\pm$ 10	

Values shown are the mean final values for work and rest as indicated.

Table 3. Mean (+ s.d.) Metabolic heat production rate and total production, sweat production, sweat loss, and potential heat loss via sweat loss.

	Metabolic Production (Kj)	Sweat Prod. (g/min.)	Sweat Loss (g/min)	Sweat Heat Loss (Kj)
NO REST	1.79 $\pm$ 0.41	18.5 $\pm$ 8.1	8.4 $\pm$ 4.5	1.19 $\pm$ 0.48
NO COOL	1.20 $\pm$ .30	15.7 $\pm$ 9.7	5.6 $\pm$ 1.7	1.47 $\pm$ 0.53
COOL	2.66 $\pm$ .68	9.7 $\pm$ 5.6	6.0 $\pm$ 3.7	2.86 $\pm$ 2.02
NO PC	1.84 $\pm$ 0.28	8.4 $\pm$ 3.1	7.6 $\pm$ 3.3	3.3 $\pm$ 1.01

Sweat Heat Loss is the potential heat removed if all sweat were evaporated at the skin.

# INTERMITTENT MICROCLIMATE COOLING STRATEGIES

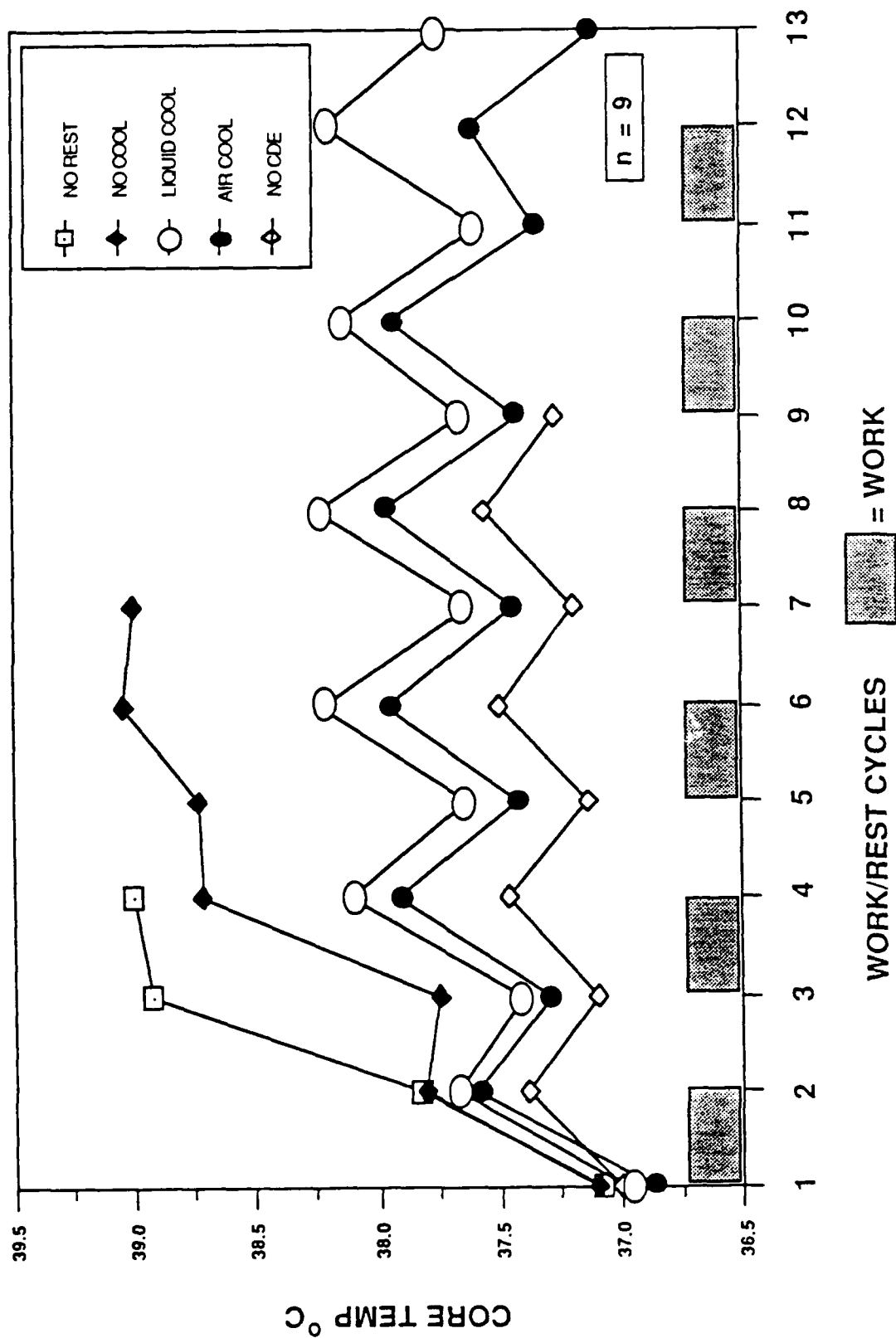


Figure 1.

1987 USAF-UES SUMMER FACULTY RESEARCH PROGRAM/  
GRADUATE STUDENT SUMMER SUPPORT PROGRAM

Sponsored by the  
AIR FORCE OFFICE OF SCIENTIFIC RESEARCH

Conducted by the  
Universal Energy Systems, Inc.

FINAL REPORT

USER-SYSTEM INTERFACE STANDARDS

Prepared by: Jerome W. Blaylock, Ph.D.  
Academic Rank: Associate Professor  
Department and Computing and Applied Sciences  
University: Texas Southern University  
Research Location: Air Force Logistics Management Center  
AFLMC/LGM  
Gunter AFS, Alabama 36114-6693  
USAF Researcher: Lt Col Phillip L. Harris  
  
Date: 30 September 1987  
Contract No: F49620-85-C-0013



# User-System Interface Standards

Dr. Jerome Blaylock

## ABSTRACT

Numerous base-level logistics application systems are being developed within the Air Force for various micro, mini, and mainframe computer systems. There do not currently exist adequate standards for the user-system interface. As a result, each system contains its own user interface. It is not unusual to find at a single workstation applications that run on a variety of micro, mini, and mainframes under different operating systems, each with its own unique user interface.

This report documents the results of an analysis of the feasibility of developing user-system interface standards for Air Force base-level logistics computer application systems. It recommends that user-system interface standards be developed for base-level logistics systems based on existing guidelines for developing user interface software that have previously been developed for the Air Force. The user-system interface standards should first be developed for IBM compatible microcomputers under MS/DOS and OS/2, and implemented in a prototype system. Other related conclusions and recommendations are provided.

## ACKNOWLEDGMENTS

The author of this report wishes to thank HQ Air Force Maintenance and Acquisition Logistics Policy Division (HQ USAF/LEYM), the Air Force Logistics Management Center, the Air Force Systems Command, and the Air Force Office of Scientific Research for sponsorship of this research. Further thanks goes to the Logistics Management Center personnel who provided information used in the preparation of this report.

The work reported in this document was sponsored by the Air Force Office of Scientific Research/AFSC under Contract F49620-85-C-0013, and HQ USAF/LEYM under Project LM870705.

## I. INTRODUCTION

I-1 Background. The mission of the Air Force Logistics Management Center (AFLMC) is to increase Air Force readiness and combat capability by conducting studies and developing, analyzing, testing, evaluating, and recommending new or improved concepts, methods, systems, or procedures to enhance logistics efficiency and effectiveness. Resources of the AFLMC include approximately one-hundred handpicked professionals from base-level logistics functions and "state-of-the-art" microcomputer and minicomputer systems. Mainframe computers are also available.

Personnel at the AFLMC observed that numerous base-level logistics computer application systems are being developed without adequate user-system interface standards. Jerome W. Blaylock, Ph.D., was selected under the 1987 Summer Faculty Research Program (SFRP) to investigate the feasibility of developing user-system interface standards for Air Force logistics systems. Dr. Blaylock is an Associate Professor of Computer Science and a Research Scientist at Texas Southern University where he has taught courses in operating systems and microcomputer assembly language programming, and conducted research in software engineering under a research grant. He has worked for the U.S. Air Force and consulted for the U.S. Navy, Department of Energy, and NASA. Dr. Blaylock has published numerous technical papers, primarily in the area of computer performance evaluation and capacity planning.

I-2 Purpose. The purpose of this report is to document the results of the investigation of the feasibility of developing user-system interface standards for Air Force base-level logistics systems, and to recommend actions and follow-on research. The work reported was performed during a ten-week period in the Summer of 1987 at Gunter AFS, Alabama. It also included visits to other Air Force bases.

I-3 Problem. Numerous logistics application systems are currently being developed within the Air Force for various micro, mini, and mainframe computer systems. Programming and life-cycle management standards exist for the development of these logistics systems. However, there does not currently exist adequate standards for user interface with these systems. User-system

interface standards apply to the development of software for the interfacing of application systems with the users of the systems. User-system interface standards are a subset of system development standards for application systems. As a result of not having adequate standards for user interface, each system contains its own unique user interface requiring extensive user training. The problem of establishing user-system interface standards is exacerbated by the fact that these logistics systems are being developed by different organizations using different software and operation systems on micro, mini, and mainframe computer systems.

## II. RESEARCH OBJECTIVES AND APPROACH

II-1 Objectives. The primary objective of the research reported in this document was to investigate and report on the feasibility of developing user-system interface standards for Air Force base-level logistics computer application systems. The design of a prototype logistics user interface system was to be investigated. An existing logistics systems could be used as a prototype, or a prototype might be developed at the AFLMC. Existing windows software packages were to be identified and the applicability of the use of windows software for logistics systems was to be evaluated. The applicability of expert systems to logistics systems could also be considered. The development of user interface standards and prototype user interface systems to be proposed as Air Force standards for logistics systems must eventually be applicable to micro, mini, and mainframe environments. Since the Zenith microcomputer environment at the AFLMC, the typical UNIX minicomputer environment, and the base-level Unisys 1100/60 mainframe environment differ significantly, it may be more practical to first establish user-system interface standards for the IBM compatible microcomputer environment (e.g. Zenith MS/DOS).

II-2 Approach. The approach taken in satisfying the above objectives was to begin by conducting a literature search of documents related to user-system interface standards. On-line search facilities available at AFLMC to the Logistics Studies Research Bibliography (LSRB) and Defense Technical Information Center (DTIC) were utilized. Next, various productional, prototype, and developmental base-level logistics systems were viewed and

their user-system interfaces observed. This required travel to other Air Force bases. Additionally, a windows software package was identified and evaluated as to its applicability to base-level logistics systems. Prototype and expert systems were also considered. Finally, a report was prepared documenting the work performed, results obtained, recommendations, and suggested follow-on research.

### III. LITERATURE SEARCH

III-1 General. A major portion of the work performed under the SFRP involved literature searches, obtaining selected literature, and the review and study of relative material on user-system interface. A significant benefit of this effort to AFLMC is the acquisition of a large volumes of pertinent literature on user-system interface and related topics (e.g. man-machine interface, human factors, ergonomics). Only a small portion of the literature is referenced in this report because of limits on the length of the report. These topics constitute a broad, highly interdisciplinary area of study. This study concentrated on the user interface of computer software, in particular, base-level logistics application software and their associated software interface packages (e.g. windows).

The two most significant publications discovered by the literature search are as follows:

a. Guidelines for Designing User Interface Software by Sidney L. Smith and Jane N. Moiser [1]. This 478 page report was prepared by The MITRE Corporation for the Electronic Systems Division, AFSC, Hanscom AFB, Massachusetts. The 944 guidelines proposed in this report will be invaluable in developing user-system interface standards at AFLMC. Dr. Sidney Smith, co-author of the report, was invited to visit AFLMC. During his visit he made a formal presentation to AFLMC and AFSSC personnel followed by a full-day of informal discussions.

b. Designing the User Interface: Strategies for Effective Human-Computer Interaction by Ben Shneiderman [2]. In this book Dr. Shneiderman presents a comprehensive survey of the specifically human factors that need to be considered in designing interactive computer systems. His goal is to

encourage greater attention to the user interface and to help develop a more rigorous science of user interface design.

III-2 Military Publications. The following is a partial list of military publications relative to system development and user-system interface:

a. MIL-STD-1472C, Military Standard: Human Engineering Design Criteria for Military Systems, Equipment and Facilities [3]. This standard contains a ten-page addition on personnel-computers interface.

b. MIL-H-46855B, Military Specification: Human Engineering Requirements for Military Systems, Equipment and Facilities [4]. This is the fundamental document governing human engineering in military systems development.

c. DOD-STD-2167, Military Standard: Defense System Software Development [5]. This standard contains requirements for the development of Mission-Critical Computer System (MCCS) Software. The standard may also be applied to non-MCCS software development and acquisition.

d. DOD-HDBK-761, Military Handbook: Human Engineering Guidelines for Management Information Systems [6]. This document originated as a joint publication of the Management Information Systems Directorate, U.S. Army Materiel Development and Readiness Command, and the U.S. Army Human Engineering Laboratory. It is now published as a DOD Military Handbook which is intended to be an aid for the inclusion of human factors considerations in the design of Management Information Systems (MIS).

e. DOD 7920.1, Life Cycle Management of Automated Information System (AIS) [7]. This document establishes joint technical and functional policy governing the life cycle management and control of AIS.

f. AFR 700-series, Information Systems. The Air Force 700-series regulations provide life-cycle guidance for information systems. AFR 700-26, Information Systems: Acquisition and Management of Small Computers [8]. This regulation provides guidance for application software development.

g. AF Manual 171-100, Automated Data Systems (ADS) Standards [9]. This six-volume manual contains design, development, programming, testing,

documentation, implementation, maintenance, and data submission standards which apply Air Force-wide.

h. AFLMC Regulation 400-1, AFLMC Project Management System [10]. This regulation establishes procedures for managing the logistics improvement study efforts of AFLMC, including procedures for the life-cycle phases of logistics computers application systems.

i. ARI Research Product, Design Guidelines for User Transactions with Battlefield Automation Systems: Prototype for a Handbook [11]. These guidelines were prepared at the U.S. Army Research Institute.

III-3 Aerospace Publications. The following are some aerospace publications related to human factors engineering and user-system interface design:

a. Human Engineering Procedures Guide [12]. This technical report was prepared at the Air Force Aerospace Medical Research Laboratory, Wright-Patterson AFB, Ohio.

b. Human Factors in the Design and Evaluation of Aviation Displays [13]. This report was prepared by the NATO Advisory Group for Aerospace Research and Development.

c. Spacelab Experiment Computer Application Software (ECAS) Display Design and Command Usage Guidelines [14]. These guidelines were prepared at the NASA/George C. Marshall Space Flight Center, Alabama.

III-4 Military Supported Work.

a. As mentioned above, the most significant publication resulting from military supported work related to user-system interface is the Guidelines for Designing User Interface Software [1]. This publication is the latest in a series of technical reports [15,16,17,18,19,20,21] prepared by MITRE for the Electronic Systems Division, AFSC, Hanscom AFB, Massachusetts.

b. Science Application, Inc. has prepared two bibliographies on human factors in computer systems for the Office of Naval Research: Human Factors in Computer Systems: A Review of the Literature [22] and A Critically Annotated Bibliography of the Literature of Human Factors in Computer Systems [23].

### III-5 Books.

a. As mentioned above, the best single book on user-system interface standards is Designing the User Interface: Strategies for Effective Human-Computer Interaction by Ben Shneiderman [2].

b. Handbook of Screen Format Design by Wilbert O. Galitz [24]. This handbook serves to enhance one understanding the basic concepts of screen design.

### IV. ANS COMMITTEE X3V1

IV-1 Committee Meeting. The AFLMC was represented by Dr. Blaylock at the American National Standards (ANS) Committee X3V1 meeting in Bloomington, Minnesota during 8-12 June 1987. At the committee meeting he participated in the meetings of Task Group 9 - User System Interface. The four and one-half (4 1/2) day meeting provided an opportunity to discuss standards with over fifty representatives from computer vendors and users, both government and business. Eight individuals attended the Task Group 9 meetings. The results of an on-line literature search conducted at AFLMC were discussed with other attendees, one of which had also conducted an on-line search. Some of the main areas of involvement of Task Group 9 are: keyboards, icons, menus, system navigation, screen formatting, cursor movement, help facilities, and direct manipulation. Committee X3V1 also interfaces with other U.S. standards organizations and the International Standards Organization (ISO).

IV-2 Recommendation. It is recommended that future Air Force participation in ANS Committee X3V1 and Task Group 9 be considered. It is suggested that AFLMC send one or more representatives to the next ANS Committee X3V1 Meeting in Asbury, New Jersey during 14-18 September 1987. Possible choices of individuals to send are Dr. Blaylock, Capt Roberts, a human factors engineer, and someone from AFLMC/LGM. Based on the experiences at this meeting and the recommendations of the AFLMC attendee(s), the decision can be made about the Air Force officially joining ANS Committee X3V1 (cost is approximately \$200.00) and any future participation. The reason for suggesting participation at another ANS Committee X3V1 meeting prior to making the decision to join is that the last meeting of Task Group 9 was not typical.



Key members were late in arriving at the committee meeting because of their participation at an ISO meeting in Japan. Task Group 9 just completed the planning stage for future work. The accomplishments of Task Group 9 through the next ANS Committee X3V1 meeting should provide useful information to facilitate making the decision about joining ANS Committee X3V1.

## V. CURRENT SYSTEMS

V-1 General. Productional and prototype base-level maintenance systems were viewed and their user interface observed at AFLMC and the Air Force Standard Systems Center (AFSSC), Gunter AFS, Alabama; Air Force Human Resources Laboratory (AFHRL), Wright-Patterson AFB, Ohio; 33 TFW, Eglin AFB, Florida; 917 TFG, Barksdale AFB, Louisiana; and General Dynamics, Ft. Worth, Texas. Figure 1 contains a list of the systems viewed at each location. Table 1 shows characteristics of the systems and their computer environments. More detailed information about each system and its user interface characteristics is contained in the project folder at AFLMC.

V-2 AFLMC. All three base-level maintenance systems viewed at AFLMC run on Zenith microcomputer systems under MS/DOS. Each system is written in a different programming language (i.e., COBOL, FORTRAN 77, BASIC) and contains unique user-system interface software internal to the computer programs in the systems. Individually, the user-system interface of each system is appropriate for the application. The AFAMS and MEETS both tend to be data entry and reporting systems, whereas, CFR is a more interactive system that conducts a dialog with a pilot.

Because of the characteristics of the CFR application and its being implemented on a Zenith 248 with a color monitor, CFR has the more impressive user-system interface of the three systems. Many of the characteristics of CFR may be used in developing user-system interface standards and a prototype system. The CFR system does not contain windows; however, it could easily be adapted to a windows environment. The use of windows does not preclude the use of menus and full-screen displays, but instead, can be used to enhance these characteristics. The desirable user-system interface characteristics not contained in the three base-level maintenance systems at AFLMC include

on-line documentation, tutorials, help facilities, skill levels, icon type busy indicators, uniform function and control (soft) key implementations, and windows.

33TFW, Eglin AFB, Florida

- . Ground Station Unit (GSU)
- . Minimum Essential Engine Tracking System (MEETS)
- . Maintenance Management Information Control System (MMICS)

917TFG, Barksdale AFB, Louisiana

- . Turbine Engine Monitoring System (TEMS)
- . Comprehensive Engine Management System Increment IV (CEMSIV)
- . Maintenance Management Information Control System (MMICS)

General Dynamics, Ft. Worth, Texas

- . Ground Station Software (GSS)
- . Ground Station Unit (GSU)
- . Comprehensive Engine Management System (CEMS)
- . Maintenance Management Information Control System (MMICS)

AFHRL, Wright-Patterson AFB, Ohio

- . Integrated Maintenance Information System (IMIS)
- . Computer Based Maintenance Aids System (CMAS)
- . Maintenance Diagnosis Aiding System (MDAS)
- . Improved Technical Data System (ITDS)
- . Authoring and Presentation System (APS)

AFLMC, Gunter AFS, Alabama

- . Automated Flying and Maintenance Scheduling (AFAMS)
- . Minimum Essential Engine Tracking System (MEETS)
- . Computerized Fault Reporting (CFR)

AFSSC, Gunter AFS, Alabama

- . Core Automated Maintenance System (CAMS)
- . Reliability and Maintainability Information System (REMIS)

Figure 1 - Base-Level Systems Viewed

Table 1 - System Characteristics

System	M E T S	A F A M S	C F R	G S U	G S S	T E M S	C M A S	C E M S I V	I M I S	M D A S	I T D S	A P S	R E M I S	C E M S	M M I C S	C A M S
Characteristics																
Status																
Prototype									X	X	X	X				
Developmental													X			X
Productional	X	X	X	X	X	X	X	X						X	X	
Computes																
Zenith (IBM Compatible)	X	X	X	X	X	X										
GRID (IBM Compatible)							X									
Harris								X								
Sun (or Sun Compatible)									X	X	X	X				
Tandam													X			
Amdahl (IBM Compatible)														X		
Unisys 1100															X	X
Operating Systems																
MS/DOS	X	X	X	X	X							X				
CP/M						X										
UNIX								X	X	X	X					
GRID							X									
Mainframe													X	X	X	X
Programming Languages																
COBOL	X				X								X	X	X	X
FORTRAN		X						X								
BASIC			X													
PASCAL							X									
C									X	X	X	X				

V-3 AFSSC. The CAMS was viewed at the AFSSC and its user-system interface observed. The CAMS is a standard Air Force base-level maintenance system which runs on the Unisys 1100/60 mainframe computer system. The CAMS is written in COBOL which interfaces with the DMS1100 database management system, TIP transaction interface package, and DPS1100 screen formatting system. The user-system interface for CAMS is significantly influenced and controlled by these software products. As a result, the user-system interface characteristics of CAMS differ significantly from those of typical

microcomputer systems. For example, CAMS does not use windows, icons, etc., and the user does not navigate through CAMS in the manner typical for microcomputer systems. In CAMS each screen corresponds to a TIP transaction and transaction program which formats the screen through DPS1100. The CAMS and its predecessor, MMICS, would probably be the most difficult of the systems viewed to convert to the user-system interface standards developed for base-level application systems.

V-4 AFHRL. The prototype systems developed and being developed at the AFHRL are impressive in the computer techniques they utilize (e.g. full-screen displays, graphics, color). However, they follow no formal user-system interface standards. Only one of the systems includes provisions for help facilities and only one system provides for different skill levels. The systems follow no function and special (soft) keys standards. They do generally follow the procedures of listing the meanings of the function keys at the bottom of the screen.

V-5 Maintenance Units. The user interface characteristics of the systems observed at Eglin AFB, Florida, Barksdale AFB, Louisiana, and General Dynamics, Ft Worth, Texas are all significantly different. No two systems viewed were developed by the same organization. At a single workstation were observed systems running on a Zenith microcomputer under both MS/DOS and CP/M, on a Harris minicomputer under UNIX, and on an Unisys 1100/60 under OS1100. At another workstation were systems running on a Zenith 100 under MS/DOS, an Amdahl mainframe under MVS, and an Unisys 1100/60 under OS1100. There appears to be no central control or user interface standards for base-level maintenance systems.

## VI. STANDARDS VERSUS GUIDELINES

VI-1 General. An investigation of the feasibility of developing user-system interface standards requires first an analysis of the differences among design standards, guidelines, rules, and algorithms. Guidelines or rules might be a preferred alternative to standards at AFLMC. The use of standard software (e.g. windows) for user-system interface is an technique for enforcing certain user-system interface standards and assisting in system development.

We will begin with definitions of design standards, guidelines, rules, and software packages taken from Sidney Smith's article "Standards Versus Guidelines for Designing Use Interface Software" [25].

VI-2 Design Standards. A series of generally stated requirements for user interface design, imposed in some formal manner (e.g. legislation, contract, management decree, regulation). MIL-STD-1472C [3,25], subsection 5.15.3.2.1 is an example of a standard.

VI-3 Design Guidelines. A series of generally stated recommendations for user interface software, with examples, added explanation, and other commentary, selected (and perhaps modified) for any particular system application, and adopted by agreement among people concerned with interface design. Guidelines for Designing User Interface Software [1] contains 944 guidelines for user-system interfaces. Both standards and guidelines are in the public domain. By contrast, application-specific design rules and user-system interface software packages are developed almost exclusively for private use [25].

VI-4 Design Rules. A series of design specifications for a particular system application, stated specifically so that they do not require any further interpretation by user interface software designers. If guidelines are not translated into design rules, each designer will decide separately in the course of applying guidelines, which will result in an inconsistent design of user interfaces.

VI-5 Design Algorithms. Computer software implementing and imposing design rules which interface with application programs to control user-system interfaces. Microsoft Windows [26] is an example of user-system interface software.

VI-6 Recommendation. Based on the above definitions and discussion, it is recommended that AFLMC develop design rules for the design and development of user-system interfaces for base-level logistics systems. Guidelines for Designing User Interface Software [1] should be used in the development of these design rules. Through an iterative process these design rules should be developed and implemented on a prototype system using existing base-level

maintenance systems as samples of systems whose user interfaces are to be evaluated and improved. The design rules and prototype system should utilize any user-system interface software package(s) proposed or adopted for use by AFLMC.

The next question is what to call these design rules. They are not to be restricted to the design of a particular application system, as is generally the case for design rules, but are to apply to all base-level logistics systems. Initially, only those systems implemented on IBM compatible MS/DOS microcomputers (e.g. Zenith) may be considered. It may be desirable to call these design rules "standards" in order to be consistent with Air Force terminology, and to eventually publish them as an Air Force Regulation or Manual. Hopefully, they will receive better acceptance and adherence than the current Air Force Standards for Automated Data System (ADS) published in AF Manual 171-100 [9]. Another alternative is to refer to the design rules as design procedures or specifications.

## VII. USER INTERFACE SOFTWARE

VII-1 Alternatives. There are three alternatives available for implementing user-system interface software:

- a. Commercially available software packages.
- b. Locally developed software routines.
- c. Individually developed software for each program.

Of these alternatives, the first is the most desirable for the following reasons:

- a. Good commercial packages tend to be more comprehensive and reliable than locally developed software because of the large number of users.
- b. Commercial packages are generally less expensive than locally developed software because of the economics of scale.
- c. Commercial packages are generally upgraded by the supplier as computer systems change (e.g. MS/DOS to OS/2).
- d. Commercial packages require little or no local maintenance.
- e. Commercial packages are readily available.
- f. Commercial packages can reduce software development costs.

Locally developed software routines are an alternative to commercial packages when such packages are not available to meet the user-system interface needs of the developing organization.

VII-2 Overhead Impact. User interface software is not only critical to system development but can also represent a sizable investment [1,25]. The average percentage of operational software devoted to implementing the user interface is estimated by Smith [1,25] as comprising 30 to 35 percent. Estimates for individual systems range from 3 to 80 percent [17]. The percentage of software development devoted to implementing the user interface, while maintaining user-system interface standards, can be minimized by utilizing a good commercially available software package. Such a package will not handle all of the user-system interface software development and guarantee adherence to standards, but will aid in the design and development of user-system interfaces. The overhead associated with the proper development of effective user interfaces is more than offset in the long-term by the benefits of increasing user-system efficiency.

VII-3 Microcomputer Packages. We will address at this time user-system interface software packages for only IBM compatible (e.g. Zenith) microcomputers. Microsoft Windows [26] is the only general-purpose application user-system interface software package identified that runs on IBM compatible microcomputers under MS/DOS. The AFLMC currently has Microsoft Windows for their Zenith microcomputers. However, the Microsoft Windows Software Development Kit is needed to give application systems the windows-based iconic user interface [27]. Future IBM and IBM compatible microcomputers will run under the OS/2 operating system which will eventually replace MS/DOS. The Microsoft Windows Presentation Manager is included as a standard part of OS/2 [28]. One restriction on the use of Microsoft Windows is that it currently interfaces with application programs written in only the following three programming languages: C, Pascal, and Assembly.

VII-4 Display Analysis Program. The Display Analysis Program [29] was developed by Dr. Thomas S. Tullis based on work he performed for his Ph.D. thesis [30]. The program is a tool for use in evaluating and redesigning alphanumeric displays, especially CRT displays. The program was utilized as a part of this SFRP effort. It is recommended that AFLMC officially acquire and

continue to utilize and evaluate this program in analyzing screens/windows proposed for new application systems.

#### VIII. CONCLUSIONS AND RECOMMENDATIONS

VIII-1 Conclusions. The development of user-system interface standards for Air Force base-level logistics computer application systems is not only feasible, but is necessary. Already, the proliferation of base-level logistics systems at individual maintenance units is such that personnel are having difficulty learning and distinguishing among the numerous systems and their difficult user-system interfaces. At a single workstation were observed base-level maintenance systems running on Zenith microcomputers under both MS/DOS and CP/M, a Harris minicomputer under UNIX, and a Unisys 1100/60 mainframe computer system under OS1100. Each of these application systems had quite different user-system interfaces. In the future it is anticipated that the number of different systems running at a single workstation will increase significantly to the point that the training required to interface with the different systems will be prohibitive and the different user-system interfaces in their aggregate will be overwhelming. An effort to develop user-system interface standards and control the proliferation of base-level logistics systems with different user interfaces is overdue and is essential to the future success of logistics systems.

Adequate guidelines exist for the development of user-system interface standards. The development of such standards should be an iterative process involving detailed analyses and comparisons of current logistics systems (initially those systems that run on IBM compatible microcomputers) and their associated user-system interfaces. As proposed standards are being developed, they should be implemented in a prototype system which, when completed, can be field-tested. The prototype system should utilize proposed software packages for user interfacing.

VIII-2 Recommendations. The following recommendations are made based on the results of the research conducted under the 1987 SFRP. Some of these recommendations are stated in the body of this report. The following recommendations includes suggestions for follow-on research.



a. Develop user-system interface design rules called "standards" for Air Force base-level logistics application systems. Initially, these standards should only apply to IBM compatible microcomputer systems (e.g. Zenith MS/DOS), but later they should be developed for all base-level logistics systems.

b. Adopt windows as a tentative standard technique for user-system interface and acquire the Microsoft Windows Software Development Kit for evaluation. If other similiar software packages are later identified, they should also be acquired and evaluated.

c. Concurrent with the development of user-system interface standards, develop a prototype system implementing these standards.

d. Future Air Force participation in ANS Committee X3V1 and Task Group 9 - User System Interface should be considered based on the experiences of AFLMC representative(s) at the next ANS Committee X3V1 Meeting (see subsection IV-2).

e. The Display Analysis Program should be acquired, utilized, and evaluated by AFLMC for analyzing alphanumeric screens/windows proposed for new application systems (see subsection VII-4).

f. The application of expert systems to base-level logistics should be investigated by AFLMC as a project separate from user-system interface standards.

The SFRP frequently results in the submission by the SFRP researcher of a proposal for a Research Initiative Program (RIP) award for follow-on research to be conducted during the following year. The maximum award under the RIP is \$20,000. Such an award could support an effort to identify the appropriate user-system interface software guidelines for base-level logistics systems that run on IBM compatible microcomputers. The selection of these guidelines would be based on an analysis of the user interface requirements for existing microcomputers base-level maintenance systems.

## REFERENCES

- [1] Smith, Sidney L. and Jane N. Mosier, Guidelines for Designing User Interface Software, MITRE, MTR-10090, ESD-TR-86-278, NTIS/DTIC No. AD A177 198, Aug. 1986.
- [2] Shneiderman, Ben, Designing the User Interface: Strategies for Effective Human-Computer Interaction, Addison-Wesley, Nov. 1986.
- [3] MIL-STD-1472C, Military Standard: Human Engineering Design Criteria for Military Systems, Equipment and Facilities, DOD, Sept. 1983.
- [4] MIL-H-46855B, Military Specification: Human Engineering Requirements for Military Systems, Equipment and Facilities, DOD, Jan. 1979.
- [5] DOD-STD-2167, Military Standard: Defense System Software Development, DOD, June 1985.
- [6] DOD-HDBK-761, Military Handbook: Human Engineering Guidelines for Management Information Systems, DOD, June 1985.
- [7] DOD 7920.1, Life Cycle Management of Automated Information Systems (AIS), DOD.
- [8] AFR 700-26, Information Systems: Acquisition and Management of Small Computers, HQ USAF, April 1986.
- [9] USAF Manual 171-100, Automated Data Systems (ADS) Standards, Vol I-VI, HQ USAF, July 1985.
- [10] AFLMC Regulation 400-1, AFLMC Project Management System, Aug 1986.
- [11] Sidorsky, R.C., et al., Design Guidelines for User Transactions with Battlefield Automation Systems: Prototype for a Handbook, ARI Research Product 84-08, U.S. Army Research Institute, NTIS/DTIC No. AD A153 231, May 1984.
- [12] Geer, C.W., Human Engineering Procedures Guide, Technical Report AFAMRL-TR-81-35, Air Force Aerospace Medical Research Laboratory, NTIS/DTIC No. AD A108 643, 1981.
- [13] Hopkin, V.D. and R.M. Taylor, Human Factors in the Design and Evaluation of Aviation Displays, Report AGARD-AG-225, NATO Advisory Group for Aerospace Research and Development, NTIS/DTIC No. AD A076 631, 1979.
- [14] NASA, Spacelab Experiment Computer Application Software (ECAS) Display Design and Command Usage Guidelines, NASA/George C. Marshall Space Flight Center, Alabama, Report MSFC-PROC-711, 1979.
- [15] Smith, Sidney L. and Jane N. Mosier, Design Guidelines for User-System Interface Software, MITRE, MTR-9420, EDS-TR-84-190, NTIS/DTIC No. AD A154 907, Sept. 1984.

- [16] Benkley, Carl W., Use of Prototyping for Man-Machine Interface Requirements Definition on the AWDS Program, MITRE, MTR-9234, ESD-TR-84-178, NTIS/DTIC No. AD A146 033, Aug. 1984.
- [17] Smith, Sidney L., User-System Interface Design in System Acquisition, MITRE, MTR-9129, ESD-TR-84-158, NTIS/DTIC No. AD A140 956, April 1984.
- [18] Smith, S.L. and A.F. Aucella, Design Guidelines for the User Interface to Computer-Based Information Systems, MITRE, MTR-8857, ESD-TR-83-122, NTIS/DTIC No. AD A127 345, March 1983.
- [19] Smith, Sidney L., User-System Interface Design for Computer-Based Information Systems, MITRE, MTR-8464, ESD-TR-82-132, NTIS/DTIC No. AD A115 853, April 1982.
- [20] Smith, Sidney L., Man-Machine Interface (MMI) Requirements Definition and Design Guidelines: A Progress Report, MITRE, MTR-8134, ESD-TR-81-113, NTIS/DTIC No. AD A096 705, Feb. 1981.
- [21] Smith, Sidney L., Requirements Definition and Design Guidelines for Man-Machine Interface in C<sup>3</sup> System Acquisition, MITRE, M80-10, ESD-TR-80-122, NTIS/DTIC No. AD A087 258, June 1980.
- [22] Ramsey, H. Rudy and Michael E. Atwood, Human Factors in Computer Systems: A Review of the Literature, Technical Report SAI-79-111-DEN, Science Application, Inc., NTIS/DTIC No. AD A075 679, Sept. 1979.
- [23] Ramsey, H. Randy; Michael E. Atwood; and Priscilla J. Kirshbaum, A Critically Annotated Bibliography of the Literature of The Human Factors in Computer Systems, Technical Report SAI-78-070-DEN, Science Applications, Inc., NTIS/DTIC No. AD A058 081, May 1978.
- [24] Galitz, Wilbert O., Handbook of Screen Format Design, QED Information Sciences, Inc., 1981.
- [25] Smith, Sidney L., "Standard Versus Guidelines for Designing User Interface Software," Behaviour and Information Technology, Vol. 5, No. 1, pp 47-61, 1986.
- [26] Microsoft Windows: User's Guide and the Desktop Applications User's Guide, Heath Zenith Data Systems, 1986.
- [27] Hart, David and Lee, "Microsoft Windows Software Development Kit," Byte, pp. 250-256, June 1987.
- [28] Vellon, Manny, "The OS/2 Windows Presentation Manager: Microsoft Windows On the Future," Microsoft Systems Journal, Vol.2 No.2, pp. 13-17. May 1987.
- [29] Tullis, Thomas S., Ph.D., Display Analysis Program User's Guide, 1986.
- [30] Tullis, Thomas Stuart, Predicting the Usability of Alphanumeric Displays, Ph.D. Thesis, Rice University, Houston, Texas, Nov. 1983.

1987 USAF-UES SUMMER FACULTY RESEARCH PROGRAM

GRADUATE STUDENT SUMMER SUPPORT PROGRAM

Sponsored by the  
AIR FORCE OFFICE OF SCIENTIFIC RESEARCH

Conducted by the  
Universal Energy Systems, Inc.

FINAL REPORT

FOURIER TRANSFORM INFRARED STUDIES OF

ETHYLENEDIAMMONIUM DINITRATE AND

1,4-BUTANEDIAMMONIUM DINITRATE

Prepared by:	John M. Bopp, Jr.
Academic Rank:	Assistant Professor
Department and University:	Nazareth College of Rochester
Research Location:	AFATL/MNE Eglin AFB, Florida 32542-5434
USAF Researcher:	Robert L. McKenney, Jr.
Date:	12 September 87
Contract No:	F49620-85-C-0013

Fourier Transform Infrared Studies of  
Ethylenediammonium Dinitrate And  
1,4-Butanediammonium Dinitrate

by

John M. Bopp, Jr.

ABSTRACT

The structure of two salts, ethylenediammonium dinitrate (EDD) and 1,4-butanediammonium dinitrate (BDD) were investigated using Fourier transform infrared spectroscopy. Spectra were taken of solid EDD in reflectance and transmittance mode to examine a solid to solid phase transition. These results were compared to data obtained using differential scanning calorimetry. Transmittance spectra were obtained of the molten state of EDD and of two of its deuterated forms. Solid and molten spectra were taken of BDD as well as of six molten samples of various deuterated forms. Attempts were made to relate infrared absorption features to specific functional groups.

### ACKNOWLEDGEMENTS

I would like to express my appreciation to the United States Air Force Systems Command and to the Air Force Office of Scientific Research for their sponsorship of this summer fellowship program. I wish to thank the staff of universal Energy Systems for their assistance.

This summer fellowship was a personally rewarding experience due to the many helpful and competent people I had the privilege to work with. Bob McKenney was generous in his support, advice and professionalism. My colleague and housemate, Steve Struck, provided an enjoyable atmosphere in the lab as well as at home. I was fortunate to have Mike Patrick, Elizabeth Deibler and Roberto Cimino as co-workers and as friends. The technical assistance of Rick Beesley and Sgt. Russ Huffman was essential in overcoming many problems. Lastly, I was immeasurably fortunate to have met Anneliese Clontz, to whom I am now engaged.

NO-A191 203

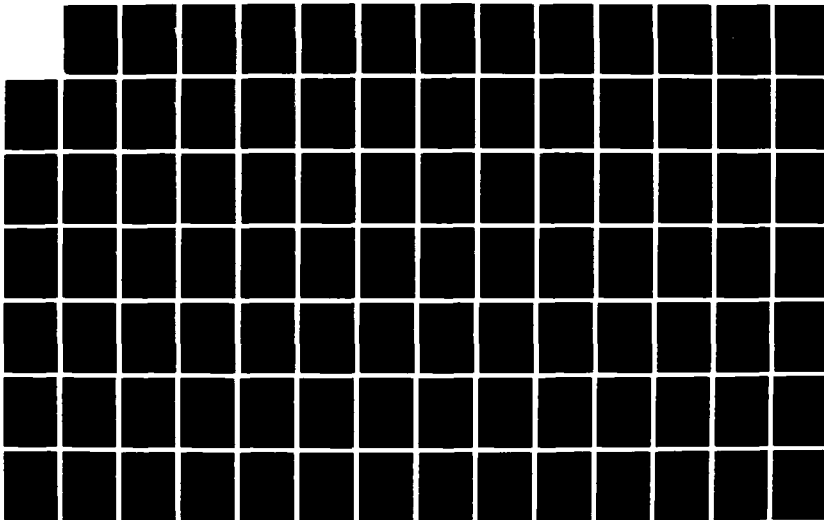
UNITED STATES AIR FORCE SUMMER FACULTY RESEARCH PROGRAM  
(1967) PROGRAM TE. (U) UNIVERSAL ENERGY SYSTEMS INC  
DAYTON OH R C DARRAH ET AL. DEC 87 AFOSR-TR-88-8212  
F49620-85-C-0013

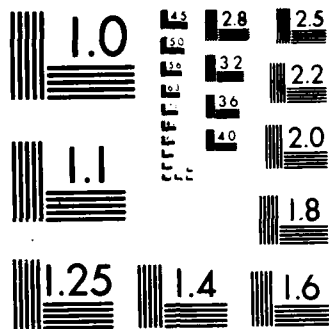
5/11

UNCLASSIFIED

F/G 5/1

ML





MICROCOPY RESOLUTION TEST CHART  
NATIONAL BUREAU OF STANDARDS 1963-A



## I. INTRODUCTION

The United States Air Force is engaged in an extensive program to develop improved explosive materials in terms of shock and thermal stability. The goal of this effort is the reduction of safety hazards attending the storage and handling of explosive materials. Several proposed new compositions include ethylenediammonium dinitrate (EDD). EDD is a high melting, oxygen deficient explosive material that forms a eutectic mixture with ammonium nitrate, an inexpensive oxidizing material. EDD has been used as an explosive for many years and its detonation characteristics have been extensively studied. Unfortunately, a dearth of effort was made at gaining a basic understanding of the thermal, structural and kinetic properties of this material. It is hoped that a study of EDD and a series of homologs could explain its thermal stability.

EDD is known to exist in two crystal structures at room temperature: it is a polymorphic material [1]. EDD is also known to undergo a solid to solid phase transition around 130C, well below its melting point of 188C. This polymorphism of EDD has implications to its utility as an explosive component. Different polymorphs of the same compound can have different sensitivities to shock as well as differing densities. Temperature and pressure can cause phase transitions which in turn lead to fracturing the crystallites. The decomposition characteristics are then altered by the change in particle size.

It is generally acknowledged that the molten state (melt) of energetic material plays an important role in thermal decomposition reactions [2,3]. Very little literature exists on the composition and structure of melts.

My recent research efforts have been in the area of solid state thermal decomposition kinetics [4]. This led to my assignment to the Energetic Materials Branch of the Air Force Armament Laboratory.

## II. OBJECTIVES OF THE RESEARCH EFFORT

Although the importance of the molten state of nitrate containing salts in their thermal decomposition processes is widely acknowledged, very little information on the melts of nitrate salts has been published. A survey of recent (1977-present) chemical literature indicates that no information on the infrared absorption characteristics of melts of ethylenediammonium dinitrate (EDD) or any of its homologs has been published. It was decided that Fourier transform infrared spectra (FTIR) of EDD, 1,4-butanediammonium dinitrate (BDD) and various deuterated species of EDD and BDD are important data and should be included in the efforts of the Air Force Armament Laboratory.

It was also decided that further investigations of the polymorphs of EDD should be performed. These investigations include FTIR spectra of the powder taken at room temperature and near the solid to solid phase transition temperature.

### III. EXPERIMENTAL

A recent journal article describes the preparation of EDD and BDD and reports a number of physical properties [5]. Samples for reflectance study were obtained by dissolving the salt in water and placing a drop of the dilute aqueous solution on a 13mm circular stainless steel mirror. The solvent was removed in vacuo leaving a residual layer of crystallites. Samples whose spectra were obtained in transmittance mode were prepared by grinding the material to a fine powder with a mortar and pestle. Toluene was then added to make a slurry. A drop of this slurry was placed on a 13mm zinc selenide plate and spread out into a thin layer. The sample was then allowed to air dry leaving a monolayer of fine powder. The Fourier transform infrared spectra (FTIR) were obtained using a Mattson Cygnus 25 FTIR Spectrometer equipped with a Bach Shearer FTIR microscope having a mercury-cadium telluride detector. The hot stage attachment was also built by Mattson Instruments, Inc. The temperature was controlled with an Omega Thermal Regulator and was monitored by a type J iron-constantan thermocouple. The spectra were acquired and processed using a Starlab Computer System.

Figures 1 through 5 show the FTIR spectra of melts of BDD and four of its deuterated forms. They are BDD deuterated at the ammonium positions and at the alpha carbons (BDD d10), deuterated at the ammonium positions (BDD d6), deuterated at the alpha carbons (BDD d4 alpha) and deuterated at the beta carbons (BDD d4 beta). These spectra were all obtained in transmittance mode. For comparison a room

temperature reflectance of BDD is given in Figure 6. The absorptions by the melts are excessively intense giving spectral features that are broad and distorted relative to absorptions by the neat solid. The spectra were all processed against the same background, though the samples may have been of differing thicknesses. As a result the percent transmission scale is not applicable. By comparing the spectra of BDD to those of its deuterated forms and by using published work, some assignments can be made relating absorptions to features of the molecules [6,7]. A table of the absorption frequencies for each compound and a tentative assignment is given in Table I.

The same data is presented for EDD. Figure 7 shows the FTIR spectrum of an EDD melt. Figure 8 is that of a sample deuterated at the ammonium positions (EDD d6) while Figure 9 is of a sample that has deuteriums on the two carbon atoms (EDD d4). Table II lists the frequencies of the absorptions and suggests possible assignments. Figures 10 and 11 show room temperature reflectance spectra of solid EDD.

Several features make the interpretation of these spectra difficult. The broad absorption of ammonium groups (3100 to 2000 wavenumbers) obscures the region in which CH absorbs. Similarly the absorption by nitrate ions is broad (1300 to 1600 wavenumbers) and swamps the high frequency end of the fingerprint region. Background carbon dioxide absorbs strongly around 2300 wavenumbers.

The evidence of the polymorphs of EDD can be seen in Figure 11. The

absorption band of the nitrate ion is split into two resolved absorptions, with maxima at 825 and 845 wavenumbers. In Figure 12, the behavior of this line is monitored as the temperature is raised from 120C to 138C. As the transition occurs, the high frequency line weakens, broadens and eventually coalesces with the low frequency line. This observation is consistent with the differential scanning calorigram of EDD in Figure 13, which shows an endothermic process occurring from 124C to 140C. When the infrared sample was allowed to cool to room temperature, the nitrate absorption was found again to split into a doublet.

#### IV. RECOMMENDATIONS

The understanding of the thermal and kinetic properties is far from complete. In addition to the ongoing research efforts at the High Explosive Research and Development facility, several grants have been awarded to academic research laboratories.

The work reported here suggests several paths of inquiry. Detailed crystallographic structures of EDD should be obtained at temperatures above and below the phase transition. This would determine the exact structures of the polymorphs of EDD and could characterize the nature of the transition.

The FTIR system employed this summer was lacking the software package to perform rapid scanning. The acquisition of such software could permit the monitoring of kinetic experiments with the FTIR. This would

in turn provide a means to determine initial processes, and the structures of intermediates and products. Such kinetic data for the thermal decomposition reactions of EDD and BDD are essential to complete the mechanistic study of the deflagration of these materials.

TABLE I

<u>BDD</u>	<u>BDD d10</u>	<u>BDD d6</u>	<u>Bdd d4 Alpha</u>	<u>BDD d4 Beta</u>	<u>Assignment</u>
747	720	722	720	722	$\text{NO}_3^-$ bend ( $\nu_4$ )
	782				
825	833	825	826	826	$\text{NO}_3^-$ rock ( $\nu_2$ )
	871				
884	920		904		
1039	1046	1039	1039	1040	CN stretch
1068	1085		1075	1061	$\text{NO}_3^-$ ( $\nu_1$ )
	1137				
1171	1181	1162			CN stretch
	1240		1224		
1308	1357	1330	1339	1311	$\text{NO}_3^-$ stretch ( $\nu_3$ )
1516			1518	1517	$\text{NH}_3^+$ bend
1615			1616	1616	$\text{NH}_3^+$ bend
1750	1766	1752	1748		$\text{NO}_3^-$ ( $\nu_1 + \nu_4$ )
2800	2729		2727		$\text{NH}_3^+$ stretch
	2827	2975			
	2877		2940		CH stretch
	2944				
	3032		3130		

TABLE II

<u>EDD</u>	<u>EDD d4</u>	<u>EDD d6</u>	<u>Tentative Assignment</u>
726	720	729	$\text{NO}_3^-$ bend ( $\nu_4$ )
825	827	825	$\text{NO}_3^-$ rock ( $\nu_2$ )
845	846		$\text{NO}_3^-$ rock ( $\nu_2$ )
909	907		$\text{NH}_3^+$
1043	1044	1041	CN stretch
1111	1113		$\text{NO}_3^-$ ( $\nu_1$ )
1185		1179	CN stretch
1367	1400	1370	$\text{NO}_3^-$ stretch ( $\nu_3$ )
1518	1507		symmetric $\text{NH}_3^+$ bend
1599	1618		asymmetric $\text{NH}_3^+$ bend
1750	1753		$\text{NO}_3^-$ ( $\nu_1 + \nu_4$ )
	1867	1891	
	1995		
2079	2109		$\text{NH}_3^+$ stretch
2200	2700		$\text{NH}_3^+$ stretch
3200	3200	3200	$\text{NH}_3^+$ stretch
3567		3590	CH stretch



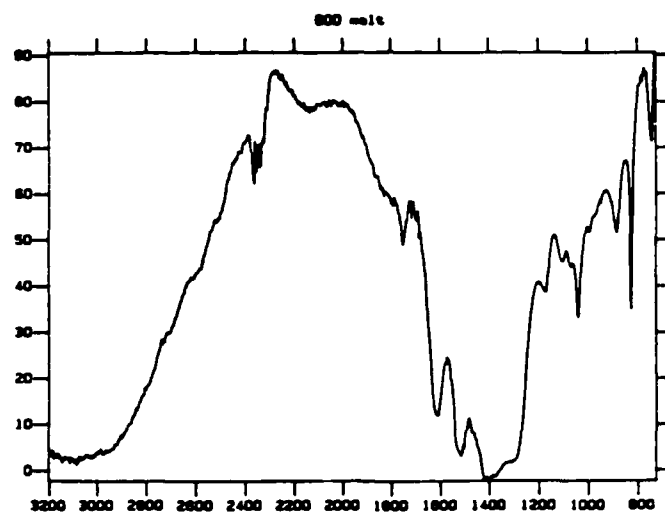


Figure 1

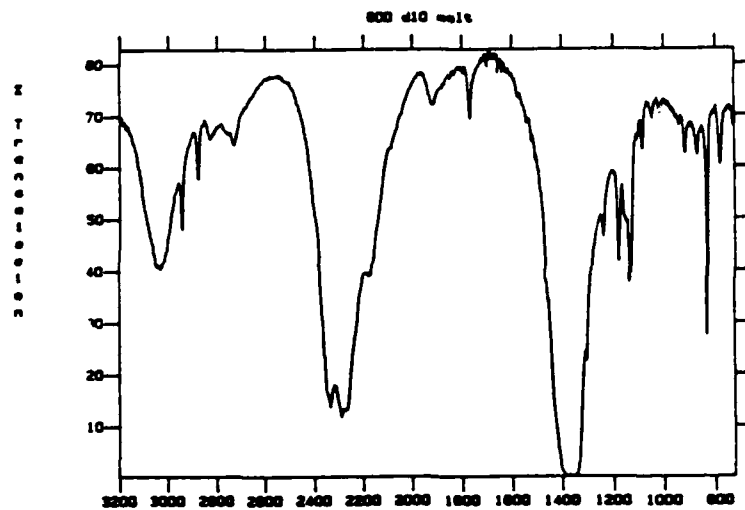


Figure 2

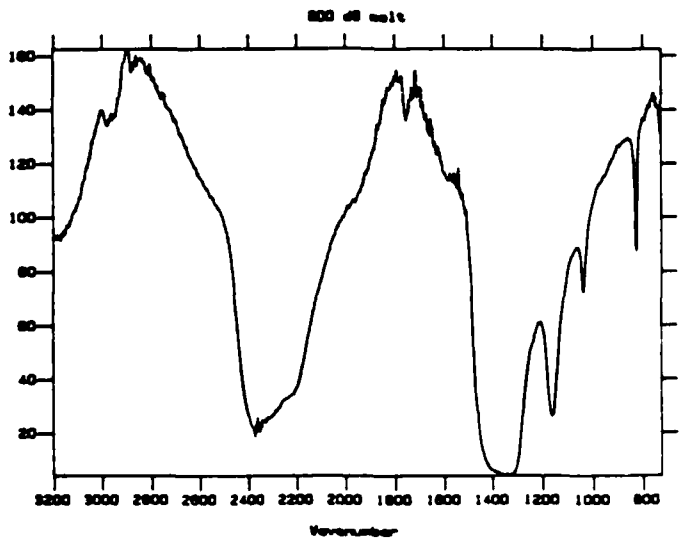


Figure 3

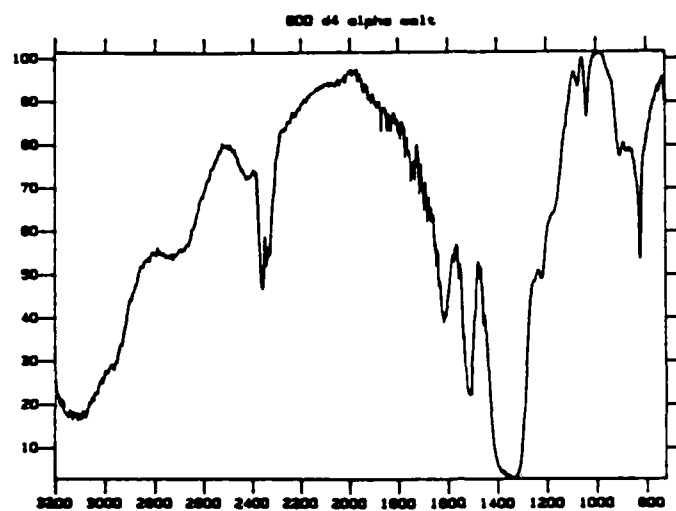


Figure 4

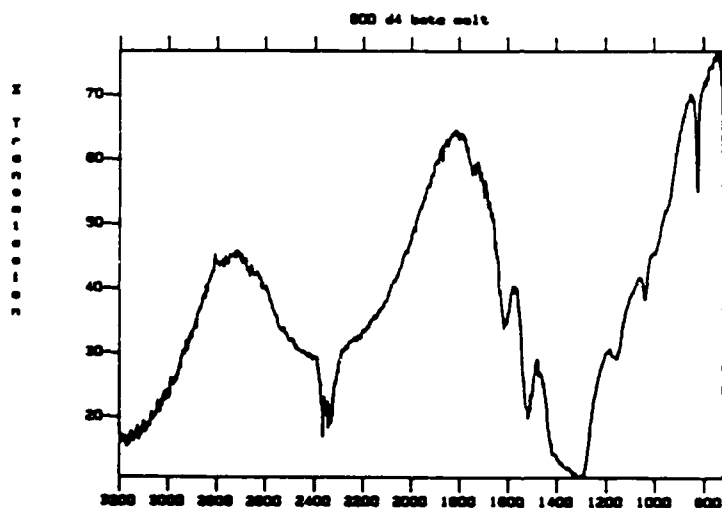


Figure 5

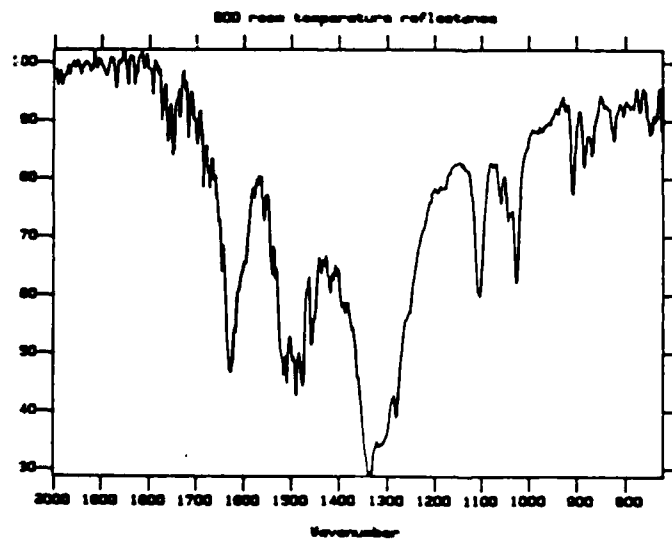


Figure 6

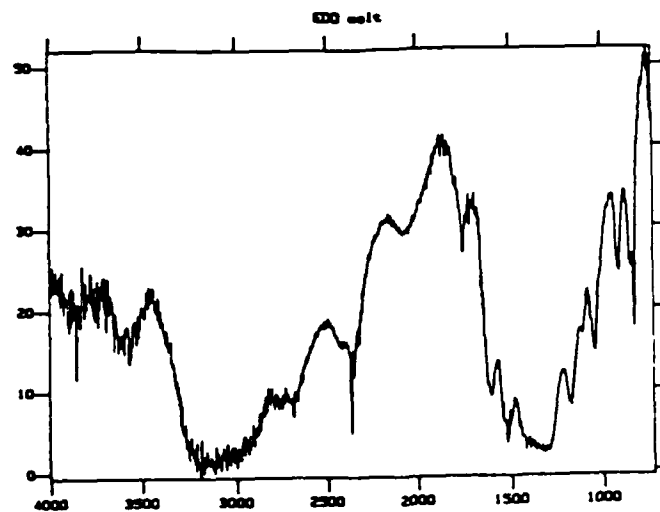


Figure 7

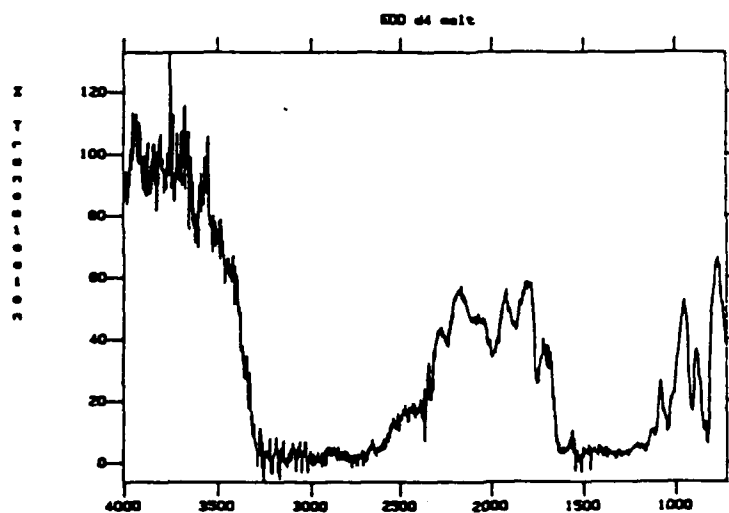


Figure 8

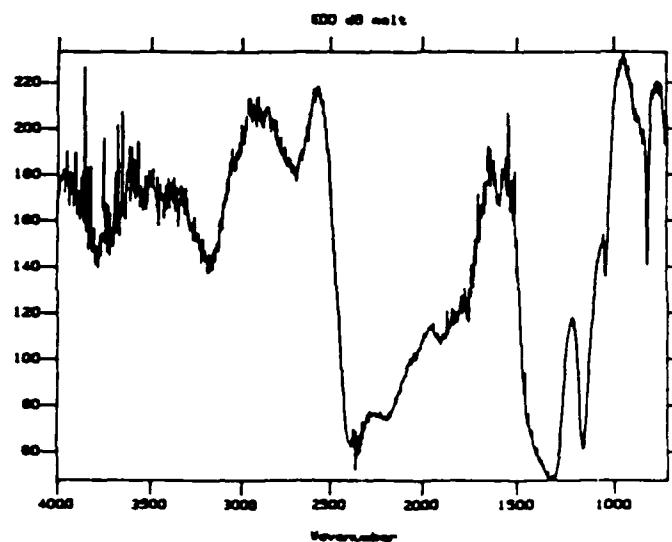


Figure 9

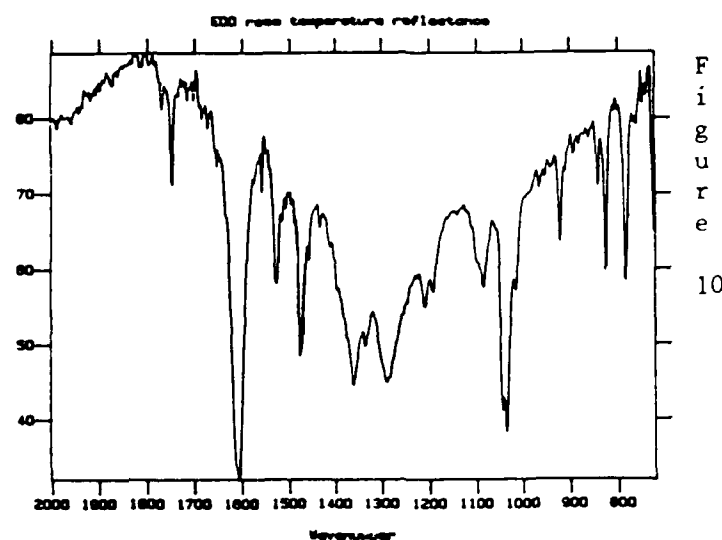


Figure 10

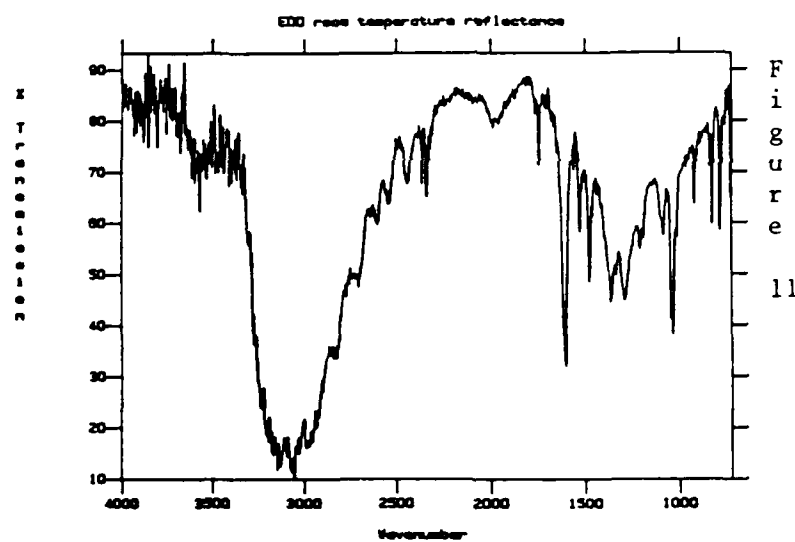
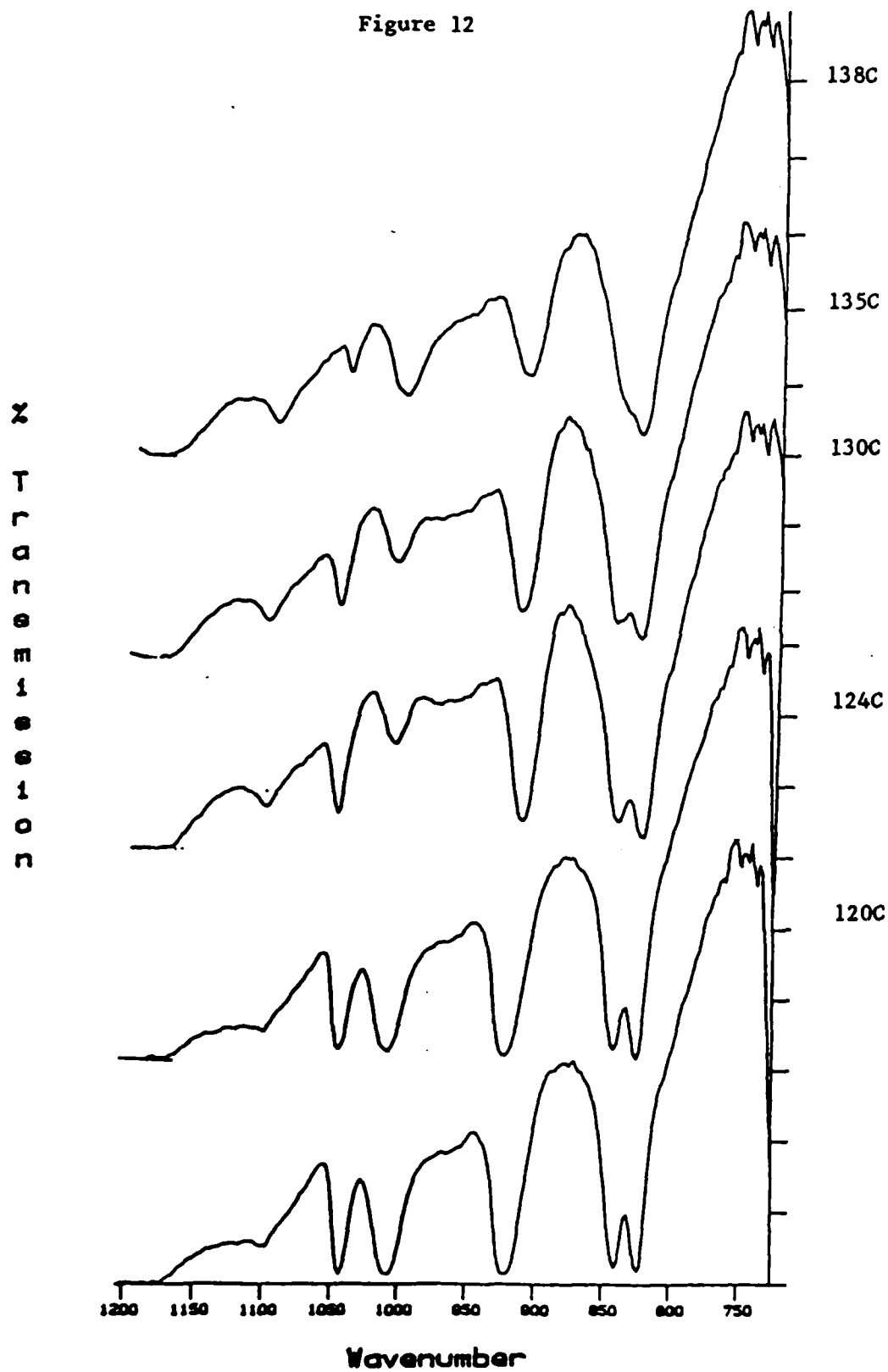


Figure 11

20-000-000367-1

Figure 12



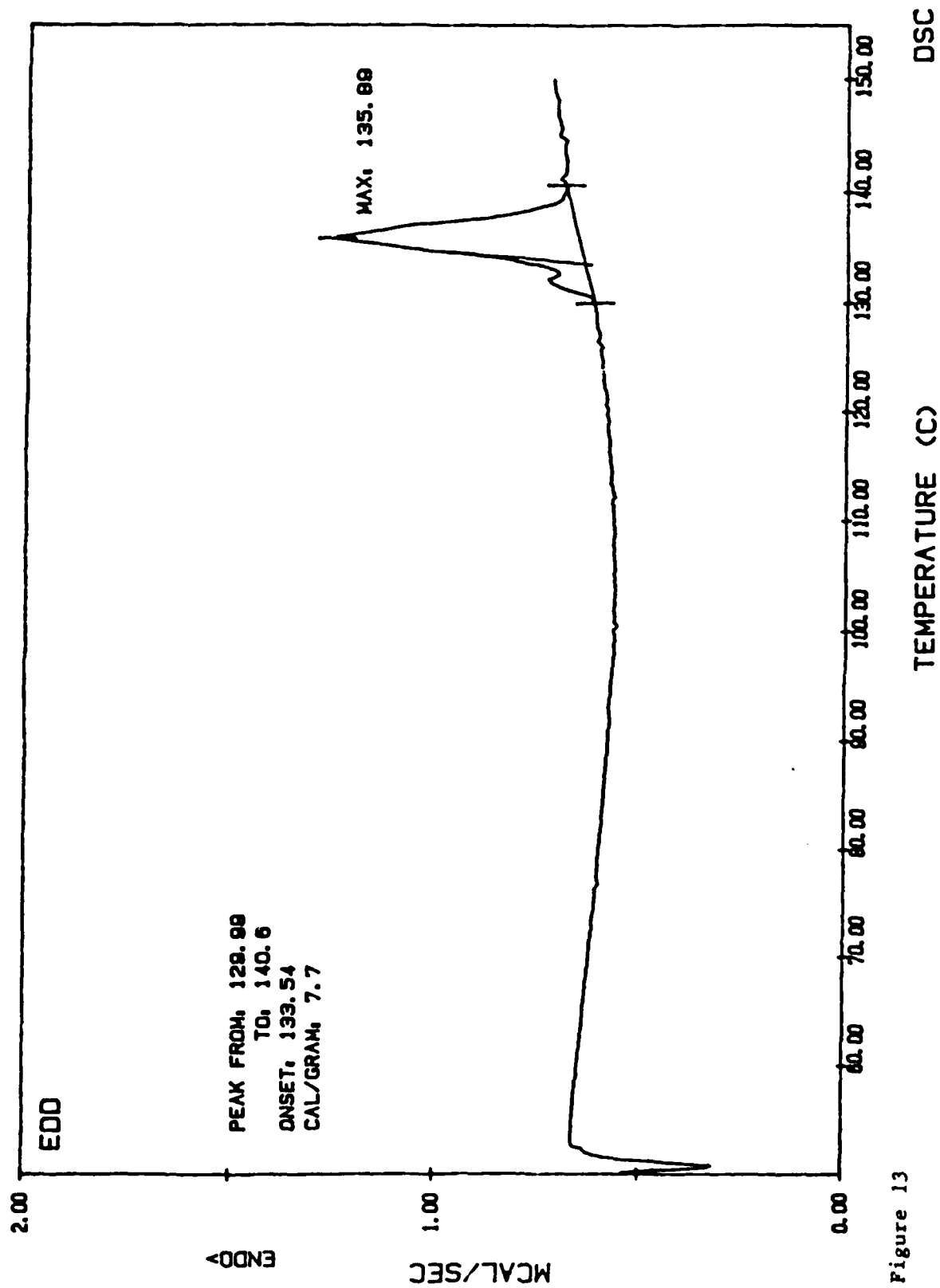


Figure 13

#### REFERENCES

1. Private communication with R. L. McKenney, Jr. Eglin, AFB.
2. Shaw R. and Walker, F.F., J. Phys. Chem. 8 Vol. 1, pp. 2572 (1977).
3. Karpowicz, R.J. and Brill, T.B., Combustion and Flame, Vol. 56, pp. 317 (1984).
4. Bopp, J.M. and Garrett, B.B., Inorg. Chem. Submitted for Publication.
5. McKenney, R.L., Struck, S.R., Hildreth, R.A. and Fryling, J.A., Journal of Energetic Materials, Vol. 5, pp. 1 (1987).
6. Silverstein, R.M., Basler, G.C., and Morrill, T.C., "Spectrometric Identification of Organic Compounds", John Wiley and Sons, New York, 1981.
7. Socrates, G., "Infrared Characteristic Group Frequencies", John Wiley and Sons, New York, 1980.

1987 USAF-UES SUMMER FACULTY RESEARCH PROGRAM/  
GRADUATE STUDENT SUMMER SUPPORT PROGRAM

Sponsored by the  
AIR FORCE OFFICE OF SCIENTIFIC RESEARCH  
Conducted by the  
Universal Energy Systems, Inc.

FINAL REPORT

A "Form and Function" Knowledge Representation  
for Reasoning about Classes and Instances of Objects

Prepared by: Kevin Bowyer  
Academic rank: Assistant Professor  
Department and Computer Science and Engineering Dept.  
University: University of South Florida  
Research Location: RADC/COES, Griffiss AFB, Rome, NY  
USAF Researcher: Jacob Scherer  
Date: July 10, 1987  
Contract No: F49620-85-C-0013



A "Form and Function" Knowledge Representation  
for Reasoning about Classes and Instances of Objects

by

Kevin W Bowyer

ABSTRACT

This report outlines an approach to combining knowledge about functionality of an object with knowledge about the geometric form of an object. The representation of geometric form allows an object to be defined as an interconnection of multiple components. Different types of connections are defined in order to allow different types of relative movement between components. The representation of intended function of an object is handled by procedural attributes attached to components of an object. The combined "form and function" knowledge representation allows modeling of classes, subclasses and specific instances of an object. The ability to model object classes allows us to investigate questions of how new subclasses and instances are learned.

### ACKNOWLEDGEMENTS

I wish to thank the Air Force Office of Scientific Research and the Air Force Systems Command for their sponsorship of the Summer Faculty Research Program and the Graduate Student Summer Support Program. These programs have had a clear positive impact on my research, and I am sure that many other participants must feel the same way. In my contacts with the Universal Energy Systems administrators, they have consistently been efficient, helpful and friendly.

RADC, as an organization, has provided a very enjoyable working environment. Their excellent computing facilities have always been readily accessible. I have had many pleasant social encounters with different staff members from both COES and IRRE, as well as many challenging technical discussions. It has been very stimulating to be surrounded by so many research oriented professionals. Jake Scherer has given just the right amount of direction and guidance for me to be able to develop my own original research plan.

## I. INTRODUCTION

My primary research accomplishments up to this time have been in the general area of artificial intelligence, with particular emphasis on modeling, image processing and vision.

RADC/COES has strong interests in natural language understanding, knowledge representation and reasoning techniques. In addition, RADC/IRRE has interests in various forms of image processing for object representation.

The overlap of my background with RADC/COES interests led to my selection and assignment to COES. The research direction initially chosen was to study fuzzy reasoning applied to natural language processing. However, this initial topic evolved through several stages to become more oriented toward basic knowledge representation. In order to understand natural language expressions concerning physical objects, it is necessary to have some representation of what the object is. One mechanism for understanding an object is to model its physical form and the functional properties which can be inferred from the physical form. To be able to reason about classes of objects as well as specific instances, the representation of physical form for the class must be fuzzy enough to incorporate many different specific instances. Thus the initial topic evolved to become a project concerned with representing knowledge about classes and specific instances of objects. Ideally, the same knowledge representation should be

useful for both natural language understanding and image understanding applications.

## II. OBJECTIVES OF THE RESEARCH EFFORT

The objective of this research effort is to explore forms of knowledge representation which blend information about intended function of an object with models of physical form of an object.

We seek first to develop a method of representing physical form which allows an object to be defined in terms of components whose interconnections may allow some range of movement.

We then seek to develop a method of modeling the intended function of an object in terms of properties satisfied by its components and connections between its components.

Combining a procedural representation of knowledge about function with a parameterized geometric model of physical form allows us to create an abstract representation for a class of objects. The ability to model object classes allows us to explore mechanisms for learning new instances and subclasses of objects.

### III. MODELING OF OBJECTS WITH NONRIGID CONNECTION OF COMPONENTS

The current state of the art in computer vision and graphics is largely limited to modeling individual instances of rigid objects. Some modeling schemes may allow objects to be defined as the composition of more primitive components, but usually still require connections between components to be rigid. For a survey of standard representation techniques for solid objects, see Requicha (1980, 1982). For a discussion of an object modeling scheme which uses generalized cylinders for components and allows flexible connections between components, see Nevatia and Binford (1977).

We envision an interesting and substantial advance in modeling geometric form of an object to be one which allows:

- (1) definition of a "component" as a rigid assembly of sub-components, and
- (2) definition of an "object" as a composition of multiple components, where
- (3) one component may be attached to another component by any of several types of "connection" (each connection type represents a different type of possible relative movement between components).

Item (1) of our criteria is, by itself, easily accomplished using any of a range of known solid modeling techniques (boundary surface representation, constructive solid geometry, plane sweep, etc.). Thus, the important issues which arise in

developing our desired object modeling system are (1) how to specify connections between individual components of an object, and (2) how to specify allowable ranges of movement associated with a given type of connection between components. These issues are, of course, interrelated and cannot be solved entirely independently of each other. A given type of attachment may automatically imply a given type of relative movement, which need only be instantiated by parameters specific to the particular connection.

For an example of how these problems might be approached, we will concentrate on representations for objects which can be understood as chairs. Individual object components can be defined by planar-face boundary surface descriptions. The simplest form of component connection is a RIGID connection, indicating a fixed attachment which allows no relative movement between components. A RIGID connection can be specified by six parameters; the names of the two components involved, two points on the surface of the first component and two points on the surface of the second component:

RIGID ( Component-A, Component-B, P-1-A, P-1-B, P-2-A, P-2-B )  
As a result of the connection, the two points on the first component are made coincident with the two points on the second component. The two coincident points implicitly specify some amount of coincident surface area between the two components, at which the components are assumed to be joined.

Using the simple scheme outlined above, we can define a

(relatively uncomfortable) straight back chair as shown in Figure 1. This chair has a total of six components; a back, a seat, and four legs. The components are joined by a total of five RIGID connections; one connection of the back to the top of the seat, and four connections of individual legs to the bottom of the seat. Each component is defined as a rectangular solid with a boundary surface definition composed of six faces.

#### IV. PROCEDURAL REPRESENTATION OF KNOWLEDGE ABOUT FUNCTION

Object representations of the type discussed in the previous section describe only geometric form. We assert that such form-only descriptions do not describe an object in a way that completely reflects a person's understanding of the object. A person easily understands the object defined in the previous section to be a chair, but uses more than the uninterpreted definition of geometric form in doing so. In understanding an object to be a chair, a person interprets the form of the object in terms of its intended function.

The intended function of an object is not explicit in the definition of its geometric form. However, the ability of an object to serve a given function generally can be inferred by the presence or absence of certain properties derivable from the geometric form. The object definition in the previous section can be understood as a chair because a collection of "chair-like" properties can be inferred from the object's form.

It has a component which could be a "seat" because it has a flat surface that could be sat on. It has a component which could be a "back" because it has a flat surface which forms a 90 degree angle with the seat surface. It has a component (or collection of subcomponents) which could form a "base" because it is capable of providing stable support for the seat. It is some collection of such interpreted functional attributes that allows the object to be understood as a chair.

Knowledge of the intended function of an object can be integrated with its geometric model by a set of attributes attached to the component and/or subcomponent definitions and their connection relations. Each attribute specifies that the component or component connection to which it is attached satisfies a particular property relevant to the object's function. Symbolically, our combined "form and function" definition of the straight back chair in Figure 1 might appear as in Figure 2. The Seat component is given the attribute SITTABLE-SURFACE, indicating that it has an approximately flat surface of the appropriate size to sit on. The Back component is given the attribute BACK-SUPPORT, indicating that it has a surface which could provide back support. The connection between the Seat and Back components is given the attribute CREATES-SITTABLE-SPACE, indicating that the connection of the two components creates an area with an appropriate combination of sittable space and back support. The Base component is given the attribute PROVIDES-STABLE-SUPPORT (Base, Seat), indicating that the Base provides stable support for the Seat.



The simple use of symbolic attributes which, by convention, indicate particular chair-like properties is sufficient to define specific instances of the "chair" class. However, a more general view is that the symbolic attributes stand for properties which can be verified by computationally examining a specific geometric model. Thus, SITTABLE-SURFACE might be the name of a procedure which tests each surface in the geometric definition of the component that it is attached to, returning "true" if a sittable surface exists, and "false" if one doesn't. It is this procedural view of representation of knowledge about function which leads us to the possibility of modeling classes of objects.

#### V. KNOWLEDGE REPRESENTATION FOR OBJECT CLASSES

A knowledge representation for a class of objects should provide the means to reason about a previously unencountered object and determine whether or not it is a member of the class. We propose to construct a knowledge representation for defining a class of objects by blending a parameterized geometric model with a procedural representation of knowledge about function. For example, we might construct a definition of the class of objects called chairs as:

```
Class-Chair -> Connected ( Back, Seat ),  
                Connected ( Seat, Base ),  
                BACK-SUPPORT ( Back ),  
                SITTABLE-SURFACE ( Seat ),
```

CREATES-SITTABLE-SPACE ( Seat, Back ),  
PROVIDES-STABLE-SUPPORT ( Base, Seat ).

This definition indicates that a chair must have connected components which can be labelled Back, Seat, and Base, that the Seat must have a sittable surface, that the Back must provide back support, that the connection of Back and Base must create a sittable area, and that the Base must provide stable support for the Seat.

Suppose that a previously unknown object is encountered. This object can be understood as a chair if some labelling of its components as Seat, Back, and Base can be found which satisfies all the procedural attributes that verify the functionality of the object. The object would then become a prototype for a specific subclass of the "chair" class, and can be given a specific name, such as "straight back chair." If another instance of this subclass is encountered later, then it can be understood not just as a "chair," but as a "straight back chair."

## VI. RECOMMENDATIONS

Brooks and Binford (1981) have described a representational scheme, used in ACRONYM, which allows modeling of specific instances, subclasses, and classes of objects. Their examples are oriented to the class of objects understood as wide-bodied passenger jet aircraft. Their representation allows for

variations in size and structure between specific instances within the class. Distinguishing between different instances of the class is handled by specialization of constraints. While component connections may occur at different places for different object subclasses or instances, all connections are assumed to be rigid. Flexible connections between components are not discussed. Also, mechanisms for learning new subclasses and instances are not discussed.

Winston et al (1983) describe an integrated representation of form and function, and methods for learning by analogy and constraint transfer. Their examples are oriented to the class of objects understood as cups. Their representation is implemented by semantic networks derived from natural language specifications entered by the user; they do not attempt to have a system which derives the semantic network by examining specific 3-D geometric models. Thus they are able to abstract away from many of the problems inherent in variations of size, structure and flexible connections between components.

Pentland (1986) discusses a representation based on superquadrics and fractals which allows simple composition of components. A brief description of modeling a chair is given which is similar to our discussion here. However, flexible connections between components and learning of new instances and subclasses are not discussed.

The research project outlined in this report explores several

important new directions. The "form and function" representation of a class of objects allowing flexible connections between components has not, to our knowledge, been attempted before. We wish to implement such a representation and then use this representation to explore issues in learning of new object instances and subclasses.

## REFERENCES

Brooks, R.A., and Binford, T.O. Representing and Reasoning About Partially Specified Scenes, Proceedings of DARPA 1980 Image Understanding Workshop, SAI-81-170-WA (1981), 95-103.

Nevatia, R. and Binford, T.O., Description and Recognition of Curved Objects, Artificial Intelligence 8 (1977), 77-79.

Pentland, A.P., Perceptual Organization and the Representation of Natural Form, Artificial Intelligence 28 (1986), 293-331.

Requicha, A.A.G., Representations for Rigid Solids: Theory, Methods, and Systems, Computing Surveys 12, 4 (1980), 437-464.

Requicha, A.A.G., and Voelcker, H.B., Solid Modeling: A Historical Summary and Contemporary Assessment, IEEE Computer Graphics and Applications (1982), 9-24.

Winston, P.H., Binford, T.O., Katz, B., and Lowry, M. Learning Physical Descriptions From Functional Definitions, Examples, and Precedents, Proceedings of AAAI '83 (1983), 433-439.

My-Chair -> RIGID (Back, Seat, Back-1, Back-2, Seat-1, Seat-2),  
 RIGID (Seat, Leg1, Seat-3, Seat-4, Leg1-1, Leg1-2),  
 RIGID (Seat, Leg2, Seat-5, Seat-6, Leg2-1, Leg2-2),  
 RIGID (Seat, Leg3, Seat-7, Seat-8, Leg3-1, Leg3-2),  
 RIGID (Seat, Leg4, Seat-9, Seat-10, Leg4-1, Leg4-2);

Back -> <A, C, G, E>, <A, B, D, C>, <D, B, F, H>,  
 <H, F, E, G>, <C, D, H, G>, <A, B, F, E>;

Seat -> <I, J, K, L>, <I, L, M, P>, <M, P, O, N>,  
 <N, O, K, J>, <L, K, O, P>, <J, I, M, N>;

Base -> Leg1, Leg2, Leg3, Leg4;

Leg1 -> <Q, T, X, U>, <U, X, W, V>, <V, W, S, R>,  
 <T, Q, R, S>, <T, S, W, X>, <R, Q, U, V>;

Leg2 -> <Y, BB, FF, CC>, <CC, FF, EE, DD>, <AA, Z, DD, EE>,  
 <Z, AA, BB, Y>, <BB, AA, EE, FF>, <Z, Y, CC, DD>;

Leg3 -> <GG, JJ, NN, KK>, <KK, NN, MM, LL>, <II, HH, LL, MM>,  
 <JJ, GG, HH, II>, <JJ, II, MM, NN>, <HH, GG, KK, LL>;

Leg4 -> <OO, RR, VV, SS>, <SS, VV, UU, TT>, <TT, UU, QQ, PP>,  
 <RR, OO, PP, QQ>, <RR, QQ, UU, VV>, <PP, OO, SS, TT>;

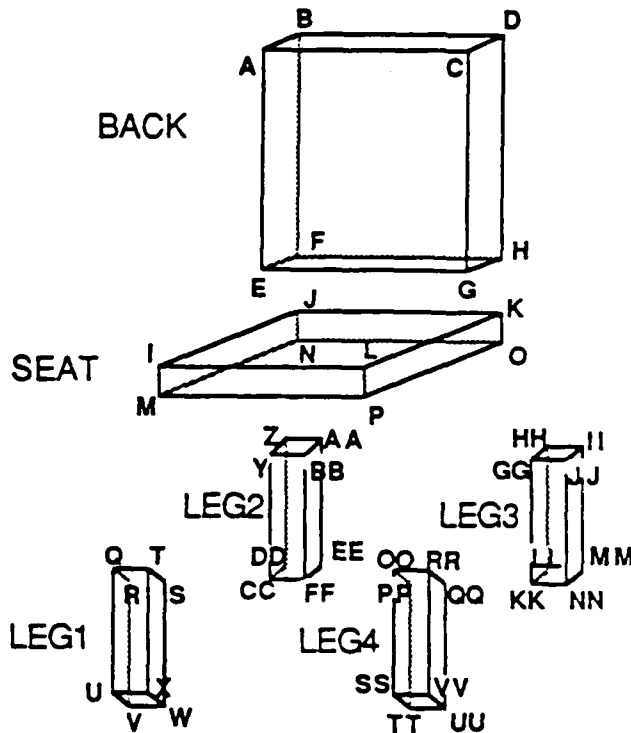


Figure 1 - Specification of a Simple Straight Back Chair

```

My-Chair -> RIGID (Back, Seat, Back-1, Back-2, Seat-1, Seat-2),
            CREATES-SITTABLE-SPACE (Seat, Back);
            RIGID (Seat, Leg1, Seat-3, Seat-4, Leg1-1, Leg1-2),
            RIGID (Seat, Leg2, Seat-5, Seat-6, Leg2-1, Leg2-2),
            RIGID (Seat, Leg3, Seat-7, Seat-8, Leg3-1, Leg3-2),
            RIGID (Seat, Leg4, Seat-9, Seat-10, Leg4-1, Leg4-2);

Back  ->  <A, C, G, E>, <A, B, D, C>, <D, B, F, H>,
          <H, F, E, G>, <C, D, H, G>, <A, B, F, E>,
          BACK-SUPPORT;

Seat  ->  <I, J, K, L>, <I, L, M, P>, <M, P, O, N>,
          <N, O, K, J>, <L, K, O, P>, <J, I, M, N>,
          SITTABLE-SURFACE;

Base  ->  Leg1, Leg2, Leg3, Leg4,
          PROVIDES-STABLE-SUPPORT ( Base, Seat );

Leg1  ->  <Q, T, X, U>, <U, X, W, V>, <V, W, S, R>,
          <T, Q, R, S>, <T, S, W, X>, <R, Q, U, V>;

Leg2  ->  <Y, BB, FF, CC>, <CC, FF, EE, DD>, <AA, Z, DD, EE>,
          <Z, AA, BB, Y>, <BB, AA, EE, FF>, <Z, Y, CC, DD>;

Leg3  ->  <GG, JJ, NN, KK>, <KK, NN, MM, LL>, <II, HH, LL, MM>,
          <JJ, GG, HH, II>, <JJ, II, MM, NN>, <HH, GG, KK, LL>;

Leg4  ->  <OO, RR, VV, SS>, <SS, VV, UU, TT>, <TT, UU, QQ, PP>,
          <RR, OO, PP, QQ>, <RR, QQ, UU, VV>, <PP, OO, SS, TT>;

```

Figure 2 - Chair Specification with Function Attributes

1987 USAF-UES SUMMER FACULTY RESEARCH PROGRAM/  
GRADUATE STUDENT SUMMER SUPPORT PROGRAM

Sponsored by the  
AIR FORCE OFFICE OF SCIENTIFIC RESEARCH

Conducted by the  
Universal Energy Systems, Inc.

FINAL REPORT

AN ANALYSIS OF INFRARED LIGHT PROPAGATION IN HOLLOW METALLIC LIGHT PIPES

Prepared by:	Lee I. Britt, M.S.
Academic Rank:	Instructor
Department and	Physics
University:	Grambling State University
Research Location:	VKF/ Space Systems Branch Arnold AFS TN 37389-5000
USAF Researcher:	Mr. Sidney Steely
Date:	14 August 87
Contract No:	F49620-85-C-0013



AN ANALYSIS OF INFRARED LIGHT PROPAGATION IN HOLLOW METALLIC LIGHT PIPES

by

Lee. I. Britt

ABSTRACT

An analysis of electromagnetic wave propagation at optical frequencies was performed using the Fourier method, for waves in hollow metallic ducts. Solutions for monochromatic plane wave propagation in hollow metallic light pipes were determined for straight cylindrical, rectangular and curved geometries. These solutions yield an infinite series representation of the generating function in each case that is characteristic of the wave guide geometry.

Useful parameters relating to the minimum loss dominant mode are pointed out in each case. Power loss considerations in each geometry lead naturally to exact expressions for attenuation in each guide. A perturbation technique is pointed out that will take into account the effects of bending in the curved cylindrical guide.

### ACKNOWLEDGEMENTS

I would like to thank the Air Force Systems Command and the Air Force Office of Scientific Research for sponsorship of this research. I am very grateful to Universal Energy Systems for help with matters of an administrative and directional nature. I wish to also thank Mr. Marshall Kingery for his assistance in locating key technical personnel.

There are a number of people in the Calspan group that helped make my experience at AEDC both rewarding and enriching. Many thanks are due to Mr. Don Williams and Mr. Ron Dawbarn for clarification of the research problem; Mr. Jim Selman and Mr. George Skinner for directions to reference materials. Mr. Reinhard Menzel for many enlightening technical discussions, and Mr. Sidney Steely for analytical suggestions.

I wish also to express my appreciation to Ms. Debora Richards for her care and diligence in typing. Special appreciation is due to my wife, Alma, and our children, Tayanna, Jamal and Le Shundra, for enduring so patiently my absence this summer.

## I. INTRODUCTION

One of the requirements of the Focal Plane Array test chamber is that it has the capability of simulating star scenes with a high degree of reliability in the laboratory. This is to be done by using selected Integrating spheres as blackbody sources, and coupling the radiant output of these spheres on to an aperture plate.

The coupling is to be done by polished metallic light pipes because most of the standard glasses and materials that make up transparent fiber optics cables do not transmit very well in the Infrared (IR) region of the electromagnetic spectrum and secondly because at cryogenic temperatures glass cables would lose their flexibility and would shatter. The metallic cables can withstand the cryogenic temperature extremes without experiencing material damage, however there is a problem with optical transmission because IR radiation injected at the entrance aperture of the light pipe experiences rapid attenuation as it propagates the length of the guide. This attenuation is even more pronounced as the bend of the guide approached more and more a torus.

In an effort to increase the efficiency of these guides an analysis is needed to provide a better understanding of the physical phenomena that occurs when IR radiation propagates in both the straight and curved geometries.

My past research efforts have been in the areas of Electronic Warfare and Electro-Optical systems analysis and evaluation. I have been involved in spectrophotomic and spectroradiometric evaluation and testing of IR sources. I have performed laser induced damage studies on selected target materials. I have also taught courses in Atomic and Experimental Physics as well as Physics For the Life Sciences.

My knowledge and familiarity with IR systems and radiometry resulted in my assignment to develop an analysis of Light Propagation in hollow metallic pipes.

## II. OBJECTIVE OF THE RESEARCH EFFORT

The study of electromagnetic wave propagation in hollow ducts was first discussed in detail by Rayleigh (1897).

The development of shortwave oscillators led to increased research and development of devices and structures that operate for the most part in the microwave region. Very few investigations however have been performed on the propagation of IR radiation in metallic ducts.

Marcatili and Schmeltzer (1964) showed that the hollow metallic circular wave guide will function very well as a conduit of optical radiation.

Garmire, McMahon and Bass (1976) point out that one geometry for low loss transmission is a rectangular aperture wide and thin, with the electric polarization parallel to the long dimension of the cross section.

The general objective here then will be to present an analysis that will give some insight to the loss mechanisms within the light pipe, and also to suggest techniques of optimizing transmission over the length of the guide. The wave equation in cartesian, cylindrical and toroidal coordinates will be examined and from their solutions information will be obtained relating to propagation and attenuation. The solutions to these equations will be obtained in a straight forward fashion when possible by the Fourier method.

## III. GENERAL THEORETICAL DEVELOPMENT

The Vector Wave equation for the electric field  $\vec{E}$  and the Magnetic

field  $\vec{H}$  is given by

$$\nabla^2 \vec{E} - \epsilon_0 \mu_0 \frac{\delta^2 \vec{E}}{\delta t^2} = 0 \quad (1)$$

And

$$\nabla^2 \vec{H} - \epsilon_0 \mu_0 \frac{\delta^2 \vec{H}}{\delta t^2} = 0. \quad (2)$$

For monochromatic plane waves propagating in a hollow metallic guide these equations may be written in terms of a transverse Laplacian operator expressed as

$$\nabla_t^2 = \frac{\delta^2}{\delta x^2} + \frac{\delta^2}{\delta y^2} = \nabla^2 - \frac{\delta^2}{\delta z^2} \quad (3)$$

which yields

$$\nabla_t^2 \vec{E} + k_c^2 \vec{E} = 0 \quad (4)$$

and

$$\nabla_t^2 \vec{H} + k_c^2 \vec{H} = 0 \quad (5)$$

where  $k_c$  is the guide cut off wave number given by  $2\pi/\lambda_c$ . When  $\vec{E}$  has a component parallel to the direction of propagation the wave is called a Transverse Magnetic (TM) wave. When  $\vec{H}$  has a component parallel to the direction of propagation the wave is called a Transverse Electric (TE) wave.

It is stated in Jackson (1962) that the TEM wave cannot exist in the hollow wave guide. Therefore we shall restrict our attention to the TM and TE wave analysis. Since (4) and (5) are connected by Maxwells' Curl and divergence equations, for each mode it is only necessary to solve for either  $\vec{E}$  or  $\vec{H}$  assuming the  $z$  dependence is given by  $\vec{E}(V_1, V_2) \text{ EXP}[i(\omega t - 2\pi z/\lambda_g)]$  and  $\vec{H}(V_1, V_2) \text{ EXP}[i(\omega t - 2\pi z/\lambda_g)]$  where  $V_1$  and  $V_2$  are coordinates.

#### IV. RECTANGULAR WAVE GUIDES

The geometry for the rectangular wave guide is shown in Fig. 1.

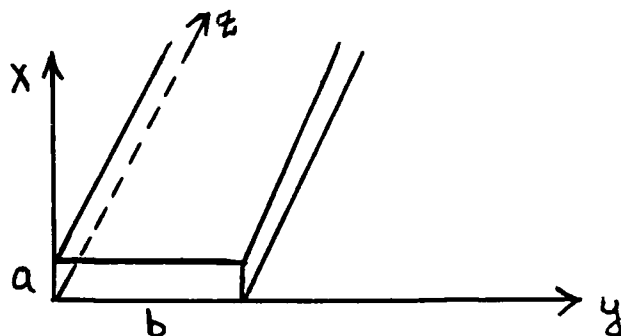


Fig. 1. Hollow, rectangular guide geometry

For this geometry we can write the scalar form of (4) and (5) which is the Helmholtz equation in cartesian coordinates. Picking TM waves the equation is

$$\frac{\delta^2 U_e}{\delta x^2} + \frac{\delta^2 U_e}{\delta y^2} + k_c^2 U_e = 0 \quad (6)$$

where here we have neglected the common exponential factor, and the subscript "e" refers to electric (E) waves and "h" to magnetic (H) waves.

Assume a solution of the form

$$E_z = U_e(x,y) \text{ EXP}[i(\omega t - 2\pi z/\lambda_c)] \quad (7)$$

where in general  $U(x,y)$  is a generating function for the E or H field.

Let

$$U_e(x,y) = X(x)Y(y) . \quad (8)$$

The boundary condition on our solution is that  $U_e(x,y)$  at the surface should vanish. This means that  $U_e(0,y) = U_e(a,y) = U_e(x,0) = U_e(x,b) = 0$ .

Inserting (8) into (6) and separating we obtain the ordinary differential equation

$$\frac{d^2X}{dx^2} + \mu^2 X = 0 \quad (9)$$

and

$$\frac{d^2Y}{dy^2} + (k_c^2 - \mu^2)Y = 0 \quad (10)$$

where  $\mu$  is the separation constant.

The solution to (9) is

$$X(x) = a_1 \cos \mu x + b_1 \sin \mu x \quad (11)$$

and the solution to (10) is

$$Y(y) = a_2 \cos \sqrt{k_c^2 - u^2} y + b_2 \sin \sqrt{k_c^2 - u^2} y \quad (12)$$

Then a solution to (8) is given by

$$U_e(x, y) = (a_1 \cos ux + b_1 \sin ux)(a_2 \cos \sqrt{k_c^2 - u^2} y + b_2 \sin \sqrt{k_c^2 - u^2} y) \quad (13)$$

By imposing the boundary conditions a solution is obtained satisfying all conditions.

$$U_e(x, y) = B_{mn} \sin \frac{m\pi x}{a} \sin \frac{n\pi y}{b} \quad (14)$$

By superposition we get

$$U_e(x, y) = \sum_{m=1}^{\infty} \sum_{n=1}^{\infty} B_{mn} \sin \frac{m\pi x}{a} \sin \frac{n\pi y}{b} \quad (15)$$

The electric field at the entrance aperture generally is some value  $f(x, y)$ , or:

$$f(x, y) = \sum_{m=1}^{\infty} \sum_{n=1}^{\infty} B_{mn} \sin \frac{n\pi y}{b} \sin \frac{m\pi x}{a} \quad (16)$$

By Fourier methods for double infinite series the coefficient is determined to be:

$$B_{mn} = \frac{4}{ab} \int_0^a \int_0^b f(x, y) \sin \frac{m\pi x}{a} \sin \frac{n\pi y}{b} dx dy \quad (17)$$



which leads to the required general solution

$$U_e(x,y) = \frac{4}{ab} \sum_{m=1}^{\infty} \int_0^a \int_0^b f(x,y) \sin \frac{m\pi x}{a} \sin \frac{n\pi y}{b} dx dy \quad (18)$$

with dominant mode given by

$$U_e(x,y) = \frac{4}{ab} \int_0^a \int_0^b f(x,y) \sin \frac{\pi x}{a} \sin \frac{\pi y}{b} \quad (19)$$

Marion (1965) has stated that in practice it is desirable to pick the wave guide dimensions such that only the dominant mode will be propagated at the operating frequency. This would optimize the transmission and eliminate multimode effects. Garmire, McMahon and Bass (1977) have shown both theoretically and experimentally that the bending loss per angle of bend in rectangular metallic wave guides is explicitly independent of wave guide height, bend radius, and light wavelength, depending only on the reflectivity of the wave guide wall. Their further work (1980) generated useful design equations which give guidance to the best choice of wave guide parameters. This makes the rectangular wave guide an attractive candidate for use as a light pipe.

In Collin (1960) it is pointed out that the power loss per unit length of guide is given by

$$2\alpha P = P_L = \frac{1}{2} R_n \oint_C [(\beta)^2 |\vec{n} \times \vec{\nabla}_t U_h|^2 + k_c^4 U_h^2] dl \quad (20)$$

For TE modes where the phase constant  $\beta^2$  is given by  $\omega^2 \mu_0 \epsilon - k_c^2$ , and the skin-effect surface resistance of a metal with permeability  $\mu$ , defined by  $R_n$  is given by  $(\omega \mu / 2\sigma)^{1/2}$ .

Also

$$P = \frac{1}{2} Z_0 k_0 \beta k_c^2 \iint_S U_h^2 da \quad (21)$$

This means that the attenuation constant,  $\alpha$ , for TE modes is given by

$$\alpha = \frac{R_n \oint_C [(\beta)^2 |\vec{n} \times \vec{\nabla}_t U_h|^2 + k_c^4 U_h^2] dl}{2 Z_0 k_0 \beta k_c^2 \iint_S U_h^2 da} \quad (22)$$

And the analogous expression for TM modes is

$$\alpha = \frac{R_n k_0 Y_0}{2 \beta k_c^2} \frac{\oint |\vec{\nabla}_t U_e|^2 dl}{\iint_S U_e^2 da} \quad (23)$$

Where the intrinsic impedance of free space,  $Z_0$  is given by  $(\mu_0 / \epsilon_0)^{1/2}$ .

These equations give the following formulas of attenuation in nepers per meter

$$\alpha = \frac{2R_n}{b Z_0 (1 - k_{c,mn}^2 / k_0^2)^{1/2}} \left[ \left( 1 + \frac{b}{a} \right) \frac{k_{c,mn}^2}{k_0^2} + \frac{b}{a} \left( \frac{\epsilon_{on}}{2} - \frac{k_{c,mn}^2}{k_0^2} \right) \right. \\ \left. \times \left( \frac{m^2 ab + n^2 a^2}{m^2 b^2 + n^2 a^2} \right) \right] \quad (24)$$

with  $\epsilon_{on} = \begin{cases} 1 & m = 0 \\ 2 & m > 0 \end{cases}$

and

$$\alpha = \frac{2R_n}{b Z_0 (1 - k_{c,mn}^2 / k_0^2)^{1/2}} \left( \frac{m^2 b^3 + n^2 a^3}{m^2 b^2 a + n^2 a^2 b} \right) \quad (25)$$

For TE and TM modes respectively.

#### V. CYLINDRICAL WAVE GUIDES

The analysis for straight cylindrical wave guides follows a similar line of development. The geometry is shown in Fig. 2.

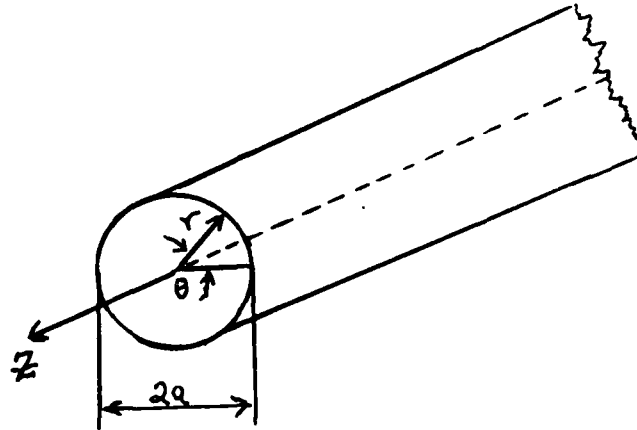


Fig. 2 Hollow Cylindrical geometry

Because of the obvious symmetry we choose a cylindrical coordinate representation of the Helmholtz equation and again pick TM waves, for the analysis.

We have

$$\frac{\delta^2 U_e}{\delta r^2} + \frac{1}{r} \frac{\delta U_e}{\delta r} + \frac{1}{r^2} \frac{\delta^2 U_e}{\delta \theta^2} + k_c^2 U_e = 0 \quad (26)$$

Assume a solution of the form:

$$E_z = U_e(r, \theta) \text{EXP}[i(\omega t - 2\pi z/\lambda_c)] \quad (27)$$

The boundary condition is  $U_e(a, \theta) = 0$ .

Let

$$U_e(r, \theta) = R(r) \theta(\theta) . \quad (28)$$

Applying the separation technique we obtain

$$\frac{d^2 \theta}{d\theta^2} + \mu^2 \theta = 0 \quad (29)$$

And also upon rearrangement

$$r^2 \frac{d^2 R}{dr^2} + r \frac{dR}{dr} + [k^2 r - \mu^2] R = 0 \quad (30)$$

Equation (29) solves easily, however (30) is a Bessels' differential equation and must be solved by series solution.

A complete solution to (26) is then

$$U_e(r, \theta) = (A_2 J_\mu(k_c r) + B_2 Y_\mu(k_c r))(A_1 \text{Cos} \mu \theta + B_1 \text{Sin} \mu \theta) \quad (31)$$

Where  $J_\mu$  and  $Y_\mu$  are Bessel functions.

Inserting the boundary condition we eventually obtain the following as solutions:

$$U_e(r, \theta) = \sum_{m=0}^{\infty} \left\{ \left[ \sum_{n=1}^{\infty} \frac{2}{\pi a^2 [J_{m+1}(k_{c,mn} a)]^2} \int_0^a J_m^2(k_{c,mn} r) \int_0^{2\pi} f(r, \theta) \cos m\theta d\theta dr \right] \cos m\theta \right. \\ \left. + \left[ \sum_{n=1}^{\infty} \frac{2}{\pi a^2 [J_{m+1}(k_{c,mn} a)]^2} \int_0^a J_m^2(k_{c,mn} r) \int_0^{2\pi} f(r, \theta) \sin m\theta d\theta dr \right] \sin m\theta \right\} \quad (32)$$

For  $m$  in the coefficient  $A_{mn}$  given by  $m = 1, 2, 3$  and

$$U_e(r, \theta) = \sum_{n=1}^{\infty} \frac{2}{\pi a^2 [J_1(k_{c,on} a)]^2} \int_0^a J_0^2(k_{c,on} r) \int_0^{2\pi} f(r, \theta) dr d\theta \quad (33)$$

For  $m = 0$  in the above expression.

The dominant mode is given by

$$U_e(r, \theta) = \frac{2}{\pi a^2 [J_1(k_{c,01} a)]^2} \int_0^a J_0^2(k_{c,01} r) \int_0^{2\pi} f(r, \theta) dr d\theta \quad (34)$$

From the general expression for attenuation, we obtain from the cylindrical guide

$$\alpha = \frac{R_m}{aZ_0} \left( 1 - \frac{k_{c,mn}^2}{k_0^2} \right)^{-1/2} \left( \frac{k_{c,mn}^2}{k_0^2} + \frac{m^2}{P'^2 - m^2} \right) \quad (35)$$

and

$$\alpha = \frac{R_m}{aZ_0} \left( 1 - \frac{k_{c,mn}^2}{k_0^2} \right)^{-1/2} \quad (36)$$

For TE and TM modes respectively. Where the  $P'_{mn}$ 's are the roots for  $k_c a$  in the expression  $dJ_m(k_c r)/dr = 0$  at  $r = a$  as required by the boundary condition for TE mode.

#### VI. THE CURVED CYLINDRICAL GUIDE

Magnus, Oberhettinger, and Soni (1966) show that the wave equation in toroidal coordinates is given by

$$\frac{\delta}{\delta \xi} \left( \frac{\sinh \xi}{\cosh \xi - \cos \eta} \frac{\delta f}{\delta \xi} \right) + \frac{\delta}{\delta \eta} \left( \frac{\sinh \xi}{\cosh \xi - \cos \eta} \frac{\delta f}{\delta \eta} \right) + \frac{1}{\sinh \xi (\cosh \xi - \cos \eta)} \frac{\delta^2 f}{\delta \phi^2} + \frac{k_c^2 C^2 \sinh \xi}{(\cosh \xi - \cos \eta)^3} f = 0 \quad (37)$$

and state that this differential equation is not separable for  $k_c \neq 0$ . This forces the use of an alternate method of solution for this case. Marcatili and Schmeltzer (1964) define a toroidal system  $(\gamma, \theta, z)$  with metric coefficients  $e_r = 1$ ,  $e_\theta = r$ , and  $e_z = 1 + r/R \sin \theta$  where  $R$  is the radius of curvature of the guide as shown in Fig. 3.

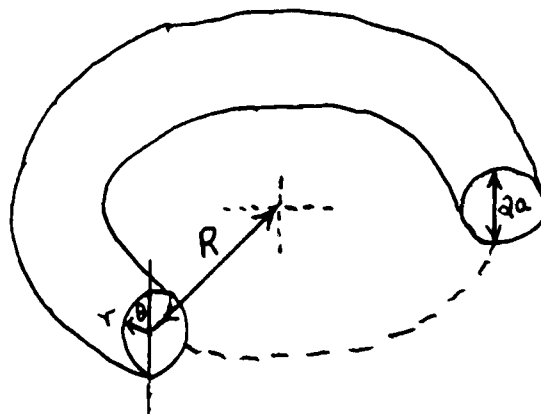


Fig. 3. Hollow, toroidal geometry

Maxwells' equations are given by

$$\frac{\delta}{\delta \theta} \left\{ \left( 1 + r/R \sin \theta \right) \mathcal{H}_z \right\} - i \gamma_c r \mathcal{H}_\theta + i \omega \epsilon r (1 + r/R \sin \theta) \xi_\theta = 0 \quad (38)$$

$$i \gamma_c \mathcal{H}_r - \frac{\delta}{\delta r} \left\{ (1 + r / R \sin \theta) \mathcal{H}_z \right\} + i \omega \epsilon (1 + r / R \sin \theta) \xi_\theta = 0 \quad (39)$$

$$\frac{\delta}{\delta r} (r \mathcal{H}_\theta) - \frac{\delta}{\delta \theta} \mathcal{H}_r + i \omega \epsilon r \xi_z = 0 \quad (40)$$

$$\frac{\delta}{\delta \theta} \left\{ (1 + r / R \sin \theta) \xi_z \right\} - i \gamma_c \xi_\theta - i \omega \mu r (1 + r / R \sin \theta) \mathcal{H}_r = 0 \quad (41)$$

$$i \gamma_c \xi_r - \frac{\delta}{\delta r} \left\{ (1 + r / R \sin \theta) \xi_z \right\} - i \omega \mu (1 + r / R \sin \theta) \mathcal{H}_\theta = 0 \quad (42)$$

$$\frac{\delta}{\delta r} (r \xi_\theta) - \frac{\delta \xi_r}{\delta \theta} - i \omega \mu r \mathcal{H}_z = 0 \quad (43)$$

Where the common factor  $\text{Exp} [i(\gamma_c z - \omega t)]$  has been left out and where  $\gamma_c$  refers to the propagation constant of the curved guide. Introduction of a parameter  $\sigma$  defined approximately by  $2 \left( \frac{2\pi a}{U_{mn} \lambda} \right)^2 \frac{a}{R}$  for  $\sigma \ll 1$  and using a first order perturbation technique yields the solutions of (37) - (42) as

$$\xi_\theta = (1 + \sigma r/a \sin \theta) E_\theta \quad (44)$$

$$\xi_r = (1 + \sigma r/a \sin \theta) E_r \quad (45)$$

$$\xi_z = (1 + \sigma r/a \sin \theta) E_z + (i\sigma/ka)(E_r \sin \theta + E_\theta \cos \theta) \quad (46)$$

$$\mathcal{H}_\theta = (1 + \sigma r/a \sin \theta) H_\theta \quad (47)$$

$$\mathcal{H}_r = (1 + \sigma r/a \sin \theta) H_r \quad (48)$$

$$\mathcal{H}_z = (1 + \sigma r/a \sin \theta) H_z + (i\sigma/ka)(H_r \sin \theta + H_\theta \cos \theta) \quad (49)$$

where  $E_r$ ,  $E_\theta$ ,  $E_z$ ,  $H_r$ ,  $H_\theta$ , and  $H_z$  refer to the uncurved guide. The validity of this technique is confirmed upon examination by letting  $R \rightarrow \infty$  in (44) - (49), thereby resulting in the curved wave guide geometry degenerating into a cylindrical system and a straight guide. The power flow in the axial  $z$  direction within the guide given by

$$P_z = \frac{1}{2} \int_0^a \int_0^{2\pi} \text{Re} [\xi_r \mathcal{H}_\theta^* - \xi_\theta \mathcal{H}_r^*] r dr d\theta \quad (50)$$

decreases along  $z$  at the rate

$$\frac{dP_z}{dz} = -2 \alpha_{mn}(R) P_z = -P_r \quad (51)$$

where  $P_r$  is the mean radial power flowing into the guide wall per unit length defined by

$$P_r = \frac{1}{2} \int_0^{2\pi} \text{Re} [\xi_\theta \mathcal{H}_z^* - \xi_z \mathcal{H}_\theta^*]_r = a \left[ 1 + a/r \sin \theta \right] a d\theta \quad (52)$$

The model therefore to some degree takes into account losses due to curvature in circular cylindrical guides, and suggests that there are optimum values for both the axial length and the radial dimension of the guides.



#### VIII. CONCLUSIONS AND RECOMMENDATIONS

The solution of the wave equation in some geometries is an infinite series that when combined with the exponential factor gives an expression for either the electric field or the magnetic field depending on the starting point for analysis (i.e. TM or TE mode analysis).

A realistic computer model of the input fields at the aperture of the wave guide should be developed to obtain an expression for  $f(x,y)$  that will improve the expression for the fields in the wave guide. Losses due to curvature in bent circular wave guides can be described partly in terms of a perturbation of the guide axis, however losses due to scattering have yet to receive ample descriptive treatment.

Since losses in the rectangular guide are minimal with respect to wave guide height, bend radius, and wavelength it could serve as an alternative to circular pipes. Whatever choice is made for the geometry, techniques should be used to make sure that only the dominant mode will be propagated at the operating frequency.

## REFERENCES

1. Collin, R. E., Field Theory of Guided Waves, New York, New York, McGraw-Hill Book Company Inc. 1960.
2. Garmire, E. T. McMahon, and M. Bass, "Propagation of Infrared Light in Flexible Hollow Waveguides," Applied Optics, January 1976, pp. 147.
3. Garmire, E. T. McMahon, and M. Bass, "Low-Loss Optical Transmission Through Bent Hollow Metal Wave-Guides," Applied Physics Letters, July 1977, pp. 92.
4. Garmire, E. T. McMahon, and M. Bass, "Flexible Infrared Wave-Guides For High-Power Transmission," IEEE Journal of Quantum Electronics, January 1980, pp. 24-23.
5. Jackson, J. D., Classical Electrodynamics, New York, John Wiley & Sons, 1975.
6. Magnus, W., Oberhettinger and Soni, R. P. Formulas and Theorems for the Special Functions of Mathematical Physics, Springer-Verlay, Berlin, 1966.
7. Marcatili, E. A. J., and R. A. Schmeltzer, "Hollow Metallic and Dielectric Wave Guides for Long Distance Optical Transmission and Lasers," The Bell System Technical Journal, July 1964, pp. 1784-1809.
8. Marion, J. B., Classical electromagnetic Radiation, New York, New York, Academic Press Inc. 1965.
9. Rayleigh, L., "On the Passage of Electric Waves Through Tubes, On the Vibration of Dielectric Cylinders," Phil. May., February 1897, pp. 125-132.

1987 USAF-UES SUMMER FACULTY RESEARCH PROGRAM/  
GRADUATE STUDENT SUMMER SUPPORT PROGRAM

Sponsored by the  
AIR FORCE OFFICE OF SCIENTIFIC RESEARCH

Conducted by the  
Universal Energy Systems, Inc.

FINAL REPORT

PHYTOTOXICITY OF SOIL RESIDUES OF JP-4 AVIATION FUEL

Prepared by:	Richard H. Brown
Academic Rank:	Associate Professor
Department and	Biology Department
University:	Ouachita Baptist University
Research Location:	USAF OEH/ECQ Brooks Air Force Base San Antonio, TX 78235
USAF Researcher:	Dr. Tom Doane
Date:	August 18, 1987
Contract No:	F49620-85-C-0013

# ABSTRACT

The toxicity of JP-4 aviation fuel soil residues was assessed in a series of soil bioassays using sorghum (*Sorghum bicolor*), bean (*Phaseolus vulgaris*), oat (*Avena sativa*), and cucumber (*Cucumis sativus*). Sorghum and bean indicated no sensitivity to JP-4 residues in soils contaminated with up to 2000 ppmw jet fuel. Oat and cucumber shoot length and fresh shoot weight was stimulated in samples contaminated with up to 2 ppmw and inhibited in soils receiving 2000 through 200,000 ppmw of JP-4. An  $ED_{50}$  is indicated between 20,000 and 200,000 ppmw of JP-4 for both oat and cucumber.

### ACKNOWLEDGEMENTS

I would like to express my appreciation to the Air Force Systems Command and the Air Force Office of Scientific Research for sponsoring this research and to Universal Energy Systems for administering the program through which this study was conducted.

The success of a challenging endeavor is seldom the result of one person's efforts and abilities. Without the concerted efforts of a number of people, this project would have suffered. Special appreciation is extended to Col. James Rock and Maj. Tom Doane for the opportunity to conduct this research, for their personal interest, and for allowing me academic freedom when possible and guidance when necessary. The assistance of Lt. Mike Spakowicz, Airman Harold Casey, Ms. Ann Potter, and Dr. Robert Frans in the acquisition of supplies and materials was invaluable. Capt. Martin Tobin is greatly appreciated for his excellent graphics. Without the assistance of Capt. Tom Lillie, Steven Naber, and Lt. Jeffery Muilenburg, statistical analysis of the acquired data would have been more difficult.

## I. INTRODUCTION:

JP-4 aviation fuel is the primary fuel used in aircraft of the United States Air Force and is composed of a complex mixture of about 300 aliphatic and aromatic hydrocarbon compounds varying in length up to  $C_{16}$ . Jettisoning of fuels, aircraft crashes, and fueling operations may effect a release of aviation fuels into the environment and as a consequence, some degree of ecological perturbation can result. It has been reported by Clewell (1980) and Bishop (1983) that upon release, those fuel components on the lower boiling light end,  $C_8$  and below, tend to evaporate leaving the heavier  $C_9 - C_{16}$  compounds as residues. The phytotoxicity of these residues in soil is the focus of this study.

Previous studies have reported the toxicity and mutagenicity of jet fuels to dogs, monkeys, mice, rats, and humans (Kinkead, 1974 and Kapp, 1979 and Knave, 1979). Still others have addressed the impact of these fuels on aquatic ecosystems (Jenkins, 1977 and Doane, 1980 and Bombick, 1982). In contrast, there has been limited research conducted on the effects of aviation fuels on terrestrial ecosystems although these effects are certainly just as important.

This research was conducted to provide for the USAF Occupational and Environmental Health Laboratory at Brooks Air Force

Base, Texas, a reference study and a functional procedure to assist in the monitoring of environmental damages resulting from fuel releases.

## II. OBJECTIVES OF THE RESEARCH EFFORT:

A number of soil bioassay procedures have been developed by Leasure (1964), Dowler (1969), Kratky (1971), Santelman (1971), Gerber (1977), Lavy (1986), and others using mortality, root length, shoot length, fresh or dry shoot weight, or some other factor to assess plant responses to a variety of chemical substances. It was my assignment to:

- a. Review the literature for current soil bioassay methods;
- b. Develop an effective bioassay protocol to be used by the USAF/OEHL to monitor damage caused by JP-4 fuel residues in soil;
- c. And to use this protocol to produce a reference study to be used for comparing the results of future assays on field samples.

## III. MATERIALS AND METHODS:

Commercial topsoil (Southland) was air dried and sieved through a number 7 U. S. Standard Sieve then adjusted to a pH between 6.5 and 7.5. One thousand gram samples of this soil were placed in large plastic bags and contaminated

with 0, 0.002, 0.02, 0.2, 2, 20, 200, and 2000 ppmw of Jp-4 aviation fuel dissolved in a methyl alcohol carrier by slowly dripping the contaminant solution into a depression in the surface of each sample. These samples were ventilated for 24 hours to allow evaporation of the carrier and the volatile components of the fuel then thoroughly mixed by closing and inverting each bag 25 times (Lavy, 1986). One hundred and twenty-five gram aliquots of each sample were transferred to a series of labeled, wax impregnated cups and watered to field capacity.

Seeds of cucumber (*Cucumis sativus* L.), oat (*Avena sativa* L.), sorghum (*Sorghum bicolor* L.) and bean (*Phaseolus vulgaris* L.) were pregerminated for 24 hours to provide seeds with uniform radicle lengths. Five (four for bean) similar sized, pregerminated seeds were planted in each of four cups per concentration per species so that the surface of each seed was level with the soil surface. These planted cups were then placed in Rheem Puffer Hubbard environmental chambers (Mod. CEC255-6) for 14 days during which the temperature was maintained at 21 degrees C. for the 14 hour days and 18 degrees C. at night. Each cup was watered daily to field capacity and the relative humidity was allowed to vary between 70 and 90 percent.

On the 14th day, all plant shoots were harvested by cutting the stem at soil surface. Shoot lengths (soil surface to



apex of the leaf providing the longest measure) and fresh shoot weights were determined and recorded. These data are summarized in Fig. 1.

Using the same procedure plus on the fifth day, the plants were watered with RA-PID-GRO 23-19-17 plant nutrient solution prepared per manufacturer's instructions, a second bioassay was conducted using cucumber and oat seeds planted in soils contaminated with 0, 2, 20, 200, 2,000, 20,000, and 200,000 ppmw of JP-4. Shoot length and fresh shoot weight data obtained from these plants are summarized in Fig. 2.

Data from all assays were analysed for means, standard deviations, standard errors, and confidence limits using an analysis of variance (ANOVA,  $p < 0.01$ ) and Duncan's multiple range test ( $p < 0.05$ ).

#### IV. RESULTS AND DISCUSSION:

In the 0 - 2000 ppmw test run, neither sorghum nor bean exhibited significant differences in growth (length or weight) at any JP-4 : soil concentration through 2000 ppmw. Due to their lack of sensitivity to the residues of this contaminant, they were excluded from subsequent tests. Oat and cucumber did show significant dose-response variations, therefore, were included in the second test series.

In the 0 - 2000 ppmw series, oat shoot length and fresh weight ~~were~~ stimulated by the presence of JP-4 residues in the 0.002 through 2 ppmw samples while growth in the 0, 20, and 200 ppmw samples were similar. A slight inhibition of growth was observed at 2000 ppmw. Data obtained in the second bioassay (0 - 200,000 ppmw series), confirmed these observations. Oat growth was significantly stimulated at 2 ppmw and inhibited by the presence of residues in each of the 2000 to 200,000 ppmw samples. Although a regression analysis was not conducted, these data indicate an ED<sub>50</sub> between 20,000 and 200,000 ppmw for shoot length and between 2000 and 20,000 for fresh shoot weight.

Cucumber growth (length and weight) was significantly increased when the plants were grown in soils contaminated by JP-4 in concentrations of 0.002 and 0.2 ppmw. Concentrations of 0, 0.02, and 2 through 200 ppmw produced similar results while plants grown in the 2000 ppmw samples exhibited significant reduction in growth. The 0.02 samples showed unexplained high variability and are believed to be of little value in this study. In the second bioassay with cucumbers, these results were again largely confirmed. Residues in soils contaminated with 2 ppmw of JP-4 resulted in significant plant stimulation, while the 0, 20, and 200 ppmw samples showed similar growth. Each of the 2000 through 200,000 ppmw samples showed continued significant decreases.

Without regression analysis, an  $ED_{50}$  for cucumber appears to be between 20,000 and 200,000 ppmw for both length and weight.

In both bioassay runs and for all species tested, the shoot length and fresh shoot weight dose-response curves were remarkably complimentary. Mortality was never of importance in this study since 100% survivorship was observed even in the 200,000 ppmw samples.

Based on the procedures used in these bioassays, a protocol for testing field samples was developed and has been presented to the United States Air Force Occupational and Environmental Health Laboratory at Brooks Air Force Base, TX.

#### V. RECOMMENDATIONS:

The results of this study indicate that toxicity to plants grown in soils containing JP-4 aviation fuel is low. This information could be of considerable value to the United States Air Force in legal actions resulting from JP-4 contamination. However, before these results can be considered absolute, several ancillary activities should be initiated. These include:

- a. One or more repetitions of the second bioassay to verify the results and through regression analysis de-

termine an appropriate ED<sub>50</sub> for each test species.

b. Conducting bioassays using other test species to determine which is most sensitive to JP-4 residues.

c. Conducting bioassays using other soil types to determine the growth medium that will produce the most consistent and informative results.

d. Testing of the protocol developed for analysis of field samples.

e. Conducting studies that compare results obtained using laboratory standard soil with results obtained using field soil samples.

f. Conducting extended studies to determine JP-4 residue persistence in various soil types.

## REFERENCES

1. Bailey, D. R., "Comparison of Oats and Lemna Oligorrhiza for Diuron Bioassay," Queensland Journal of Agricultural and Animal Sciences, Vol. 27, 1970, pp. 395-400.
2. Behrins, R., "Quantitative Determination of Triazine Herbicides in Soils by Bioassay," Residue Reviews, Vol. 32, 1970, pp. 355-369.
3. Bishop, E. C., M. Macnaughton, R. deTreville, and R. Drawbaugh, Rationale for a Threshold Limit Value (TLR)<sup>R</sup> for JP-4 Jet B Wide Cut Aviation Turbine Fuel, USAFOEHL Report No. 83-128EH111DGA, Brooks Air Force Base, TX, 1983.
4. Bombick, D. W. and L. G. Arlian, Comparative Toxicity of Selected Aviation Fuels as Measured by Insect Bioassay, USAFAMRL Report No. AFAMRL-TR-82-31, Wright-Petterson Air Force Base, OH, 1982.
5. Clewell III, H. J., The Effect of Fuel Composition Ground-fall From Aircraft Fuel Jettisoning, USAFAFESC Report No. ESL-TR-81-13, Tyndall Air Force Base, FL, 1981.
6. Doane, T., USAFOEHL Guide to Aquatic Bioassay Techniques, Terminology, and Capabilities, USAFOEHL Report No. 80-18, Brooks Air Force Base, TX, 1980.

7. Dowler, C. C., "A Cucumber Bioassay Test for the Soil Residues of Certain Herbicides," Weed Science, Vol. 17, Weed Science Society of America, 1969, pp. 309-310.
8. Gerber, H. R., "Biotests for Herbicide Development," Crop Protection Agents - Their Biological Evaluation, (N. R. McFarlane, ed.), Academic Press, N. Y., 1977, pp. 307-321.
9. Hurle, K., "Biotests for the Detection of Herbicides in the Soil," Crop Protection Agents - Their Biological Evaluation, (N. R. McFarlane, ed.), Academic Press, N. Y., 1977, pp. 285-306.
10. Jacques, G. L., and R. G. Harvey, "Persistence of Dinitro-aniline Herbicides in Soil," Weed Science, Vol. 27, Weed Science Society of America, 1979, pp. 660-665.
11. Jayakumar, R., and A. Mohamed Ali, "Response of Cucumber, Finger Millet, Foxtail Millet, and Sunflower to Soil Residues of Atrazine and 2, 4-D," Indian J. Weed Science, Vol. 16, 1984, pp. 133-135.
12. Jenkins, D., S. A. Klein, and R. C. Cooper, "Fish Toxicity of Jet Fuels--I. The Toxicity of the Synthetic Fuel JP-9 and its Components," Water Research, Vol. 11, 1977, pp. 1059-1067.

13. Kapp, R. W. and C. E. Piper, In Vitro and In Vivo Mutagenicity Studies Jet Fuels, A Final Report, Hazelton Laboratories America, Vienna, VA, 1979.
14. Kimball, K. D. and S. A. Levin, "Limitations of Laboratory Bioassays: The Need for Ecosystem Level Testing," Bioscience, Vol. 35, 1985, pp. 99-129.
15. Kinkead, E. R., L. C. DiPasquale, E. H. Vernot and J. D. MacEwen, Chronic Toxicity of JP-4 Jet Fuel, Report No. 11, AFAMRL-TR-74-125, Wright-Patterson Air Force Base, OH, 1974.
16. Knave, B., P. Mindus, and G. Struwe, "Neurasthenic Symptoms in Workers Occupationally Exposed to Jet Fuel," Acta Psychiatrica Scandinavica, Vol. 60, 1979, pp. 39-49.
17. Kohn, G. K., "Bioassay as a Monitoring Tool," Residue Reviews, Vol. 76, Springer-Verlag, N. Y., 1980, pp. 99-129.
18. Kratky, B. A. and G. F. Warren, "The Use of Three Simple, Rapid Bioassays on Forty-two Herbicides," Weeds Research, Vol. 11, 1971, pp. 257-262.
19. Lavy, T. L. and P. W. Santelmann, "Herbicide Bioassay as a Research Tool," Research Methods in Weed Science, 3rd Ed. (N. D. Camper, ed.), Southern Weed Science Society, Champaign, IL, 1986, pp. 201-217.

20. Leasure, J. K., "Bioassay Methods for 4-Amino-3, 5, 6-trichloropicolinic Acid," Weeds, Vol. 12, Weed Society of America, 1964, pp. 232-233.
21. Santelmann, P. W., J. B. Weber, and A. F. Wiese, "A Study of Soil Bioassay Technique Using Prometryne," Weed Science Vol. 19, 1971, pp. 170-174.



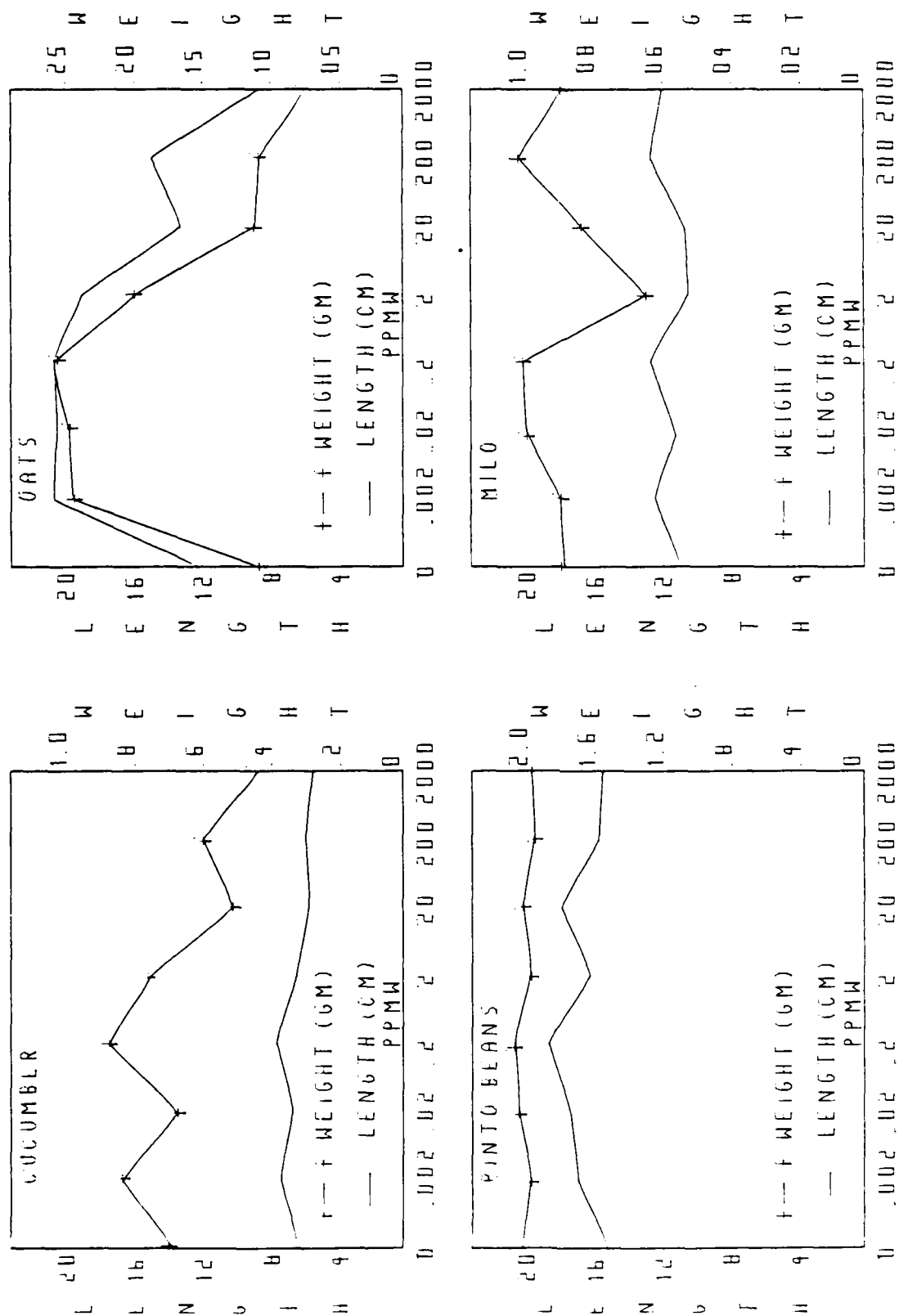


Fig. 1. Fresh shoot length and weight response of cucumber, oat, pinto bean, and milo sorghum to residues of JP-4 jet fuel applied to soil in varying concentrations. (assay #1)

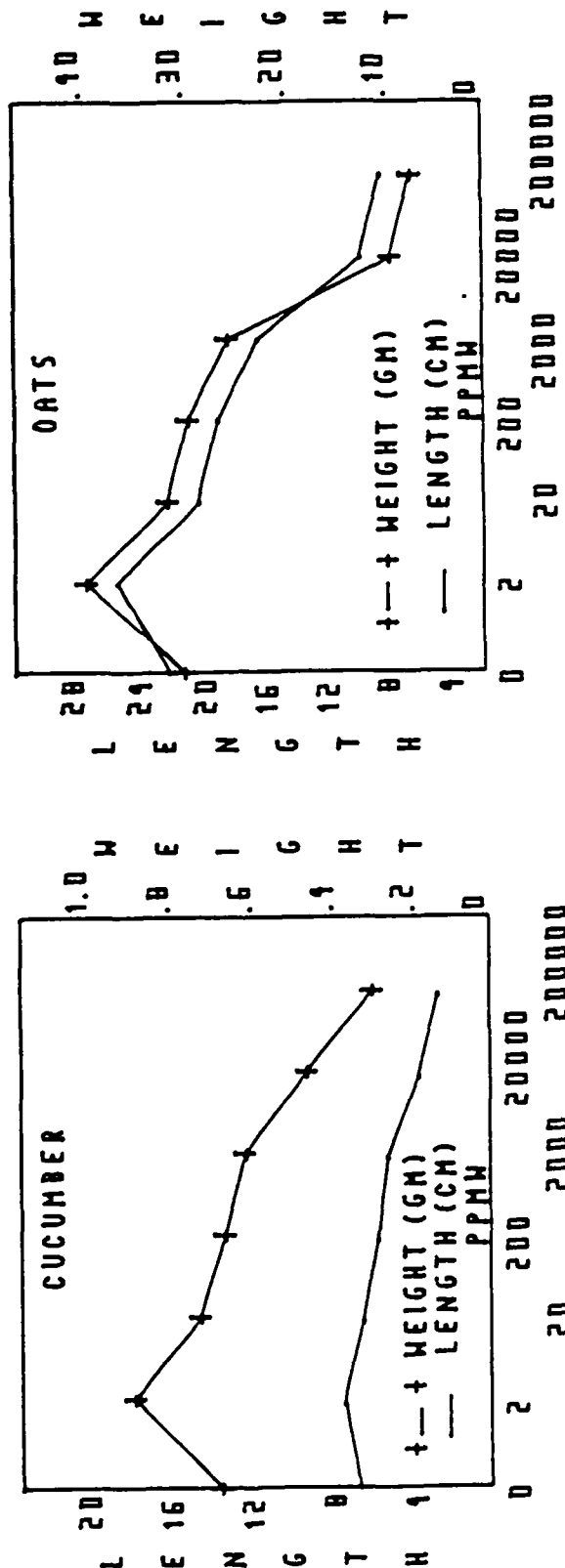


Fig. 2. Fresh shoot length and weight response of cucumber and oats to residues of JP-4 jet fuel applied to soil in varying concentrations. (assay #2)

1987 USAF-UES SUMMER FACULTY RESEARCH PROGRAM

GRADUATE STUDENT SUMMER SUPPORT PROGRAM

Sponsored by the

AIR FORCE OFFICE OF SCIENTIFIC RESEARCH

Conducted by the

Universal Energy Systems, Inc.

FINAL REPORT

DYNAMICS OF A METALLIC JET

Prepared by:	Robert A. Buchl, Ph.D.
Academic Rank:	Assistant Professor
Department and	Department of Physics & Astronomy
University:	University of Wisconsin - Eau Claire
Research Location:	USAF Armament Laboratory Eglin AFB FL 32542-5434
USAF Researcher:	William H. Cook Chief, Computational Mechanics Section
Date:	3 Aug 87
Contract No:	F49620-85-C-0013

# DYNAMICS OF A METALLIC JET

by

Robert A. Buchl

## ABSTRACT

The dynamics of a shaped charge metallic jet is discussed for two cases, jet formation and jet penetration into a semi-infinite target. The equations of motion which govern a metallic jet are presented which incorporate a velocity gradient and the Bernoulli hydrodynamic equation. The equations of motion are solved analytically and describe jet elongation and jet penetration. Jet particulation and the energy expenditure in the penetration process are considered.

### Acknowledgements

I wish to thank the Air Force Systems Command and the Air Force Office of Scientific Research for sponsorship of this research. Universal Energy Systems must be mentioned for their concern and help to me in all administrative and directional aspects of this program.

My experience was rewarding and enriching because of many different influences. William H. Cook provided me with support, encouragement, and a truly enjoyable working atmosphere. The concern of Mr Ronald B. Boulet and his secretarial staff was greatly appreciated. Dr S. C. Lambert's interest was encouraging throughout the duration of this research project. His arranged guided tour of Eglin AFB was very interesting.

## I. INTRODUCTION

In the early 1800's a primitive shaped charge effect was known in both Germany and Sweden. Almost forgotten, it was revived in the 1880's by Dr Charles Munroe, working at the Naval Torpedo Station in Newport, Rhode Island. He discovered that if a block of guncotton with countersunk letters was detonated against a steel surface, the letters became embedded. Later, the process was called the Munroe or shaped charge effect.

For over thirty years, it has been known that the collapse of a conical metal shell due to a highly compressive shock wave generates a jet along the symmetry axis of the cone. The jet is followed by a slug due to the residual cone mass. A consequence of the detonation of a shaped charge is the high speed shock wave which compresses the cone under tremendous pressure. The subsequent developed metallic jet is composed of metal particles from the cone and travels at hypervelocity speeds.

An early theory of jet production and penetration by a shaped charge was based on the assumptions of ideal incompressible hydrodynamics. The formation of a jet and its subsequent penetration into a target can be considered to be two independent processes. In a typical shaped charge jet, it is known that the jet velocity decreases from the front of the jet to its rear as the jet propagates.

Extensive previous work has been accomplished in regard to the

characteristics of shaped charge jets. A vast amount of data and analytical discussion has been reported in the literature as a result of many experiments and investigations. Among the objects measured are the standoff distance, the distance from the base of the cone to the target, and how it affects the penetration. Other features of interest are cone size, initial speed of the penetration, depth of penetration into a semi-infinite target, and jet breakup.

## II. OBJECTIVES OF THE RESEARCH EFFORT

The object of this research effort is to conduct a study of the dynamic behavior of a metallic shaped charge jet. It is proposed to utilize a mathematical modeling approach in conjunction with known experimental features of a metallic jet, especially the velocity gradient.

The structure of the investigation will be based upon physical laws that explain the behavior of a jet. Previous experimental data has established that a constant velocity gradient exists for a traveling jet.

The primary objective of this report is to provide a rigorous description of a hypervelocity metallic jet for two cases. One case is a jet formation process without regard to target penetration. The other facet will be to analyze jet penetration into a semi-infinite target.

The physical behavior of a metallic jet provides equations whose

solutions account for the instantaneous length, mass, and velocity of the jet. Besides material constants like density, dynamic yield strengths, etc., the velocities of the front and rear of the jet are of interest.

Extensive research effort regarding shaped charge jets has been published previously. This investigation will complement previous work.

In this paper, we neglect any deviation from perfect axial alignment called waver of the jet. Breakup is a phenomenon that a jet of excessive length breaks up into fragments. We will assume a homogeneous uniform jet of a variable length and mass. An estimate of the time of particulation when a jet is extended to its limit and begins to breakup will be considered.

### III. DYNAMICS OF JET FORMATION

A hypervelocity metallic jet is generated by the uniform collapse of a metallic cone. A detonation wave propagated through an explosive cast outside the cone causes the jet to propagate along the symmetry axis. The high compression forces acting on the cone metal causes the formation of a high-speed jet.

In this section, the effort is to consider the jet during its formation stage as it is increasing in both velocity and length. It is assumed the emerging jet has a constant density even though its mass and length increase with time due to the impacting together of the walls of



the cone. Actually, the rear portion of a jet, called a slug, has more mass per unit length than the front leading portion of the jet.

However, an average density can account for this jet feature.

The equation of motion of a jet mass  $m$  and center of mass velocity  $v = \dot{x}_{cm}$  is given by

$$d(mv) / dt = Y_1 A \quad (1)$$

where  $Y_1$  is the dynamic stress at the rear (tail) of the jet where it is formed inside the cone and  $A$  is the cross-sectional area of the jet. The product  $Y_1 A$  is the accelerating force on the left end of the expanding jet and directed along its longitudinal direction.

The density of a jet of length  $l$  is

$$\rho_j = m / Al \quad (2)$$

Differentiating the density expression with respect to time results in the condition

$$\dot{m} / m = \dot{l} / l \quad (3)$$

which relates the changing mass with the changing length of the jet, assuming the jet cross-sectional area is constant throughout its length. Therefore, the jet equation of motion may be expressed as

$$l \dot{v} + \dot{l} v = Y_1 / \rho_j \quad (4)$$

A continuous metallic jet is capable of supporting an internal

pressure. The pressures inside a metallic jet are extremely high and the jet may be treated as having hydrodynamic properties. It is conventional to use Bernoulli's equation for a jet treated as a dynamic fluid. We write Bernoulli's equation in regard to the points at the front and rear of the jet as

$$\frac{1}{2}\rho_j \dot{x}_2^2 + Y_2 = \frac{1}{2}\rho_j \dot{x}_1^2 + Y_1, \quad (5)$$

where  $Y_1$  and  $Y_2$  are the dynamic stresses at the points having instantaneous velocities  $\dot{x}_1$  and  $\dot{x}_2$ , respectively, as seen in Fig. 1.

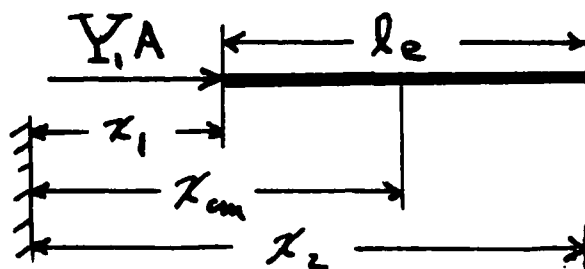


FIG. 1 Instantaneous Length of Jet

The center of mass of a uniform jet will lie at its midpoint. According to the illustrated jet in Fig. 1, its length is  $l = x_2 - x_1$ , and with the center of mass coordinate  $x_{cm} = x_1 + l/2$ , it is found with  $\dot{l} = \dot{x}_2 - \dot{x}_1$ , that the center of mass velocity is given by

$$v = \dot{x}_1 + \frac{1}{2}\dot{l} = \dot{x}_2 - \frac{1}{2}\dot{l}. \quad (6)$$

The Bernoulli expression, therefore, along with the velocity relationships, Eq. (6), leads to the expression

$$v\dot{l} = (Y_1 - Y_2) / \rho_j. \quad (7)$$

Experimentally, it is known that there exists a constant velocity gradient in a variable length jet. The jet velocity decreases, monotonically from tip to tail, in the jet formation process.

It will be assumed that the relationship between the center of mass velocity and the instantaneous jet length may be written in the differential form as

$$dv = \alpha dl \quad , \quad (8)$$

where  $\alpha$  is a constant and its magnitude is related to the velocity gradient as will subsequently be shown. Henceforth, the problem of describing a metallic jet in our formulation results in combining together the three expressions, Eqs. (4), (7), and (8), to form a differential equation for the expanding jet length which is

$$\alpha l_e \dot{l}_e = Y_2 / \rho_j \quad . \quad (9)$$

The initial condition of the jet is that its length is  $l_0$  at time  $t = 0$ . It is remarkable that the jet fluid stress  $Y_2$  at the front end of the jet appears in Eq. (9), even though the jet is generated at its left end as shown in Fig. 1.

The expression, Eq. (9), has the solution

$$l_e(t) = \left( l_0^2 + \frac{2Y_2 t}{\alpha \rho_j} \right)^{1/2} \quad , \quad (10)$$

which illustrates the lengthening of the jet with time.

The length of a jet will increase up to a length at which the particulation process begins. The rate of length change of the jet is

$$\dot{l}_e = \frac{Y_2}{\alpha \rho_j} \left( l_0^2 + \frac{2Y_2 t}{\alpha \rho_j} \right)^{-1/2} \quad (11)$$

The mass of the jet at any time  $t$ , using Eqs. (3) and (11), will be determined by

$$\int_{m_0}^m \frac{dm}{m} = \frac{Y_2}{\alpha \rho_j} \int_0^t \frac{dt}{l_0^2 + \frac{2Y_2 t}{\alpha \rho_j}} \quad (12)$$

which may be expressed as

$$m = \frac{m_0}{l_0} \left( l_0^2 + \frac{2Y_2 t}{\alpha \rho_j} \right)^{1/2} \quad (13)$$

where  $m_0$  is the initial mass of the jet at time  $t = 0$ . The expression, Eq. (13), shows the jet gains mass with increasing time. The velocity of the center of mass of the lengthening jet may be expressed as

$$v(t) = \left( \frac{Y_1}{Y_2} - 1 \right) \alpha l_e(t) \quad (14)$$

which, if this velocity is to be compatible with the velocity expression, Eq. (8), requires that the tail pressure be twice the tip pressure at the front of the jet,  $Y_1 = 2Y_2$ . This pressure condition precisely gives rise to the observed velocity gradient.

It is easily seen from previous expressions that the front and rear velocities of the jet are given by the relations

$$\dot{x}_{2,1} = \alpha l_e(t) \pm \frac{Y_2}{2\alpha \rho_j l_e(t)}, \quad (15)$$

where the plus, minus signs are to be used for the front, rear velocities, respectively.

The velocity gradient is explicitly illustrated by subtracting the two equations, Eqs. (15). It is seen that the velocity gradient expression is

$$\frac{Y_2}{\alpha \rho_j} = \frac{\dot{x}_2 - \dot{x}_1}{1/2}, \quad (16)$$

which fixes the value of  $\alpha$ . Cumulative jet length of a FXR (flash X-ray) picture as a function of jet velocity shows that  $\alpha$  may be determined from

$(Y_2/\alpha \rho_j) = (9 - 3.3)(\text{mm}/\mu\text{sec})/(1/1100 \text{ mm}) = 6.27 \times 10^3 \text{ mm}^2/\mu\text{sec}$ , if the strength of the jet tip  $Y_2$  and the density are known.

The acceleration of the jet is not constant, but can easily be expressed at a time derivative of the velocity in Eq. (14).

The preceding discussion of an expanding jet reveals that the length, mass, and velocities are explicit functions of time.

The next section involves the dynamics of a metallic jet as it encounters a target and the subsequent penetration process.

#### IV. DYNAMICS OF JET PENETRATION

A shaped charge jet may give rise to hypervelocity impact. The jet penetration is illustrated in Fig. 2. Basically, the idea is to consider that both the jet and the target behave as ideal incompressible fluids at the high pressures involved.

A typical metallic jet has a bulb at its tip moving with a speed of about 8 mm/ $\mu$ sec, and the rest of the jet following. The high pressure at the penetrating tip causes strong outward flow of both jet and target material.

At the initial time, the jet will have an initial speed, length, and mass before penetration. As the penetration process begins, the equation of motion governing the jet is

$$d(mv)/dt = -Y_2^c A \quad (17)$$

The stresses produced by the jet upon the target material are much greater than the yield strengths of most materials. The term  $-Y_2^c A$  is the force exerted upon the jet by the target and gives rise to a deceleration of the jet as it penetrates into the target material.

Paralleling the discussion in regard to jet formation, we introduce the velocity gradient and assume a constant density jet. The equation of motion, using the velocity relation  $dv = \beta dl$ , becomes

$$l_c \ddot{v} + \beta l_c \dot{l}_c = -Y_2^c / \rho_j \quad (18)$$

where  $l_c$  denotes the contracting jet length due to the penetration process. Inserting the Bernouilli relation, Eq. (6), it is seen that the length of the penetrating jet satisfies the differential equation

$$\beta l_c \dot{l}_c = -U_1^c / \rho_j \quad (19)$$

It has been shown that for jet velocities in excess of 4 mm/ $\mu$ sec, a hydrodynamic theory is valid so that both the jet and target have fluid properties. The solution of Eq. (19) shows that the length of the jet behaves explicitly with time as

$$l_c(t) = \left( l_0^2 - \frac{2U_1^c t}{\beta \rho_j} \right)^{1/2} \quad (20)$$

It is seen from the expression, Eq. (20), that it is the pressure at the tail of the jet that determines its length, although the decelerating force is applied at the tip (right) end where the jet encounters the target.

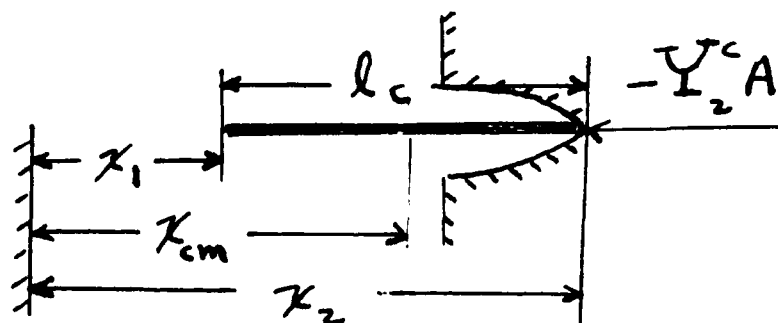


FIG. 2 Jet Penetration

A penetration time for a jet may be estimated from the length expression, Eq. 20. Setting the jet length to zero, an estimation time for total penetration is approximately  $t = (\beta \rho_j l_0) / (2Y_1^c)$ .

The length of the jet according to the expression, Eq. (20), is decreasing at the rate

$$\dot{l}_c = - \frac{Y_1^c}{\beta \rho_j} \left( l_0^2 - \frac{2Y_1^c t}{\beta \rho_j} \right)^{-1/2}. \quad (21)$$

The instantaneous mass of the jet from Eq. (3) is found to be

$$m = \frac{m_0}{l_0} \left( l_0^2 - \frac{2Y_1^c t}{\beta \rho_j} \right)^{1/2}, \quad (22)$$

showing the decrease of mass with time.

The velocity of the center of mass of the jet is formed from combining Eqs. (7) and (21). It follows that

$$v(t) = \left( \frac{Y_2^c}{Y_1^c} - 1 \right) \beta l_c(t), \quad (23)$$

and therefore, the pressure at the front of the jet will be twice the pressure at the rear of the jet,  $Y_2^c = 2Y_1^c$ , so that  $v = \beta l_c$ . In the penetration phase, it is easily shown that the value of  $\beta$  must be determined from  $Y_1^c / (\beta \rho_j) = (\dot{x}_2 - \dot{x}_1) / (1/l)$ . During the jet penetration, the rear of the jet is moving faster than the front as the whole jet decelerates.



The Bernouilli equation applied at the jet-target interface is

$$\frac{1}{2} \rho_j \dot{x}_2^2 + Y_2 = \frac{1}{2} \rho_t \dot{x}_t^2 + Y_t, \quad (24)$$

which accounts for the dynamic yield strength of the target. The target material of density  $\rho_t$  has a penetration rate  $\dot{x}_t$  given by

$$\dot{x}_t = \left( \frac{\rho_j}{\rho_t} \right)^{1/2} \dot{x}_2, \quad (25)$$

if the strengths in Eq. (24) are neglected. The penetration velocity for a decelerating jet, using  $\dot{x}_2 = V + \dot{l}/2$  becomes

$$\dot{x}_t(t) = \left( \frac{\rho_j}{\rho_t} \right)^{1/2} \left[ \beta l_c(t) - \frac{Y_1}{2 \beta \rho_j l_c(t)} \right]. \quad (26)$$

The penetration distance as a function of time is

$$P(t) = \int_0^t \dot{x}_t(t) dt, \quad (27)$$

which upon integration becomes

$$P(t) = \left( \frac{\rho_j}{\rho_t} \right)^{1/2} \left\{ \frac{\beta^2 \rho_j}{3 Y_1} [l_0^3 - l_c^3(t)] + \frac{1}{2} [l_c(t) - l_0] \right\}, \quad (28)$$

and satisfies  $P(0) = 0$ , zero penetration at the initial time. Maximum penetration of a semi-infinite target follows from the expression, Eq. (28), when the length of the metal jet is depleted. Therefore,

$$P_{max} = l_0 \sqrt{\frac{\rho_j}{\rho_t}} \left( \frac{\beta^2 \rho_j l_0^2}{3Y_t} - \frac{1}{2} \right). \quad (29)$$

It seems that the strength of the target is not directly connected with the penetration distance. However, that is due only to its neglect by utilizing the approximate expression, Eq. (25). During the penetration process, the jet is depleted from tip to tail until the primary penetration process is completed. A residual secondary penetration process occurs due to the fact that the kinetic energy imparted to the target by the jet must be dissipated.

The energy conservation in a shaped charge jet penetration process is of interest. The incident kinetic energy of a penetrating jet is equal to the sum of the plastic work done plus the remaining kinetic energy of the jet plus the outgoing kinetic energies of the jet and target material.

We construct a model to calculate the plastic work done in forming a paraboloidal shaped cavity as shown in Fig. 3. The plastic work performed by the internal stresses  $\sigma^{ij}$  on an element of volume is

$$dW = \sigma^{ij} \frac{de_{ij}}{dt} dt dz, \quad (30)$$

where the strain rate is related to the derivatives of the velocity components by

$$\dot{e}_{ij} = \frac{1}{2}(v_{i,j} + v_{j,i}) \quad . \quad (31)$$

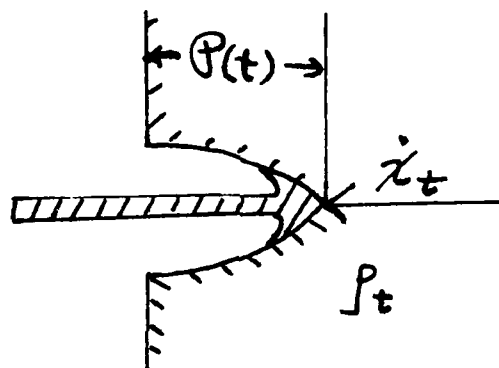


FIG. 3 Hydrodynamic Penetration of Target

The stress tensor  $\sigma^{ij}$  is taken as constant in the form

$$\sigma^{ij} = -P_t g^{ij} \quad . \quad (32)$$

A parabolic penetration boundary with azimuthal symmetry may be described by the parabola  $y^2 = ax$ , where  $a$  is an adjustable parameter.

Setting  $\vec{v} = \hat{i}\dot{x} + \hat{j}\dot{y}$  along with  $\dot{x} = \dot{x}_t$ , it follows that the strain rate is given by the divergence of the velocity field as

$$\nabla \cdot \vec{v} = - \frac{a \dot{x}_t}{2y^2} \quad . \quad (33)$$

Writing the volume element as  $d\tau = \pi y^2 dx$ , it is possible to express the plastic work done as

$$W = \frac{1}{2} a \pi Y_t \rho_{max}^2 \quad . \quad (34)$$

A hypervelocity copper jet of original length  $l_0 = 30$  cm and area  $A = 0.6$  cm<sup>2</sup>, impacting at 6 mm/ $\mu$ sec on an iron target, delivers a kinetic energy of approximately 5 M joules. Out of this total amount of incident kinetic energy, part of it goes into the energy necessary to do the plastic work, Eq. (34), and the remaining energy is connected with the kinetic energies of the outgoing target and jet material.

A shaped charge jet with high tip velocity and a much lower tail speed causes the jet to stretch to a considerable length at the large standoff distance. The jet length necessary for deep penetration is limited by particulation; the jet breaks up into segments. Methods of delaying the particulation process include studies by hydrocode simulation, with both one- and two-dimensional codes, and empirical formulas.

## V. RECOMMENDATIONS

The metallic jet has characteristics of slug formation, variable cross-sectional area, breakup and waver. In a true sense, these items would influence the discussion of further work. The penetration process is in general a very difficult problem. Calculations usually proceed to estimate the volume of the cavity produced, and to account for energy division into strain energy and kinetic energy. Targets of both finite and semi-infinite width are of interest.

It is recommended by the author that the analysis of a shaped charge jet be extended to include the following items:

- a. Particulation of a jet which is a jet breakup phenomenon.
- b. Elaboration of the penetration model presented in this work in regard to a rigorous treatment of viscous plastic flow. Energy dissipation of the jet and particulation during the penetration phase are of special interest.

## REFERENCES

Birckhoff, G., D. P. MacDougall, E. M. Pugh and G. I. Taylor,  
Journal of Applied Physics 19, P. 563 (1948).

Pack, D. C., and W. M. Evans, Proceedings of Physical Society,  
(London) 64, P. 298 (1951).

Backman, M. E., and W. Goldsmith, International Journal-  
of Engineering and Science 16, PP. 1-99 (1978).

Eichelberger, R. J. and E. M. Pugh, Journal of Applied Physics 23,  
P. 537 (1952).

Pugh, E. M., R. J. Eichelberger and N. J. Rostoker,  
Journal of Applied Physics 23, (1952).

Di Persio R., J. Simon and T. H. Martin, "A Study of Jets from  
Scaled Conical Shaped Charge Liners,"  
Ballistic Research Laboratories Report  
No. 1298 (August, 1960).

Held, M., "Propellants, Explosives, Pyrotechnics" 10, P. 125  
(1985).

Cook, M. A., Journal of Applied Physics 30, P. 725 (1959)

Eichelberger, Journal of Applied Physics 27, P. 63 (1956).

Singh, S., Proceedings of Physical Society, (London) 70, P. 867 (1957).

Anderson, C. E. Jr., "A Short Course on Penetration Mechanics,"  
Southwest Research Institute (1986).

Abrahamson, G. R. and J. N. Goodier, Journal of Applied Physics 34,  
P. 195 (1963).

Sokolnikoff, I. S., Tensor Analysis-Theory and Applications to  
Geometry and Mechanics of Continua, New York, John Wiley & Sons, Inc.,  
(1964).

Sokolnikoff, I. S., Mathematical Theory of Elasticity, New York,  
McGraw-Hill Book Company, (1946).

Chou, P. C. and W. J. Flis, "Propellants, Explosives, Pyrotechnics" 11,  
PP. 99-114 (1986).

1987 USAF-UES SUMMER FACULTY RESEARCH PROGRAM /  
GRADUATE STUDENT SUMMER SUPPORT PROGRAM

Sponsored by the

AIR FORCE OFFICE OF SCIENTIFIC RESEARCH

Conducted by the

Universal Energy Systems, Inc.

FINAL REPORT

Reactions of Nitryl Chloride with Aromatic Substrates  
in Chloroaluminate Melts

Prepared by : Charles M. Bump, Ph. D.  
Academic Rank : Assistant Professor  
Department and : Department of Chemistry  
University : Hampton University  
Research Location: FJSRL/NC  
US Air Force Academy  
Colorado Springs, CO 80840  
USAF Researcher : Dr. John S. Wilkes  
Date : 27 August 1987  
Contract No. : F49620-85-C-0013



Reactions of Nitryl Chloride with Aromatic Substrates  
in Chloroaluminate Melts

by

Charles M. Bump

ABSTRACT

An ionic liquid composed of 0.667 mole fraction aluminum chloride and 0.333 mole fraction 1-methyl-3-ethyl imidazolium chloride was employed as the solvent for electrophilic aromatic nitration using nitryl chloride ( $\text{NO}_2\text{Cl}$ ). Nitrations of toluene, benzene, chlorobenzene, acetophenone, and nitrobenzene were studied. In addition, the reaction of nitryl chloride with methylethylimidazolium chloride and with aluminum chloride was investigated. Even weakly deactivated aromatic substrates were nitrated in this study. Only nitrobenzene was not successfully nitrated. The imidazolium chloride moiety itself reacted with nitryl chloride to give chloronitromethylimidazoles on hydrolysis. Aluminum chloride reacted with the nitryl chloride to give a compound which may be nitronium tetrachloroaluminate ( $\text{NO}_2^+ \text{AlCl}_4^-$ ). This compound successfully nitrated benzene.

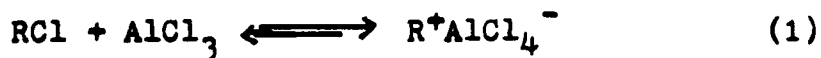
### ACKNOWLEDGEMENTS

I would like to thank the Air Force Systems Command and the Air Force Office of Scientific Research for the sponsorship of this research. I would also like to thank Universal Energy Systems, Inc. for actively calling my attention to this program by their on-campus visit to Hampton University.

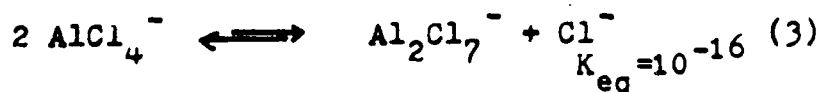
It is a pleasure to recognize the help of several individuals at the Frank J. Seiler Research Lab who made my work easier and more enjoyable: Dr. John S. Wilkes and Major Steve Lander for their encouragement and direction, especially in the early stages of this project, Mr. J. Lloyd Pflug for his gc/mass spec analysis of several samples, Dr. John Rovang for running Al-27 magnetic resonance spectra, Mrs. Lisa Cooke for showing me the reaction and analysis techniques, Mr. Steve Keeley for showing me how to prepare the ionic liquid used as the solvent for my reactions, and my colleagues Dr. Norman E. Heimer, Dr. Albert Hershberg, and Dr. Maurice Neveu for their helpful discussions throughout the research period.

## I INTRODUCTION

Aluminum chloride / 1-methyl-3-ethylimidazolium chloride mixtures are ionic liquids at room temperature for apparent mole fractions of aluminum chloride from 0.333 to 0.667. Once the liquid is prepared, there is no longer free aluminum chloride present - rather it is converted to mixtures of tetrachloroaluminate ( $\text{AlCl}_4^-$ ) and heptachloroaluminate ( $\text{Al}_2\text{Cl}_7^-$ ). The precise amount of these species present depends on the relative amount of aluminum chloride added to methylethylimidazolium chloride. The following reactions describe the relevant reaction chemistry:

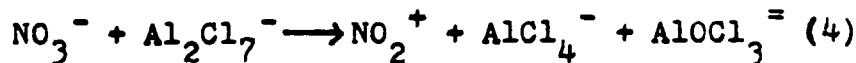


From equations (1) and (2) it is intuitively clear that a ratio of two moles of aluminum chloride per mole imidazolium chloride (ie. 0.667 mole fraction aluminum chloride) results in the aluminum being present almost exclusively as heptachloroaluminate. In addition to equations (1) and (2) there is an equilibrium shown below:

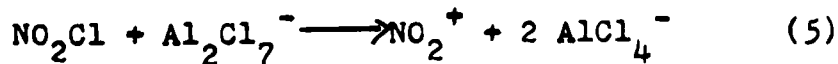


Equilibrium (3) is analagous to the dissociation of water. A wide variety of Lewis acidity is available for these

ionic liquids. These ionic liquids, or molten salts, have been studied as battery electrolytes in on-going research at the Seiler Lab. There is also an interest in using the molten salt as a solvent/catalyst for electrophilic reactions - where the Lewis acidity of the reaction medium can be carefully controlled. Friedel-Crafts type electrophilic substitution of aromatic compounds represents an obvious reaction that may be amenable to the use of ionic liquids as solvent. Alkylations and acylations have already been studied in this medium. Nitration reactions are particularly interesting from the point of view of producing "high energy compounds" for use as fuels and explosives. Nitrations of aromatic compounds have been carried out using nitrate salts such as sodium or potassium nitrate as the nitrating agent. However, the ionic liquid is consumed by the formation of the nitronium ion rather than serving as an inert solvent/catalyst.



It was hoped that nitryl chloride ( $\text{NO}_2\text{Cl}$ ) would not follow that pattern.



The purpose of my work was, then, to investigate the nitration of aromatic compounds using nitryl chloride.

If time permitted, nitrosyl chloride ( $\text{NOCl}$ ) and acetyl nitrate ( $\text{CH}_3\text{CO}_2\text{NO}_2$ ) were also to be examined as nitrating agents in the molten salt medium.

My background is in a combination of organic synthesis and electroanalytical chemistry. I have synthesized the "Picket Fence Porphyrin" myoglobin model of J. P. Collman et al. and studied the electron transfer properties of the metal-free porphyrin ligand by polarography, cyclic voltammetry, and controlled potential coulometry. My experience in both synthetic chemistry and electrochemistry resulted in my assignment to work on organic reactions in room temperature molten salts.

## II OBJECTIVES OF THE RESEARCH EFFORT

The successful nitration of aromatic compounds by the nitrate ion in an ionic liquid of apparent mole fraction 0.667 aluminum chloride added to methylethylimidazolium chloride had the side effect of consuming the melt as reagent rather than allowing it to serve as a solvent/catalyst. Clearly, dinitration (or trinitration) to more energetic material could not be achieved in a "one pot reaction" merely by adding more nitrating agent. The ultimate goal of the nitration research was to produce trinitrobenzene from benzene by only adding more nitrating agent to introduce successive nitro groups.

My goal at the outset of the 1987 Summer Faculty

Research Program (SFRP) was to examine other nitrating agents that might permit the melt to fill the role of solvent/catalyst in the production of nitroaromatic compounds. Specifically, I would look at nitryl chloride, nitrosyl chloride, and acetyl nitrate as sources of the nitro group. Further, I was to determine the range of aromatic compounds that could be successfully nitrated by each system. On the discovery that nitryl chloride reacted with the melt, I undertook to determine the nature of that reaction by combining nitryl chloride with the melt and with its individual components.

My investigation of nitryl chloride took the entire research period, so it was planned that I continue my investigation at Hampton University under the Research Initiation Program.

### III THE NITRATION OF AROMATIC COMPOUNDS USING NITRYL CHLORIDE IN CHLOROALUMINATE MELTS

Nitryl chloride was generated following the procedure of Kaplan and Shechter<sup>1</sup>. Since it is a gas at room temperature (B.P. =  $-16^{\circ}$  C), nitryl chloride was collected in a dry ice/acetone bath maintained at  $-80^{\circ}$ . Four 50 ml pear shaped flasks were connected to a cow fraction cutter to allow simultaneous collection of nitryl chloride in all flasks. Approximately 0.5 ml of pale yellow liquid nitryl chloride was obtained in each flask. The flasks

were then fitted with gas inlet tubes, the stopcocks open to the atmosphere, and the flasks allowed to warm to ambient temperature. The stopcocks were then closed, sealing approximately one millimole of nitryl chloride vapor in the flask. The exact amount was determined by taring the flasks before the nitryl chloride was generated. Nitryl chloride was stored overnight in a freezer at  $-20^{\circ}$  overnight prior to use.

The aluminum chloride/methylethylimidazolium chloride melt was prepared in an oxygen free, anhydrous glove box by adding 6.46g of aluminum chloride very slowly to 3.54g of 1-methyl-3-ethylimidazolium chloride. The resulting 10.00g of melt had an apparent mole fraction of aluminum chloride of 0.667. A measured amount of melt was added to a glass ampoule and stoppered inside the glove box. The aromatic compound was introduced to the melt via a one hundred microliter syringe outside of the glove box just prior to the start of the reaction.

The flask containing nitryl chloride was cooled in a dry ice/acetone bath to  $-80^{\circ}$  and a magnetic stirring bar plus the melt containing the aromatic substrate were added. The reaction mixture was held at  $-30^{\circ}$  for ten minutes and then allowed to warm to ambient temperature.

The ratio of aromatic : melt : nitrating agent was maintained throughout this study as 1 : 1.5 : 1.5 .

Reactions were quenched with water after three hours

and brought to pH 10 by 6N KOH. An internal standard of bromobenzene or m-xylene was added and the alkaline solution extracted with ether. The ether was diluted to 5.00 ml and a fifty microliter aliquot of that solution diluted again to 5.00 ml. In that manner, an ether solution nearly millimolar in total aromatic concentration was produced. That solution was injected into a gas chromatograph for identification and quantification of reaction products. Product identification was made on the basis of retention times of authentic compounds and gc/mass spectra. Quantification was made on the basis of response factors of authentic compounds with respect to an internal standard<sup>2</sup>.

Results are summarized on the following page. All reactions were performed in duplicate. Gas chromatographic assays represent the average of three determinations. From the tabulated results, two conclusions are self-evident: 1) that if nitryl chloride was added to the melt before benzene was introduced, a reaction between nitryl chloride and the melt took place which precluded the nitration of benzene, and 2) that if the aromatic substrate was dissolved in the melt and then combined with nitryl chloride, only the most highly deactivated compound, nitrobenzene, failed to give a nitrated product. For both nitrobenzene and acetophenone, the nitration of the aromatic substrate must be in competition with the reaction of nitryl chloride and



NO-A191 203

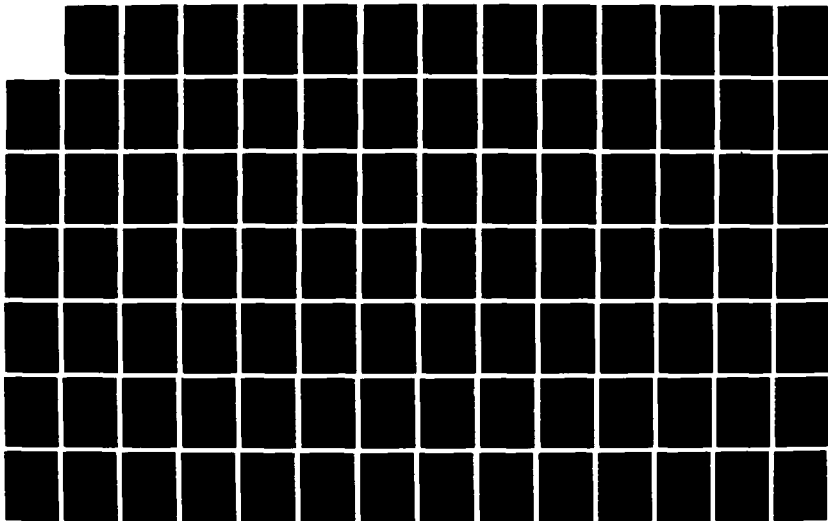
UNITED STATES AIR FORCE SUMNER FACULTY RESEARCH PROGRAM  
(1987) PROGRAM TE. (U) UNIVERSAL ENERGY SYSTEMS INC  
DAYTON OH R C DARRAN ET AL. DEC 87 AFOSR-TR-88-8212  
F49620-85-C-0013

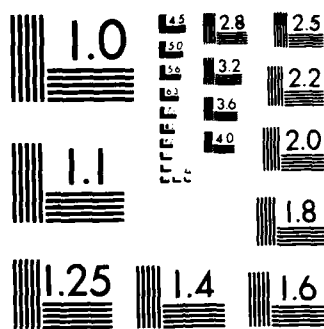
6/11

UNCLASSIFIED

F/G 5/1

NL





MICROCOPY RESOLUTION TEST CHART  
NATIONAL BUREAU OF STANDARDS 1963 A

# NITRATION OF AROMATIC COMPOUNDS WITH NO<sub>2</sub>Cl

reaction	product	% yield of product		
		trial 1	2	avg.
benzene + melt, then NO <sub>2</sub> Cl	benzene	0.0	18.1	9.1
	dichloro benzene	11.5	10.8	11.2
	nitro benzene	44.2	44.9	44.6
NO <sub>2</sub> Cl + melt, then benzene	benzene	62.5	51.7	57.1
	chloro benzene	0.0	28.7	14.4
	nitro benzene	0.0	0.0	0.0
toluene + melt, then NO <sub>2</sub> Cl	toluene	7.7	15.6	11.7
	o-chloro toluene	*	19.5	19.5
	o-nitro toluene	17.1	11.9	14.5
	p-nitro toluene	17.6	12.2	14.9
	total o,p nitro toluenes	34.7	24.1	29.2
	o/p ratio	.97	.98	.98
chloro benzene + melt, then NO <sub>2</sub> Cl	chloro benzene	31.4	0.0	15.7
	dichloro benzene	6.6	14.0	10.3
	chloro nitro benzene	45.3	35.5	40.4
acetophenone + melt, then NO <sub>2</sub> Cl	aceto phenone	66.5	56.5	61.5
	m-nitro aceto phenone	4.2	6.5	5.4
nitro benzene + melt, then NO <sub>2</sub> Cl	nitro benzene	82.7	46.2	64.5
	m-dinitro benzene	0.0	0.0	0.0

the melt. In the case of nitrobenzene, the reaction with the melt is apparently the more favored one, while for acetophenone the deactivated aromatic can win that competition at least part of the time. The nitration of acetophenone, albeit in poor yield, is especially significant since heretofore nitryl chloride has not been successful in nitrating that compound in the more traditional organic solvents<sup>3</sup>.

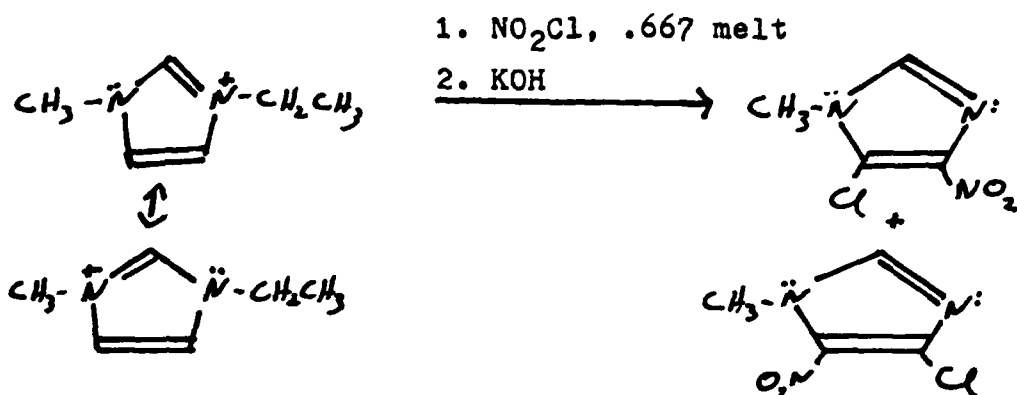
The o/p ratio of the nitrotoluene isomers formed during the nitration of toluene is appreciably lower than that usually associated with nitration in mixed nitric and sulfuric acid<sup>4</sup>. That clearly suggests that the free nitronium ion ( $\text{NO}_2^+$ ) is NOT the active nitrating species in the molten salt system. In reactions with nitryl chloride and titanium tetrachloride or aluminum trichloride in more traditional organic solvents, Olah proposed that the active nitrating agent is a complex between the nitryl chloride and the Lewis acid<sup>5</sup>. In the present study, the nearly even distribution of o and p nitrotoluenes suggests that the active nitrating agent is sterically hindered against attack at the o position - a suggestion which is not inconsistent with Olah's complex.

#### IV THE REACTION OF NITRYL CHLORIDE WITH 1-METHYL-3-ETHYLIMIDAZOLIUM CHLORIDE

The failure of benzene to nitrate on combination with the melt and nitryl chloride that had stirred alone for three hours gave preliminary evidence that a reaction between them must be consuming the nitryl chloride.

A larger than usual amount of the melt and nitryl chloride was allowed to react for three hours before quenching the reaction with water and bringing the pH to 10 with 6N KOH. Addition of concentrated HCl to pH 7 resulted in the formation of the gelatinous  $\text{Al}(\text{OH})_3$  which was removed by filtration through a sintered glass fritted funnel. Evaporation of the filtrate to dryness produced a yellow oil and white crystals presumed to be KCl. Acetonitrile was used to selectively dissolve the yellow oil and leave behind the KCl. The acetonitrile solution was then dried over anhydrous magnesium sulfate and the solvent removed on a rotory evaporator.

The resulting yellow oil had an infrared spectrum similar to that of 5-chloro-1-methyl-4-nitroimidazole in the Sadtler Library of Infrared Spectra. Subsequent gc/mass spec analysis of another sample of the reaction product indicated the presence of both 5-chloro-1-methyl-4-nitroimidazole and its isomer 4-chloro-1-methyl-5-nitroimidazole. This reaction may be formulated schematically as:



This reaction is analogous to the one observed between the melt and elemental chlorine<sup>6</sup>. The parallel with chlorine extends to the addition reaction of these compounds. Nitryl chloride adds to cyclohexene to give 1-chloro-2-nitrocyclohexane<sup>7</sup>.

It is also interesting to note that in the present study, the ethyl groups of the imidazolium chloride are lost preferentially by the action of KOH.

A reaction takes place with methylethylimidazolium chloride alone and nitryl chloride even at  $-80^\circ$ . The reaction mixture initially turns red with the evolution of heat. On standing, it becomes yellow and ultimately turns colorless. The product of that reaction has not been analyzed but it is presumed to follow the pattern established by the reaction of nitryl chloride with the whole melt.

#### V REACTION OF NITRYL CHLORIDE WITH ALUMINUM CHLORIDE

In order to completely test the aluminum chloride/methylethylimidazolium chloride melt for reaction with

nitryl chloride, the reaction of aluminum chloride with nitryl chloride was also studied. Literature precedent for a reaction was not encouraging. Only sulfur trioxide gave a Lewis acid-Lewis base reaction with nitryl chloride. All other Lewis acids suffered oxidation-reduction reactions or no reaction at all was observed<sup>8</sup>.

In our hands, solid aluminum chloride showed little evidence of reaction with nitryl chloride at  $-80^{\circ}$ . When the reaction mixture was allowed to warm to ambient temperature overnight, the white aluminum chloride turned yellow. Aluminum-27 nmr measurements in acetonitrile and in nitromethane established the presence of tetrachloroaluminate and aluminum chloride by their respective chemical shifts relative to  $\text{Al}(\text{H}_2\text{O})_6^{+3}$ <sup>9</sup>. From the area under the peaks, 80% of the aluminum present was  $\text{AlCl}_4^-$  and the remaining 20%  $\text{AlCl}_3$ . Vacuum sublimation of a sample of this yellow powder resulted in a yellowish white solid with a loss of 20% of its starting mass. Thus the 80/20 distribution of tetrachloroaluminate and aluminum chloride has been obtained by two independent means.

The identity of the cation for the tetrachloroaluminate was probed by UV-visible spectroscopy. The nitronium ion spectrum was generated by mixing fuming nitric and sulfuric acids and also by using commercially available

nitronium tetrafluoroborate. ( $\text{NO}_2^+\text{BF}_4^-$ ). The spectrum of the yellowish-white powder in acetonitrile and in tetramethylene sulfone was similar to, but not identical with that of the nitronium ion. Presumably the nitronium ion is contaminated with another species - perhaps  $\text{NO}^+$ .

The unpurified yellow powder was allowed to react with both benzene and with nitrobenzene on a qualitative basis. Benzene was converted to nitrobenzene and a very small amount of nitrobenzene was changed to dinitrobenzene.

#### VI CONCLUSIONS / RECOMMENDATIONS

- A The usefulness of nitryl chloride as a nitrating agent in aluminum chloride/methylethylimidazolium chloride melts is diminished by the reaction of nitryl chloride with the imidazolium chloride moiety.
- B The product of the reaction between nitryl chloride and aluminum chloride has the capability of being an effective nitrating agent - especially if it is  $\text{NO}_2^+\text{AlCl}_4^-$ . Then, the addition of a stoichiometric amount of aluminum chloride would re-establish heptachloroaluminate as the exclusive anion in the reaction mixture. Both the identity and the reactivity of this compound should be further examined.
- C A competitive nitration between toluene and benzene with nitryl chloride in the melt was attempted. In



order for the analysis of such data to be useful, the products must be limited to nitration or chlorination. In our hands, 45 minutes was sufficient time for both nitration and chlorination of the same molecule, thereby making the mathematical evaluation of the relative rates of nitration prohibitively difficult. Since nitrobenzene, chlorobenzene, nitrotoluene, and chlorotoluene as well as the unreacted aromatics are all reducible, it would be desirable to monitor their concentrations electrochemically in situ for the competitive nitration reaction.

- D The ten week period expired before the nitrating capability of nitrosyl chloride and of acetyl nitrate could be explored. The suitability of these compounds as nitrating agents should be investigated.
- E The results obtained here represent duplicate experiments. They need to be repeated to provide data suitable for publication in refereed journals.
- F The ratio of aromatic substrate : melt : nitrating agent has been kept at 1 : 1.5 : 1.5 . No effort has been made to determine if this is an optimum ratio. In fact, acetophenone forms a complex with aluminum chloride that effectively lowers the Lewis acidity of the melt and hence its reactivity. With more of the ionic liquid present, such a

reaction would have a smaller effect on the Lewis acidity of the melt and its reactivity.

## REFERENCES

1. Ralph Kaplan and Harold Shechter, *Inorganic Synthesis*, (1953), 4, 52.
2. Mary A. Kaiser and Frederick J. Debbrecht in Modern Practice of Gas Chromatography, ed. Robert L. Grob, Wiley Interscience, New York, 1977, pp.199-202.
3. Charles C. Price and Carlton A. Sears, *J. Amer. Chem. Soc.*, (1953), 75, 3276.
- 4a. P. B. D. de la Mare and J. H. Ridd, Aromatic Substitution: Nitration and Halogenation, Academic Press, New York, 1959.
- b. William M. Weaver in The Chemistry of the Nitro and Nitroso Groups, ed. Henry Feuer, part 2, Wiley Interscience, New York, 1970, pp. 1-49.
5. George A. Olah, Industrial and Laboratory Nitrations, ACS Symposium Series 22, American Chemical Society, Washington, DC, 1976, p. 1 cited in K. Schofield, Aromatic Nitration, Cambridge University Press, New York, 1980, p. 93.
6. Charles C. Price and Carlton A. Sears, *J. Amer. Chem. Soc.*, (1953), 75, 3277.
7. J. A. Boon, S. W. Lander, J. A. Levisky, J. Lloyd Pflug, Lisa M. Skrzynecki-Cooke, and John S. Wilkes, *Proc. Joint Int. Symp. on Molten Salts*, October 1987.
8. H. H. Batey and H. H. Sisler, *J. Amer. Chem. Soc.*,

(1952), 74, 3408.

9. J. J. Delpuech in NMR of Newly Accessible Nuclei, vol. 2,  
Chemically and Biochemically Important Elements,  
ed. Pierre Laszlo, Academic Press, New York, 1983,  
pp. 153-195.

1987 USAF-UES SUMMER FACULTY RESEARCH PROGRAM/

Sponsored by the  
AIR FORCE OFFICE OF SCIENTIFIC RESEARCH

Conducted by the  
Universal Energy Systems, Inc

FINAL REPORT

CHEMISTRY FOR THE SPACE PROGRAM

Prepared by:	Allan R. Burkett
Academic Rank:	Associate Professor of Chemistry
Department and	Division of Natural Sciences
University:	Dillard University
Research Location:	Edwards Air Force Base Air Force Astronautics Laboratory/CX Applied Research and Energy Storage
USAF Researcher:	Dr. Stephen Rodgers
Date:	August, 1987
Contract No:	F49620-85-C-0013

## CHEMISTRY FOR THE SPACE PROGRAM

by

Allan R. Burkett

### ABSTRACT

This report consists of a review of what has been done in four broadly defined areas of the space program as well as some speculation on likely productive lines of work for future researchers. The areas reviewed are: (1) Interaction of Atmospheric Free Radicals with the Space Station, (2) Hiding a Craft from IR Detectors, (3) Solar Energy Trapping, and (4) Regeneration of Necessities. The most promising lines of research are in the use of metallopolymers for energy trapping and electrode coatings, and in the use of transition metal complexes in reduction of carbon dioxide.

### ACKNOWLEDGMENTS

I would like to acknowledge the Air Force Systems Command, Air Force Office of Scientific Research, and Edwards Air Force Base for sponsoring this project. Specific accolades must go to Dr. Stephen Rodgers, Lt. Walter Lauderdale, Jolain Lamb, and Louis Dee for their valuable assistance in this work.

## CHEMISTRY FOR THE SPACE PROGRAM

### I. INTRODUCTION

The Astronautics Laboratory at Edwards Air Force Base formally came into existence in March, 1987. Previously it was designated the Rocket Propulsion Laboratory. The change in name reflects a broadened research interests into all areas of astronautics. The particular division to which I have been assigned (AFAL/CX) is the applied research and energy storage component of the laboratory.

My research interests have been in the area of inorganic photochemistry, with emphasis on transition metal chemistry and chemistry of M-M bonded systems. This compliments the research group I am working with, as the group contains a physical organic chemist, an organic chemist, a spectroscopist, and a theoretician.

### II. OBJECTIVES OF THE RESEARCH EFFORT

The Federal Government and its agencies are planning to build a manned space station in the next 20 years or so.<sup>1,2</sup> There is considerable basic chemical research to be done prior to this undertaking that can improve both living conditions and survivability of the astronauts manning such a craft. The primary objective of my effort is to identify specific research projects for future investigators.

Some areas initially identified as having potential for fruitful investigation were: degradation of construction materials by exoatmospheric free radicals, recycling of carbon dioxide and regeneration of necessities such  $O_2$  and  $H_2O$ , trapping solar energy chemically and storing it chemically for reuse, and hiding a craft from infrared detection. The overall aims of the project are to compile what has been done in these



areas and to lay the foundation for fundamental research.

### III. Interaction of Atmospheric Free Radicals with the Space Station

One aspect of damage to a space craft in relatively close earth orbit is the chemical action of free radicals on exposed surfaces for long periods of time. The 20-30 year expected life of a space station provides more than enough time for exoatmospheric free radicals to damage the craft.

Table I<sup>a</sup>  
CONCENTRATION OF GASES AT 500 Km

Cmpd	Atoms/m <sup>3</sup>	Moles/m <sup>3</sup>
N <sub>2</sub>	2 E11	3 E-13
O <sub>2</sub>	4 E09	7 E-15
O	2 E13	3 E-11
H	8 E10	1 E-13
He	3 E12	5 E-12

(a) United States Standard Atmosphere, NASA, Washington, D.C.  
Oct 1976 at 500 Km

Only oxygen atoms have significant exoatmospheric concentration at the expected altitude of 300-500 Km (Table I). Flux densities for atomic oxygen have been estimated<sup>3</sup> at  $10^{17} - 10^{19}$  atoms m<sup>-1</sup> sec<sup>-1</sup>. This implies  $2 \times 10^{-7}$  moles of external material impacted every second or about 5 moles per year on exposed surfaces. This is not a major concern for the main structure of the space station because reaction rates are smaller than the collision frequency.

Results from experiments<sup>4-6</sup> done on the fifth and eighth shuttle flights have shown that actual thickness loss is material dependent. Materials containing carbon, hydrogen, oxygen, or nitrogen have relatively high reaction rates. Various perfluorinated and silicone polymers are less reactive by a factor of approximately 50. Metals, with the excep-

tion of silver and osmium, are relatively stable from a macroscopic viewpoint.<sup>3</sup>

Projections from the main station, particularly solar power systems, will require protection from exoatmospheric oxygen. Two types of solar power systems have been given priority.<sup>7</sup> The first is a solar dynamic system which collects solar radiation in concentrators, and this energy is subsequently used to drive heat engines that generate electrical power. The second is a solar voltaic system which directly converts solar energy to electrical power.

The solar dynamic system has reflector and absorber surfaces. The performance of these surfaces is extremely sensitive to changes in their optics, and degradation of optical surfaces by atomic oxygen over the lifetime of a space station can be expected. Reflectors coated with silver are particularly susceptible to attack. They must be overcoated with a material (magnesium fluoride is currently used<sup>7</sup>) thick enough to prevent diffusion of atomic oxygen and protect the silver. Solar voltaic systems extensively use thin films as solar cell supports and in addition use silver or copper foil to connect the solar cells to the electrical network.<sup>8</sup>

It appears that the extensive use of silver metal and thin films in solar power systems make them particularly vulnerable to attack by atomic oxygen. The development of surface protective coatings for these systems appears to be the most efficient way to solve the problem.

#### IV. Hiding a Craft from IR Detectors

One particular point about space satellites is that they are relatively easy to detect in the IR region of the electromagnetic spectrum, particularly when detection devices are located in other satellites.

From a military viewpoint, it is useful to be able to 'hide' from IR detection. Two concepts that can achieve this are: (1) Cooling the surface of the craft by pumping the surface heat into a heat sink, then radiating the energy into space at a slow rate, or radiate away from detection devices, or both. (2) Surrounding the craft in an IR absorbing envelope.

The difficulty in drawing heat from the surface of the craft to some central location, then cooling the 'hot spot', is the amount of material required to perform the task. Assume 500 g of ice is heated from  $-250^{\circ}\text{C}$  (23 K)  $500^{\circ}\text{C}$  (773 K).

Table II(b)  
Physical Constants for Water

Temp deg C	Specific Heat cal/g/deg	Phase	Enthalpies cal/g
-250 to -180	.146		
-188 to -78	.285	$\text{H}_2\text{O}(\text{s})$	Heat of fusion 79.9
-78 to -18	.463		
-11 to -2	.490	$\text{H}_2\text{O}(\text{l})$	Heat of vap 540
100 to 500(c)	.5		

(b) Handbook of Chemistry and Physics, 49th Edition, The Chemical Rubber Company, Cleveland Ohio

(c) A composite value for a temperature range from 100 -  $500^{\circ}\text{C}$  and pressures from 1 to 12 atmospheres.

Table III  
Heat absorbed on heating water from  $-250 - 500^{\circ}\text{C}$

Temperature Range ( $^{\circ}\text{C}$ ) or phase transition	Specific heat or enthalpy ( $\text{cal g}^{-1}$ )		
-250 - -188	.144 x 62 deg	x 500 g	= 4256 cal
-188 - -78	.285 x 110 deg	x 500 g	= 15675 cal
-78 - -18	.436 x 60 deg	x 500 g	= 13890 cal
-18 - 0	.490 x 18 deg	x 500 g	= 4410 cal
$0^{\circ}(\text{s}) - 0^{\circ}(\text{l})$	79.7 x 500 g		= 39850 cal
0 - 100	1.00 x 100 deg	x 500 g	= 50000 cal
100(l) - 100(g)	540 x 500 g		= 270000 cal
100(g) - 500(g)	.5 x 400 deg	x 500 g	= 100000 cal
Total	500000 cal		

Using the data in Table II we find that only 500 Kcal of energy will be absorbed by the ice/water/steam under these conditions (Table III).

This absorbs too little energy to be practical. Using other materials, e.g. ethylene glycol, will not materially improve the performance because the amount of heat absorbed per unit mass will always be impractically low.

Another idea along similar lines is to use a reversible, entropy driven reaction to remove heat from the surface of a craft. Spontaneous, endothermic reactions must evolve gases or convert starting materials into liquid solutions to absorb enough heat to be useful. Reactions of this type would not be readily reversible and could be used only once. Furthermore, from the calculation above, it is clear that circa 500g of chemicals cannot absorb enough energy from a craft weighing two or three tons to have any reasonable chance of successfully cooling the surface.

However, a chemical system is possible if it is deemed desirable to hide a craft temporarily from IR detectors. For the purpose of this discussion, it is assumed that a orbiting satellite is a cube 10 m to a side and behaves as a blackbody radiator at about 300 K. The essential properties of such an emitter<sup>9</sup> are that the spectral radiant exitance is between 2-8  $\mu\text{m}$  and that the energy output is between  $1 \times 10^{-3}$  and  $8 \times 10^{-13} \text{ J cm}^{-2} \text{ sec}^{-1}$ .

A mixture of water, carbon dioxide, (waste products from the space station) and methanol almost completely blanket this spectral range. The extinction coefficients at the various wavelengths are given in Table IV.

To achieve an optical density of 3.0 (.1 %T), it is necessary to have about 15 moles of each material between the craft and the detector. (From Beer's Law,  $bc = 3/\text{extinction coefficient}$ , or  $bc = 15$  assuming the extinction coefficient  $= 20 \text{ M}^{-1} \text{ cm}^{-1}$ . Declare an arbitrary volume of  $10 \text{ m}^2$  by 1 cm  $= 100 \text{ L}$ ;  $100 \text{ L} \times .15 \text{ M} = 15 \text{ mole}$ . The 15 mole of substance does not, of course have to be confined to the 1 cm path length, but can

occupy any distance between the craft and the detector.) This is essentially pound quantities of each substance.

The delivery system can be fairly simple. The condensed phases of water, carbon dioxide, and methanol can be stored in a box. The box contains a lid that can be uncovered with automatic control devices. When used, the box will be positioned between the satellite and the detector. When the lid is opened, exposing a 'side' containing many pinholes, the condensed phases of the 'smoke screen' will evaporate. The gaseous molecules will escape through the pinholes with a translational vector pointed in the direction of the detector.

Table IV  
IR Extinction Coefficients for  $H_2O$ ,  $CO_2$ , and  $CH_3OH$

Compound	Wavelength ( $\mu m$ ) micrometer	extinction coefficient ( $M^{-1} cm^{-1}$ )	Source
$CO_2$	2.6	29	Sadtler Spectrum No. 4166P (gas)
	2.8	21	
	4.2	67	
	4.7	18	
$CH_3OH$	~3.6	25	Sadtler Spectrum No. 41665P (gas)
	~9.5-10	34	
$H_2O$	~5-7	5	Provided by L. Dee at AFAL/CX <sub>on</sub> a Nicole S5X at 4 $cm^{-1}$ resolution

#### V. Solar Energy Trapping

Most of the energy in solar radiation is confined to the visible and low energy UV portion of the spectrum.<sup>9,10</sup> Systems which absorb strongly in this range can be particularly useful for solar energy conversion.

The primary goal of chemists and engineers interested in solar energy conversion to date has been in the area of solar cells, and the need for ever more efficient solar cells will remain well into the next

century. It is, however, useful to look at other methods of trapping the energy. Recent studies have shown the practicality of using solar energy to generate chlorine free radicals in thermally excited states.<sup>11</sup> The energy return from recombination to  $\text{Cl}_2$  can be as high as 15% greater than the bond energy. The feasibility study demonstrated that the energy of bond formation plus the extra thermal energy can be usefully recovered to perform such functions as heat fuel for attitude jets.

Bis- $\pi$ -cyclopentadienyltricarbonylmolybdenum undergoes photochemical cleavage of the Mo-Mo bond in the visible portion of the electromagnetic spectrum to form  $n^5\text{-C}_5\text{H}_5\text{Mo(CO)}_3$  radicals.<sup>12,13</sup> Other M-M bonded systems have absorption bands in the visible region of the spectrum, and radical formation upon irradiation is typical behavior.<sup>14</sup>

Compounds like these have not been considered in the past for trapping and storing chemical energy, and the field is wide open for research. Several concepts in the area of metallopolymer are possible.

Metallopolymer are relatively new types of compounds.<sup>15-29</sup> These compounds exhibit a variety of interesting properties including: (1) Rectifying properties when bound to an electrode<sup>16,17</sup>, (2) Transient storage of photochemically produced oxidative and reductive equivalents,<sup>27,29</sup> (3) Uses in photoelectrodes<sup>20,22,24</sup>, and (4) Photosensitization of semiconductors.<sup>20</sup>

These advances lead to the idea of placing a M-M bonded system on or in a polymer system (See Figure 1). When such a system absorbs energy corresponding to the M-M bond, it will be possible to cleave this bond to form radicals. Previous work using specific polydentate ligands indicates that by carefully selecting the other ligands bonded to the metal, it should be possible to hold the two metal radical fragments away from each other and prevent recombination conformationally.<sup>30,31</sup> Recom-

bination at the desired time can then be effected either catalytically or thermally depending upon the relative thermodynamic and kinetic factors.

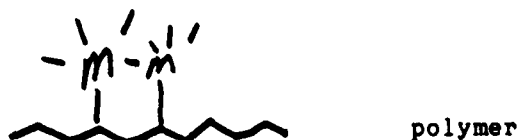


Figure 1  
A M-M bonded system linked to a polymer chain.

Another possibility is to use a M-M bond to cross link a polymer chain (Figure IIa). Entropy effects will tend to straighten out the chain upon cleavage of the M-M bond, preventing recombination by increasing the distance between metal atoms (Figure IIb). This type of system can also be useful if the M-M bond disproportionates into  $M^+$  and  $M^-$  fragments.

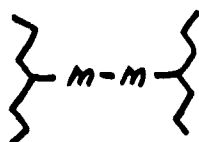


Figure II a



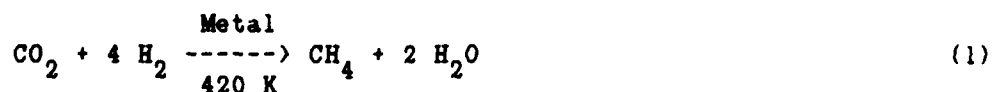
Figure II b

## VI. Regeneration of Necessities

A major problem in a closed system such as a space state is resupply of oxygen, water, food, etc. The more necessities that can be manufactured on board, the better. The major starting material for on board manufacture is  $CO_2$ . Each individual exhales 400 L - 800 L (18 - 36 mole) of carbon dioxide each day which must be removed from the breathing air. Solid amine resins have shown the ability to absorb  $CO_2$  at ambient temperatures and desorb  $CO_2$  upon heating.<sup>32</sup> This provides a convenient collection method.

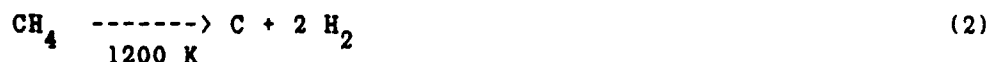
What follows is a brief overview of various attempts by NASA to reduce carbon dioxide, either as the gas or the carbonate. Products of these processes are water (which can be electrolyzed to yield oxygen), carbon (which can be converted to activated charcoal for removing trace impurities from ambient air), methane (which can be further reduced or used as a fuel), or carbon monoxide (which can be used to make methanol, a fuel, or further reduced).

A promising reducing system is the Sabtier Process.



At a  $\text{H}_2:\text{CO}_2$  molar ratio of 4:1, Jackson<sup>33</sup> has shown that thermodynamic considerations imply a minimum operation temperature of 150 C°. Efficient conversion at these temperatures requires proper choice of catalyst. The transition metals Ru, Rh, or Ir are the most effective for reduction. A 0.5% Ru on alumina mixture was the best of these.<sup>34</sup> The  $\text{H}_2:\text{CO}_2$  molar ratio that gives optimum<sup>35</sup> conversion is 4.35:1. Hydrogenation catalysts are poisoned by halogen and sulfur containing compounds.<sup>33</sup> Activated charcoal can be used to purify the  $\text{CO}_2$  as activated charcoal is a poor  $\text{CO}_2$  absorber<sup>36</sup>.

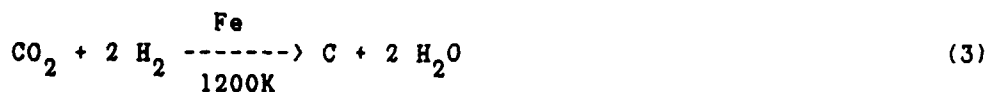
Methane from this reaction can be further reduced,



to give carbon and hydrogen. The hydrogen can then be recycled in reaction (1) and the carbon used to make activated charcoal. This particular reaction (2) is not well understood. The mechanism is unknown, although a free radical mechanism seems likely,<sup>37</sup> and no good catalyst has been found to lower the conversion temperature, although many have been tried.<sup>38,39</sup>



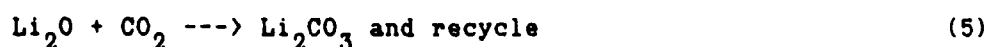
A similar reduction method is the Bosch reaction



which occurs at a higher temperatures (600 - 1000 C°) than the Sabtier reaction. At the high temperature end a 98% conversion occurs, but side reactions forming methane ( $\text{C} + 2 \text{H}_2 \rightarrow \text{CH}_4$ ) and carbon monoxide ( $\text{C} + \text{CO}_2 \rightarrow 2 \text{CO}$ ) pose a problem, although these can be recycled. Difficulties have also arisen with carbon build-up on the nickel steel wool catalyst.<sup>40</sup>

There is a definite need to look for a more efficient catalyst<sup>41,42</sup> for reaction (3). The difficulty with carbon build up on the catalytic surface needs to be solved, perhaps by providing a more attractive surface for the condensation of gaseous carbon atoms.

An electrochemical process has been tried that converts carbon dioxide in the form of a carbonate salt directly to oxygen.



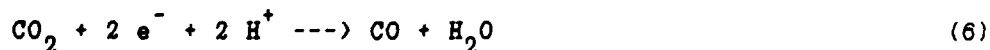
The carbon is deposited on the cathode and the oxygen is collected at the anode.<sup>43</sup>

The difficulty lies primarily in the fact that high the temperatures necessary for electrolysis lead to corrosion of heat resistant materials used in cell construction.

In addition to the efforts by NASA, a relatively large amount of research has been done on the electrochemical, photochemical, and photo-assisted electrochemical reduction of water, carbon dioxide, and carbonates in both aqueous and organic media. Part of this effort is summarized in references 44-59 and in the references contained therein.

This chemistry involves complexes of ruthenium,<sup>44,-46,50,51</sup> titanium,<sup>49</sup> nickel,<sup>52-58</sup>, and cobalt<sup>54,58</sup> as catalytic agents to effect reduction. Photoefficiency for the photo-assisted reactions is often quite poor, although some systems<sup>44,60</sup> have superior photoefficiencies with quantum yields > 0.85.

Pure electrochemical methods have considerably more promise as a pathway to CO<sub>2</sub> reduction. Although an attractive approach, electrochemical techniques usually require large negative overvoltages for the reaction:



The standard potential for reaction (6) is -0.1 V and is - 0.52 V at pH 7. Experimental results in dimethylformamide and in acetonitrile (both vs a standard calomel electrode) are -2.21 V and -2.10 V respectively.

The use of transition metals as catalytic agents can significantly lower the required overvoltage.<sup>50,59</sup> Meyer has shown<sup>50</sup> that potentials as low as -1.2 V can be achieved when 'electron reservoir' ligands such as polypyridyl provide the initial reduction site.

It is clear that transition metal complexes acting as electro-catalysts in homogeneous solution is a promising line of research. The results thus far obtained show that: (A) the problem of CO<sub>2</sub> reduction in homogeneous solution using soluble transition metal catalysts is more reasonable than once thought and accessible to a reasonable number of reducing agents, and (B) reduction to CO or HCOO<sup>-</sup> is possible depending on the reducing system.<sup>50</sup>

## References

1. Holloway, P.F., 'Space Station Technology,' JBIS, 1983, 36, 409
2. Freitag, R.F., 'The US Space Station Program,' JBIS, 1986, 39, 80
3. Leger, L.J., Visentine, J.T., 'A Consideration of Atomic Oxygen Interactions with the Space Station', J. of Spacecraft and Rockets, 1986, 23, 505
4. Leger, L.J., Spiker, I.K., Kuminecz, J.F., Ballentine, T. J., and Visentine, J.T., 'STS Flight 5 LEO Effects-Background Description and Thin Film Results,' AIAA Paper 83-2631, Oct. 1983
5. Leger, L. J., Visentine, J.T., and Kuminecz, J.F., 'Low Earth Orbit Atomic Oxygen Effects on Surfaces,' AIAA Paper 84-0548, Jan. 1984
6. Visentine, J. T., Leger, L. J., Kuminecz, J. F., And Spiker, I.K., 'STS-8 Atomic Oxygen Effects Experiment,' AIAA Paper 85-0451 Jan. 1985
7. Hord, R.M., Ed; Handbook of Space Technology: Status and Projections, CRC Press, Inc. Boca Raton, FL, 1985, p 87-105
8. For a more complete description see Reference 3, p 510 511
9. Wolfe, W. L., and Zissis, G. J. eds., The Infrared Handbook, IRIA-ERIM, pp 1-15 - 1-17, Figures 1-1, 1-2, 1-7, 1-9, 1978
10. Thekaekara, M. P., 'Evaluating Light from the Sun', Optical Spectra, pp 32-35 March, 1972
11. Hurlock, S. C., et. al., 'Radiation Augmented Propulsion Feasibility', AFRPL Paper TR-85-068
12. Burkett, A.R., Meyer, T.J., Whitten D.G., 'Light Catalyzed Substitution and Disproportionation in  $[n^5-C_5H_5Mo(CO)_3]_2$ ,' J. of Organomet Chem, 1974, 67, No. 1, p 67-73
13. (a) Wrighton, M.S. and Ginley, D.S., 'Photochemistry of  $_5$ Metal-Metal Bonded Complexes. III. Photoreactivity of Hexacarbonylbis( $n^5$ -cyclopentadienyl)di-molybdenum(I) and Ditungsten(I), J. Am. Chem. Soc., 97, No. 15, p 4246-4251, 1975 (b) Meyer, T.J., and Caspar, J.V., 'Photochemistry of Metal-Metal Bonds,' 1985, Chemical Reviews, 85, No. 3, p 187-218 (c) Caspar, J.V., and Meyer, T.J., Mechanistic Aspects of the Photochemistry of Metal-Metal Bonds. Evidence for the Intervention of Two Different Primary Photoproducts in the Photochemistry of bis( $n^5$ -cyclopentadienyl)tetracarbonyldiiron,' J. Am. Chem. Soc., 1980, 102, No. 26, p 7794-7795
14. Grinley, D.S. and Wrighton, MS. Photochemistry of Metal-Metal Bonded Complexes. IV. Generation of  $d^0$  and  $d^1$  Mononuclear Fragments via Homolytic Cleavage in Heteronuclear Metal Carbonyls, J. Am. Chem. Soc., 1975, 98, No. 13, p 4908-4911 and references therein.

15. Meyer, T.J., 'Redox Properties of Polymetallic Systems,' Advances in Chemistry Series, 1976, V1976, No. 150, p 73-84
16. Abruna, H.D., Denisevich, P., Umaha, M., Meyer, T.J., and Murray, R.W., 'Rectifying Interfaces Using Two-Layer Films of Electrochemically Polymerized Vinylpyridine and Vinylbipyridine Complexes of Ruthenium and Iron on Electrodes,' J. Am. Chem. Soc., 1981, 103, No. 1, p 1-5
17. Ellis, C.D., Murphy, W.R. Jr., Meyer, T.J., 'Selectivity and Directed Charge Transfer through an Electroactive Metallopolymer Film,' J. Am. Chem. Soc., 1981, 103, No. 25, p 7480-7483
18. Sullivan, B.P., Calvert, J.M., and Meyer, T.J., 'Electropolymerization and Reductive Chloride Loss Techniques in Preparing Metallopolymer Films on Electrode Surfaces,' Abstracts of Papers of the American Chemical Society, 1981, 182, p 123
19. Denisevich, P., Abruna, H.D., Leidner, C.R., Meyer, T.J., and Murray, R.W., 'Electropolymerization of Vinylpyridine and Vinylbipyridine Complexes of Iron and Ruthenium-Homopolymers, Copolymers, Reactive Polymers,' Inorganic Chemistry, 1982, 21, No. 6, 2153-2161
20. Calvert, J.M., Caspar, J.V., Binstead, R.A., Westmoreland, T.D., and Meyer, T.J., 'Metallopolymer Photochemistry. Photophysical, Photochemical, and Photoelectrochemical Properties of (bby)<sub>2</sub>Ru(II) Sites Bound to poly(4-vinylpyridine),' J. Am. Chem. Soc., 1982, 104, No. 24, p 6620-6627
21. Westmoreland, T.D., Calvert, J.M., Murray, R.W., and Meyer, T.J., 'A Photoelectrode Based on Visible Photolysis of a Metallopolymer Film,' J. Chem. Soc., Chem Commun., 1983, No. 2, p 65-66
22. Westmoreland, T.D., Calvert, J.M., Murray, R.W., and Meyer, T.J., 'A Photo-Electrochemical Cell Based on Oxidative Quenching in a Metallopolymer Film,' ACS Symposium Series, V2983, No. 211, p 552
23. Margerum, L.D., Ellis, C.D., Murray, R.W., and Meyer, T.J., 'Electrode-metallopolymer Interfaces by Oxidative Electropolymerization,' ACS Symposium Series, V1983, No. 211, p 541
24. (a) Westmoreland, T.D., Calvert, J.M., Murray, R.W., and Meyer, T.J., 'A Photo-Electrode Based on Visible Photolysis of a Metallopolymer Film,' J. Chem. Soc-Chem. Comm., 1983, 1983, No. 2, p 65-66  
 (b) Eggleston, D.S., Goldsby, K.A., Hogson, D.J., Meyer, T.J., 'Transient Storage of Photochemically Produced Oxidative and Reductive Equivalents in Soluble Redox Polymers,' Journal of Physical Chemistry, 1986, 90, No. 5, p 728-730
25. Surridge, N.A., Linton, R.W., Hupp, J.T., Bryan, S.R., Meyer, T.J., and Griffis, D.P., 'Characterization of Metal-Complex-Containing Organic Polymeric Films by Secondary Ion Mass Spectrometry', Anal. Chem., 1986, 58, No. 12, p 2443-2447

26. Vining, W.J. and Meyer, T.J., 'Redox Properties of the Water Oxidation Catalyst  $(\text{Bpy})_2(\text{H}_2\text{O})\text{RuORu}(\text{H}_2\text{O})(\text{Bpy})_4^{2+}$  in Thin Polymeric Films - <sup>2</sup>Electrocatalytic Oxidation of  $\text{Cl}^-$  to  $\text{Cl}_2^-$ ,' Inorg Chem, 1986, 25, No. 12, p 2023-2033
27. Margerum, L.D., Meyer, T.J., and Murray, R.W., 'Selective Incorporation of Pendant Redox Sites into Preformed Polymers,' J. Phys. Chem., 1986, 90, No 12, p 2696-2702
28. Surridge, N., Hupp, J.R., Younathan, J., McClanahan, S.F., Danielson, E., and Meyer, T.J., 'Photoinduced Charge Separation and Storage in Soluble Polymers and Polymeric Films,' J. of the Electrochem. Soc., 1987, 134, No. 3, p 130.
29. Margerum, L.D., Murray, R.W., and Meyer, T.J., 'Transient Storage of Photochemically Produced Oxidative and Reductive Equivalents in Soluble Redox Polymers,' J. Phys. Chem., 1986, 90, No. 5, 728-30
30. Askham, F.R., Stanley, G.G., and Marques, E.C., 'A New Type of Transition-Metal Dimer Based on a Hexaphosphine Ligand System:  $\text{Co}_2(\text{CO})_4(\text{eHTP})_2^{2+}$  (eHTP =  $(\text{Et}_2\text{PCH}_2\text{CH}_2)_2\text{PCH}_2(\text{CH}_2\text{CH}_2\text{PEt}_2)_2$ ),' J. Am. Chem. Soc., 1985, 107, p 7423
31. Laneman, S.A., and Stanley, G.G., 'An Open-Mode Nickel Dimer Based on a Binucleating Hexaphosphine Ligand System. Solid-State and Solution Conformations,' Inorganic Chemistry, 1987, 26, p 1177
32. Parker, J.F., Jr and West, V.R. Eds, Bioastronautics Data Book, NASA p-446, Washington, 1972, p 836
33. Jackson, J.K., 'Test results, operational ninety-day Manned Test of a Regenerative Life Support System; NASA-CR-111881, NASA, Washington, D.C., May 1971
34. Thompson, E.B. Jr., 'Investigations of Catalytic Reactions for Carbon Dioxide Reduction,' Report No. FDC-TDR-G422, Wright-Patterson AFB, OH, 1964-1967
35. Yajatm, M.M., and Barker, R.S., 'Parametric study of Life Support Systems', NASA-CR-73282, NASA, Washington, D.C., January, 1969
36. Parker, J.F., Jr and West, V.R. Eds, Bioastronautics Data Book, NASA p-446, Washington, 1972, p 836
37. Shantarovich, P.S. and Pavlov, B.V., 'The Mechanism of the Decomposition of Methane', Zhur. Fiz. Khim., 30, 1956, p 811-820
38. Masao K.K., 'Decomposition of  $\text{CH}_4$  on the Surface of Platinum', Rev. Phys. Chem. Japan, 1937, 11, p 82-95
39. Spektor, B.V., 'Thermal Decomposition of Methane', Zhur. Priklad. Khim., 1956, 29, p 1078-1082)

40. Armstrong, R.C., 'Life Support Systems for Space Flight of Extended Time Periods' NASA-CR614, NASA, Washington, D.C., 1966
41. Holmes, R.K., King, C.D., and Keller, E.E., 'Bosch Carbon Dioxide Reduction Development. Interim Report.', 1974, NASA CR-143959, NASA, Washington, D.C.
42. Manning, M.P. and Reid, R.C., 'Carbon Dioxide Reduction by the Bosch Process,' Am. Soc. Mech. Eng., 1975, 75-ENAS-22
43. Stein, P.J., 'Research and Development Program for the Combined Carbon Dioxide Removal and Reduction System' Contract NASA-4154, NASA, Washington D.C. 1965
44. Dressick, W.J., Meyer, T.J., and Durham, B. 'An Excited State Photo-electrochemical Cell for the Production of Oxygen Based on Oxidative Quenching of  $\text{Ru}(\text{bipy})_3^{2+}$ ,' sr. J. Chem., 1982, 22, No. 2, p 153-157
45. Dressick, W.J., Meyer, T.J., Durham, B., Rillema, D.P., 'Excited-state Photoelectrochemical Cells for the Generation of Hydrogen and Oxygen Based on  $\text{Ru}(\text{bpy})_3^{2+}$ ,' Inorganic Chem., 1982, 21, No. 9, p 3451-3458
46. Sullivan, B.P., and Meyer, T.J., 'Photoinduced Irreversible Insertion of  $\text{CO}_2$  into a metal-Hydride bond,' Journal of the Chemical Society-Chemical Communications, 1984, No. 18, p 1244-1245
47. Ulman, M., Aurian-Biajeni, B., and Halmann, M., 'Fuel from Carbon Dioxide: an Electrochemical Study,' Chemtech, 1984, 1, p 235-239
48. Viliyakumar, K.M and Lichtin, N.M., 'Reduction of Carbon Dioxide by Hydrogen and Water Vapor over Metal Oxides Assisted by Visible Light,' J. Catal., 1984, 90, No. 1, 173-177
49. Halmann, M., Katzir, V., Borgarello, E., and Kiwi, J. 'Photoassisted Carbon Dioxide Reduction on Aqueous Suspensions of Titanium Dioxide,' Sol. Energy Mater., 1984, 10, p 85-91
50. Bolinger, M.C., Sullivan, B.P., Conrad, D., Gilbert, J.A., Story, N., Meyer, T.J., 'Electrocatalytic Reduction of Carbon Dioxide Based on Polypyridyl Complexes of Rhodium and Ruthenium,' J. Chem. Soc.-Chem. Comm., 1985, No. 12, 796-797
51. O'Toole, T.R., Margerum, L.D., Westmoreland, T.D., Vining, W.J., Murray, R.W., Meyer, T.J., 'Electrocatalytic Reduction of  $\text{CO}_2$  at a Chemically Modified Electrode,' J. Chem. Soc.-Chem. Comm., 1985, No. 20 p 1416-1417
52. Belev, M., Collin, J.P., Ruppert, R, and Sauvage, J.P., 'Electrocatalytic Reduction of Carbon Dioxide by Nickel Cyclam<sup>2+</sup> in Water: Study of the Factors Affecting the Efficiency and the Selectivity of the Process,' J. Am. Chem. Soc., 1986, 108, No. 24, 7461-7467
53. Takezawa, N., Terunuma, H., Shimokawabe, M, and Kogayashi, H, 'Methanation of Carbon Dioxide: Preparation of Nickel/Magnesium Oxide' Appl. Catal., 1986, 23, No. 2, p 291-298

54. Pearce, D.J. and Pletcher, Derek, 'A Study of the Mechanism for the Electroanalysis of Carbon Dioxide Reduction by Nickel and Cobalt Square Planar Complexes,' J. Electroanal. Chem. Interfacial. Electrochem., 1986, 197, p 317-330
55. Hawecker, J., Lehn, J.M., and Ziessel, R., 'Photochemical and Electrochemical Reduction of Carbon Dioxide to Carbon Monoxide Mediated by (2,2'-bipyridine)tricarbonylchlororhenium(I) and Related Complexes as Homogeneous Catalysts,' Helv. Chim. Acta., 1986, 69, No. 8, p 1990-2012
56. Hukkanen, H and Pakkanen, T.T., 'Photochemical Catalytic Reduction of Carbon Dioxide by Visible Light using Tris(2,2'-bipyridine)ruthenium (II) and (2,2'-bipyridine)tricarbonylchlororhenium as Photocatalysts,' Inorg. Chim. Acta., 1986, 114, No. 2, p L43-L45
57. Daniele, S., Ugo, P., Bonempelli, G, and Fiorani, M., 'An Electrochemical Investigation on the Nickel-promoted Conversion of Carbon Dioxide to Carbon Monoxide,' J. Electroanal. Chem. Interfacial Electrochem., 1987, 219, p 259-271
58. Fisher, B. and Eisenberg, 'Electrocatalytic Reduction of Carbon Dioxide by Using Macrocycles of Nickel and Cobalt,' J. Am. Chem. Soc., 1980,102, p 7361-7362
59. Amatore, C. and Saveant, J.M., 'Mechanism and Kinetic Characteristics of the Electrochemical Reduction of Carbon Dioxide in Media of Low Proton Availability, J. Am. Chem. Soc., 1981,103, p 5021-502
60. Neyhart, G.A., Marshall, J.L., Dressick, W.J., Sullivan, B.P., Watkins, P.A., and Meyer, T.J., 'Excited State Photoelectrochemical Production of  $H_2O_2$  and  $Br_2$ ,' J. Chem. Soc. Chem. Comm. 1982, p915-917

1987 USAF-UES SUMMER FACULTY RESEARCH PROGRAM

GRADUATE STUDENT SUMMER SUPPORT PROGRAM

Sponsored by the  
AIR FORCE OFFICE OF SCIENTIFIC RESEARCH

Conducted by the  
Universal Energy Systems, Inc.

FINAL REPORT

BAYESIAN TESTABILITY DEMONSTRATION

Prepared by:	Ronald V. Canfield
Academic Rank:	Professor
Department and	Department of Mathematics
University:	Utah State University
Research location:	Rome Air Development Center
	Systems Reliability and Engineering Division
	R and M Techniques Branch
USAF Researcher:	Jerome Klion
Date:	17 August 1987
Contract No:	F49620-85-C-0013



# BAYESIAN TESTABILITY DEMONSTRATION

by

Ronald V. Canfield

## ABSTRACT

The purpose of this work is to explore the use of Bayesian methods in testability demonstration. The primary focus is on prior information. The role and sources of prior information are discussed. A general method of quantifying prior information is developed based on the intuitive concepts of location and equivalent sample size. Two testability demonstration plans are derived. The first uses standard Bayesian risk concepts. This method requires extensive tables or graphs. The second plan introduces an alternative by controlling the maximum risk similar to the classical non Bayesian tests. Implementation of this method is much simpler than the standard test. Similarity of the new test to the non Bayesian fixed sample test suggests that a simple Bayesian sequential test is possible.

#### ACKNOWLEDGMENTS

The author wishes to thank the Air Force Systems Command, Air Force Office of Scientific Research for their sponsorship of the Summer Faculty Research Program. Special thanks are given to the personnel at the Reliability and Maintainability Branch of the Systems Reliability and Engineering Division of the Rome Air Development Center for their support and assistance in the research and preparation of this report. Jerome Klion was particularly helpful in giving my research practical direction.

I. INTRODUCTION: Technological advances considerably enhance the ability of systems to perform complex and previously impossible tasks. Accompanying this enhancement is tremendous growth in system complexity. The necessity for efficient maintenance and testing for such systems has motivated introduction of automated diagnostic equipment such as Built-In-Test (BIT). Specifications for system performance now include testability requirements. Present testability demonstration tests designed for different applications are impractical from both time and economic aspects. It is necessary to find more efficient and cost effective means of demonstrating testability. Bayesian methods offer the potential of improving efficiency of demonstration tests by incorporating information which is independent of test samples into the decision process. This problem is of particular interest to the author because of previous research experience in quantification of prior information for Bayesian analysis.

II. OBJECTIVES OF THE RESEARCH EFFORT: The purpose of this work is to explore the use of Bayesian methods in testability demonstration. The primary focus is on prior information. The sources of prior information are to be identified and a general method quantifying the information into a prior density function is to be developed. In order to anticipate possible problems which may be encountered in carrying out a Bayesian demonstration, a plan will be derived. In the process of this derivation it was learned that the test would involve the use of extensive tables which will require numerical solutions of equations. Therefore a new objective was defined to derive an alternative test based on the concept of control of maximum risk rather than average risk as used by existing Bayesian tests.

III. GENERAL BACKGROUND: There are many possible measures of testability such as fraction of faults detected (FFD), false alarm rate (FAR), can not duplicate rate (CND), percent fault coverage (PFC), and fraction of faults isolatable (FFI) [1]. The variable fraction of faults isolatable is used in this report. However this work is applicable to any measure for which detection can be measured as a Bernoulli random variable, e.g.,  $X = 0$  or  $1$  indicating for example no isolation and isolation respectively of a known fault.

Notation. The following notation is used throughout this paper.

$n$	sample size
$Y$	the number of faults isolated in a test sequence
$\pi$	the true FFI of the BIT design
$h(\pi)$	prior density function of $\pi$
$g(y \pi)$	conditional density function of $Y$ given $\pi$
$\pi_0$	specified fault coverage
$\pi_1$	lowest fault coverage acceptable to the consumer
$H_0: \pi \geq \pi_0$	the statistical hypothesis to be tested
$I_1$	Fisher's information in single random fault observation or $E_{\pi}((\partial g(y \pi)/\partial \pi)^2)$ where the sample size for $y$ is 1
$E_{\xi}(\cdot)$	expected value of $(\cdot)$ with respect to the random variable $\xi$
$\beta(\gamma, \lambda)$	$\Gamma(\gamma)\Gamma(\lambda)/\Gamma(\gamma + \lambda)$ (the beta function)

Assumptions. Given a system composed of  $N$  component parts, if a failure occurs it is assumed that there are  $N$  possible causes of that failure. The number of potential faults ( $N$ ) in the system is assumed to be very large. The number simulated or observed in a test is assumed to be a small fraction of the total number ( $N$ ) in the system. It is further assumed that simulated or observed faults represent a random sample of the population of potential faults. Under these assumptions the isolation of a fault is a Bernoulli random variable so that the number of faults isolatable ( $Y$ ) is a binomial random variable. Since  $Y$  is a sufficient statistic for  $\pi$ , it will be used in the test developed in this report.

II. THE PRIOR DISTRIBUTION. The prior distribution serves to transfer information which is not contained in the sample into the decision process. This distribution represents a quantification of the prior information. Sources and use of prior information are discussed in this section. Because it is not possible to avoid the use of judgement in determining the prior, an intuitive basis for prior information is developed to aid in choosing the prior. An intuitive basis will make the process of quantification more repeatable.

Sources of Prior Information. Information concerning the

testability of a given BIT design can come from a variety of sources external to the test sample results. This information can be divided into two categories, (a) information specific to the system to be tested, e.g., design procedures followed, tools used, preliminary test results on system components and, (b) information obtained from similar systems, e.g., previous demonstration test results, field performance. Category b represents "experience."

Consider the information in category a. The primary source of this information is the BIT design and ad hoc testability tasks undertaken during the design and production process. BIT coverage is designed into a system. This design coverage represents a predicted FFI. Additional considerations for prediction of testability attributes has been studied and reported by the ARINC Research Corporation [2]. Predictions are not perfect as experience has shown that performance rarely achieves the level predicted. However the predictions represent prior information which may be modified as experience dictates. In addition to design information there may be tests performed on major components of the BIT circuitry or on a system prototype. Ideally these may represent tests on the system itself. However it should be expected that when such components are integrated into a system, some ambiguities or unanticipated performance may occur. Although this test information could be used to modify a predicted value, it seems in general that there is not enough information from such sources to justify its usage for testability measurement. This kind of information can be used however to characterize quality or content of diagnostic information at the component level. Definition of quality or content of diagnostic information is given later.

Consider now information in category b, i.e., experience with similar BIT systems. To reduce reliance on purely subjective factors in the use of this information it is important to have documented information. Documented prior experience serves as a common denominator among persons who may become involved in the test process. For each system documented the information should include as a minimum

- (i) design information , e.g., type of BIT
- (ii) fault coverage predicted from design information and

the method of prediction/assessment

(iii) demonstration test results

(iv) field performance data for the system

This kind of documentation will result in a data bank which can be used to modify a coverage value predicted by design information and to characterize information content. BIT designs have been used effectively by manufacturers to reduce the cost of testing chips. Documentation similar to the type suggested above has been carried out to aid engineers in the design of VLSI chips [3]. Albert, et. al. [4] has studied a great many BIT designs which have military application. The study focused on the development of methodologies to verify that designs meet specified requirements. Design performance was not part of the study. It does however suggest that such information could be assembled into a useable form for Bayesian analysis. The observation was made in [4] that standardization of methodologies is at least as necessary as finding better techniques. Standardization can be even more important to the effectiveness of Bayesian analysis. Bayesian methods depend on prior information. A data bank as described previously will provide much more information per BIT system if fewer systems are used.

An Intuitive Basis for Prior Information. Bayesian methods require a prior distribution of the population parameters. In this particular application it is FFI. To quantify prior information is to select a statistical distribution which represents what is known (or not known) about the parameter. The results should be repeatable; that is, similar results should be obtained if a different group does the quantifying. This can be difficult if the concepts which link information to an analytical form are not intuitive. This is especially important in the present application because much of the information concerning BIT design may be held by individuals who are not necessarily familiar with statistical distributions.

In most applications a two parameter prior distribution is sufficiently flexible to represent prior information. This indicates that the intuitive basis for prior information must involve two concepts. The concepts suggested here are "location" and "equivalent sample size."

Definition of location. Since BIT coverage is designed there is a design goal and a method of predicting or assessing the coverage. This goal represents location information. The most used measure of location is the mean value. Its use is likely motivated more from mathematical convenience (e.g., normal distribution theory) than intuitive appeal. In this application mathematical convenience has little impact so that additional measures can be considered. For most individuals the "most likely value" seems to a more natural measure of location. This measure translates to modal value (M) in a statistical distribution.

Definition of equivalent sample size (ESS). Information content of a random sample with known density function is given by Fisher's information measure. The symbol  $I_1$  is used in this report to represent Fisher's information in a sample of size 1 from the Bernoulli population. The information content in the prior has been defined [5] in a manner similar to Fisher's information. Let  $V = \partial \ln(h(\pi)) / \partial \pi$ . Prior information is defined  $E(V^2)$ . It is the average squared slope of the prior density. Thus  $V^2$  can be interpreted as the information in  $h(\pi)$  at  $\pi$ . Dividing  $V^2$  by Fisher's information at  $\pi$  in a single random sample gives the equivalent sample size of  $h(\pi)$  at  $\pi$ . ESS is defined as

$$ESS = E_{\pi}(V^2 / I_1) \quad (1)$$

For a single Bernoulli sample  $I_1^{-1} = (\pi(1 - \pi))$  so that (1) becomes

$$ESS = E_{\pi}(V^2 \pi(1 - \pi)). \quad (2)$$

If prior information from different sources have the same mode the information is consistent. Under this condition the ESS for the combined prior information is the sum of the ESS from each source.

Choice of Prior Distribution. Prior information as formulated previously and the basis for information developed are used in this section to determine a prior distribution. There are many unique situations which can dictate different approaches to choosing the prior distribution. The approach taken here serves as an example

which can be adapted to many different situations.

Choosing a prior is simplified if a parametric family of priors can be found which has sufficient flexibility to represent all possible realizations of prior experience. From the standpoint of mathematical compatibility with the likelihood function the conjugate prior is a natural choice. For the binomial likelihood function this is the beta family of distributions with density

$$h(\pi) = \pi^{\gamma-1} (1-\pi)^{\lambda-1} / \beta(\gamma, \lambda) \quad \pi, \gamma, \lambda > 0 \quad (3)$$

This family seems to have the desired flexibility for representation of information. The mode of the beta is given by

$$M = (\gamma - 1) / (\gamma + \lambda - 2) \quad (4)$$

and the variance is

$$\sigma^2 = \gamma\lambda / ((\gamma + \lambda)^2 (\gamma + \lambda - 1)) \quad (5)$$

Fisher's information for a single Bernoulli sample is

$$I_1 = (\pi(1-\pi))^{-1} \quad (6)$$

Using (2) and (6) it follows that

$$ESS = \gamma + \lambda - 2 \quad (7)$$

It is informative to consider (7) with  $\gamma = \lambda = 1$ . Given these values  $h(\pi)$  is a uniform density function. In the sense that the posterior density is the same as the likelihood function, this prior is noninformative. Note that  $ESS = 0$ , which is logically consistent.

Choosing the parameters of the beta prior. The principles used to determine parameter values from prior information are illustrated in an example in this section. Suppose the following prior information is available

Category (a)

(1) predicted FFI = 0.90 (from design)



(2) a total of 30 prior tests performed at the component level on several components of the system with all faults isolated

(3) 2 prior generated faults isolated on a system prototype

Category (b)

(1) the data in table 1 represents information extracted from a fictitious testability data bank. Data on systems with similar BIT design and use environment is given.

Table 1. Prior Testability Data.

System	Predicted FFI	Demonstrated FFI	Field FFI
1	0.70	0.60	0.57
2	0.85	0.73	0.65
3	0.75	0.70	0.60
4	0.90	0.80	0.75
5	0.95	0.81	0.69
6	0.65	0.62	0.51

The starting point for setting M is the design value 0.90. The additional information in category a lends credibility to this prediction. Information content of prior data is measured in terms of ESS. The two samples on a prototype represent real system tests and so the ESS contribution is taken to be 2. Additional information from category a includes 30 prior tests of a few isolated components of the system at the component level of BIT circuitry. If these observations were made at the system level they could represent 30 bonafide samples of the system BIT. However it can be expected that incorporation into the system may impair the BIT circuitry at the component level. Therefore it is decided to assume ESS = 10 from this information. To summarize category a information, M = 0.90 and total ESS = 12.

The information from category b will now be used to modify M and ESS. A plot of column 3 table 1 (Y axis) against predicted FFI in column 2 table 1 (X axis) is shown in figure 1. A regression of X on Y yields the model  $Y = 0.14 + 0.7X$ . From this equation prior experience suggests that systems with design FFI 0.90 has demonstrated FFI approximately 0.78. In light of the prior tests in category a,

the decision is made to use  $M = 0.80$ .

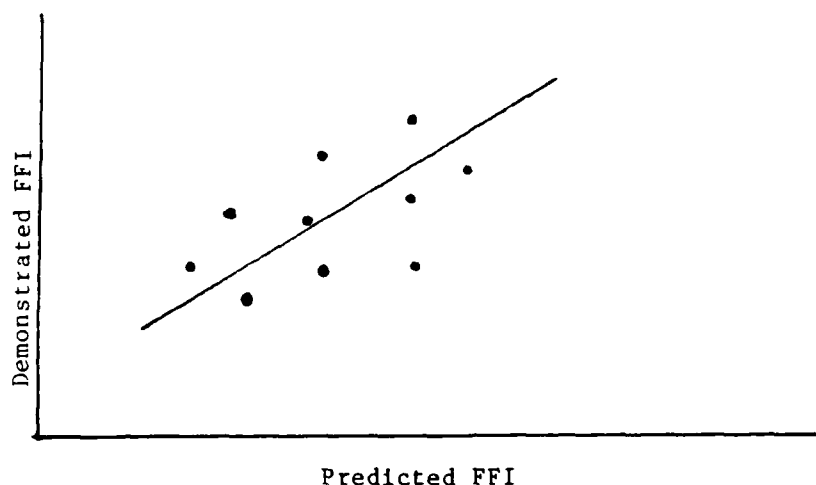


Figure 1. Plot of demonstrated FFI vs. predicted FFI.

If an assumption of homogeneous variance for the regression model is reasonable, it is possible to extract additional information from category b. For least squares regression coefficients the estimated variance of a prediction at  $X = X_0$  is

$$S_{\hat{Y}|X_0}^2 = (1 + 1/n + (X_0 - \bar{X})^2 / \sum (X_i - \bar{X})^2) S_E^2$$

where

$$S_E^2 = \sum (\hat{Y}_i - \bar{Y}_i)^2 / (n - 2)$$

For the data in table 1 using  $X_0 = 0.90$ ,  $S_{\hat{Y}|X_0}^2 = 0.03965$  Equations (4) and (5) are used to determine the  $\gamma$  and  $\lambda$  for a beta prior with  $M = 0.80$  and  $\sigma = 0.03965$ . The resulting solutions are  $\gamma = 8$  and  $\lambda = 2$ . It follows from (7) that  $ESS = 8$  for this information. It is concluded from all of the prior data that the basis for determining the parameters of the prior density is

$$M = 0.80 \quad (8)$$

and

$$ESS = 2 + 10 + 8 = 20. \quad (9)$$

It follows from (4) and (7) that  $\gamma = 17$  and  $\lambda = 5$ .

III. BAYESIAN TESTABILITY DEMONSTRATION: Two Bayesian tests are outlined in this section based upon FFI as a measure of testability. The number of faults isolated in a random sample ( $Y$ ) is the assumed data. A beta prior is used with parameter values computed from the

prior information given in (8) and (9). The methods apply to any Bernoulli based measure of testability.

Test Format. A testability demonstration is a test of the hypothesis  $H_0: \pi \geq \pi_0$ . The alternative is assumed to be the region of the parameter space of  $\pi$  complimentary to  $H_0$ . In general a statistical test is based upon a test statistic ( $Y$ ) selected because it contains the sample information relating to the test parameter. The test is carried out by determining a critical region, i.e., a subset of the space of  $Y$ . If the observed value of  $Y$  is in the critical region, the hypothesis is rejected. For the application in this report  $Y$  is the total number of faults isolated in  $n$  trials. The critical region is of the form  $Y \leq c$  where  $c$  is called the critical value.

There are two unavoidable errors which may occur when testing  $H$ . It is possible to (a) reject  $H$  when it is true or (b) accept  $H$  when it is not true. The probability of error a will be called the producer's risk and the probability of error b will be called the consumer's risk in this report. The frequency of occurrence of these errors is controlled by choice of  $c$  and the sample size of the test ( $n$ ). Classical non Bayesian tests are characterized by the maximum risks associated with the possible test errors. In general these risks are functions of the parameter values within  $H$  or the alternative. The usual procedure is to choose the test sample size ( $n$ ) and the critical value ( $c$ ) to limit the maximum possible risks. For the producer the maximum risk is

$$\alpha = \max_{\pi \geq \pi_0} \Pr(\text{rejecting } H_0 | \pi) = \sum_{y=0}^c \binom{n}{y} \pi_0^y (1 - \pi_0)^{n-y} \quad (10)$$

The consumer's risk is usually controlled by selecting a subset of the alternative to  $H_0$  in which an error would be serious (e.g.,  $\pi \leq \pi_1$ ) and limiting the maximum consumer's risk within the subset to

$$\beta = \max_{\pi \leq \pi_1} \Pr(\text{accepting } H_0 | \pi) = \sum_{y=c+1}^n \binom{n}{y} \pi_1^y (1 - \pi_1)^{n-y} \quad (11)$$

The format of a Bayesian test is similar however the parameter being a random variable permits many different risk definitions. Several are

given in Coppola [6]. The expected risk (EBR) and a new method called the expected maximum risk (EMR) are considered in this report.

Risk as it is used in decision theory brings together the concepts of loss and opportunity to experience the loss. Even though the loss for a particular bad decision may be great, if the opportunity to make that bad decision is limited, the risk may be small. Opportunity is measured by the prior density and loss is given by the probability of the errors  $a$  and  $b$  discussed previously. Overall risk in Bayes hypothesis testing is given in [7]. However this test is not satisfactory in most applications as the producer and consumer have competing interests. It is usually desirable to control each risk separately. A form which closely reflects the desires of the test engineer [6], is based on the average conditional risks for the producer and consumer. A testability demonstration plan is derived for this method of risk control. It is designated expected Bayes risk or EBR. The expected maximum risk (EMR) is introduced as an alternative method to control risk.

Expected Bayes risk (EBR). The EBR for the producer is the conditional probability of rejecting a good system and for the consumer it is the conditional probability of accepting a bad system. These risks can be computed mathematically as

$$\alpha = \int_{\pi_0}^1 \Pr((\text{rejecting } H_0 | \pi) | \pi \geq \pi_0) h(\pi) d\pi \quad (12)$$

and

$$\beta = \int_0^{\pi_1} \Pr((\text{accepting } H_0 | \pi) | \pi \leq \pi_1) h(\pi) d\pi \quad (13)$$

where

$$\begin{aligned} \Pr((\text{rejecting } H_0 | \pi) | \pi \geq \pi_0) &= \frac{\sum_{y=0}^c g(y|\pi)}{\int_{\pi_0}^1 h(\pi) d\pi} \\ &= \frac{\sum_{y=0}^c \binom{n}{y} \pi^y (1-\pi)^{n-y} \beta(\gamma, \lambda)}{\int_{\pi_0}^1 \pi^{\gamma-1} (1-\pi)^{\lambda-1} d\pi} \end{aligned}$$

and

$$\begin{aligned} \Pr((\text{accepting } H_0 | \pi) | \pi \leq \pi_1) &= \frac{\sum_{y=c+1}^n g(y|\pi)}{\int_0^{\pi_1} h(\pi) d\pi} \\ &= \frac{\sum_{y=c+1}^n \binom{n}{y} \pi^y (1-\pi)^{n-y} \beta(\gamma, \lambda)}{\int_0^{\pi_1} \pi^{\gamma-1} (1-\pi)^{\lambda-1} d\pi} \end{aligned}$$

The risks are controlled by choice of the values  $\alpha$  and  $\beta$ . The test parameters  $c$  and  $n$  are determined by simultaneous solution of (12) and

(13). Numerical methods are required to solve the above equations for  $c$  and  $n$ .

It is possible to provide tables/graphs for use in the design and test of demonstration hypotheses. Because of the number of test parameters tables will be extensive, graphical methods can be more efficient.

Expected maximum risk (EMR). An alternative risk definition is given in this section. It is intended to be more closely associated with the concept of risk control held by test engineers than the risk of the previous section. EBR while limiting the average risk can permit large risk for some values. EMR controls the maximum risk.

Risk computations involving prior densities assume that the prior is an absolute quantification of prior information. It represents exactly what is known about the test parameter. As a matter of practical importance, most priors are less than perfect. They are subject to "sampling variation" similar to sample statistics. In addition to the natural variation of prior data the result of quantification from the same prior data introduces variation. Different groups of analysts given the same prior information may not arrive at the same prior density. An intuitive approach to selecting the prior as discussed previously will contribute significantly to a reduction of that variation but cannot eliminate it.

It is informative to examine the risks (12) and (13) in light of the accuracy of the prior density and "worst case" protection. Discussion is centered on the producer's risk, however the principles apply as well to the consumer's risk. Note from (12) that risk opportunity is incorporated by weighting the conditional risk  $\Pr((\text{rejecting } H_0 | \pi) | \pi \geq \pi_0)$  with the prior density  $h(\pi)$ . Risk opportunity is also inherent in the conditional risk through the second conditioning event  $\pi \geq \pi_0$ . It is inappropriate to permit prior information to influence the "worst case" conditional risk. Opportunity is not a factor in this determination. Given inaccuracies of prior information this principle seems even more reasonable. Therefore the conditional risk  $\max \Pr((\text{rejecting } H_0 | \pi) | \pi \geq \pi_0)$  is determined assuming no prior information, i.e., a uniform distribution of  $\pi$  is assumed over  $(0,1)$ . It follows that

$$\max_{\pi \geq \pi_0} \Pr((\text{rejecting } H_0 | \pi) | \pi \geq \pi_0) = \sum_{y=0}^c \binom{n}{y} \pi_0^y (1 - \pi_0)^{n-y} / (1 - \pi_0)$$

Opportunity is provided by the weighting factor  $h(\pi)$  so that EMR for the producer is given by

$$\alpha = \int_{\pi_0}^1 \max_{\pi \geq \pi_0} \Pr((\text{rejecting } H_0 | \pi) | \pi \geq \pi_0) h(\pi) d\pi = \quad (14)$$

Similarly the consumer's EMR is defined

$$\beta = \int_{\pi_0}^1 \max_{\pi \leq \pi_1} \Pr((\text{accepting } H_0 | \pi) | \pi \leq \pi_1) h(\pi) d\pi = \quad (15)$$

Equations (14) and (15) can be rewritten

$$\alpha_0 = k_0 \alpha = \sum_{y=0}^c \binom{n}{y} \pi_0^y (1 - \pi_0)^{n-y} \quad (16)$$

and

$$\beta_1 = k_1 \beta = \sum_{y=c+1}^n \binom{n}{y} \pi_1^y (1 - \pi_1)^{n-y} \quad (17)$$

where

$$k_0 = (1 - \pi_0) \beta(\gamma, \lambda) / \int_{\pi_0}^1 \pi^{\gamma-1} (1 - \pi)^{\lambda-1} d\pi \quad (18)$$

and

$$k_1 = \pi_1 \beta(\gamma, \lambda) / \int_0^{\pi_1} \pi^{\gamma-1} (1 - \pi)^{\lambda-1} d\pi \quad (19)$$

Note that (16) and (17) are essentially the same as (10) and (11) except that the risk bounds are adjusted to reflect the prior information. It is intuitively logical that when no prior information is available (i.e.,  $\gamma = \lambda = 1$ ) (14) and (15) should coincide with the classical test. This is the case since  $\alpha_0 = \beta_1 = 1$  for  $\gamma = \lambda = 1$ .

Assuming large samples a normal approximation for  $Y$  can be used to compute  $c$  and  $n$ . The resulting solutions are

$$c = 1 + n \pi_0 - z_{\alpha_0} \sqrt{n \pi_0 (1 - \pi_0)} \quad (20)$$

and

$$n = ((z_{\beta_1} \sqrt{\pi_1 (1 - \pi_1)} + z_{\alpha_0} \sqrt{\pi_0 (1 - \pi_0)}) / (\pi_0 - \pi_1))^2 \quad (21)$$

where  $z_q$  is the  $q$ th quantile of a standard normal distribution. Determination of  $c$  and  $n$  for this case is very simple compared with the EBR method. EMR uses existing normal probability tables. Tables of the incomplete beta integral exist but may not be in sufficient detail or range of values necessary for application in testability. However tables can be prepared for the integrals in (18) and (19)

using the numerical approximations for the beta integral in [8].

The approximations (20) and (21) are useful when the prior probabilities of the errors associated with the two risks are sufficiently large. If for example  $\Pr(\pi \leq \pi_1)$  is less than  $\beta$  from prior information alone, there is no need for further testing. The system should be accepted. Equations (20) and (21) cannot be used under this condition because they force risk levels  $\alpha$  and  $\beta$  which are mathematically inconsistent with the formula. It is possible to determine the precise values of  $\Pr(\pi \geq \pi_0)$  and  $\Pr(\pi \leq \pi_1)$  for which (20) and (21) apply. Considerations given later suggest that ESS be limited which will in effect avoid this problem.

Example. This example uses equations (14)-(21) to compute  $n$  and  $c$  from  $M$  and ESS. Only the results of the calculations are shown. Test parameters are assumed to be  $\alpha = \beta = 0.10$ ,  $\pi_0 = 0.90$  and  $\pi_1 = 0.80$ . Results of the computations for 5 different priors are given in table 2.

Table 2.  $n$  and  $c$  values for 5 different priors

ESS	M	$\gamma$	$\lambda$	$k_0$	$k_1$	$\alpha_0$	$\beta_1$	$n$	$c$
—	—	1	1	1.0000	1.0000	0.1000	0.1000	80	70
10	0.80	9	3	1.1173	1.2960	0.1117	0.1296	66	57
20	0.80	17	5	1.9175	1.3652	0.1917	0.1365	50	42
20	0.85	18	4	0.6580	2.1600	0.0658	0.2160	59	51
20	0.90	19	3	0.2844	3.8660	0.0284	0.3866	55	47

A Sequential Bayesian Test. Sequential tests are known to provide significant savings in average sample size when compared with fixed sample test of the same size and power. Due to the difficulties of testability demonstration it seems worthwhile to consider sequential tests. A Bayesian sequential test is given in [9]. The test seems to have found little application, probably due to the difficulty in computing the test parameters. By contrast the non Bayesian sequential test is a very simple test and when used with truncation is well accepted by test engineers [10]. The Bayesian test based on EMR control developed in this report reduces the Bayesian test to a standard fixed sample test with modified error probabilities  $\alpha_0$  and  $\beta_1$ . This simplification suggests that a sequential test could be used for this portion of the demonstration to increase test efficiency.

Test Sample Size, ESS and Information. Table 2 demonstrates the influence of mode on the test sample size  $n$  for a fixed ESS. This effect is common to all Bayesian tests. As the mode of a prior increases ( $M \geq 0.5$ ) the information content increases. This in turn gives the prior more influence which reduces the number of test samples required to control the risks. If for example  $\Pr(\pi \leq \pi_1)$  is sufficiently small there is no risk in accepting  $H$  with no data.

The term dominance has been used to describe the relative influence relationship between the prior information and the data as expressed by the likelihood function [7]. In reliability applications the tendency is to have prior dominance due to expense of testing. It appears from the previous example that it will be relatively easy to unintentionally impose complete dominance of the prior because of the sensitivity of information content of a prior to the mode when it is near 1. For example a mode of 0.95 may be suggested for the prior. However when combined with an ESS of 20 no additional samples are required to satisfy risks of  $\alpha = \beta = 1$ . Realizing the practical limitations on prior information accuracy it seems inappropriate to permit a decision based on prior information alone. There may be some situations in which such action may be acceptable but in general these cases would seem to be exceptions. The need to provide some direction to control dominance of the prior density is evident. The control can be expressed as a limitation on ESS as a function of  $M$ ,  $\alpha$  and  $\beta$ .

IV. RECOMMENDATIONS. The purpose of this study was to investigate the use of Bayesian analysis in testability demonstration. The study covers availability and use of prior information. Two demonstration plans are developed in detail so that strengths and weaknesses can be compared. Significant contributions have been made in two areas. First the introduction of equivalent sample size of the prior provides an intuitive method of quantifying prior information. Second, risk control by limiting the expected maximum risk greatly simplifies the test format when compared with the standard Bayesian test.

(1) It is recommended that efforts be made to set up a repository of field information and previous demonstrations on BIT and other fault diagnosis methods which can be used as prior information for future demonstrations.



(2) Guide lines should be established to control the maximum amount of information which can be supplied by the prior. A table or graph can be used to express the guide lines.

(3) The operating characteristics over a limited range of prior densities and hypotheses should be studied for the standard Bayesian test and the new test based on control of expected maximum risk so that test comparisons may be made.

(4) Bayes sequential tests based on control of expected maximum risk should be developed and the operating characteristics should be compared with the fixed sample alternative.

#### REFERENCES

1. Klion, J., A Rational and Approach for Defining and Structuring Testability Requirements, Griffiss AFB, NY, Rome Air Development Center, RADC-TR-85-150, 1985
2. ARINC Research Corp., Predictors of Organizational-Level Testability Attributes, Annapolis, MD, ARINC Research Corp., Pub. 1511-02-2-4179, 1986
3. Hudson, C.L., Jr., Introduction to Design for Test for VLSI Circuits, Plymouth, Minnesota, Honeywell, Inc., 1986
4. Albert, J.H., M.J. Partridge, and R.J. Spillman, Built-In-Test Verification Techniques, Griffiss AFB, NY, Rome Air Development Center, RADC-TR-86-241, 1987
5. Canfield, R.V. and Teed J.C., "Selecting the prior distribution in Bayesian statistics", IEEE Trans. on Rel. Oct. 1977 Vol R-26:283-285
6. Coppola, A., Bayesian Reliability Tests Made Practical, Griffiss AFB, Rome Air Development Center, RADC-TR-81-106, 1981
7. Zacks, S., The Theory of Statistical Inference, NY, John Wiley and Sons, 1971
8. Abramowitz, M. and I.A. Stegun, (ed.), Handbook of Mathematical Functions, Washington D.C., National Bureau of Standards, Applied Math. Series 55, 1964
9. Mann, N.R., R.E. Schafer and N.D. Singpurwalla, Methods for Statistical Analysis of Reliability and Life Data, NY, John Wiley and Sons, 1974
10. Balaban, H., Maintainability Prediction and Demonstration Techniques, Vol. 2, Griffiss AFB, NY, Rome Air Development Center RADC-TR-69-356, 1970
11. Martz, H.F. and R.A. Waller, Bayesian Reliability Analysis, NY, John Wiley and Sons, 1982

1987 USAF-UES SUMMER FACULTY RESEARCH PROGRAM/

GRADUATE STUDENT SUMMER SUPPORT PROGRAM

Sponsored by the

AIR FORCE OFFICE OF SCIENTIFIC RESEARCH

Conducted by the

Universal Energy Systems, Inc.

FINAL REPORT

HYPERTEXT AND THE INTEGRATED MAINTENANCE INFORMATION SYSTEM (IMIS)

Prepared by: Patricia Ann Carlson

Academic Rank: Professor

Department and  
University: Rhetoric  
Rose-Hulman Institute of Technology

Research Location: AFHRL/LRC  
Wright-Patterson AFB  
Dayton, Ohio 45433

USAF Researchers: Robert Johnson  
Donald Thomas  
David Gunning

Date: August 10, 1987

Contract No.: F49620-85-C-0013

# HYPERTEXT AND THE INTEGRATED MAINTENANCE INFORMATION SYSTEM (IMIS)

by

Patricia Ann Carlson

## ABSTRACT

The Integrated Maintenance Information System (IMIS) concept is to provide the technician with all logistical, operational, technical, training, and diagnostic information for aircraft repair. Because of the sheer amount of information being integrated, user overload is a significant concern.

The traditional solution to this problem of presenting complex information in a timely fashion is to design a consistent display format and to employ standard commands. At a deeper level, however, questions of information integration become issues of information engineering and the nature of knowledge structures.

At this level, the definition of user interface takes on a more sophisticated meaning. The hypertext concept considers a body of knowledge as a database -- potentially, a highly organized, compressed structure of richly interconnected "chunks" -- and allows for flexible indexing and retrieval by implementing a "smart" interface (a programmable "idea processing" mechanism).

Hypertext, as the backbone for development philosophy, permits advanced design features -- such as enhanced functionality, customized views, and improved knowledge synthesis and representation -- which, in turn, increase the user's ability to interact productively with information.

#### ACKNOWLEDGEMENTS

I wish to thank the Air Force Systems Command and the Air Force Office of Scientific Research for sponsorship of this research. Also, I wish to thank the Air Force Human Resources Laboratory, Logistics and Human Factors Division personnel at Wright-Patterson AFB under the command of Colonel Donald C. Tetmeyer for a rewarding and professionally enriching summer. In particular, I wish to acknowledge Mr. Bertram Cream (Division Technical Director) for serving as my Effort Focal Point.

Many people helped to make my experience both pleasant and challenging. David Gunning suggested the topic of "hypertext" and supplied the initial reading and bibliography. Robert Johnson (the IBC Branch Head) provided ideas for focusing the topic. Donald Thomas (Senior Scientist) provided help with the specifics of the project as well as guidance for the overall approach. To all these people, I express my gratitude for encouragement and support.

## I. INTRODUCTION:

The Air Force Human Resources Laboratory (AFHRL), Logistics and Human Factors Division is working on a prototype information management system for aircraft maintenance. The following excerpt summarizes the functionality envisioned for the full Integrated Management Information System (IMIS) concept:

The system will display graphic technical instructions, provide intelligent diagnostic advice, provide aircraft battle damage assessment aids, analyze in-flight performance and failure data, analyze aircraft historical data, and access and interrogate on-board built-in-test capabilities. It will also provide the technician with easy, efficient methods to receive work orders, report maintenance actions, order parts from supply, and complete computer-aided training lessons and simulations. The portable computer will make it possible to present quality information by taking advantage of the computer's ability to interact with, and tailor information to, technicians with varying levels of expertise. (IMIS, 1986)

For the past few years, I have focused my research on methods to improve technical documentation. I have been particularly interested in document design -- a discipline concerned with the substance, structure, syntax, and style of text written for a specific function.

In the past I have done research projects in document design under the NASA/ASEE (American Association for Engineering Education) Summer Faculty Research Program. Much of my work has been in the area of system design for online technical and instructional data. Representative areas of my research include:

- o Screen format for online text -- including issues of menu design, error messages, and data entry.
- o User support requirements in large, complex computing facilities.
- o Rhetoric and software problems in the design of a dynamic book.

- o Modeling user interaction with text under a variety of conditions and constraints.

## II. OBJECTIVES OF THE RESEARCH EFFORT:

Large-scale and long-term research projects, especially those which seek to incorporate (and even to drive) the leading edge in hardware technology and software engineering have a potential to lose their identity over time and/or become different things to different working groups. In addition, ambitious projects which seek to pull together a number of on-going and emerging technologies run the risk of becoming a collage rather than a composite. By its very nature, the IMIS project faces both identity warp and loose integration as development takes place over time.

I was asked by my HRL/LRC colleagues to assess the potential for the hypertext concept to serve as a unifying philosophy for IMIS.

Ideally, a unifying design philosophy provides a global frame of reference and has these characteristics:

- o Mirrors the deep structure of the project's goals and objectives.
- o Is clear enough to provide direction, but flexible enough to accommodate meaningful change.
- o Is understandable and acceptable to all constituencies of the design and development team.
- o Precipitates practical benefits for the end user, such as ease-of-use, consistency of delivery, improved job performance.
- o Demonstrates advantages for the total system, such as lower overhead and improved integration.

My project as a participant in the 1987 Summer Faculty Research Program

(SFRP) was to investigate the benefits of integrating hypertext into the IMIS project. This report is a condensed summary of my findings. The results of my study are reported in a paper document modeled on hypertext. In other words, the full document is both a repository of information and a demonstration of principle.

### III. THE HYPERTEXT CONCEPT:

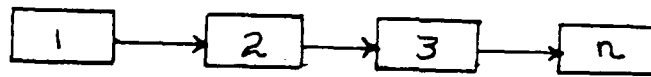
a. Hypertext is based on the notion that human idea processing occurs through association. Although the idea was discussed by H.G. Wells (1938) and more fully expounded by Vannevar Bush, President Roosevelt's Science Advisor (1945), the term itself originated with Ted Nelson (1974). Despite their radically different intellectual backgrounds, all three men describe hypertext as an electronic means for enhancing four categories of idea processing:

- o Reading: goal-oriented (information seeking) navigation through a large, unstructured library of information - casual browsing through a pool of text and graphics.
- o Annotating: recording ideas dynamically generated while reading text (including critiquing); explicating difficult passages; storing user-produced mnemonic aids; communicating with the library manager and/or other users.
- o Collaborating: electronic conferencing and/or multiple authoring of complex documents.
- o Learning: accommodating varying learning styles, varying speeds of ingesting materials, and personalized structuring of bodies of information.

A hypertext system uses online capabilities to overcome the limitations of the linear nature of printed text. Paper text (or flat text) provides only two-dimensions of information processing: linear and hierarchical.



## LINEAR TEXT



## HIERARCHICAL FLOW OF INFORMATION

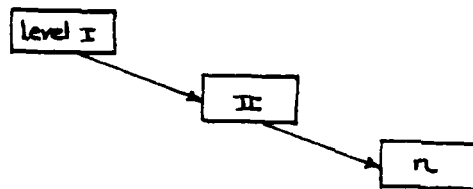


Figure 1: 2-D Information Processing

A hypertext system more closely models the deep structure of human idea processing by creating a network of nodes (modules) and links (webs), allowing for three-dimensional navigation through a body of data.

- o Modules: pools of information collected in one anthology, labelled or typed, and electronically stored as nodes in a database.
- o Webs: the pattern or links among the nodes. The links can be predefined by the hypertext system designer or the user(s) can establish the links as part of walking through the information domain.

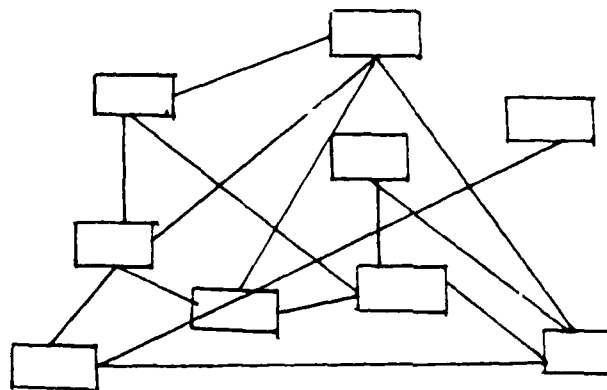


Figure 2: 3-D Information Processing

The pattern of links (the web) represents the internal logic or knowledge structure.

b. "Hypertext" received some attention in the '60s and '70s -- with a few major systems being designed and either fully or partially implemented (Englebart, 1963; Nelson, 73). During the late '70s and the '80s, increasing attention has been given to the concept as a potential method for dealing with a number of problems engendered by the information explosion.

As background for my project, I read numerous accounts of the hypertext philosophy and of hypertext-based systems. From this reading, I isolated two central components crucial to any hypertext system. I then used the questions surrounding these essential elements as the focal points for my research.

- o a database: which can be -- (1) a large, loosely structured library of documents which have been placed online directly from hardcopy, (2) a highly organized, compressed, structure of richly interconnected "chunks," which have meaningful boundaries between sets and subsets and logical relationships among elements, (3) a variation of organization somewhere between these two extremes. (See Section V below.)
- o an assistance processor: a retrieval mechanism (or a collection of retrieval mechanisms) for effective access to and management of the database. (See Section VI below.)

As a rule-of-thumb, one can say that there is a reciprocity between the amount of design put into each element. Relatively unformatted libraries require more complicated software in the retrieval mechanisms, if the user requires fine-grained applications. Text which has been specifically preprocessed for the system service requires less

complicated software.

In addition, based on my research, I made the following four observations on hypertext:

**Classic Hypertext:** Theoreticians of hypertext have promoted the system as an enhancement for reading and learning a complex body of knowledge and for capturing ideas spontaneously created by the mind during the reading process. On this level, hypertext becomes a macro literary system, consisting of a very large online library (envisioned by the most enthusiastic of hypertext supporters as a global knowledge representation) in which inter-document links are machine supported and all reading, writing, collaboration among users, and criticism/annotation take place via the hypergraph (Conklin, 1987). This vision of hypertext is best suited to a situation where the user: (1) is under little stress and few constraints, (2) is engaged in a fairly complex, open-ended problem, and (3) is intelligent and inquisitive enough to appreciate "free-planing" through a large information structure.

**Applied Hypertext:** Recently, hypertext has been used in systems intended for more utilitarian purposes. These applications exploit hypertext for a range of specific uses; therefore, each system has its own collection of functions and features.

Two categories of applications are:

- o **Problem Exploration Tools:** systems which support early unstructured thinking on a problem, in which many disconnected ideas come to mind, such as early authoring and outlining (idea processing), problem solving, and software development. (Example applications include Issue Based Information Systems (IBIS) -- which organizes electronic conferencing -- and the various electronic outline processors and notecard packages commercially available).

- o Browsing/Structured Reading/Reference: Read-only systems for teaching, for reference, and for public distribution of information. (Example applications include Emacs INFO Subsystem, the Symbolics Document Examiner, and TIES, an application that allows museum-goers to browse through explanations while viewing exhibits.)

Advantages: Whether one defines hypertext as the classic, free-form adjunct to creativity or as a relatively structured performance aid (as it manifests itself in many applications), the model improves information processing in the following ways:

- o Provides electronic support for techniques of processing information which humans have developed over centuries of dealing with written representations of bodies of knowledge.
- o Enhances conventional information processing by improving current-traditional procedures (e.g. indexing and footnotes) and by adding capabilities (backtracking through text, unlimited branching, layering information, task- or user-specific paths).
- o Allows for representation of internal logic patterns within a body of information by emulating the AI concept of semantic networks. (Most hypertext systems allow the user to view the hypergraph through a graphics representation of the web.)

Disadvantages: Drawbacks to hypertext come in two forms: those which are limitations of current implementations and those which appear to be intrinsic to the concept itself (Conklin, 1987).

- o Disorientation: freedom and flexibility create confusion unless there are many navigational aids in the user interface.
- o Modularization: determining what constitutes a node (establishing sets and subsets); addressing issues of style, structure, substance, syntax for individual frames (establishing contextuality, readability, consistent meaning).
- o Cognitive Overhead: in a free-form system, the user must constantly make meta-level judgments about the flow of ideas; even in relatively structured systems, the user runs the risk of needing to monitor too many levels or modes of presentation.

#### IV. HUMAN TEXT PROCESSING:

a. The essence of hypertext is not a new idea. It is, however, an idea whose technology has arrived. Because of this, hypertext has increasingly become a buzz word in the information industry and is used to cover a range of ideas. As an illustration, the program for a small, one-day conference on "Writing for the Computer Industry" (MIT, August 15, 1987) lists the following presentations:

- o "Using Hypertext to Document Software Applications"
- o "Nonlinear Writing in a Linear World"
- o "Case Study for Volume One of Inside Macintosh: Merging Linear Authoring and Nonlinear Associative Use for Technical Documentation"
- o "Designing an Interface for Writers and Users of Hypertext"
- o "Using an Object-Oriented Programming Language to Extend the Capabilities of a Hypertext System"
- o "Hypertext and the Teaching of Writing"

However, this exposure should not imply that hypertext is a gimmick. To the contrary, the concept appears to be a convenient and correct cognitive model for many of the issues facing modern information processing. In addition, it has two qualities essential to a field paradigm: (1) it is simple at its root, (2) it has seemingly infinite expansibility and adaptability.

b. In order to suggest what benefits accompany an electronic hypertext system, I examined its leading competitor: the current-traditional method of dealing with information -- a hardcopy, linear prose representation.

Because of my experience with document design, I contend that most

articles on hypertext overstate the case against "flat" text. They concentrate on the inflexibility of the printed word, the sequential nature of the presentation, and the sheer bulk of text mandated by conventional composition patterns, such as the paragraph.

However, few documents are read from cover-to-cover in the lock-step, serial fashion depicted by hypertext advocates. To the contrary, good documents are designed to facilitate rapid perusal. Furthermore, sophisticated readers know how to navigate through a text without savoring each individual word.

Skilled readers have a number of strategies and tactics for extracting meaning quickly from paper documentation. Some examples of functionality gained through training or experience include:

- o Various methods of perusal -- e.g. thumbing, glancing, skimming, and browsing.
- o Individual markup techniques -- e.g. writing in the margin or on the end papers corrections, summaries, mnemonic devices, commentary, conversion of prose to tables and graphs, lists, cross-references, key terms, diagrams, indexing aids.
- o Placing bookmarks or "dog ears," marking trails in various manners.
- o Intuiting place and content through visuo-spatial cues.
- o The psychological benefit of tactile contact with paper documentation (a form of hand-eye-brain relationship not yet fully researched).

In addition, modern methods of document design greatly increase ease-of-use, timeliness of information, and accessibility in a paper delivery system. Design techniques include:

- o Alternatives to the paragraph as the basic unit of prose (e.g. structured writing and information mapping, other devices for information compression).
- o Improved printing and graphics technology, including the

emergent capabilities of desktop publishing.

- o Improved techniques for indexing, referencing, and branching.
- o Integrated graphics which signal knowledge structure (e.g. visual table of contents and logos as signposts).
- o Mapping presentation to user needs (e.g. task orientation versus reference function).

Any electronic information delivery system must be able to -- at a very minimum -- duplicate the capabilities provided by the combination of an experienced reader and a well-designed text. Anything less degrades the system: leaving at best, an electronic page-turner; at worst, even less than the paper version. Furthermore, in order to justify abandoning the conventional method and medium, an electronic system should offer improvements, such as increased flexibility, reduction in storage, and convenient document development/maintenance.

As a framework for the remainder of my work, I concentrated on the natural analogy between the two elements of the traditional, paper system (skilled reader and structured text) and the two elements of a hypertext system (assistance processor and designed -- or modularized -- documentation).

#### V. ASSISTANCE PROCESSOR ISSUES:

- a. The assistance processor is a retrieval mechanism (or collection of retrieval mechanisms) used for effective access to and management of the collection of "chunks" making up the information domain.

Some requirements for IMIS information retrieval software include:

- o Duplicate the reader's capabilities (both strategic and tactical) for using paper text.
- o Demonstrate increased functionality over paper-based information delivery system in a particular application environment.
- o Support various constituencies in the user community (in the case of IMIS: aircraft technicians, trainers, documentation managers, weapon systems vendors, etc.)
- o Accommodate modes (types of information delivered -- e.g. technical, logistical, training, etc.), facilitate graceful transition among modes, and integrate into an easily used synthesis (meta-modes).
- o Point toward the integration of expert systems and other AI functions.
- o Incorporate -- even on a rudimentary level -- filters based on content analysis and navigational devices based on logic representations.

b. I examined three specific areas where intelligent retrieval mechanisms are intrinsic to the full IMIS concept:

- o Tailoring Individual Views: Accommodating the end user is important for system acceptance. IMIS can best serve its users by having layers of interfaces, which are progressively more sophisticated and increasingly more personalized (perhaps through user programming). Level I allows the user to select font characteristics, suppress generic content (e.g. generalized system greetings and messages), and otherwise make decisions about items of personal preference, ease-of-use, and comfort (for example, right handed versus left handed operations). Level II allows choices dealing with session management style, annotation, and navigational aids in a predefined web. Level III allows the advanced user to change the sequence of information (to leave the predetermined link network and to create an individualized web).
- o Modes and Meta-modes: Full IMIS integrates a number of functions (job aiding, training, troubleshooting, collecting logistical data, displaying personnel management information, etc.). Deciding how these functions might be bundled in the user interface is crucial to the total IMIS knowledge synthesis.
- o Document Management and Text Maintenance: the technician is not the only user who will benefit from IMIS. Automation results in more effective and efficient management of technical orders by supporting: (1) collection of usage data, (2) electronic mail/error reporting, (3) automated field testing of TOs, (4) gleaning individual views (networks of links) for patterns which might be useful to the whole user community, (5) faster and more



consistent updating and corrections, (6) improved turnaround time on user error reports.

## VI. TEXT DESIGN ISSUES:

a. A paper-based information delivery system is improved if the material has been preprocessed for the reader. This same idea of designing information so that it accommodates the user's needs and reflects the structure of the knowledge domain should be applied to online information delivery systems.

Some issues in information design for a hypertext system include:

- o Determining the boundaries of modules (in essence, defining what constitutes a node and allowing for composite nodes while sustaining contextuality).
- o Screen design issues (e.g., format, menu structure, error messages, text screen design, data entry, etc.).
- o Definition of internal logic (webs to structure the domain).
- o Authoring system capabilities (leading ultimately toward end-to-end technical order automation).
- o Integration of graphics.
- o Employing visuo-spatial control of information.
- o Documentation management enhancements (leading toward end-to-end automation).

b. I examined three specific areas where substantial benefits could be realized from carefully designed content nodes.

- o Authoring System: HRL/LRC has developed an authoring system -- Authoring and Presentation System (ASP) -- to help in placing technical orders on line. Nevertheless, human judgment is required for structuring the tracks (or layers of information). This segment of my research suggested some ways in which this overhead might be lessened by exploiting the effort already expended in the carefully written paper job guides (Duffy, 1985).
- o Logic Analysis/Content Analysis: Both topics are ambitious when

applied to natural language text. True automated content analysis of documentation may be years away. Nevertheless, text can be stored in such a way as to make its underlying structure explicit. For example, the Standard Generalized Markup Language (SGML) identifies the type for each segment and may be used to generate maps from which logic patterns can be inferred. Such graphic representations serve as navigational aids in the pool of information.

- o Visuo-spatial Management of Information: User overload is a major human factors concern in any information integration system. Although little scientific evidence supports the contention that visuo-spatial (e.g. use of icons) representation and retrieval is easier than symbolic (words and numbers), the success of workplace metaphors in commercial systems warrants considering spatial management devices in the IMIS interface.

## VII. IMPLEMENTATION SCENARIOS:

- a. By necessity, any large design project is undertaken by addressing the parts of the larger problem. Integration takes place as the various pieces are developed because of management expertise and an organizational master plan.

IMIS research takes place on several different levels. Proof of concept, development, and implementation involve parallel research on several software and hardware projects. A partially ruggedized, portable computer/display unit (PCMAS), an authoring system for creating online technical orders (AFS), and a fault isolation system for troubleshooting (MDAS) are examples of issues in hardware design, software tools, and AI applications currently being examined by aggregates of military, civil service, and contractor personnel.

However, for the IMIS concept to work, the various parts must fit seamlessly together in the user interface and the system should exhibit a graceful transition through three important stage of growth: Integrated

PCMAS and MDAS, Intermediate IMIS, and Full IMIS.

I selected the issue of user interface -- as manifested in screen design -- as a reasonable and observable indicator of how hypertext serves as a development backbone for IMIS.

b. In this section of my project, I applied some of the notions discussed in the above sections. Specifically, I devised an implementation scenario by suggesting interface designs for specific phases of integration. In order to work methodically, I constructed a taxonomy of expected/required functionality and of screen types for the identified stage of IMIS. I then prepared candidate screens for areas of the taxonomy.

This study did not collect user acceptance data; however, my conclusions do touch on the advantages -- from a human factors point of view -- for various IMIS constituencies accruing from my simulations of interface design.

#### VIII. RECOMMENDATIONS:

Hypertext is still more of a notion than a developed idea. Nevertheless, I recommend using it as a central thread upon which to string the IMIS system precisely because of its emergent quality. Although a simple concept at its root, hypertext offers many higher-level design advantages.

We are now seeing only the beginnings of hypertext reflected in

commercial products, but it seems safe to predict that the notion of three-dimensional idea processing will capture the imagination of the software industry the way top-down programming dominated software engineering/management a few years ago. In a hypertext survey report done for MCC, the author asks his reader to ". . . come away from this paper excited, eager to try using hypertext for yourself, and with the sense that you are there at the beginning of something big, something like the invention of the wheel, but something that still has enough rough edges that no one is really sure that it will fulfill its promise" (Conklin, 1987).

More specifically, I recommend continued work in five areas:

- o Treating documentation as a database opens IMIS up to all the novel approaches to information retrieval currently under development (Armstrong, 1987). Not only does this keep options open, it also increases the likelihood that designers can squeeze more functionality out of the system without increasing the overhead.
- o Hypertext mirrors human information processing and, therefore, has ties with AI research (e.g. semantic networks) and second-generation expert systems (modeling heuristics rather than rules). Hypertext, as a backbone for IMIS, allows for integration of future developments in these areas.
- o Unification of design principles comes through awareness and acceptance. Therefore, hypertext should be promoted in a variety of ways. An in-house advocacy group could collect and discriminate information. Other support mechanisms include a demonstration project (perhaps a hypertext on hypertext), position papers on IMIS and hypertext, and bringing in outside lecturers/consultants, perhaps even sponsoring a conference on hypertext.
- o Unification can encourage early prototyping -- that is, specific images of what the finished system might look like. Scenarios depicting the functionality of IMIS (Brandt, 1986) should now incorporate more concrete representations of information integration -- specifically, candidate interfaces (including mockups of screen designs). Such simulations serve as a "look ahead" device for guiding research and focusing development work; as such, they serve as a feedback loop in the process.

- o Hypertext is an alluring idea having both theoretical and pragmatic dimensions. In addition, it addresses many of the problematic areas in modern information management. As such, it will undoubtedly be exploited by industry. HRL/LRC should monitor commercial applications for innovative uses of the concept.

• REFERENCES

Armstrong, Anne A., Navigating with Search Software, Federal Computer Week, July 13, 1987, Vol. 1, no. 16, pp. 26-27, ff.

Brandt, Craig M., et al., Training Technology Scenarios for an Integrated Automated Job Aiding/Training System, Draft Version, 1986. Systems Exploration, Inc. Contract No. F33615-85-C-0010.

Bush, Vannever, As We May Think, The Atlantic Monthly, July 1945, Vol. 176, no. 1, pp. 101-108.

Conklin, Jeff, A Survey of Hypertext, MCC Technical Report No. STP-356-86, Rev. 1, February 9, 1987.

Duffy, Thomas, Preparing Technical Manuals: Specifications and Guidelines, in The Technology of Text: Principles for Structuring, Designing, and Displaying Text, Vol. 2, David H. Jonassen, Ed. Englewood Cliffs, New Jersey, Educational Technology Publications, 1985, pp. 370-392.

Engelbart, D. C., A Conceptual Framework for the Augmentation of Man's Intellect, in Vistas in Information Handling, F. Howerton, Ed. Washington, D.C., 1963, pp. 1-29.

IMIS: Integrated Maintenance Information System -- A Maintenance Information Delivery Concept, unpublished paper, AFHRL LSC, Wright-Patterson AFB, August 1986.

Nelson, T.H., Computer Lib/Dream Machines, Chicago, Illinois, Hugo's Book Service, 1974.

Nelson, T.H., A Conceptual Framework for Man-Machine Everything, AFIPS National Computer Conference and Exposition Proceedings, 1973, Vol. 42, Montvale, New Jersey, AFIPS Press, pp. M21-M26.

Wells, H.G., World Brain, Garden City, New York, Doubleday, Doran & Co., 1938.

1987 USAF-VES SUMMER FACULTY RESEARCH PROGRAM/  
GRADUATE STUDENT SUMMER SUPPORT PROGRAM

Sponsored by the  
AIR FORCE OFFICE OF SCIENTIFIC RESEARCH

Conducted by the  
Universal Energy Systems, Inc.

FINAL REPORT

SUPPLEMENTAL TO THE FINAL REPORT

Prepared by: Awo-Sun Chu, Ph.D.  
Academic Rank: Associate Professor  
Department and: Department of Physics and  
Computational Sciences  
University: Talladega College  
Research Location: AFMAL/MLPO  
Wright-Patterson AFB  
Dayton, OH 45433-6533  
USA Researcher: Patrick A. Hemenger, Ph.D.  
William L. Mitchell, Ph.D.  
Date: 17 Aug 87  
Contract No. F49620-85-3-0013



# Dopant diffusion in nipi Semiconductor Superlattices

by

Kwo-Sun Chu

## ABSTRACT

Matrix elements of dopant diffusion tensor parallel and perpendicular to the crystal growth direction in a nipi semiconductor superlattice are obtained using the time expansion of the momentum autocorrelation function technique. Truncation of the series is justified by a self-consistent scheme in which the concept of the memory of the system is employed. Superlattice potential is taken as the superposition of the space charge potential and the host substrate lattice potential. Numerical calculations are carried out for Si and Be doped GaAs superlattice.

### Acknowledgements

The authors would like to express their sincere appreciation to the Air Force Office of Scientific Research, Air Force Systems Command for the financial support which made this research possible. Thanks is also extended to the University Energy Systems for their services rendered and to the Materials Laboratory, Air Force Wright Aeronautical Laboratories for their support and hosting of this investigation.

## I. INTRODUCTION

My research interests are diversified in many aspects of theoretical physics. Theoretical formulations of physical problems and their practical applications are my forte. I had the opportunities to become involved in particles interacting with quantum fields in semiconductor, molecular statistical theory of polar correlation function, phase transition, and transport properties in liquid crystals and multicomponent systems, classical nucleation, and kinetic theories of stratospheric aerosols' evolution and thermodynamic properties, fluid dynamic behavior of aerosol deposition in the human lung, laser scattering and Freederick's transition, mechanical properties of metal alloys, etc.

The recently developed in-house research program in semiconductor superlattices in the Materials Laboratory brought me to the joint summer research efforts in the theoretical investigation of this relatively new field.

## II. OBJECTIVES OF THE RESEARCH EFFORT

The long-range goals of this research are (1) to achieve the high performance of device applications using specially tailored electronic and optical properties of synthetic semiconductor superstructure materials, and (2) to establish the foundation for non-linear optics studies of semiconductor superlattices and their potential.

new innovative device applications

The short-range preliminary objectives are

- (a) Feasibility studies of semiconductor superlattices in general,
- (b) Investigation of computational methods in band theory, in particular, the adaptability of the Linear Muffin-Tin Orbitals (LMTO) method to superlattice structures,
- (c) Analyzing the LMTO software package for the band structure calculations and entering it into the Materials Laboratory computer facilities for future usage.

During our course of investigation, upon the decision of a group composed of two in-house researchers, two summer faculty members, and one contractor, our initial tasks focused on the nipi superlattice band structures and non-linear optical absorption. With these guidelines, the following immediate objectives were developed to acquire the necessary background information for the band structure calculations of nipi superlattices. They are

- (d) To obtain dopant diffusivity in nipi superlattices,
- (e) To procure the time evolution of dopant distribution during annealing, and thus, the final dopant profile in nipi superlattices.

### III. RESEARCH RESULTS FOR PUBLICATION

- (a) Dopant Diffusion in nipi Semiconductor Superlattices
- (b) Time Evolution of Dopant Distribution during Annealing

DOPANT DIFFUSION IN NIP1 SEMICONDUCTOR SUPERLATTICES\*

by

A.S. Chu,\*\* W.C. Mitchell, and P.M. Hemenger

Materials Laboratory, Air Force Wright Aeronautical Laboratories,  
Wright-Patterson Air Force Base, Ohio 45433-6533

\* Research sponsored by the Air Force Office of Scientific Research/AFSC, United States Air Force, under Contract W-49(2)-63-0-0013

\*\* Air Force Office of Scientific Research Summer Faculty Fellow.  
Permanent Address: Department of Physics and Computational Sciences,  
Talladega College, Talladega, Alabama 36180

# ABSTRACT

Matrix elements of dopant diffusion tensor parallel and perpendicular to the crystal growth direction in a nipi semiconductor superlattice are obtained using the time expansion of the momentum autocorrelation function technique. Truncation of the series is justified by a self-consistent scheme in which the concept of the memory of the system is employed. Superlattice potential is taken as the superposition of the space charge potential and the host substrate lattice potential. Numerical calculations are carried out for Si and Be doped GaAs superlattice.

## 1. INTRODUCTION:

Dopant concentrations and distributions are the main ingredients in the band structures of doped superlattices (SL's), in addition to, the artificially imposed superlattice periodicity. The doping profile consequently, gives rise to a large number of novel properties of the SL's, such as, tunability of the carrier concentration, of the band gap, of the sub-band separation, and of the optical absorption coefficient. In turn, many device applications can result from these intriguing phenomena, as well as from the heterostructure superlattices.

The dopant profile is reached through the diffusion mechanism, which was shown in a doped bulk semiconductor.<sup>1-4</sup> Early efforts in the transport measurements of compositional superlattices were made by Esaki et al.<sup>5,6</sup> Recent studies of the effects of dopant diffusion<sup>7-11</sup> on the quantum well destruction phenomenon, superlattice fabrication, the annealing process, and photoluminescence have been carried out. Neither calculated nor measured dopant diffusion coefficients in SL's superlattices were reported. The steady enhancement of heteroepitaxy techniques in superlattice growth increasingly requires knowledge of dopant diffusion coefficients. It is the purpose of this report to reveal our findings of such transport properties.

Since the transport coefficients can always be expressed in terms of certain time autocorrelation functions, one would naturally proceed to solve this type of problem by solving an associated memory function equation which describes the time evolution of the time autocorrelation



function, or by establishing a proper Fokker-Planck equation and solving it to obtain the transition probability between two states. In a superlattice structure, however, these approaches are becoming more too complicated and difficult. An alternative method for this purpose must be used.

One widely used technique is the time expansion of the autocorrelation function.<sup>12-18</sup> with this approach, the transport coefficients can be calculated directly through the dynamical variables of the system. The results have proven to be in remarkably good agreement with the computer experiments<sup>16-20</sup> of the Monte Carlo procedure and molecular dynamics.

## II. Time Expansion of the Momentum Autocorrelation Function.

Let us consider dopant diffusion in a semiconductor superlattice of nipi structure. Let  $V(r)$  denote a one-body potential experienced by a referenced dopant particle in the superlattice. This particle can be either a neutral donor or acceptor or an ionized donor or acceptor; however, we will deal with that later. The diffusion coefficient can be calculated from the momentum autocorrelation function

$$D = (3m^2)^{-1} \int_0^\infty \langle \vec{p}(0) \cdot \vec{p}(t) \rangle dt \quad (1)$$

where  $m$  is the mass of the dopant particle, the  $\vec{p}(t)$  is its momentum at different times.  $\langle \dots \rangle$  indicates the equilibrium time average. Since  $\vec{p}$  is a dynamic variable, it obeys the equation of motion and its evolution in time is governed by

$$\vec{p}(t) = e^{iLt} \vec{p}(0) \quad (2)$$

where  $e^{iLt}$  is the time displacement and  $L$  is the Liouville's operator. Expansion of the time displacement operator into a power series yields

$$\begin{aligned} \langle \vec{p}(0) \cdot e^{iLt} \vec{p}(0) \rangle &= \sum_{n=0}^{\infty} \langle \vec{p}(0) \cdot (iL)^n \vec{p}(0) \rangle \frac{t^n}{n!} \\ &= \langle p^2 \rangle + \langle \vec{p} \cdot \dot{\vec{p}} \rangle + \langle \vec{p} \cdot \ddot{\vec{p}} \rangle \frac{t^2}{2!} + \langle \vec{p} \cdot \dddot{\vec{p}} \rangle \frac{t^3}{3!} + \dots \end{aligned} \quad (3)$$

where the dots denote the different time derivatives.

Due to the fact that the momentum autocorrelation function and the ensemble average is taken, irregardless of which particle at which time is being used as a reference particle, all the coefficients of the odd terms of  $t$  in equation (1) should vanish. So we have, for example, the first order term

$$\langle \vec{p} \cdot \dot{\vec{p}} \rangle = 0 \quad (4)$$

This is always true when the dispersion of a dynamic variable is a stationary process. From the equipartition theorem, we have

$p^2 = 3mk_B T$ . The time derivative of it lead to equation (4). This can also be derived directly from the properties of the vector representation of the random process defined in the Hilbert space. A clear picture of equation (4) on its physical basis can be shown by writing

$$\langle \vec{p} \cdot \dot{\vec{p}} \rangle = m \left\langle \frac{d\vec{r}}{dt} \cdot (-\nabla H) \right\rangle \quad (5)$$

Assuming that the hamiltonian depends upon the coordinates only through the potential, one has

$$\langle \vec{p} \cdot \dot{\vec{p}} \rangle = -m \left\langle \frac{d\vec{r}}{dt} \cdot \nabla V \right\rangle = -m \left\langle \frac{dV}{dt} \right\rangle = 0 \quad (4)$$

If the isolated system is at its equilibrium state, the ensemble average of the time derivative of the potential vanishes. The time derivative of equation (4) gives

$$\langle \dot{p}^2 \rangle = - \langle \vec{p} \cdot \ddot{\vec{p}} \rangle \quad (5)$$

and the time derivative of the equation of motion gives

$$\ddot{p}_i = \frac{d}{dt} \left( - \frac{\partial H}{\partial \dot{q}_i} \right) = - \frac{\partial}{\partial q_i} \frac{dV}{dt} \quad (6)$$

Since

$$\frac{dV}{dt} = \sum_j \frac{\partial V}{\partial q_j} \dot{q}_j = \sum_j \frac{p_j}{m} \frac{\partial V}{\partial q_j} \quad (7)$$

Then

$$\ddot{p}_i = - \sum_j \frac{p_j}{m} \frac{\partial^2 V}{\partial q_i \partial q_j} \quad (8)$$

The quantity  $p_i p_i$  is then

$$p_i \ddot{p}_i = - \sum_j \frac{p_i p_j}{m} \frac{\partial^2 V}{\partial q_i \partial q_j} \quad (9)$$

where the subscripts  $i$  and  $j$  denote the coordinates and momenta.

Letting  $i$  be the  $x$ -component of the observed diffusing molecules, we have

$$P_x \ddot{P}_x = -\frac{P_x^2}{m} \frac{\partial^2 V}{\partial x^2} - \frac{P_x P_y}{m} \frac{\partial^2 V}{\partial x \partial y} - \frac{P_z P_x}{m} \frac{\partial^2 V}{\partial z \partial x} \quad (12)$$

because of the statistical independence, or uncorrelation, among the momentum components and the potential derivatives, the ensemble average of all the terms except the first one in equation (12) vanish. Therefore,

$$\langle P_x \ddot{P}_x \rangle = -\langle \frac{P_x^2}{m} \rangle \langle \frac{\partial^2 V}{\partial x^2} \rangle = -k_B T \langle \frac{\partial^2 V}{\partial x^2} \rangle \quad (13)$$

The second identity is obtained by the equipartition theorem, and thus

$$\langle \dot{P}^2 \rangle = -\langle \dot{\vec{P}} \cdot \ddot{\vec{P}} \rangle = k_B T \langle \nabla^2 V \rangle \quad (14)$$

Since equation (14) is independent of time, we have

$$\langle \dot{\vec{P}} \cdot \ddot{\vec{P}} \rangle = 0 \quad (15)$$

Taking the time derivative of equation (15) yields

$$\langle \ddot{P}^2 \rangle = -\langle \dot{\vec{P}} \cdot \dddot{\vec{P}} \rangle \quad (16)$$

The time derivative of equation (10) gives

$$\ddot{P}_i = -\sum_j \left\{ \frac{\dot{P}_j}{m} \frac{\partial^2 V}{\partial q_i \partial q_j} + \frac{P_j}{m} \frac{\partial^2 V}{\partial q_i \partial q_j} \frac{dV}{dt} \right\} \quad (17)$$

Substituting equation (9) into equation (16), yields

$$\ddot{P}_i = -\sum_j \left\{ \frac{\dot{P}_j}{m} \frac{\partial^2 V}{\partial q_i \partial q_j} + \sum_K \frac{P_j P_K}{m^2} \frac{\partial^3 V}{\partial q_i \partial q_j \partial q_K} \right\} \quad (18)$$

Thus

$$\dot{P}_i \ddot{P}_i = - \sum_j \frac{1}{m} \frac{\partial V}{\partial q_i} \frac{\partial V}{\partial q_j} \frac{\partial^2 V}{\partial q_i \partial q_j} + \sum_{j,k} \frac{P_j P_k}{m^2} \frac{\partial V}{\partial q_i} \frac{\partial^3 V}{\partial q_i \partial q_j \partial q_k} \quad (19)$$

Again, taking i as the x-component of the observed diffusing molecule, one have

$$\begin{aligned} \dot{P}_x \ddot{P}_x = & - \frac{1}{m} \left( \frac{\partial V}{\partial x} \right)^2 \frac{\partial^2 V}{\partial x^2} - \frac{1}{m} \frac{\partial V}{\partial x} \frac{\partial V}{\partial y} \frac{\partial^2 V}{\partial x \partial y} - \frac{1}{m} \frac{\partial V}{\partial x} \frac{\partial V}{\partial z} \frac{\partial^2 V}{\partial x \partial z} \\ & + \frac{P_x^2}{m^2} \frac{\partial V}{\partial x} \frac{\partial^3 V}{\partial x^3} + \frac{P_y^2}{m^2} \frac{\partial V}{\partial x} \frac{\partial^3 V}{\partial x \partial y^2} + \frac{P_z^2}{m^2} \frac{\partial V}{\partial x} \frac{\partial^3 V}{\partial x \partial z^2} \\ & + 2 \frac{P_x P_y}{m^2} \frac{\partial V}{\partial x} \frac{\partial^3 V}{\partial x \partial x^2 \partial y} + 2 \frac{P_y P_z}{m^2} \frac{\partial V}{\partial x} \frac{\partial^3 V}{\partial x \partial x \partial y \partial z} + 2 \frac{P_z P_x}{m^2} \frac{\partial V}{\partial x} \frac{\partial^3 V}{\partial x \partial x^2 \partial z} \end{aligned} \quad (20)$$

The statistical independence between the components of momentum, and between the momentum and the coordinates, again give the ensemble average of equation (20)

$$\begin{aligned} \langle \dot{P}_x \ddot{P}_x \rangle = & - \frac{1}{m} \left\{ \left\langle \left( \frac{\partial V}{\partial x} \right)^2 \frac{\partial^2 V}{\partial x^2} \right\rangle + \left\langle \frac{\partial V}{\partial x} \frac{\partial V}{\partial y} \frac{\partial^2 V}{\partial x \partial y} \right\rangle + \left\langle \frac{\partial V}{\partial x} \frac{\partial V}{\partial z} \frac{\partial^2 V}{\partial x \partial z} \right\rangle \right\} \\ & + \frac{K_B T}{m} \left\{ \left\langle \frac{\partial V}{\partial x} \frac{\partial^3 V}{\partial x^3} \right\rangle + \left\langle \frac{\partial V}{\partial x} \frac{\partial^3 V}{\partial x \partial y^2} \right\rangle + \left\langle \frac{\partial V}{\partial x} \frac{\partial^3 V}{\partial x \partial z^2} \right\rangle \right\} \end{aligned} \quad (21)$$

Combining terms and simplifying equation (21) yields

$$\begin{aligned} \langle \dot{P}_x \ddot{P}_x \rangle = & - \frac{1}{2m} \left\langle \frac{\partial V}{\partial x} \frac{\partial}{\partial x} \left[ \left( \frac{\partial V}{\partial x} \right)^2 + \left( \frac{\partial V}{\partial y} \right)^2 + \left( \frac{\partial V}{\partial z} \right)^2 \right] \right\rangle \\ & + \frac{K_B T}{m} \left\langle \frac{\partial V}{\partial x} \frac{\partial}{\partial x} \left[ \frac{\partial^2 V}{\partial x^2} + \frac{\partial^2 V}{\partial y^2} + \frac{\partial^2 V}{\partial z^2} \right] \right\rangle \\ = & - \frac{1}{2m} \left\langle \frac{\partial V}{\partial x} \frac{\partial}{\partial x} (\nabla V)^2 \right\rangle + \frac{K_B T}{m} \left\langle \frac{\partial V}{\partial x} \frac{\partial}{\partial x} (\nabla^2 V) \right\rangle \end{aligned} \quad (22)$$

Similarly

$$\langle \ddot{\vec{p}}_y \ddot{\vec{p}}_y \rangle = -\frac{1}{2m} \left\langle \frac{\partial V}{\partial y} \frac{\partial}{\partial y} (\nabla V)^2 \right\rangle + \frac{K_B T}{m} \left\langle \frac{\partial V}{\partial y} \frac{\partial}{\partial y} (\nabla^2 V) \right\rangle \quad (23)$$

and

$$\langle \ddot{\vec{p}}_z \ddot{\vec{p}}_z \rangle = -\frac{1}{2m} \left\langle \frac{\partial V}{\partial z} \frac{\partial}{\partial z} (\nabla V)^2 \right\rangle + \frac{K_B T}{m} \left\langle \frac{\partial V}{\partial z} \frac{\partial}{\partial z} (\nabla^2 V) \right\rangle \quad (24)$$

Finally, we have

$$\langle \ddot{\vec{p}}^2 \rangle = \frac{1}{2m} \langle \nabla V \cdot \nabla (\nabla V)^2 \rangle - \frac{K_B T}{m} \langle \nabla V \cdot \nabla (\nabla^2 V) \rangle \quad (25)$$

The time derivative of equation (14) leads to

$$\langle \vec{p} \cdot \ddot{\vec{p}} \rangle = -\langle \dot{\vec{p}} \cdot \dot{\vec{p}} \rangle = 0 \quad (26)$$

Again, the time derivative of equation (26) gives

$$\langle \vec{p} \cdot \ddot{\vec{p}} \rangle = -\langle \dot{\vec{p}} \cdot \ddot{\vec{p}} \rangle = \langle \ddot{\vec{p}}^2 \rangle \quad (27)$$

Following the same procedure, one can easily show that all the odd terms of  $t$  in equation (3) vanish and that all the even terms can be calculated through the potential. Thus, equation (3) reduces to

$$\begin{aligned} \langle \vec{p}(0) \cdot \vec{p}(t) \rangle &= 3 m K_B T - K_B T \langle \nabla^2 V \rangle \frac{t^2}{2!} \\ &\quad - \left[ \frac{K_B T}{m} \langle \nabla V \cdot \nabla (\nabla^2 V) \rangle \right. \\ &\quad \left. - \frac{1}{2m} \langle \nabla V \cdot \nabla (\nabla V)^2 \rangle \right] \frac{t^4}{4!} \\ &\quad - \dots \end{aligned} \quad (28)$$

Note that the upper limit of the integration of the time correlation function in equation (1) is a relative term. This means that a sufficiently large time  $\tau$  must be chosen in order to insure that the contribution of the time correlation function to the integration for  $t > \tau$  is negligible. In other words, at  $t = \tau$ , the diffusing particle has completely lost the memory of its past history, i.e.,

$$\langle \vec{p}(0) \cdot \vec{p}(\tau) \rangle = 0 \quad (29)$$

There is no correlation between  $\vec{p}(0)$  and  $\vec{p}(\tau)$  over the ensemble average. It is well-known that in condensed matter, the momentum auto correlation function decays rapidly as  $\tau \sim 10^{-12}$  s. Let  $\tau_c$  denote the average time interval between particle collisions. In low density systems, such as in gases,  $\tau$  is usually much larger than  $\tau_c$  in order to consider that the particles behave as diffusing particles with a certain degree of memory rather than as newtonian particles whose displacements and velocities are explicit functions of time. Harris and Rice<sup>21</sup> demonstrated that, in a real fluid, there is a shorter relaxation time and memory than in a dense rigid sphere fluid, and also, that the relaxation time and memory in the dense rigid sphere fluid are shorter than in the same system and have a lower density. It is clear that, in a real fluid, transfer of energy occurs continuously through the potential energy of interaction. Significant energy exchanges must occur at a rate greater than that corresponding to the collision rate of the rigid sphere at the same density as in the real fluid. In crystalline solids, potential energy overcomes thermal energy. In the crystalline phase, materials possess not only the short-range order

as in the liquid phase, but also the long-range order. When a dopant makes a jump, diffusing from its lattice site, the associated energy is transmitted immediately to all directions through interactions of interatomic potentials. A much faster restoration to its equilibrium state than to the liquid phase is expected. From Harris and Rice's conclusion, it is justified to say that, in a crystalline solid phase,

has the same order of magnitude as  $\tau_0$ . However, in general,  $\tau$  is considered microscopically large compared with  $\tau_0$  and macroscopically small compared with the laboratory time scale.

Using equation (28) with  $t = \tau$  and truncating at an arbitrary term, one can easily solve the equation of a polynomial of even orders for  $\tau$ . In general, the number of roots represents the number of intersections the momentum autocorrelation function meets with the time axis. The amplitude of the momentum autocorrelation function usually damps rapidly after only a few oscillations. Substituting the obtained  $\tau$  in equation (1), one can calculate the diffusion coefficient  $D$ . Identifying this  $D$  with the one derived from the fluctuation and dissipation theorem, i.e.,

$$D = \frac{k_B T}{m} \tau_0 \quad (30)$$

$\tau_0$  then can be determined from equation (30), and it should be approximately equal to the calculated  $\tau$ . Thus, equation (30) serves as a safeguard to our calculations. We now truncate equation (28) further to a higher order term and perform the calculation for a new  $\tau$  and a new  $D$ . We compare the new  $D$  with the previous  $D$  to check whether they are close enough (within a few percent difference). If



the result is negative, we continue the same procedure until the difference becomes positive and within range.

## II. Anisotropic Dopant Diffusion Tensor

Matrix elements of a diffusion tensor can be calculated by

$$D_{ij} = \frac{1}{3m^2} \int_0^\infty \langle \vec{P}_i(0) \cdot \vec{P}_j(t) \rangle dt \quad (31)$$

where  $i, j$ , denote the components of the coordinate system. Due to the independence of the motion along mutually perpendicular directions, one has

$$\langle \vec{P}_i(0) \cdot \vec{P}_j(t) \rangle = 0 \quad (32)$$

Thus, a diagonal matrix of diffusion tensor results

$$\vec{D} = \begin{pmatrix} D_{\perp} & 0 & 0 \\ 0 & D_{\perp} & 0 \\ 0 & 0 & D_{\parallel} \end{pmatrix} \quad (33)$$

where  $D_{\perp}$  is the diffusivity perpendicular to the crystal growth direction (parallel to the doping layers, and  $D_{\parallel}$  is the diffusivity parallel to the crystal growth direction (perpendicular to the doping layers). They differ by the interatomic potentials along the normal to the doping layers and the crystal symmetry.

Böhler<sup>12</sup> obtained the periodic potential along the direction,  $x$ , of crystal growth due to the space charges of localized donors and

acceptors in the n-layers and p-layers respectively by solving Poisson's equation,

$$V_1(z) = V_0(z - \lambda d) \quad -\frac{d}{2} < z - \lambda d < \frac{d}{2} \quad (2)$$

with  $\lambda = 0, +1, +2, +3, \dots$  and

$$\begin{aligned} V_0(z) &= \frac{2\pi e^2}{K} n_D z^2 & |z| \leq \frac{dn}{2} \\ &= \frac{2\pi e^2}{K} n_D dn \left( |z| - \frac{dn}{4} \right) & \frac{dn}{2} \leq |z| \leq \frac{dn}{2} + d_i \\ &= \frac{2\pi e^2}{K} \left\{ n_D dn \left( \frac{dn}{4} + d_i \right) - n_A \left[ \left( \frac{d}{2} - |z| \right)^2 - \frac{d_p^2}{4} \right] \right\} \\ & & \frac{dn}{2} + d_i \leq |z| \leq \frac{d}{2} \end{aligned}$$

where  $d = d_n + d_p + 2d_i$  is the thickness of the nipi superstructure and  $d_n$ ,  $d_p$ , and  $d_i$  are the respective thicknesses of the n, p, and i (intrinsic) layers.  $K$  is the dielectric constant of the host semiconductor.  $n_D$  and  $n_A$  are donor and acceptor doping concentrations with  $n_D d_n = n_A d_p$ .

The crystal bonding characteristics of semiconductors commonly used as substrate for nipi superlattice, such as, GaAs, display both covalent and ionic bond nature.<sup>23</sup> The percentage contribution of each type of bonding can be calculated from the electronegativity of the elements.<sup>24</sup> The fundamental roles played by the dopants, however, are space-charged ions. The widely used empirical potential for covalent bonds is the Lennard-Jones potential. It is inversely proportional to the 6th and 12th powers of the interatomic separation. Compared with the inverse 1st power in the ionic potential, the latter has much larger long-range effects and the ionic behavior of its interactions between dopant ions

and the host atoms is much more dominant. Thus, we adopt the pair ionic potential and their summation as the lattice potential experienced by the dopant ions, i.e.,

$$V_{ij}(r_{ij}) = \alpha_{ij} e^{-r_{ij}/\rho_{ij}} - z_i z_j \frac{e^2}{r_{ij}} \quad (36)$$

where the subscript indicates the interaction between the  $i$ th and  $j$ th ions, and also the types of atoms.  $r_{ij}$  is the separation of them.  $\alpha_{ij}$  and  $\rho_{ij}$  are the repulsive potential parameters between the  $i$  and  $j$  types of atoms.  $z_i$  and  $z_j$  are the valence electrons transfer to (-) or from (+) the atoms to complete the crystal bonds. In general,  $|z_i| = |z_j| = 1$ .  $e$  is the electronic charge.

The one-body potential experienced by the observed diffusion ion due to the host lattice, then, is the summation of the above pairwise potentials,

$$V_i = \sum_j^{n_0} \alpha_{ij} e^{-r_{ij}/\rho_{ij}} - |z_i z_j| \sum_j \frac{(\pm) e^2}{r_{ij}} \quad (37)$$

The second summation includes the  $n_0$  nearest neighbors and the remaining  $(N - n_0)$  pairs of ions.  $N$  is the total number of host atoms. Dopant number concentrations, for practical reasons, vary from  $10^{17} \text{ cm}^{-3}$  to  $10^{19} \text{ cm}^{-3}$ . Compared with the host semiconductor concentration,  $10^{23} \text{ cm}^{-3}$ , they do not perturb the crystal structure and cohesive energy much. Since the net force vanishes at the equilibrium state, the repulsive force has to equal the attractive force for every atom in the crystal. Thus, we can replace the parameters  $\alpha_{ij}$  and  $\rho_{ij}$  by

the  $\alpha$  and  $\rho$  of the host semiconductor. If we let  $\beta_{ij} = \beta_{ij}/R$ , where  $R$  is the nearest-neighbor separation, equation (37) becomes

$$V_i = n_o \alpha e^{-R/\rho} - \beta \frac{|z_i z_j| e^2}{R} \quad (38)$$

For the nearest neighbors,  $\beta_{ij} = 1$ . The constant  $\beta = \sum_j \left( \frac{z_i z_j}{R_{ij}} \right)$  is the Madelung constant of the crystal structure. The total lattice cohesive energy may be written as

$$E = \frac{N}{2} \left( n_o \alpha e^{-R/\rho} - \beta \frac{|z_i z_j| e^2}{R} \right) \quad (39)$$

The factor  $1/2$  is to eliminate the pairwise repetition. At the equilibrium state  $dE/dR = 0$ ; therefore,

$$\alpha = \frac{\beta |z_i z_j| e^2}{n_o R^2} \rho e^{R/\rho} \quad (40)$$

Using the experimental data of the bulk modulus and their extrapolated value at absolute zero temperature, one can determine the parameter  $\rho$ . Then, using equation (40),  $\alpha$  can be calculated. Since the entropy is constant at absolute zero, the bulk modulus is given by  $B = V d^2 E / dV^2$ .  $N_o$  denotes the number of atoms contained in a volume of  $\rho^3$ . The total volume,  $V$ , occupied by the total number of atoms, then, is  $V = \frac{N}{N_o} \rho^3$ . The value of  $N_o$  can be a fraction because not every primitive cell is cubic.  $N_o$  can be calculated easily from the number of atoms contained in a conventional unit cell  $a^3$ , with  $a$  as the lattice constant, and the relation between  $R$  and  $a$  in its particular structure.

Since

$$\begin{aligned}\frac{d^2 E}{dV^2} &= \frac{d^2 E}{dR^2} \left( \frac{dR}{dV} \right)^2 + \frac{dE}{dR} \frac{d^2 R}{dV^2} \\ &= \frac{d^2 E}{dR^2} \left( \frac{dR}{dV} \right)^2 \quad (\text{at equilibrium})\end{aligned}$$

one yields

$$\frac{N_0 \beta |z_i z_j| e^2}{8 R^4} \left( \frac{R}{\rho} - 2 \right) = B$$

The matrix elements  $D_{||}$  and  $D_{\perp}$  of the diffusion tensor can be

calculated from

$$\begin{aligned}D_{||} &= \frac{K_B T}{m} \tau_{||} - \frac{K_B T \tau_{||}^3}{18 m^2} |z_i z_j| \langle \nabla^2 (V_i + V_j) \rangle \\ &\quad - \left[ K_B T \langle \nabla (V_i + V_j) \cdot \nabla (\nabla^2 (V_i + V_j)) \rangle - \right. \\ &\quad \left. \frac{1}{2} \langle \nabla (V_i + V_j) \cdot \nabla (\nabla (V_i + V_j))^2 \rangle \right] \frac{\tau_{||}^5}{3 m^3 5!} \\ &\quad - \dots \dots \dots \\ D_{\perp} &= \frac{K_B T}{m} \tau_{\perp} - \frac{K_B T \tau_{\perp}^3}{18 m^2} |z_i z_j| \langle \nabla^2 V_i \rangle \\ &\quad - \left[ K_B T \langle \nabla V_i \cdot \nabla (\nabla^2 V_i) \rangle - \right. \\ &\quad \left. \frac{1}{2} \langle \nabla V_i \cdot \nabla (\nabla V_i)^2 \rangle \right] \frac{\tau_{\perp}^5}{3 m^3 5!} \\ &\quad - \dots \dots \dots\end{aligned}$$

The directional correlation times  $\tau_{||}$  and  $\tau_{\perp}$  are solved from corresponding equations, which were given in equation (28). Diffusion along the crystal growth direction suffers the additional space charge potential  $\phi(z)$ , while diffusion along the slip layer direction does not. This effect results in the anisotropy of transport. The ensemble averages involved in the above equations can be carried out in two ways. Those involving  $\phi$ , say  $\langle \nabla \phi \rangle$ , are taken in the one-body

frame system,

$$\langle X(V_1) \rangle_1 = \frac{\int X(V_1) e^{-V_1/K_B T} dz}{\int e^{-V_1/K_B T} dz} \quad (45)$$

Those involving  $V_2$ , say  $Y(V_2)$ , are taken in the two-body frame system,

$$\langle Y(V_2) \rangle_2 = \frac{\int Y(V_2) g(r) d^3r}{\int g(r) d^3r} \quad (46)$$

In equation (45), the Boltzmann factor is used as the weighting factor while in equation (46), the radial distribution function is used.

Ensemble averages of cross terms in equation (43) are treated by

$$\langle X(V_1) Y(V_2) \rangle = \langle X(V_1) \rangle_1 \langle Y(V_2) \rangle_2 \quad (47)$$

where  $\langle \rangle = \langle \rangle_1$  is the one-body average frame system,  $\langle \rangle_2$  indicates the two-body average frame system. Since, within the scope of this work, we do not have knowledge of the acquired radial distribution function, an alternative approach can be taken. The Madelung constant is determined entirely upon the crystal structure. It contains the contributions of all atoms at every separation from a reference lattice site, starting from the nearest neighbors. We divide the Madelung constant by the total number of atoms. For each term of the summation in the constant, there is a weighting factor  $1/j$  to replace the radial distribution function at the same configurational space.  $j$  represents the total number of atoms at a distance of the  $j$ th neighborhood from the referred atom. For example,

$$\begin{aligned}
\langle \nabla^2 V_i \rangle &= N \langle \nabla^2 V_{ij} \rangle \\
&= N \left[ \left( \frac{N_i}{N} \right) \frac{\alpha}{\rho^2} e^{-R/\rho} - \sum_j \left( \frac{N_j}{N} \right) 2 |z_i z_j| \frac{(\pm) e^2}{\beta'_{ij} R^3} \right] \\
&= n_0 \frac{\alpha}{\rho^2} e^{-R/\rho} - 2 |z_i z_j| \frac{e^2}{R^3} \left( \sum_j \frac{(\pm) N_j}{\beta'_{ij}} \right) \quad (4) \\
&= n_0 \frac{\alpha}{\rho^2} e^{-R/\rho} - 2 \beta |z_i z_j| \frac{e^2}{R^3}
\end{aligned}$$

where  $N_j/\beta'_{ij} = \beta_{ij}$ , which was defined previously for the Madelung constant. Based on the crystal's discrete atomic distribution and the specific lattice structure, we are able to form  $\beta_{ij}/\alpha$ . This fraction is a weighting factor to measure the percentage contribution of these  $N_j$  atoms to the quantity of which the average is taken. Due to the rapid decay of the repulsive term, we have considered only the nearest neighbor's contribution. This approach for determining the averages is plausible to substitute for the continuous radial distribution function for the probability of finding the pairwise distribution in crystalline structures.

#### IV. Application to Si and Ge Doped GaAs nipi Superlattice

The substrate semiconductor has a zincblende crystal structure. Physical constants<sup>25</sup> needed for carrying out numerical calculations are listed in Table 1 at  $T = 300$  K.

a	( $10^{-8}$ cm)	5.65325
n		4
r	( $10^{-8}$ cm)	2.44793
N		$8R^3/a^3$
$\sigma$	( $10^{11}$ dynes/cm <sup>2</sup> )	7.69 (7~0)
K		11

Table 1. Physical Constants of GaAs semiconductors at 300 K.

The dopant masses, valences, and crystal bonding are taken from the periodic table and reference (24). The Madelung constant for the zincblende lattice sum calculation is  $\beta = 1.6361$ . Using the developed formulism, we calculate  $D_{||}$ ,  $D_{\perp}$ , and the apparent diffusion coefficient  $D$  and list them in Table 2 at  $T = 300$  K.

$D_{  }$ ( $10^{-7}$ cm <sup>2</sup> /s)		
$D_{\perp}$ ( $10^{-7}$ cm <sup>2</sup> /s)		
$D = \frac{D_{  }}{3} + \frac{2D_{\perp}}{3}$		

Table 2. Diffusivities of Si and Be Doped GaAs nipi Superlattice



## 7. MEMARKS

The calculation of the diffusion tensor in a semiconductor superlattice can be carried out through dynamical quantities of the diffusion particles in terms of various derivatives of interaction potentials. Microscopic properties are related to macroscopic properties by the ensemble average of the system. All possible diffusion mechanisms occurring concurrently in a condensed phase are taken into consideration by using the momentum autocorrelation function expression for the diffusivity. This is true because there is only one net momentum at an instant, no matter how many diffusion mechanisms may be involved. The truncation of the time expansion is well justified by introducing the correlation time  $\tau$  for self-consistency. The procedure for the calculation is straight-forward. The accuracy of the results relies on the modeling of interaction potentials. There is no experimental values reported in the literature<sup>27</sup> for our comparison to test the validity of our approach. However, our theoretical expressions do reveal agreement by the first order terms with those derived from the fluctuation and dissipation theory. The findings of this work, thus, are useful for future reference in this field of study.

#### IV. RECOMMENDATIONS

To make our summer efforts and research results prolific, and to bring the maximum benefit of my participation in the SERP, I would like to make the following recommendations:

- (a) Continue long-term interactions between the Materials Laboratory and myself to achieve the goals and objectives set forth in this SERP project.
- (b) Carry out the quantitative differential reflectivity measurements on bulk semiconductors with the presently developed technique to test the validity of its application in nipi superlattices. The rationale is that there is no experimental data in nipi superlattices to compare with.
- (c) Use the results of (b) to obtain final band profiles using the current demonstrated approach. Relate the results here with those known electrical properties to see whether better interpretations are given.
- (d) Repeat procedures (b) and (c) in Si and Ge doped GaAs nipi superlattices and other reported nipi superlattices.
- (e) Compile the LUTS programs now existing in the Materials Laboratory into computer files. Perform calculations on the band structures of the known band structures. Organize all the data into a systematic format for problems for solution. Keep this organized data in the SERP's permanent files for future calculations in new bulk semi-conductors and nipi superlattices to compare with reported data.

AD-A191 203

UNITED STATES AIR FORCE SUMMER FACULTY RESEARCH PROGRAM  
(1907) PROGRAM TE. (U) UNIVERSAL ENERGY SYSTEMS INC  
DAYTON OH R C DARRAH ET AL. DEC 87 AFOSR-TR-88-0212

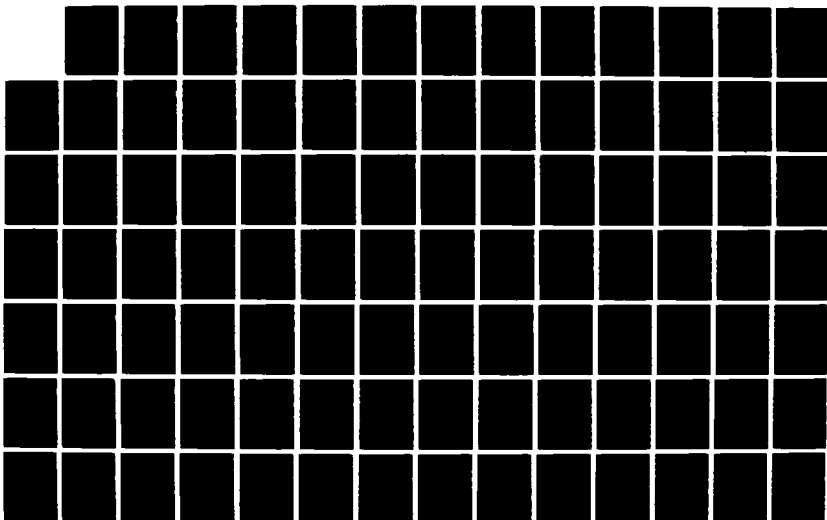
7/11

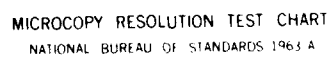
UNCLASSIFIED

F49620-85-C-0013

F/G 5/1

ML





MICROCOPY RESOLUTION TEST CHART  
NATIONAL BUREAU OF STANDARDS 1963 A

In particular, this package will be used extensively by the Materials Laboratory in the near future for band structure calculations of all new synthetic semiconductor superlattice materials of interest to the Lab. These include the compositional and doped nipi superstructures. Once the author's modified generalized LMTD theory for superlattice band structure calculations is complete, all this can be implemented.

- (f) Grow nipi superlattices with the upcoming MBE facility of the Materials Laboratory to test the theoretical methods completed this summer and to verify the theories to be developed in the proposed work of (g).
- (g) Support the author's SER/AFOSR sponsored Fall 1984 proposal on the band structure calculations of semiconductor superlattices, in particular, using a modified LMTD approach. Since the foundation work of the proposed research has been laid out during the summer, initial research support is necessary for the fruitful completion of this fall endeavor.

# REFERENCES

1. Seidel, T.E., and MacBae, A.C., Trans. AIME 245, 491 (1968).
2. Wood, R.F., and Giles, G.S., Phys. Rev. 223, 2928 (1961).
3. Ghez, R., Cehrlein, A.S., Sedgwick, T.O., Morehead, R.F., and Lee, Y.H., Appl. Phys. Lett. 45, 881 (1984).
4. Koroi, D.S., and Hemenger, P.M., Appl. Phys. Lett. 50, 155 (1986).
5. Esaki, L., Change, D.L., Howard, W.E., and Hideout, V.L., Proc. 11th Int. Conf. Phys. Semiconductors, warsaw, Poland, 431 (1972).
6. Tsu, R., and Esaki, L., Appl. Phys. Lett., 19, 246 (1971).
7. Tan, T.Y., and Gosele, U., J. Appl. Phys. 61, 1541 (1987).
8. Irvine, S.J.C., Giese, J., Gough, J.S., Blackmore, C.W., Royle, A., Mullin, J.B., Chew, M.G., and Cullie, A.G., J. Cryst. Growth, 77, 437 (1986).
9. Yamauchi, Y., Uwai, K., and Mikami, O., Jpn. J. Appl. Phys. 23, L785 (1984).
10. Wilson, S.R., Paulson, W.M., Gregory, R.R., Hamdi, A.R., and McDaniel, R.D., J. Appl. Phys., 55, 4152 (1964).
11. Ibid, "Laser-Solid Interactions and Transient Thermal Processing of Materials", Elsevier Publ., New York, 309 (1965).
12. Chu, A.S., and Koroi, D.S., J. de Phys., 36, 99 (1975).
13. Chu, A.S., and Koroi, D.S., Mol. Cryst. Liq. Cryst., 57, 109 (1981).
14. Perico, A., and Luenza, M., J. Chem. Phys., 63, 3100 (1965).
15. Aragon, S., Sergio, R., and Pecora, R., J. Chem. Phys., 62, 5346 (1965).
16. Brunett, R., and Jacoboni, L., Phys. Rev. B, 29, 5739 (1984).
17. Karada, K., Yamanaka, A., Tanigaki, K., and Iada, T., J. Chem.

Phys., 76, 1550 (1982).

18. Brown, D., and Clarke, J.H.P., J. Chem. Phys., 46, 644 (1967).
19. Rahman, A., Phys. Rev. A, 13, 405 (1964).
20. Levesque, D., and Verlet, L., Phys. Rev. A, 2, 2114 (1970).
21. Harris, S.A., and Rice, S.A., J. Chem. Phys. 31, 1055 (1959).
22. Bohler, G.H., J. Vac. Sci. Technol. 16, 851 (1979).
23. Demarco, J.J., and Weiss, F.J., Phys. Lett. 13, 209 (1964).
24. Pauling, L., The Nature of Chemical Bond, 3rd Ed., Cornell University Press, Ithaca, N.Y. (1960).
25. Blakemore, J.S., J. Appl. Phys., 53, 12 (1982).
26. Tosi, M.P., Soli. Stat. Phys., 10, 1 (1964).
27. Blakemore, J.S., Gallium Arsenide Semiconductors (key papers in physics; No. 1), AIP, New York, (1987).

1987 USAF-UES SUMMER FACULTY RESEARCH PROGRAM/

GRADUATE STUDENT SUMMER SUPPORT PROGRAM

Sponsored by the

AIR FORCE OFFICE OF SCIENTIFIC RESEARCH

Conducted by the

Universal Energy Systems, Inc.

FINAL REPORT

NONLINEAR OPTICAL EFFECTS IN FIBERS AND SMALL CRYSTALS

Prepared by:	Dr. David Y. Chung
Academic Rank:	Professor
Department and	Department of Physics and Astronomy
University:	Howard University
Research Location:	The Frank J. Seiler Research Laboratory Nonlinear Optics Division USAF Academy Colorado Springs, CO 80840-6528
USAF Researcher:	Major James R. Rotge'
Date:	7 August 1987
Contract No:	F49620-85-C-0013



# ABSTRACT

A number of small optical cells were constructed and tested for the purpose of studying small one-dimensional crystals. The optical properties of two types of needle-shaped crystals (natural and synthetic) were studied in some detail. Preliminary tests show that the small cell method developed here has potential for future applications of these new classes of optical materials. This method can also be applied to studies of nonlinear effects in one-dimensional crystals, e.g., harmonic generation, Raman and Brillouin Scattering.

#### ACKNOWLEDGEMENTS

I wish to thank the Air Force Systems Command and the Air Force Office of Scientific Research for sponsoring this research. The administrative and directional help from Universal Energy Systems, Inc., is highly appreciated.

I would like to thank Major Jim Rotge' for suggesting this area of research and for his collaboration and guidance, and Major Richard Cook and Captain Raymond Motes for their many helpful discussions and encouragement.

I would also like to thank Drs. George Brost and Mohamed El-Hewie for many interesting discussions. Also, I would like to acknowledge the technical support from Captain K. Pugh of the Department of Electrical Engineering, USAF Academy, and all the FJSRL laboratory staff, especially Mr. Bobby Hatfield and Mr. Duane Dunlap.

Finally, I am very grateful for the typing of this manuscript by Ms. L. Kelly.

## I. INTRODUCTION

The nonlinear properties of optical fiber and other crystals are of particular interest to Air Force research and device applications programs. Optical fibers offer low loss and can support high intensity over long interaction lengths. This provides an opportunity for studying and making use of nonlinear optical processes at low power levels. Also, second harmonic generation in glass fiber was discovered recently.<sup>1,2</sup> This was considered a forbidden process because of inversion symmetry in the glass structure. Therefore, it is of considerable interest to study both theoretical and experimentally why and how this second harmonic generation can exist in fibers at all. Once this is known, one might then produce the type of fiber suitable for future applications in nonlinear devices.

There are many nonlinear optical materials for many different applications. The material requirements are widely different for diverse applications, such as optical logic, optical signal processing, optical switching, optical memories, modulation and frequency conversion. In addition to the nonlinear optical properties, the material's ability to be formed into specific geometric configurations such as thin films and fiber is also an important factor in device applications.

My research interests have been in the area of fiber optics and nonlinear effects in crystals.<sup>3,4</sup> Therefore, it was a wonderful opportunity to perform experiments at the Nonlinear Optics Division of the Frank J. Seiler Research Laboratory at the USAF Academy.

In this project we concentrated on the study of small needle-shaped crystalline materials and the nonlinear effect in fibers. The results of this research will be very useful for possible device applications in future optical technology.

## II. OBJECTIVES OF THE RESEARCH EFFORT

The major objectives are as follows:

a. To study the nonlinear effect in different optical fibers. To investigate the possible harmonic generations by coupling different wavelengths of laser light and very short light pulses into the fiber. Raman and Brillouin scatterings are possible means of detecting the effects.

b. To study a totally different kind of optical fiber, namely the type grown by nature. To characterize these fibers using various optical tests and to explore possible future applications.

Since there are no existing optical cells which can be used for the small fiber crystals, we concentrated our efforts to develop an appropriate means for efficient light coupling using fiber optics technology for (b) mentioned above.

Due to the unexpected delay in the delivery of the Quantronics laser (for (a)), we were not able to perform this part of the project. This aspect of the research is to be pursued by the Frank J. Seiler Research Laboratory personnel after delivery of the Nd:YAG laser system and appropriate fiber specimens.

### III. THE DESIGN AND TESTING OF THE SMALL OPTICAL CELL

#### 1. EXPERIMENTAL ARRANGEMENT:

In the earlier experiment for studying optical properties of magnetic fluids<sup>3</sup>, a method using small capillary tubing was developed for liquid samples. Here, we used the same concept and technology to study small fiber crystals. Several techniques and variations of the small cells were tried and will be described in the subsections below.

a. In Figure 1, we used a single mode fiber with the outer jacket removed and glued it on a small piece of glass slide. The end of the fiber was cut so that the light can be coupled in and out with good efficiency. Also, the end of the fiber was made to stick out of the slide by 3 mm for easy access of coupling with the small crystals to be described later in this section.

To ensure good coupling of light in and out of the system (fiber-crystal-fiber) we need to align the fiber optics with the crystal as precisely as possible. In the earlier experiment for liquid samples,<sup>3</sup> this was achieved by guiding (or sliding) A and B along the edge of slide D. A small capillary tube (C) contained the liquid sample and was also glued onto a small piece of a glass slide. The light could then be coupled from A to C and then from C to B. When the fiber ends A and B were immersed in the capillary tube C containing a liquid sample, we were able to achieve excellent coupling of laser light in and out of the liquid sample.

In order to extend the same idea to solid samples, further improvement of the fiber coupler is needed. Depending on the size of the needle shaped crystals, we can use the same capillary tube C for the solid samples and, with a drop of index matching fluid, some light can be made to couple in and out of the crystal sample. However, considerable light is scattered from both ends of the crystal. This makes polarization and spectroscopic studies of the crystal difficult. Therefore, other methods described below were also tried.

b. In Figure 2, two glass slides, with fiber attached (A and B) were arranged at an angle as shown. The sample crystal (C) was carefully placed between them so that the two fiber ends were slightly bent. The coupling of light was made again with matching fluid. With this arrangement the scattered light, which is mostly in the forward direction, is minimized. This method has some degree of success, but optical coupling in and out of the crystals is still insufficient, especially for smaller crystals. The following improvements were made.

c. Instead of using the matching fluid in the capillary tubing, we replaced it with UV cured epoxy (Norland optical adhesive 61) between the fiber and the crystals. This optical alignment was done under the optical microscope. Once optimum coupling was obtained by careful adjustment of the relative position of the fiber end with the crystal, a drop of epoxy was applied to the junction. A UV lamp ( $\sim 4W$ ) was used to cure the epoxy while the optical alignment was maintained. The same procedure could then be repeated to couple the other end of the crystal to a fiber, or the light output from the crystal could go directly into the monochromator input for spectroscopic studies as shown in Figure 3.

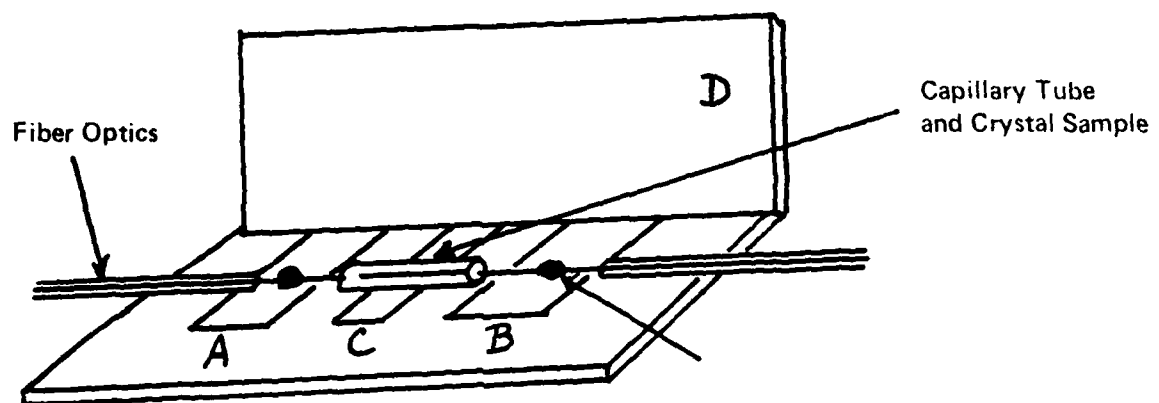


Figure 1. Small cell using fiber optics

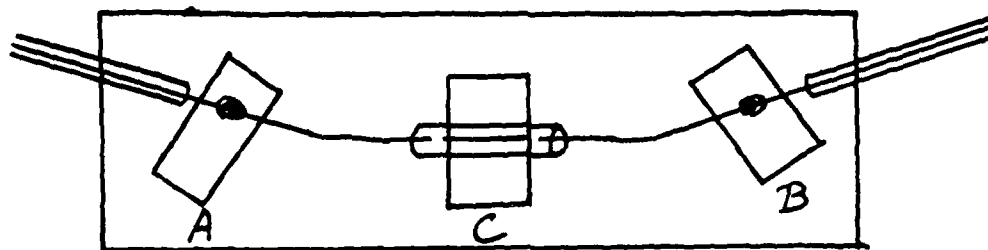


Figure 2. Small cell with bending light path

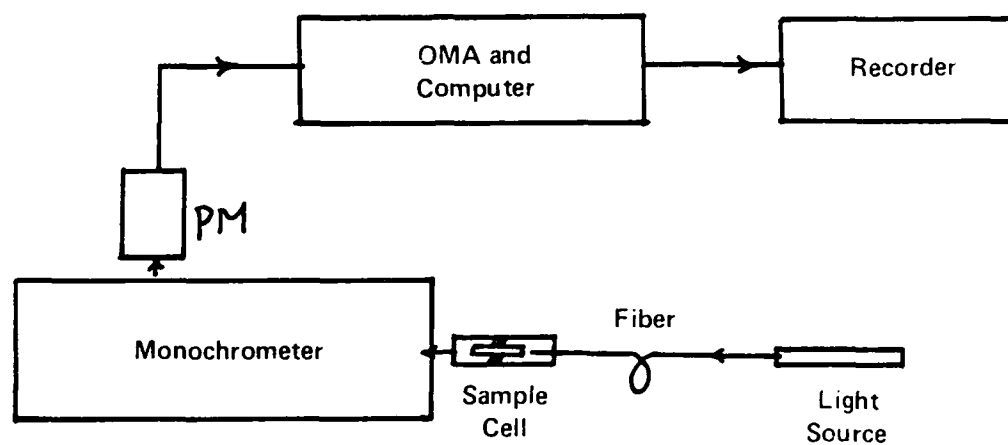


Figure 3. Experimental arrangement for spectroscopic studies

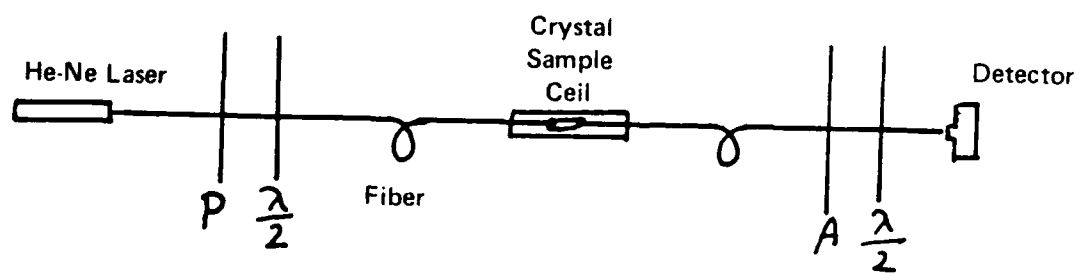


Figure 4. Experimental arrangement for polarization studies



The advantage of using method b is that one crystal sample can be easily changed with another. However, method c gives better light coupling.

## 2. SOME PRELIMINARY RESULTS:

These different coupling schemes were compared and preliminary results are summarized as follows:

### a. A Bundle of Small Crystals:

For naturally grown crystals, sometimes a bundle of smaller crystals were stuck together into a larger one. This type of crystal is characterized by its larger diameter (a few hundreds  $\mu\text{m}$  in diameter) and randomly oriented in the optical axis. This crystal has the advantage of ease of handling due to its large size and is convenient for optical spectroscopic analysis.

The method in Figure 1 was used for light coupling; occasionally the UV cure method can also be applied. With the use of a white light source (as shown in Figure 3), the optical spectrum can then be studied. Only preliminary tests on Gypsum (from Nova Scotia, Canada) were done with and without the small crystals. The results show the potential usefulness of this method.

b. Smaller Crystals:

For smaller crystals (a few  $\mu\text{m}$  in diameter), we can study both the polarization and spectroscopic properties using the cell shown in Figure 2. Due to its small diameter, it is difficult to couple a lot of light into the crystal. However, preliminary results on Scolecite (Oregon) showed that it is sufficient to study the optical properties in some detail.

IV. RECOMMENDATIONS:

1. Several small cells using capillary tubes and fiber optical technology were constructed and tested. They were shown to be very useful for spectroscopic and polarization studies of small single crystals. This approach is highly recommended for the study of both natural and artificially grown needle shaped crystals. However, only preliminary results were obtained. We hope to continue to study the small crystals using the method developed here with our mini-grant applications.

2. The nonlinear effects in optical fibers and small crystals were not carried out fully this summer because of the late delivery of the Quantronix laser. With the establishment of the small cell method for handling the small crystals, we can now efficiently couple laser power into small crystal/fiber samples for observations of possible nonlinear optical effects.

#### REFERENCES

1. D.H. Auston, et. al., "Research on Non-linear Optical Materials: An Assessment," Applied Optics, Vol 26, No. 2, p. 211 (1987).
2. Ulf Osterberg and Walter Margulis, "Experimental Studies on Efficient Frequency Doubling in Glass Optical Fibers," Optics Letters, Vol. 12, No. 1, p. 57 (1987).
3. David Y. Chung, T.R. Hickman, R.P. dePaula and J.H. Cole, "Magneto-Optics of Ferrofluids, Using Fiber Optics," J. of Magnetism and Magnetic Materials, Vol. 39, No. 1-2, p. 71 (1983).
4. H. Ong, "Charge Density Waves in One-Dimensional Conductor,  $\text{NbSe}_3$ ," Phys. Rev. B.27, No. 2, p. 1417 (1983).

1987 USAF-UES SUMMER FACULTY RESEARCH PROGRAM/  
GRADUATE STUDENT SUMMER RESEARCH PROGRAM

Sponsored by the  
AIR FORCE OFFICE OF SCIENTIFIC RESEARCH

Conducted by the  
Universal Energy Systems, Inc.

FINAL REPORT

The Effect of Model Flexibility on the Accuracy  
of Aerodynamic Coefficients Determined from  
Free-Flight Ballistic Tests

Prepared by:	Dr. Robert W. Courter
Academic Rank:	Associate Professor
Department and	Mechanical Engineering Department
University:	Louisiana State University
Research Location:	AFATL/FXA Eglin AFB, FLorida 32542
USAF Researcher:	Mr. Gerald L. Winchenbach
Date:	July 24, 1987
Contract No.:	F49620-85-C-0013

The Effect of Model Flexibility on the Accuracy  
of Aerodynamic Coefficients Determined from  
Free-Flight Ballistic Tests

by

Dr. Robert W. Courter

ABSTRACT

The objective of the present research was to determine the influence of ballistic model flexibility on aerodynamic coefficients determined from free-flight ballistic tests by parameter estimation methods based on rigid body theory. General equations defining the dynamic behavior of a flexible body were derived. Body flexibility introduced two additional types of terms into the normal rigid-body equations: inertia coupling terms and aerodynamic coefficient terms. The inertia coupling terms were evaluated by performing a simulation study of a high fineness-ratio penetrator configuration. Preliminary results indicate that flexibility within normal structural limits does not influence the body trajectory or the accuracy of the aerodynamic coefficients determined from rigid body theory.

## ACKNOWLEDGEMENT

The author would like to express his thanks to the Air Force Office of Scientific Research, the Air Force Systems Command and Universal Energy Systems, Inc. for providing him with the opportunity to become involved in the aeroballistic research activities of the Air Force Armament Laboratory at Eglin AFB, Florida. He especially appreciates the friendly, helpful attitude of the lab personnel and the accessibility to outstanding research facilities.

He would especially like to thank the following people who helped make the summer's activity so rewarding: to Chief Scientist Dr. Sam Lambert for arranging a laboratory tour and for always having the welcome mat out; to Branch Chief Stephen Korn for strongly supporting the research effort; to Research Colleague and Section Chief Gerald Winchenbach for suggesting the research project and providing all the support anyone could ask for; to Project Engineer Greg Abate for being there for help whenever he was called on and to Graduate Student Thomas Harkins for doing most of the computer work and countless other tasks of value. It was a most exciting summer.

## **I. INTRODUCTION:**

The aerodynamicist has at his disposal a variety of experimental and analytical methods with which to determine the aerodynamic characteristics of a flight configuration. One of these methods involves the application of sophisticated parameter estimation techniques in conjunction with experimental data acquired in an instrumented free-flight ballistic range. The U. S. Air Force carries out such aerodynamic research in the Aeroballistic Research Facility (ARF) at Eglin AFB, a 750-foot range instrumented with fifty, two-plane shadowgraph and timing stations from which projectile linear position and angular orientation as a function of time can be determined. These data then form a trajectory which is matched with analytical predictions by appropriate estimations of the aerodynamic coefficients of the flight item being tested. The quality of the aerodynamic characteristics which are determined from such range data analyses depends heavily on the analytical models which are used to "fit" the experimental data. The models currently incorporated into the ARF parameter estimation algorithms include the standard six-degree-of-freedom rigid body equations of motion with aerodynamic forcing functions tailored to the particular configuration being studied. The ARF staff has been successful in determining the aerodynamics of a wide variety of configurations with these algorithms.

Data from a recent test series involving high fineness ratio penetrators have suggested that model flexibility may influence the results of free-flight range test programs. Two important factors are immediately obvious: (1) a flexing model will possess a time-dependent inertia distribution which could lead to dynamic coupling, and (2) a flexing model may alter the flow field in which it flies to the extent that aerodynamic loads are affected. Since the present algorithms in the ARF parameter estimation program do not account for either of these effects, the accuracy of aerodynamic predictions may be compromised in tests of slender, flexible configurations.

## **II. OBJECTIVES OF THE RESEARCH EFFORT:**

It is the objective of the present summer research program to begin an investigation to determine the effects of ballistic model flexibility on the quality of aerodynamic predictions from the ARF.

The purposes of the research are:

1. Establish a method of analysis of flexible free-flight models.
2. Determine through simulation the effect that body flexibility has on penetrator trajectory using rigid-body aerodynamic coefficients of a typical high fineness ratio penetrator.



### III. METHODOLOGY:

The emphasis of the present program is to discover if body flexibility affects the quality of aerodynamic coefficient estimates from ballistic range data. The work accomplished is entirely analytical, and it incorporates the simplest possible methods. The approach can be outlined as follows:

1. The equations of motion of a flexible body are derived. In this derivation an arbitrary "flexed" displacement is assumed and the dynamic equations for this "flexed" mass element determined. However, only bending deformations are considered in the analysis which follows. A high fineness ratio circular cylinder is selected as a typical penetrator configuration for which torsion and tension-compression deformations are negligible in comparison with bending deformations.
2. The purpose of ballistic data analysis is to determine the loads which were necessary to produce the trajectory measured. This means that the loads are not known *a priori*. Without loads the forced vibration of the slender body cannot be determined. In the present case the elastic effects are accounted for by determining the free-free vibration of the model with the NASTRAN finite element computer code using a bar-element model.
3. The "elastic inertia" terms which evolve from the derivation in part 1 are evaluated based on a normalized fundamental mode shape from the NASTRAN analysis. Higher order

modes are available, but only the fundamental mode is considered initially. An arbitrary time-dependent amplitude function is included in the description of the fundamental mode. This function has a frequency equal to the fundamental natural frequency of the cylinder.

4. The equations of motion containing the elastic inertia-coupling terms are then solved for a trajectory using a fixed set of geometric parameters, aerodynamic coefficients and initial conditions. They are first solved without any elastic effects to establish a "baseline" trajectory. Then they are solved with the elastic effects using the elastic amplitude as a parameter.
5. Comparisons of the trajectories generated in part 4 indicate the elastic effects of interest, such as resonant conditions, phase shift and significant amplitude value.

In the following sections the details of each of the steps outlined above will be given.

#### **IV. DERIVATION OF EQUATIONS:**

The dynamic equations of motion of a flexible body can be derived by considering a typical differential mass element positioned at an arbitrary location relative to the center of mass of the body. The body itself is translating and rotating relative to an inertial axis

system. Such a configuration is shown in Figure 1. Here the absolute location of the mass element with respect to the origin of the inertial axis system is given as the vector sum of the radius vector of the center of mass,  $\mathbf{R}_O$ , the position of the "rigid body" mass element from the center of mass,  $\boldsymbol{\rho}$ , and the elastic displacement of that mass element from its rigid body position,  $\boldsymbol{\xi}$ .

$$\mathbf{R} = \mathbf{R}_O + \boldsymbol{\rho} + \boldsymbol{\xi} \quad (1)$$

The corresponding velocity and acceleration of this mass element are, respectively,

$$\dot{\mathbf{R}} = \dot{\mathbf{R}}_O + \dot{\boldsymbol{\rho}} + \dot{\boldsymbol{\xi}} \quad (2)$$

$$\ddot{\mathbf{R}} = \ddot{\mathbf{R}}_O + \ddot{\boldsymbol{\rho}} + \ddot{\boldsymbol{\xi}} \quad (3)$$

The description of a vector rate in a moving axis system must include both the rate of change of vector length and the rate of change of vector direction. Typically,

$$\dot{\mathbf{V}} = \overline{\dot{\mathbf{V}}} + \boldsymbol{\omega} \times \mathbf{V} \quad (4)$$

where  $\overline{\dot{\mathbf{V}}}$  represents the vector change relative to the moving axis system and  $\boldsymbol{\omega} \times \mathbf{V}$  represents the vector change induced by axis rotation. Applying this principle to Equation (3) above yields the following equation for the acceleration vector:

$$\begin{aligned}
\ddot{\mathbf{R}} = & \ddot{\mathbf{R}}_0 + \ddot{\mathbf{p}} + 2\boldsymbol{\omega} \times \dot{\mathbf{p}} + \dot{\boldsymbol{\omega}} \times \mathbf{p} \\
& + \boldsymbol{\omega} \times \boldsymbol{\omega} \times \mathbf{p} + \ddot{\boldsymbol{\xi}} + 2\boldsymbol{\omega} \times \dot{\boldsymbol{\xi}} \\
& + \dot{\boldsymbol{\omega}} \times \boldsymbol{\xi} + \boldsymbol{\omega} \times \boldsymbol{\omega} \times \boldsymbol{\xi}
\end{aligned} \tag{5}$$

Now the equations of motion of the body can be defined in terms of the mass element acceleration, the mass element position relative to the body center of mass and the applied forces and moments on the body. The translational and rotational equations of motion become, respectively,

$$\int \ddot{\mathbf{R}} \, dm = \Sigma \mathbf{F} \tag{6}$$

$$\int \mathbf{r}_0 \times \ddot{\mathbf{R}} \, dm = \Sigma \mathbf{r}_0 \times \mathbf{F} = \Sigma \mathbf{M} \tag{7}$$

Equations (6) and (7) in conjunction with Equation (5) are general. However, in this initial analysis of the flexibility problem the full equations will not be used. It will be assumed that all terms involving the x-component of  $\boldsymbol{\xi}$  are zero (no flexibility in tension-compression). Also, it will be assumed that the other components of  $\boldsymbol{\xi}$  act independently and normal to the x-axis (torsional flexibility is neglected). The full scalar expansions of Equations (6) and (7) with these simplifications are too lengthy to include here. The equations reduce to the rigid-body form when the inertia coupling terms produced by deformation of the penetrator structure, called the "elastic inertia" terms, are eliminated. These equations are very complicated and require considerable algebraic manipulation before integration can take place. They also represent a much more complicated physical

model than we are prepared to deal with here. A simplified set of equations is presented in the following section.

## V. FREE-FREE VIBRATION ANALYSIS:

The determination of the dynamic behavior of an elastic body depends on knowledge of the loads applied to that body. In the present case, however, the loads are unknown. In fact the objective of ballistic testing is to determine the loads from free-flight trajectory analysis. Therefore, we must resort to indirect methods to determine the deformation vector,  $\xi$ , which appears in the dynamic equations.

The technique which will be used is that of free-free natural vibration. Here the body is assumed to vibrate at its natural frequency under a net forcing load of zero. The results of this type of analysis are the natural frequencies and mode shapes of the structure. The mode shapes are determined in terms of an arbitrary time-dependent amplitude function. That is

$$\xi = \dot{A}_0 \sin(\Omega t) F(x,y,z) \quad (8)$$

where  $\dot{A}$  is the amplitude magnitude,  $\Omega$  is the natural frequency and  $F(x,y,z)$  is the mode shape. The NASTRAN finite element computer code is used to determine the free-free vibrational characteristics of the model structure. A high fineness ratio circular cylinder was selected as a representative flexible body because of the simplicity with

which it can be modeled in the NASTRAN program. The uniform cylinder was assumed to be made of 40 equal bar elements. A comparison of the computer solution for this case with the natural frequencies determined by direct analytical methods showed a discrepancy of under 1 percent. Figure 2 is a typical single-plane fundamental bending mode shape for a slender circular cylinder. This normalized function is used to determine the mass integrals of the "elastic inertia" terms which appear in the equations of motion and are defined in Appendix 1. Note that the mode shown in Figure 2 can be very well represented analytically by a 4th-order polynomial equation. For mode shapes which are not so amenable to analytical representation the integrals must be evaluated numerically.

## VI. SIMULATION PROGRAM:

In the preceding sections the general equations for dynamic analysis of an elastic free-flight body have been described. The initial attempt at elastic analysis reported here will be for the simplest possible case. This case will be that of **single-plane bending** of a high fineness ratio circular cylinder. The general equations of motion thus become:

$$\begin{bmatrix} 1 & 0 & 0 & 0 & 0 & 0 \\ 0 & 1 & 0 & 0 & 0 & 0 \\ 0 & 0 & 1 & 0 & 0 & 0 \\ 0 & 0 & 0 & a_{44} & 0 & a_{46} \\ 0 & 0 & 0 & 0 & a_{55} & a_{56} \\ 0 & 0 & 0 & a_{64} & a_{65} & a_{66} \end{bmatrix} \begin{Bmatrix} u \\ v \\ w \\ p \\ q \\ r \end{Bmatrix} = \begin{Bmatrix} A \\ B \\ C \\ D \\ E \\ F \end{Bmatrix} \quad (9)$$

$$\begin{aligned}
\text{where } A &= (F_{xg} + F_{xa})/m + rv - qw \\
B &= (F_{yg} + F_{ya})/m + pw - ru \\
C &= (F_{zg} + F_{za})/m + qu - pv \\
D &= L + p(qK_x - 2K_z - 2L_{zz}) + qr(2K_z + J_{zz}) \\
&\quad + (q^2 - r^2)K_y + qr(I_{yy} - I_{zz}) \\
E &= M - q(pk_y + 2K_z + 2L_{zz}) - pr(2K_z + J_{zz}) \\
&\quad - (p^2 - r^2)K_x - pr(I_{xx} - I_{zz}) \\
F &= N + r(pk_y - qK_x) + 2(qK_y + pK_x) \\
&\quad + pq(I_{xx} - I_{yy}) \\
a_{44} &= I_{xx} + 2K_z + J_{zz} \\
a_{46} &= -K_x \\
a_{55} &= I_{yy} + 2K_z + J_{zz} \\
a_{56} &= -K_y \\
a_{64} &= -K_x \\
a_{65} &= -K_y \\
a_{66} &= I_{zz}
\end{aligned}$$

In these equations  $u$ ,  $v$ ,  $w$ ,  $p$ ,  $q$  and  $r$  are the translational and angular rates, respectively, and  $I_{ij}$  are the conventional inertia terms. The "elastic inertia" terms are defined as follows:

$$K_i = \int x_i \xi_z dm ; \quad L_{zz} = \int \xi_z \xi_z dm ; \quad J_{zz} = \int \xi_z^2 dm$$

The aerodynamic forces and moments,  $F_{x_a}$ ,  $F_{y_a}$ ,  $F_{z_a}$ ,  $L$ ,  $M$ , and  $N$  are expanded in terms of stability derivatives which are typical of the slender penetrator configuration. Since the study involves a comparison of theoretical trajectories for the rigid and elastic bodies, the accuracy of these aerodynamic coefficients is not critical as long as the form of the aerodynamic model is consistent.

The simulation program is a straight-forward application of the fourth-order Runge-Kutta numerical integration algorithm to solve the twelve equations of motion for the state variables  $u$ ,  $v$ ,  $w$ ,  $p$ ,  $q$ ,  $r$ ,  $\phi$ ,  $\theta$ ,  $\psi$ ,  $x$ ,  $y$ ,  $z$ . Graphical and numerical output can be directed to the computer screen or to the printer.

The procedure followed in developing the results shown in the next section is:

1. For a given set of aerodynamic characteristics perform a rigid-body run to establish a baseline for comparison.
2. Using a NASTRAN run to determine mode shape and natural frequency for the slender cylinder configuration, evaluate the "elastic inertia" terms.
3. Make trajectory runs using the elastic equations of motion and the "elastic inertia" terms determined in step 2. The arbitrary elastic amplitude is varied from run to run to determine its influence on the results.



## VII. RESULTS AND CONCLUSIONS:

It has been determined that the angular resolution possible from ballistic range data is of the order of 0.5 degrees. Using this criterion the minimum discernable bending amplitude for a typical slender cylinder (fineness ratio = 35) is 0.02 inches. An amplitude range of 0.02 to 0.12 inches, the latter corresponding to a 3 degree angular deflection, was selected for the initial flexibility study reported here. A set of aerodynamic coefficients consistent with a fineness ratio 35 penetrator flying at a nominal Mach number of 5 was used in the simulation program.

Figure 3 shows the characteristics of the penetrator trajectory for the rigid body case. Simulations for the elastic body case using the same aerodynamic coefficients were performed over the range of amplitudes indicated above. There was no discernable difference in the trajectories, even for the most severe case of bending.

It is impossible to reach any broad conclusions from the foregoing simulation comparisons. It has been shown that the elastic inertia coupling does not influence the trajectory within the limitations imposed by the simplifications made in the analysis (i.e., symmetrical configuration of certain fineness ratio with single plane bending). Time and data limitations have precluded a thorough analysis of the problem. Nevertheless, the results of this limited study do tend to give the analyst confidence in the

aerodynamic coefficients determined from rigid body analysis of free-flight ballistic range data.

#### VIII. RECOMMENDATIONS:

The initial phase of the investigation into elastic body effects on ballistic range data analysis has been completed. However, a definitive resolution of the problem has not been reached. The work should be completed along the following lines:

1. The simulation comparisons begun with this research should be extended to include additional fineness ratios and flexibility amplitudes. This would make possible the definition of flexibility boundaries within which rigid body theory is secure.
2. Using the elastic body equations of motion a general theory should be derived which establishes the body and flight conditions which could lead to aberrations in range-determined aerodynamic coefficients.
3. Using rigid body equations of motion an aerodynamic forcing function driven by body flexibility effects should be determined. The goal here is to seek a forcing function which could adequately account for body flexibility within the framework of rigid body dynamics.

The principal goal of the continuation of the present work is to determine ballistic testing boundaries within which the current rigid body theory may be safely used to determine aerodynamic coefficients. This goal not only involves finding limits of the present data reduction scheme, but it also includes defining aerodynamic forcing functions which would account for flexibility while still allowing use of the rigid body dynamic theory. The author intends to propose this extension of the summer project to AFOSR under the Mini-Grant Program.

## REFERENCES

Halcomb, John R., MSC NASTRAN, Verification Problem Manual, The Macneal-Schwendler Corporation, Los Angeles, June, 1984.

Meirovitch, L. and J. Bankovskis, Dynamic Characteristics of a Two-Stage, Variable Mass, Flexible Missile with Internal Flow, NASA CR-2076, June, 1976.

Meirovitch, L., Elements of Vibration Analysis, McGraw-Hill, New York, 1975.

Nissim, E. and N. Gilon, The Aeroelastic Equations of a Slender Body, Israel Journal of Technology, 1972, Vol. 10, No. 1-2.

Schaeffer, H., MSC NASTRAN Primer - Static and Normal Modes Analysis, Schaeffer Analysis Corp., Mont Vernon, NH, 1958.

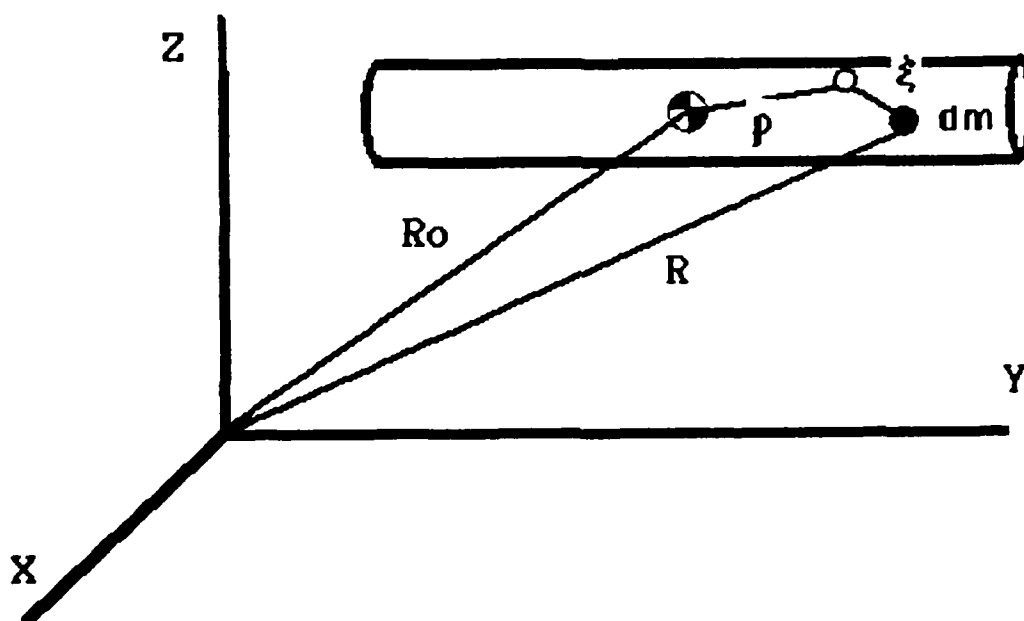


FIGURE 1. ELASTIC BODY TERMINOLOGY

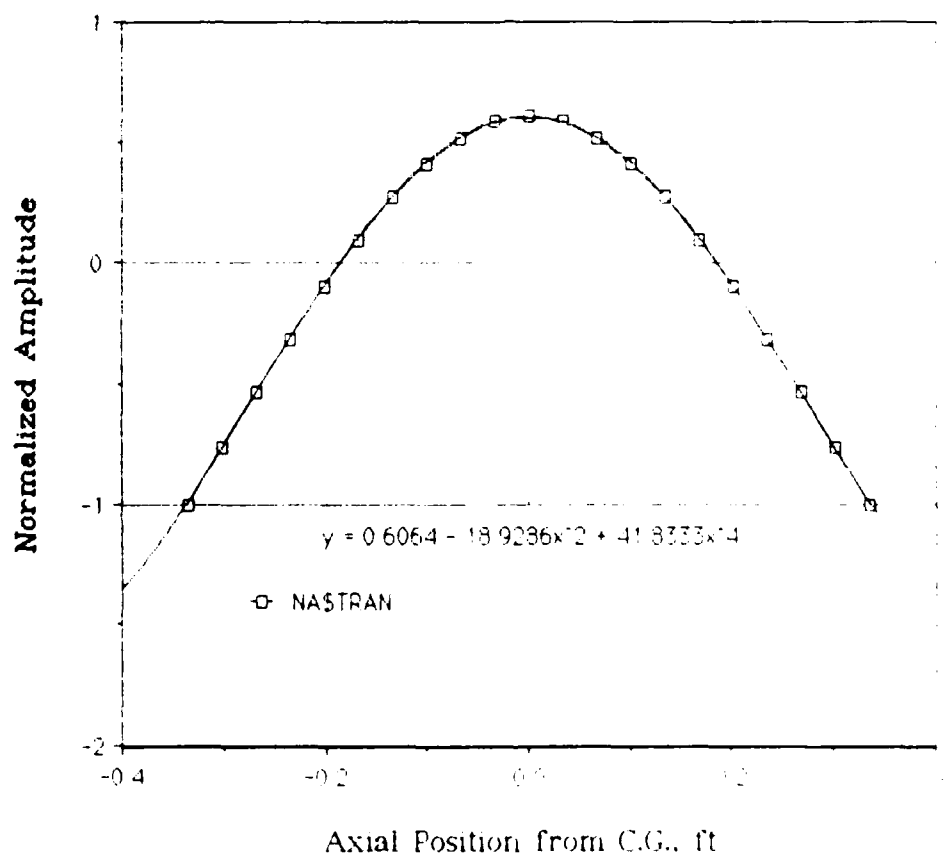


FIGURE 2. FUNDAMENTAL BENDING MODE

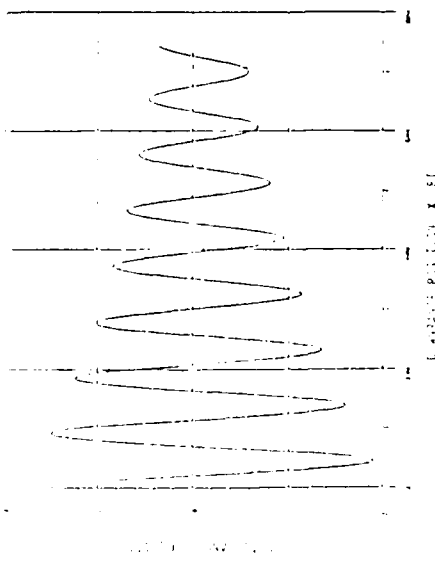
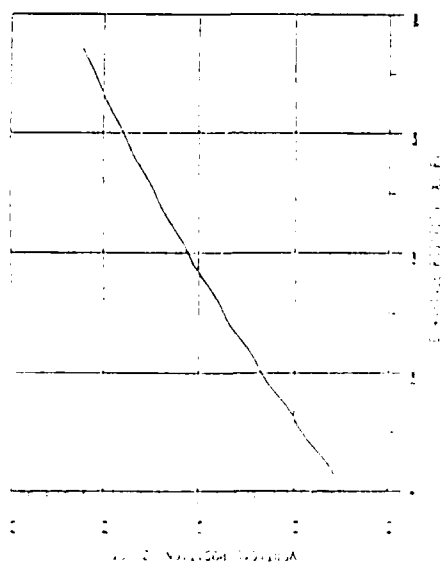
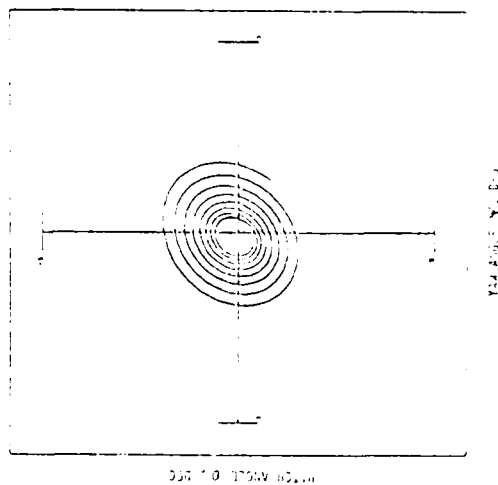
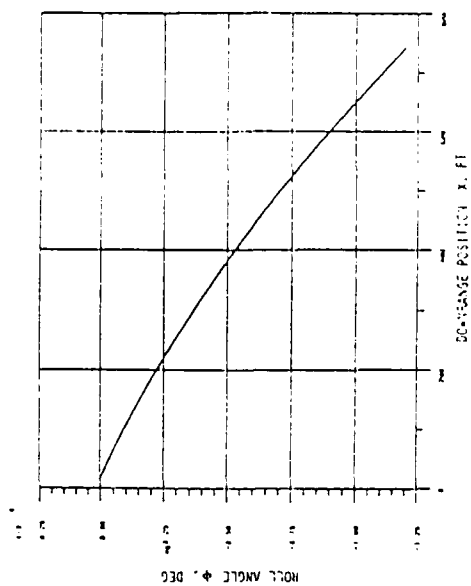


FIGURE 3. RIGID BODY AND ELASTIC BODY TRAJECTORY

1987 USAF-UES SUMMER FACULTY RESEARCH PROGRAM

GRADUATE STUDENT SUMMER SUPPORT PROGRAM

Sponsored by the  
AIR FORCE OFFICE OF SCIENTIFIC RESEARCH

Conducted by the  
Universal Energy Systems, Inc.

FINAL REPORT

TUNABLE ABSORPTION IN SUPERLATTICES

Prepared by: Bruce A. Craver, Ph.D.  
Academic Rank: Associate Professor  
Department and: Physics Department  
University: University of Dayton  
Research Location: AFWAL/MLPO  
Wright Patterson AFB, OH 45433  
USAF Researcher: Dr. Dave Zelmon and Dr. Ken Hopkins  
Date: 11 Aug., 1987  
Contract No: F49620-85-C-0013



# TUNABLE ABSORPTION IN SUPERLATTICES

by

Bruce A. Craver

## ABSTRACT

A review of the theory of superlattices and quantum wells, and the theory of optical absorption in these structures, was conducted. A comparison is made between the mechanisms for tunable absorption in quantum wells and doping superlattices. For quantum wells, tunable absorption is achieved by the quantum confined Stark effect, and in nipi's by a tunneling-assisted absorption, i.e. Franz-Keldysh effect, induced by an internal electric field arising from the superlattice potential caused by ionized donors. Suggestions concerning the future research direction of the nonlinear optics group are offered.

### Acknowledgements

I wish to thank the Air Force Systems Command and the Air Force Office of Scientific Research for the sponsorship of this work. Universal Energy Systems should be thanked for their efforts to ensure that this was a stimulating and productive association.

I wish also to express my appreciation to Drs. Pat Hemenger, Ken Hopkins and Dave Zelmon for the support and encouragement provided to an uninitiated in the area of superlattices. Our regular meetings and discussions were invaluable in clarifying my understanding and focusing my efforts.

## I. INTRODUCTION:

The USAF has a strong interest in the development of a wide range of fast, low-power electro-optical circuit devices for application in optical computing and in image processing and manipulation. The design of such devices will depend upon nonlinear optical effects. Nonlinear optical materials are ones for which the fundamental electrical and optical properties such as the conductivity, refractive index, absorption, i.e. the dielectric function, depend on the electric field  $F$  in the material. Most often this dependence is either on the field strength itself, or on the intensity or square of the field strength. Materials exhibiting such nonlinear behavior are capable of fast switching or changes in state, modulation or tuning of its properties, and self-interaction effects.

At the University of Dayton, I had previously worked on problems in nonlinear optics for the USAF. This work was largely in the area of nonlinear self-optic effects such as self-induced total internal reflection, optical limiting, self-(de)focusing and nonlinear lenses. I have also carried out detailed calculations of nonlinear absorption in semiconductors arising from the effects due to hot electrons created under intense irradiation.

## II. OBJECTIVES:

The nonlinear optics effort within the group with which I worked was relatively new, and there had been little opportunity to develop expertise with the subject of superlattices (SLs). Nevertheless, it was clear from their survey that SLs exhibit nonlinear optical behavior, and a potential for application to a wide range of electro-optical devices such as tunable light sources, lasers, and spatial light modulators. Furthermore, a new in-house molecular beam epitaxy (MBE) machine is expected to be operational by the end of the year. For these reasons it was decided that I should begin to work in the area of SLs.

The ultimate goal of this in-house effort is to develop superlattice structures for eventual incorporation into a spatial light modulator, whose operation is envisioned to depend on the absorption of the SL. Consequently, my first objective was to familiarize myself with the fundamental theory of absorption by a SL, and in particular the mechanisms by which the absorption coefficient  $\alpha$  can be tuned or modulated. This would entail an extensive review of the literature, with an eye toward determining what types of measurements, at what temperatures, and on what materials such work has been done. In addition, I am to provide some guidance in the direction of the research to be conducted at Wright Patterson Materials Lab. It is desirable to find an

area of research which is directly relevant to the goals of the USAF, and yet does not duplicate efforts being carried out by others.

### III.

(a) Superlattices (SLs) are spatially periodic structures along one direction in space, assumed to be the z-axis. The unique feature of SLs is the capability for control of the production of such devices to within a few crystalline monolayers, so that it is possible to tailor the device for a variety of applications (QE-22, 1986; Chemla, 1985; Dohler, 1986). My literature review suggests that the two tunable absorption mechanisms which have been demonstrated experimentally, and are most likely to show progress toward a spatial light modulator, are exciton effects and tunneling-assisted absorption. To describe these it is useful to classify SLs into two major groups, compositional and doping (or nipi) SLs.

Compositional SLs are constructed from alternating layers of materials with different bulk band gaps, one of the most exhaustively studied of which is  $\text{GaAs}/\text{Al}_x\text{Ga}_{1-x}\text{As}$ . Although there are several possible band alignments, depending on the materials used, that of GaAs/AlGaAs is the one we shall use as the prototype for absorption in compositional SLs. The

spatial behavior of the band gap is illustrated in Fig. 1. Notice that this structure results in potential wells for the electrons and holes which are within the same layer. In contrast, the doping SLs are constructed by alternately doping a single semiconductor material n-type and p-type along the SL axis. The space charge of ionized impurity sites then produces a SL potential which modulates the band edges. A schematic representation is shown in Fig. 2. Note that in contrast to the compositional SL the nipi produces potential wells for electrons and holes which are in alternating spatial regions, thereby localizing them in different regions of the SL.

Both types of SLs have demonstrated tunable absorption, i.e. the ability to modulate  $\alpha$ , in a spectral range near the band edge, but by different mechanisms (Chemla et al, 1983; Miller et al, 1985; Dohler et al, 1982; Dohler and Ruden, 1984). In compositional SLs such as GaAs/AlGaAs the tuning is via excitonic effects. In bulk GaAs at very low temperature there is a strong absorption peak at the band edge due exciton formation. This effect is completely obscured at higher temperatures by broadening due to ionization by phonons. However, electrons and holes in the GaAs wells of the SL are forced to stay closer together, thereby lowering the exciton energy. This actually allows one to see these exciton peaks at room temperature. This absorption occurs at an energy equal to the energy of

formation of an exciton, which in turn depends on the parameters of the GaAs quantum wells (QW), and can be determined by design. Furthermore, this exciton energy can be changed by applying an electric field, which effectively changes the average separation of the electrons and holes, and their average positions in the well. It is then possible to shift the spectral location of this strongly absorbing peak into a previously nearly transparent region by applying an external electric field. This is referred to as the quantum confined Stark effect (QCSE).

The nipi's achieve the same result by a quite different means (Dohler et al, 1982). It can be most easily thought of as a Franz-Keldysh effect, i.e. absorption below the band edge in the presence of an electric field. An electron absorbs a photon with energy less than the band gap, and then tunnels through the remaining barrier to the conduction band. The absorption coefficient  $\alpha$  then depends on the electric field. In the nipi there are internal fields associated with the SL potential that induce absorption below the band edge. One can then view  $\alpha$  as dependent on the amplitude of the spatially oscillating SL potential, or effective band gap, which in turn is dependent on the doping levels and layer thicknesses.

Here also one has the ability to tune  $\alpha$ . The amplitude of the SL space charge potential, and equivalently the

effective band gap of the nipi, depends on the density of charge carriers in the two regions. As the excitation of the SL, i.e. the carrier density in the doped regions, increases it partially neutralizes the ionized impurity sites, reducing the SL potential amplitude, and thus altering  $\alpha$ . The carrier concentrations can be modified by electro-injection or photoexcitation. The unique feature of nipi's that makes this possible is the spatial separation of electrons and holes, which greatly increases their recombination lifetimes. It is clear then that by altering the carrier concentration in the doped regions one can induce relatively large changes in  $\alpha$  near the band edge with rather modest changes in the carrier density. Once again it is possible to shift the absorption edge into a previously transparent spectral region.

(b) Although my main effort was concentrated on tunable absorption I have also begun some simple modeling of the band structure of a SL by using a generalization of the Kronig-Penny (KP) type of analysis. The intent here was to try to understand the formation of the subband structure of SLs from first principles, and to see if it would shed any light on the so-called effective mass approximation (EMA) or the question of band offsets or discontinuities. In this model one represents the SL by a periodic sequence of a combination of wells and potential barriers of differing heights and widths. Each SL period is envisioned to be a



series of an arbitrary number of potential barriers and associated wells corresponding to one set of parameters followed by a series of an arbitrary number of barriers and wells corresponding to a different set of parameters. The barriers and wells of a given type model the lattice potential of a specific semiconductor, and the free electron mass is used. I have completed a derivation of the lattice momentum-energy band dispersion curve, but have not yet studied the resultant band structure.

#### IV. RECOMMENDATIONS

As noted previously, both mechanisms for tunable absorption have been demonstrated. There has been an extensive amount of work done on the QCSE and nonlinear excitonic effects in QW or compositional SLs (QE-22, 1986 and sources cited therein), and a rudimentary modulator has been demonstrated (Wood et al, 1984). However, recent work on doping SLs have shown tunable photoluminescence (Dohler et al, 1986), electro-luminescence (Hasnain et al, 1986), electroabsorption (Chang-Hasnain et al, 1987), and optically induced absorption (Simpson et al, 1986) in doping SLs in GaAs at room temperature. These demonstrate the validity of the concepts of use of nipi's in room temperature light modulators.

There are, in addition, several other features that make nipi's attractive. In principle, they can be made from any semiconductor that can be doped both n- and p-type, and since they are made from a single material there is an absence of boundary effects and lattice mismatch problems. One can also engineer and modulate the effective band gap essentially from zero to the bulk band gap, implying a range of tunability  $\alpha$  spanning several orders of magnitude. In view of this, and the already existing large effort in compositional SLs, it is recommended that USAF pursue work on the doping SLs. In particular, it should concentrate on optically and electrically modulated absorption at room temperature, initially in GaAs, but also consider materials such as InP, GaP, InAs and Si. There has been some recent work on these materials (Gal et al, 1986; Kitamura et al, 1987; Kobayashi et al, 1986; Yuan et al, 1987; Priester et al, 1987), but at 80 K and lower. It is in this direction where the efforts could best complement the existing work in this field rather than duplicate it.

In support of this effort I will be making a proposal for a mini-grant to carry out modeling of the absorption coefficient for nipi structures, as in Dohler (1982 and 1984), and to then compute the reflectance and transmittance through such nonlinearly absorbing devices. The modeling would consist of writing computer codes to calculate  $\alpha$  from a given set of SL parameters, and to optimize the design.

Ultimately, one wishes to find the transmittance of such devices. This is not a straightforward question since with strong absorption there will also be a spatial dependence of the excitation of the sample, and hence of  $\alpha$ . What is needed is a self-consistent treatment of these effects. We propose to carry out such an exact calculation by using the method of invariant imbedding to determine the transmittance and reflectance of a nonlinear absorbing medium. It is anticipated that this would give different results from the standard exponential attenuation, which assumes an  $\alpha$  independent of position. This could also affect the analysis and interpretation of experiments to measure  $\alpha$ .

## REFERENCES

QE-22(9), Sep., 1986. The entire issue is devoted to the physics and applications of semiconductor quantum wells and superlattices. There one can find an exhaustive set references.

Chang-Hasnain, C.J., G. Hasnain, N.M. Johnson, G. Dohler, J.N. Miller, J.R. Whinnery, and A. Dienes, "Tunable electroabsorption in gallium arsenide doping superlattices," 1987, Appl. Phys. Lett., Vol. 50(14), pp. 915-917.

Chemla, D.S., T.C. Damen, D.A.B. Miller, A.C. Gossard and W. Wiegmann,, "Electroabsorption by Stark effect on room-temperature excitons in GaAs/GaAlAs multiple quantum well structures," Appl. Phys. Lett., 1983, Vol. 42(10), pp. 864-866.

Chemla, D.S., Quantum wells for photonics," Physics Today, May, 1985, Vol. 38(5), pp. 56-64.

Dohler, G.H., H. Kunzel and K. Ploog, "Tunable absorption coefficient in GaAs doping superlattices," Phys. Rev. B, 1982, Vol. 25(4), pp. 2616-2626.

Dohler, G.H., and P.P. Ruden, "Theory of absorption in doping superlattices," Phys. Rev. B, 1984, Vol. 30(10), pp. 5932-5944.

Dohler, G.H., "Light generation, modulation, and amplification by n-i-p-i doping superlattices," Optical Engineering, 1986, Vol. 25(2), pp. 211-218.

Dohler, G.H., G. Fasol, T.S. Low, J.N. Miller and K. Ploog, "Observation of tunable room temperature photoluminescence in GaAs doping superlattices," Solid State Comm., 1986, Vol. 57(8), pp. 563-566.

Gal, M., J.S. Yuan, J.M. Viner, P.C. Taylor and G.B. Stringfellow, "Modulated-reflectance spectroscopy of InP doping superlattices," Phys. Rev. B, 1986, Vol. 33(6), pp. 4410-4413.

Hasnain, G., G.H. Dohler, J.R. Whinnery, J.N. Miller and A. Dienes, "Highly tunable and efficient room-temperature electroluminescence from GaAs doping superlattices," Appl. Phys. Lett., 1986, Vol. 49(20), pp. 1357-1359.

Kitamura, K., R.M. Cohen and G.B. Stringfellow, "Doping superlattices in GaP," J. Appl. Phys., 1987, Vol. 61(4), pp. 1533-1536.

Kobayashi, H., Y. Yamauchi, H. Kawaguchi and K. Takahei, "Nonlinear optical absorption of InP doping superlattices," Jap. J. Appl. Phys., 1986, Vol. 25(10), pp. L804-L807.

Miller, D.A.B., D.S. Chemla, T.C. Damen, A.C. Gossard, W. Wiegmann, T.H. Wood and C.A. Burrus, "Electric field dependence of optical absorption near the band gap of quantum-well structures," Phys. Rev. B, 1985, Vol. 32(2), pp. 1043-1060.

Priester, C., G. Allan, M. Lannoo and G. Fishman, "Theoretical approach for a n-i-p-i silicon," Phys. Rev. B, 1987, Vol. 35(6), pp. 2904-2908.

Simpson, T.B., C.A. Pennise, B.E. Gordon, J.E. Anthony and T.R. AuCoin, "Optically induced absorption modulation in GaAs doping superlattices," Appl. Phys. Lett., 1986, Vol. 49(10), pp. 590-592.

Wood, T.H., C.A. Burrus, D.A.B. Miller, D.S. Chemla, T.C. Damen, A.C. Gossard and W. Wiegmann, "High-speed optical modulation with GaAs/GaAlAs quantum wells in a p-i-n diode structure," Appl. Phys. Lett., 1984, Vol. 44(1), pp. 16-18.

Yuan, J.S., M. Gal, P.C. Taylor and G.B. Stringfellow, "Doping superlattices in organometallic vapor phase epitaxial InP," Appl. Phys. Lett., 1985, Vol. 47(4), pp. 405-407.

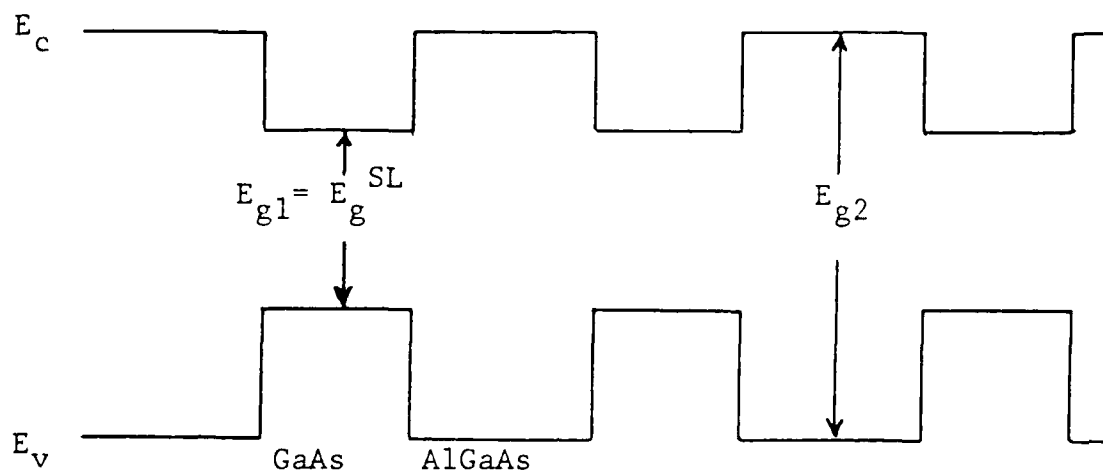


Fig. 1 Spatial variation of the band edges in a GaAs/AlGaAs compositional SL.  $E_g^{SL}$  is the band gap for the SL;  $E_{g1}$  and  $E_{g2}$  are the band gaps of the respective bulk materials.

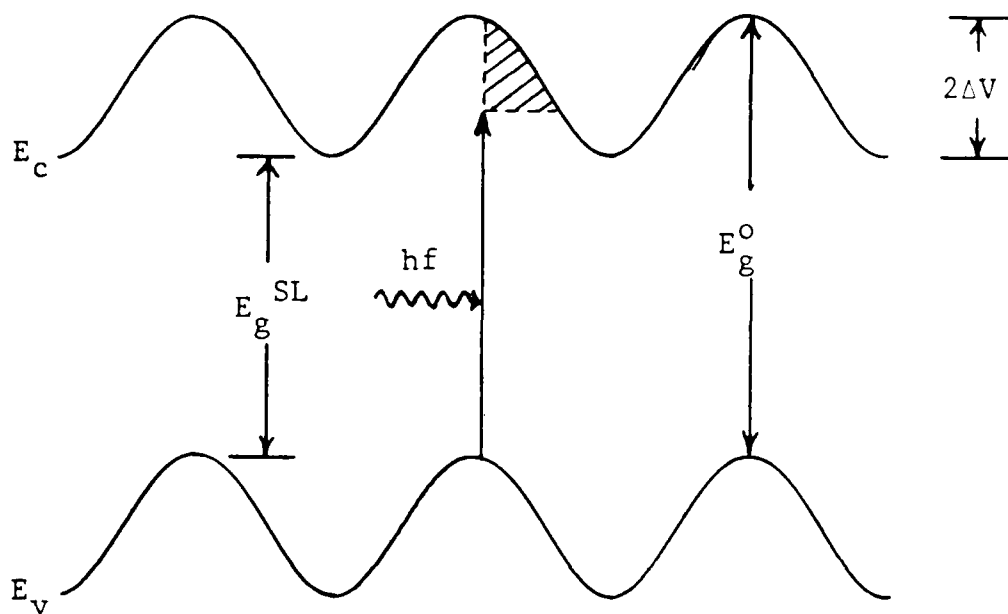


Fig. 2 Spatial variation of the band edges in a doping (n-i-p-i) SL.  $E_g^0$  is the band gap of the bulk material,  $E_g^{SL}$  is the effective band gap of the SL, and  $\Delta V$  is the amplitude of the oscillation in the superlattice potential. Absorption of a photon with energy less than  $E_g^0$  is illustrated. The shaded region schematically represents the region through which the electron must tunnel.



1987 USAF-UES SUMMER FACULTY RESEARCH PROGRAM  
GRADUATE STUDENT SUMMER SUPPORT PROGRAM

Sponsored by the  
AIR FORCE OFFICE OF SCIENTIFIC RESEARCH

Conducted by the  
Universal Energy Systems, Inc.

FINAL REPORT

Prepared by:	William K. Curry
Academic Rank:	Assistant Professor
Department and	Computer Science
University:	Rose-Hulman Institute of Technology Terre Haute, Ind
Research Location:	Wright-Patterson AFB Dayton, Ohio
USAF Researcher:	Captain Bruce Edson
Date:	7 August 1987
Contract No:	F49620-85-C-0013

Computer Simulation of Adaptive Resource  
Management in Real-Time

by  
William K. Curry

ABSTRACT

Using computer simulation, a study was made of the management of limited, specialized resources, under real-time response constraints. The primary focus was the automatic control and assignment of Electronic Counter Measure (ECM) resources for an aircraft operating in a hostile electronic environment. Techniques from the fields of Artificial Intelligence and Object-oriented system design were utilized in an attempt to maintain this real-time response in a very large space of possible situations. We also attempted to create a system with adaptive characteristics to allow for simple, unassisted "learning" of the proper responses to unanticipated situations.

### Acknowledgments

I wish to thank the Air Force Wright Aeronautical Laboratories (AFWAL), the Air Force Systems Command, and the Air Force Office of Scientific Research for their sponsorship of these efforts. I also wish to thank Universal Energy Systems for their handling of the administrative portion of the Summer Faculty Research Program.

I greatly appreciate the excellent manner in which Capt. Bruce Edson provided needed support, resources, and technical assistance. The technical support provided by Lt. Richard Ricart was also of great help in my efforts.

## I. INTRODUCTION:

The increasing density of the enemy threat environment in Electronic Warfare (EW), and the increasing sophistication of the threat radars used, have combined to make the field of Electronic Counter Measures (ECM) one in which response time and the effectiveness of resource allocation have become critical factors [1]. When a hostile presence is detected there is a short period of time during which an ECM technique can be expected to succeed. The difficulty is compounded by these ECM resources being specialized, in the sense that a particular technique may or may not be an effective deterrent in a given threat situation. These constraints suggest that as much of the decision process as possible should be automated.

The problem presented by automated control is that computer software has generally relied on static responses to previously anticipated input patterns. Thus systems are, in general, unable to adapt to new types of inputs or unanticipated input combinations within real-time constraints, if at all. In the case of an ECM system, this limitation may force the aircraft crew back into a slow, manual decision making mode and thereby jeopardize the mission and/or the aircraft. It is to this problem that this research was directed.

The Software Development Group of the Avionics Lab of AFWAL has been studying the application of new computer system design concepts generated by the fields of Artificial Intelligence (AI) and Software Engineering, to the solution of complex and highly constrained systems such as these.

My fields of interest, and subjects which I have been teaching for the past two years are AI and Software Engineering. This problem was therefore of interest to me because concepts from both areas had to be enlisted to create a successful system. The AI concepts were needed to provide for the system's adaptation mechanisms. Software Engineering techniques were utilized to provide the flexibility, maintainability, and efficiency required by real-time military software.

## II. OBJECTIVES OF THE RESEARCH EFFORT:

Several AI techniques being developed enable software systems to undergo very simple learning processes. If an ECM control system can be developed which, by use of these learning techniques, will adapt to its current environment and "learn" the proper response to an unexpected threat, then the system might be relied upon in new situations to, at worst, degrade gracefully in its performance and at best, generate an effective response. If a generated response was found to be effective it could also store that information for later addition to the pool of knowledge known by all ECM systems.

The initial research goal was to produce a computer simulation of the problem, modeling the mechanisms by which a system such as this could adapt to new inputs correctly while giving a resource allocation recommendation on a real-time basis. Due to the real-time constraints placed on this system, the capability was needed to produce both a good, quick response when fast response was critical and an optimal response when the processing time was available. Since a system such as this would most likely have a long maintenance period, thus it was also important to consider simplicity and maintainability in our implementation.

In an attempt to generalize the problem area to a non-militarized, generic, resource management problem, it was

decided to map the ECM environment, using as much detail as possible, to the problem of an imaginary creature, labeled an EWOK, trying to survive in a hostile world. Whereas the aircraft has threats, the EWOK has predators, the aircraft has ECM tools, the EWOK has various techniques of confusing or evading his enemies, etc. In our EWOK world the number, type, and current activity of the predators combine to produce an overall situation. This situation is evaluated by our EWOK, which then responds with a defensive strategy consisting of one or more techniques. The natural constraints placed on the EWOK's responses were found to have a reasonable correspondence to the constraints placed on the aircraft's ECM system. For example the aircraft may release a flare, while the EWOK may release an odor, but both actions are limited by distance, time, threats against which they may prove effective, and the number of times during a single encounter they may be used.

### III.

The system was developed on an LMI (Lisp Machines Inc.) Lisp machine using the ZetaLisp dialect [3] of the LISP programming language. In order to make the system as portable as possible, with the exception of the user interface, only Common Lisp [2] constructs were used. To help manage the system's complexity and to introduce added flexibility, the system was designed with an object-oriented approach and implemented using Flavors [3].

In order to provide the EWOK with both the capability to quickly evaluate the current environment and to perform simple learning functions when needed, it was decided to use concepts from Fuzzy Cognitive Map structures to translate environment situations to EWOK responses. Fuzzy Cognitive Map structures are fuzzy signed digraphs having a feedback mechanism. Digraphs are used to represent causation (i.e. A being present and B being present causes C to be assumed, while C and D being present may inhibit E's assumption, etc.). These causation connections are signed because both positive (causal increase) and negative (causal decrease) relationships can be represented, and they are called fuzzy because the strengths of the connections are allowed to change as the system perceives a stronger or weaker causal relationship between the nodes. B. Kosko [4] gives a fuller explanation of FCM's structure make-up and operation. This ability to change the causal strength between two items during system operation provides the simple learning



mechanism which we felt could be utilized in creating an adaptable system.

Our particular use of FCM type knowledge representation involved, as with Kosko's FCMs, the assigning of causal (activation inducing) connection values between the various system entities. We, however, did not treat the collection of these connection values as a mapping matrix on which matrix operations could be applied to achieve input/output transformations. We chose to pass the individual connection values between the system entities wrapped in the body of system object messages. The values were treated more as a confidence in the need to fire (become active) for the receiving entity. The input values received were additive and when an entity received a high enough confidence level from its environment to fire, it became active and sent confidence values to any other system entities its activation influenced.

The system objects communicate via message passing. In order to control the complexity of the system's message passing, it was designed using some of the concepts found in the work of P. Green [5] on Activation Frameworks. When one of the intermediate objects, such as a technique classification object, receives an input message, it doesn't immediately process that message but instead places it in an input queue and increases a "queue potential" value associated with the object. When the object receives a "process" message, it then processes and/or routes each message in its input queue as needed. Messages are passed

only up to the object directly above the sender or to the object directly below the sender in the system hierarchy. This design accomplishes two purposes. First, the number of objects which an individual object must communicate with is reduced, making the system's data flow simpler. Secondly, if a response from some of the lower level objects is never needed then the time to process their messages may never be expended, making real-time response more attainable.

#### IV.

The system is built around a collection of objects, the four primary objects of the system being the environment object, the EWOK object, the weight table object, and the user interface object. All other system objects are subservient to one of these primary objects.

The environment object communicates with a collection of threat objects representing the EWOK's predators. The threat objects contain all of the information needed to uniquely identify their type, what they are currently doing, and how dangerous their current activity is to the EWOK.

The EWOK object represents the actual creature. It communicates with three types of subservient objects, state objects, mission objects, and technique classification objects. The state objects are used to model EWOK internal

conditions which may influence the response to a threat. For example if the EWOK is healthy he may choose an active defense technique against a threat, such as fighting, whereas if he is not healthy he may simply try to flee from the threat. These objects correspond to conditions that may exist onboard the aircraft, such as low fuel, aircraft damage, etc.

The mission objects keep track of what the EWOK is trying to accomplish and how important it is for him to accomplish it. These objects, when active, influence the class of responses the EWOK considers first when a threat appears. This is the area in an ECM system where the relative importance of crew safety and mission completion are evaluated.

The technique classification objects are used to break the EWOK's defenses into major categories, such as expendables which have quantity limitations, territorial techniques which depend on surrounding terrain, etc., with each category requiring different preconditions in the EWOK and the environment before its techniques are applicable. Each technique classification object knows about and communicates with its own group of defense techniques objects. These classifications were created so as to have a one-to-one correspondence to the ECM technique classifications used by the Air Force.

The weight table object is where the connection strengths of the system's entries are kept. When an object needs to send another object a message indicating the sender has fired

(become active) it sends the weight table object a "weight" message to determine the strength of the connection between sender and the receiving object.

V.

The system is menu driven with top level options of setting environment characteristics or talking to the EWOK. If the user opts to set environment characteristics then a second set of options is presented allowing him to turn on/off threats or modify threat characteristics. When a threat is turned on or a currently active threat has its characteristics changed, update messages are sent to the EWOK via the environment object.

When the user opts to communicate with the EWOK he is also given a second menu of options. Capabilities are provided for querying for and/or modifying the EWOK internal state and mission/goal factors which are active, and for asking the EWOK to produce a response to its current environment.

When the EWOK is asked to respond to its current environment, a defense is selected for each of the threats currently active in the environment. The selection process is a function of how dangerous the current threat is to the EWOK, which defense techniques the EWOK has left in its repertoire, and whether a quick answer is needed or the

optimal answer can be found. If the quick answer is needed, selections are made on the basis of a high level estimate of which defense groups would be the most effective in dealing with the current threats. If time permits a optimal answer, then all messages in the EWOK's object input buffers are processed and a steady internal state achieved prior to the selection of the highest priority defense group.

#### VI. RECOMMENDATIONS:

There are two primary additions which should be made to the system to complete it. Parts of the system may need to go through a redesign process in order to accomplish these additions, thus making them non-trivial modifications. There are also several areas which need further investigation before the system can be justified as a reasonable analogy to the original ECM resource management control problem.

The original intent of the effort was to build a system that, via modifications to the connection strengths in the FCM, could undergo a simple learning process to become more effective in dealing with known threats and to arrive at reasonable responses to new threats. At present, this feedback modification of the connection strengths has not been implemented.

The other critical gap is that, to provide the feedback needed for the above learning process, the environment must be able to automatically respond to the EWOK's use of techniques. This is an area which was not explored. The system thus provides only manual modification of the environment.

More study is needed into whether the greatest advantage can be gained by passing connection values inside of system messages or by dealing with the collection of values as one large transformation matrix. More study is also needed into the best mechanism to produce a "good" response when the processing time is not available to produce a "best" response.

Several details in the original problem were not carried into the simulation due to lack of time. These include the importance of aircraft mission phase (ingress, operations, egress) on the response needed, the fact that there are usually more than one friendly aircraft on a mission, whereas our system implements only one EWOK, and the detailed time factors involved in the interplay of an aircraft and the surrounding threat population.

In future versions the Flavors constructs used to implement the system's object structures could be replaced with the Loops object-oriented environment's constructs, since Loops is becoming more standard in this area.

## REFERENCES

- [1] D. Curtis Schleher, Ph.D., Introduction to Electronic Warfare, ARTECH House, Inc., 1986
  
- [2] Guy L. Steele, Jr., Common Lisp The Language, Digital Press, 1984
  
- [3] Richard M. Stallman, David Moon, Daniel Weinreb, Lisp Machine Manual, Sixth Edition, Lisp Machines, Inc., 1984
  
- [4] B. Kosko, "Adaptive Inference in Fuzzy Knowledge Networks", Proceedings of the IEEE International Conference on Neural Networks, San Diego, June 1987
  
- [5] Peter E. Green, "AF: A Framework for Real-Time Distributed Cooperative Problem Solving", Artificial Intelligence Research Group, Worcester Polytechnic Institute

1987 USAF-UES SUMMER FACULTY RESEARCH PROGRAM  
GRADUATE STUDENT SUMMER SUPPORT PROGRAM

Sponsored by the  
AIR FORCE OFFICE OF SCIENTIFIC RESEARCH

Conducted by the  
Universal Energy Systems, Inc.

FINAL REPORT  
EFFECT OF WIND AND TURBULENCE ON AN ARTIFICIALLY  
GENERATED STRATO-MESOSPHERIC PLASMA

Prepared by:	Phanindramohan Das
Academic Rank:	Professor
Department and	Department of Meteorology
University:	Texas A&M University
Research Location:	USAF - ESD/ATA Hanscom AFB, MA 01731-5000
USAF Researcher:	Lt. Col. William W. Lana
Date:	29 September 87
Contract No:	F49620-85-C-0013



Effect of Wind and Turbulence on an Artificially  
Generated Strato-Mesospheric Plasma

by  
Phanindramohan Das

ABSTRACT

The important principles relating to the generation of an Atmospheric Ionization Mirror (AIM) in the strato-mesospheric regions are reviewed. An equation on plasma evolution which includes ionization by high power microwave breakdown, and plasma loss by attachment to neutral particles, recombination, and by advection due to neutral air motion, is analyzed for relative importance of these factors in determining the steady-state condition of the artificially ionized region. The theory predicts that for a steady-state AIM to be possible, extremely weak winds are desirable.

The climatology of the middle-atmospheric winds is reviewed: it is found that strong winds are the rule in this region, with speeds close to  $200 \text{ m s}^{-1}$  being on record. There also are wide variations of winds both in space and time. While winds with speeds less than a few meters per second are desirable for a steady AIM, actual winds of several tens of meters per second need to be allowed for in an experimental design of an AIM.

### ACKNOWLEDGMENTS

I wish to thank the Air Force Systems Command and the Air Force Office of Scientific Research for sponsorship of this research. I also appreciate the concern and help provided by Universal Energy Systems in all administrative and directional aspects of the program.

The work atmosphere and the encouragement provided by Col. Bill Lana at the ESD/ATA set me on the path toward a very rewarding ten (or so) weeks of research and study. It was his amiability and that of Maj. Rich Arlen that helped me fit into the working environment of a predominantly military organization. On the technical side, the frequent discussions with Paul Kossey, Don Hunton and John Hechscher of Air Force Geophysical Laboratories (AFGL) helped me formulate my research problem which was entirely a new one for me. I must also mention the superb Research Library of AFGL, and its staff without whose constant help this research would have been immensely more difficult, if not impossible.

I also appreciate the concern of Mrs. Jackie Strong in typing and preparing the paper for me so as to enable me to meet the deadline.

## I. INTRODUCTION:

Natural ionization in the upper atmospheric layers, collectively known as the ionosphere, has played a vital role in long-range radio communication until the advent of the communication satellites. Even with the availability of satellites a major fraction of long-range communication still is dependent on the natural ionosphere. There also are important military needs of communication, guidance and control that are served by upper atmospheric ionization. However, the natural ionosphere is often not dependable as a medium for radiowave propagation because of its natural variability, including its susceptibility to sudden catastrophic disturbances due to solar flares. Ideas toward developing methods to control the ionospheric region or, if feasible, to create an artificial ionization region are, therefore, very attractive for military applications.

The idea of ionospheric modification, albeit for a purpose different from those alluded to above, dates back to 1937 when Bailey suggested that by irradiating the ionospheric region by powerful radiowaves at the electron gyrofrequency one should be able to produce an ionospheric glow discharge. This suggestion stayed afloat (Bailey, 1938; Bailey and Goldstein, 1958) until Clavier (1961) demonstrated its severe limitations. In the meantime, Soviet scientists (Ginsburg and Gurevich, 1960; Gurevich, 1965) made a comprehensive analysis of the nonlinear effects on the ionosphere likely to be produced by powerful electromagnetic waves. While these studies made reference to the problems of gas discharges and microwave breakdown, they did not specifically suggest the possibility of forming an ionized region in the atmosphere by microwave breakdown. Such a possibility as well as an atmospheric experiment was proposed by Lombardini (1965) who used the laboratory data of Brown and Rose (1957) and calculated power thresholds needed to produce atmospheric breakdown by using VHF radio waves.

While the Soviet scientists can claim no originality in experimental laboratory work on microwave breakdown, nor in suggesting atmospheric ionization by microwaves, they should be credited with providing a comprehensive theoretical and laboratory attack which was strongly

motivated by the possibility of forming an artificial ionization region (AIR) in the strato-mesospheric region ( $\sim 30-80$  km). Gurevich (1972) presented an analysis leading to the suggestion that a small patch of ionization could be formed and maintained by using a beam of high-power microwaves. This analysis was further refined by Gurevich (1979) and Borisov and Gurevich (1980) and a lucid presentation was made by Gurevich (1980) who described the complete concept of breakdown in the interference region of two intersecting, pulsed microwave beams. Various aspects of the concept have since been theoretically examined and laboratory experiments have been performed to validate the concept [see references in Duncan (1987)]. However, no facility has been built to test the concept in the atmosphere, apparently because of prohibitive cost and the gigantic nature of the engineering undertaking.

Recently, there has been a growing interest in the U.S. toward studying the feasibility of generating an AIR [renamed Artificial Ionization Mirror (AIM)] somewhere in the upper atmosphere. One of the concepts that is being considered seriously is that of using high-power microwave (HPM) beams to cause an electrical breakdown in the strato-mesospheric region. It is perceived that the Soviet studies on the concept, while appearing to be theoretically sound, need to be examined carefully, especially with respect to practical factors, before an engineering experiment is undertaken in the free atmosphere. Such factors are physical and chemical as well as meteorological in nature. The research reported here pertains to the last, and possibly a very important, category.

The most important meteorological factors that bear upon the proposed AIM are the winds - neutral winds, to be more specific - since in the middle atmosphere electrodynamic transport processes are negligible. The winds, however, arise in three different forms, namely: (1) the prevailing winds due to the temperature (and consequent pressure) gradients caused by solar heating - with their attendant seasonal variations, (2) periodic fluctuations in the prevailing winds caused by wave disturbances such as tidal waves (TW) and internal gravity waves (IGW), and (3) turbulent fluctuations with their attendant diffusive effect. The space-time variability of these winds is apparently very

complex and should strongly impact upon the maintenance if not the generation of an AIM.

## II. OBJECTIVES OF THE RESEARCH EFFORT:

The general objective of this research, as indicated above, is to assess the effect of neutral winds and turbulence on the generation and maintenance of an AIM in the strato-mesospheric region. Such an assessment is necessarily dependent on the conceptual engineering model which, for the purpose of this report, is that of Gurevich (1960), Borisov (1982), Borisov and Gurevich (1980, 1983) and Borisov, et al. (1983) with minor extensions and modifications. This model, as can be recalled, is based on the concept (validated in the laboratory) of electrical breakdown in air caused in the interference field of two intersecting, pulsed HPM beams. In the following section, the relevant details of the model are reviewed so as to show the manner in which the winds and turbulence will affect the maintenance of the AIM.

Despite the complex and far-reaching implication of the neutral-air motion on the maintenance of an AIM, Soviet scientists appear to have disposed of the question just by giving highly idealized analytical solutions to a time-dependent equation for electron density. Only a minimal effort has been made to examine the engineering implication of the winds and their spatial and temporal variation. This research addresses some of these implications. More specifically, the objectives pursued under this SFRP fellowship are:

- (i) to review the available information on middle atmospheric winds and their spatial and temporal variations, and
- (ii) to make a preliminary assessment of the impact of the above on an artificially ionized region (on an AIM, to be more specific) in the middle atmosphere.

## III. CONCEPTUAL MODELS OF AN ARTIFICIAL IONIZATION MIRROR (AIR):

As originally proposed by Lombardini (1965), following the laboratory data of Brown and Rose (1957), the breakdown field in air can be

written

$$E_b = Ap (1 + \omega^2/v_c^2)^{1/2}, \quad (1)$$

where  $E_b$  is the r.m.s. breakdown field in  $V m^{-1}$ ;  $A$ , a constant;  $p$ , the pressure in Pa;  $v_c$ , the collision frequency in  $s^{-1}$ ; and  $\omega$  is the frequency of the radio waves in radian  $s^{-1}$ . Following McDonald, et al. (1963) one can approximate

$$v_c = 3.98 \times 10^7 p$$

which can be inserted in (1). On the other hand, for a given r.m.s. field  $E_0$  under far-field approximation at the height  $h_0$ , produced by a vertically pointing antenna, the vertical variation of the field can be written

$$E(z) = E_0(h_0) (1 + z/h_0)^{-1} \quad (2)$$

in which atmospheric absorption has been neglected. Since atmospheric pressure and, consequently,  $E_b$  decreases exponentially with height according to (1) while  $E(z)$  decreases linearly according to (2), it should be possible to use a ground-based transmitter with appropriate amount of power to cause microwave breakdown at a predetermined height,  $h_b$ , say.

In addition to obtaining a method for estimating the height of the breakdown, Lombardini also obtained a method of determining the height at which the maximum rate of increase in ionization can be achieved with a given field  $E > E_b$ .

Lombardini's work, while being remarkable for its pioneering nature, apparently was ignored, obviously for the engineering demand his suggestions would make for an atmospheric experiment. For ionizing breakdown at the height of 60 km, for example, his calculations showed a needed HPM ("heater") power, at the frequency of 1 GHz, of 1.2 GW with an antenna gain of  $10^6$ . Later research shows that Lombardini's estimates are too optimistic. In terms of power gain product,  $P_T G$ , where  $P_T$

is the transmitted power and  $G$  is the antenna gain, the requirement estimated recently is  $\gtrsim 4 \times 10^{15}$  W while Lombardini's estimates work out at  $P_T G = 1.2 \times 10^{15}$  W.

Even though the power gain products needed for middle atmospheric breakdown were attainable, Lombardini's concept of a single beam HPM breakdown would suffer from a low predictability of the height of breakdown and the ionization to be attained because of the natural variation of atmospheric density and the background ionization. Of course, the need of extreme transmitter power, self-absorption of the heater beam in the ionization generated, and potential plasma instabilities immediately establish a preference for short pulses of HPM as the breakdown agency (Gurevich, 1972, 1979). In addition, Borisov and Gurevich (1980) and Gurevich (1980) prefer intersecting pulsed beams of high-power microwaves for upper-atmospheric breakdown. It is this concept and its variants that dominate the thinking on the generation of an AIM.

The concept of Borisov and Gurevich is schematically shown in Fig. 1: (a), explaining the general concept, and (b), giving a detailed structure of the breakdown region. The beams which, because of a very small width, are essentially parallel are made to intersect at an angle  $\psi$  which is adjustable. The phases of the waves in the individual beams as well as the pulses are adjusted so as to interfere in the region of interest which is indicated on the diagram (a) as the ionization layer. The detailed structure of the ionization region depicted in diagram (b) shows that the breakdown occurs in bands which are regions of additive interference. The axes of the consecutive bands are apart by a distance,  $a$ , where

$$a = \lambda / \sin(\psi/2) \approx 2\lambda / \psi \quad (3)$$

the last expression being valid when  $\psi \ll 1$ . The thickness of the band will depend on the field strength in the beams as well as the strength of diffusion. For weak diffusion Gurevich (1980) gives a thickness

$$d \sim (0.1 - 0.2)\lambda . \quad (4)$$

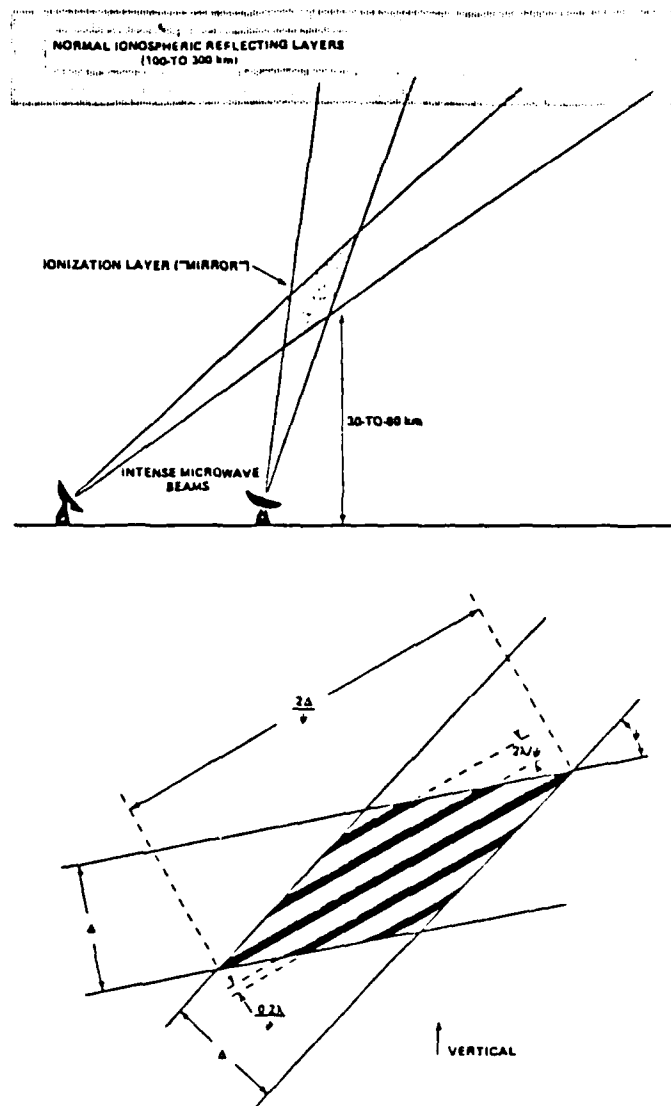


Fig. 1. Schematic representation of the intersecting beam concept of generation (and maintenance) of an AIM [from Field (1987)].



Another important aspect of the AIM engineering concept is the specification of pulse width and repetition rate. Since the power density requirement for breakdown is large, the most economical way of operating an AIM is considered to be to establish the AIM with a pulse of relatively large duration,  $\tau_{est}$ , and then maintain it with pulses of shorter duration  $\tau_m$ . The rationale for this approach can be seen as follows. In the beginning the ionization needs to be built up from ambient electron density; if the required operating minimum plasma density is  $N_{min}$ , the ionization in the first pulse is driven to a value  $N_{max}$  somewhat above  $N_{min}$ . When the establishment pulse is turned off, deionization processes, such as attachment and recombination, will decrease the plasma density to  $N_{min}$  in time  $\tau_D$  when the maintaining pulse is turned on. The duration of maintenance pulse  $\tau_m$ , will be much shorter than  $\tau_{est}$  since the breakdown will occur at a much higher initial electron density of  $N_{min}$ . The period  $\tau_m + \tau_D = 1/F$  determines the pulse repetition period  $F$ . The process described here is schematically shown in Fig. 2.

A second concept for generating an AIM has also been presented in the Soviet literature. Novikov and Sergeichev (1982), with a view to reducing the required pulse power, suggests that the antenna dimensions be increased so as to focus the beams to a very small width. With such an approach, breakdown fields can be achieved by using a small power in the individual pulses. In order to increase the dimensions of the mirror, then, the beams can be slewed in a manner analogous to the raster used in forming TV pictures. At a given point of intersection, as schematically shown in Fig. 3 a mirror cell is formed and a mirror can be synthesized from a number, say  $J$ , of longitudinal cells and  $K$  transverse cells.<sup>1</sup> The principal constraint is that the beams must return to the first cell every duty period,  $\tau_m + \tau_D$ . Defining the duty fraction  $D_F \equiv \tau_m / (\tau_m + \tau_D) = \tau_m F$  we can see the limitation to be

$$JK \leq 1/D_F. \quad (5)$$

---

<sup>1</sup>Here, "longitudinal" means in the plane of intersection, and "transverse," means normal to the plane of intersection of the beams.

## ESTABLISHMENT AND MAINTENANCE PULSES

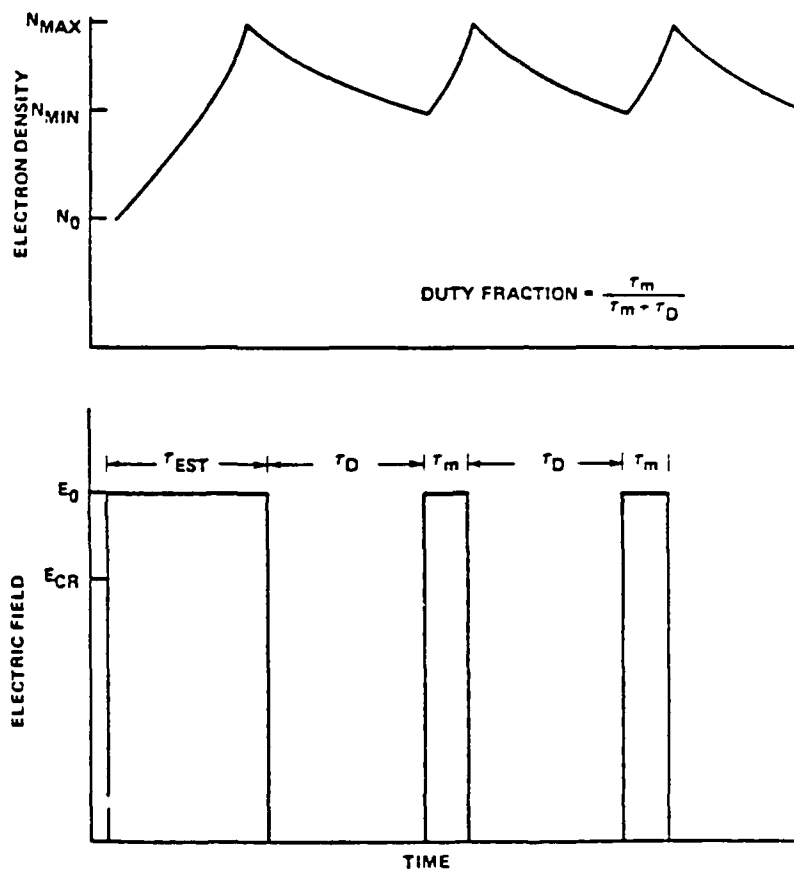


Fig. 2. A schematic representation of pulse duration and repetition in establishing and maintaining an AIM [from Field (1987)].

## MULTI-CELL MIRROR FROM SCANNING BEAM

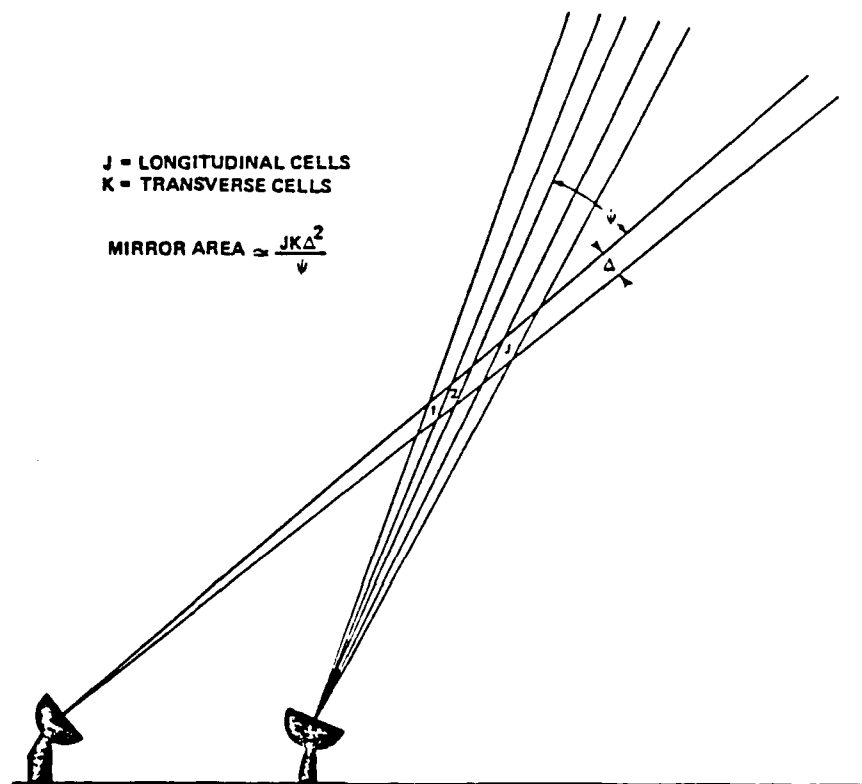


Fig. 3. Conceptual method of generating a multicell AIM by the scanning of intersecting beams [from Field (1987)].

For the convenience of subsequent discussion we may note that there are two apparent advantages in the multi-cell approach: (1) the peak power in an individual pulse is reduced greatly, and (2) it will be easier to generate an essentially horizontal mirror. These advantages are gained at the cost of (1) antennas of larger diameters, and (2), for a given mirror size, a smaller  $D_F$  is needed to maintain the mirror from many small cells than to maintain it from a single large one. A smaller  $D_F$  may be achieved by shorter  $\tau_m$  (higher power) or a longer  $\tau_D$  (lower rate of deionization - at a greater height, for example).

In the sequel we shall refer to the above engineering concepts as single-cell AIM and multi-cell AIMs, respectively.

#### IV. EFFECT OF NEUTRAL AIR MOTION ON AIM

a. Theory. The effect of various factors, including neutral air motion, is approached through an equation of continuity for plasma concentration. In writing such an equation Gurevich (1972), Borisov and Gurevich (1980), and Borisov, et al. (1983), have included a term representing the advective change in plasma concentration. I shall rewrite their equation in a slightly different manner so as to include the effect of fluctuating winds. The equation takes the following form:

$$\begin{aligned} \frac{\partial N}{\partial t} + \vec{V} \cdot \nabla N + \bar{w} \frac{\partial N}{\partial z} + \nabla \cdot (\overline{N \vec{V}}) + \frac{\partial}{\partial z} (\overline{w N}) \\ = (\nu_i - \nu_a)N + D_a \nabla^2 N - \alpha_r N^2, \end{aligned} \quad (6)$$

in which, formally speaking,  $N$ ,  $\vec{V}$ ,  $\bar{w}$ ,  $\overline{N \vec{V}}$  and  $\overline{w N}$  can be treated as an average over a suitable time scale. The symbols are

- $N$ , electron concentration ( $\text{vol}^{-1}$ )
- $\vec{V}$ , winds in the x-y plane defined below,
- $w$ , wind in the z direction defined below,

$v_i$ , ionization rate under the applied electric field,  
 $v_a$ , rate of loss of electrons by attachment to neutral particles,  
 $D_a$ , ambipolar diffusion constant,  
 $\alpha_r$ , recombination coefficient,  
 $t$ , time, and  
 $\nabla_3 \equiv \left( \frac{\partial}{\partial x}, \frac{\partial}{\partial y}, \frac{\partial}{\partial z} \right) \equiv \left( \nabla, \frac{\partial}{\partial z} \right),$

where  $x, y$  are cartesian coordinates in the plane normal to the bisector of the angle between the intersecting beams, along which the coordinate is  $z$ . Equation (6) is physically awkward and has only a formal meaning: while the time scale of the variation of  $N$  is on the order of milliseconds due to deionization and diffusion, the wind observations are on time scales of minutes and hours. Thus any observable interaction of neutral air motion with the above time scales of variation predominantly has to be treated in an advective sense (that is, in terms of  $\vec{V} \cdot \nabla N$  and  $\bar{w} \partial N / \partial z$ ). The fluctuations, on the other hand have to be theoretically deduced with an a posteriori verification. It is no wonder, therefore, that the Soviet scientists completely ignored the terms involving wind fluctuations. A good example of the Soviet approach is given by Borisov, et al. (1983) who treat the problem as a one-dimensional one and in a steady state in the sense of an average over a pulse repetition period:

$$D_a \frac{d^2 N}{dx^2} - v_x \frac{dN}{dx} + (v_i - v_a - \alpha_r N)N = 0, \quad (7)$$

in which  $v_i$  needs to be determined from a coupled equation for the electric field, and the  $x$ -axis is in the plane of the beams. In addition  $v_x$  is the  $x$ -component of the wind. This equation then is put into a non-dimensional form:

$$\frac{d^2 n}{dX^2} - K_v \frac{dn}{dX} + (K_i - K_a)n - K_r n^2 = 0, \quad (8)$$

where

$$\begin{aligned} n &= N/N_0, & N_0 &= \epsilon_0 m(\omega^2 + \nu_e^2) \sin^2(\psi/2)/e^2 \\ k_x &= \text{x-component of the wave vector } \vec{k}, \\ X &= k_x x, \\ K_v &= \nu_x/D_a k_x, \\ (K_i, K_a) &= (\nu_i, \nu_a)/D_a k_x^2 \\ K_r &= \alpha_r N_0/D_a k_x^2. \end{aligned}$$

In the above  $m$  = electron mass,  $\omega$  = angular frequency of heater wave,  $\nu_e$  = electron collision frequency,  $e$  = electronic charge and  $\epsilon_0$  = electric permittivity of free space. On the basis of a set of optimal conditions developed by Gurevich (1980), Borisov, et al. (1983) generated the parameter values shown in Table I. It should be remarked that  $K_v$  is based on a wind of  $40 \text{ m s}^{-1}$ ; other quantities needed for computing  $K_v$  and other  $K$ 's are based on standard atmospheric values. The surprising result to the effect that  $K_v$  is invariant with height is due to their using optimal conditions when  $k_x$  and  $D_a$  become inversely related through collision frequency.

Table I\*

Height (km)	$\omega_{\text{opt}}(\text{s}^{-1})$	$k_{x(\text{opt})}(\text{m}^{-1})$	$(\tau_m F)_{\text{opt}}$	$K_a$	$K_r$	$K_v$
30	$7.4 \times 10^{10}$	120	$3.0 \times 10^{-5}$	300	6000	120
40	$1.6 \times 10^{10}$	27	$6.5 \times 10^{-6}$	65	1300	120
50	$4.4 \times 10^9$	7	$1.8 \times 10^{-6}$	17	350	120
60	$1.3 \times 10^9$	2	$5.0 \times 10^{-7}$	5	100	120

\*Explanation:  $\omega_{\text{opt}}$ , optimal angular frequency at which  $k_{x(\text{opt})}$  is the (x-component of) wave vector.

Table I immediately suggests that while ambipolar diffusion is small and possibly negligible, the effect of wind becomes very important except perhaps at the lowest levels where recombination dominates the loss process. At the upper levels ( $h > 60 \text{ km}$ ) recombination becomes

weak and winds become very important.

Borisov and Gurevich (1980) and Borisov, et al. (1983) sought to analyze the effect of the winds by obtaining analytical solutions of (8). With drastic simplification (and somewhat questionable linearization), Borisov, et al. arrived at the conclusion that a steady-state AIM (in the sense of an average over a pulse repetition period) cannot be achieved unless

$$v_x < 6.6 \times 10^2 (\tau_m F)_{\text{opt}}^{1/2} \text{ m s}^{-1},$$

the subscript "opt" standing for the optimal condition. The values of  $(\tau_m F)_{\text{opt}}$  cited for an AIM at 60 km is  $5 \times 10^{-7}$  s which makes

$$v_x < 0.46 \text{ m s}^{-1}.$$

The physical meaning of these conditions is quite obvious: "The wind carries off the ionization, and later is restored by a diffusion process." For a given wind condition, this condition can be met by increasing the duty fraction - principally by increasing  $\tau_m$ . I shall come back to this point later on. In the meantime we should note that even at 30 km where  $(\tau_m F) \sim 3 \times 10^{-5}$ ,  $v_x$  needs to be less than  $3.6 \text{ m s}^{-1}$ .

b. Middle atmospheric winds. As alluded to earlier, the information on middle atmospheric winds can be organized in terms of the prevailing (seasonal) winds and their fluctuations. CIRA (1972) presents the wind observations in terms of models - the one for the zonal (W-E) winds being expressed as

$$u = u_0 + u_1 + u_2 + u_{QB}$$

where  $u$  is the total mean wind for an observation time at a given point,  $u_0$ , the seasonal (say, monthly) mean component,  $u_1$  and  $u_2$ , respectively, are the 24- and 12-hour tidal components, and  $u_{QB}$  is the so-called quasi-biennial oscillation. In the following discussion we shall

exclude  $u_{0g}$  for an obvious lack of importance in our problem.

A meridional view of  $u_0$  over the globe for the month of January is shown in Fig. 4 which is constructed partly by interpreting Northern Hemispheric July data as that of Southern Hemispheric January. It needs to be emphasized that the meridional cross-section is constructed out of data having insufficient longitudinal distribution. However, fortunately, the North American region is very well represented.

A meteorological discussion of the  $u_0$ -field is of little significance to the study - the only important point being that of estimating maximum wind speeds in the altitude range from about 30 to 100 km. We observe broad wind speed maxima in the 30-80 km altitude range with intense speed maxima between 60 and 70 km. The maximum speeds at these heights, according to Fig. 4, are  $80 \text{ m s}^{-1}$  for westerlies and  $50 \text{ m s}^{-1}$  for the easterlies.

Strong as they are in the averaged global view, the prevailing zonal westerly maxima are stronger, according to CIRA (1972), in the winter months over North America, often being over  $100 \text{ m s}^{-1}$ . In the spring and fall months the zonal winds are lighter - maxima with  $40 \text{ m s}^{-1}$ . Summer months however show maximum zonal speeds of  $60 \text{ m s}^{-1}$  - easterlies below 80 km and westerlies above 90 km - in the latitude belt from  $30^\circ$ - $60^\circ$  over North America.

Before I discuss the tidal contributions ( $u_1, u_2$ ) to the zonal winds, I should mention the meridional (N-S) component of the prevailing winds, which also has appreciable average speeds, the maxima in the North American Middle Atmosphere being of the order of  $15 \text{ m s}^{-1}$ . In other words, all in all, we often should expect maximum wind speeds well above  $100 \text{ m s}^{-1}$  in the N. American Middle Atmosphere. In fact, we should expect even stronger winds in the northernmost latitudes in view of wind speed reports of  $184 \text{ m s}^{-1}$  and  $198 \text{ m s}^{-1}$  from stations in the North European region.

The gross picture of tidal contributions to the winds is that of amplitudes of the diurnal as well as semi-diurnal components being on the order of  $10 \text{ m s}^{-1}$  both in the zonal (W-E) and meridional (N-S) components. The tidal contribution can easily reach  $100 \text{ m s}^{-1}$  in the lower thermosphere. A set of individual zonal wind profiles in this



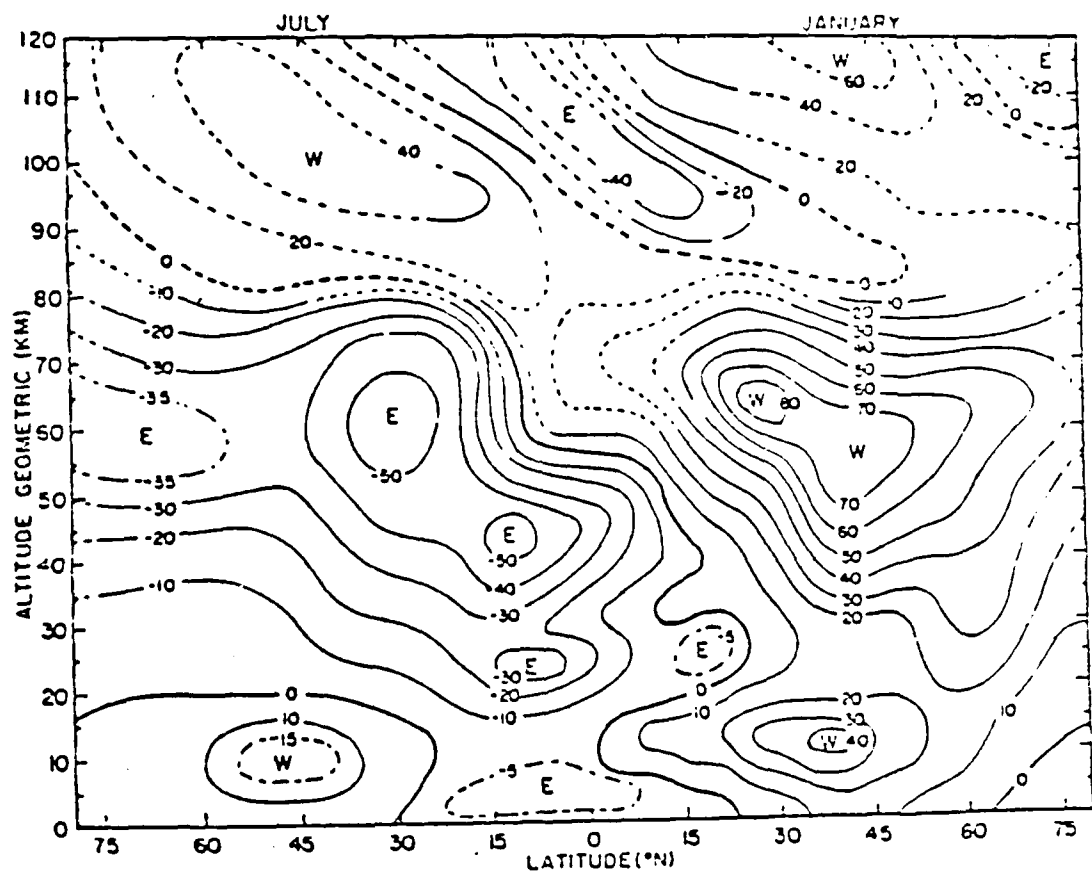


Fig. 4. Mean January and July Zonal Winds to 120 km between Equator and 75°N [from CIRA (1972)].

region of the atmosphere presented by CIRA (1972) (see Fig. 5) proves the point.

Gravity wave contribution to middle-atmospheric winds and turbulence. CIRA (1972), has not explicitly discussed the role of vertically propagating gravity waves on the vertical distribution of zonal winds. Hirota (1984) displays a mean meridional cross-section of the annual range of the zonal winds based on CIRA (1972) and points out a distinct minimum in the mesopause region. Indeed, individual zonal wind cross-sections themselves tend to show zonal speed minima in the mesopause region. Hirota presents statistical analyses in which he isolates the fluctuations, presumably due to gravity waves, of the zonal winds and temperatures, and confirms the presence of waves with vertical wavelengths of the order of 10 km. The amplitude of gravity-wave fluctuation of the zonal winds are estimated at about  $10 \text{ m s}^{-1}$ . Unfortunately the data used by Hirota does not go up to the mesopause.

An explanation of the rapid decrease of zonal wind speed above 60 km ( $\sim$  stratopause) is based on breaking gravity (and, possibly, tidal) waves in the mesosphere (Houghton, 1978; Lindzen, 1981; and others). For our purpose, there are two aspects of gravity-wave breakdown that are important: (1) the rapid fluctuation in the winds that a breaking, sharp-crested wave will cause, and (2) the turbulent diffusion that breaking gravity waves will generate. At present, there is no clear idea of the extent of middle atmospheric turbulence and how much of it is due to gravity waves. There are some estimates - about  $200 \text{ m}^2 \text{ s}^{-1}$  by Lindzen (1981) at 85 km, and a vertical profile of eddy viscosity:

$$D_{\text{eddy}}(z) = 400 \times 10^2 - 110 \text{ km}/40 \text{ km} (\text{m}^2 \text{ s}^{-1}),$$

due to Matsuno (1982). These are large values - much larger than the expected ambipolar diffusion of the order of a few  $\text{m}^2 \text{ s}^{-1}$  that is expected at 85 km height. At present it remains intriguing as to how much of the gravity-wave generated neutral-air turbulence can contribute to the enhancement of plasma diffusion.

c. Discussion of the effect of neutral-air motion on AIM. The

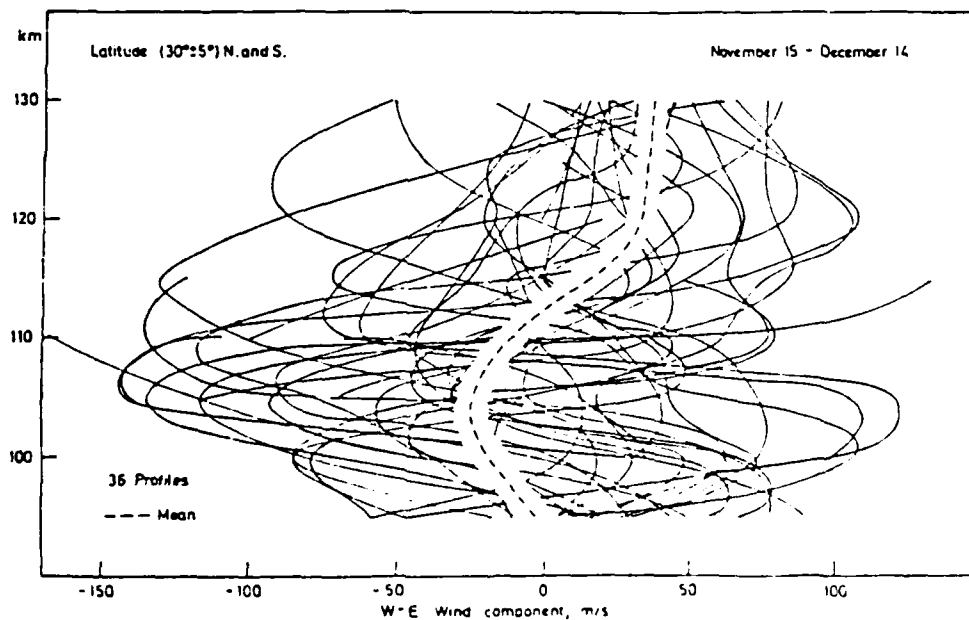
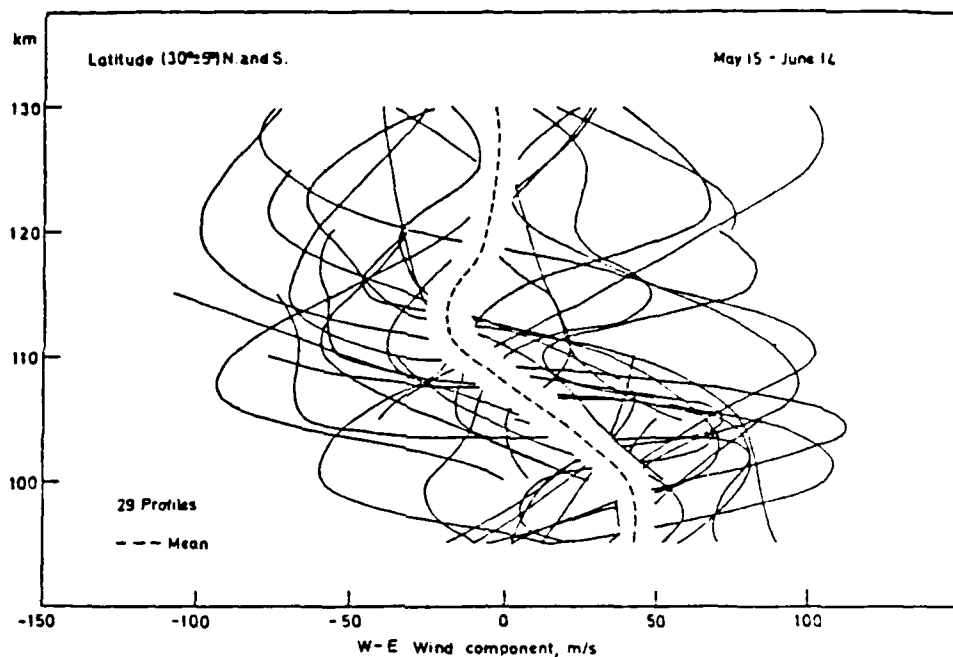


Fig. 5. Zonal wind profiles from chemical trail experiments at  $30 (\pm 5)^\circ$  latitude N and S for launchings held 15 May - 14 June and 15 November - 14 December. Data from the S. Hemisphere are shifted by 6 months to correspond in season. The dashed lines are mean profiles [from CIRA (1972)].

most striking feature of the Middle Atmospheric winds is extreme variability as well as strength, which demands very careful planning of small-scale experiments such as that of an AIM. Obviously, if we are thinking of centimeter-length microwaves as the breakdown agency, which would make ion streaks of widths on the order, at best, of centimeters, we find them bodily displaced considerably between pulses: with a  $100 \text{ m s}^{-1}$  wind and a pulse repetition period of  $10^{-3} \text{ s}$ , we expect a displacement of 10 cm between pulses. Thus if diffusion is low, as it will be under molecular conditions, the concept of starting an AIM with a pulse of duration  $\tau_{\text{est}}$  and then maintaining it with a pulse with  $\tau_m \ll \tau_{\text{est}}$  will be virtually untenable. In other words, the design of an AIM experiment should be based on  $\tau_{\text{est}}$  alone.

The large displacement of the AIM plasma in neutral winds appears to favor the multicell method of generating an AIM, although with pulses of duration  $\tau_{\text{est}}$  rather than  $\tau_m$ , since this method will tend to generate a broader plasma environment. In addition, at least conceptually, higher altitudes are preferred where the recombination and attachment are relatively small so that longer pulse repetition periods and longer wavelengths can be used. I do not have, at present writing, the design parameters needed for the mesopause heights - 80-90 km - which appear very attractive as an experimental height for an AIM. This altitude range may have an additional attraction in having a large turbulent diffusion due to gravity-wave dumping, although it is not clear what fraction, if any, of the turbulent energy generated will participate in the mixing of irregularities on the scale of a few centimeters.

#### V. RECOMMENDATIONS:

a. In view of the conclusion reached above, any experimental design of an AIM must include, ab initio, the effect of winds; since such a design will possibly be preceded by a computer simulation of the physics and dynamics of an HPM-induced plasma, such simulation must include realistic winds - neutral air motion - on various space-time scales.

b. Conceptually as well as theoretically speaking, diffusion is likely to have considerable beneficial importance in the maintenance of a plasma patch of relatively uniform consistency. In the Middle Atmosphere the molecular (ambipolar) diffusion is likely to be too small for the purpose. On the other hand turbulent eddies are generated on a rather large scale. While certainly participating in mixing processes in general, the eddies will need to cascade into the scale of the wavelength of the heater beam before being able to augment the diffusion on that scale. Maekawa, et al. (1987), for example, suggest that a large amount of gravity-wave energy is absorbed in the height range 85-90 km. A method must be found for translating this energy into a coefficient of diffusion on the scale of a wavelength of an HPM.

c. With respect to breaking vertically propagating waves in the mesosphere, the identification of their source is not unequivocal. For the purpose of siting an AIM experiment, it will be desirable to identify preferred regions of high gravity wave activity, presuming that such preferred regions exist. This means analyzing available MST radar wind data specifically for this purpose.

d. I have not had any experience with chemical trail experiments but must ask, naively perhaps, if any attempt has been made to measure small-scale diffusion in the chemical trails. If so, with what results? If not, are there data that can be analyzed toward such a purpose?

## REFERENCES

- Bailey, V. A., On Some Effects Caused in the Ionosphere by Electric Waves. Phil. Mag., 1937, Vol. 23, pp. 929-960.
- Bailey, V. A., Generation of Auroras by Means of Radio Waves. Nature, 1938, Vol. 142, pp. 613-614.
- Bailey, V. A., and L. Goldstein, Control of the Ionosphere by Radio Waves. J. Atmos. Terr. Phys., 1958, Vol. 12, p. 216.
- Borisov, N. D., and A. V. Gurevich, High Frequency Pulsed Air Breakdown in Intersecting Radio Beams. Geomagnetism and Aeronomy, 1980, Vol. 20, pp. 587-591.
- Borisov, N. D., and A. V. Gurevich, Reflection of Radio Waves from an Artificial Ionized Region. Geomagnetism and Aeronomy, 1983, Vol. 23, pp. 441-444.
- Borisov, N. D., O. A. Gel'fond, and A. V. Gurevich, Structure of an Artificial Ionized Layer in the Atmosphere. Sov. J. Plasma Phys., 1983, Vol. 9, pp. 610-616.
- Brown, S. C., and D. Rose, Microwave Gas Discharge Breakdown in Air, Nitrogen and Oxygen. J. Appl. Phys., 1957, Vol. 28, pp. 561-
- CIRA, COSPAR International Reference Atmosphere, Berlin, Akademie-Verlag, 1972.
- Clavier, P. A., Man-Made Heating and Ionization of the Upper Atmosphere. J. Appl. Phys., 1961, Vol. 32, pp. 570-577.
- Duncan, L. M., Soviet Literature Review, Los Alamos, Los Alamos National Laboratory, 1987.
- Field, E. C., Jr., Subionospheric Reflecting Layer Produced by Intense Electromagnetic Beams, Los Angeles, Pacific-Sierra Research Corporation, 1987.
- Ginsburg, V. L., and A. V. Gurevich, Nonlinear Phenomena in a Plasma Located in an Alternating Electric Field. Sov. Phys. Usp., 1960, Vol. 3, pp. 115-146.
- Gurevich, A. V., Contribution to the Theory of Nonlinear Effects during Radio Wave Propagation in the Ionosphere. Geomagnetism and Aeronomy, 1965, Vol. 5, pp. 49-56.

- Gurevich, A. V., Isothermal Ionization of the Atmosphere under the Effect of Radio Waves. Geomagnetism and Aeronomy, 1972, Vol. 12, pp. 556-564.
- Gurevich, A. V., Ionization of the Lower Ionosphere under the Effect of Strong Radio Pulses. Geomagnetism and Aeronomy, 1979, Vol. 19, pp. 428-432.
- Gurevich, A. V., An Ionized Layer in a Gas (in the Atmosphere). Sov. Phys. Usp., 1980, Vol. 23, pp. 862-865.
- Hirota, I., Climatology of Gravity Waves in the Middle Atmosphere. Dynamics of the Middle Atmosphere, J. R. Holton and T. Matsuno, Eds., Tokyo, Terra Scientific Publishing, 1984, pp. 65-75.
- Lindzen, R. S., Turbulence and Stress owing to Gravity Wave and Tidal Wave Breakdown. J. Geophys. Res., 1981, Vol. 86, pp. 9707-9714.
- Lombardini, P. P., Alteration of the Electron Density of the Lower Ionosphere with Ground-Based Transmitters. Radio Sci., 1965, Vol. 69D, pp. 83-94.
- Matsuno, T., A Quasi-one Dimensional Model of the Middle Atmosphere Circulation Interacting with Gravity Waves. J. Meteor. Soc. Japan, 1982, Vol. 60, pp. 215-226.
- McDonald, A. D., D. V. Gaskell, and H. N. Gitterman, Microwave Breakdown in Air, Oxygen, and Nitrogen. Phys. Rev., 1963, Vol. 130, 1841-1850.

1987 USAF-UES SUMMER FACULTY RESEARCH PROGRAM/

FACULTY SUMMER SUPPORT PROGRAM

Sponsored by the  
AIR FORCE OFFICE OF SCIENTIFIC RESEARCH

Conducted by the  
Universal Energy System, Inc.

FINAL REPORT

Analysis and Modeling of the Thermal Response of an Autoclave  
for Expert System Control of Carbon-Epoxy Composite Fabrication

Prepared by:	Bruce A. DeVantier
Academic Rank:	Assistant Professor
Department and	Civil Engineering and Mechanics
University:	Southern Illinois University at Carbondale
Research Location:	AFWAL/MLBC Wright Patterson AFB Dayton, OH 45433
USAF Researcher:	Francis Abrams
Date:	23 August 87
Contract No:	F449620-85-C-0013



Analysis and Modeling of the Thermal Response of an Autoclave  
for Expert System Control of Carbon-Epoxy Composite Fabrication

by

Bruce A. DeVantier

ABSTRACT

An analysis is performed to determine the thermal properties of an autoclave used for the production of epoxy based carbon fiber composites. The emphasis in the work is the development of a model of autoclave response for use in model simulation of a process response to expert system control. The model developed is capable of reproducing the response of a small autoclave currently used during expert system control of the epoxy curing process. Verification is made by comparing the model prediction to test measurements made during an autoclave heatup and cooldown. The computer coding for the thermal model is in both FORTH and FORTRAN languages. The FORTH version is included because the expert system control shell is written in this language, and the possibility of real time application is considered. The FORTRAN version is used in a process simulation mode, in conjunction with an epoxy composite curing model, and the language choice is necessary because of compatibility with the curing model. The model has been tested in this simulator mode, and realistic response was noted. Five parameters are used to fit the autoclave response in the heating and cooling modes. The parameters result from a lumped mass formulation and include thermal masses of the autoclave solid structure and the internal gas, as well as heat transfer coefficients. The values of these fitted constants reveals a relatively stable control system, with a damped response due to significant loss of heat to surroundings in comparison to the thermal masses involved.

### Acknowledgements

I wish to acknowledge the financial and logistic aid provided by the Air Force Systems Command, the Air Force Office of Scientific Research, and Universal Energy Systems for making this work possible. The opportunities provided are and will continue to be of immeasurable value to me personally and professionally.

The direction and advice of Francis Abrams were key to my progress, and I will be always indebted to her for the time she took out of her very busy schedule. Comments and evaluations from Dr. William Lee were very helpful to my understanding of the computational and physics-related aspects of the program. The general guidance of Major Steve Leclair was also of great value. Finally, I wish to thank Charles Norfleet, whose contributions were that of a colleague rather than a graduate student under direction. His constant help was and is greatly appreciated.

## I. INTRODUCTION:

The use of artificial intelligence as an engineering tool has recently expanded greatly. The branch of artificial intelligence known as expert systems has been shown to be useful in the field of process control. The Nonmetallic Materials Branch of the Materials Laboratory at Wright Patterson Air Force Base has been investigating expert system control of the curing of thermoset resin carbon composites in conjunction with the Manufacturing Processes Branch of the same laboratory.

The control of the composite curing process requires the use of an autoclave for the temperature and pressure control of the process. The normal process is controlled by a unit utilizing electronic analog control of the servo mechanisms regulating process control variables. The imposition of specific schedules of pressure and temperature can be effected by a microprocessor in the control unit. The autoclave can be operated in a scheduled or manual mode. The expert system controls the control unit by mimicry of the control strategy which would be used by an individual with expertise in composite fabrication and autoclave control. Use of the expert system control has been demonstrated to decrease the processing time and improve the reliability of controlled curing.

This investigator has worked on the development of computational process models for composite fabrication. The usefulness of process models to development of expert system control in composite processing has been demonstrated in control simulations with computational models. Simple lumped parameter models have been utilized by this investigator to simulate

thermal response of composites during curing, and this experience has provided a framework for extended investigations with the Materials Laboratory.

## II. OBJECTIVES OF THE RESEARCH EFFORT:

The control of composite curing by an expert system represents an extra level of control complexity for the process. The potential for control instability will depend upon the physical characteristics of the autoclave and the autoclave control device settings. It appears that a simple lumped parameter description of the thermal response characteristics can be utilized in the assessment of autoclave response to control. With a simple model such as this it would also be possible to predict in real time if control problems were a possibility.

The objectives of the study were to develop a simulation model for autoclave response to control settings, determine the thermal characteristics of the autoclave currently used with the expert system, and assess the possibility of process control instability for the current physical system and other possible configurations of the expert system with different autoclaves. After the model was developed and verified it was to be used in a process simulation to determine if

## III. MODEL DEVELOPMENT

The control mechanisms for the autoclave used in this study were a common control device known as a proportional-integral-derivative (PID) controller.

NO-A191 203

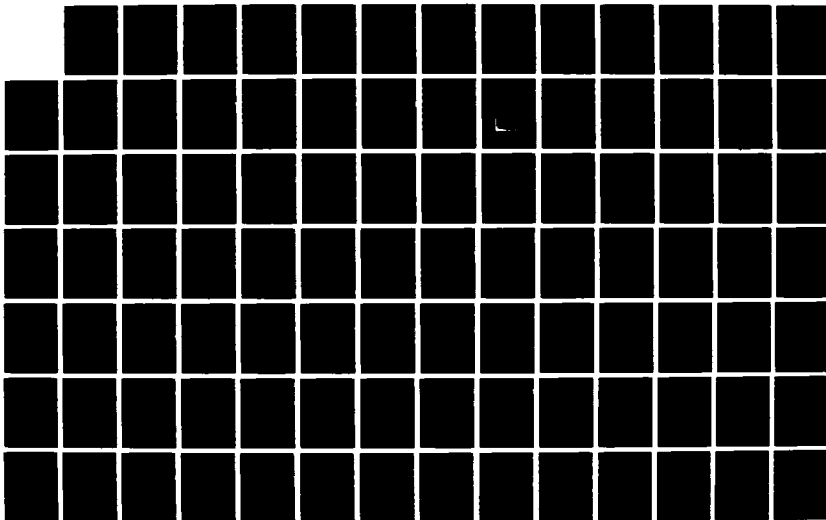
UNITED STATES AIR FORCE SUMMER FACULTY RESEARCH PROGRAM 8/11  
(1987) PROGRAM TE. (U) UNIVERSAL ENERGY SYSTEMS INC  
DAYTON OH R C DARRAH ET AL. DEC 87 AFOSR-TR-88-0212

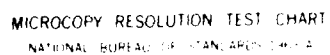
UNCLASSIFIED

F49620-85-C-0013

F/O 3/1

NL





MICROCOPY RESOLUTION TEST CHART  
NATIONAL BUREAU OF STANDARDS-1963-A

controller. The parameter controlled in this case is gas temperature inside the autoclave. A temperature goal known as a set point is chosen, and the controller sends output to the heating or cooling devices which controls their output so that the set point temperature is smoothly reached. The output of the PID is dependent upon a relative deviation from the set point  $\epsilon$  described by the following equation

$$O = G \left( \epsilon + \frac{1}{R} \int \epsilon dt + r d\epsilon/dt \right) \quad (1)$$

where  $O$  is the output in fraction of maximum,  $G$  is the gain of the PID device,  $R$  is the reset of the integral portion, and  $r$  is the rate coefficient of the differential portion. The deviation is given by

$$\epsilon = (T_s - T) / T_r \quad (2)$$

where  $T_s$  is the set point,  $T$  is the sensed temperature, and  $T_r$  is the possible temperature range over which the autoclave can operate.

In general PID controllers can control a device at any level of output up to its maximum output. However, for the current autoclave all mechanisms are operated as on/off devices. The output from the PID is sent to pressure control valves which operate heating and cooling according to the following linear transformation

$$P = 9 + 12 O \quad (3)$$

where P is the control valve pressure. Thus the conversion is a linear variation over a 12 psi range. The pressure settings control heating and cooling by the following schedule: 1) cooling unit on for  $P < 8.5$  psi, 2) first bank of heaters on for  $P > 10$  psi, and 3) additional second bank of heaters on for  $P > 13$  psi. The settings provide an asymmetric control about the zero output level of 9 psi with an effective dead range of action of 1.5 psi. The control panel allows for dead range specification on the PID itself, but this capability is not utilized because the pressure control has an overriding dead range. It should be noted that the actual output of the PID produces output over a range of -50 to 50 % output, but the simulation model uses equation (3) with a range of -100 to 100% for ease in considering output of the separate heating and cooling modes full rates.

The heating banks are rated at 20 kW each and were taken to be operating at just under their rating so that the output in English units was 950 BTU/min for each bank. The cooling unit is tube and fin heat exchanger using a reservoir of 55 F cooling water.

The lumped mass approach to thermal modeling requires that material of the same type be modeled as having a single representative temperature and react as a whole to thermal stimuli. The approach taken was to treat the gas inside the autoclave as a single mass and the autoclave housing and heaters as another single mass. An energy balance for the gas can be described by the following differential equation

$$C_g \frac{dT_g}{dt} = HA (T_a - T_g) - Q_1 \quad (4)$$



where  $T_g$  is the gas temperature,  $C_g$  is the thermal capacity of the gas,  $HA$  is the product of the heat transfer coefficient of the heaters/autoclave to the gas and their area,  $T_a$  is the autoclave/heater temperature,  $t$  is time, and  $Q_1$  is the loss of energy to surroundings.  $Q_1$  is modeled by the following relation

$$Q_1 = HA_1 ( T_a - T_e ) \quad (5)$$

where  $T_e$  is the effective ambient temperature to which heat is lost. An energy balance for the autoclave/heater leads to the following differential equation:

$$C_g \frac{dT_a}{dt} = Q_i - HA ( T_a - T_g ) \quad (6)$$

where  $C$  is the autoclave/heater thermal mass, and  $Q$  is the heat input (negative for cooling) from the heaters or coolers. The value for  $Q$  is the specified heater rates in the heating mode, but an overall heat exchange expression must be used in cooling which takes the form

$$Q_i = UA ( T_a - 55 ) \quad (7)$$

where  $UA$  is the overall heat exchange coefficient multiplied by the effective area.

It is worthwhile to note that  $Q$  might more reasonably be considered as a loss from the autoclave/heater, because heat must pass from the gas to the autoclave body before passing to the ambient air. The reason the model is formulated as given is due to the inadequacy of treating the heaters and autoclave body as one thermal mass. The temperature of the heating banks will obviously be higher than the autoclave body when the heaters are on, and the body has a significant lag in response in the initial heat up. However, it was felt that considering a third thermal mass would make the model more complicated than justified, because this step would have required two extra heat exchange coefficients and an extra thermal mass which would have made the determination of the coefficients difficult in any sort of optimal sense.

### III. MODEL VALIDATION AND RESULTS

The model was validated and the modeling coefficients were fit by comparing model output to measured gas temperatures in the autoclave in response to a series of set points. Figure 1 is a plot of measured temperature and model predictions for the test data. The codes for the model in both FORTRAN and FORTH are presented in the Appendix.

The initial response to the first set point is much slower for the actual temperature than for the model prediction. This is apparently due to the great difference in temperature between the heaters and the autoclave body in the initial heat up. In fact the controller has difficulty in this stage, because an initial rush of warm gas hits the controller thermocouple sensor so that the controller feels it has reached the set point. The gas

loses energy to the autoclave body as it circulates, and thus the controller acts in an unstable manner. This has been detected in all of the expert system cure runs. The autoclave response model cannot predict this behavior, because it does not distinguish between the heater and autoclave body as thermal masses. Note however that after the first set point, the agreement between the model and the measurements is good.

The values of the model constants used to produce Figure 1. are  $C_a = 5.5$ ,  $HA = 20$ ,  $C_g = 19.8$ ,  $HA_1 = 3.0$ , and  $UA = 0.9$  with all units in the English system (BTU, Fahrenheit, and minutes). These values are not optimized, but they should not change drastically if an optimization algorithm could be found. A no-derivative Newton-Raphson search for the constants in a nonlinear least squares algorithm was applied to the model, however it could not produce convergence because of the discontinuity of derivatives caused by the on-off nature of the heating and cooling.

The ratio of any  $C$  and  $HA$  in the thermal balance equations represents a characteristic time of response of a body to heat input through the  $HA$  term. The larger the characteristic time, the longer will be the lag in response. The none of the thermal lags is greater than a few minutes so that the interaction with the feedback loop of the PID should not be significant. Also, the heat loss time constant is not negligible, and it acts to stabilize the system and work against unstable response. It is important to remember that this is a small autoclave in the sense of many industrial curing settings, and the stable real time control is not guaranteed in larger systems.

The model was tested in conjunction with a cure process model previously used to test the expert system control rules. The autoclave thermal response model performed more realistically than the original assumption that the set point was reached exactly, especially in the cool down phase when the cooling unit could not provide enough cooling to reach the set points prescribed by the expert system. Results are not presented for brevity's sake.

#### IV. RECOMMENDATIONS

The analysis of the thermal response of the PID controlled autoclave appears to be stable except in the initial heat up stage. In light of the stabilizing effect of losses to the ambient and the unstable initial response the following recommendations can be made.

1) Further analysis should be done of larger autoclaves including those with true proportional control, 2) the cause of the spurious response of the initial heating stage be examined to isolate the cause, 3) further model simulations with the expert system be run with a hypothetical large autoclave in an attempt to find those cases in which control might be unstable, and 4) examine the response of large autoclaves with respect to the validity of lumped mass analysis.

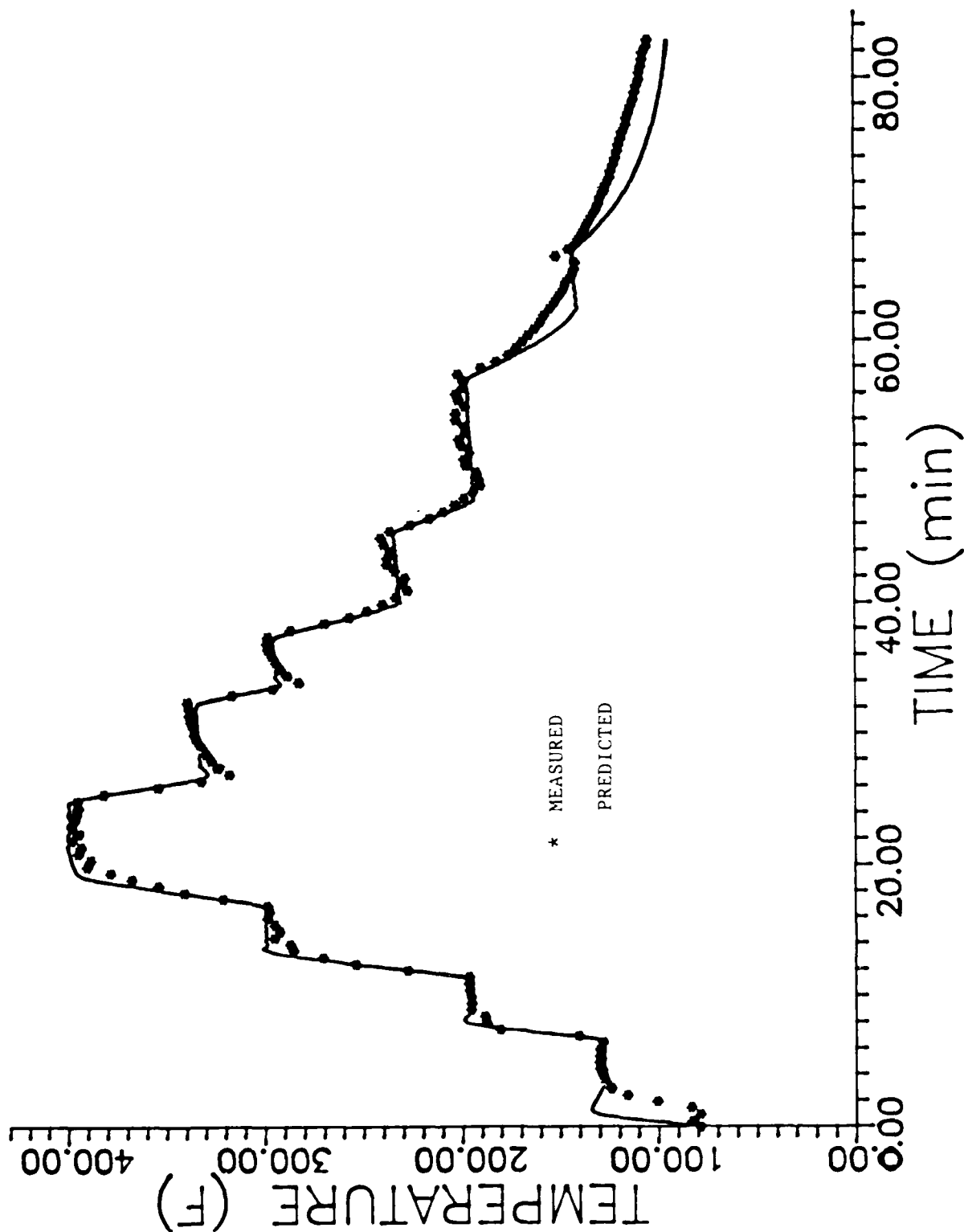


Figure 1. Model Prediction vs. Measured Autoclave Response

# V. APPENDIX COMPUTER CODES

```

SUBROUTINE AUTSIM(SET,AUT,AMASS)
IMPLICIT REAL*8 (A-H,O-Z)
DIMENSION T(2),AA(20),PLAG(100)
COMMON/TIMBK/ TIME,XEND
DATA H /0.01D0/, P1 /8.50D0/, DEADR /0.0D0/,
IP2 /10./, P3/13.D0/, Q0 /1900.D0/, Q1 /950.D0/
OPEN(50,FILE='CHARST.DAT')
READ(50,80) (AA(I),I=1,20)
READ(50,*) CA,CAH,UA,HA,HALOSS,GAIN,RESET,RATE,FLAG
CLOSE (50)
X=0.00
EPS0=0.00
EPS1=0.00
SUMEPS=0.00
T(1)=AUT
T(2)=AMASS
KOUNT=0
DT0=663.D0
LAG=NINT(TLAG/H)
DO 11 M=1,LAG
  PLAG(M)=9.000
11 CONTINUE
DO 100 K=1,10000
  KOUNT=KOUNT+1
  DIF=T(1)-SET
  EPS=DIF/DT0
  EPS2=EPS1
  EPS1=EPS0
  EPS0=EPS
  DEPSDT=(3.D0*EPS0-4.D0*EPS1+EPS2)/2.D0/H
  IF(KOUNT.EQ.1) DEPSDT=0.00
  SUMEPS=SUMEPS+H/2.D0*(EPS0+EPS1)
  OUTPUT=-GAIN*(EPS+RATE*DEPSDT+SUMEPS/RESET)
  IF(ABS(OUTPUT).LT.DEADR) OUTPUT=0.00
  IF(OUTPUT.GT.1.) OUTPUT=1.00
  IF(OUTPUT.LT.-1.) OUTPUT=-1.00
  PNOW=OUTPUT*6.D0+9.000
  IF(LAG.EQ.0) GO TO 115
  NLAG=LAG-1
  DO 101 KK=1,NLAG
    PLAG(LAG-KK+1)=PLAG(LAG-KK)
101 CONTINUE
  PLAG(1)=PNOW
  P=PLAG(LAG)
115 IF(LAG.EQ.0) P=PNOW
  KK=K-1
  IPRINT=MOD(KK,20)
  IF(X.LT.1.D-5) GO TO 95
  TIME=TIME+H
  IF(IPRINT.GT.0) GO TO 95
  WRITE(2,50) TIME,T(1),T(2),PNOW,EPS,SUMEPS,SET,DIF,OUTPUT
95 CALL RK5(X,T,H,CAH,CAH,UA,HA,HALOSS,P,P1,P2,P3,Q0,Q1)
  IF(X.GE.XEND) GO TO 100
100 CONTINUE
60 FORMAT(9(1X,F9.3))

```

```

90  FORMAT(20A4)
200 AUT=T(1)
    AMASS=T(2)
    RETURN
    STOP
    END
    SUBROUTINE YPS(YT,YP,CAH,CA,UA,HA,HALOSS,P,P1,P2,P3,Q0,Q1)
    IMPLICIT REAL*8 (A-H,O-Z)
    DIMENSION YT(2),YP(2)
    QLOSS=HALOSS*(YT(1)-100.00)
    YP(1)=(HA*(YT(2)-YT(1))-QLOSS)/CA
    IF(P.LT.P2.AND.P.GE.P1) GO TO 40
    IF(P.LT.P1) GO TO 60
    IF(P.LT.P3) GO TO 50
    Q=Q0
    GO TO 70
50  Q=Q1
    GO TO 70
40  Q=Q.D0
    GO TO 70
60  Q=UA*(55.D0-YT(1))
70  YP(2)=(Q-HA*(YT(2)-YT(1)))/CAH
    RETURN
    END
    SUBROUTINE RK5(X,Y,H,CAH,CA,UA,HA,HALOSS,P,P1,P2,P3,Q0,Q1)
    IMPLICIT REAL*8 (A-H,O-Z)
    REAL*8 K(6,2),Y(2),YT(2),YP(2)
    DO 100 J=1,2
    YT(J)=Y(J)
100  CONTINUE
    CALL YPS(YT,YP,CAH,CA,UA,HA,HALOSS,P,P1,P2,P3,Q0,Q1)
    DO 150 J=1,2
    K(1,J)=YP(J)
150  CONTINUE
    DO 200 J=1,2
    YT(J)=Y(J)+H/4.D0*K(1,J)
200  CONTINUE
    CALL YPS(YT,YP,CAH,CA,UA,HA,HALOSS,P,P1,P2,P3,Q0,Q1)
    DO 250 J=1,2
    K(2,J)=YP(J)
250  CONTINUE
    DO 300 J=1,2
    YT(J)=Y(J)+H/8.D0*(K(1,J)+K(2,J))
300  CONTINUE
    CALL YPS(YT,YP,CAH,CA,UA,HA,HALOSS,P,P1,P2,P3,Q0,Q1)
    DO 350 J=1,2
    K(3,J)=YP(J)
350  CONTINUE
    DO 400 J=1,2
    YT(J)=Y(J)+H/3.D0*(2.D0*K(2,J)+K(3,J))
400  CONTINUE
    CALL YPS(YT,YP,CAH,CA,UA,HA,HALOSS,P,P1,P2,P3,Q0,Q1)
    DO 450 J=1,2
    K(4,J)=YP(J)
450  CONTINUE

```

```

      DO 500 J=1,2
      YT(J)=Y(J)+H/15.00*(3.00*K(1,J)+9.00*K(4,J))
500  CONTINUE
      CALL YPS(YT,YP,CAH,CA,UA,HA,HALOSS,P,P1,PC,P3,00,01)
      DO 550 J=1,2
      K(5,J)=YP(J)
550  CONTINUE
      DO 600 J=1,2
      YT(J)=Y(J)+H/7.00*(6.00*K(5,J)-12.00*K(4,J)+12.00*K(3,J)+2.00*K(2,
      J)-3.00*K(1,J))
600  CONTINUE
      CALL YPS(YT,YP,CAH,CA,UA,HA,HALOSS,P,P1,PC,P3,00,01)
      DO 650 J=1,2
      K(6,J)=YP(J)
650  CONTINUE
      DO 700 I=1,2
      Y(I)=H/90.00*(7.00*K(1,I)+32.00*K(3,I)+12.00*K(4,I)+32.00*K(5,I)+7
      1.00*K(6,I))+Y(I)
700  CONTINUE
      X=X+H
      RETURN
      END

```



## Screen # 1

```
( RUNGE-KUTTA IDIM IS #-1 OF SIM. ODE'S LOOP IS # )
```

```
! CONSTANT IDIM 5 CONSTANT STEP/PS 10E FCONSTANT P3
23E FCONSTANT GAIN 15E FCONSTANT RESET 3E FCONSTANT RATE
3E FCONSTANT DEADBAND 8.5E FCONSTANT P1 10E FCONSTANT P2
19E3 FCONSTANT QINI 95E1 FCONSTANT QIND FVARIABLE UA
FVARIABLE EPS-3 FVARIABLE EPS-1 FVARIABLE EPS-2 VARIABLE PRNT#
VARIABLE STEP# FVARIABLE QINOUT FVARIABLE TMASS-AIR
FVARIABLE TMASS-AUT FVARIABLE HTOGCF FVARIABLE INTEGRD
FVARIABLE TSET FVARIABLE TOIF0 CREATE DUMM 1024 ALLOT
FVARIABLE P FVARIABLE WOUT FVARIABLE HALQSS
HANDLE PIDDAT
PIDDAT FILENAME PID1.DAT
PIDDAT MAKE-FILE .STATUS
PIDDAT OPEN-FILE .STATUS
--)
```

## Screen # 2

```
: PROMPT0 ." ACTIVATE 2087, DOSINT, AND ARRAY SCREENS IF YOU
      ." HAVE NOT YET" OR ." THEN USE RKS AND LOAD SCREEN 1" OR :
: PROMPT1 ." NOW USE OYIDX AND LOAD SCREEN 1" OR :
: PROMPT2 ." NOW USE RKS AND LOAD SCREEN 2" OR :
: PROMPT3 ." NOW USE PID AND LOAD SCREEN 3" OR :
```

```
( THIS DRIVER NAME " & THIS SCREEN # PROBLEM SPECIFIC )
```

```
OR OR PROMPT0
```

## Screen # 3

```
: EQUATION ." ODES OF AUTOCLAVE HT WITH PID CONTROL :
: IOS T8.5E 0 Y F1 T8.5E 1 Y F1 2E X F1 7.5E XEND F1 1E-1
      H F1 3 STEP# 1 :
: HEADING OR ." RUNGE-KUTTA SOLUTION OF " OR EQUATION OR OR :
: LABELS 8 SPACES ." TIME 20 SPACES ." TEMP-AIR
      15 SPACES ." AUTOCLAVE TEMP" OR OR :
: INIT-COND X F0 5. LOOP 3 DO 3 SPACES : X F1 5. LOOP OR OR :
: DISKIOS X F0 DUMM 4 + F1 LOOP 3 DO 1 X F0
      DUMM 1 1+ 3 + + 1 + F1 LOOP 1 PRNT# 1 :
: PR#) PIDCAT 4 PRNT# WRITE DROP DROP :
: INITIAL IOS DISKIOS HEADING LABELS INIT-COND :
: STORE-#S PRNT# 3 0 DO PIDCAT 24 DUMM 1 24 + 4 + WRITE
      DROP DROP LOOP :
: DIFF-EQ INITIAL SOLVE PR# STORE-#S PIDCAT CLOSE-FILE
      .STATUS :
```

## Screen # 1

```

3 STEP# : 0E EPS-0 F1 0E EPS-1 F1 0E EPS-2 F1 0E INTGRND F1
00E HTCOEF F1 19.6E TMASS-AIR F1 5.5E TMASS-AUT F1
0.9E UA F1 663E TDIF0 F1 3E HALOSS F1
: TAIR 0 Y F0 ;
: EPS EPS-1 F0 EPS-2 F1 EPS-0 F0 EPS-1 F1 TSET F0 TAIR F-
TDIF0 F0 F1 EPS-0 F1 ;
: CHANGE-SET TSET F1 EPS ;
: INTGERS EPS-0 F0 EPS-1 F0 F+ 2E F1 H F0 F+ INTGRND F0 F+
INTGRND F1 ;
: DEPSDT EPS-0 F0 3E F+ EPS-1 F0 4E F+ F- EPS-2 F0 F+ H F0 F+
2E F1 ;
: OUTPUT EPS-0 F0 DEPSDT RATE F+ F+ INTGRND F0 RESET F1 F+
GAIN F+ %OUT F1 ;
: OUT.P %OUT F0 6E F+ 9E F+ P F1 ;
-->

```

## Screen # 2

```

: HEATING P F0 P2 F1 IF 0E QINOUT F1 ELSE P F0 P3 F1
IF QINI QINOUT F1 ELSE QINC QINOUT F1 THEN THEN ;
: COOLING P F0 P1 F1 IF 0E QINOUT F1
ELSE UA F0 1 YTEMP F0 1E1 F- F+ QINOUT F1 THEN ;
: QINOUT OUTPUT %OUT F0 FABS DEADBAND F1 IF 3E QINOUT F1 ELSE
%OUT F0 0E F1 IF HEATING ELSE COOLING THEN THEN
OUT.P ;
: LOSS 0 YTEMP F0 100E F- HALOSS F0 F+ ;

```

```

--

```

## Screen # 3

```

: YP0 1 YTEMP F0 0 YTEMP F0 F- HTCOEF F0 F+ LOSS F-
TMASS-AIR F0 F1 ;
: YP1 QINOUT QINOUT F0 1 YTEMP F0 2 YTEMP F0 F- HTCOEF F0 F+
F- TMASS-AUT F0 F1 ;
: DY10X DUP 0 = IF DROP YP0 ELSE 1 = IF YP1 THEN THEN ;
: OFFSET PRNT# 0 8 * LOOP * 1 + ;
: PRNT X F0 FDUP E. OFFSET DUMM + F1 LOOP 0 DO 1 Y F0 FDUP
OFFSET 1 1+ 8 * + DUMM + F1 3 SPACE E. LOOP 0 DO 1 ;
: RESULTS STEP# 0 STEP#R MOD 0 = IF PRNT# 3 1+ PRNT#
PRNT THEN STEP# 0 1+ STEP# 1 EPS INTGERS ;
OR OR PROMPTC

```

Screen # 1

( RUNGE-KUTTA IDIM IS #-1 OF SIM. ODE'S LOOP IS # )

( RKS SETUP )

IDIM 1+ CONSTANT LOOP

FVARIABLE XEND FVARIABLE H FVARIABLE X FVARIABLE YTEMP

IDIM FARRAY K0 IDIM FARRAY K1 IDIM FARRAY K2 IDIM FARRAY K3

IDIM FARRAY K4 IDIM FARRAY K5 IDIM FARRAY Y IDIM FARRAY XTEMP

( NOTE THAT WORD RESULTS MUST DEFINE OUTPUT IN DYIOX )

( DYIOX MUST BE SUPPLIED AS A SEPARATE SCREEN FILE )

: ?DONE X F0 XEND F0 F+ :

CR CR PROMPT1

Screen # 2

: MAKEK0 LOOP 0 DO I DYIOX F0UP I K0 F1 H F0 F+ 4E F1 I Y F0  
F+ I YTEMP F1 LOOP X F0 H F0 4E F1 F+ XTEMP F1 ;: MAKEK1 LOOP 0 DO I DYIOX F0UP I K1 F1 I K0 F0 F+ 5E F1 H F0  
F+ I Y F0 F+ I YTEMP F1 LOOP ;: MAKEK2 LOOP 0 DO I DYIOX F0UP I K2 F1 I K1 F0 2E F1  
F+ H F0 F+ I Y F0 F+ I YTEMP F1 LOOP  
XTEMP F0 H F0 4E F1 F+ XTEMP F1 ;: MAKEK3 LOOP 0 DO I DYIOX F0UP I K3 F1 9E F+ I K0 F0 3E F+  
F+ 15E F1 H F0 F+ I Y F0 F+ I YTEMP F1 LOOP  
XTEMP F0 H F0 4E F1 F+ XTEMP F1 ;: MAKEK4 LOOP 0 DO I DYIOX F0UP I K4 F1 3E F+ I K3 F0 12E F+  
F+ I K2 F0 12E F+ F+ I K1 F0 2E F+ F+ I K0 F0  
3E F+ F+ 7E F1 H F0 F+ I Y F0 F+ I YTEMP F1 LOOP  
XTEMP F0 H F0 4E F1 F+ XTEMP F1 ;

: MAKEK5 LOOP 0 DO I DYIOX I K5 F1 LOOP ;

3 LOAD

Screen # 3

: KISUBJ MAKEK0 MAKEK1 MAKEK2 MAKEK3 MAKEK4 MAKEK5 ;

: STEPXY LOOP 0 DO I K0 F0 7E F+ I K2 F0 32E F+ F+ I K3 F0  
12E F+ F+ I K4 F0 32E F+ F+ I K5 F0 7E F+  
F+ H F0 F+ 30E F1 I Y F0 F+ I Y F1 LOOP  
X F0 H F0 F+ X F1 ;

: GETXY X F0 XTEMP F1 LOOP 0 DO I Y F0 I YTEMP F1 LOOP ;

: SOLVER GETXY KISUBJ STEPXY ;

: SOLVE BEGIN SOLVER RESULTS ?DONE UNTIL QUIT ;

CR CR PROMPT3

## Screen # 1

```

( ARRAY HANDLING SCREENS      2 CONSTANT FWSIZE
( ARRAY--CREATES AND EXECUTES INTEGER VECTORS )

: ARRAY CREATE DUP , 1+ WSIZE * ALLOT
  DOES> DUP ROT DUP DUP 0< ABORT" INDEX ERROR" ROT 0
    ABORT" INDEX ERROR" 1+ WSIZE * + ;

( FARRAY--SAME AS ARRAY EXCEPT FOR FLOATING POINTS )
: FARRAY CREATE DUP , 2+ FWSIZE * ALLOT
  DOES> DUP ROT DUP DUP 0< ABORT" INDEX ERROR" ROT 0
    ABORT" INDEX ERROR" FWSIZE * WSIZE * + ;

( USAGE FOR MATRIX ALLOCATION: ( #ELEMENTS-1 NAME -- ) )
( USAGE AFTER NAME DEFINITION: ( ELEMENT*-1 NAME -- ADDR ) )

2 LOAD

```

## Screen # 2

```

( MATRIX OR 2ARRAYS IN INTEGER AND FLOATING POINT )

: ZINDERR SWAP DUP DUP 0< SWAP 3 PICK 0< OR
  ABORT" COL INDEX ERROR" SWAP ROT DUP 0< ROT
  ROT SWAP OVER OVER WSIZE + 0< 3 PICK OR
  ABORT" ROW INDEX ERROR" ;

: 2ARRAY CREATE DUP , OVER , 1+ SWAP 1+ * WSIZE * ALLOT
  DOES> ZINDERR SWAP WSIZE * + ROT 2+ WSIZE * + DROP ;

: 2FARRAY CREATE DUP , OVER , 1+ SWAP 1+ * 1 + FWSIZE * ALLOT
  DOES> ZINDERR SWAP FWSIZE * + ROT FWSIZE * WSIZE 2* + +
  DROP ;

( USAGE FOR MATRIX ALLOCATION: ( #ROWS-1 #COLS-1 NAME -- ) )
( USAGE AFTER NAME DEFINITION: ( ROW*-1 COL*-1 NAME -- ADDR ) )

```

1987 USAF-UES SUMMER FACULTY RESEARCH PROGRAM/

GRADUATE STUDENT SUMMER SUPPORT PROGRAM

Sponsored by the

AIR FORCE OFFICE OF SCIENTIFIC RESEARCH

Conducted by the

Universal Energy Systems, Inc.

FINAL REPORT

A STUDY OF SERVICE DEMAND DISTRIBUTION AND TASK ORGANIZATION

FOR THE ANALYSIS OF ENVIRONMENTAL SAMPLES AND ASSOCIATED

SUPPORT SERVICES AT THE USAF OCCUPATIONAL AND ENVIRONMENTAL

HEALTH LABORATORY - BROOKS AFB, SAN ANTONIO, TEXAS

Prepared by: Don E. Deal, Ph.D. and Gary Lake

Academic Rank: Assistant Professor

Department and Industrial Engineering

University: University of Houston

Research Location: USAF/OEHL

Brooks AFB

San Antonio, Texas 78235

USAF Researcher: Mr. Frank Marcie

Date: 30 August 1987

Contract No: F49620-85-C-0013

A STUDY OF SERVICE DEMAND DISTRIBUTION AND TASK ORGANIZATION FOR  
THE ANALYSIS OF ENVIRONMENTAL SAMPLES AND ASSOCIATED SUPPORT  
SERVICES AT THE USAF OCCUPATIONAL AND ENVIRONMENTAL HEALTH  
LABORATORY - BROOKS AFB, SAN ANTONIO, TEXAS

by

Don E. Deal  
Gary Lake

ABSTRACT

A review of historical data was undertaken to assess the trends in and present status of the laboratory's ability to accomodate sample analysis workloads, short term projections for the growth in requests for analysis were also made for major sample classes. From numerous interviews with key supervisory and bench personnel, a list of problems and concerns was compiled which together comprised a substantial group of throughput-limiting elements. Workload projections were then analyzed in conjunction with these problem area data and with OEHL long term plans to produce a number of recommendations for increased efficiency. These recommendations focus on glass washing turn-around, acquisition of vital personnel, lab automation, and management of contract lab participation.

### ACKNOWLEDGEMENTS

I want to express my appreciation to the Air Force Systems Command and the Air Force Office of Scientific Research for sponsorship of this research program.

Our efforts would have proved far less rewarding had it not been for the responsiveness of OEHL personnel at all levels; I would like to thank the chemists, assistant analysts, and supervisors for their frank responses to our inquiries. Special thanks should go to Mr. Frank Marcie for his assistance in explaining day to day lab operations, outlining long term plans and in relating lab operation history. I also wish to extend my deepest appreciation to Col. James Rock for his continual support and guidance during our investigations. Finally, sincere thanks are extended to my graduate assistant, Mr. Gary Lake, who provided valuable support in all phases of our assignment.

## I. INTRODUCTION:

The USAF Occupational and Environmental Health Laboratory at Brooks AFB is engaged in a variety of activities encompassing the monitoring, modeling and control of elemental factors within and surrounding the Air Force occupational environment. These activities are targeted at maintaining a minimum feasible impact on the natural environs and at providing a maximum feasible level of safety for personnel in the workplace. To these ends, the USAF/OEHL is chartered with a wide range of duties which include the evaluation of industrial procedures and occupational hazards, review of environmental standards and legislation, and comprehensive analysis of air, water and soil samples and industrial materials.

The laboratory is currently nearing the terminal stages of an expansion program brought about by an increased demand for its services, chiefly in the area of chemical analysis of industrial and environmental samples. Yet, while additional workspace and new analytical equipment has been secured, little, if any, growth in personnel has been realized to help meet the challenge of increased workload and the increasing importance of the laboratory's function. Not only has there been a steady increase in the demand for traditional analytical services, but also a widening in scope of services requested; and in some of these new areas the growth rate has been explosive (e.g., asbestos analysis). Moreover, substantial efforts are now being undertaken to engage a new and comprehensive quality assurance program.

Given the confluence of these factors and a limited ability to acquire additional personnel, the OEHL strategy for meeting projected workloads will focus on efforts to automate and modernize operations and, where possible, to eliminate bottlenecks. The first steps to be taken in this direction will naturally center on the identification of problem areas and consideration for their criticality in terms of existing operating parameters and planned enhancements.



Areas of personal research interest which have resulted in my summer assignment to the OEHL are heuristics for optimization, system modeling, human factors analysis and facilities layout planning.

## II. OBJECTIVES OF THE RESEARCH EFFORT:

In order to gain as much information as possible regarding service demand and system operating characteristics, an exploratory phase was to be undertaken during which we would obtain a general overview of laboratory operations and determine what records of pertinent data existed. Historical data would be collected and analyzed to establish the distribution of and growth trends in sample analysis requests, and paralleling this task, interviews would be conducted with supervisory and bench personnel to gain more detailed, qualitative information concerning sample processing procedures.

Subsequent to these efforts, we would initiate an evaluation phase in which the information gathered would be reviewed en masse. In this phase we sought to:

- (1) project near-term growth in sample requests received for the various major sample classes and the request total;
- (2) identify significant output-limiting elements;
- (3) identify possible areas of concern and prioritize personnel responses regarding operational problems;
- (4) review plans for upgrade of operations, specifically with respect to how these plans confronted the factors given in (1),(2), and (3) above.
- (5) compile a list of recommendations targeted at planning and operations.

### III. FINDINGS:

Historical data reflecting total samples received, number of priority samples, and proportions processed in-house and through contract labs were collected for a 3-year period from May 1984 to April 1987. Priority samples are those for which special processing arrangements between the lab and field are made in advance; such samples may have short "lifetimes", and analysis results are of some immediacy. All samples are categorized according to a two-letter code which identifies the physical form (sample code) and preservation group (work center code) of the sample (see Table 1 below). Codes are assigned by the Sample Control section upon log-in.

---

TABLE 1: SAMPLE CONTROL CODES

SAMPLE CODES

F - Biological  
G - Oxygen & Gas  
H - Industrial Hygiene  
M - Bulk Industrial Materials  
N - Non-potable Water  
O - Other  
P - Potable Water  
S - Soil & Vegetation  
U - Urine

WORK CENTER CODES

A - Oxygen Demand  
B - Oils & Greases  
C - Nitrogen & Phosphorous  
D - Cyanide  
E - Phenols  
F - Metals  
G - Other Water  
H - Pesticides  
J - Clinical  
K - Industrial Hygiene & Special Analysis  
T - Trace Organics

---

Figure 1 on the following page depicts the month by month count of samples received over the period of interest. The charted linear growth trend in Figure 1 suggests an additional 2500 samples per year logged in to the laboratory. Figure 2 presents a breakdown in the 3-year total of samples received over the major sample/work center codes. Although there are approximately 45 sample categories, we can see in Figure 2 that fifteen of these groups account for 90% of all

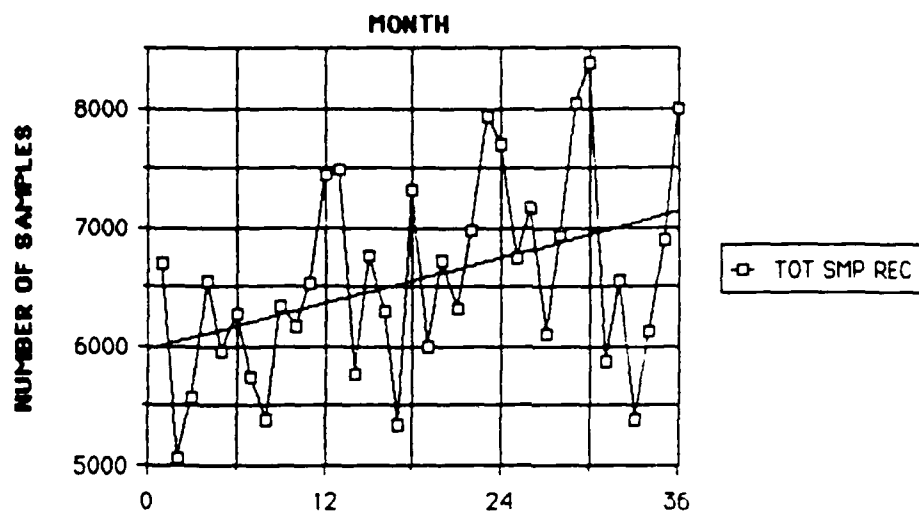


FIG. 1: TOTAL SAMPLES RECEIVED (MAY 84-APR 87)

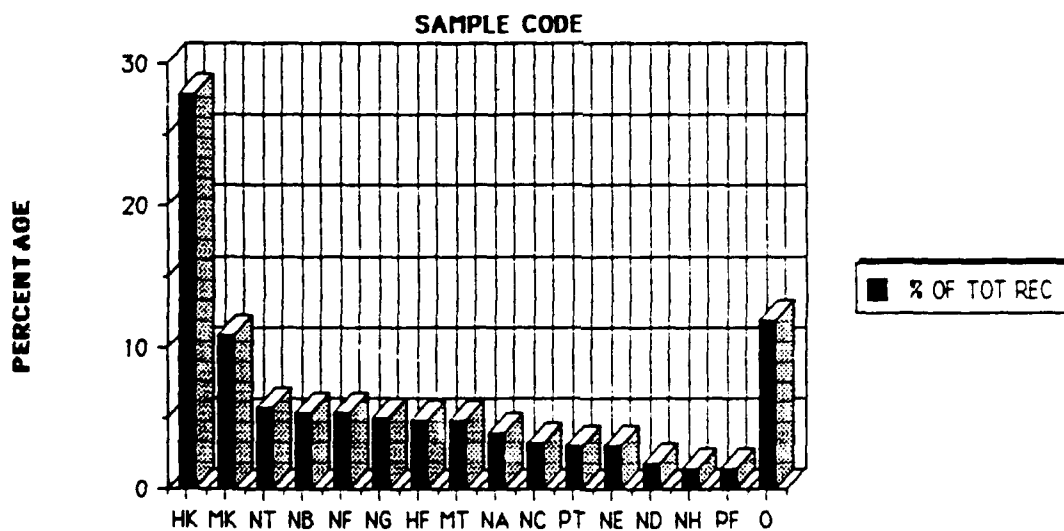


FIG. 2: PERCENT OF TOTAL SAMPLES RECEIVED (MAY 84-APR 87)

requests received, with the HK group alone representing nearly 30% of the total (the HK category consists of air samples analyzed for asbestos at one work station and those analyzed for organic constituents at another station). We also reviewed the individual 36-month histories of requests for analysis in these fifteen major categories in order to obtain an estimate in the growth of samples received independent of that inferred from Figure 1. This analysis produced a per-year increase in samples logged of 4000-4500. This figure correlated well with data for the most recent past and represents, we feel, a more reasonable expectation for sample growth in the near-term future.

Figure 3 shows the monthly count in samples allotted to in-house analysis and contract labs; the trend lines there suggest that the OEHL has been able or willing to retain 60% of the growth while assigning the balance of the annual increase to the various contract laboratories. This willingness to take on the majority of the increased workload has not been without effect, however. Reviewing the number of analyses performed per work day averaged over each month in the 36-month period of focus (Figure 4), we see that except for the banner month of April 1987 the trend in analyses completed has been more or less flat for the most recent two and a half years (samples received and analyses performed are entirely distinguishable counts; some samples may require only a single analysis, while others may demand several analyses). The resulting effect is portrayed in Figure 5 where data representing the month by month average length of time a sample resides in the AF lab is charted. We should note that the slope of the trend line superimposed there is positive, but skewed by the effect of the unusually productive output of April 1987. We have inferred from this data an annual increase in the average turn-around time for a sample processed in-house of 1/2 to 3/4 days per year.

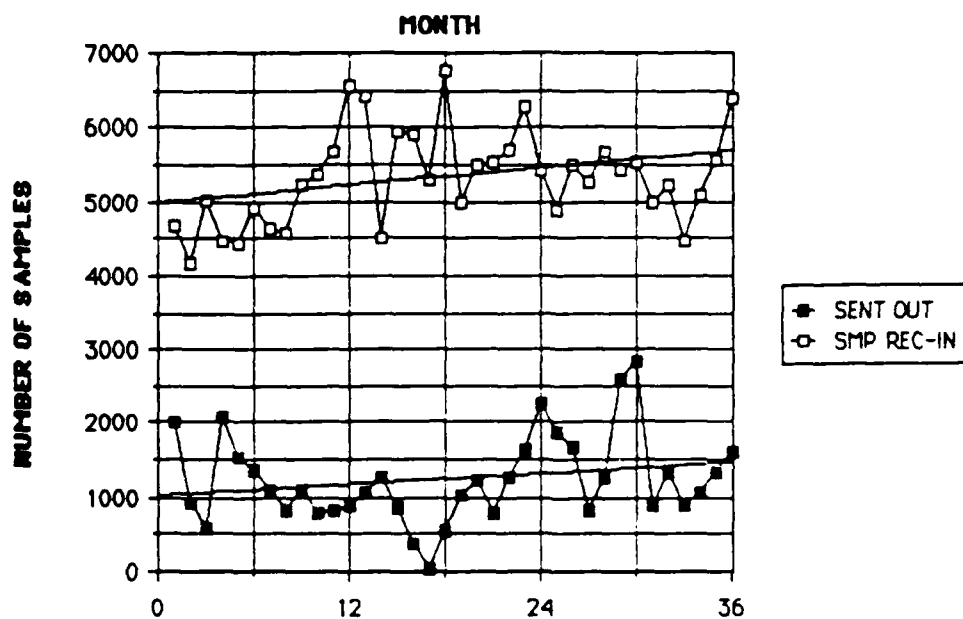


FIG. 3: SAMPLES RECEIVED IN-HOUSE AND TRANSSHIPPED

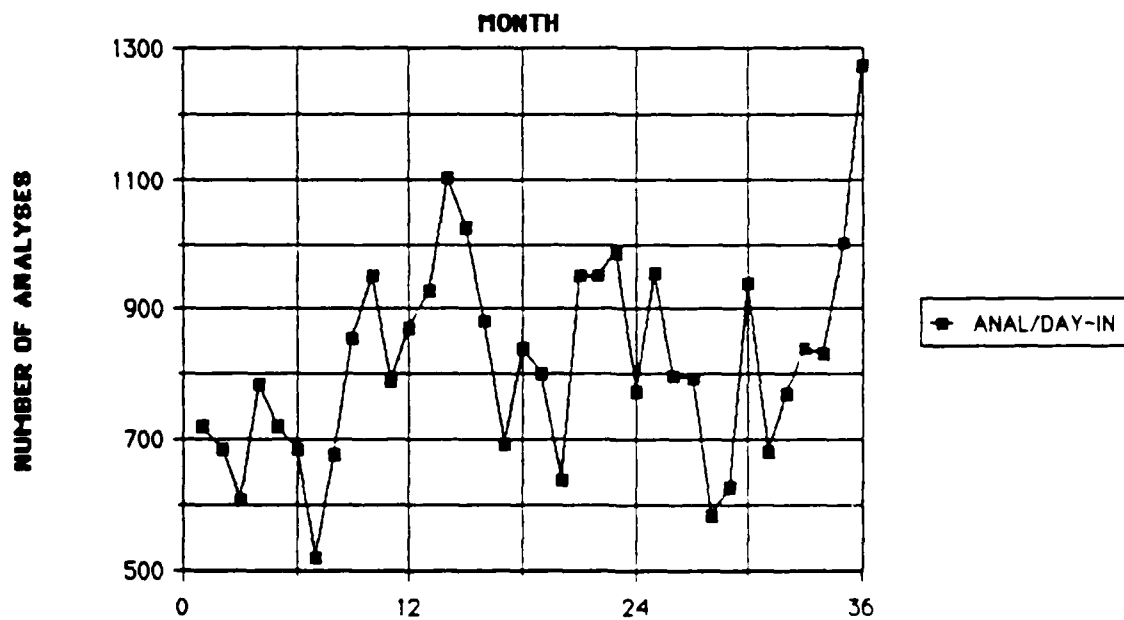


FIG. 4: AVG. NO. OF ANALYSES COMP./ WK. DAY (IN-HOUSE)

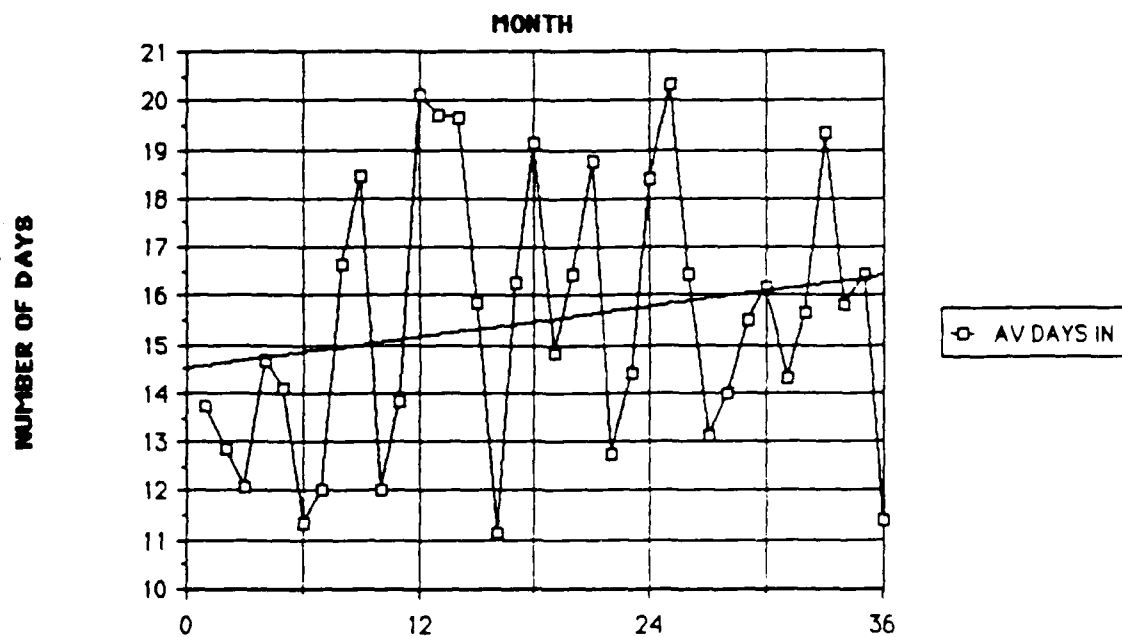


FIG. 5: AVG. NO. OF DAYS IN LAB/SAMPLE (IN-HOUSE)

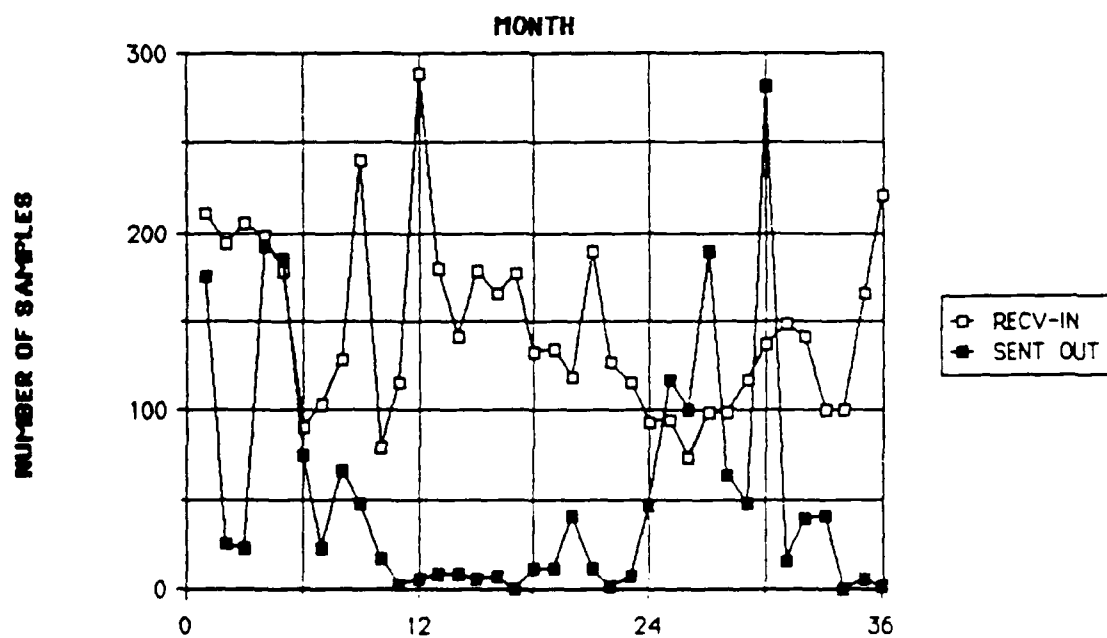


FIG. 6: PT SAMPLES REC. IN-HOUSE & TRANSSHIPPED

Our analysis of the processing of priority samples uncovered no significant problems in this area. Only about 1% of all samples received are given priority designations, and a frequency histogram of processing times over three years for these requests indicated that they are given the attention they require in the vast majority of cases.

We next returned our focus to the histories of the high-volume sample categories, reviewing these histories for anomalous data. We found three cases in which there appeared unusual events or trends. In the first instance (sample class PT, Fig. 6), an erratic apportionment of samples between contract labs and the OEHL was observed. The reader can see in Figure 6 that for the period from month 12 to month 24, the number of samples sent to outside labs for analysis was very small; however, over months 25 to 30, the in-house total dipped while the proportion contracted out climbed dramatically. The cause for this situation seems to have been a brief period during which there were recurrent instrument problems. Supervisory people advised us that these problems had been dealt with, and this seems borne out by the data as the last six months show a resurgence in the level of in-house processing. Figure 7 depicts the volumes of samples processed in-house and transshipped to contract labs for code HF. The function representing the sample count transshipped exhibits significant fluctuations for the last twelve months, while the preceding year and a half indicates a small and stable level of contracted samples. Moreover, the accompanying curve for the volume processed in the OEHL shows a declining trend over the last twelve months with dramatic decreases in the most recent two months. Finally, in Figure 8 we present similar data for air samples coded HK. The trends of the two curves very clearly indicate a converging effect over the the previous 18 months; the number of samples retained for analysis in-house has noticeably decreased while the contract lab apportionment shows steady growth to a maximum for the 3-year period. Recall that HK air samples include those analyzed for asbestos content at one station and those for organic constituents at another. The organics analysis station

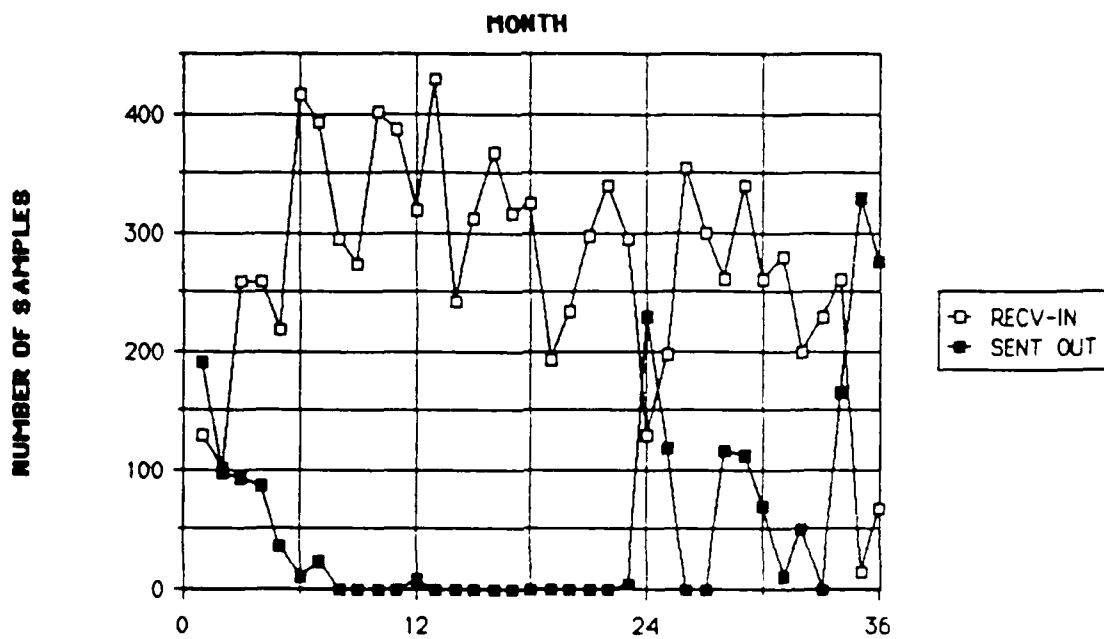


FIG. 7: HF SAMPLES REC. IN-HOUSE & TRANSSHIPPED

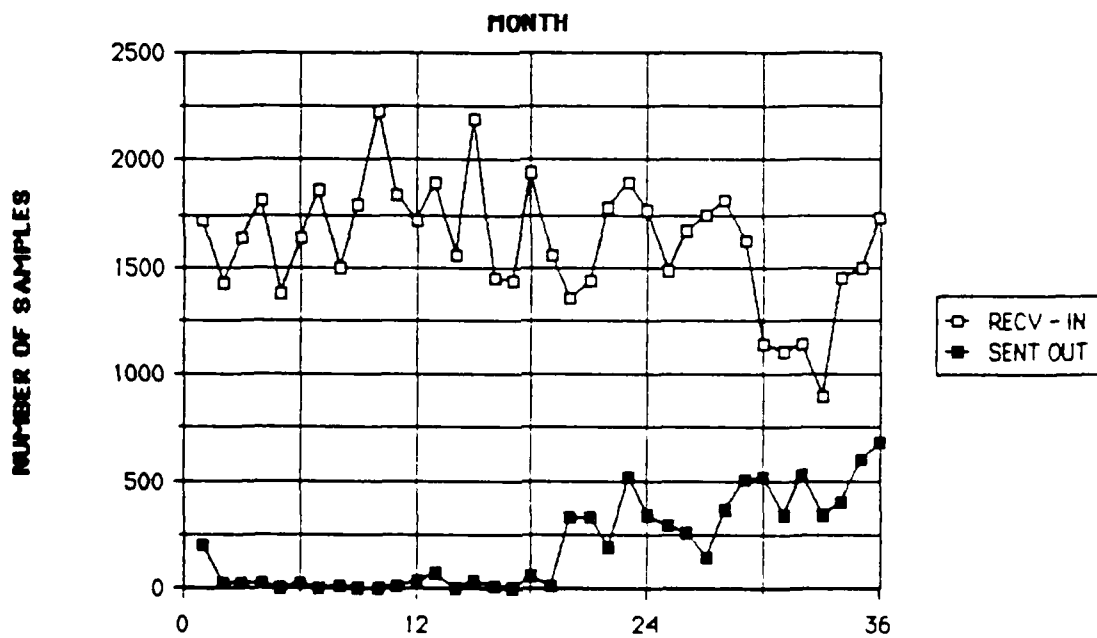


FIG. 8: HK SAMPLES REC. IN-HOUSE & TRANSSHIPPED



rarely sends samples out; therefore, the trend we see resides largely within air asbestos sample data. We are aware that physical expansion activities have caused some disruption in normal operations. The air asbestos people, in fact, stated that they had made location changes two or three times within recent months; but we feel that this does not adequately account for the trends we see developing. There is some indication that analytical work in this area is physically taxing; long periods are spent counting fibers while peering through a microscope, and personnel have complaints with back and eye fatigue. Management should be wary of cumulative physical effects and possible morale deterioration in this group. Efforts to obtain appropriate remote monitoring and special seating equipment should be supported. There are possibly other factors contributing to the apparent decline in productivity in air asbestos sample processing; we encourage supervisors to investigate this issue further.

As stated earlier, interviews were conducted at the various work stations in order to ascertain task complexities and the general network flow of samples and accompanying data from station to station, but more specifically to elicit information from bench personnel reflecting their concerns and perceptions of operational shortcomings. Table 2 represents a listing of responses received; items are given in priority order based on number of responses, with a "1" indicating highest priority. We should note that some of these items represent factors over which lab management has only very limited control. We mention them briefly here, but do not address them in detail in our recommendations and conclusions section (other items under management influence will be treated in that section). Calls to and from the field are frequently necessary to clarify requests and to obtain additional data or pass on results of analyses performed. Item 7 typically represents an unawareness on the part of the requesting source as to the effort involved in performing a quantitative versus qualitative analysis; the source may, indeed, need assistance in deciding what he or she actually requires. Coordination between the lab and source may be time-consuming, but

is a reality in service organization operations. We feel that no recommendations should be made with regard to items 6 and 7. We are cognizant of the constraints on the lab administration to obtain additional personnel (Item 9), whether it be military or civil service. Although very few groups made explicit mention of workforce shortage, several suggested indirectly that this was a problem. We were informed that a consultant study had, in fact, been conducted in recent years resulting in a recommendation for the hiring of several tens of new workers. This simply does not appear to be a viable option. It is likely that this recommendation was made based on the existing structure of work flow at that time --- that is, without knowledge of the possibility of a concerted automation upgrade plan. We do suggest in the following section that a small number of key personnel be acquired, but we are optimistic that with a sincere resolve to modernize routine lab functions that the need for a substantial increase in the workforce level will be obviated.

---

TABLE 2 : PROBLEM AREA RESPONSES

<u>ITEM NO.</u>	<u>PRIORITY</u>	<u>ITEM DESCRIPTION</u>
1	1	Glassware washing (turn-around times excessive)
2	1	Considerable time taken up in doing routine, repetetive calculations & QA
3	2	Ergonomic issues
4	2	Work sheet/report forms require too much redundant information and excessive information transcription
5	3	Down time and/or repair time for automated instrumentation excessive
6	3	Number of calls to or from field
7	4	Requesting source asks for more detailed analysis than really required (e.g., quantitative rather than qualitative)
8	4	Frequent turnover of recently trained personnel
9	4	Insufficient number of people
10	4	Missing paper work

---

#### IV. CONCLUSIONS AND RECOMMENDATIONS:

In this final section we bring together results of our data analysis, employees' problem area responses and our own personal observations to summarize the status of lab operations and to offer some recommendations for lab enhancements. We will first address a number of items individually, then turn to the issue of lab operations upgrade efforts. This issue encompasses several of the concerns registered in the employee interviews and is of paramount importance to the future existence of the laboratory.

A. GLASSWARE WASHING. There are two glass washing operations servicing separate areas of the laboratory. We visited the newer facility in the expansion wing of the building, and our recommendations are based on observations at that location. Bench personnel in several areas expressed a concern regarding timely availability of glassware used in their analytical procedures. In some of those areas large backlogs and/or lengthy turn-around times were at least partially attributable to a glassware shortage. We should emphasize that purchase of additional glassware inventory presents no long term solution to this problem; since the demand rate exceeds the recycle time, this action would serve only to introduce an interim period of glassware availability after which conditions would revert to those prevalent now. Our primary recommendations focus directly on those tasks constituting the preparation of glassware for re-use: acid-bathing and rinsing (by hand) and oven baking. Obviously, glassware must be sterilized to prevent the introduction of contaminants into sample material. This is accomplished by soaking glass items in an acid bath for a short period, after which they are scrubbed and rinsed, then baked at 325F for an hour and a half in special ovens. A bottleneck in current operations is the lack of requisite facilities for accomodating additional acid baths; glassware tends to stack up in carts in the washing area where they wait to go into one of two small acid bath tubs. We see a need for two more tubs, with accompanying construction of a new hood to handle ventilation and limit

spill damage. While space might appear to be a problem, we noted that there was a pulsonic washer at that location which was not in working condition and which was considered only of marginal use to the person in charge of washing (he explained that with loading and unloading, the machine saved little time in rinsing operations and that, when run with any soap solution, left a residue on the glass). If the pulsonic washer is not to be employed on a routine basis, we recommend it be removed; this will free up a significant fraction of the space needed for a new hood and acid baths. Additional room, if needed, could be taken from existing counter space; we observed that 10-15% of the counter top area was ill-used, accomodating material which should not be placed in the washing area to begin with. This included a small warming oven and several unopened boxes of new glassware (these items should be removed to appropriate alternate locations whether or not a new hood is planned). Another factor contributing to lengthy turn-around times concerns the baking process. While glass items require baking only for 1.5 hours at 325F, it takes the ovens three to four hours (nearly half a work day) to heat up to this temperature. Steps should be initiated to decide whether the two existing ovens can be "refurbished" to provide needed temperatures more quickly, or whether newer, better models should be purchased. Finally, in our visit to this facility we noted that an employee had been temporarily assigned as part-time help to this area. This assignment produced a noticeable improvement in washing operations. If possible, permanent employ of one full-time person to the two washing operations should be considered; he or she could spend one-half day at each location, where they would assist in rinsing and glass pick-up and delivery.

B. ERGONOMIC ISSUES: We touched on some of these items near the end of the previous section (see discussion of air asbestos operations). We add here that a large majority of the responses categorized as ergonomic issues concerned room temperatures in the new expansion wings of the laboratory. Temperatures were uncomfortably warm in several areas; in fact, in glassware washing five fans were running during our visit. Moreover, temperatures were sufficiently high

in some instances to inhibit proper operation of automated analytical equipment. Management is aware of this control problem and steps are being taken toward its correction. We emphasize here the need to deal with this issue promptly.

C. REPLACEMENT OF RETIRING EMPLOYEES: At least four persons with considerable lab experience will be eligible for retirement in the coming year. These include chiefly bench and section supervisory personnel. Considerations dictate that action be taken soon as to evaluation of OEHL options regarding these people and positions. It should be determined which personnel the lab desires to retain and which desire to stay and in what capacity, particularly in light of plans for the major changes in lab operations which are now being formulated and reviewed. Management should be mindful of the lead time required for identifying and evaluating candidates for hire and the time needed for new-hires to reach productive functioning. Given current workforce numbers, we strongly support replacement in those positions left vacant by retiring employees.

D. LAB AUTOMATION & OPERATIONS UPGRADE: Lab performance over the next 2-3 years will be of critical importance to the future of the OEHL. Since the relinquishment by the EPA of regulatory control over laboratories to state governments, several states have seen fit to set their own guidelines for lab operations. This has, of course, added a whole new dimension of complexity to the logistics of standards compliance; out of this has grown the possibility of decentralizing OEHL functions. Though such a decentralization would no doubt result in increased operating costs and lower quality of services delivered, the OEHL must exhibit renewed determination and capability to manage operations under these conditions in order to stem this possibility. The central theme in this new management must be the enhancement of automated capabilities; to a large degree, plans have been made and steps taken in this direction. We will now review the key elements in the automation and operations upgrade effort.

(1) Automation of analytical tasks should begin in those areas with high sample request

volumes; additional purchase of automated instruments should proceed as funds are made available. The recent lab expansion has been accompanied by several major purchases of top-line analytical equipment; thus, this facet of the upgrade strategy is well under way. We reiterate here that with the significant growth in requests for analysis in the asbestos areas, management should be particularly attentive to innovative developments which might assist analysts there.

(2) Links between automated analytical equipment and computer systems should be established. Software should be purchased or developed which interprets and stores data coming in from these instruments and which computes and stores, from this data, report level information for sample analyses results. New computer hardware and system software have just been delivered; we are hopeful that with some customizing this system will accomodate this objective.

(3) An area that we felt was not addressed in our review of the automation upgrade plans concerns the management of quality assurance data. The issue of compliance with EPA and state standards has greatly magnified the role of the lab's QA section. They are assigned the task of monitoring and interpreting agency requirements and assuring that lab performance reflects the accuracy demanded by these and other bodies. This entails frequent and comprehensive quality testing and detailed record-keeping. In fact, extensive record-keeping procedures are now being initiated. Though necessary, this effort will place monumental pressure on both QA and bench personnel to handle large amounts of information, while still getting work out. Record-keeping, computation, and review will be done primarily by hand until an appropriate data management system can be put in place. Results of interviews indicated estimated decreases in sample throughput as high as 25% would follow initiation of these procedures. While we believe figures of 5-10% are more realistic, it is clear that the lab can ill afford to suffer such a drop in sample processing rates for an extended period. A priority objective must be established now to determine what requirements are appropriate and what software exists or can be written to meet these requirements.

(4) An essential element to the upgrade effort is the data base system. The utility of practically

all elements discussed to this point depend on the ability of users to post and retrieve data in usable form. First hand experience suggests that the present system for data storage and retrieval is entirely inadequate; reports that should have taken at most hours to obtain required several days. System upgrade plans at present include what was termed a "pseudo data base"; management should be convinced that a system with such a description will satisfy their needs before building other elements around it. We recommend that the data base system adopted address the following objectives: (a) accomodation of general-purpose report generation requests; (b) support of special or non-routine report production; (c) accomodation of an interface between the sample control and automated analysis systems to facilitate reporting of analysis results. This last item could be particularly important. We noted in our interviews and reported in our tally of problem-area responses that an incredible amount of time was consumed in the transcription of information (e.g., from work sheet to final report form). A goal might be to have pre-designed forms called up on a terminal screen on which the analyst enters a lab ID number; sample description data and analysis results would be filled in automatically. The analyst could then review the information and have it printed out, ready for his signature. Finally, it should also be kept in mind that data base capabilities should be amenable to the special requirements of QA.

Clearly, the above points regarding lab automation and upgrade goals comprise a major effort. We feel that these goals cannot be realized by enlisting present personnel on a part-time or as-able basis. We suggest that a small team of full-time people be acquired whose sole responsibility will be support of these objectives. We estimate that the magnitude of this effort requires approximately four people: 1 systems programmer, 1 data base programmer, 1 applications programmer, and 1 electronics systems technician.

E. MANAGEMENT OF CONTRACT LAB WORK ALLOCATION: As noted earlier, the OEHL is authorized the employ of contract laboratories to assist them in the handling of sample analysis workloads

At present, requests for send-out of samples are made by bench personnel and submitted to a section chief who then determines the number to be contracted out and to which of the five laboratories samples will be sent. During the most recent period no real budget was effected for costs associated with these services, although expenditures were in the neighborhood of one million dollars per year. We have attempted to make a rough estimate of the costs for analyses contracted out in the coming year based on our earlier projections of growth in sample requests received and accepting the premise that incorporation of new QA record-keeping procedures will negatively impact sample throughput in-house. Assuming a 5% decrease in samples processed, we calculate that 3200 samples which would otherwise be analyzed in-house will be sent out. Adding to this an estimated 4250 samples in yearly growth, we obtain a figure of 7250 more samples processed through contract labs in the coming year. At an average of \$50 per sample, this suggests an increment in expenditures of \$375,000 --- a sizable increase over the present base of \$1,000,000.

Facing a possible increase in costs of this magnitude and uncertainties in budgeting, management should focus on prudent use of monies that are recieved. We recommend that a mathematical model be developed, incorporating decision rules reflecting sample-to-contract lab assignment constraints, which seeks to maximize utility of funds budgeted for this support work. The model should be designed to run on a routine basis, delivering sample quantities, by type, which are to be transshipped to each laboratory. Model decision-making would employ such information as in-house sample backlogs and priorities and contract lab turn-around times, fees and price break structures. Use of this tool would relieve the supervisor of the tedium of manual assignment of samples to labs and yield assignment policies which represent nearer-optimum use of allocated funds. Such a model will be the subject of a proposal we plan to submit as a follow-on to the initial efforts outlined in this report.



1987 USAF-UES SUMMER FACULTY RESEARCH PROGRAM

GRADUATE STUDENT SUMMER SUPPORT PROGRAM

Sponsored by the  
AIR FORCE OFFICE OF SCIENTIFIC RESEARCH  
conducted by the  
Universal Energy Systems, Inc.

FINAL REPORT

Prepared by:	Suhrit K. Dey
Academic Rank:	Professor
Department and	Mathematics
University:	Eastern Illinois University
Research Location:	Arnold Air Force Base
	Computational Fluid Dynamics
	Tennessee
USAF Researcher:	Dr. George Kyle Cooper
Date:	September 15, 1987
Contract No:	F49620-85-C-0013

Vectorized Perturbed Functional Iterative Scheme (VPFIS) for  
Numerical Solution of Nonlinear Partial Differential Equations.

by

Suhrit K. Dey

ABSTRACT

Perturbed functional iterative scheme (PFIS) was developed in [1] and applied successfully to solve nonlinear partial differential equations. With the advent of a new era of supercomputers and vector processors the algorithm of PFIS has been modified. This modified scheme could solve implicit approximations of nonlinear partial differential equations in an explicit mode of computation so that no Jacobian is computed and no factorization of matrices is needed. It displays a superlinear rate of convergence. Two dimensional Euler-type nonlinear hyperbolic partial differential equations have been successfully solved using vectorized PFIS. An implicit version of this code has also been formed. In comparison with other implicit finite difference codes, the present code does not require inversion of any block matrices. Also, the algorithm of the present scheme appears to be much simpler.

# ACKNOWLEDGEMENT

This work has been supported by the summer research grant ('87) from the Universal Energy System (UES).

I thank Mr. M. Kingery from AEDC for his support in this work and Dr. G. K. Cooper of Sverdrup Technology, Inc./AEDC Group who was my excellent research colleague and helped me in every possible way for the success of this work.

## I. INTRODUCTION:

A perturbed functional iterative scheme (PFIS) has been developed in [1] which adds unique perturbation parameters to nonlinear Jacobi and/or Gauss-seidel iterations. Whereas Newton's method is based upon a complete linearization of a nonlinear system, the present method linearizes only the diagonal elements and this linearization is damped out as convergence is approached. Thus, most nonlinear properties of the system have been preserved during the mode of application of the method.

In the summer of '87 a modified vectorized algorithm of PFIS has been developed and has been implemented the supercomputer CRAY. Excellent results have been found with regard to the solution of 2D nonlinear hyperbolic Euler type models.

## II. OBJECTIVES OF THE RESEARCH EFFORTS

The primary objective was to look into the fact whether vectorized PFIS could reduce computational complexities which are often associated with most implicit CFD codes dealing with the solution of various 2D and/or 3D flow models. This objective has been partially fulfilled. An example is given in the appendix B.

For two dimensional Euler-type equations, two versions of this code have been formed. One requires an explicit mode of computation and the other uses inversion of scalar matrices for each vector. Thus, if there are  $IJ$  number of field points, a  $J \times J$  matrix is inverted for each  $i = 1, 2, \dots, I$  vectors. No block-matrices were required.

The algorithm is given in details in the appendix A.

### III. RECOMMENDATIONS

Both theoretical and computational studies should be conducted in the future to understand:

- (i) Convergence properties of the vectorized algorithm of PFIS.
- (ii) Numerical solution of 2D Euler's equation with various initial/boundary conditions.
- and (iii) Extension of these studies to 3D flow models.

Since the method is much simpler than most implicit finite difference codes and has a superlinear rate of convergence, such studies should be quite helpful to the researchers in CFD.

The final objective should be to develop a code for general Navier-Stokes Equations since VPFIS could solve implicit finite difference approximations using an explicit mode of computations.

# REFERENCES

1. Dey, S. K. Numerical Solution of Nonlinear Implicit Finite Difference Equations of Flow Problems by Perturbed Functional Iterations Computational Fluid Dynamics Edited by W. Kollmann Hemisphere Publishing Corporation, New York, 1980, pp. 543-602.
2. Peyret, R and Taylor, T.D. Computational Methods for Fluid Flow, Springer-Verlag, New York, 1983.

# APPENDIX A: ALGORITHM OF VPFI5 (EXPLICIT & IMPLICIT)

## (a) Algorithm of Explicit VPFI5

Let us consider two coupled nonlinear equations.

$$U = F(U, V) \quad (a)$$

$$V = G(U, V) \quad (b)$$

where

$$U_i = (U_{i1} \ U_{i2} \ \dots \ U_{iJ})^T$$

$$U = (U_1 \ U_2 \ \dots \ U_I)^T$$

$$V_i = (V_{i1} \ V_{i2} \ \dots \ V_{iJ})^T$$

$$V = (V_1 \ V_2 \ \dots \ V_I)^T$$

$$i = 1, 2, \dots, I$$

Thus, there are  $IJ$  number of field points and at each point we need to compute

$U_{ij}$  and  $V_{ij}$  ( $i=1, 2, \dots, I$ ;  $j=1, 2, \dots, J$ ).

In the element form, (a) and (b) are  $U_{ij} = F_{ij}(U, V)$ ,  $V_{ij} = G_{ij}(U, V)$ .

First make an initial guess  $U^0, V^0$ . At some  $(k+1)$ th iteration for each

$i=1, 2, \dots, I$ , compute each #1, #2 ... #10 for  $j=1, 2, \dots, J$

(Note  $U_{ij}^k$  = value of  $U_{ij}$  at the  $k$ th iteration).

$$\tilde{F}_{1j} = F_{1j}(U_1^{k+1}, U_2^{k+1} \dots U_{i-1}^{k+1}, U_i^k \dots U_I^k; \quad (1)$$

$$V_1^{k+1}, V_2^{k+1} \dots V_{i-1}^{k+1}, V_i^k \dots V_I^k)$$

( $F_1$  is known now)

$$\tilde{G}_{1j} = G_{1j}(U_1^{k+1}, U_2^{k+1} \dots U_{i-1}^{k+1}, U_i^k \dots U_I^k; \quad (2)$$

$$V_1^{k+1}, V_2^{k+1} \dots V_{i-1}^{k+1}, V_i^k \dots V_I^k)$$

( $G_1$  is known now)

$$\frac{\partial F_{1j}^{k+1,k}}{\partial U_{1j}} = \frac{\partial F_{1j}}{\partial U_{1j}}(U_1^{k+1} \dots U_{i-1}^{k+1}, \tilde{F}_1, U_{i+1}^k \dots U_I^k; V_1^{k+1} \dots V_{i-1}^{k+1}, \tilde{G}_1, V_{i+1}^k \dots V_I^k) \quad (3)$$

$$\frac{\partial G_{1j}^{k+1,k}}{\partial V_{1j}} = \frac{\partial G_{1j}}{\partial V_{1j}}(U_1^{k+1} \dots U_{i-1}^{k+1}, \tilde{F}_1, U_{i+1}^k \dots U_I^k; V_1^{k+1} \dots V_{i-1}^{k+1}, \tilde{G}_1, V_{i+1}^k \dots V_I^k) \quad (4)$$

$$\hat{F}_{1j} = F_{1j}(U_1^{k+1} \dots U_{i-1}^{k+1}, \tilde{F}_1, U_{i+1}^k \dots U_I^k; \quad (5)$$

$$V_1^{k+1} \dots V_{i-1}^{k+1}, \tilde{G}_1, V_{i+1}^k \dots V_I^k)$$

$$\hat{G}_{1j} = G_{1j}(U_1^{k+1} \dots U_{i-1}^{k+1}, \tilde{F}_1, U_{i+1}^k \dots U_I^k; \quad (6)$$

$$V_1^{k+1} \dots V_{i-1}^{k+1}, \tilde{G}_1, V_{i+1}^k \dots V_I^k)$$

$$\alpha_{1j}^{k+1} = (\hat{F}_{1j} - \tilde{F}_{1j}) / (1 - \partial F_{1j}^{k+1,k}) \quad (7)$$

$$\beta_{1j}^{k+1} = (\hat{G}_{1j} - \tilde{G}_{1j}) / (1 - \partial G_{1j}^{k+1,k}) \quad (8)$$

$$U_{1j}^{k+1} = \alpha_{1j}^{k+1} + \tilde{F}_{1j} \quad (9)$$

$$V_{1j}^{k+1} = \beta_{1j}^{k+1} + \tilde{G}_{1j} \quad (10)$$



Convergence criterion is:

$$\max_{ij} (|\alpha_{ij}^k| + |\beta_{ij}^k|) < \epsilon$$

for some  $k > K$ ,  $\epsilon$  = a preassigned positive number arbitrarily small.

b) Algorithm of Implicit VPFIS

Solve

$$U_{ij} = F_{ij}(U, V)$$

$$V_{ij} = G_{ij}(U, V)$$

$$i = 1, 2, \dots, I; \quad j = 1, 2, \dots, J$$

At some  $(k+1)$ th iteration, compute for  $j=1, 2, \dots, J$  for each  $i=1, 2, \dots, I$

$$\tilde{F}_{ij} = F_{ij}(U_1^{k+1} \dots U_{i-1}^{k+1}, U_i^k, U_i^k; V_1^{k+1}, \dots, V_{i-1}^{k+1}, V_i^k, \dots, V_I^k) \quad (1)$$

( $F_i$  is known now)

$$\hat{F}_{ij} = F_{ij}(U_1^{k+1} \dots U_{i-1}^{k+1}, \tilde{F}_i^k, U_{i+1}^k \dots U_I^k; V_1^{k+1}, V_i^k, \dots, V_I^k) \quad (2)$$

$$\alpha_i^{k+1} = M_i^{-1}(\hat{F}_i - \tilde{F}_i), \quad \text{if} \quad F_{ij,im} = \frac{\partial F_{ij}}{\partial U_{im}}, \quad \text{then}$$

$$M_i = \begin{bmatrix} 1 - F_{i1,i2} & -F_{i1,iJ} & \dots & -F_{i1,iJ} \\ -F_{i2,i1} & 1 - F_{i2,i2} & \dots & -F_{i2,iJ} \\ \vdots & \vdots & \ddots & \vdots \\ -F_{iJ,i1} & -F_{iJ,i2} & \dots & 1 - F_{iJ,iJ} \end{bmatrix} \quad (3)$$

All derivatives are evaluated at  $(U_1^{k+1} \dots U_{i-1}^{k+1}, \tilde{F}_i^k, U_{i+1}^k \dots U_I^k;$

$V_1^{k+1}, \dots, V_{i-1}^{k+1}, V_i^k \dots V_I^k)$

$$U_{ij}^{k+1} = \alpha_{ij}^{k+1} + \tilde{F}_{ij} \quad (4)$$

$$(\alpha_i^{k+1} = (\alpha_{i1}^{k+1} \quad \alpha_{i2}^{k+1} \dots \alpha_{iJ}^{k+1})^T)$$

$$\begin{aligned} \tilde{G}_{ij} = G_{ij}(U_1^{k+1} \dots U_i^{k+1}, U_{i+1}^k \dots U_I^k; \\ V_1^{k+1} \dots V_{i-1}^{k+1}, V_i^k \dots V_I^k) \end{aligned} \quad (5)$$

$$\begin{aligned} \hat{G}_{ij} = G_{ij}(U_1^{k+1} \dots U_i^{k+1}, U_{i+1}^k \dots U_I^k; \\ V_1^{k+1} \dots V_{i-1}^{k+1}, \tilde{G}_i, V_{i+1}^k \dots V_I^k) \end{aligned} \quad (6)$$

$$\beta^{k+1} = N_i^{-1}(\hat{G}_i - \tilde{G}_i)$$

where

$$N_i = \begin{bmatrix} 1 - G_{i1,i2} & -G_{i1,iJ} & \dots & -G_{i1,iJ} \\ -G_{i2,i1} & 1 - G_{i2,i2} & \dots & -G_{i2,iJ} \\ \vdots & \vdots & \ddots & \vdots \\ -G_{iJ,i1} & -G_{iJ,i2} & \dots & 1 - G_{iJ,iJ} \end{bmatrix} \quad (7)$$

Derivatives are evaluated at

$$\begin{aligned} (U_1^{k+1} \dots U_i^{k+1}, U_{i+1}^k \dots U_I^k; \\ V_1^{k+1}, \dots, V_{i-1}^{k+1}, G_i, V_{i+1}^k \dots V_I^k) \\ V_{ij}^{k+1} = \beta_{i+1}^k + \tilde{G}_{ij} \end{aligned} \quad (8)$$

Criterion for convergence is:

$$\max_{ij} (|\alpha_{ij}^k|, |\beta_{ij}^k|) < \epsilon$$

for some  $k > K$ ,  $\epsilon$  is positive and arbitrarily small.

## APPENDIX B: THE TWO-DIMENSIONAL HYPERBOLIC MODEL

We solved the following two-dimensional model applying both explicit and implicit versions of PFIS:

$$U_t + UU_x + VU_y = f(U, V, t)$$

$$V_t + UV_x + VV_y = g(U, V, t)$$

using various initial/boundary conditions.

We chose  $f$  and  $g$  such that analytical solutions are known. These nonlinear hyperbolic Euler-type equations were solved numerically using both explicit and implicit versions of vectorized PFIS. Both schemes generated the same results. The maximum error was of the order  $0.5E-02$ . No artificial viscosity was needed to maintain computational stability. The codes appeared to be much simpler and used no more computer time than other existing implicit codes used at AEDC

[Ref. Dr. G. K. Cooper].

1987 USAF-UES SUMMER FACULTY RESEARCH PROGRAM/

GRADUATE STUDENT SUMMER SUPPORT PROGRAM

Sponsored by the

AIR FORCE OFFICE OF SCIENTIFIC RESEARCH

Conducted by the

Universal Energy Systems, Inc.

FINAL REPORT

AN EIGHT-DOMAIN FRAMEWORK FOR UNDERSTANDING INTELLIGENCE  
AND PREDICTING INTELLIGENT PERFORMANCE

Prepared by:	Ronna F. Dillon/Catherine Aubertin
Academic Rank:	Professor /Graduate Student
Departments:	Educational Psychology, Psychology, and Psychiatry
University:	Southern Illinois University
Research Location:	Air Force Human Resources Laboratory, Manpower and Personnel Division, Test and Training Branch (AFHRL/MOEL)
USAF Researcher	Dr. William C. Tinne
Date:	September 21, 1987
Contract No:	F49620-85-C-0013

AN EIGHT-DOMAIN FRAMEWORK FOR UNDERSTANDING INTELLIGENCE  
AND PREDICTING INTELLIGENT PERFORMANCE

by

Ronna F. Dillon  
Catherine Aubertin

ABSTRACT

This paper describes my participation in the 1987 Summer Faculty Research Program in the Test and Training Branch of the Air Force Human Resources Laboratory at Brooks Air Force Base. My activities centered on elucidation of an eight-domain model of aptitude and use of the model in (a) conceptualizing and writing materials for a national research symposium on measuring and predicting professional competence across a range of professions and for a biennial conference on individual differences in cognition and learning, and (b) undertaking a program of research on the importance of measures of each domain for predicting school and job performance among Air Force recruits. The eight-domain framework taps processing capacity, processing speed, declarative knowledge, information-processing components, information-processing metacomponents, rule induction skill, verbal and visuospatial knowledge manipulation skills, and cognitive flexibility.

### ACKNOWLEDGEMENTS

I would like to acknowledge the sponsorship of the Air Force Systems Command, Air Force Office of Scientific Research, the Air Force Human Resources Laboratory, and the Manpower and Personnel Division of AFHRL. The scientific assistance of Dr. Lloyd Buntch, Dr. Raymond Christal, Dr. William Tinne, and Dr. Dan Woltz of AFHRL is gratefully acknowledged. I also would like to acknowledge the programming and data reduction assistance of Mr. Richard Walker and Ms. Janice Hereford (OAO Corporation under contract to AFHRL).

## I. INTRODUCTION:

A major manpower and personnel mission of scientists affiliated with the Air Force Office of Scientific Research is elucidation of the fundamental information processes underlying intelligent performance among Air Force personnel. During the past 15 years, I have been involved in a program of research aimed at conceptualization and validation of a robust framework for understanding intelligence.

During the period of my AFOSR/UES Summer Faculty Fellowship, my aptitude framework has guided two types of activities. The first effort involves implementation of a large-scale research program, based on my eight-domain framework, with scientists in the Air Force Human Resources Laboratory's (AFHRL) Learning Abilities Measurement Program (LAMP). The program of research couples experimental tests from five aptitude domains I have conceptualized and studied in my laboratory with three aptitude domains operationalized by LAMP scientists. The LAMP tests have focused on working memory, access to information stored in a long-term state, and declarative knowledge. To these domains, I add measures of information-processing stages and strategies, metacomponential processes, transformational rule induction ability, abilities to manipulate different types of stored knowledge, and the multiple dimensions of cognitive flexibility. For each domain, new methods and new measures are used.

The second facet of this work involves expanding and synthesizing knowledge with respect to the aptitudes underlying intelligent performance by conceptualizing and submitting materials for a major symposium at the 1988 Convention of the American Educational Research

Association and by developing and conducting the first in a biennial series of conferences in individual differences and learning.

## **II. OBJECTIVES OF THE RESEARCH EFFORT:**

The activities I coordinated during my participation in the 1987 Summer Faculty Research Program (SFRP) embodied three objectives. First, I conceptualized and wrote a prospectus for a symposium to be sponsored by Division I, Research in the Professions, for the 1988 Convention of the American Educational Research Association. The symposium centers on new ways of measuring and predicting professional competence. Second, I conceptualized and wrote a prospectus for a biennial conference series on individual differences in cognition and learning, to be carried out in collaboration with Dr. William C. Tonne at AFHRL. Third, I planned a program of research, and the initial two studies were executed. This work is guided by my eight-domain aptitude framework. These initial studies were designed to ascertain the amount of variance in the Armed Services Vocational Aptitude Battery (ASVAB) that could be accounted for by models derived from the framework.

## **III. SCIENTIFIC BACKGROUND FOR THE SYMPOSIUM, CONFERENCE,**

### **AND RESEARCH PROGRAM:**

The study of human intelligence has suffered from certain limitations. Most conceptualizations of intelligence have been quite narrow, centering on a small number of domains (i.e., often only one domain), with the domains being narrowly conceived. For example, researchers may devote their attention to one type of ability (e.g., spatial ability) or, more narrowly, to only one aspect of ability, such as dynamic spatial ability or mental rotation. As a consequence, our knowledge of the nature of intelligence has not broadened as might



otherwise have been the case. Moreover, typical frameworks for predicting intelligent performance yield less-than-satisfactory estimates of who will succeed in given military, academic, or occupational training programs or in particular professional settings.

The investigation of human intelligence is motivated by two complimentary goals, both necessitating accurate measurement of intellectual processes. The theoretical goal is to advance knowledge regarding the nature of mental representations. The importance of the applied goal of enhancing prediction of training, academic and/or occupational success in military selection and classification cannot be overstated. Scientists cannot advance knowledge regarding the nature of intelligence or improve prediction of success in military enlisted or officer training programs in the absence of sensitive measurement of information-processing and learning abilities. The need for improved prediction of who will succeed in military careers, and for possession of mechanisms for distinguishing average potential from the potential for excellence is clear. Resources are saved on the part of students or enlisted personnel to the extent that diagnosticians can avoid selecting learners for programs in which they are not likely to succeed or selecting individuals for jobs in which they are not likely to perform well. Resources also are saved on the part of the military organization if attrition and the associated personnel and other costs therewith can be minimized.

Despite the major importance of accurate selection mechanisms for training and job placement, sizable rates of attrition continue to constitute a major problem in the military sector. An increasing number of psychologists are displaying an interest in developing improved

testing procedures (cf. Dillon, 1986, in press; Sternberg, 1984). These investigators contend that typical psychometric assessments rarely account for satisfactory amounts of variance in measures of academic success or other criterion measures of interest (e.g., Dillon, 1985-a, 1986; Jencks, 1977; Matarazzo, 1972; McCall, 1977; Wechsler, 1975). Moreover, diagnostic and prescriptive information available from traditional assessments is imprecise. This imprecision exists because models used for prediction are comprised of predictors taken from one or more test scores, which measure only the products of performance. Thus, no information is available with respect to strengths and limitations in the processes underlying performance. The importance of such information is clear. Very different patterns of information-processing strengths and limitations underlie the same test score.

A robust conceptual framework for measuring and understanding intelligence, and for predicting intelligent performance is needed. Clearly, a crucial need exists for enhanced prediction of success of training among Air Force personnel, and a theoretical model will provide the framework necessary for implementation of the needed testing program.

I am pursuing this goal with scientists in the LAMP group. My work involves developing a robust framework for understanding aptitude and predicting intelligent performance. The framework couples LAMP's working memory, long-term memory, and declarative knowledge clusters with five clusters I have studied. The five clusters from my battery tap componential processes, transformational rule induction, manipulation of stored verbal and visiospatial knowledge, metacomponential processes, and cognitive flexibility.

### Eight-Cluster Framework of Human Abilities

Work in the LAMP program currently focuses nicely on three domains of abilities. The domains are working memory, long-term memory, and declarative knowledge.

#### Working Memory -- Processing Capacity

Two approaches to the study of working memory, and the alternative conceptions of memory driving each type of research, are of considerable interest. One conception of working memory, based on the processing workspace model (Baddeley & Hitch, 1984), refers to a limited-capacity structure, capable of processing typically 3-9 units of information at a time. Present work by members of LAMP centers on this approach to working memory. Interest here is in the dimensionality of working memory and relations between working memory and performance on tests of other aptitudes. Christal (1987) reports that factor analyses of working memory and reasoning tasks yield a processing capacity factor that subsumes reasoning tests used in the battery. These analyses point to the important role of working memory capacity in information processing across a range of cognitive tasks.

A second approach to working memory, based on activation capacity models (e.g., Anderson, 1987), centers not on the capacity of working memory but instead characterizes working memory as a state of fluctuating activation patterns reflecting traces in long-term memory. According to this latter view, the network of traces that comprise long-term memory each have resting activation levels. Working memory is defined in this regard as that portion of memory currently in a highly active state. Thus, working memory reflects those contents that are the subject of processing at a given time.

### Long-Term Memory -- Processing Speed

The second domain being investigated in the LAMP program is processing speed on measures that involve access to information stored in long-term memory. Retrieval from long-term memory, by means of a name matching task, and search through long-term memory, using a semantic matching task, are of particular interest. Scientists in the LAMP group isolate latencies associated with retrieval and search processes and use these latencies as predictors in models of learning. Again, interest is in relations among indices of long-term memory and measures of other aptitudes. Moreover, interest is in the role of long-term memory, along with the other aptitude clusters, in predicting intelligent performance among Air Force personnel.

### Knowledge

Declarative Knowledge measures constitute the third aptitude domain. Success in a given area of technical training clearly necessitates possession of the facts, data base or knowledge used in the particular discipline of interest. The importance of declarative knowledge to successful performance in any field has not been disputed. Rather, the issue is that measures of such knowledge alone fail to account for adequate amounts of variance in measures of intelligent training or job performance. A study recently completed in my laboratory (Dillon & Reznick, 1986) on third-year medical students underscores the limitations of declarative knowledge measures for enhancing scientists' understanding of intelligence among students at advanced levels of training or experience. Moreover, the study permits disentangling of the relative contributions of declarative knowledge, rule induction skills, and information-processing components.

In the study, medical students participating in a surgical clerkship were given sets of inductive reasoning items. Ongoing eye movement patterns were recorded. The incremental validity of models coupling eye movement measures of information processing with a measure of medical declarative knowledge (i.e., the Medical College Admissions Test; MCAT Science score) was compared to models based on rule induction skill alone (i.e., score on common-content, familiar-rule figural analogies) and medical declarative knowledge alone. Data indicated that medical declarative knowledge alone accounted for 40% of the variance in surgical clerkship performance, while analogy performance alone accounted for 22% of the variance in criterion performance. Declarative knowledge and information-processing activities were coupled by recording eye movement patterns during solution of a set of analogies for which item elements were related by rules based on medical knowledge (e.g., two symptoms to a diagnosis, two symptoms to a medical procedure). Information-processing measures used with medical declarative knowledge were the percentage of total row (i.e., large, nonredundant) scans to total scans (a positively weighted variable) and the number of times the subject broke main-array processing to attempt confirmation (a negatively weighted variable). For these advanced medical students, intelligent performance was reflected in the ability to process relatively large amounts of information in a nonredundant manner and to induce and apply item rules before attempting to confirm these rules by processing the response set. Coupling declarative knowledge with information-processing performance components increased the R<sup>2</sup> to an extremely high 77%.

In the collaborative work designed to follow the SFRP effort, the breadth of technical knowledge a learner brings to the testing situation will be assessed through evaluation of scores on the Armed Services Vocational Aptitude Battery (ASVAB). An additional motivation for using the ASVAB as a measure of breadth of relevant declarative knowledge is to demonstrate the significant increase in the amount of variance in measures of intelligent performance (i.e., criterion measures of interest) that can be accounted for when prediction models are based on measures of the other five aptitude domains studied in this collaborative effort along with declarative knowledge.

#### Componential Processes

The fourth domain being elucidated in this collaborative program of research involves my first cluster of new aptitude dimensions. Tests in this domain reveal the operation of componential, or fundamental information-processing operations. Isolation of encoding, rule inference, rule application, and confirmation activities is accomplished by means of a paradigm I developed that involves use of a partial screen technique, with movement between computer screens being under the experimental subject's control (see Dillon, 1987-a). Complex reasoning items are decomposed into distinct information-processing stages for item administration, and each stage is displayed on a separate computer screen. Subject's move forward and backward between stages, processing information about each stage as many times and for as much time as necessary for item solution.

The procedure is designed to yield information to corroborate data available through my eye movement paradigm (see Dillon, 1982, 1986, in press-a, in press-b for reviews of this work). The eye movement work

involves recording eye scan patterns during solution of intact, complex reasoning items. Stage difficulties and characteristics have been manipulated to yield information regarding the nature of intellectual processes (Dillon, 1982, 1987-a, 1987-b). Four levels of individual differences in information-processing components have been isolated that underlie, and thus significantly predict, intelligent performance. These levels tap individual differences in (a) execution of distinct information-processing stages, (b) the order in which processing steps are executed, (c) execution of optional strategy elements, and (d) changes in performance over time. In addition, the contribution of relevant declarative knowledge, abilities to induce or deduce the transformational rules governing relations among stimulus elements, and abilities to manipulate stored verbal, visiospatial, and, as relevant, quantitative stored knowledge were isolated in this work.

Through research in my laboratory (e.g., Dillon, 1982, 1985-a, 1986, 1987-a, 1987-b, 1987-c; Dillon & Reznick, 1986; Dillon & Stevenson-Hicks, 1981; Dillon & Wisher, 1981), I have demonstrated that eye movement measures of information processing, recorded during solution of inductive reasoning items, account for markedly greater amounts of variation in measures of academic achievement than do scores taken from the same items, with  $R^2$ s in the .20s for test scores and in the mid-.40s to high-.70s for information-processing measures.

#### Transformational Rule Induction

The fifth domain of interest in this collaborative work is the ability to induce transformational rules in solution of reasoning tasks. Following research done in my laboratory (e.g., Dillon, 1987-a, 1987-b; Dillon & Reznick, 1986), the work reported herein involves disentangling

the role of rule induction processes from declarative knowledge and from other information-processing activities by recording examinees' scores on test items tapping pure induction (i.e., using highly familiar content and transformational rules). For example, a colleague and I (Dillon & Reznick, 1986) reported a significant contribution of induction, apart from declarative knowledge and information-processing componential skills, to achievement among third-year medical school students.

#### Manipulation of Stored Verbal and Visiospatial Knowledge

The sixth domain to be investigated in this collaborative program of research centers on learners' abilities to manipulate stored verbal and visiospatial knowledge. Specifically, since intelligent behavior nearly always necessitates skills at manipulating multiple knowledge bases, both verbal and visiospatial manipulation skills should be important. That is, most types of reasoning and cognitive problem solving require access to verbal and visiospatial stored knowledge. I use the term "knowledge manipulation" because the stimulus elements and the attributes of these elements, as well as the rules governing relations between sets of elements, involve familiar information. The examinee's task is to be able to use this verbal and visiospatial information that already is possessed to ascertain relations among sets of stimuli and to distinguish stimulus elements that are similar from elements that are dissimilar based on familiar rules. In previous work, I have demonstrated that facilities at manipulating familiar verbal and visiospatial knowledge bases contribute significantly to intelligent performance (Dillon, 1985-b). Verbal and visiospatial processing proficiencies each contribute to prediction of performance. Moreover,



when learner's demonstrate a preference for processing one type of item content over the other type of content, these preferences are related to differences in performance on complex verbal and visiospatial reasoning tests. In addition, the extent to which these fundamental information-processing proficiencies and preferences relate to job choice, or occupational specialization with the Air Force is of interest.

#### Metacomponential Processes

Metacomponential operations concern those mental activities in which learners engage when they are thinking about their mental processes, developing macrostrategies concerning sets of items having similar features or demands, planning to engage in problem solving, and/or monitoring solution processes. The various components of this seventh domain are of interest in our collaborative research.

With respect to differences in learners' thoughts about their own cognitive processes, I am have adapted an instrument from Sternberg and Wagner's (1986) notion of tacitly acquired occupational knowledge. Examinees rate the importance they attribute to a variety of activities with respect to managing their own lives, managing others, and managing their careers. These ratings then are compared to expert ratings or prototypes. Sternberg and Wagner (1986) report that differences in this tacitly acquired knowledge distinguish novices from experts. In addition, my colleagues and I (Dillon, Travis, & Loschen, 1987) have assembled a set of items that tap aspects of tacit knowledge that are general across medical professionals, and a set of items of specific relevance to the demands of medical professionals in private practice, items relevant specifically to professionals in the public sector (e.g.,

hospital administration), and items relevant specifically to academic physicians. Individuals in the different sectors become increasingly different in the manner in which they prioritize professional demands, in a manner that is consistent with the different professional outlets. In addition, as expected, general occupational knowledge indices have greatest predictive power in early career years, and specific occupational knowledge measures have greatest predictive validity for distinguishing experienced professionals across career outlets.

Macrostrategies are executive planning processes that are relevant to sets of items having similar features or demands. In previous research in my laboratory (Dillon, under review-b), subjects were assigned to either a blocked or a mixed item presentation format. In the blocked format, items were grouped for presentation on the basis of similar transformational rules. Under the mixed condition, items were ordered randomly for presentation. I recorded eye movement patterns during item solution. Results indicate that macrostrategy development is reflected in information processing that is characterized by thorough encoding and by truncated rule application and confirmation processing. Once specific stimulus elements are encoded and the subject infers that a general class rule governs relations among stimulus elements, the remaining information-processing stages are executed in abbreviated fashion. In a different set of studies (Dillon, 1985-b), I found that general planning and monitoring activities are important aptitudes on the part of novices as well as relatively expert examinees.

### Flexibility

The eighth domain of cognitive aptitudes that is of interest in this collaborative research program centers on the multidimensional

construct of cognitive flexibility. Academic and professional success necessitates possession of many and varied abilities and skills. Beyond possession of specific skills, I believe an important set of skills underlying intelligent (i.e., successful) performance involves cognitive flexibility.

I have undertaken a program of research centered on development of a multifaceted theory of flexibility and determination of the relations of flexibility to measures of success among students and professionals. In my terms (Dillon, 1987; Dillon, Lyster, & Aubertin, 1987), flexibility involves the abilities to (a) select the type of strategy designated by the experimenter when more than one approach is potentially appropriate, (b) generate more than one strategy in solving test items or problems that have more than one possible solution strategy, (c) maintain processing efficiency when solving items having different attributes that are randomly ordered for presentation, and (d) change approach when the task demands change.

Despite the considerable recent interest in cognitive flexibility that has been displayed in the literature (e.g., Cooper, 1980, 1982; Cooper & Mumaw, 1985; Gitomer, 1984; Lesgold, Feltovich, Glaser, & Wang, 1981; Lohman & Kyllonen, 1985; Schneider & Fisk, 1986; Scribner, 1984), no framework exists for studying flexibility. I have undertaken a program of research to develop a multifaceted theory of flexibility and to determine its relation to success among students and professionals. I believe flexibility involves the ability to generate multiple strategies for cognitive problems or test items that can be solved in more than one way, analyzing and/or synthesizing incomplete information to maximize interpretations possible, the ability to maintain

information-processing efficiency during solution of items that require different types of transformational rules for their solution, and the ability to change set in order to generate new and different solutions to problems that follow sets of items that were different than the current item. With respect to the first dimension of flexibility, the experimenter tells the subject which type of strategy or classificatory scheme to use, whereas in the fourth type of flexibility, the task demands change across items, with only one type of transformational rule governing a particular item.

The ability to generate multiple strategies in solution of items that can be solved in more than one way (Dillon, 1987-d, 1987-e), and the ability to maintain processing efficiency as the demands of a task change (Dillon, 1987-e) are two dimensions of cognitive flexibility that have been found to play an important role in processing among college students and medical personnel. In this collaborative effort, we are interested in examinees' abilities to generate multiple strategies and to change set; i.e., to maintain processing efficiency when given a different kind of test item after having solved a set of items with demands that were similar to one another.

### III. SFRP ACTIVITIES

#### A. SYMPOSIUM

##### Objectives of the Symposium

This symposium will bring together researchers from the diverse fields of medical education, vocational/technical education, military selection and classification, and professional education, permitting analysis and synthesis of theoretical underpinnings and practical significance of a wide range of assessment paradigms. Thus, the

symposium materials will be generalizable across professions. To ensure cohesiveness among symposium participants, all presenters are asked to address a common set of focus questions, as noted below.

1. Describe the aptitude or ability dimensions you feel most importantly underlie success in the area you are measuring.
2. Describe the method you are proposing for studying these cognitive or other bases of individual difference.
3. Discuss the manner in which the method connects with theories of abilities.
4. Discuss the practical utility of the method, including routine psychodiagnostic utility, stability of measurements, and predictive validity.
5. Discuss the manner in which the method is responsive to particular constraints or circumstances of testing in the environment in which you have done your research.

Moreover, selection of topics/contributors has been accomplished to permit several interesting comparisons, including (a) goals, concerns, and constraints that are common across areas, (b) concerns and constraining factors that are specific to each area, (c) differences in predicting academic training success versus occupational training success, (d) differences in predicting student performance versus professional competence, and (e) issues in long- versus short-term prediction.

#### Significance

A professional forum for bringing together common issues in intelligence measurement and performance prediction across professions and for delineating unique constraints within technical and professional areas is needed. This goal of this symposium, enabling contributors to address a common set of questions, is to provide such a forum.

#### B. CONFERENCES

##### Objectives of the Program

The objectives of this program are to bring together top DOD and university researchers for a forum in which the latest research in

individual differences in cognition and learning can be discussed, provide technical reports to inform the DOD community of the high calibre work underway, and provide a highly visible, professional outlet for informing the scientific community about the nature of these activities.

#### Outcomes

There will be three principle outcomes of this ongoing program. The first outcome will be a biennial conference in individual differences in cognition and learning. The second outcome will be a technical report of the proceedings from each conference. The final outcome will be an edited book containing chapter contributions derived from each presentation.

A complete list of topics for the first conference is given below:

- (A) Newly conceptualized individual difference dimensions, including cognitive flexibility, and occupational knowledge
- (B) Models of intelligence
- (C) Discourse comprehension
- (D) New work in enlisted, aircrew, and officer selection
- (E) Predicting success in medical training
- (F) Predicting success in other professional and occupational settings
- (G) Development of expertise in electronics
- (H) Development of expertise in communications
- (I) Development of expertise in mathematics and computer programming
- (J) Development of expertise in medicine
- (K) Individual differences underlying officer advancement
- (L) Tacit acquisition of occupational knowledge in selected aspects of science and industry
- (M) New techniques in computerized assessment of individual differences
- (N) Psychophysiological and electrophysiological techniques in individual differences measurement
- (O) Comprehensive performance-based examinations in medicine and other academic areas
- (P) Using multiple raters and multiple criterion measures to predict success in training
- (Q) Job sampling

### Significance

No set of scholarly meetings and publications has brought together the newest developments in individual differences in cognition and learning among university and DOD researchers in a unified and ongoing manner. This program of conferences and scholarly publications is designed to meet this need.

### C. RESEARCH PROGRAM ON EIGHT-DOMAIN APTITUDE FRAMEWORK AND INTELLIGENT PERFORMANCE

#### Approach

Two studies have been conducted during the Summer Research Faculty Program period using Air Force recruits as examinees. These data point to the robustness of the model of aptitude we propose. Work conducted under the the SFRP is discussed below. By the end of the 1987 Summer Research Faculty Program period, data collection and analysis was completed on one study, and data collection was completed on a second study. These studies focus of the robustness of my five domains of the eight-domain aptitude framework with respect to understanding intelligent performance among Air Force recruits.

Study 1. Test calibration. Test difficulties, test lengths, and other relevant constraints were evaluated in Study 1, for tests tapping each domain in the framework. The appropriateness of all tests for the Air Force population was established.

Study 2. Aptitude Testing. Study 2 was designed to ascertain the variance in intelligent performance, using ASUAB scores as criterion measures, accounted for by componential, metacomponential, and flexibility domains of the aptitude framework.

Results. Data were analyzed to determine the amount of variance in ASVAB accounted for by clusters of aptitudes. Data were analyzed separately by domains and also across domains. With respect to information-processing components, the percentage of time spent forming rules with respect to the relations among stimulus elements was positively related to performance, while the amount of time spent processing the response set in attempt at response solution was negatively related to performance, as was the number of times subjects chose to view the screen containing the response set. With respect to metacomponential skills, metamemory, tacitly acquired occupational knowledge and other practical intellectual skills all contribute significantly to ASVAB performance. Data indicate that  $R^2$ s are in the .45-.62 range for models based on individual domains, and  $R^2$ s for models based on sets of domains are in the .60-.85 range. Regarding flexibility, data on the number of strategies generated by subjects when more than one strategy is appropriate for a given test item are being analyzed. Preliminary analyses of data indicate that Air Force recruits differ considerably in this aspect of flexible information processing. We expect that this aptitude will play an important role in ASVAB performance.

#### V. RECOMMENDATIONS:

The summer research period has provided time for test construction, data collection and analysis for one study and data collection for a second study. Given the extremely large amount of data collected and the need to continue this data collection in additional studies using technical training and performance criteria that are just becoming available, it is necessary to follow up the SFRP effort with a continued



research initiative. The collaborative research activities described in this section center on elucidation of the role of eight domains of aptitudes in intelligent performance among Air Force recruits and determination of the robustness of the eight-domain framework. The work is divided into two phases. Phase 1 centers on analysis and evaluation of data collected on 900 Air Force recruits on the framework (Study 2 of the SFRP period). These data were collected during the last 2 weeks of the Summer Faculty Research Program period. Phase 2 involves collection of data on an additional 900 examinees to ascertain the robustness of the framework by evaluating the variance accounted by the battery on two new criterion measures, in addition to ASVAB. Total testing time for the entire battery is 3 hours.

Phase 1 Objectives:

Phase 1 centers on analysis and interpretation of data from Study 2, collected during the latter part of the SFRP period. The aptitude dimensions measured in this collaborative research tap newly conceptualized cognitive dimensions from work conducted largely in my laboratory. These tests needed to be adapted both to the subject population and the testing system on which the Air Force data were to be collected. Several weeks were required to complete this large-scale effort. As a result, data from Study 2 were not available until after the completion of the SFRP period. These data must be analyzed and interpreted during the initial portion of the RIP period. Phase 1 is expected to be completed during the first two months of the RIP project period.

### Phase 2 Objectives:

Phase 2 centers on ascertaining the predictive power of our eight-domain framework, and incremental validity of tests in the battery relative to domains tapped in the LAMP battery alone. Moreover, the use of new practical and important criterion measures, in addition to ASVAB, will provide data with respect to the robustness of the aptitude framework. Two studies will be conducted.

Study 1. Data from 900 examinees will be collected on the eight-domain aptitude battery. In Study 1, end-of-training scores will be collected at the completion of basic training. These scores will serve as criterion data and will be used in prediction models with ASVAB scores. The importance of using criterion measures that tap actual technical training is addressed.

Study 2. Study 2 is an optional, but desired, part of the collaborative aptitude testing work being done with members of the LAMP group. For Study 2, the eight-domain battery will be administered to a set of examinees. For these experimental subjects, criterion data will be derived from examinees' performance on computer-based tutors, developed by LAMP scientists. I will work with LAMP scientists once Study 1 is underway to determine the availability of experimental subjects to take the eight-domain battery of tests and also complete the tutor-based learning activities.

### Expected Results

All eight aptitude domains have been shown to contribute significantly to prediction of intelligent academic, technical, and occupational performance. This collaborative effort constitutes the first attempt to complete a large-scale effort aimed at elucidating the

role of a comprehensive set of information-processing componential and metacomponential activities on intelligent performance measured by actual learning and performance criteria.

The findings of this collaborative work are expected to corroborate and extend work completed to date. Specifically, no work has been reported to date that couples memory phenomena with information-processing componential, metacomponential and flexibility processes in predicting intelligent performance in a naturally occurring training/occupational context. Prediction models derived from these dimensions are expected to be significantly more powerful than models based on separate sets of the domains.

In addition, no efforts have been reported to use computerized tutor-based learning dimensions as criterion measures. This step is expected to provide a valid criterion of learning that has appropriate range to permit sound predictions of the power of the aptitude battery derived from the eight-domain framework.

#### Significance

Maximum prediction of the quality of performance among Air Force personnel is essential if we are to make wise use of human and material resources. For such prediction to occur, scientists must contribute a robust model of aptitude and valid means of assessing the results of training. Toward this end, I couple important and robust information-processing componential and metacomponential skills with knowledge and memory processes being investigated by LAMP scientists and make use of the newest advances in criterion measurement.

## References

- Anderson, J. R. (1987). Skill acquisition: Compilation of weak-method problem solutions. Psychological Review, 94, 192-210.
- Baddeley, A. D., & Hitch, G. (1974). Working memory. In G. B. Bower (Ed.), Advances in learning and motivation (Vol. 8). New York: Academic Press.
- Christal, R. E. (1987). A factor-analytic study of tests of working memory. Unpublished manuscript.
- Cooper, L. A. (1980). Spatial information processing: Strategies for research. In R. Snow, P-A. Federico, & W. E. Montague (Eds.), Aptitude, learning, and instruction: Cognitive process analyses. Hillsdale, NJ: Erlbaum.
- Cooper, L. A. (1982). Strategies for visual comparison and representation: Individual differences. In R. J. Sternberg (Ed.), Advances in the psychology of human intelligence. Hillsdale, NJ: Erlbaum.
- Cooper, L. A., & Mumaw, R. J. (1985). Spatial aptitude. In R. F. Dillon (Ed.), Individual differences in cognition (Vol. 2). New York: Academic Press.
- Dillon, R. F. (1982). Individual differences in eye fixations within and between stages of inductive reasoning. (Tech. Rep. No. 82-2). Carbondale, IL: Southern Illinois University.
- Dillon, R. F. (1985-a). Predicting academic achievement with models based on eye movement. Journal of Psychoeducational Assessment, 3, 157-165.
- Dillon, R. F. (1985-b). Tests of three new aptitudes: Information-processing proficiency and preference, metamemory, and

- practical problem solving. (Tech. Rep. 85-1) Carbondale, IL: Southern Illinois University.
- Dillon, R. F. (1986). Information processing and testing. Educational Psychologist, 20(3), 1-27.
- Dillon, R. F. (1987-a). An information-processing framework for understanding intelligent performance. Manuscript submitted for publication.
- Dillon, R. F. (1987-b). Metacomponents of intelligence. Manuscript submitted for publication.
- Dillon, R. F. (1987-c). The future of aptitude testing. Invited colloquium at the Air Force Human Resources Laboratory, San Antonio, July.
- Dillon, R. F. (1987-d). The multidimensional nature of cognitive flexibility. Manuscript submitted for publication.
- Dillon, R. F. (in press-a). New approaches to aptitude measurement. In R. F. Dillon & J. W. Pellegrino (Eds.), Testing: Theoretical and applied perspectives. New York: Praeger.
- Dillon, R. F. (in press-b). Information processing and intelligent performance. In R. J. Sternberg (Ed.), Advances in the psychology of human intelligence (Vol. 5). Hillsdale, NJ: Erlbaum.
- Dillon, R. F., Lyerla, R., & Aubertin, C. A. (1987). Flexibility: Its contribution to intelligent academic performance. Paper presented at the Ninety-seventh Annual Convention of the American Psychological Association, New York, August.
- Dillon, R. F., & Reznick, R. K. (1986). Development of a new system of measurement. In Proceedings of the 1986 Meeting of the Military Testing Association. Mystic, CN: Military Testing Association.

- Dillon, R. F., & Stevenson-Hicks, R. (1981). Effects of item difficulty and method of test administration on eye scan patterns during analogical reasoning. (Tech. Rep. No. 1). Carbondale, IL: Southern Illinois University, Eye Movement Research Laboratory.
- Dillon, R. F., Travis, T. A., & Loschen, E. (1987). Flexibility as a measure of intelligence among psychiatry clerks. Unpublished manuscript.
- Dillon, R. F., & Wisher, R. A. (1981). The use of scanning indices to predict performance on technical school qualifying tests. Applied Psychological Measurement, 5(1), 43-49.
- Gitomer, D. H. (1984). A cognitive analysis of a complex troubleshooting task. Unpublished doctoral dissertation. University of Pittsburgh.
- Jencks, C. (1977). Who gets ahead? New York: Basic Books.
- Lesgold, A. M., Feltovich, P. J., Glaser, R., & Wang, Y. (1981, September). The acquisition of perceptual diagnostic skill in radiology (Tech. Rep. No. PDS-1). Learning Research and Development Center, University of Pittsburgh.
- Lohman, D., & Kyllonen, P. (1985). Individual differences in solution strategy on spatial tasks. In R. F. Dillon & R. R. Schmeck (Eds.), Individual differences in cognition (Vol. 2). New York: Academic Press.
- Matarazzo, J. D. (1972). Wechsler's measurement and appraisal of adult intelligence (5th ed.). Baltimore: Williams & Wilkins.
- McCall, R. B. (1977, July 29). Childhood IQ's as predictors of adult educational and occupational status. Science, 197, 482-483.

- Schneider, W., & Fisk, A. D. (1986). Attention theory and mechanisms for skilled performance. In R. A. Magill (Ed.), Memory and control of motor behavior. Amsterdam: North Holland.
- Scribner, A. (1984). Cognitive studies of work. The Quarterly Newsletter of the Laboratory of Comparative Human Cognition, 6(1, 2).
- Sternberg, R. J., & Wagner, R. K. (1986). Practical intelligence: Origins of competence in the everyday world. Cambridge: Cambridge University Press.
- Wechsler, D. (1975, January). Intelligence defined and undefined: a relativistic appraisal. American Psychologist, 30(2), 135-139.

1987 USAF-UES SUMMER FACULTY RESEARCH PROGRAM/

SPONSORED BY THE  
AIR FORCE OFFICE OF SCIENTIFIC RESEARCH  
CONDUCTED BY THE  
UNIVERSAL ENERGY SYSTEMS, INC.

FINAL REPORT

MICROSTRUCTURAL DEVELOPMENTS IN TITANIUM ALUMINIDES:

A STUDY OF DYNAMIC MATERIAL MODELING BEHAVIOR

Prepared By:	Ravinder M. Diwan, Ph.D.
Academic Rank:	Professor
Department and	Mechanical Engineering Department
University :	Southern University
Research Location:	AFWAL/MLLM, Materials Laboratory Wright-Patterson AFB, OH
USAF Researcher:	Dr. Harold L. Gegel
Date:	August 7, 1987
Contract No:	F49620-85-C-0013



MICROSTRUCTURAL DEVELOPMENTS IN TITANIUM ALUMINIDES:

A STUDY OF DYNAMIC MATERIAL MODELING BEHAVIOR

BY

RAVINDER M. DIWAN

ABSTRACT

The material behavior of the TiAl system, PREP-HIP Ti-48Al-1V, has been investigated by dynamic material modeling using the flow stress data from constant strain rate hot compression tests for strain rates ranging from  $10^{-4}$  to  $10^{-1} \text{ s}^{-1}$  and temperatures from  $1000^{\circ}\text{C}$ - $1250^{\circ}\text{C}$ . Phases were identified which are related to the transformation temperatures of the alloy in phase equilibria; also, stability and instability regimes in the processing or stability maps were identified. The results indicate the presence of twins in the  $\gamma$ -phase, very small amounts of dispersed  $\alpha_2$ -phase, significant amounts of cross slip and shear bands with possible texture effects, and, at certain strain rates and temperatures, formation of subgrains was observed.

The TiAl system is characterized by the presence of strong directional bonding of the  $\gamma$ -intermetallic phase and its related strengthening effects. The structural morphology and quantitative parameters need to be further investigated at higher temperatures above  $1250^{\circ}\text{C}$  to analyze completely the constitutive and mechanical behavior of this system. Mechanical instabilities in certain regions are seen to be more dominant than metallurgical instabilities because of the strong thermodynamic stability of  $\gamma$ -TiAl.

### ACKNOWLEDGEMENTS

The author would like to acknowledge the support of the Air Force Systems Command, the Air Force Office of Scientific Research, and Universal Energy Systems, Inc., which made possible this research, conducted at the Air Force Wright Aeronautical Laboratory, Wright-Patterson AFB, OH.

The author also wishes to acknowledge Dr. H. L. Gegel, Processing Science, Processing and High Temperature Materials Branch, Materials Laboratory for his invaluable support and scientific discussions to apply metallurgical synthesis to dynamic material modeling. The author is also grateful to members of the Processing and High Temperature Materials Branch, Ms. K. A. Lark, Mr. J. C. Malas, Mr. L. M. Matson, Mr. J. T. Morgan, and Mr. W. T. O'Hara for their scientific discussions and technical contributions. Dr. Gegel is the WUD - 49 (Work Unit Directive #49), In-House Research Group Leader. Mr. W. T. O'Hara is the Research Focal Point and the Program Administrator.

The author also wishes to acknowledge Mr. Rodney Darrah, Summer Faculty Research Program Manager, UES, Inc. for his support and operation of the Summer Faculty Research Program. The support and the input of the technical staff of UES, Inc. and of the facilities at the Materials Laboratory is greatly appreciated. The author is also grateful to Drs. S. M. Doraivelu and M. G. Mendiratta, UES, Inc., and R. Srinivasan, Wright State University for their contributions and stimulating discussions. Thanks are expressed to Ms. D. Goodman for carrying out X-ray diffraction work and to Mr. J. Henry for his assistance in SEM and electron microprobe work. Thanks are also expressed to Mrs. H. L. Henrich for typing and editorial assistance in preparation of this report.

## I. INTRODUCTION:

The TiAl systems are important materials of interest to the Air Force for high temperature applications. An approach<sup>1-3</sup> of dynamic material modeling (DMM) is a significant tool that can help in defining "processing windows" for safe processing of this material and its application.

The Processing Science Group of the Metals and Ceramics Division of Wright-Patterson Air Force Base Materials Laboratory is particularly concerned about the analytical modeling of deformation processes and material flow to aid in the understanding of structural evolution and their arrangements in a fabricated product. The DMM analysis of titanium aluminides is in initial stages and metallurgical understanding of the system is still being developed. Special attention is required to understand the concepts of stability from both a mechanical as well as metallurgical viewpoint. Dynamic material modeling is based upon combining the disciplines of thermodynamics and continuum mechanics to describe the overall material behavior. Once a framework for analysis has been established by DMM, a detailed study of microstructural developments is of great value in properly understanding the behavior of these materials during hot deformation.

This research was carried out to analyze the microstructural dynamics related to deformation processing. This work is based upon the use of established concepts of quantitative stereology and microstructural analysis which is applicable to the study of microstructure evolution during deformation processing and to the analysis of structure-property relations which result as a consequence of the thermomechanical history that the finished component has experienced.

## II. OBJECTIVES OF THE RESEARCH EFFORT:

Development of microstructures and the constitutive behavior of a workpiece material depends on the effects of stress, temperature, strain levels and strain rates during processing. Engineering alloys are complex, dynamic materials systems which present a challenge for structural analysis and scientific interpretation of observations made about the processing behavior of the workpiece after being subjected to an arbitrary thermomechanical history. Assessment of these characteristics has been accomplished earlier in some aluminum based 2024-SiC alloys,<sup>4</sup> nickel based alloys,<sup>5</sup> and titanium based Ti6Al4V<sup>6</sup> and Ti-based 6242 alloys.<sup>7,8</sup> The Ti-Al based alloys of the  $\gamma$ -composition aluminides or the  $\alpha_2$ -phase composition aluminides have not been assessed thoroughly using the dynamic material modeling analysis approach. Thus, the dynamic study of material modeling methodology will be used to investigate microstructural evolution and the intrinsic workability of Ti-48Al-1V  $\gamma$ -aluminide to determine the conditions for stable material flow. This information will be presented as a stability map to support analytical process modeling and the selection of optimum processing conditions.

This research has the overall objective to determine the role of microstructure in the constitutive modeling of plastic flow of selected titanium-based aluminide composition. The study of these systems is made difficult due to incomplete information in phase stabilities, phase boundaries in Ti-Al systems, effects of alloying elements, grain sizes, and conditions of the base ingot metallurgy I/M or the powder metallurgy P/M. These parameters should be evaluated as the final

formability of the material depends strongly on the initial state which is determined by the processing history.

Using a software tool known as the MIS system, various stability plots for PREP-HIP Ti-48Al-1V material at 0.4 and 0.5 strain levels were generated. These were used to select certain specimens for microstructural analysis in addition to the detailed characterization of the as-received HIP'd material. These studies were carried out to determine if a "limit" strain concept might govern the amount of deformation which is permissible during each stage of processing.

Research in this project also included phase identification and characterization by X-ray diffraction, scanning electron microscopy and electron microprobe analysis. Microstructural evaluation and DMM analysis were conducted with the aim of understanding the intrinsic workability and microstructural evolution during hot deformation. In addition, and to recommend further directions to continue this work; an attempt is being made to devise conditions of stable constitutive flow to shorten the cycle time of alloy development, on the assumption that materials science and processing science should be conducted in parallel in order to develop an alloy system which can be economically and reliably fabricated into an aerospace component.

### III. APPROACH AND EXPERIMENTAL PROCEDURES

#### (A) Equilibrium Thermodynamics and Phase Analysis

The limitation of unconfirmed information of phase boundaries and phase stabilities of the titanium-aluminum

system and effects of material processing at elevated temperatures has to be recognized in a total dynamic material modeling of this system. This recognition first of all requires that all phases be identified for qualitative thermodynamical and mechanical behavior and their morphological characteristics to understand the overall behavior of the workpiece material as it deforms.

J. L. Murray<sup>9</sup> of the National Bureau of Standards has made a recent account and equilibrium diagram of the titanium- aluminum system. For Ti-48Al-1V (considering binary composition of 48 at.% Al), the as received alloy was subjected to X-ray diffraction analysis using the diffraction pattern of this PREP-HIP as-received material. This pattern was indexed to analyze for the presence of  $\alpha_2$  and  $\gamma$ -phases. The relative strength of  $\alpha_2$  peak is weak, so, for further confirmation, some additional work was done using the microprobe characterization. This data will be reported later.

The as received PREP-HIP Ti-48Al-1V material (2240°F/15 ksi/4 hr.) was subjected to isothermal constant strain-rate compression testing which was performed over a range of temperatures from 1000°C-1250°C and a range of strain-rates from  $10^{-4}$ - $10^{-1}$  s<sup>-1</sup> for each temperature. The test specimens were air cooled and utilized for microstructural analyses, and the flow stress data were used to develop the contour plots needed for dynamic material modeling using the MIS computer programs.

(B) Dynamic Material Modeling

In dual or multiphase systems, several atomic processes are possible and combine to create new structures and provide the degrees of freedom needed for stable plastic flow. Stability is determined by the condition that the excess entropy production rate,  $1/2 \dot{\sigma}^2$ , is greater than zero. Simple compression testing can be used for dynamic material modeling as long as "steady" state can be approached asymptotically with time.

The present study had utilized test specimens which were 0.25" in diameter x 0.375" in height; the compression specimens were coated with glass for lubrication and strain-rate tested at constant strain-rate to study the flow behavior and microstructural evolution.

The flow curves show an approaching steady state or some flow softening. The typical slight barrelling in several specimens is seen on microscopic examination to indicate microstructurally observed cracking at end regions. The investigations are not complete, and more detailed analysis and compression testing of this material is required to characterize the overall microstructural evolution and to evaluate the constitutive phenomena and model the microstructural behavior.

The DMM stability maps were generated using MIS program and some analysis was also done using a modified system developed by UES called MME (Material Modeling Environment)

departures and perturbations in composition to achieve appropriate alloy and processing development.

(D) Microstructural Analyses

The "as-received" and "processed" specimens after the compression testing are cut longitudinally in mid plane and these sections are used to prepare metallographic specimens for microstructural analyses by optical and scanning electron microscopy. The specimens were polished and etched using standard metallographic procedures. The 98-2 + H<sub>2</sub>O<sub>2</sub> molybdenum acid composition etch was found to give better contrast of the  $\alpha_2$ -phase and when used with the differential interference contrast DIC technique and polarized light. The microstructural analyses were also conducted to confirm the presence of the phases using scanning electron microscope SEM and electron microprobe analysis.

Some optical micrographs indicated regions of interlamellar  $\alpha_2 + \gamma$  structures, however, in these regions  $\alpha_2$  could not be firmly identified due to the small activation volumes of the  $\alpha_2$  phase. Some results obtained earlier<sup>11</sup> using TEM were also assessed in interpretations of the microstructural analysis of these materials.



to generate the appropriate surfaces. The contour plots for 0.4 and 0.5 strain levels were investigated by using metallographic methods to detect microstructural changes, which might explain the cause of an indicated mechanical instability and to arrive at certain suitable test specimen conditions that require microstructural analyses.

(C) Operative Mechanisms and Their Analysis

Each material has its specific deformation and recovery processes. The stability maps which characterize the intrinsic workability of an alloy system would depend on how the various atomic processes combine several processing features to control the efficiency of material flow. The "as-received" and "processing" microstructures during material flow need to be characterized to understand microstructural evolution during stable material flow.

The initial microstructures were recognized to be  $\alpha_2$ -Ti<sub>3</sub>Al, an ordered hexagonal structure of the type DO<sub>19</sub> and  $\gamma$ -TiAl, an ordered fcc structure of the type L1<sub>0</sub>. These phases that were observed for the Ti-48Al-1V composition range alloys are to be understood as having strong directional bondings and of limited range in their compositions. Additions of transition elements, T-metals, produce different strengthening effects compared to non-transition elements, B-metals.<sup>10</sup> Interaction of strengthening effects of certain "control system" compositions should be analyzed along with

#### IV. EXPERIMENTAL OBSERVATIONS AND RESULTS:

Metallographic examination of the as-received PREP-HIP Ti-48Al-1V material indicated a large variability in the grain size of the  $\gamma$ -grains which could be due to the variability and distribution in the preconsolidated PREP-alloy powder size. The hcp  $\gamma$ -TiAl phase shows nearly equiaxed grains with the presence of twins and some porosity. The volume percent of the second phase is very small and in some cases is indistinguishable.

The as received PREP-HIP Ti-48Al-1V specimens were further examined for the  $\alpha_2$ -phase using different chemical etchants, and the SEM and EDAX techniques. The effects of thermomechanical treatments and possible interlamellar localized regions were seen in some of the SEM micrographs. These observations were investigated further to identify the chemical analysis of different regions in the matrix phase, possible platelets, and light and dark regions using the EDAX technique. However, the bright white second phase particles were very small in amount, and no differences were observed in the EDAX pattern results.

The appearance of the bright white phase and the possibility of interlamellar structure was further examined using different chemical etchants. The 98-2 + H<sub>2</sub>O<sub>2</sub> molybdic acid etch provided a better contrast for the second phase. This phase is sparingly seen as thin platelets along some of the grain boundaries of the predominant  $\gamma$ -phase. Stress effects, and the presence of twins was also clearly seen. Some of the fine, second phase particles are also seen dispersed in the structure, and the possibility of the interlamellar  $\alpha_2$  +  $\gamma$  phases also exists.

X-ray diffraction provided some evidence of the second phase as the  $\alpha_2$ -phase  $\text{Ti}_3\text{Al}$ . The X-ray diffraction pattern of the as-received material was indexed for the  $\alpha_2$  and  $\gamma$  phases. Several clear peaks of the  $\gamma$ -TiAl phase were seen and a shallow peak corresponding to the  $\alpha_2$ - $\text{Ti}_3\text{Al}$  phase was also observed. To confirm the presence of the  $\alpha_2$ -phase, results of the thin foil transmission electron microscopy<sup>11</sup> were assessed. These results revealed a microstructure consisting of mostly single phase  $\gamma$  equiaxed grains. A number of widely separated  $\gamma$  grains were also observed which contained thin  $\alpha_2$  lamella. Some  $\gamma$  grains also consisted of a high density of dislocations, twins, and stacking faults. Since most of the contiguous  $\gamma$  grains did not contain the  $\alpha_2$ -phase, it is believed that the high temperature flow processes will be essentially governed by a large volume of  $\gamma$  grains.

The electron microprobe results of the PREP-HIP as-received material and several constant strain-rate tested specimens were found to show the composition of the bright white phase to be approximately Al  $\approx$  36 at.%, Ti  $\approx$  60 at.%, and V  $\approx$  4 at.%. This is seen to be corresponding to the composition of the  $\alpha_2$ - $\text{Ti}_3\text{Al}$ ; an ordered phase as shown in the Ti-Al phase diagram, with a composition of Ti with Al  $\approx$  35 at.% composition. The matrix composition of the  $\gamma$ -phase was found to be Al  $\approx$  48 at.%, Ti  $\approx$  49 at.%, and V  $\approx$  3 at.%. This is found to agree with the composition of the  $\gamma$ -TiAl; as shown in the Ti-Al phase diagram, with a composition of Ti with Al  $\approx$  49 at.%.

As indicated earlier, the  $\alpha_2$  and  $\gamma$  intermetallic phases found in the Ti-48Al-1V alloy are characterized by the presence of strong directional bonding which would primarily affect the ductility and hot workability of this alloy. Microhardness tests on the as-received and

some of the compression tested specimens were observed to give lower hardness values of the  $\alpha_2$ -phase compared to those of the  $\gamma$ -phase. However, enough readings could not be taken for the  $\alpha_2$ -phase in various specimens due to very small amounts of the  $\alpha_2$ -phase, and difficulty in getting good phase contrast in the microstructures for hardness testing.

Several of the contour plots generated using the MIS code for the Ti-48Al-1V at the 0.4 and 0.5 strain level showed that many specimens had remained either in the stability or in the instability regions at both strain levels. However, some specimens experienced a transition as these were deformed and had gone from the stable regions to the unstable regions. This indicates that some "critical" strain level should be maintained and should not be exceeded for certain temperature and strain rate conditions to ensure safe processing. More testing and verification needs to be done in this direction.

Detailed optical and scanning electron micrographic examinations were conducted of several compression tested specimens. These were analyzed, using the results of stability maps and contour plots, in relation to the phase equilibria information to see the effects of kinematic variables, temperature, and strain-rate on the microstructural evolutions. The Ti-Al phase diagram shows a phase transformation at  $\approx 1125^\circ\text{C}$ , so it is possible that at or above  $1125^\circ\text{C}$  different behaviors might be observed. Conditions are considered as low temperature when  $T \leq 1125^\circ\text{C}$ , and as high temperature when  $T \geq 1150^\circ\text{C}$ ; strain rates are considered as low strain rates when  $\dot{\epsilon} \leq 10^{-3}\text{s}^{-1}$ , and as high strain rates when  $\dot{\epsilon} \geq 10^{-2.8}\text{s}^{-1}$ .

Under the high strain rate conditions ( $\dot{\epsilon} \geq 10^{-2.8} \text{ s}^{-1}$ ), and at or below  $\approx 1125^\circ\text{C}$  transformation temperature, the structures are seen to be generally exhibiting the presence of microscopic cracks at one edge, some barrelling, the presence of porosity and very similar banded grain structure, due to the deformations of the  $\alpha_2$ - and  $\gamma$ -phases, as verified by the optical and scanning electron micrographic analysis. These conditions have contributed to power dissipation mainly through stored energy as atomic defects. Some specimens in the tensile regions at the barrelling portions have shown the presence of microscopic cracks. Microstructures under these conditions would have significant dislocation interactions and hardening of the matrix phase.

Now, considering conditions of low temperatures at or below  $\approx 1125^\circ\text{C}$ , but under the low strain rate conditions, ( $\dot{\epsilon} \leq 10^{-3} \text{ s}^{-1}$ ), the typical microstructure of a specimen was examined for  $1100^\circ\text{C}$ ,  $10^{-4} \text{ s}^{-1}$ . More analysis needs to be done in this particular set of low temperatures, low strain rate region.

At the lower strain rates ( $\dot{\epsilon} \leq 10^{-3} \text{ s}^{-1}$ ), and the higher temperature conditions ( $T \geq 1150^\circ\text{C}$ ), there is a possibility of the ordered  $\alpha_2$ -phase to transform to the softer  $\alpha$ -phase. The power dissipation, under these conditions, can be through the energy dispersive processes that involve diffusional flows, transformation and recovery mechanisms. Processes involving dynamic recovery and polygonization are clearly seen.

Further examination of the several specimens at higher temperatures ( $T \geq 1150^\circ\text{C}$ ), and higher strain rate conditions ( $\dot{\epsilon} > 10^{-3} \text{ s}^{-1}$ ), revealed some subgrain formation that is indicative of the possibility of dynamic recovery. Slip bands in the matrix are also observed along with the clear presence of subgrain formations.

The overall study of microstructural developments of the Ti-48Al-1V in the selected range of test conditions indicates metallurgical stability, though mechanical instabilities are seen as porosity, and crack propagation are observed in some specimens. Dynamic microstructural synthesis is attempted in the PREP-HIP Ti-48Al-1V system and it is seen that typical low temperature, high strain-rate hardening processes predominate. The hard matrix of the  $\gamma$ -phase containing very small amounts of the dispersed  $\alpha_2$ -phase, as confirmed for several test specimens examined, have not shown any enhanced dynamic recrystallization, though some partial recrystallization might have occurred in some specimens. Microscopic cracking, is seen in many of the low temperature ( $T \leq 1150^\circ\text{C}$ ), high strain rate ( $\dot{\epsilon} \geq 10^{-2}\text{S}^{-1}$ ) conditions in the barrelled, tensile end regions of the specimens.

The dynamic material modeling approach used in this research, detailed in several other references, has pointed out the conditions of stability of the PREP-HIP Ti-48Al-1V in processing flow, and has also clearly shown a region of mechanical instability around  $\approx 1150^\circ\text{C}$ . Furthermore, a transition in the stability, instability regions is seen close to  $\approx 1125^\circ\text{C}$ . The processing-stability maps also indicated development of stability regions close to  $\approx 1250^\circ\text{C}$ . Earlier works of Ashby and Frost,<sup>12</sup> and Raj,<sup>13</sup> in developing the models of power dissipation, are significant in the understanding of several atomic and structural mechanisms in simple engineering alloys. However, the complex nature and the unique characteristics of the intermetallic phases present in this alloy make this system very distinct. Power partitioning has been shown in this Ti-48Al-1V  $\alpha_2 + \gamma$  alloy system to

be due to the dynamic recovery and polygonization processes related to the subgrain formations. This system has not shown any grain boundary sliding or superplasticity behavior mechanisms.

From some related work carried out by M. G. Mendiratta<sup>11</sup> of Universal Energy Systems, Inc., and work carried out in-house by K. A. Lark,<sup>14</sup> it is observed that the microstructures in the cast-HIP Ti-48Al-1V system show enormous variability in the grain structures. The presence of the  $\alpha_2$ -phase dispersed in small amounts in the  $\gamma$  matrix has been confirmed in this work by metallography, SEM, and electron microprobe analysis and has also been established in the TEM work of Mendiratta.<sup>11</sup> But as the  $\alpha_2$ -phase in this Ti-48Al-1V system is found in very small amounts, the hot deformation processes are seen to be affected mainly by the behavior of the  $\gamma$ -TiAl phase

In another related work by R. Srinivasan,<sup>15</sup> on compression testing of isoforged Ti-48Al-1V at temperatures from 1150°C-1350°C and at strain rates from  $10^{-3}$  to  $10^0 \text{ s}^{-1}$ , it was observed that all of the compression tested specimens at and below 1300°C had become elliptical in shape, but this anisotropy had nearly disappeared for specimens tested at 1350°C. No metallographic analysis of the structures has been carried out for this system. It is possible that the combined effects of temperature and strain rates on the Poisson's ratio, initial structure and texture relationships of the material would have caused this behavior. It should also be noted from the present work that the PREP-HIP Ti-48Al-1V, using the DMM analysis has indicated the onset of a stability region at  $\approx 1250^\circ\text{C}$ .

This strongly suggests that the PREP-HIP Ti-48Al-1V work should be continued to investigate the microstructure behavior at, and above,

1250°C to include the peritectoid reaction at  $\approx 1285^\circ\text{C}$ .

#### V. RECOMMENDATIONS:

1. The present microstructural and DMM analyses have shown a transition in the stability behavior of the system at  $\approx 1125^\circ\text{C}$ . Further studies are needed to analyze more completely the dynamic material modeling and to suitably select the most favorable processing conditions for this alloy.

2. The present study has also shown the onset of stability regions at  $\approx 1250^\circ\text{C}$ . In order to fully analyze and enhance the power dissipation through metallurgical processes, the PREP-HIP Ti-48Al-1V alloy should be further investigated to include the temperature of  $1250^\circ\text{C}$  and in the range of  $1250^\circ\text{C}$ - $1400^\circ\text{C}$ . This is recommended and is of special interest, noting that at  $\approx 1285^\circ\text{C}$  and above, the peritectoid reaction in the Ti-Al system could result into the transformed  $\beta$ -phase.

3. A study should be carried out of the phase behavior and the transformation at  $\approx 1285^\circ\text{C}$  using differential thermal analysis DTA and differential scanning calorimetry. This would be of fundamental importance in understanding the microstructural evolution and development of any  $\beta$ -phase. These and other related studies should be conducted to develop the material data base for the application and processing of the titanium aluminide alloy systems.

4. It is noted that the PREP-HIP Ti-48Al-1V shows a large variability in the microstructural grain size of the  $\gamma$ -phase matrix grains, with very small dispersions of the  $\alpha_2$ -phase. Due to this statistically complex nature of this system, more detailed quantitative analyses of this Ti-48Al-1V system are required.



5. A study of the microstructure-related mechanisms in deformation processing and DMM analysis to evaluate the stability processes should be carried out to relate the effect of variations in the characteristics and distribution of the preconsolidated alloy powder sizes.

6. This study has shown a transition in material flow conditions, such as in going from stability regions in processing-stability maps at the 0.4 strain level to instability regions at the 0.5 strain level. This suggests a "critical" strain level at which deformation processing should be stopped. This concept should be studied with more comprehensive and detailed analysis of this system.

7. The present study showed the presence of the  $\alpha_2$ -phase in very small amounts. It is of fundamental interest and is strongly recommended, that the effect of the  $\alpha_2$ -phase be analyzed in the dual  $\alpha_2 + \gamma$  phase titanium aluminides. This could be achieved by selecting the various base compositions of the alloy such that a range in the volume fractions of the second  $\alpha_2$ -phase could be precipitated in the system which might enhance the stable material flow by microstructure related dynamic metallurgical processes during deformation processing.

8. The evaluation of the several power partitioning processes in the titanium aluminide system, using some "control system" alloy chemistries, should be carried out with variations in a certain range of the volume fractions of the dispersed second phases, that are (a) softer or (b) harder than the matrix phase. Such a study of the detailed microstructural effects would be very useful in the clearer understanding of deformation processing of these materials and in the application of dynamic material modeling for the control and selection of more efficient processing conditions.

## REFERENCES

1. H. L. Gegel, J. C. Malas, S. M. Doraivelu, J. M. Alexander, J. S. Gunasekera, "Material Modeling and Intrinsic Workability for Simulation of Bulk Deformation," To be published, FGU 2nd International Conference for Applied Plasticity, University of Stuttgart, Germany, August 24-28, 1987.
2. H. L. Gegel, "Synthesis of Atomistics and Continuum Modeling to Describe Microstructure," Presented, and to be published -- ASM's Materials Science Seminar - Computer Simulation in Materials Science, Orlando, Florida, October 4-5, 1986.
3. H. L. Gegel, "Material Behavior Modeling - An Overview," American Society for Metals, Metals Park, in Conference Proceedings Experimental Verification of Process Models, Ed. by C. C. Chen, ASM 1983, pp. 3-32.
4. V. Y. R. K. Prasad, H. L. Gegel, J. C. Malas, J. T. Morgan, K. A. Lark, S. M. Doraivelu, and D. R. Barker, "Constitute Behavior and Dynamic Modeling of Hot Deformation of a P/M 2024 Al Alloy with 20 Vol.% SiC Dispersion," AFWAL/MLLM, Materials Laboratory, Wright-Patterson AFB, Ohio, Internal Report: Final Report for the period May 1983-December 1983, AFWAL-TR-84-4076, November 1984.
5. General Electric IR&D - Research conducted by General Electric Company on nickel based alloys.
6. S. M. L. Sastry, R. J. Lederich, T. H. Mackay, and W. R. Kerr, "Superplastic Forming Characterization of Titanium Alloys," Journal of Metals 35, 48-53 (1983).
7. P. Dadras and J. F. Thomas, Jr., "Characterization and Modeling for Forging Deformation of Ti-6Al-2Sn-4Zr-2Mo-0.1Si," Met. Trans. A, 12, 1867-1876 (November 1981).

8. Y. V. R. K. Prasad, H. L. Gegel, S. M. Doraivelu, J. C. Malas, J. T. Morgan, K. A. Lark, and D. R. Barker, "Modeling of Dynamic Material Behavior in Hot Deformation: Forging of Ti-6242," Met. Trans. A, 15, 1883-1892 (October 1984).
9. J. L. Murray, "The AlTi (Aluminum Titanium) System," 26.98154 Equilibrium Diagrams, published by the National Bureau of Standards.
10. E. W. Collings and H. L. Gegel, Eds., "Physical Principles of Solid Solution Strengthening in Alloys," Proc. ASM-TMS (AIME) Symposium, Plenum Press, New York, 1975, pp. 147-182.
11. M. G. Mendiratta, Private Communication - transmission electron microscopy of the PREP-HIP Ti-48Al-1V.
12. H. J. Frost and M. F. Ashby, "Deformation-Mechanism Maps" - The Plasticity and Creep of Metals and Ceramics, Pergamon Press 1982.
13. R. Raj, "Development of a Processing Map for Use in Warm-Forming and Hot-Forming Processes," Met. Trans. A, 12, 1089-1097 (June 1981).
14. K. A. Lark, In-house Research, Private Communication.
15. R. Srinivasan, Private Communication, Compression Test Behavior of Isoforged Ti-48Al-1V.

1987 USAF-UES SUMMER FACULTY RESEARCH PROGRAM/  
GRADUATE STUDENT SUMMER SUPPORT PROGRAM

Sponsored by the  
AIR FORCE OFFICE OF SCIENTIFIC RESEARCH  
Conducted by the Universal Energy Systems, Inc.

FINAL REPORT

ADA AND ARTIFICIAL INTELLIGENCE APPLICATIONS  
FOR ELECTRONIC WARFARE

Prepared by:	Verlynda S. Dobbs
Academic Rank:	Assistant Professor
Department and	Computer Science and Engineering
University:	Wright State University
Research Location:	WPAFB, Avionics Laboratory, Electronic Warfare, AAWA-1
USAF Researcher:	William McQuay
Date:	September 1, 1987
Contract No:	F49620-85-C-0013

ADA AND ARTIFICIAL INTELLIGENCE APPLICATIONS  
FOR ELECTRONIC WARFARE

by

Verlynda S. Dobbs

ABSTRACT

The appropriateness of Ada for artificial intelligence applications for electronic warfare (EW) was investigated. The investigation included a review of current efforts and the implementation of a prototype system for an EW application. The system, which applied bidirectional heuristic search techniques to the generation of flight paths through a military hostile environment was successfully implemented in Ada. Results provided data for the comparison of two bidirectional heuristic search techniques.

## I. INTRODUCTION

For much of the past decade, the question of the appropriateness of Ada for artificial intelligence (AI) has been debated. [SCH80,REE85,WAL86,BAK87] Discussions of the question have focused on a variety of language features including flexibility, portability, maintainability, efficiency, readability and writeability. No consensus has been reached, although many proponents of Lisp and other nonprocedural languages are convinced that Ada is not suitable for AI. To disprove this theory, researchers are currently experimenting with building packages, generics and program units in Ada to facilitate AI functions. In this manner it may be possible to demonstrate that Ada can provide superior, or at least adequate, facilities for AI.

My research interests are in the application of heuristic search techniques to real world problems and software engineering. The EW Division of the USAF Wright Aeronautical Laboratories at Wright Patterson Air Force Base is interested in encouraging the use of Ada in software for weapon systems and in the use of AI techniques in weapon systems.

## II. OBJECTIVES

There were two main objectives for this effort. The first objective was to prepare a summary of the AI efforts that have been and are currently being implemented in Ada. The second objective was to implement in Ada a prototype of a flight path generator using heuristic information about threat locations.

NO-A191 203

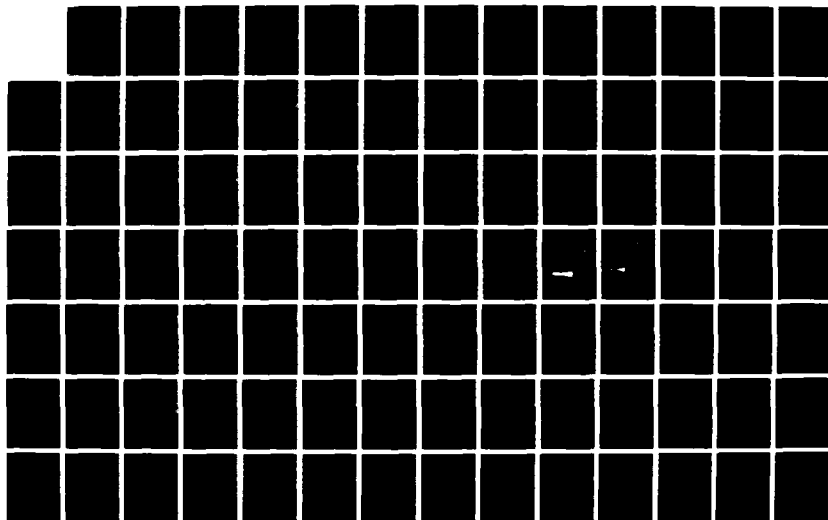
UNITED STATES AIR FORCE SUMMER FACULTY RESEARCH PROGRAM  
(1987) PROGRAM TE. (U) UNIVERSAL ENERGY SYSTEMS INC  
DAYTON OH R C DARRAN ET AL. DEC 87 AFOSR-TR-88-0212  
F49620-85-C-0013

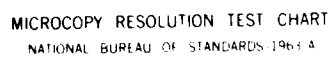
9/11

UNCLASSIFIED

F/G 5/1

ML







Part III reviews background information on Ada and Lisp, discusses current research efforts applying Ada to AI, and analyzes functions needed by EW applications. Part IV reviews search techniques and flight path generators, Part V describes an Ada implementation of an EW function, and Part VI makes recommendations.

### III. BACKGROUND

There are two basic approaches taken by programming languages: the procedural approach and the non-procedural approach. Languages traditionally used for AI research, such as Lisp, take the non-procedural approach, while languages like Ada and Pascal are procedural. Lisp, which was developed in the early 1960s as an interactive development environment, is based on the manipulation of list structures. Programs and data are both represented as list structures. It is, therefore, possible to create functional abstractions on the fly, embed them in other data structures, and pass them as arguments to other abstractions. Data structures and programs evolve as more is learned about the nature of the problem and the approach to its solution. Non-procedural languages score high on flexibility and writeability, but are basically not maintainable, portable, readable or efficient.

Ada was designed for programming real-time embedded computer applications. Ada enforces a programming discipline which encourages good programming practices. Control structures and data structuring tools provide more standard

ways of expressing solutions to problems. The redundant specification in the language provides a high level of consistency checking. These consistency checks increase confidence that the coding of the algorithm is correct. Ada makes it possible to extend the language by providing packages which can be used to encapsulate new data types and the operations defined for them. Ada scores high on maintainability, portability, and readability, and its efficiency continues to increase.

#### Current Efforts

The widespread use of Ada for AI applications is dependent upon the demonstration by the Ada community of its effectiveness. In that spirit, efforts are ongoing in Ada in the areas of expert systems [ADK86,LAV86], distributed knowledge based systems [BRA86,FRA86], pattern directed processing [REE85], and semantic networks [SCH86]. Several of these efforts are discussed in the paragraphs below.

Adkins [ADK86] and LaVallee [LAV86] both report building inference engines in Ada. Adkins was basically not pleased with his results. He implemented the inference engine as a collection of tasks, each task representing one rule. Working code was produced, but only with great difficulty. LaVallee, who reported favorable results, implemented the inference engine as a single task. Rule firing rates, which were in excess of 500 per second on a single MC68000 processor, compared favorably to the reports of Kary and Juell [KAR86] for systems in C and Lisp on a Vax. The C-

based system ran between 50 and 1000 logical inferences per second (LIPS may be less than a complete rule per second), while the Lisp-based system performed at one LIPS or less. LaVallee plans to continue investigating additional parallelism.

A software architecture that facilitates the construction of distributed expert systems using Ada has been described by Brauer [BRA86] and Frank [FRA86]. This architecture, which is being developed for the Space Station, allows monitoring and diagnosis of sensors and built-in test equipment. The basic concept of the architecture is a modular software unit that contains both a data processing component and an AI component. This unit acts as an interface between Ada and a knowledge-based component.

Efforts of Reeker, Kreuter and Wauchope [REE85] have been directed toward adding useful AI programming tools to Ada, specifically tools for pattern-directed string processing. Algorithms for pattern matching are being evaluated, considering, among other things, the basic efficiency of each of the algorithms and the efficiency of its implementation in the Ada environment. The methods for pattern matching are being tried with both character strings and lists. Preliminary results are positive and indicate that providing pattern-directed packages for various data types is not only feasible, but quite worthwhile.

A method of implementing semantic networks in Ada is described by Scheidt, Preston and Armstrong [SCH86].

Although semantic networks appear to be the most promising technique for knowledge representation, their use in real world problems has been limited by their implementation in specialty or AI languages. The effort attempts to rectify this situation by developing a viable and highly robust semantic network in Ada. This effort was highly successful.

Another example of a system implemented in Ada that applies AI techniques to a real world problem is discussed in Parts IV and V of this paper.

#### Electronic Warfare Functions

An ultimately flexible weapon system would be capable of providing many of the functions which are now performed by the crew. These include sensing of the environment; interpretation of conflicting, incomplete, or corrupted sensory data; integration of sensory data; overall situation assessment; planning and real-time decisions for mission and survival achievement; and control of weapon system functions. The system must function in an environment that contains vast amounts of raw data where the data is unintentionally corrupted via natural phenomena or intentionally corrupted via friendly or enemy jamming and deception missions.

EW processing spans many different disciplines (passive radio frequency (RF) and infrared (IR) sensor interpretation, active RF and IR countermeasures techniques, etc.) where the sensors must operate in different environments with different requirements for information extraction, interpretation and

reaction. The EW system must respond to a dense and dynamic environment. Systems implementing functions such as those described above will operate primarily in numeric environments. These EW systems, which need to be maintainable, portable, readable, and efficient, can be effectively implemented in Ada.

#### IV. ELECTRONIC WARFARE APPLICATION

This effort incorporates a new bidirectional heuristic search technique [DAV87] into a flight path generator for a high performance platform through a military hostile environment. The sections of this part review both search techniques and flight path generators.

##### Search Techniques

Most AI solutions to problems contain a search component that is often the critical inner loop of the solution. Therefore, it is imperative that searching be done in as efficient a manner as possible.

Searching has traditionally been performed blindly, either breadth first or depth first. These blind searches continue to generate all successors (expand) nodes in some predetermined order until a goal node is found. An exponential explosion occurs in both the time and the space required to find a solution.

The size of the search tree can be reduced by using more informed search techniques. Heuristics (rules of thumb) can be used to estimate a new node's distance from a goal. The

next node chosen for expansion will then be the node believed to be the closest to a goal. Consequently, time and space will not be wasted on nodes that show very little promise.

To help avoid an exponential explosion, a heuristic function  $h$ , whose two arguments are state space nodes, is provided.  $h$  returns an estimate of the path cost between its arguments and is used by the search algorithm to determine the best node to expand next.

Heuristic search algorithms take one of two basic approaches. Unidirectional search algorithms, which build one search tree of nodes rooted at the start, expand nodes from the start until a goal node is found. Bidirectional search algorithms maintain two search trees of nodes rooted at the start and the goal. The nodes on these trees are those so far generated by the algorithm, and the path from a root to a leaf represents the least cost path the algorithm has yet found connecting root and leaf. The leaves, called open nodes, are candidates for expansion. The algorithm attempts to expand leaves in such a pattern that the two trees "meet" as soon as possible, at which point the problem is solved and a route from start to goal may be reported.

In order to determine which open node  $n$  to expand next, there is an evaluation function of the form

$$f(n) = (1 - w) * g(n) + w * h_o(n), \quad 0 \leq w \leq 1. \quad (1)$$

Here  $g(n)$  is the cost of the search tree path from node  $n$  to its corresponding root,  $h_o$  is the heuristic component of  $f$

(derived in some fashion from the function  $h$  mentioned above), and  $w$  is a weight fixed to some value deemed to be effective. Small values of  $f(n)$  indicate that  $n$  is more likely to be on a low cost solution path than do large values. During each cycle of the search algorithm, an open node with minimal  $f$ -value is selected from the appropriate search tree for expansion. Its successors are generated. If one of the successors is on the opposite search tree, the algorithm halts. Otherwise  $f$  is evaluated for each of the successors and they are appropriately placed on a search tree. The algorithm recycles.

One of the fastest bidirectional search algorithms reported in the literature is DNODE, due to Politowski and Pohl [POL84]. In this algorithm  $h_o(n)$  in equation (1) is set to  $h(n,d)$ , where  $d$  is a leaf on the opposite search tree of maximal depth (highest  $g$ -value).  $d$  is called the "d-node". At node expansion time, the depth of each new node is compared with that of the current d-node on the same tree. Whenever a deeper node is found, it is used to replace the current d-node. At change of direction time, every node on the newly active open list has its  $h_o$ -value updated if the opposite d-node has been changed. Although this updating at change of direction time is somewhat expensive, experiments show that, at least in sliding block puzzles, DNODE is faster than most other bidirectional search algorithms as well as the most common unidirectional search algorithm. [GOL86]

A new bidirectional search algorithm, which is an

improvement to DNODE, eliminates the heuristic calculations at change of direction time. Statistics for Improved Dnode in the sliding block puzzle domain document its good performance. [DAV87] Unfortunately, these algorithms have been analyzed and compared primarily using puzzles of various types. It is desirable to apply these algorithms to a real-world application.

### Flight Path Generators

The problem space for a flight path generator (FPG) can be represented as a grid aligned along the x-y axis. The FPG is given a starting location (the start), a destination location (the goal), and a description of threats to be avoided (the costs associated with the edges of the graph). A flight path is generated from the start to the destination based on avoiding the threats and producing a short path.

Flight path generators have traditionally been implemented using two approaches that produce radically different results. [LIZ84] These approaches lie on the opposite ends of the efficiency spectrum. The first approach uses dynamic programming techniques. This approach produces optimum paths primarily with respect to the smallest cost in terms of threat interaction and, secondarily, with respect to distance travelled. Unfortunately, this approach is extremely expensive in terms of computer resources because it examines every possible alternative and makes use of the total threat environment.



The second approach uses only local information at each endpoint of a leg of the flight. A fixed number of new legs within a given angle are examined. The best leg is chosen based only on the amount of threat interaction of this set of legs. This approach is very fast since it is based solely on the limited local information. However, the approach produces relatively poor routes because it ignores the threat data of the global environment.

Due to the weaknesses of these methods, most automated route planning has not been feasible. Good paths were only produced by examining all possible alternatives. The artificial intelligence technique of applying heuristics can be used effectively to reduce the number of alternatives to be examined. A unidirectional search algorithm has been used to generate paths based on static threat data. [LI284] This algorithm (A\* [HAR68]) will produce better routes than the local approach above and is faster than the dynamic programming approach. Unfortunately, it may still be too slow if rapid turnaround is required. DNODE has been shown to be faster than A\* [GOL86], and Improved Dnode faster than DNODE [DAV87] in the sliding block puzzle domain. These DNODE-based algorithms have been targeted for use in this flight path generator.

#### V. THE FLIGHT PATH GENERATOR

The development of the flight path generator demonstrates the use of AI techniques in a real-world problem

and further validates the results of previous AI research on bidirectional search algorithms.

### Goals of Project

The project goals were to apply bidirectional heuristic search techniques (specifically DNODE and Improved Dnode) to a real-world problem, to verify the performance of Improved Dnode versus DNODE, and to perform the implementation in Ada. The first goal emanates from the desire of computer scientists to see a reduction in the time lag between the research and development of new techniques and the actual use of those techniques. A natural fallout of using the new techniques is the further substantiation of the related research. The last goal is a result of the US Air Force's interest in having software development related to weapon systems performed in the language that is the Department of Defense's "single, common, high-order programming language, effective immediately." [DOD87]

### Development

The FPG was developed in Vax Ada on a Vax 11/780 running the VMS operating system. Prior to actual development, heuristics had to be identified, path cost calculations determined and sample threat data generated for the environment [LIZ84] as described in the paragraphs below.

The threat data is classified by type, each type having two specific characteristics: a radius and a threat cost. Threats are scattered throughout the grid and are located by

their x and y coordinates. The grid consists of arbitrary units and size.

The heuristic calculation for a node n (the  $h_o$  part of the f-value) is based on a straight line that connects node n to the opposite d-node ( $d_{opp}$ ).

$$h_o = \text{threat coefficient} * (\sum \text{costs of intersected threats}) \\ + \text{distance}(n, d_{opp}) \quad (2)$$

Multiplication of the accumulated threat cost by a threat coefficient (t-coeff) greater than zero causes threat avoidance to be of greater importance relative to path length.

The path cost to reach a node n (the g part of the f-value) is calculated using the straight line that connects node n to its parent node.

$$g(n) = g(\text{parent}(n)) + \text{threat coefficient} * (\sum \text{costs of intersected threats}) + \text{distance}(\text{parent}(n), n) \quad (3)$$

### Parameter Tuning

An important part of any problem using heuristic search is identifying appropriate heuristics. Lizza [LIZ84] suggests two heuristics for flight path generation. An adaptation of one of them was chosen for this implementation. Many parameters effect the quality of the paths generated and combine to form the complete heuristics. These include the leg length, the path deflection angle (equal to the "look

ahead" distance or the radius of awareness), the maximum number of possible legs generated from each endpoint within the angle of deflection, the value of  $w$  (the heuristic weight), the number of node expansions before direction is changed and the threat coefficient. Tuning the parameters requires finding effective combinations of these variables. "Best" combinations will vary depending on the requirements for the path.

Trying all combinations of these parameters was not feasible for this project. Therefore, the parameters were fixed or varied as shown in Table I. Several additional parameters are included in the table for reference.

### Results

The statistics kept for each path generated included the number of nodes expanded, the number of heuristic calculations, the CPU time (found not reliable), the conflict cost (sum of costs of threats intersected by the generated path), the  $g$ -value (includes length and conflict cost of the generated path), and the path length. DNODE and Improved Dnode were both run 1080 times using various combinations of the parameters in Table I. In general, paths improved (shorter length, lower conflict cost) as the number of legs per arc increased and the length of the legs decreased. However, a price is paid for the improved paths in terms of CPU time. DNODE, using a weight of .5, produced the paths of lowest conflict cost but the CPU time averaged ten times that of the other weights. Examples of some of the paths

generated are shown in Figures 1-2.

Table I. Parameter Values for Flight Path Generator

PARAMETER	CATEGORY	VALUES			
leg length	varied	10	5		
path deflection angle	fixed	90	degrees		
legs per arc	varied	3	6		
weight	varied	.5	.75	1.0	
nodes expanded before change of direction	fixed	10			
g threat coefficient	fixed	20			
h threat coefficient	fixed	1			
number of threat categories	fixed	radius	2.0	4.0	6.0
		cost	0.3	0.2	0.1
		density	0.4	0.4	0.2
grid size	fixed	100	x 50		
threat density	varied	.04	.08	.12	.16 .20 .24
start location	varied	0,0	0,12.5	0,25	
			0,37.5	0,50	
goal location	varied	100,36	100,18		

Examining the number of nodes expanded (X) and the number of heuristic calculations (h-calcs) for Improved Dnode versus DNODE shows overall a slight improvement in X and a greater improvement in h-calcs. This supports the previous research [DAV87]. Averages for the statistics from both Improved Dnode (D1) and DNODE for each weight are shown in Table II. The numbers are given in the form D1/DNODE with

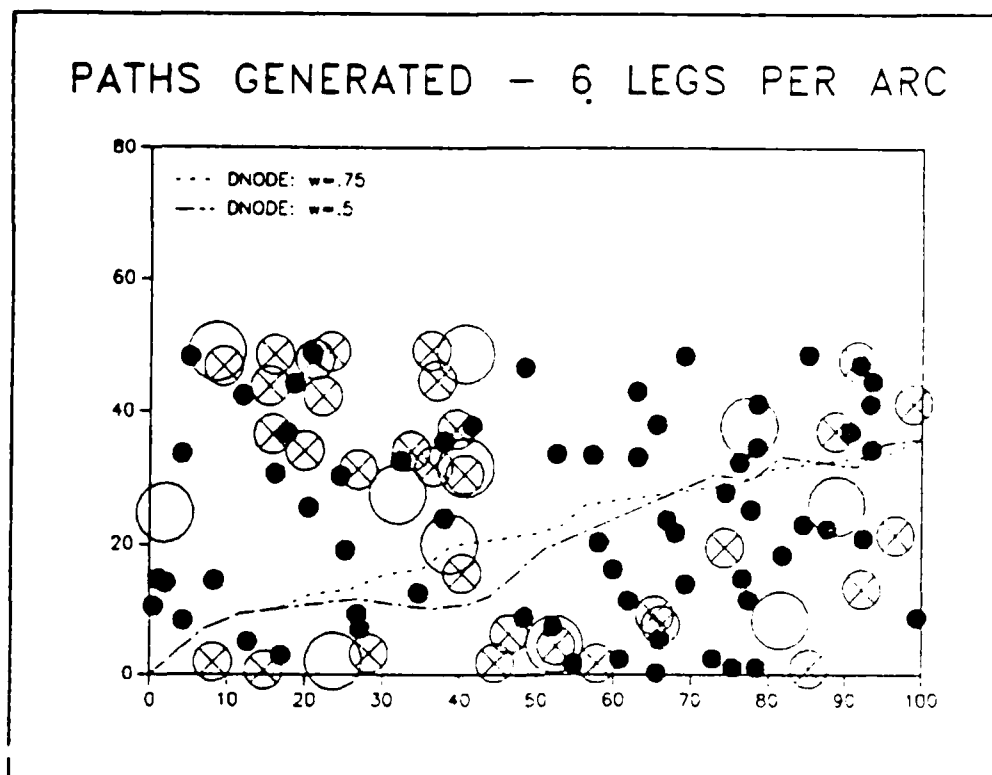


Figure 1. Paths Generated Using DNODE

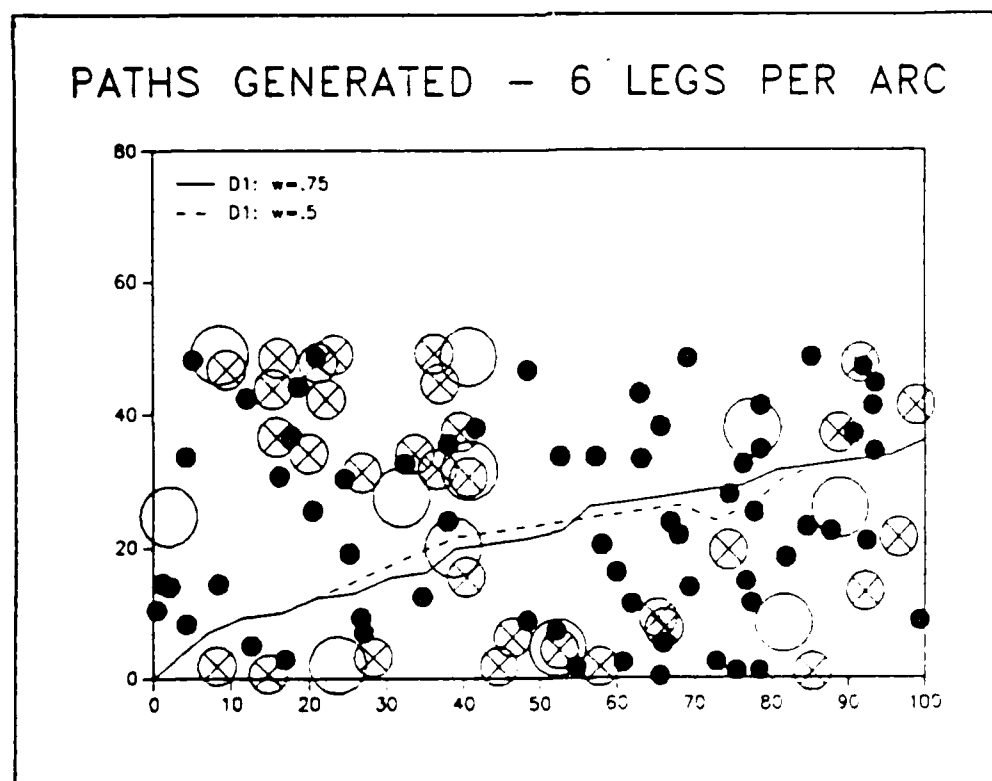


Figure 2. Paths Generated Using Improved Dnode

the ratio shown in parenthesis.

Table II. FPG Results fo D1/DNODE

WEIGHT	X	H-CALCS	CONFLICT COST	PATH LENGTH
1.0	18.5/18.3 (1.01)	71.4/93.3 (0.77)	1.42/1.43 (0.99)	107.5/106.4 (1.01)
.75	18.6/18.4 (1.01)	71.9/94.1 (0.76)	1.08/1.09 (0.99)	107.9/107.0 (1.01)
.50	36.7/93.9 (0.39)	136.7/729.7 (0.19)	0.96/0.92 (1.04)	110.4/107.6 (1.03)
ALL	24.6/43.5 (0.57)	93.4/305.7 (0.31)	1.15/1.14 (1.01)	108.6/107.2 (1.01)

#### VI. RECOMMENDATIONS

Systems such as those for EW, that use AI techniques to solve problems primarily in numeric environments can be effectively implemented in Ada. A set of tools for designing and implementing EW systems in Ada would be extremely useful. Additional efforts which involve building EW prototypes in Ada would aid in identifying tools to be developed.

The incorporation of AI techniques into solutions of real world problems has been hampered by the use of speciality and AI languages for their implementation. Ada provides the vehicle for moving these techniques out of the research laboratories. Successful integration of AI techniques into Ada would create adaptable software packages that are highly suitable for solving real world problems.

### ACKNOWLEDGEMENTS

I would like to extend my thanks to the Air Force Systems Command, the Air Force Office of Scientific Research, and the Avionics Laboratory for the opportunity to perform this work. I appreciate all the assistance given me by AAWA-1 and especially William McQuay and Charles Ambuske.

### REFERENCES

- ADK86 Adkins, M., "Flexible Data and Control Structures in Ada," 2nd Annual Conference on Artificial Intelligence and Ada, Fairfax, Virginia, November 12, 1986.
- BAK87 Baker, L., "Ada & AI Join Forces," AI Expert, April, 1987.
- BRA86 Brauer, D., "Ada and Knowledge-Based Systems: A Prototype Combining the Best of Both Worlds," First International Conference on Ada Programming Language Applications for the NASA Space Station, Houston, Texas, June 2-5, 1986.
- DAV87 Davis, H., V. Dobbs and N. Thibeault, "Speed Improvement for Bidirectional Heuristic Search Algorithms," Fifth International Conference on Systems Engineering, Dayton, Ohio, September 9-11, 1987.
- DOD87 Department of Defense Directive, "Computer Programming Language Policy," Number 3405.1, April 2, 1987.
- FRA86 Frank, M., "Using Ada to Implement the Operations Management System as a Community of Experts," First International Conference on Ada Programming Language Applications for the NASA Space Station, Houston, Texas, June 2-5, 1986.
- GOL86 Golden, D. "A Domain Independent Method of Comparing Search Algorithm Run-Times," Masters Thesis, Wright State University, 1986.
- HAR68 Hart, P., N. Nilsson and B. Raphael, "A Formal Basis for the Heuristic Determination of Minimum Cost Paths," IEEE Transactions on Systems Science and Cybernetics, SSC-4 (2), 1968.
- KAR86 Kary, D. and P. Juell, "TRC: An Expert System Compiler," Sigplan Notices 21 (5), 1986.



- LAV86 LaVallee, D., "An Ada Inference Engine for Expert Systems," First International Conference on Ada Programming Language Applications for the NASA Space Station, Houston, Texas, June 2-5, 1986.
- LIZ84 Lizza, C., "Generation of Flight Paths Using Heuristic Search," Masters Thesis, Wright State University, 1984.
- POL84 Politowski, G. and I. Pohl, "D-node Retargeting in Bidirectional Heuristic Search," Proceedings of the National Conference on Artificial Intelligence, 1984.
- REE85 Reeker, L., J. Kreuter and K. Wauchope, "Artificial Intelligence in Ada: Pattern-Directed Processing," AFHRL-TR-85-12, May, 1985.
- SCH80 Schwartz, R. and P. Melliard-Smith, "The Suitability of Ada for Artificial Intelligence Applications," SRI International, May, 1980.
- SCH86 Scheidt, D., D. Preston and M. Armstrong, "Implementing Semantic Networks in Ada," 2nd Annual Conference on Artificial Intelligence and Ada, Fairfax, Virginia, November 12, 1986.
- WAL86 Wallace, D., "An Evaluation of Ada for AI Applications," First International Conference on Ada Programming Language Applications for the NASA Space Station, Houston, Texas, June 2-5, 1986.

1987 USAF-UES SUMMER FACULTY RESEARCH PROGRAM/  
GRADUATE STUDENT SUMMER SUPPORT PROGRAM

Sponsored by the  
AIR FORCE OFFICE OF SCIENTIFIC RESEARCH  
Conducted by the  
Universal Energy Systems, Inc.

FINAL REPORT

Computational Simulation of  
Transonic Store Separation

Prepared by: F. Carroll Dougherty  
Academic Rank: Assistant Professor  
Department and University: Department of Aerospace Engineering Sciences  
University: University of Colorado, Boulder  
Research Location: Arnold Engineering Development Center,  
Arnold Air Force Station  
USAF Researcher: Dr. John A. Benek  
DATE: September 25, 1987  
Contract No: F49620-85-C-0013

Computational Simulation of  
Transonic Store Separation

by

F. Carroll Dougherty

ABSTRACT

The preliminary development of a numerical simulation capability using finite-difference techniques for flows about aircraft carrying stores is described. Since a single global mesh about the aircraft with stores is very difficult to generate, a multiple overset mesh approach called the chimera scheme is used. In the chimera scheme, a complex configuration such as a wing with stores beneath it is mapped with a global mesh about the main component, the wing, and with minor overset meshes generated about each additional component such as the stores. The minor meshes can be overset on the global mesh without matching any boundaries, so they can be freely moved with respect to the global mesh. Therefore, the time-accurate simulation of a moving store beneath a wing is possible without regridding the configuration. This research effort involves coding the three-dimensional chimera grid package for moving meshes, then coupling the grid management routines with a time-accurate Euler flow solver.

### ACKNOWLEDGMENTS

I would like to thank the Air Force Systems Command and the Air Force Office of Scientific Research for this research opportunity. I would also like to thank UES for their administrative help, and, in particular, Mr. Marshall Kingery, who served as my point of contact with the Air Force.

My work would not have gone as well if it hadn't been for the help and support of the people in the Computational Fluid Dynamics section, Propulsion Wind Tunnel Facility, Arnold Engineering Development Center: Jim Jacocks, head of the Computational Fluid Dynamics group, Jack Benek, and Norman Suhs. Their suggestions, comments, and arguments were a great help in the restructuring of the codes. Bill Dietz, Bill Thomson, and Keith Jordan also were very helpful with the computer systems.

I. INTRODUCTION: Today's high speed aircraft are intended to carry a variety of stores either externally or submerged, and are rated as to their ability to deliver these stores to their targets reliably and accurately without loss of aircraft performance. Store-induced aerodynamic drag can significantly downgrade aircraft performance, however, while aerodynamic interactions may cause the released stores to scatter, run into each other, or impact the aircraft. It is necessary, then, to develop reliable methods to predict the aerodynamics of store/airframe interactions.

Wind tunnel tests can provide useful data regarding store carriage, but are severely limited by the scaling effects and design considerations when store release data are required. Analytical results are impossible to compute because of the nonlinearity inherent in the problem of store separation. Flight testing is an option, but without extensive analytical or experimental results to rely on, these tests can be unpredictable, expensive, and dangerous. Current computational techniques can accurately predict the trajectories of stores in a known flow field or with known loading, but are unable to predict the separation motion when the stores are interacting with the flow field of the releasing aircraft (ref. 1,2). An additional capability to predict the motion of the stores as they are released from an aircraft is needed.

Finite-difference codes have been very successful in simulating nonlinear flow fields, both for steady and nonsteady computations. A major obstacle to this computational approach, however, is the difficulty in developing effective discretization processes for complex

configurations like the aircraft carrying stores. A single global mesh about an aircraft/store configuration could be generated, but it is unlikely to be computationally efficient, especially for viscous flow simulation. Moreover, allowing the stores to move would require a new mesh to be generated after each movement.

Composite grid schemes use two or more simple meshes to map a complex configuration. The use of a multiple grid approach can yield better grid resolution, simplify the application of boundary conditions, and ease the task of grid generation. Some of the disadvantages to composite meshes are that the flow solvers must be modified, and that the bookkeeping that tracks the relationships among the meshes can be complicated. The two most common of the composite schemes are the patched and overset mesh approaches (ref. 3). Patched grids connect along common surfaces; overset grids are superimposed on a global mesh in regions of interest. Because the minor overset meshes are independent of each other and the global mesh, they can be moved with respect to the global grid.

Both patched and overset mesh approaches have been used with three-dimensional finite-difference flow solvers to simulate the steady flow about store configurations (ref. 4-7). Because of the freedom of motion in the chimera scheme, an overset mesh approach, it has been chosen to simulate the flow about moving stores. First demonstrated in two dimensions (ref. 7), the combined overset mesh package and time-accurate Euler flow solver computed solutions for one body moving with respect to a larger object. These two-dimensional tests showed that the time accuracy was adequately maintained, the bookkeeping routines were

capable of tracking the moving grids correctly, and that the simulation of the flow field aerodynamics was clearly possible.

The chimera grid scheme has been evolving jointly between NASA Ames Research Center and Arnold Engineering Development Center. The author, now at the University of Colorado, has been involved with the development of the package since its inception, and is the principal investigator for all the moving versions. It was logical for the next phase, the development of the three-dimensional store separation simulation code, to take place at the AEDC facilities.

II. OBJECTIVES OF THE RESEARCH EFFORT: Two primary objectives were defined for this research effort:

- \* To couple a three-dimensional overset grid code, the chimera grid scheme, with a time-accurate, finite-difference Euler code to create a complete package for time-accurate simulation for flows about moving bodies.
- \* To obtain results showing the effects of aerodynamic interaction between bodies such as three simple stores clustered together or a single store under a wing, both before and after separation.

III. APPROACH: A three-dimensional version of the two-dimensional moving chimera code was to be coupled with a three-dimensional Euler code, ARC3D, an interpolation routine, and a trajectory package. The new code, called HYDRA for the many-headed monster in Greek mythology, would be able to simulate the steady or unsteady flows about multiple or complex configurations. Specific details about the main routine and the

four modules mentioned above are contained in the following sections.

Main Routine: The HYDRA main routine had to initialize the program variables, control the time step loop, call the program modules, and regulate the output files. The program modules were divided into two subroutine calls: the call to a routine, MULTI, which set up the trajectory and chimera packages, and the call to the subroutine SOLVE to manage the flow solver and interpolation calculations. The time step loop could be started at the beginning, or could be started from a stored restart file. The type and amount of output was determined by input parameters. Parameters for sizing arrays were determined for the coupled programs, and consistent COMMON blocks were created at this level of the HYDRA code.

Trajectory Routine: For this initial effort, a simple routine computing the three-dimensional translation and rotation as a function of small changes in  $x$ ,  $y$ ,  $z$ ,  $\theta$ ,  $\phi$ , and  $\psi$  was used. The direction changes were pre-determined by the user. Eventually, a routine that would integrate the forces and moments about the moving body for the new position would have to be included.

Chimera Package: A very preliminary version of the three-dimensional moving chimera code existed at the beginning of the research effort. The code, PEGSUSM, had to be debugged, generalized for more configurations, and thoroughly checked to see that the bookkeeping that worked in two dimensions would also work in three. The package had to be able to deal with simple multiple body configurations with one body moving away from the rest. The bookkeeping had to track the moving grid in relation to the stationary grids, keep current with the changes in the boundary interfaces between the grids, and compute the new



interpolation data for the interfaces after each movement. COMMON blocks had to be rearranged to reflect the coupling with the other modules, and the capability to use solid state disk (SSD) storage devices had to be built into the routines. An additional effort to make the PEGSUSM package very fast (relative to the flow solver) was also undertaken.

Flow Solver: The steady state ARC3D code, vectorized and modified for multiple meshes by Dr. J. A. Benek of CALSPAN/AEDC, formed the base code for this module. The outer levels of the code, the time step loop, initialization routines, and some output controls, had to be stripped from the program. Time-dependent terms had to be added for time-accurate calculations, and, although not used in this effort, the viscous terms and routines were also modified for the coupled program. Subroutines computing the forces and moments on each body surface also had to be included. Again, COMMON blocks and parameter statements were changed, and the SSD storage capabilities had to be built into the control routine SOLVE. The SOLVE subroutine also had to manage the interpolation and update routines for the boundary interfaces between the meshes.

Interpolation Routines: The same routines used in J. A. Benek's steady state calculations (ref. 6) were to be used in this effort. The boundary values on the interfaces were computed using tri-linear interpolation. The coefficients for the interpolation calculations were computed in the chimera grid package and passed via COMMON blocks to the interpolation routines. The updating of the interfaces had to be changed from the steady state code, and had to be controlled by the subroutine SOLVE. Parameters and COMMON blocks were also changed.

Simple geometric shapes were used throughout the debug and testing phases of the research effort. Spheres, cubes, and planform wings alone and in relation to each other were the predominant choices. If time had permitted, a simple store beneath first a flat plate, then a simple wing, would have been used for demonstration calculations.

IV. RESULTS: The work was completed in steps. The first step was to write the main routine and initialization routines for the grid package information. Then the changes were made to the PEGSUSM code to link it with the new main routine. The trajectory routine was added, and the combined codes were tested for moving and nonmoving multiple grids. The next step was to add the initialization routines, parameters, and COMMON blocks for the flow solver modules to the main routine. The flow solver code was stripped of its outer levels, modified for the new parameters and COMMON blocks, then joined to the HYDRA code. The new update subroutines were added to the SOLVE routine, and the interpolation subroutines were also modified for the coupled code. Finally, the force and moment subroutines were added to the HYDRA code.

Spheres and cubes embedded inside larger Cartesian grids were used to test the three-dimensional moving chimera package. The bookkeeping successfully tracked the smaller grids through translations and rotations with respect to the outer grids. Boundary interfaces between grids were easily maintained during movements, and additional interpolation points along the interfaces, first thought necessary, were found to be not needed, saving CPU time and storage. The SSD storage capability was built in with a switch input by the user and was carefully checked out. The PEGSUSM package was changed to use

considerably less computer time per call by the addition of several improved search and stencil walk routines. Vectorization was built in where possible, as well. The resulting package was about two orders of magnitude faster than the previous code for the same number of points. It also used about one third the time per iteration as the flow solver, which was judged quite good for a demonstration calculation.

The flow solver additions were checked in two stages: first steady state calculations, then unsteady. A simple wing designed to be run as an infinite wing to mimic two-dimensional calculations was used alone and overset on a larger cylindrical grid. The airfoil shape was a NACA 64A010. Steady state computations made on both the single and overset grids appeared correct. Figure 1 shows the Mach contours for the single mesh for a freestream Mach number of 0.8 and angle of attack of 1 degree. Pressure contours for the same case are shown in figure 2. Mach contours for a multiple mesh case run with a freestream Mach number of 0.8 and zero degrees angle of attack are shown in figure 3. Solutions on both meshes were plotted in the regions of overlap. The dotted curves in the corners of the plot are the outer boundary of the smaller mesh. All solutions matched well with other calculations done with different codes.

After the time-dependent terms were added to the flow solver, simple plunge and oscillating plunge cases were tried with the same meshes. Unfortunately, one or more errors were uncovered and remained unresolved at the end of the research effort. When the force and moment routines were added to help debug the code, the steady state solutions also seemed suspect. The same bugs in the code could have been causing the slight error in the steady state and larger error in the unsteady

computations. An error might also exist in the force and moment calculations, as well.

VI. RECOMMENDATIONS: The Computational Fluid Dynamics section plans to implement a number of changes in their existing and upcoming codes based on the work covered by this effort. They also plan to use the corrected code as a base for store separation from cavitites. The author plans to apply for a mini grant to continue work on the code and with the people in the CFD section. Once the remaining errors have been found, demonstration cases with simple configurations such as the store under a wing, or three stores clustered together with one store moving would be computed. The code would then be expanded to allow more than one body in a configuration to move. If time permitted, a trajectory routine integrating the forces and moments on a body could be substituted for the simple routine currently in use.

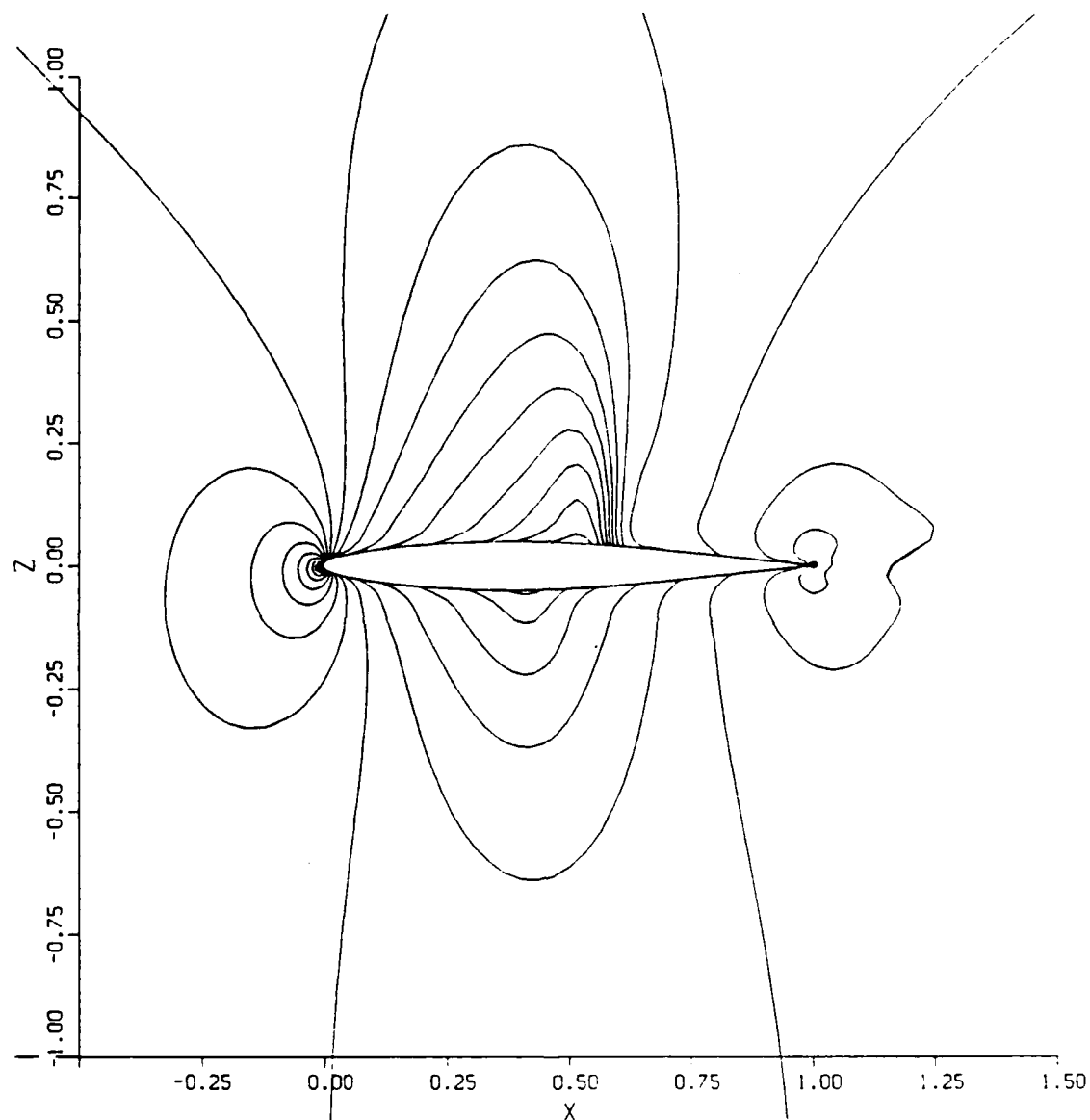


Figure 1. Mach contours for NACA 64A010 airfoil for  $M_\infty = .8$ ,  $\alpha = 1.0^\circ$ , single grid.

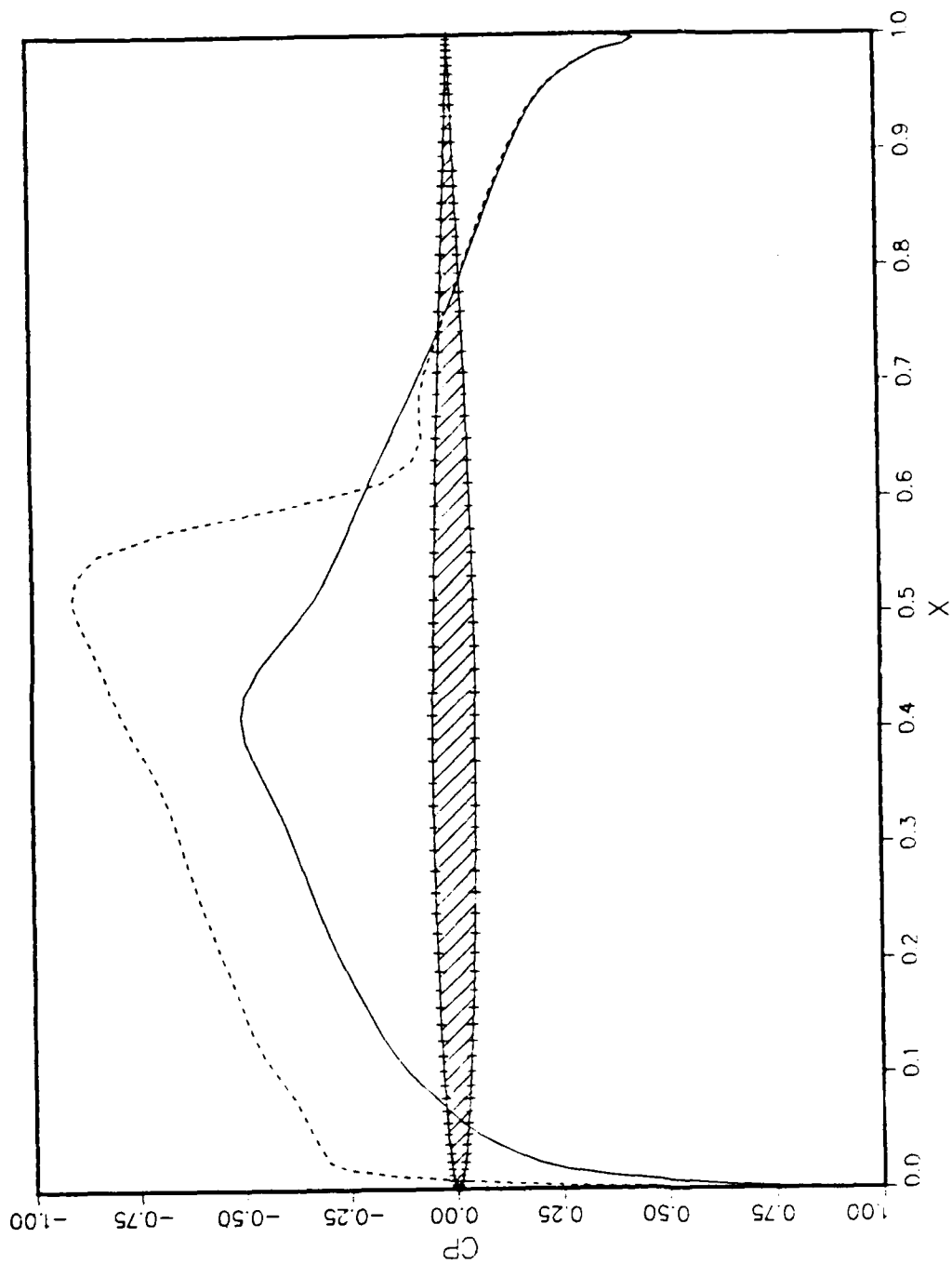


Figure 2. Pressure distribution for MACA 64A010 for  $M_{\infty} = .8$ ,  $\alpha = 1.0^\circ$ , single grid.

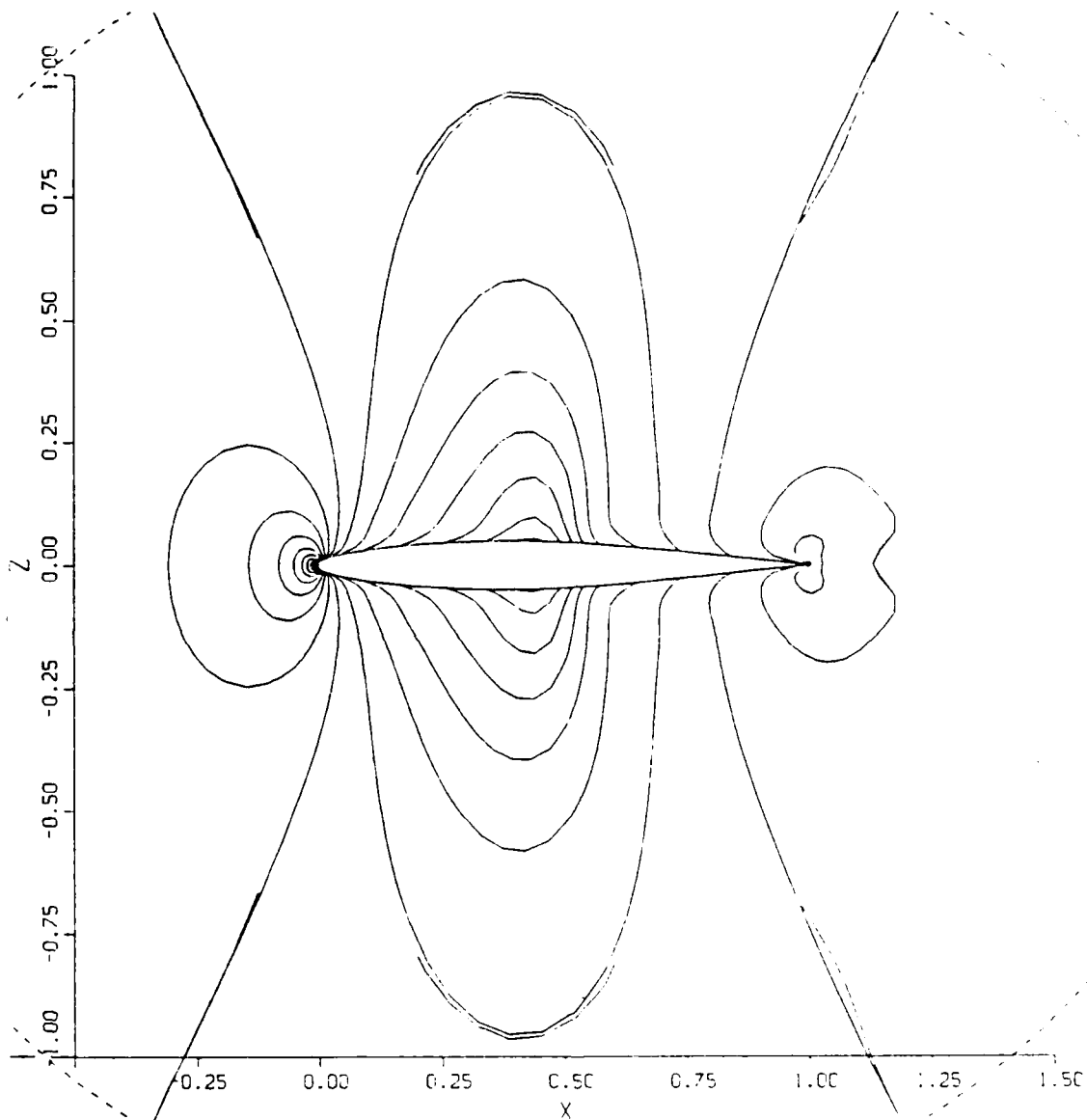


Figure 3 Mach contours for multiple mesh calculation about a NACA 64A010 at  $M_\infty = .8$ ,  $\alpha = 0^\circ$ .

#### REFERENCES

1. Keen, K. S., "Improvements in Predicting Techniques for Store Loads and Trajectories," Proc. Seventh Aircraft/Stores Compatibility Symposium, April 1986.
2. Arnold, R. J. and Epstein, C. S., "Store Separation Flight Testing," AGARD Flight Test Techniques Series, Vol. 5, AGARD-AG-300-Vol5, April 1986.
3. Steger, J. L. and Benek, J. A., "On the Uses of Composite Grid Schemes in Computational Aerodynamics," NASA TM 88372, November 1986.
4. Belk, D. M., Janus, M. J., and Whitfield, D. L., "Three-Dimensional Unsteady Euler Equation Solutions on Dynamic Grids," AIAA Paper 85-1704, July 1985.
5. Cottrell, C. S. and Lijewski, L. E., "A Study of Finned, Multi-body Aerodynamic Interface at Transonic Mach Numbers," AIAA Paper 87-2480, August 1987.
6. Benek, J. A., Donegan, T. L., and Suhs, N. E., "Extended Chimera Grid Embedding Scheme with Applications to Viscous Flows," AIAA Paper 87-1126-CP, July 1987.
7. Dougherty, F. C., Benek, J. A., and Steger, J. L., "On Applications of Chimera Grid Schemes to Store Separation," NASA TM 88193, October 1985.



1987 USAF - SUMMER FACULTY RESEARCH PROGRAM/  
GRADUATE STUDENT SUMMER SUPPORT PROGRAM

Sponsored by the  
AIR FORCE OFFICE OF SCIENTIFIC RESEARCH

Conducted by the  
Universal Energy Systems, Inc.

FINAL REPORT

GUIDED WAVES IN MILLIMETER WAVE CIRCUIT DESIGN

Prepared by:	John M.Dunn
Academic Rank:	Assistant Professor
Department and	Electrical and Computer Engineering
University:	University of Colorado, Boulder
Research Location:	RADC/EEAA Hanscom AFB Lexington, MA
USAF Researcher:	Robert Mailloux
Date:	August 15, 1987
Contract No:	F49620-85-C-0013

## GUIDED WAVES IN MILLIMETER WAVE CIRCUIT DESIGN

by

John M. Dunn

### ABSTRACT

Guided waves are investigated as a way to overcome a number of problems currently encountered in millimeter wave circuits. At the present time, microstrip elements are exclusively used in such circuits. Guided waves have a number of advantages for certain applications. For example, they exhibit lower power loss than do microstrip lines. Typical loss figures are given for a GaAs substrate. A typical circuit would use guided waves to transfer power and information from one major sub-section to another. The microstrip would be reserved for use in relatively small areas. Such a circuit will therefore employ both guided wave and microstrip elements. In order for guided waves to be effectively used, it is necessary that one can be efficiently launched from a microstrip. One possible method capable of monolithic integration is given. Another advantage of guided waves at high frequencies, is the possibility of a broadband antenna. The broader bandwidth comes from the fact that the antenna does not utilize a resonant element. A possible design of such an antenna is given, along with a number of design considerations. The emphasis in this report has been one of using simple physical concepts to examine the feasibility of the approach. No effort has been made to carry out sophisticated mathematical analysis. Instead order of magnitude calculations have been used whenever possible.

### Acknowledgements

Thanks go to the Air Force Systems Command and the Air Force Office of Scientific Research for sponsorship of this research. This work would not have been possible without the help of a number of people. Arthur Yaghian pointed the existence of the program out to me and encouraged me to apply. Bob Mailoux provided support and encouragement as my supervisor. I had a number of helpful conversations with Richard Soref and Boris Tomasic. Finally, I would to thank the support staff of the electromagnetics directorate for making my stay a pleasant one.

## I. INTRODUCTION:

This report examines a number of issues in guided waves in MMIC's (monolithic, millimeter wave, integrated circuits). It is anticipated that guided waves will play an increasingly important role in such circuits, as the operating frequency range is increased into the EHF regime, thirty to three hundred GHz (giga-Hertz).

The antenna section of the electromagnetics directorate at the Rome Air Development Center is very concerned with the design and development of millimeter wave radar systems. In particular, antenna arrays must be designed which are capable of being produced monolithically, in which all the parts of the array are manufactured on the same substrate. In this manner, it is expected that the price of phased array technology will be reduced to a low enough level that widespread deployment is possible. My research interests are in the area of electromagnetic wave propagation and scattering, in particular, in the design and testing of millimeter wave antennas and components. It was therefore natural for me to work in the antenna group in order to see if my background in wave propagation could be put to use to help overcome a number of difficulties which presently plague millimeter wave systems. The traditional methods employing microstrip elements have a number of increasing important drawbacks as the operating frequency is increased into the millimeter wave range. The use of guided waves may have a number of advantages over the microstrip for certain applications. Therefore, the goal of my research this summer has been to conduct a preliminary investigation into the feasibility of using guided waves, and to determine their advantages and disadvantages over more traditional microstrip technology.

## II. OBJECTIVES OF THE RESEARCH EFFORT:

Traditionally, designers of MMIC's have used microstrip elements for passive electromagnetic components: transmission lines, antennas, and resonators. The primary reason for doing so has been one of cost. Microstrip elements can be made by photolithographic etching, and are therefore inexpensive to produce. There are however a host of problems in using microstrip elements, which tend to be magnified as the operating frequency is increased. Microstrip elements operate in the quasi-TEM mode, for which it is necessary that the thickness of the substrate region be thin. Higher order modes become important if this is not the case. Concentrating the fields in a thin region has some adverse affects, however.

The field concentration is large around the metal boundaries, which increases the power loss. This loss can become very substantial at high frequencies. A second problem is that antenna elements made of microstrip patches are inherently narrow band if the substrate is thin. A bandwidth of only a few percent is expected in the millimeter wave region. Thus, MMIC design using microstrip elements will become more and more difficult as the operating frequency is increased.

Is there any alternative to the microstrip which becomes more attractive as the frequency of operation is pushed higher? If one goes beyond the EHF region, the infra-red and optical regimes are reached. The microstrip is not a viable concept in optics; the losses are too high, and the fabrication too difficult. Instead, the light propagates inside dielectric waveguides. Devices such as lenses and resonators are designed by using high frequency approximate techniques, the most common of which is geometrical optics. This report examines the possibility of utilizing these optical concepts at millimeter wave frequencies. Guided waves can propagate inside the substrate region without the need of a microstrip guiding structure. Instead, they are confined by controlling the lateral dimensions of the substrate region, or by exciting them in a narrow beam. They have a number of advantages over the more traditional microstrip guiding structure. In particular, they exhibit low loss, and can be used in the design of broadband antennas.

My research goals this summer were to investigate the possibility of using guided waves in MMICs for a number of applications: power and signal transfer over relatively long distances in the circuit, broadband antenna design, and a high  $Q$  resonator. In addition, it was felt to be important to examine the problem of a microstrip to guided wave transition, as the best design of a MMIC may well incorporate both microstrip and guided wave elements. The microstrip element can still be used for phase shifters, tuning, and signal transfer within a small portion of the circuit. The project originally started as an investigation into a possibilities of an alternative to the microstrip antenna which offered broader bandwidth. Gradually, it was realized that guided waves may have many other uses.

The basic approach used in the research carried out this summer was to examine the physical concepts involved, backed up by simple "back of the envelope" calculations where possible. This approach was adopted for two reasons. First of all the program only lasted ten weeks. It was therefore not possible to work on one problem in much detail. Developing a computer code for one aspect of the work, or designing one experiment could easily take up the entire summer. Since the issue of guided wave propagation had

not been looked at for MMICS's, it was felt that in ten weeks it would be more productive to develop an overview and fill in the details later. The second reason for following this approach is that simple formulas and physical concepts give the researcher an order of magnitude estimate of the usefulness of the idea. If the numbers look reasonable, a more detailed analysis can be carried out on specific aspects when time permits.

The report is broken up into a number of sections. The first section describes the basic physical properties of guided waves, particularly in gallium arsenide (GaAs). Sections then follow describing the design of a way to launch the guided wave from the microstrip, and on applications of the guided waves, including a broadband antenna, and high  $Q$  resonator.

### III). BASIC PROPERTIES OF GUIDED WAVES

A number of basic properties of guided waves will be discussed in this section. An understanding of these properties is essential if useful devices are to be designed. A guided wave is an electromagnetic wave, which propagates in the substrate region of a MMIC. For example, in figure 1, the substrate region is made up of GaAs. It is bounded on one side by a copper layer, on the other by free space or vacuum. The guided wave is confined to travel in the GaAs layer. The energy of the wave attenuates with distance exponentially as one travels away from the substrate into free space. It is not necessary to have the substrate bounded by a conductor for the guided wave to propagate. It is common to call this type of wave a surface wave. This has not been done in this report because it is felt that by using the word "surface" the wave is assumed to be trapped close to the interface between the substrate and vacuum region. This is not the case. The energy of the wave can extend down through the entire thickness of the substrate. It is a surface wave only in the sense that the energy does not radiate out from the substrate into the vacuum. There are a number of waves in layered media problems which can more properly be called surface waves, such as lateral waves. These waves are not important in the present discussion.

There is a vast amount of literature discussing various aspects of these waves (Collin, Walther). This section summarizes the results that are relevant to the discussion of guided waves in MMIC's. Let the electrical parameters of the substrate in figure 1 be denoted by:  $\epsilon_s = \epsilon_0 \epsilon_r$ , and  $\mu_s = \mu_0 \mu_r$  where  $\epsilon_0$  and  $\mu_0$  are the permittivity and permeability of free space respectively. The conductivity of the substrate region

is denoted by  $\sigma_s$ . (MKS units are used throughout this report.) Cartesian coordinates are used, with the substrate oriented parallel to the  $x - y$  plane. The interface between the conductor and substrate is at  $y = 0$ , the interface between the air and substrate is at  $y = h$ . It is assumed that the wave travels from left to right, in the positive  $x$  direction. The problem does not depend on the  $z$  coordinate by symmetry. It is apparent that Maxwell's equations can be split into two independent cases, each case having only three non-zero field components. The TM wave only has non-zero  $E_z$ ,  $H_x$ , and  $H_y$  components; the TE case only has non-zero  $H_z$ ,  $E_x$ , and  $E_y$  components. Maxwell's equations must be solved for these two types of waves. They can only exist under certain conditions.

The TM case is examined first. Because there is only one non-zero component of the magnetic field, it is convenient to look at it. It is:

$$\begin{aligned} H_{0z} &= A e^{-\gamma_0(y-h)} e^{i\beta x} \\ H_{sz} &= B \cos(\gamma_s y) e^{i\beta x} \end{aligned} \quad (1)$$

$\exp(-i\omega t)$  time dependence is assumed. The subscript 0 refers to a quantity in the air region,  $s$  refers to a quantity in the substrate region. Maxwell's equations require that:

$$\begin{aligned} -\gamma_0^2 &= k_0^2 - \beta^2 \\ \gamma_s^2 &= k_s^2 - \beta^2 \end{aligned} \quad (2)$$

$k_0$  is the wavenumber of free space:  $k_0 = \omega \sqrt{\mu_0 \epsilon_0}$ .  $k_s$  is the wavenumber of the substrate:  $k_s = k_0 \sqrt{\epsilon_r}$ . The real part of  $\gamma_0$  must be greater than zero in order to get a trapped wave. The real part of  $\beta$  is greater than zero in order to make sure that the wave is traveling in the positive  $x$  direction. Various boundary conditions must be satisfied if equation (1) is to be a solution to the problem. It is found that a non-zero solution can result only if:

$$\epsilon_r (\gamma_0 h) = (\gamma_s h) \tan(\gamma_s h) \quad (3)$$

From equation (2):

$$(\gamma_0 h)^2 + (\gamma_s h)^2 = (\epsilon_r - 1) (k_0 h)^2 \quad (4)$$

The conductivity of the substrate has been set to zero in equations (3) and (4). This does not lead to serious errors for most practical cases. These equations must be solved for  $\gamma_0$  and  $\gamma_s$ .  $\beta$  can then be found from equation (2). Equation (3) is transcendental, and a closed form, analytical solution is therefore not possible. A graphical technique can be used to obtain a good idea of what the solution looks like.

Equation (4) makes a circle of radius  $k_0 h \sqrt{\epsilon_r - 1}$  when  $\gamma_s h$  is plotted against  $\gamma_0 h$ . The intersection of this circle and the curve in equation (3) gives the desired solution, as shown in figure 2. The curve labelled  $TM_0$  corresponds to the  $TM_0$  mode. Notice that a point of intersection exists no matter what the size of the circle. There is therefore no cutoff in frequency for the  $TM_0$  mode. Higher order modes can propagate if the circle is large enough that it intersects other branches of equation (3). For example, if:  $k_0 h \sqrt{\epsilon_r - 1} \geq \pi$ , the  $TM_1$  mode will also propagate.

The same procedure can be carried out for the TE polarization. It is now convenient to use the single electric field component:

$$\begin{aligned} E_{0z} &= A e^{-\gamma_0(y-h)} e^{i\beta x} \\ E_{sz} &= B \sin(\gamma_s y) e^{i\beta x} \end{aligned} \quad (5)$$

where the relationship between  $\gamma$  and  $\beta$  given by equation (2) still holds. In order for the boundary conditions to be satisfied it is necessary that:

$$\gamma_0 h = -\gamma_s h \cot(\gamma_s h) \quad (6)$$

This equation must be solved simultaneously with equation (4) to obtain the propagation constant  $\beta$ . The first branch of equation (5) is labelled  $TE_1$  in figure 2. The intersection of this curve and the circle gives the propagation constant. Notice that the  $TE_1$  mode has a lower cutoff, below which the mode cannot propagate. For GaAs, cutoff occurs at  $k_0 h = 0.455$ .

It is instructive to look at the phase velocity ( $\omega/\beta$ ) of the modes. From equation (2):

$$\frac{v}{c} = (1 + \gamma_0^2/k_0^2)^{-1/2} \quad (7)$$

$c$  is the speed of light in vacuum ( $3 \times 10^8$  m/sec).  $v$  is the speed of the wave in the GaAs. The phase velocity of the mode is less than that in vacuum. As the thickness of the substrate goes to zero, the velocity approaches  $c$ . As the thickness of the substrate goes to infinity, the velocity approaches  $c/\sqrt{\epsilon_r}$ , the velocity of light in the substrate. Figure 3 shows the phase velocities for the  $TM_0$  and  $TE_1$  modes in GaAs, for which  $\epsilon_r = 12.9$ . It is clear from figure 3 why a microstrip line does not couple effectively to a surface wave under normal circumstances. The microstrip line uses a quasi-TEM wave, the velocity of which is the speed of light in the substrate, 278c for GaAs. If the substrate is thin, the



TM<sub>0</sub> surface wave has a velocity almost that of  $c$ . It is this velocity mismatch which prevents the waves from coupling the one another.

It is possible to estimate the losses occurring in a surface wave. Losses can be grouped into two categories: those due to the finite conductivity of the ground plane, and those due to the non-zero loss tangent of the GaAs. The losses of the first type are typically much greater than those of the second. The specific case of a TM<sub>0</sub> mode is examined. Because the ground plane is a good conductor, it is possible to use the well known approach of estimating the losses by the use of an impedance boundary condition at the ground plane [Walther]. To give a specific example, if  $k_0 h < .3$ , then for GaAs with a copper ground plane ( $\sigma = 5.7 \times 10^7$  (S/m) for copper), the loss for the TM<sub>0</sub> mode is:

$$\alpha = 0.285 \sqrt{f_g} / h_{mm} \quad (\text{dB/m}) \quad (8)$$

$\alpha$  is the decay length.  $f_g$  is the frequency in GHz.  $h_{mm}$  is the thickness of the GaAs in millimeters. For example, if  $f = 100$  GHz, and  $h = 0.142$  mm, then  $\alpha = 20$  dB/m. This should be compared with the conductor losses in a microstrip line. Assume a line with an impedance of 50  $\Omega$ . Using the formulas from Gupta [ref], it is found that the ratio of the width of the strip to its height is 0.748. Assume that the thickness of the microstrip conductor is 5 micrometers, and the substrate thickness is  $4 \times 10^{-4}$  meters. The decay length is found to be:

$$\alpha = 16.3 \sqrt{f_g} \quad (\text{dB/m}) \quad (9)$$

For example at 100 GHz,  $\alpha = 163$  dB/m. The reason for the much greater conductor loss in the microstrip is due to the fact that the substrate must be kept thin, and that the fields are therefore concentrated closer to the conductor.

The dielectric loss for GaAs is negligible. The loss tangent [Pucel] is  $1.1 \times 10^{-4}$  at 10 GHz. From Gupta, this gives a decay length for the microstrip:

$$\alpha = \frac{76.24 \tan \delta}{\lambda} \quad (\text{dB/m}) \quad (10)$$

where  $\tan \delta$  is the loss tangent. Thus:  $\alpha = 0.25$  dB/m. Similar results are found for the case of surface waves.

Therefore, it is clear a principle advantage of a surface wave is its low loss when compared to the quasi-TEM wave on a microstrip. In some situations such as power transfer, a surface wave could have distinct

advantages at high frequencies. It should be noted that it is possible for a surface wave to exist without a ground plane. In this case the  $TE_0$  mode has no lower cutoff. If such a wave could be launched efficiently, it would have extremely low loss, as the only loss mechanism is heat dissipation in the dielectric.

#### IV. EXCITATION OF GUIDED WAVES:

This section examines the issue of guided wave excitation. The important parameter in such a study is that the final design must be capable of being monolithically fabricated. This is important if low cost is to be achieved in an actual working environment. Traditional designs for guided wave launchers have not had to deal with this issue, the wave being launched from horns or prism couplers. These designs are not suitable for monolithic integration. The section of the circuit which employs microstrip technology, for example the amplifier and phase shifter regions, must be electrically thin. Otherwise higher order modes will propagate, leading to strong coupling between various parts of the circuit, a highly undesirable effect. The guided wave section will therefore have to be substantially thicker than the microstrip region. Any transition from microstrip to guided wave must incorporate such a change in thickness.

There are two possible approaches. Either the fields in the microstrip region could couple into the guided wave region by small holes in the conductor, or the coupling could be made by a gradual thickening of the substrate layer. The first method has a number of problems. The coupling from each hole must be small. This means a large interaction length is needed if a substantial amount of energy is to be coupled into the guided wave. The microstrip must be terminated, which will lead to a large reflection of the remaining energy in the microstrip. Finally, the structure could be very sensitive to frequency changes. For these reasons, the second method is preferred. The substrate is gradually widened out to a thickness which will support a surface wave, figure 4. In order to have a transition with a small return loss over a large frequency range, the transition must be gradual. How gradual is not known at this time as a detailed theoretical analysis is necessary. A few simple observations can be made, however, to show that such a scheme appears to be reasonable.

The first objective in the design of the transition is to match the impedances of the microstrip line and the guided wave. The impedance of the microstrip line depends on the height of the substrate, and the width of the line. The values can easily be varied between 0 and 100 Ohms for a GaAs substrate (Gupta).

It is necessary for the width of the line and the height of the substrate to be much less than a substrate wavelength for the formulas to apply. The impedance for the  $TM_0$  mode is given by:

$$Z = \frac{377}{\epsilon_r} \left( \frac{c}{v} \right) \quad (\Omega) \quad (11)$$

For GaAs, impedances between 30 and 105  $\Omega$  are possible for the  $TM_0$  mode, although it is not possible to go above 50  $\Omega$  if it is required to keep below cutoff of the  $TE_1$  mode. There is therefore substantial overlap in the range of impedances of the microstrip and the guided wave cases.

The next factor to look at is the fields in the coupling region. The fields under the microstrip are almost TEM, with the electric field directed vertically, and the electric field horizontally, at right angles to the direction of propagation (Bahl and Bhartia). It is therefore not possible to excite TE modes by this configuration. The  $E_x$  component of the electric field is much smaller than the  $E_y$  component for the TM waves. Their ratio is given by:

$$|E_x/E_y| = \frac{\gamma_s}{\beta} \tan(\gamma_s y) \quad (12)$$

The  $E_x$  field is smallest close to the ground plane. At the interface with the vacuum region,  $y = h$ :

$$|E_x/E_y| = \epsilon_r \sqrt{1 - (v/c)^2} \quad (13)$$

The ratio can vary a great deal depending on the parameters chosen. The fact that the ratio is small close to the conductor aids in the transition from microstrip to guided wave.

The guided wave launched from the microstrip must be directed somehow. This can be accomplished in one of two ways. The thick region of the substrate in which the guided wave travels could be of finite width, perhaps only a wavelength or two wide. The wave would thus be prevented from spreading out laterally. The geometry would be what is called a raised ridge waveguide in the optics community. The second possibility consist of flaring the microstrip out into a horn at the transition, as shown in figure 4. The guided wave will travel out in a beam, in the same manner that a horn antenna works for microwaves in free space. It is thus not necessary that the wave travel in a substrate with a narrow width. This could have a number of advantages in monolithic fabrication.

## V. APPLICATIONS:

A number of possible applications of guided waves are discussed in this section. Because of their low loss, guided waves have an obvious advantage over microstrip lines. At first sight, the increased loss of microstrip lines at higher frequencies may not seem that worrisome, because the size of the circuit is going down as the inverse of the frequency, and the loss is increasing only as the square root of the frequency. This conclusion neglects a number of important factors. The loss is actually increasing at a higher rate, as the surface roughness of the conductor becomes increasingly important at higher frequencies. The second problem is that even in a completely monolithic design, some sections of the circuit must be a considerable distance away from others, and the circuit must communicate with another circuit. These distances will not keep getting indefinitely smaller because of packaging and power dissipation considerations. Guided waves are a good candidate in these situations.

Another application for guided waves is in the area of antenna design. Currently, microstrip antennas are being used as the standard antenna in MMIC applications. They have a number of serious limitations, however. They are narrow band, typically only having a bandwidth of a few percent unless special efforts are made (Bahl and Barthia). It is possible that a type of guided wave antenna may give much greater bandwidth at higher frequencies. A possible geometry is shown in figure 5. The microstrip line excites a guided wave by means of the methods discussed in the last section. If the substrate is terminated, the wave will travel on into free space. The guide can end at right angles, or it can end at an angle of forty five degrees as shown in figure 5. If it is terminated by a right angle, the wave will launch out of the end of the dielectric. If terminated at forty five degrees, it will launch at right angles to the guide.

This type of antenna has a number of inherent advantages. It does not rely on any resonance in the structure. It therefore is inherently broadband in nature. It is not necessary to metallize any of the surfaces. It therefore is low loss. A number of constraints must be observed, however. The guide cut at forty five degrees works essentially as a ray optics antenna. It is therefore essential that the thickness of the dielectric waveguide be several wavelengths. In other words, the guide should be overmoded. (For the endfire case, this may not be necessary.) A certain amount of energy will be reflected back from the interface. This will go as:  $\left[ (\sqrt{\epsilon_r} - 1) / (\sqrt{\epsilon_r} + 1) \right]^2$ . For  $\epsilon_r = 12.9$ , this gives 32 percent of the power reflected. This is not an acceptable level for most applications. There are two possible solutions to this

0.1/ $D$  to 0.4/ $D$  is possible. Assuming, for example:  $k_0/\beta = 0.5$ ;  $f = 100\text{GHz}$ ;  $k_0 = 2.1 \times 10^3\text{m}^{-1}$ ;  $\epsilon_r = 12.9$ . If  $R = 1\text{ cm}$ ,  $\alpha = .41D$ , and  $L = 3D$ , then:  $Q = 1500$ . This is the unloaded  $Q$ . There are small gaps in the reflectors appearing at one end of the resonator in order that energy may be coupled in and out. Such a  $Q$  compares favorably with the  $Q$  of order 100 possible using a microstrip. It does not take more space to make such a resonator, but this may not be that much of a sacrifice at millimeter wave frequencies. It should be noted that the intrinsic upper limit to the  $Q$  for a GaAs substrate is about 10,000, because of the loss tangent of the material.

## VI. RECOMMENDATIONS:

The work carried out this summer has been an effort to examine the feasibility of using guided waves in MMIC's. The work has been of a preliminary nature, using physical arguments and order of magnitude calculations. What is now needed is a careful experimental and theoretical study of the problems.

The best place to start is to construct a microstrip to guided wave transition using the guidelines presented in this report. This should be possible to do using relatively modest laboratory facilities. The electrical parameters of the transition should be carefully measured using a network analyzer if available. It is planned to submit a proposal, in which the measurement process will be described in greater detail. The next step is to build the proposed broadband antenna using the network analyzer again to measure the electrical parameters. In addition, it is important to measure the radiation pattern of the antenna if the equipment is available.

It is important to carry out a careful theoretical study of the transition as an aid to understanding the physics involved and thereby improve the design. This type of problem has not been analyzed before, but the problem is similar in concept to a number of well known problems. Techniques used in the analysis of waveguide transitions and the design of horns should be applicable. Details of the methods will be supplied in the proposal.

Finally, if time permits, it would be nice to build a resonator to see if the concept is indeed viable at millimeter wave frequencies.

problem. The first is to use a substrate with a lower dielectric constant. For example, if  $\epsilon_r = 2.1$ , then 3 percent of the power is reflected, a much better match. Another possibility is to place a  $1/4$  thick matching layer on top of the antenna. This will decrease the bandwidth, however. The antenna will take up more space than a microstrip which is typically only  $1/2$  a wavelength long. At high frequencies, however, the premium placed on wide bandwidth and high radiation efficiency may well outweigh the extra space used. If the antenna were three wavelengths by three wavelengths, this would still only be a fraction of a centimeter of area at millimeter wave frequencies.

Another possible application for surface waves is that of a high  $Q$  resonator or filter. Such a resonator may be desirable at the input and output stages of an amplifier. At lower frequencies, ceramic resonators have become popular. They can give  $Q$ 's greater than 1000 (Wakino et al.). However, their size becomes a problem at millimeter wave frequencies; they are too small to be cheaply used. A guided wave could be used instead. It is contained in a Fabrey-Perot resonator in a way similar to optics, figure 7. The essential difference is that such a device would be built into the circuit monolithically, and a distributed Bragg reflector would be used instead of metal mirrors. The Bragg reflector consists of metallic strips etched on top of the guide. These strips are spaced so that the guided wave cannot pass underneath them. The theory of Bragg reflection is well developed (Yariv, Elachi). A small amount of the wave is reflected back from each strip. If the spacing is chosen right, the reflection from each strip will add coherently to produce a large reflection. This spacing must satisfy the Bragg condition, for which:

$$\beta D = \pi \quad (14)$$

$D$  is the length between centers of the strips. Assuming a substrate of GaAs at 100 GHz,  $D = 1.36$  mm.

It is of interest to calculate the  $Q$  of the resonator. To do this accurately requires a detailed analysis. However, a simple order of magnitude estimate may be obtained by assuming a  $TM_0$  mode propagating between two mirrors. The  $Q$  is defined to be the ratio of the energy in the volume divided by the power lost through the ends of the resonator, and multiplied by the angular frequency. If the energy is assumed to be uniformly distributed:

$$Q \sim (k_0^2 \epsilon_r R / \beta) \exp(2\alpha L) \quad (15)$$

$R$  is the length of the resonator.  $\alpha$  is the decay length in the Bragg region of the strips.  $L$  is the length of the strip region. In order to find  $\alpha$ , a detailed analysis is necessary. It appears an  $\alpha$  in the range of

## REFERENCES

Bahl, I.J., and P. Bhartia, Microstrip Antennas, Norwood, MA, Artech House, 1980.

Collin, R.E., Field Theory of Guided Waves, N.Y., N.Y., McGraw-Hill, 1960.

Elachi, C., "Waves in Active and Passive Periodic Structures: A Review," Proceedings of the IEEE, December, 1976, Vol.64, No.12, pp. 1666-1698.

Gupta, K.C., R. Garg, and R. Chadha, Computer-Aided Design of Microwave Circuits, Norwood, MA, Artech House Inc., 1981.

Pucel, R., "Design Considerations for Monolithic Microwave Circuits," IEEE Transactions on Microwave Theory and Techniques, June, 1981, vol. MTT-29, No.6, pp. 513-534.

Wakino, K., T. Nishikawa, H. Tamura, and T. Sudo, "Dielectric Resonator Materials and their Applications," Microwave Journal, June, 1987, pp. 133-150.

Walther, C.H., Traveling Wave Antennas, NY, NY, Dover, 1965.

Yariv, A., Optical Electronics, NY, NY, Holt, Rinehart, and Winston, 1985.

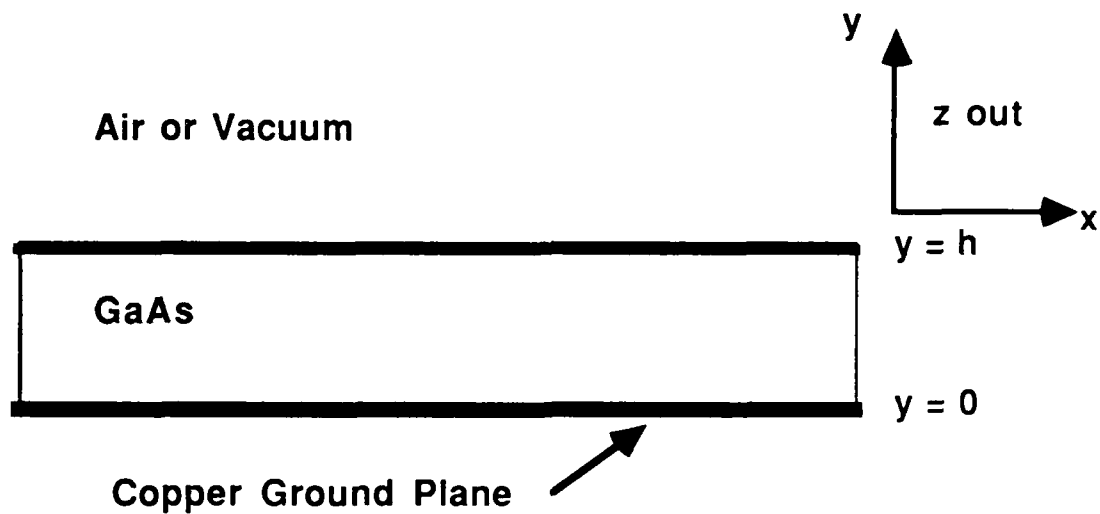


Figure 1: Guided wave geometry.

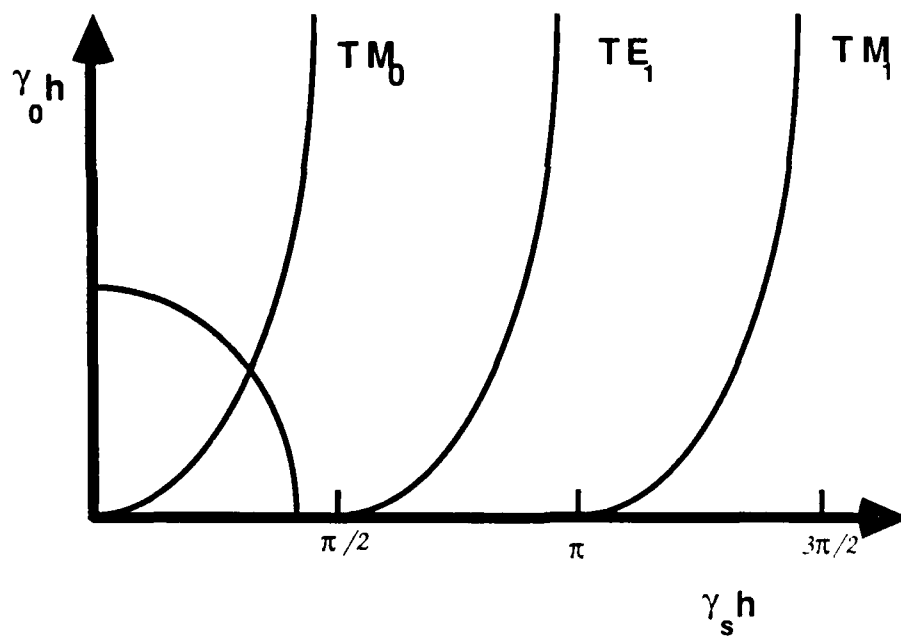


Figure 2: Graphical solution of the transcendental equations. The point of intersection gives the mode value. The radius of the circle is  $k_0 h \sqrt{\epsilon_r - 1}$ .



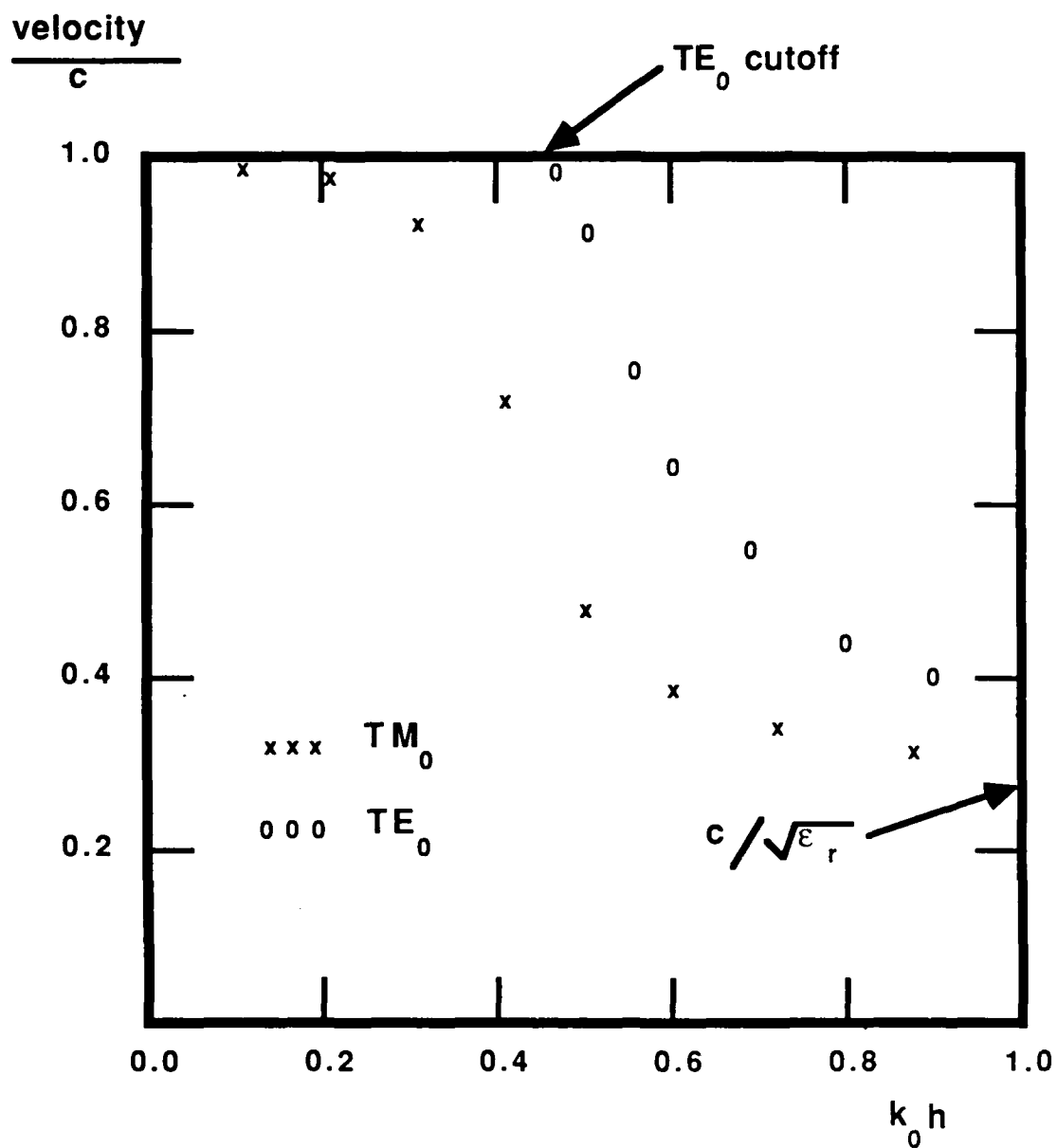


Figure 3: Graph of the wave velocity vs.  $k_0 h$  for the  $\text{TM}_0$  and  $\text{TE}_1$  modes.

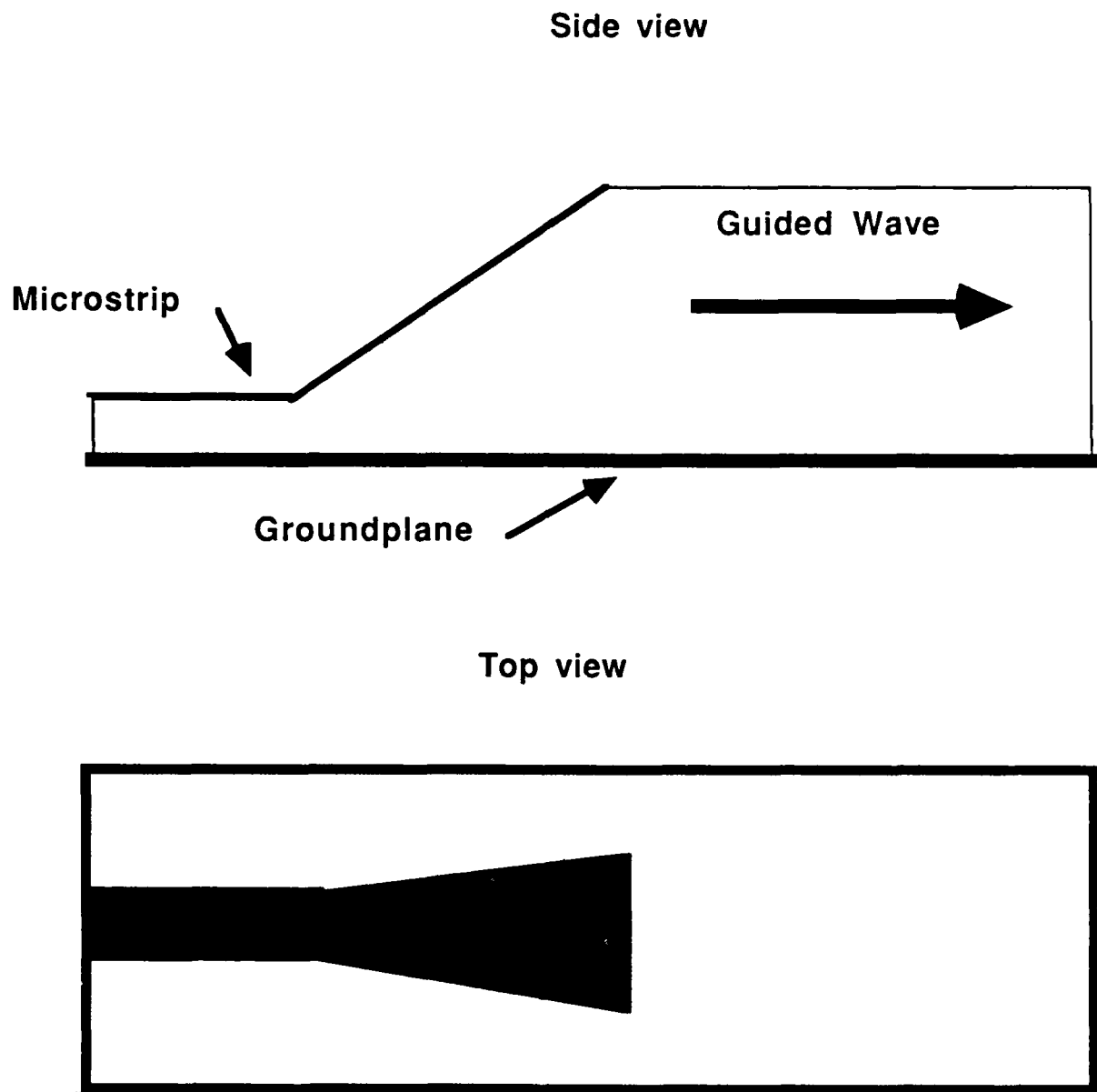


Figure 4: Microstrip to guided wave transition using gradual transition.

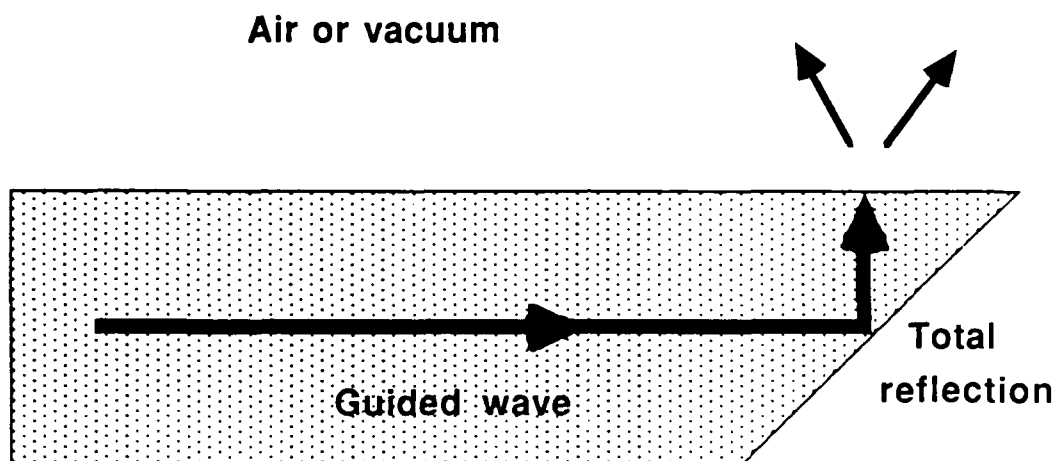


Figure 5: The guided wave is internally reflected to form a broad band antenna.

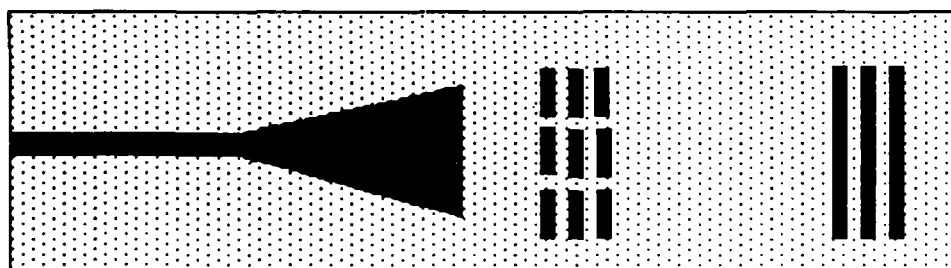


Figure 6: High Q resonator. The side view looks like that in figure 4.

1987 USAF-UES SUMMER FACULTY RESEARCH PROGRAM

GRADUATE STUDENT SUMMER SUPPORT PROGRAM

Sponsored by the

AIR FORCE OFFICE OF SCIENTIFIC RESEARCH

Conducted by the

Universal Energy Systems, Inc.

FINAL REPORT

SLEW-COUPLED STRUCTURAL DYNAMICS IDENTIFICATION AND CONTROL

Prepared by:	Thomas A. W. Dwyer, III, Ph.D.
Academic Rank:	Associate Professor
Department and University	Aeronautical and Astronautical Engineering Department University of Illinois at Urbana-Champaign
Research Location	AFWL/ARBC Kirtland AFB, NM 87117-6008
USAF Researcher	Captain Robert D. Hunt, USAF
Date	28 September 1987
Contract No:	F49620-85-C-0013

Slew-Coupled Structural Dynamics Identification and Control

by

Thomas A. W. Dwyer, III

ABSTRACT

Dynamic system identification and control algorithms are derived in this report for slew-induced deformation shaping of elastic rotational structures.

In particular, the importance of the coupling matrix between rotational and vibrational accelerations is exhibited, for use both in structural system identification and for the control of acquisition, tracking and pointing maneuvers.

A possible experiment for the validation of such identification and control algorithms on available Air Force Laboratory facilities is also described.

### Acknowledgments

The methods leading to the research program described in this report were formulated during the author's tenure as a Summer Faculty Research Fellow in the ARBC Branch of the Air Force Weapons Laboratory, in the Summer of 1967.

The author wishes to thank the collaboration of Kenneth C. Jenks and James W. Wade, who accompanied him under the auspices of the Graduate Student Summer Support Program. Their own work under the author's supervision is reported elsewhere.

The author and his students also hereby thank Captains Robert D. Hunt and James W. O'Connor, Lieutenant Mark Ponti, Mr. Dave Founds and Dr. Craig Myers of AFWL/ARBC for their valuable advice and support.

## 1. INTRODUCTION

The research program in progress at the Space Systems Laboratory, directed by this investigator at the University of Illinois, addresses among other topics the interactions among structural dynamics, optical alignment when needed, and boresight pointing control of space-based weapons systems or scientific instruments.

The activity herein discussed is thus intended to support the larger scope of research on control and structures interaction for target acquisition, tracking, pointing and fire control which has been receiving increased attention, such as in [1] and [2].

Much of the work pushing performance in this area has been at the analytical level. Feasibility demonstrations thereof on prototype real systems are therefore of great interest to the technical community as a guide to future research directions to be taken.

In particular, AFWL (Air Force Weapons Laboratory) interests in this area include ACE (Active Controls Experiment), ABES (Aluminum Beam Expander Experiment) and the new tentatively named SPICE project (Space Integrated Controls Experiment). Likewise the proposed ASTREX (Advanced Space Structures Research Experiments) program at AFAL (Air Force Astronautics Laboratory) addresses such topics [3], [4].

The research program described herein in furtherance of such interests is focused on the eventual experimental demonstration of a specific controls and structures interaction technique, presently labeled "Slew-Induced Deformation Shaping Control." The method used is the injection (feedforward) of commanded boresight kinematics information into structural control equations, to force the coupled rigid (e.g., boresight) and flexible (e.g., support structures and

optics) dynamics to evolve in a constrained manner: the result is that low bandwidth correction of slew torque commands is thereby made possible to permit precision slewing despite slew-excited structural deformation, with weak structural control augmentation.

## 2. SLEW-COUPLED DYNAMICS

Algorithmically, the methods proposed herein can be most simply described in terms of rotating a beam. Let then  $u(x, t)$  denote the lateral deflection at a position  $x$  from the center of an Euler-Bernoulli beam. Let also  $\phi_i(x)$  denote a cantilever mode shape and  $q_i(t)$  a corresponding generalized coordinate for the half beam, so that one has:

$$u(x, t) = \sum_i q_i(t) \phi_i(x)$$

If the beam rotates about its center, with an angular attitude of  $\theta(t)$  radians, then the (linearized) dynamical model given below,

$$J\ddot{\theta} + c\dot{\theta} + k\theta + \underline{d}^T \ddot{\underline{q}} = \tau_j + \tau_1 + \tau_2 + \dots + \tau_n \quad (2.1)$$

$$M \ddot{\underline{q}} + C\dot{\underline{q}} + K\underline{q} + \underline{d}\ddot{\theta} = \underline{u}_1 + \underline{u}_2 + \dots + \underline{u}_n \quad (2.2)$$

where  $J$  is the hub (e.g., rate table) inertia plus the undeformed beam moment of inertia about the central axis;  $c$ ,  $C$ ,  $k$ ,  $K$  are respectively the axial and structural damping and stiffness coefficients, and  $\underline{d}$  is the coupling coefficient between the rotational and the vibrational dynamics;  $\underline{u}$  stands for



the beam half length;  $B$  and  $\underline{b}$  are respectively the modal coupling coefficients of the structural torque actuators  $\tau = \text{col } \{\tau_i, y\}$  along the beam, and of transversal forces  $f$  symmetrically applied to the beam tips. Finally, by  $\tau_0$  is meant a central torque at the hub (e.g., rate table).

The structural mass matrix  $M$ , structural stiffness matrix  $K$ , the structural torque and force coupling matrices  $B$  and  $\underline{b}$ , and also the coupling matrix  $\underline{d}$  between structural dynamics and slew dynamics can be computed in terms of integrals of the assumed cantilevered mode shapes  $\phi_i(x)$  and mode slopes  $d\phi_i(x)/dx$ , as is shown in [5] and [6]. The analytical modeling of the structural damping matrix  $C$  is not as easily obtained, and is the object of current research at AFWL, in collaboration with Sandia National Laboratories [7].

For the demonstration of the proposed slew-induced deformation shaping control techniques described herein, good estimates of  $M$ ,  $C$ ,  $K$ ,  $\underline{d}$ ,  $J$ ,  $c$ ,  $k$  are needed, as is shown in the algorithms in [8], [9], [10], [11], also to be reviewed in the last section of this proposal. The first needed task is therefore the development of a system identification scheme, described next.

### 3. SLEW-COUPLED SYSTEM IDENTIFICATION

By suitable adaptation of the parameter estimation procedure given in [12], [13], let there be only centrally applied variable torque commands  $\tau_0$ , so that  $\tau_i = 0$  for all  $i \geq 1$  (i.e.,  $\underline{\tau} = 0$ ), and  $f = 0$  in Eqs. (2.1) and (2.2). It shall be assumed that the undeformed system's central moment of inertia  $J$  has been independently determined such as by geometric means, from static knowledge of the rate table and beam dimensions, or by other static means.

### 3.1 SLEWING DYNAMICS IDENTIFICATION

If the effective central torque  $\tau_c$ , defined as shown below,

$$\tau_c = \tau_o - c\dot{\theta} - k\theta \quad (3.1)$$

is directly sampled, as well as angular accelerometer and structural accelerometer readings, at times  $t_j$ ,  $j = 1, \dots, m$ , then the coupling matrix  $\underline{d}$  can be obtained by batch least squares solution of the equation below,

$$G^T(t_1, \dots, t_m) \underline{d} = \underline{u}(t_1, \dots, t_m) \quad (3.2)$$

where the  $n \times m$  matrix  $G = [\underline{g}_1 | \underline{g}_2 | \dots]$  has its  $j$ -th column given below,

$$\underline{g}_j = \ddot{\underline{q}}(t_j) \quad (3.3)$$

and the matrix  $\underline{u} = \text{col } \{u_j\}$  has its  $j$ -th entry given as shown:

$$u_j = \tau_c(t_j) - J \ddot{\theta}(t_j) \quad (3.4)$$

Here  $m$  is the number of time samples and  $n$  is the number of assumed modes. If  $m \geq n$  one then has:

$$\hat{\underline{d}} = [GG^T]^{-1} G \underline{u} \quad (3.5)$$

If only the commanded central torque  $\tau_0$  can be directly measured, then the axial damping and stiffness coefficients  $c$  and  $k$  can be simultaneously estimated with the structural acceleration coupling coefficient matrix  $\underline{d}$ : in this case samples of angular attitude  $\theta$  and angular rate  $\dot{\theta}$  must be available, either by optical or gyroscope readings. Then  $\underline{d}$  is replaced by  $\text{col}\{\underline{d}, c, k\}$  in Eq. (3.2), where the  $j$ -th column  $\underline{g}_j$  of  $G$ , which is now  $(n + 2) \times m$ -dimensional, is then given as shown below,

$$\underline{g}_j = \text{col}\{\ddot{\underline{q}}(t_j), \dot{\theta}(t_j), \theta(t_j)\} \quad (3.6)$$

while the effective central torque  $\tau_0$  is replaced by the commanded central torque  $\tau_0$  in the definition of the  $j$ -th entry  $u_j$  of  $\underline{u}$ . One must now have  $m \geq n + 2$ , to compute the counterpart of Eq. (3.5), with  $\underline{d}$  replaced by  $\text{col}\{\underline{d}, c, k\}$ .

### 3.2 STRUCTURAL DYNAMICS IDENTIFICATION

Once the coupling coefficient matrix  $\underline{d}$  between Eqs. (2.1) and (2.2) has thus been estimated, the structural matrices  $M$ ,  $C$ ,  $K$  can likewise be obtained by least squares solution of the equation below,

$$[M \ C \ K] H(t_1, \dots, t_m) = -\hat{\underline{d}} \underline{u}^T(t_1, \dots, t_m) \quad (3.7)$$

where the  $j$ -th column of the  $m \times 3n$  matrix  $H = [\underline{h}_1 | \underline{h}_2 | \dots]$  is given as follows,

$$\underline{h}_j = \text{col}\{\ddot{q}(t_j), \dot{q}(t_j), q(t_j)\} \quad (3.8)$$

while the  $j$ -th entry of the  $m \times 1$  matrix  $\underline{\alpha} = \text{col}\{\alpha_j\}$  is given by sampled angular accelerometer readings:

$$\alpha_j = \ddot{\theta}(t_j) \quad (3.9)$$

If  $m \geq 3n$  then one finds:

$$[\hat{M} \hat{C} \hat{K}] = -\hat{d} \underline{\alpha}^T [H H^T]^{-1} \quad (3.10)$$

### 3.3 TUNING THE IDENTIFICATION ALGORITHMS

For the existence of generalized inverses in Eqs. (3.5) and (3.10), not only must one have a sufficient number of time samples as given above, but also the torque inputs  $\tau_o(t_j)$  must yield linearly independent columns in the matrices  $G$  and  $H$ .

The choice of excitation waveforms is still a subject of research in the discipline of system identification, but for our eventual experimental purposes they can be expected to be obtainable by trial, preceded by simulation studies using prior estimates of the system model coefficients from mode shape integrals.

It should also be noted that no tip structural actuation forces  $f$  nor distributed beam actuation torques  $\tau_i$  are necessary above. These other possible control sources would come into play only in the experimental estimation of the actuator modal coupling gain matrices  $\underline{b}$  and  $\underline{p}$  in Eq. (3.2), after estimation of the other coefficient matrices from central torque excitations.

#### 4. SLEW-INDUCED DEFORMATION SHAPING CONTROL

Structural deformation coupling effects on boresight pointing can be canceled by several means, all of which are generally effective only if accurate values are known for the structural parameters, which are therefore to be previously identified, as discussed in the previous section.

##### 4.1 SLEW TORQUE SHAPING

If  $\hat{\theta}^*(t)$  denotes the angular attitude profile of a desired pointing maneuver, then the corresponding commanded torque profile can have the form below,

$$\tau_o^* = \tau_o^* + \tau_e - a_1(\hat{\theta} - \hat{\theta}^*) - a_0(\hat{\theta} - \hat{\theta}^*) \quad (4.1)$$

where one has the commanded rigid body torque  $\tau_o^*$

$$\tau_o^* = J\ddot{\theta}^* + c\dot{\theta}^* + k\theta^* \quad (4.2)$$

and the structural interaction correction  $\tau_e$ ,

$$\tau_e = \hat{d}^T \hat{z} \quad (4.3)$$

where hats denote estimated constants and signals. The feedback gains  $a_1$  and  $a_0$  are selected to dampen transients due to initial boresight attitude and

rate errors from  $\theta^*$  and perturbations due to unmodeled central disturbance torques.

One limitation of the slew torque control law above is that of the slew actuator bandwidth requirements imposed by the structural interaction correction torque  $\tau_e$ . Two low bandwidth alternatives to direct generation of  $\tau_e$  from structural accelerometers or other structural sensors are outlined below, derivations of which can be found in [8], [9], [10], [11], themselves inspired in recent work on the control robots with elastic joints, such as in [14].

#### 4.2 STRUCTURAL DEFORMATION SUPPRESSION

Suppression of slew-induced structural excitation can be obtained by simultaneous feedforward into the structural actuators of boresight angular acceleration commands, by choosing  $\underline{r}$  and  $f$  in Eq. (2.2) to yield the following "strong" structural control:

$$\hat{A}(\hat{\underline{r}} + \hat{\underline{D}} f) = \underline{u}_0^* - A_1 \hat{\underline{q}} - A_0 \hat{\underline{q}} \quad (4.4)$$

where the rigid body feedforward term  $\underline{u}_0^*$  is given below:

$$\underline{u}_0^* = -\hat{\underline{d}} \ddot{\theta}^* \quad (4.5)$$

Again hats everywhere denote estimated quantities, while the feedback gain matrices  $A_0$  and  $A_1$  are selected for fast damping of initial transients or for reduction of the effects of unmodeled structural disturbances. In this case one may set

$$\tau_0 = 0 \quad (4.6)$$

in Eq. (4.1) if the transient structural excitations can be tolerated, thus yielding a low bandwidth slew torque  $\tau_0$ .

One limitation of the slew control scheme proposed above is the structural actuator dynamical range requirements imposed by the feedforward term  $\hat{d}\ddot{\theta}^*$  in the case of rapid retargeting maneuvers, as discussed by the author in the case of rail gun fire control in [6]. A low bandwidth and low amplitude control scheme can then be employed instead, as is discussed next.

#### 4.3 STRUCTURAL DEFORMATION SHAPING

As is shown in [8], [9], [10], [11], it is possible to shape, rather than suppress, the slew-induced structural excitation, whereby the deformations are made to be proportional to the commanded slew acceleration, after decay of a fast transient. For this, the structural tip forces  $f$  and distributed beam torque commands  $\underline{t}$  are chosen to yield the following "weak" structural control: in Eq. (4.5), the term  $\underline{u}_0^*$  is replaced by  $\underline{u}_1^*$  defined below,

$$\underline{u}_1^* = -\hat{M}\hat{K}^{-1}\hat{d}\ddot{\theta}^{*(4)} - \hat{C}\hat{K}^{-1}\hat{d}\ddot{\theta}^{*(3)} \quad (4.7)$$

where the parenthetical superscript  $(n)$  denotes the  $n$ -th time derivative.

With the slew feedforward term  $\underline{u}_1^*$ , the forced structural response to the slew-induced excitation is then shown in the above-mentioned references to be given by  $\underline{q}(\text{forced}) = \underline{q}^*$ , where  $\underline{q}^*$  is expressed below in terms of the commanded slew acceleration:

$$\underline{q}^* = -\hat{K}^{-1} \hat{d} \ddot{\theta}^* \quad (4.8)$$

The full structural control with correction for the error  $\underline{q} - \underline{q}^*$  is then given by the following modification of Eq. (4.4):

$$(\underline{u}_1 + \underline{bf}) = \underline{u}_1^* - A_1(\dot{\underline{q}} - \dot{\underline{q}}^*) - A_0(\underline{q} - \underline{q}^*) \quad (4.9)$$

In this case the low bandwidth structural distortion correction torque  $\tau_e$  in Eq. (4.1) is seen to have the following form, after decay of fast structural transients by virtue of  $A_0$  and  $A_1$ :

$$\tau_e = -\hat{d}^T \ddot{\underline{q}}^* \quad (4.10)$$

#### 4.4 TUNING THE CONTROL ALGORITHMS

It is important to observe that the factor  $\hat{K}^{-1}$  has the effect of greatly reducing the magnitude of the structural shaping control  $\underline{u}_1^*$  compared with  $\underline{u}_0^*$ , as well as still yielding a low bandwidth slew torque correction in the form of Eqs. (4.10) with (4.8), where only rigid body information is used, compared with Eq. (4.3), where the full and persistently excited modeled structural frequency spectrum is present.

A trade-off that does appear here, however, is the need for commanded angular jerk rate information, which increases the real time signal processing complexity of target tracking, but is of no concern for target acquisition (retargeting).



In fact, as shown in [8], [9], [10], [11], successively weaker structural actuator inputs can be alternatively generated, at the cost of the need for successively higher derivatives of commanded slew rates, there being therefore designer-selected trade-offs among slew actuator bandwidth, structural actuator dynamical ranges and the signal processing complexity of boresight tracking.

Finally, it is shown in the above-mentioned references that multi-axial slewing can be likewise accommodated, wherein nonlinear control laws come into play, while "sliding mode" methods of variable structure control can also be used for increased robustness with respect to model errors, as is shown in [15].

## 5. EXPERIMENTAL REQUIREMENTS

The simple beam slewing model used in the preceding sections can be implemented on existing or proposed experimental testbeds, e.g., the AFAL-supported C. S. Draper Laboratories' four spoke hub, or with the ACE or SPICE facilities under current development at AFWL.

A simple beam is to be horizontally placed on a rate table equipped with a central variable torque actuator or with opposing tip forces such as AFAL/Draper's, or equivalently with linear motors around the rate table, such as at AFWL. A rotational accelerometer is to be centrally co-located with the central slew torque axis.

The beam is to be symmetrically placed, with identical transversal accelerometers at each tip. Additional structural accelerometers could also be placed along the beam, for multi-mode sensing, or else distributed piezo-

electric sensors could be bonded with the beam. Integrated or directly sensed transverse modal deflections and deflection rates are also needed, both for parameter estimation and structural feedback control.

The apparatus described above is sufficient for system identification. For demonstration of slew-induced deformation shaping control it is necessary to also use co-located PMA's (Proof Mass Actuators), such as the combined accelerometers and VCA's (Voice Coil Actuators) available from Harris Corporation [16].

Likewise, PVF2 (Polyvinylidene Fluoride) piezoelectric membranes are presently used for distributed beam control on the AFAL/Drapeer apparatus, and similar ceramic sensors and actuators are being presently used for flexible robot research at Sandia National Laboratories, co-located with AFWL.

As to the beam itself, current ACE experimental work being done at AFWL on the "ACE Quadrapod", wherein eight spare truss beams are available, presently concerns the determination of the effectiveness of viscoelastic constrained layer damping to obtain prescribed damping ratios and structural stiffness characteristics.

The successive use of two such ACE Quadrapod legs, one treated for damping augmentation, and one untreated, should yield the by-product result of determining the effect of such passive damping augmentation on the "off-diagonal" system mass matrix coupling, given by  $\underline{d}$  in Eqs. (2.1) and (2.2), between the structural dynamics and the "slew dynamics" of the beam.

The rate table to be used could then be the one presently available for the proposed SPICE experiments at AFWL, with required sampled data acquisition and processing executable with a presently available and co-located dedicated VAX computer.

The alternative or supplemental use of the existing AFAL/Draper apparatus would of course entail no new hardware, but would be more suited to eventual extension of such demonstrations to a distributed control formulation, presently less developed at the theoretical level. Moreover, slew torques in that apparatus are presently commanded with tip forces rather than hub forces, thereby bringing additional beam flexibility considerations to bear on slew torque command generation, even for system identification.

## 6. SUMMARY

It has been shown herein how the knowledge of the coupling matrix between slew acceleration and structural acceleration serves two functions: one is the estimation of other elastic structural parameters, and the other is the synthesis of feedforward rotational dynamics information to weak structural actuators for slew-induced deformation shaping, thereby permitting low bandwidth correction of slew torque commands.

Potential usefulness to ATP/FC applications has also been discussed, as well as the feasibility of testing and evaluation thereof by simple experiments relying on available Air Force Laboratory facilities.

# REFERENCES

- [1] First NASA/DOD Technology Conference (UNCLASSIFIED, Norfolk, VA, Nov. 18-20, 1986).
- [2] Second NASA/DOD Technology Conference (SECRET, Colorado Springs, CO, Nov. 17-19, 1987).
- [3] AFRPL Workshop on Advanced Space Structures and Controls Experiments (UNCLASSIFIED, Edwards AFB, Jan. 22-23, 1987).
- [4] AFAL ASTREX Workshop (SECRET, Edwards AFB, Aug. 20, 1987).
- [5] J. L. Junkins and J. D. Turner, Optimal Spacecraft Rotational Maneuvers, Elsevier, New York, 1986.
- [6] J. W. Wade and T. A. W. Dwyer, III, "Boresight Disturbance Modeling and Control of a Space-Based Electromagnetic Rail Gun," American Control Conf. (Atlanta, GA, June 15-17, 1988).
- [7] Dr. Dan Segalman, Sandia National Laboratories (Kirtland AFB, NM), unpublished report.
- [8] T. A. W. Dwyer, III, "Rapid Retargeting Maneuvers," Technical Report AAE 86-7 (UIUC ENG 86-0507), University of Illinois, Nov. 1986.
- [9] M. F. Lembeck, T. A. W. Dwyer, III and S. A. Volinsky, "A Prototype Expert System for Intelligent Pointing and Tracking Control," Proc. 2nd IEEE Internat. Symp. on Intelligent Control (Philadelphia, PA, Jan. 18-20, 1987).
- [10] T. A. W. Dwyer, III, "Tracking and Pointing Maneuvers with Slew-Excited Deformation Shaping," Proc. AIAA Guidance, Navigation and Control Conf. (Monterey, CA, Aug. 17-19, 1987), AIAA Paper 87-2599-CP.
- [11] T. A. W. Dwyer, III, "Automatically Reconfigurable Control for Rapid Retargeting of Flexible Pointing Systems," SPIE Symp. on Space Station Automation III (Boston, MA, Nov. 1-3, 1987).
- [12] J. L. Junkins, Optimal Estimation of Dynamical Systems, Sijthoff-Noordhoff Co., Alpen van den Rijn, The Netherlands/Rockville, MD, 1978.
- [13] S. L. Hendries, S. Rajaram, M. P. Kamat and J. L. Junkins, "Identification of Mass, Damping and Stiffness Matrices for Large Linear Vibratory Systems," AIAA/AAS Astrodynamics Conf. (San Diego, CA, Aug. 4-11, 1982), Paper AIAA-82-1406.
- [14] K. Khorasani and M. W. Spong, "Invariant Manifolds and their Application to Robot Manipulators with Flexible Joints," Proc. IEEE Internat. Conf. on Robotics and Automation (St. Louis, MO, March 1985, 1985), pp. 975-983.

- [15] T. A. W. Dwyer, III, H. Sira-Ramirez, S. Monaco and s. Stornelli,  
"Variable Structure Control of Globally Feedback-Decoupled Deformable  
Vehicle Maneuvers," Proc. 26th IEEE Conf. on Decision and Control (Los  
Angeles, CA, Dec. 9-11, 1987).
- [16] Dr. John W. Shipley, Harris Corporation: private communication.

1987 USAF-UES SUMMER FACULTY RESEARCH PROGRAM/  
GRADUATE STUDENT SUMMER SUPPORT PROGRAM

Sponsored by the  
AIR FORCE OFFICE OF SCIENTIFIC RESEARCH

Conducted by  
UNIVERSAL ENERGY SYSTEMS, INC.

FINAL REPORT

The Effects of Metal Mutagens on the Synthesis and  
Accumulation of Macromolecules

Prepared By:	Dr. Kiah Edwards III
Academic Rank:	Professor
Department and University:	Biology Department Texas Southern University
Research Location:	USAF/OEHL Brooks Air Force Base
USAF Researcher:	Dr. Bruce Poittrast
Date:	13 September 1987
Contract No.:	F49620-85-C-0013

THE EFFECTS OF METAL MUTAGENS ON THE SYNTHESIS AND  
ACCUMULATION OF MACROMOLECULES

KIAH EDWARDS, III

Cellular and Molecular Biology, Department of Biology,  
Texas Southern University  
Houston, Texas 77004

ABSTRACT

In an effort to further elucidate the profound effects of environmental pollutants on biological systems, this study was undertaken to determine the effects of metal ions on the rate of synthesis and accumulation of total RNA using rabbit uterine DNA. Eight of the metals (cadmium, cesium, cobalt, copper, lead, mercury, selenium and silver) enhanced the initiation of RNA synthesis at concentrations that inhibited overall RNA synthesis. These data indicate that metal mutagens and carcinogens not only decrease the fidelity of DNA replication but also exert their effects at the level of RNA initiation and total RNA synthesis. Additional findings indicate the inhibitory effects of cadmium on the synthesis of protein in rabbit uterine secretions.

#### ACKNOWLEDGEMENTS

The author wishes to express his appreciations to Universal Energy Systems, Dayton, Ohio, for sponsoring this research project and for exposing me to opportunities available in federal environmental research laboratories. Special thanks are extended to Dr. Bruce Poitrast and Colonel Rock of the Occupational and Environmental Health Laboratory at Brooks Air Force Base, San Antonio, Texas.



## INTRODUCTION

Some metals have been shown to react with electron donor sites on nucleic acids and alter the synthesis of gene products, cause base substitution and point mutations and promote carcinoma and/or tumorous growth. Others such as lead, cadmium and copper have been implicated in the stimulation of RNA synthesis (1), inhibition of DNA synthesis (2), misincorporation of bases during DNA replication (3) and superinducing the synthesis of specific proteins while suppressing others (4). Earlier data (5) have indicated that potassium is essential for the transcription of T4 phage DNA and is believed to enhance the activity of the RNA polymerase by promoting the activity of sigma factor and the premature release of elongated RNA chains. Despite this very dramatic effect of metals on DNA synthesis and RNA synthesis few studies have been conducted on the in vivo effects of metals on uterine tissues. In an attempt to study the effects of lead, cadmium and other metals on the synthesis of uterine proteins, the activities of several species of macromolecules critical to the synthesis of proteins were studied, both in vivo and in vitro. Blastokinin, a protein that is found in the uterine fluid of mammals and serves as biochemical marker for the progesterone-mediated stimulation of uterine endometrium during early pregnancy in rabbits, was a specific protein studied (6). Blastokinin has been indicated to have a profound effect on the growth of rabbit blastocysts in vitro and in vivo. Because of the abundance of blastokinin in rabbits, its hormone dependent synthesis and the fidelity of its regulation, both replication and transcription, the synthesis of this protein could serve as an outstanding indicator of mutagenic and carcinogenic environmental contaminants, such as metals. An attempt was made to correlate the in vitro data with the in vivo findings. The results presented in this paper indicated that the heavy metals

inhibited the overall synthesis of RNA, while stimulating the initiation of RNA synthesis and suppressed the accumulation of blastokinin and total proteins in the uterine secretions. The in vitro data indicated, also, that metals required for nucleic acid synthesis also suppress the activity when used in varying concentrations.

## MATERIALS AND METHODS

### Endometrial Flusings

Young, sexually-mature New Zealand White rabbits were obtained from a commercial supplier and maintained under laboratory conditions at least seven days prior to use. Estrous does/or those at progressive stages of pregnancy, were killed by cervical dislocation. The uteri were rapidly excised, washed with chilled saline and cut open along the mesometrial surface. The exposed endometrium was scraped from the surface with a scalpel blade, and the tissue used for extraction. Total time of recovery was usually less than two minutes at 40°C.

### Extraction and Fractionation of DNA

DNA was extracted from tissue (uterine endometrium before and during pregnancy), following the phenol method of Kirby (7). In some preparations the chloroform-isoamyl alcohol method was used to determine if specific DNA;s are selectively lost during deproteinization with phenol (8). Homogenized tissues were resuspended in 0.15M NaCl, 0.015M sodium citrate, pH 7.0 (SSC) and lysed by adding sodium lauryl sulfate (SLS) (Final concentration 0.4%) to teh mixture and stirring for 15-20 minutes. The lysate was extracted twice at room temperature with an equal volume of phenol preequilibrated with SSC and centrifuged at 20,000 xg for one hour. The aqueous supernatent was dialyzed,

overnight, against SSC at 4°C on a magnetic stirrer. Thereafter, it was subjected to sequential digestion first with ribonuclease T1 (Grade III: Sigma Chemical Co.) at a final concentration of 300 g/ml for 2 hours at 37°C with 50 g/ml pancreatic RNase (Calbiochem) for one hour at 37°C and finally with 200 g/ml pronase (Calbiochem) for two hours at 40°C in 2 x SSC. Sometimes the supernatant was digested with pronase and RNase prior to dialysis. After two more SLS-phenol extractions, 2 volumes of 05% ethanol were added, the DNA collected by winding, redissolved in 0.1 x SSC, dialyzed and stored at 4°C.

These procedures yielded DNA of about 300 million daltons, as determined by analytical band sedimentation (9) from previous extractions. The T4 DNA was a gift from Dr. Errol Archibald, Morehouse College, Atlanta, Georgia.

#### In vitro Synthesis of RNA

The experiments to determine the effects of metal mutagens on the synthesis of RNA were carried out using rabbit uterine DNA as a template. Each metal (cadmium, lead, silver, cesium, etc.) was tested at a minimum of six different concentrations, 0.1-2mM, for effects on overall RNA synthesis. The effects of the metals was monitored by the incorporation of <sup>3</sup>H-AMP and <sup>32</sup>P-GMP into RNA. The reaction mixture (0.2ml) for measuring the overall rate of RNA synthesis consisted of 10mM Tris (pH 8.1); 20mM-mercaptoethanol; 10mM mgCl<sub>2</sub>, <sup>3</sup>H-ATP, GTP, CTP, and UTP at 0.25 mM each; 10 g rabbit DNA and 10 g RNA polymerase. Background counts were determined with reaction mixtures devoid of enzymes or DNA. The overall determination of incorporation was assayed on filters with the Beckman LS 800 system and plotted, the percent incorporation of <sup>3</sup>H-AMP versus the concentration of metal. The enzymes and RNA precursors were obtained from New England Nuclear, Boston.

### In vivo Synthesis of RNA

In order to study in vivo protein we injected a saline (0.85%) suspension of the metal into the lumen of one uterine horn and for the control, the saline carrier alone into the other horn. The uterine fluids were harvested on day five of pregnancy and the protein content analyzed by cellulose chromatography and the Lowry method. The endometrium from each uterus was scraped and the total RNA, protein and DNA determined. These data compliment the findings pertaining the levels of blastokinin found in the uterine cavity.

### Column Chromatography

Blastokinin was separated from other proteins in uterine flushing using column chromatography. Approximately 2 ml of sample were loaded onto a 1 x 20cm column of Sephadex G-200 and 0.1 ml fractions collected at 10°C. The samples were monitored at 750 nm. The amount of blastokinin per milligram of total protein was determined using the Lowry method (10) and pooled fractions were further characterized using Sephadex 6B.

### Determination of Proteins and Nucleic Acids

To determine the amount of protein in uterine flushings, 0.2 ml of sample was mixed with the Lowry reagent and the absorbance read in the Gilford 250 Spectrophotometer at a wavelength of 250nm, using Bovine Serum Albumen (BSA) as a standard. RNA and DNA were determined using the modified Resorcinol and Diphenylamine Assays (11) respectively.

## RESULTS AND DISCUSSION

### In vitro Procedures

The experiments to determine the effects of metals on the synthesis of RNA, using rabbit uterine DNA as a template, were monitored by the incorporation of  $^3\text{H}$ -adenosine monophosphate into acid precipitable molecules. Each heavy metal (cadmium, lead, mercury, silver, cobalt and cesium) was tested at a minimum of six different concentrations, 0.1-2.0mM for effects on total RNA synthesis and the rate of initiation. The overall synthesis of total RNA was inhibited by all six of the metals and the order of greater inhibition for each of the metals was:  $\text{Ag}^+ > \text{Hg}^{++} > \text{Pb}^{++} > \text{Cs}^+ > \text{Cd}^{++} > \text{Co}^{++}$  and occurred in the same order with either template. The inhibitory effects were apparent with increasing concentrations of metals and in some instances precipitates were observed in the reaction vessels, especially silver and mercury. Table 1 clearly indicates the effects of increasing concentrations of metals on RNA synthesis to a maximum of total inhibition.

The effects of metals in the rate of RNA initiation was measured in vitro by the incorporation of  $^{32}\text{P}$ -Adenosine and  $^{32}\text{P}$ -Guanosine Triphosphate because both of these nucleotides are incorporated at the 5' ends of newly synthesized RNA polymers and guanosine residues specifically in the cap of heterogeneous RNA. Some of the radiolabel in the RNA polymer represents the poly ( $\text{A}^+$ ) tails found at the 3' end of messenger RNA molecules. At the concentrations of metals that inhibited total RNA synthesis, stimulation of RNA transcription was evident by the incorporation of  $^{32}\text{P}$ -ATP and  $^{32}\text{P}$ -GTP. The rate of initiation was greater with  $^{32}\text{P}$ -ATP than with  $^{32}\text{P}$ -GTP at concentrations of metals which produced 50-60% overall RNA inhibition. These effects were evident with both DNA templates (Tables 1 and 2). The effects of

TABLE 1

EFFECTS OF METAL CHLORIDES ON RNA SYNTHESIS, USING RABBIT DNA AS TEMPLATE

## PERCENT INCORPORATION

Metal Chloride	Concentration (mM)	$^3\text{H}$ -AMP	$^{-32}\text{H}$ -ATP	$^{32}\text{H}$ -GTP
Control	Saline	100.0	100.0	100.0
HgCl <sub>2</sub>	0.10	44.6	150.0	138.6
AgCl <sub>2</sub>	0.10	43.8	148.0	133.4
CdCl <sub>2</sub>	0.33	50.0	186.4	130.1
PbCl <sub>2</sub>	0.10	45.0	160.0	140.0
CoCl <sub>2</sub>	0.75	44.0	319.0	160.0
CsCl	0.15	40.0	142.0	161.0
MgCl <sub>2</sub>	38.0	54.0	68.0	70.0
MnCl <sub>2</sub>	5.0	50.0		

several metals that are not considered to be mutagenic or carcinogenic were examined under similar conditions using both DNA templates. The concentration of each metals ( $Mn^{++}$ ,  $Mg^{++}$ ,  $Li^{++}$ , K) was greater than the heavy metals and at concentrations that inhibited total RNA synthesis by 50-60% there was no evidence of stimulation of initiation (Table 1). The incorporation of  $^{32}P$ -ATP and  $^{32}P$ -GTP into RNA decreased and a more pronounced effect was observed on the incorporation of  $^{32}P$ -ATP (Tables 1 and 2). Results also indicate that concentrations of these metals that inhibited total RNA synthesis by 5-10% also caused decreased chain initiation. These results clearly indicated that the effects on the incorporation of  $^{32}P$ -ATP were greater than on  $^{32}P$ PGTP incorporation during the initiation of RNA transcription. The results also suggest that metal mutagens promote RNA initiation at new sites on the DNA template while light metals used in this study do not. The order of inhibition of these metals on RNA synthesis may be explained by the affinity of the metal for the pyrimidine and purine bases of the template. Density gradient data have shown that heavy metals, such as lead, silver, cesium and mercury bind to the nitrogenous bases and accentuate changes in the buoyant density. This study further suggests that some forms of cancer may be caused by heavy metals binding to the DNA template and affording new sites for the initiation of RNA transcription and producing RNA chains out of sequence and/or activating foreign genes that have been incorporated into the genome.

To determine if heavy metals would affect the transcription of RNA in vivo, we examined the effects of cadmium chloride, a carcinogen and teratogen, on the synthesis of a specific uterine protein, blastokinin. Sexually mature new Zealand White rabbits were mated and sacrificed at progressive stages of pregnancy. The uteri were flushed with chilled phosphate buffer, excised and

TABLE 2

EFFECTS OF METAL CHLORIDES ON RNA SYNTHESIS, USING T4 DNA AS A TEMPLATE

PERCENT INCORPORATION				
Metal Chloride	Concentration (mM)	$^3\text{H}$ -AMP	$^{-32}\text{H}$ -ATP	$^{32}\text{H}$ -GTP
Control	Saline	100.00	100.00	100.0
HgCl <sub>2</sub>	0.10	44.00	148.21	133.20
AgCl <sub>2</sub>	0.10	43.80	145.00	121.10
CdCl <sub>2</sub>	0.33	48.40	160.20	127.11
PbCl <sub>2</sub>	0.10	62.0	134.00	118.20
CoCl <sub>2</sub>	0.75	46.21	230.04	141.00
CsCl	0.15			
MgCl <sub>2</sub>	38.0	40.10	43.10	60.00
MnCl <sub>2</sub>	5.0	43.01	49.50	72.30



cut along the mesometrial surface. The uterine flushings were chromatographed and analyzed. The data indicate that four major classes of proteins are present in the uterine flushings of 5-day pregnant rabbits. The four major peaks represent high molecular weight proteins, hemoglobin, albumin and blastokinin. In the 5-day control blastokinin represents 54% of the total protein in uterine flushings. However, when animals are injected with cadmium chloride, at levels that inhibit total RNA synthesis in vitro, there is a decrease in the amount of total protein in 5-day flushings as well as a decrease in the amount of blastokinin (Table 3). These findings may reflect a stimulation of RNA transcription and an increase in the premature termination of the RNA chains, even though the concentration is higher than the amounts normally found in human (14).

Further studies are required to establish the effects of heavy metals on the in vivo synthesis of RNA and proteins in eukaryotic systems. However, the effects of lead and cadmium have been reviewed thoroughly in the laboratory (12, 13, 14) and humans (15) and it is known to be transferred across the placenta in pregnancy in humans (15), in the rat (16) guinea pig (17) and the mouse. These studies have clearly demonstrated the deposition of lead in the bone and indicate that it may affect the synthesis of macromolecules (proteins, etc.) and affect the developing embryos in pregnant mothers (18, 19).

TABLE 1 and 2

The effects of heavy metal salts on total RNA synthesis and the initiation of RNA transcription. Total RNA synthesis was measured by the incorporation of  $^3\text{H}$ -ATP while initiation was monitored by the amount of radioactive  $^{32}\text{P}$ -ATP or  $^{32}\text{P}$ -GTP.

TABLE 3

The effects of cadmium on the synthesis of uterine proteins. The RNA and DNA determinations are expressed as micrograms per milligram of protein. Cadmium was used at 50 ppm, 100 ppm and 0.33 mM; however, the table indicates the effects at 0.33 mM. Ctrl = Control; Ttl = Total; Preg. = Pregnancy.

TABLE 3

EFFECTS OF \*CADMIUM ON THE SYNTHESIS OF UTERINE PROTEINS

Stage of Preg. (Days)	Protein (mg)		RNA (mg/mg)		DNA (mg/mg)		Blastokinin (% Ttl. Prot.)	
	Ctrl.	CdCl <sub>2</sub>	Ctrl.	CdCl <sub>2</sub>	Ctrl.	CdCl <sub>2</sub>	Ctrl.	CdCl <sub>2</sub>
Estrus	2.26	2.26	18.0	--	188.0	--	--	--
3	2.35	2.33	54.0	--	436.0	--	19.60	--
4	2.40	2.46	171.0	--	520.0	--	38.45	--
5	2.41	2.26	100.0	--	520.0	--	54.26	33.6
6	2.42	2.30	96.0	--	512.0	--	37.00	--
7	2.40	2.41	68.0	--	439.0	--	30.55	--
8	2.37	2.40	38.0	--	307.0	--	10.21	--
9	2.12	2.10	32.0	--	288.0	--	7.93	--
10	2.10	2.10	--	--	268.0	--	--	--

# REFERENCES

1. Hoffman, D. and S. Niyogi. 1977. Science 198:513.
2. Witschi, H. 1970. Biochem. J. 120:623.
3. Bassler, R. 1965. C. R. Searic. Soc. Biol. 159:1620.
4. Luke, M., L. Hamilton and T. Hollocher. 1975. Biochem. Biophys. Res. Commun. 62:497.
5. Richardson, J. 1970. J. Mol. Biol. 49:235.
6. Krishnan, R. and J. C. Daniel. 1967. Science 158:490.
7. Kirby, K. S. 1957. Biochem. J. 66:495.
8. Skinner, D. and L. Triplett. 1967. Biochem. Biophys. Res. Comm. 28:892.
9. Studier, F. 1965. J. Mol. Biol. 63:409.
10. Amveller, G. 1985. Histochemistry 83:413.
11. Donald, J., M. Cutler and M. Moore. 1986. Environ. Res. 41:420.
12. Angell, N. and J. Lavery. 1982. Am. J. Obstet. Gynecol. 142:40.
13. Daniellson, B., L. Dencker and A. Lindgreen. 1983. Arch. Toxicol. 54:97.
14. Harris, P. and M. Holley. 1986. Pediatrics 49:606.
15. Green, M. and N. Gruener. 1974. Res. Commun. Chem. Pathol. Pharm. 8:735.
16. Kelman, B. and B. Walter. 1980. Proc. Soc. Exp. Biol. Med. 163:278.
17. Clarren, S., D. Bowden and S. Astley. 1987. Teratology 35:345.
18. Neubert, D., I. Chahoud, T. Platzek and R. Meister. 1987. Arch. Toxicol 60:238.
19. Baranski, B. 1987. Environ. Res. 42:54.

### FIGURE 1

The effect of increased concentrations of heavy metal salts on the synthesis of RNA 0----0  $\text{AgCl}_2$ , x----x  $\text{PbCl}_2$ , .----.  $\text{CsCl}$ , []----[]  $\text{CdCl}_2$ , {}----{}  $\text{CoCl}_2$ . The incorporation of  $^3\text{H}$ -ATP is used as the measure of synthesis.

### FIGURE 2

The effect of non-mutagenic or carcinogenic metal salts on total RNA synthesis using rabbit DNA as template.

### TABLE 1

The effect of heavy metal salts on total RNA synthesis and the initiation of RNA transcription. Total RNA synthesis was measured by the incorporation of  $^3\text{H}$ -ATP while initiation was monitored by the amount of radioactive  $^{32}\text{P}$ -ATP or  $^{32}\text{P}$ -GTP.

1987 USAF-UES SUMMER FACULTY RESEARCH PROGRAM

GRADUATE STUDENT SUMMER SUPPORT PROGRAM

Sponsored by the

AIR FORCE OFFICE OF SCIENTIFIC RESEARCH

Conducted by the

UNIVERSAL ENERGY SYSTEMS, INC.

FINAL REPORT

- PROJECT 1 :      Scaling Laws of Two-Dimension  
                  Nozzle Plumes.
- PROJECT 2 :      Design of a Mechanism to Control  
                  Turbulence Levels in Wind Tunnels.

Prepared by :            Marco A. Egoavil, PhD

Academic Rank :        Associate Professor

Department and        Mechanical Engineering,  
University :            University of Puerto Rico

Research                USAF/ARNOLD  
Location :              Arnold AFB, TN 37389

USAF Researcher :      Project 1 : Tom Bentley  
                          Project 2 : Daryl Sinclair

Date :                  September 7, 1987

Contract No. :         F49620-85-C-0013

## SCALING LAWS OF 2-D NOZZLE PLUMES

by

Marco A. Egoavil

### ABSTRACT

The design of high performance aircraft features two dimensional nozzle with known infrared radiation characteristics. Mean velocity and temperature profiles of rectangular outlet nozzles plumes having different aspect ratios and nozzle geometries must be established.

Scaling laws for the calculation of 2-D nozzle plumes under a free velocity field have been developed. The modeling technique used by other investigators in solving the problem under static conditions, has been extended to the present case, which involves 2 different boundary conditions of free stream velocities.

The main element of the model is a scaling factor as a fraction of the axial distance of the plume. The present study proposes that the representation of the scale factor be taken as follows : a straight line equation for the constant velocity free stream field; a second degree equation for the boundary layer velocity free stream field; and the third degree equation for the 2-D nozzle plume flow field.

The plume flow field and the external flow have a matching region that is defined by applying the conservation of mass equation.

The validation of the proposed method is part of the proposal that will be presented to the Air Force by the University of Puerto Rico.

## ACKNOWLEDGEMENTS

First of all, I appreciate the opportunity to develop this research project, assigned to me by the Air Force Systems Command and the Air Force Office of Scientific Research.

I would like to extend my thanks to Universal Energy Systems for their support in all the administrative and directional aspects of this program, and to express my recognition to Marshall Kingery, my effort focal point at Arnold Engineering Development Center. Without Mr. Kingery's support, it would not have been possible to run the experiments.

Tom Bentley afforded an enjoyable working atmosphere, guided me to clear paths to solving problems and encouraged the writing of a proposal as a follow-up to this research, while Wallace Luchuk provided moral and technical assistance to obtain wind tunnel experimental data.

The influence of Daryl Sinclair was invaluable in the planning of the Wind Tunnel Experiments and of the second proposal that I intend to submit to the Air Force at a later date.



## I. INTRODUCTION

Present high performance aircraft features two dimensional nozzles. To design two dimensional nozzle of minimum size and weight, the plume infrared (IR) radiation characteristic should be known. It is required to know mean velocities and temperature profiles of rectangular jets having different aspect ratios and nozzle geometries. Significant advances have been made analitically and experimentally in this area. but there is a need for simple analysis and formulas to treat a number of mixing problems and to predict complete turbulent jet flow fields. Applying Navier-Stokes equations solves the problem completely. However, when in presence of turbulent mixing, engine swirling and by pass-air mixing, such coding could be very laborious and computer resource might be overly expensive to run.

My research interest have been in the area of turbulent flow, combustion and computational gas dynamics. As a result of my extensive experience as a Mechanical Engineer and my deep interest in research, I was given the opportunity for the AEDC assignment to work with Mr. Tom Bentley of Sverdrup/AEDC during the Summer 1987 Air Force Research Program.

## II. OBJECTIVES OF THE RESEARCH EFFORT

The objective of this research is to theoretically predict a 2-D nozzle plume behavior when exhausted into a non-stationary air flow field.

This problem has been studied and solved by Chu, et al [1] for a simple 2-D-Nozzle for IR Analysis at static boundary conditions. The solution is obtained through a model constructed by splitting a properly scaled axisymmetric plume and inserting a rectangular section of

constant properties lines in between. This scaling method, applied to the boundary conditions, either to a free constant velocity field, or to a boundary layer field will provide the required data upon applying mass continuity law to the external stream flow and the plume flow field.

The output of this project will be compared with experimental and computational data obtained at the Arnold Engineering Development Center.

### III. MODELING TECHNIQUE

The technique is based on detailed flowfield properties of axisymmetric nozzle plumes. A scale factor obtained by the modeling is applied to the above properties in order to determine the flow characteristics of the 2-D nozzle plume.

The method is based on the application of conservation of mass law  $\rho VA$ , where the product of density  $\rho$ , times velocity  $V$  is replaced by the scale factor  $f$ . This scale factor follows a certain empirical law, represented by a linear equation, a second degree equation or a third degree equation in accordance with the type of flow. The present study proposes the use of a straight line equation for the constant velocity flow, a second degree equation for the boundary layer velocity flow field and the third degree equation for the 2-D nozzle plume flow field.

A single calculation of an axisymmetric plume can provide the solution of a number of 2-D nozzle of different configurations through a wide range of aspect ratios. This is only achieved when the nozzle pressure ratio and nozzle half angle remain the same.

#### III.1 THREE CASES OF NON-AXISYMMETRIC NOZZLE PLUMES

CASE I - Static External Flow - Synthesis of Chu's et al [1] work.

Mass flow rate entering the plume :

$$m = \rho VA = f \times A = f \times AR \times d^2$$

Scale factor  $f$  representation :

$$f = a + bX + cX^2 + dX^3$$

$a$ ,  $b$ ,  $c$  and  $d$  are obtained with the following boundary conditions :

$$X = 0, \quad f = 1, \quad f' = f'_1$$

$$X = X_c, \quad f = f_a, \quad f' = 0$$

$$f = 1 + f'_1 X + (3f'_1 - 2f'_1 X_c - 3) (X/X_c)^2 + (2 + f'_1 X_c - 2f'_1) (X/X_c)^3$$

Fig. 1 represents a synthesis of this case. It shows a basic axisymmetric plume, a phantom plume obtained by using the scale factor and an output plume showing the 2-D nozzle plume.

Fig.2 shows the equivalent section areas at a distance  $X$ .

Referring to figure 1, plume output, and to figure 2, the area at any distance  $X$  is :

$$\text{Area} : ARxd^2 = (PI)/4 (fd)^2 + Wd$$

$$\text{Solving for } W : W = d (AR - (PI/4) f^2)$$

#### CASE II - Free Constant External Velocity Field

The boundary condition of free constant velocity field is represented by the outside cylinder of diameter DIA in figure 3.

The mass flow rates at any section of the plume are represented by  $m_1$ ,  $m_2$  and  $m_3$ .

The section is at a distance  $X$  and has unit width  $\Delta X$ .

$m_1$  is the inlet axial mass flow rate.

$m_2$  is the mass flow rate due to the external flow.

$m_3$  is the outlet axial mass flow rate in the plume.

Mass conservation law :

$$m_1 + m_2 = m_3 \quad (1)$$

$$\rho_1 V_1 A_1 + \rho_2 V_2 A_2 = \rho_3 V_3 A_3$$

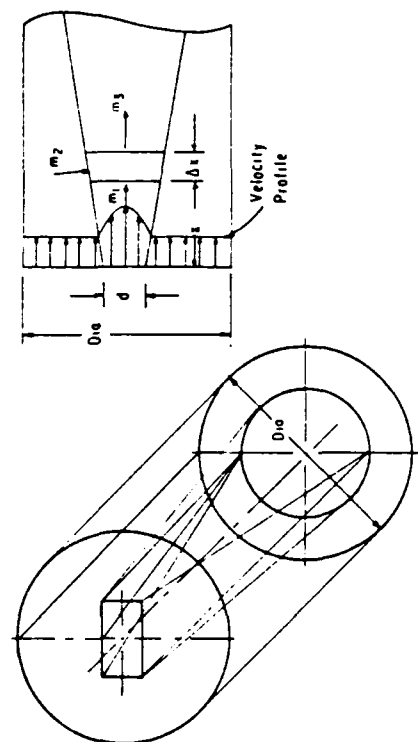


Fig 3 External cylinder representing the free constant velocity field

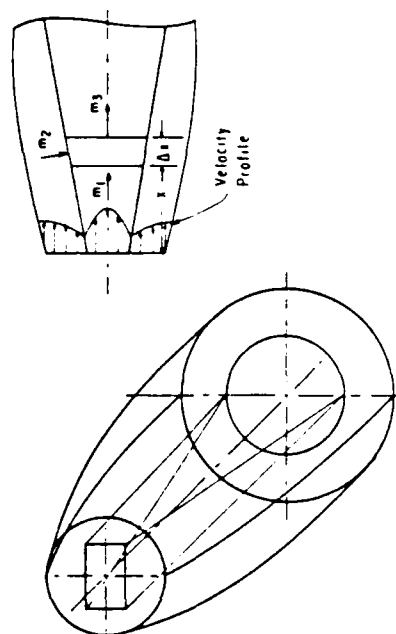


Fig 4 Paraboloid representing the free boundary type velocity field

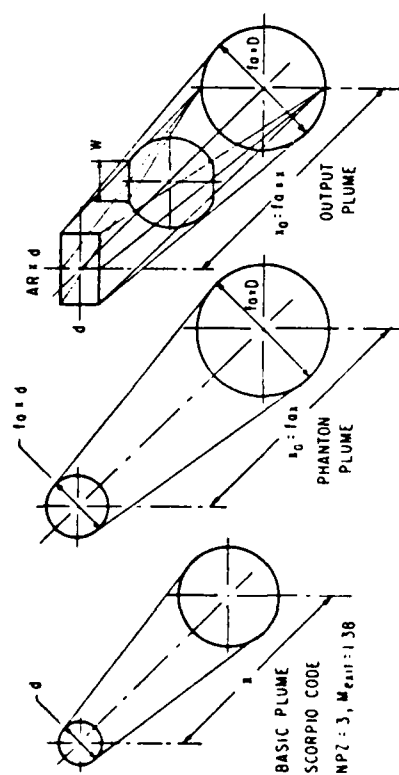


Fig 1 Synthesis of Chu, Wun and Der's Research



Fig 2 Equivalent section areas at a distance x

$$f_1 A_1 + f_2 A_2 = f_3 A_3 \quad (2)$$

Assuming a straight line law for the scale factor  $f_2$  :

$$f_2 = a_1 + b_1 X$$

Boundary conditions :

$$X = 0, \quad f_2 = 1, \quad a_1 = 1$$

$$X = X_s, \quad f_2 = f_s$$

$$f_s = 1 + b_1 X_s$$

$$b_1 = (f_s - 1)/X_s$$

$$f_2 = 1 + ((f_s - 1)/X_s) X$$

Assume a third order equation for  $f_3$  :

$$f_3 = a_3 + b_3 X + c_3 X^2 + d_3 X^3 \quad (3)$$

If  $f_2 = 0$  that is, static external flow, then :

$f_1 = f_3$  which is Chu's case.

Therefore, the scale factor  $f_1$  for the constant velocity external flow case is :

$$f_1 = (f_3 A_3 - f_2 A_2)/A_1 \quad (4)$$

where

$$A_1 = ARd^2 \text{ for the first station}$$

$$A_2 = (2ARd + (PI) fd)$$

$$A_3 = ((PI)/4) (fd)^2 + Wd$$

$$A_1 = A_3 \text{ after the first station}$$

#### CASE III - External Velocity Field of Boundary Layer Type

The boundary condition of free boundary velocity field type is represented by the paraboloid segment of radius  $r_1$  and  $r_2$  as shown in Figure 4.

The mass conservation applied to CASE II is valid for the present case, that is :

$$m_1 + m_2 = m_3$$

$$f_1 A_1 + f_2 A_2 = f_3 A_3$$

Assuming a second degree equation for the scale factor  $f_2$  :

$$f_2 = a_2 + b_2 X + c_2 X^2 \quad (5)$$

$$X = 0 \quad f_2 = 1 \quad f' = f'_2 \quad a_2 = 1$$

$$f'_2 = 2 b_2 c_2 X \quad b_2 = f'_2$$

$$X = X_s \quad f_2 = f_s$$

$$f_s = 1 + f'_2 X_s + c_2 X_s^2$$

$$c_2 = (f_s - 1 - f'_2 X_s) / X_s^2$$

$$f_2 = 1 + f'_2 X + ((f_s - 1 - f'_2 X_s) / X_s^2) X^2$$

$$f_2 = 1 + f'_2 X + (f_s - 1 - f'_2 X_s) (X/X_s)^2$$

#### IV. EXPERIMENTAL AND COMPUTATIONAL KNOWN DATA

There appears to be no data available on plumes with Mach numbers approaching unity before 1949. However in that year Corrsin, et al [18] made measurements of the mean total head and temperature fields in a round turbulent jet with various initial temperatures at low velocity turbulent jets.

Since that date up to present, many investigators [5] to [18] have reported analytical and experimental research on round and 2-D nozzle plumes. Their results could be very useful to prove the validity of the present research, but unfortunately there are no appropriate results, one for the round nozzle and other for the rectangular nozzle with matching conditions, as required to prove the theory. Therefore, it is convenient to generate our own input data. The Arnold Engineering Development Center has schedule to run test to measure actual temperature profiles in the 2-D nozzle plume of an F-100 engine. They also will run their Navier-Stokes Code to obtain temperature profiles in

round nozzle plumes under the same initial and boundary conditions of the running of the F-100 engine. The engine output data will be used as the input data in the follow up of this research. The output of the present study as compared with the output of the N.S. code will show how accurate the present theory is.

#### V. CONCLUSIONS AND RECOMMENDATIONS

A simple modeling technique for predicting detailed flow properties in a 2D-nozzle plume exhausting into a free stream of air has been presented. The follow up of this project is part of the proposal that will be presented to the Air Force by the University of Puerto Rico.

The proposal will have three basic objectives :

- a. Provide a physically realistic means by which the equivalent axi initial conditions can be obtained. This will include appropriate consideration of the external flow field.
- b. Provide a mapping scheme by which the transition region of the 2D nozzle flow can be calculated given the equivalent axi case. Particular attention will be given to the region at or near the nozzle exit so as to obtain physically realistic flow properties.
- c. Show evidence of validation of the proposed technique.

#### REFERENCES

1. Chu, C. W., Der J. Jr. and Wan W., "A Simple 2D-Nozzle Plume for IR Analysis," AIAA Paper No. 80-1808, August 1980.
2. Chu C. W. and Der J. Jr., "ADEN Plume Flow Properties for Infrared Analysis," AIAA Paper No. 82-4006, June 1981.
3. Chu C. W. and Der J. Jr., "Modeling of 2D-Nozzle Plume for IR Signature Prediction Under Static Conditions," AIAA Paper 81-1108, June 1981.
4. Chu C. W., "A Simple Analytical Method for Predicting Axisymmetric Turbulent Jet Flowfields in a Free Stream," AIAA Paper 82-0251, January 1985.
5. Van Glahn, U. H., Goodykoontz, J., and Wasserbauer, C., "Velocity and Temperature Decay Characteristics of Inverted-Profile Jets," AIAA Paper 86-0312, January 1986.
6. Dash, S. M., Wolf, D. E. and Sinha N., "Parabolized Navier-Stokes Analysis of Three Dimensional Supersonic and Subsonic Jet Mixing Problems," AIAA Paper 84-1525, June 1984.
7. Jiji, L.M., and Moghadam, S. M., "Theoretical and Experimental Investigation of Three Dimensional Buoyant Turbulence Jets," Heat Transfer 1982, Vol. 2 Grigull, E. Hahne, K. Stephan and J. Straub, Eds., Hemisphere Publishing, New York, 1982, p.p. 425-430.
8. Vatsa, V. N., Werle, M. J., Anderson, O. L. and Hankins Jr., G. B., "Solutions for Slightly Over-or Under-Expanded Hot Supersonic Jets Exhausting into Cold Subsonic Mainstreams," AIAA Paper 81-0257, January 1981.
9. Saheli, F. P., "Experimental and Analytical Evaluation of Three



NO-A191 203

UNITED STATES AIR FORCE SUMMER FACULTY RESEARCH PROGRAM  
(1987) PROGRAM TE. (U) UNIVERSAL ENERGY SYSTEMS INC  
DAYTON OH R C DARRAH ET AL. DEC 87 AFOSR-TR-88-0212

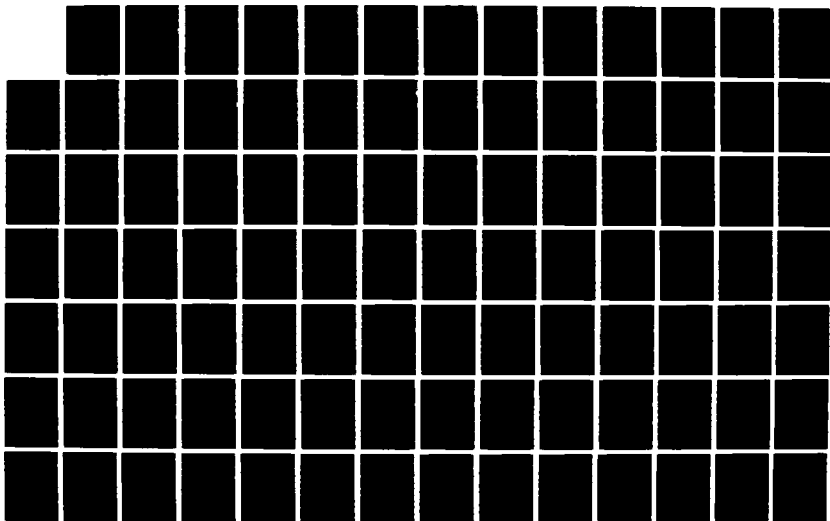
10/11

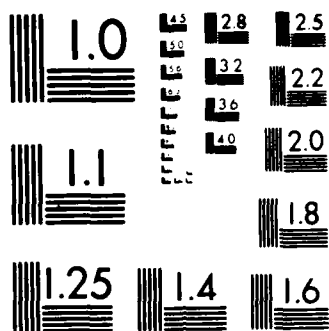
UNCLASSIFIED

F49620-85-C-0013

F/B 5/1

ML





MICROCOPY RESOLUTION TEST CHART  
NATIONAL BUREAU OF STANDARDS-1963-A

Dimensional Exhaust Plumes," AIAA Paper 80-1399, July 1980.

10. Steven, H. L., "Installed Trubine Engine Survivability Criteria (ITESC) Technical Report AFWAL-TR-80-2070, Pratt & Whitney Aircraft Group, West Palm Beach, Florida, August 1980.

11. Robinson, C. E., Roux J. A. and Bertraud W. T., "Infrared Measurements on an Exhaust Plume from an Axysmmetric Nozzle/Afterbody Model at Transonic Mach Numbers," ARO, Inc., Report AEDC-TR-78-55, March 1979.

12. Barton, J. M., Birch S. F., Paynter G. C. and Crouch R. W., "An Experimental and Numerical Study of Three Dimensional Turbulent Jets," AIAA Paper 78-994, Las Vegas, Nevada, 1978.

13. Narain, J. P., "Momentum Fluz Development From Three-Dimensional Free Jets," Journal of Fluids Engineering, Paper No. 76-FE-E, July 3, 1975.

14. Kurn, A. G., "Observations of the Flow from a Rectangular Nozzle," Tech. Rept. 74043, Royal Aircraft Establishment, March 1974.

15. Tomich, J. F., and Weger, E., "Some New Results on Momentum and Heat Transfer in Compressible Turbulent Free Jets," AIChE Journal, Vol. 13, No. 5, Sept. 1967, p.p. 948-954

16. Weinstein, A. S., Osterle J. F. and Forstall W., "Momentum Diffusion From a Slot Jet Into a Moving Secondary," ASME, Paper No. 55-A-60, November 1955.

17. Capone, F. J. and Berrier, B. L., "Investigation of Axisymmetric and Nonaxissymmetric Nozzles Installed as a 0.10-Scale F-18 Propotype Airplane Model," NASA Technical Paper 1638, June 1980.

18. Corrsin, Sand Mahinder S. U., "Further Experiments on the Flow and heat Transfer in a Heated Turbulent Air Jet," NACA TN No. 1865, 1949.

DESIGN OF A MECHANISM TO GENERATE  
WIND TUNNEL TURBULENCE

by

Marco A. Egoavil

ABSTRACT

Hardware to obtain variable turbulence levels for wind tunnel testing has been developed. The final goal of this project is to increase the turbulence level in the 4T Wind Tunnel of the Arnold Engineering Development Center to a value that is at least twice its background turbulence level.

Mechanisms have been designed, manufactured and tested in the Acoustic Research Tunnel (ART) of the AEDC. Six jets of 1/8 inches diameter at pressures varying from 10 psig to 30 psig in the stilling chamber were tested. The Mach number in the stilling chamber was of the order of 0.02. A second set of test using 17 oscilating tags of 2.0 in x 2.0 in x 1/16 in was obtained.

The turbulence level percentage was 3.16% without jets, 21.3% using 6 jets and 12.2% using tags. Further experimental data is necessary.

The follow up of the present study will be described in a proposal that will be presented to the U.S.A. Air Force by the University of Puerto Rico. In that project, present results will be used to design a mechanism to increase the turbulence level in the 4T Wind Tunnel. The successful results obtained in this research, are an indication that the follow up project can be developed in a simple and economical way.

## I. INTRODUCTION

The designers of aircraft, turbomachining and of engineering equipment have to consider types of flows which are not conventional. These are turbulent flows with a wide range of intensities from weak to very strong. Turbulent intensities levels of 2% can be encountered in subsonic and supersonic wind tunnels.

The designer of aircraft is interested in the effects of the turbulence levels on the maximum lift coefficient of aircraft wings. The study of the effects of turbulence is difficult, but interesting research efforts on that subject are in progress.

My research interest have been in the area of turbulent flow, combustion and computational gas dynamics. My extensive experience as a Mechanical Engineer and my research interests contributed to my assignment to work with Mr. Daryl Sinclair of Calspan/AEDC during the summer 1987 Research Program. Mr. Filiberto Santiago graduate student of Mechanical Engineering of the University of Puerto Rico was my research assistant in this project.

## II. OBJECTIVES OF THE RESEARCH EFFORT

The present report describes the research activities which are directed toward three objectives :

- (1) Obtain design information on turbulence generation through tests run at the Acoustic Research Tunnel of the Arnold Engineering Development Center. This objective has been partially accomplished during the past summer as described later.
- (2) Set the basis of the methodology of the design of turbulence generation in wind tunnels.
- (3) Design of a mechanism to increase the turbulence level background

of the 4T Wind Tunnel of the AEDC.

### III. APPROACH

Two experimental methods to generate turbulence level in the ART were devised. The use of jets as active turbulence generator was tested. Tags as passive turbulence generator gave the researchers information on how turbulence can be controlled. This approach was decided following the most generally accepted technical definition of what turbulence is. Theodore Von Karman quoted from G.I. Taylor in 1937 the following definition : "Turbulence is an irregular motion which in general makes its appearance in fluids, gaseous or liquid, when they flow past solid surfaces or even when neighboring streams of the same fluid flow past or over one another."

Flow past over solid surfaces can be considered flow over tags, plus some vibrational effects of each tag makes the method efficient to generate turbulence. The fluid flow over one another is represented by the action of an air flow supplied by jets and making the flow perpendicular to the main air flow causes such disturbance to it, that the turbulence is increased easily.

The Acoustic Research Tunnel was selected because of its availability and low cost in running tests. The ART is a transonic wind tunnel of a 6 inch square test section and 20.5 x 20.5 inches stilling chamber. It has a number of flanged sections that make it convenient to easily install the designed mechanism. As it is an indraft tunnel, the stagnation pressure is atmospheric and produces Mach numbers in test section of the order of 1.

### III.1 Turbulence Generation by Jets

The assemble of the following design of turbulence generation by jets developed by the present investigators is shown in Appendix A, drawing 01. This specifications of the design are as follows :

Maximum number of jets	14
7 jets at each vertical wall	
Jet's diameter	1/8"
Distance between jets	2.5"
Test air pressure in jets	5, 10, 15, 22 psig
Distance from jets to probes	26.5 inches
Air supply pressure at manifold	90 psi

The resources necessary to fabricate, install and test the turbulence generator are 400 man-hours, \$300.00 in materials and \$3,500 GFE (Electric Power).

### Results and Conclusions of the Use of Jets

Due to the limited space allowed to the report, the complete research with tables and graphs is shown in the report of Santiago [1] in this same volume.

The conclusions can be summarized as follows :

- (1) Using the 14 jets was of no avail due to the low pressure of 5 psig reached on each jet which did not generate any turbulence.
- (2) Using the calibration curve [1], the variation of the turbulence given by  $V_{rms}$  in millivolts versus the static pressure yield, Figure 1, it states that the turbulence wind tunnel background decreases by increasing the static pressure.
- (3) The variation of the turbulence through the probe section is shown in Figure 2. It shows a uniform turbulence variation through the cross section with a slight increase close to the floor. This increase disappears when the grid and jets are used, showing that there is a very good mix between the two fluids, the jets' air flow and wind tunnel main

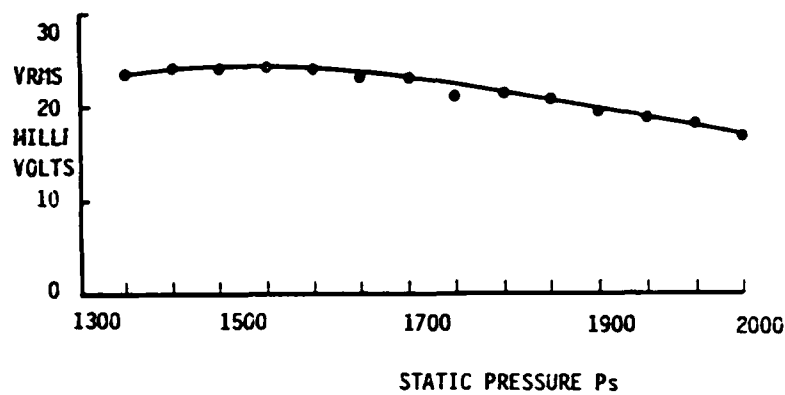


Fig. 1 Turbulence VRMS vs. Static Pressure

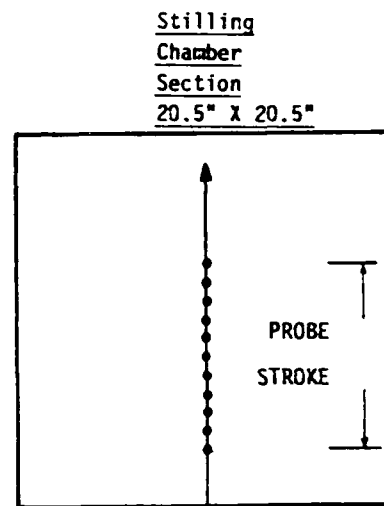
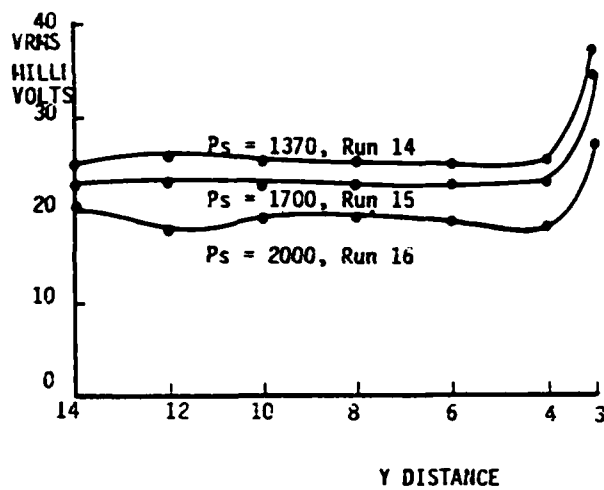


Fig. 2 Turbulence through the Stilling Chamber

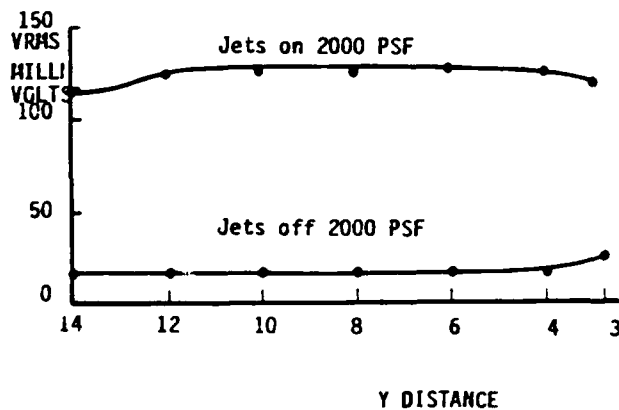


Fig. 3 Turbulence with Jets on and with Jets off



stream.

(4) Figure 3 shows the increase of turbulence using jets. The following comparisons are for runs 23 and 24 which are shown in reference [1]. The experimental values and results are repeated here.

TABLE 1 EXPERIMENTAL DATA

RUN	P(t)	P(s)	Dp	T(t)	Vdc	Vrms	JETS	TAGS	GRID	Pmani fold
	Psfa	Psfa	in water	F	Volts	Milli Volts	No	No	-	Psfa
23	2033	2000	0.045	84	3.82	17.5	0	0	YES	0
24	2033	2000	0.045	82	3.26	114.0	6	0	YES	5223
1	2031	2000	0.040	88	3.26	70.1	0	17	YES	0

TABLE 2 COMPUTED DATA, Reference [1]

RUN	P(s) s.c. psfa	T(s) s.c. R	M s.c.	V s.c. ft/sec	Turb (%) s.c.
23	2032.77	543.9	0.013	14.68	3.16
24	2032.39	541.9	0.021	23.63	21.30
1	2030.79	547.9	0.012	13.89	12.20

The experimental data states that there is an increase of :  
 $21.3/3.16 = 6.7$  times in the turbulence between tests 24 and 23, using jets and without the use of jets, respectively. These figures show that the use of jets to generate turbulence is extremely successful. The use of tags is also successful, but to a lesser degree, as shown later.

(5) Further experimentation is suggested, for example, using 14 jets with 20 psig, 30 psig and 40 psig on each jet. An increase in the

diameter of the jets is also suggested.

### III.2 Turbulence Generation by Tags

The tags used were plastic plates of 2.0 square inches. The position of each tag is shown in Appendix A, drawing 102.

The specifications of the design are as follows :

Number of tags : 17  
2 Perpendicular rows of tags.  
Material of Tags : Cellophane  
Dimension of tags : 2.0 x 2.0 x 1/16 in  
Length of tag holder : 1 in  
Distance from tags to probes : 26.5 in

### Results and Conclusions of the Use of Tags

Complete results of the use of tags are shown in reference [1].

Results of run 1 of 8-5-87 are repeated in table 1.

The main conclusion is :

(1) The turbulence generation using tags was increased by  $12.2/3.16 = 3.9$  times.

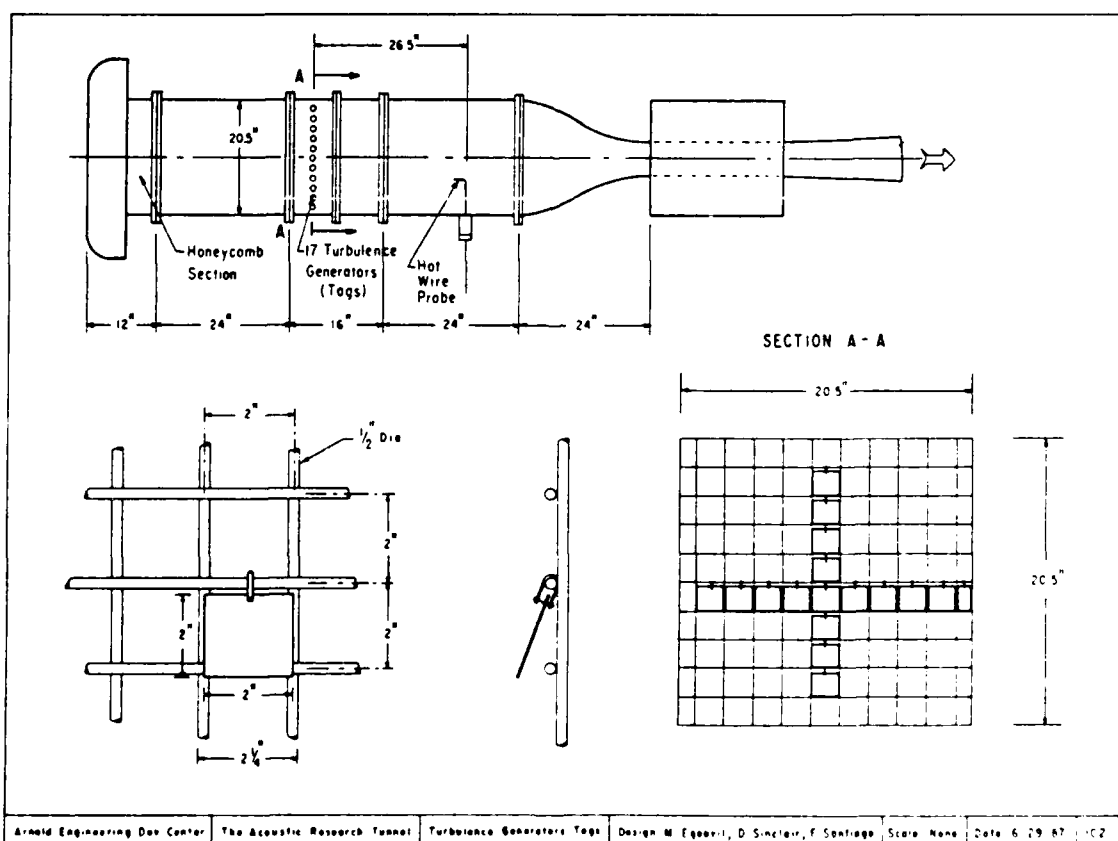
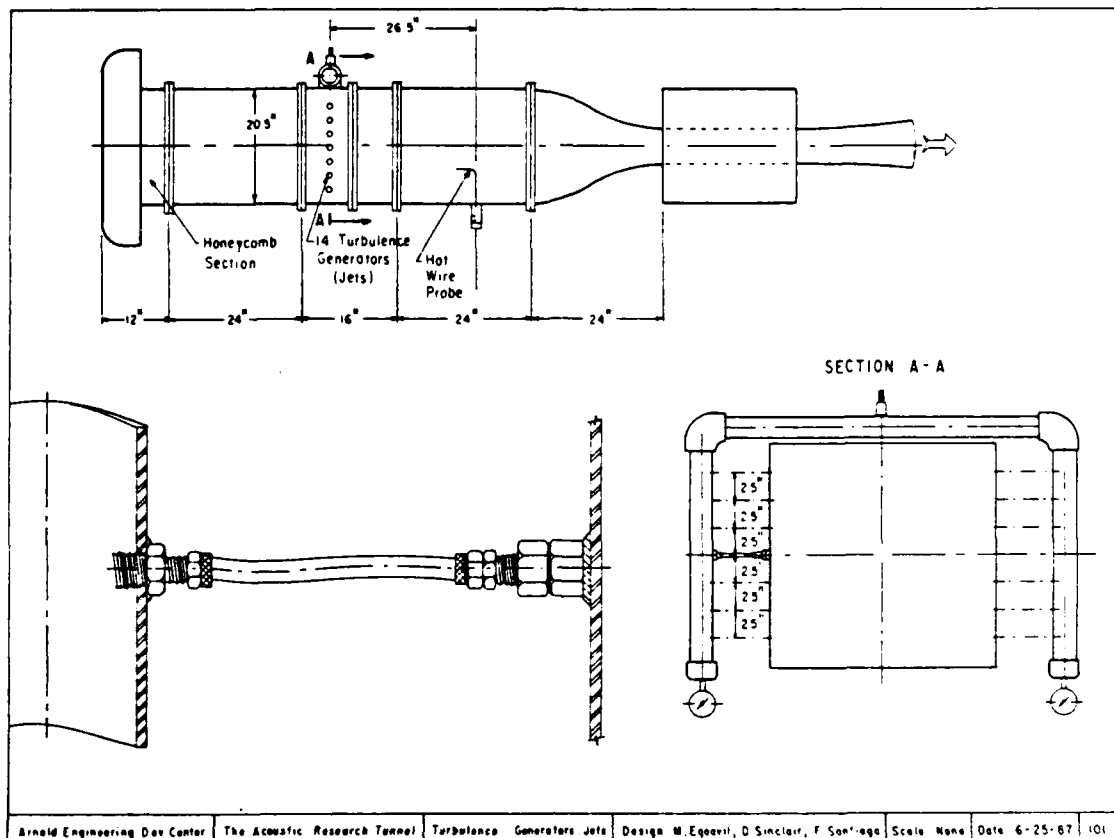
### IV. RECOMMENDATION

The follow up of this project is to set the basis of the methodology of the design of mechanisms to control the turbulence level in wind tunnels and to apply it to increase the turbulence of the 4T wind tunnel. The successful conclusions shown in this report are an indication that the design will be relatively simple and economical to develop.

### REFERENCE

1. Filiberto Santiago, "Design of a Mechanism to Generate Turbulence Level in Wind Tunnel", Graduate Student Summer Support Program Report, USAF/ARNOLD, 1987

# APPENDIX A



1987 USAF-UES SUMMER FACULTY RESEARCH PROGRAM/  
GRADUATE STUDENT SUMMER SUPPORT PROGRAM

Sponsored by the  
AIR FORCE OFFICE OF SCIENTIFIC RESEARCH

Conducted by the  
Universal Energy Systems, Inc.

FINAL REPORT

Computation of Rutherford Scattering Cross Sections

Prepared by: Dr. Ira T. Elder  
Academic Rank: Professor  
Department and Mathematical Sciences  
University: Eastern New Mexico University  
Research Location: AFWL/AWYS  
Kirtland AFB  
Albuquerque, NM 87117-6008

USAF Researcher: Dr. Paul Nelson

Date: 31 Aug 87

Contract No: F49620-85-C-0013

# Computation of Rutherford Scattering

## Cross Sections

by

Ira T. Elder

### ABSTRACT

Computation of Rutherford (or Coulomb) cross sections for scattering from angular bin to bin involved computing a triple (iterated) integral. The triple integration was performed numerically using an adaptive Simpson's quadrature formula programmed in FORTRAN. Three copies of the numerical integrator were necessary in order to prevent a subroutine from attempting to call itself recursively. An error tolerance was specified to help control and estimate the error. The adaptive method refines (generates subintervals) until the error tolerance is satisfied or to a maximum number of subintervals. The computed cross sections were used in the code PTRAN for transport of charged and neutral particles.

### Acknowledgements

I wish to thank the Air Force Systems Command, Air Force Weapons Laboratory and the Air Force Office of Scientific Research for sponsorship of this research. Universal Energy Systems must be mentioned for their concern and help to me in all administrative and directional aspects of this program

Having been in a full time academic administrative position for two years I found my summer research appointment to be particularly rewarding. It provided me the time and associates to once again be involved in research. Dr. Paul Nelson provided me with support and direction and suggested publications, journals and books which helped in the research. The help of Lt. Dave Ek was invaluable in becoming familiar with the computer system. The concern of Capt. Billy Smith and Maj. David Boyle was greatly appreciated. The encouragement and help of all these people clearly added to every aspect of this research project.

## I. INTRODUCTION

The Particle Beam Systems Section of the Space Applications Branch (AWYS) of the Applied Technology Division (AWY) at the USAF Weapons Laboratory is concerned with the transport of charged and neutral particles in various materials. In particular there is an interest in having a computer code which models the transport of neutral as well as charged particles.

My research interests have been in a variety of topics in numerical analysis, with one of these areas being the numerical solutions of two-point boundary-value problems which result in using an invariant imbedding technique with the transport equation. As a result, I was familiar with the transport equation and some of its components such as angular flux, scattering and cross sections. As a result, my being familiar with the transport equation and numerical analysis contributed to my assignment to the Particle Beam Systems Section of the Applied Technology Division.

## II. OBJECTIVES OF THE RESEARCH EFFORT

During my pre-summer visit to the Air Force Weapons Laboratory it was decided that I would join a team of researchers in developing a computer code for one-dimensional plane-parallel geometry azimuthally symmetric coupled transport of charged and neutral particles. Because no such general code existed, this seemed to be a particularly worthwhile project.

My assignment as a participant in the 1987 Summer Faculty Research Program (SFRP) was to develop and test codes (subroutines) for computing cross sections. It was decided to use Rutherford scattering for determining these cross sections and an adaptive Simpson's quadrature to perform the numerical integrations.

### III.

In order to find the macroscopic Rutherford scattering cross section, one must compute an integral of the form

$$\int_{I_i} \int_{I_j} \int_0^{2\pi} \sigma(\mu_0) d\phi d\mu d\mu'$$

where  $\mu_0 = \mu\mu' + \sqrt{1-\mu^2}\sqrt{1-\mu'^2}$  is the scattering angle cosine,

$$\sigma(\mu_0) = \frac{b^2}{16} \frac{1}{(n + \sin^2 \frac{\alpha}{2})^2},$$

$I_i$  and  $I_j$  are fixed subintervals of  $[-1,1]$ ,  $b$  is a parameter depending upon the masses and charges of the two particles and their relative velocities, the angle  $\alpha$  is related to  $\theta_0 = \cos^{-1}\mu_0$ ,  $0 \leq \theta_0 \leq \pi$  by  $\sin(\alpha - \theta_0) = \frac{M_1}{M_2} \sin\theta$  where  $M_1$  and  $M_2$  are the masses of the moving and stationary particles, respectively.

The basic one dimensional numerical integrator used was an adaptive Simpson's method. Our adaptive procedure is defined as follows. Compute the integral  $Q_1$  over the entire interval using Simpson's method. Then divide the interval in half and apply Simpson's method to each half yielding  $Q_{11}$  and  $Q_{12}$ . If  $Q_1 - (Q_{11} + Q_{12}) > \epsilon$  where  $\epsilon$  is



a specified error tolerance, then accept  $Q_{11} + Q_{12}$  as the result. If not, set aside the right half interval and proceed in the same manner for the left half interval as for the original interval. We continue with this refinement until the error tolerance is satisfied or until a specified number of refinements has occurred. This is necessary because the number of function evaluations increases rapidly as we use more refinements.

The adaptive process refines often when the integral of the Rutherford cross section function is difficult to approximate and uses few refinements when it is easy. Due to the forward-peaked elastic scattering of Rutherford scattering, it was essential to use an adaptive method and as a result on several angular bins (subintervals) the method refined the interval to the maximum number allowed.

Though the basic idea of using a one-dimensional integrator for a three dimensional is simple, it is somewhat tricky to code the process so as not to evaluate the integrand more than absolutely necessary, and so that the one-dimensional integrator does not attempt to call itself recursively. One has to use three copies of this subroutine and then define functions which call them in the proper order.

While the results of computing the cross sections were acceptable, there are however some difficulties. Computation of the cross sections can require a considerable amount of computer time. This is particularly true when demanding several digits of accuracy or when specifying

a "small" error tolerance. At this point there is no natural way of determining a prior workable value of the error tolerance.

The cross sections were used in the code PTRAN, the computational transport program, and the results seemed to be reasonably accurate. But it should be mentioned that the cross section calculations were the most time consuming computations in PTRAN.

#### IV. RECOMMENDATIONS

Because the Rutherford cross section package uses considerable computer time in order that the cross sections have sufficient number of digits of accuracy so that a reasonable amount of accuracy will occur in the rest of the code PTRAN, it is probably best to separate the Rutherford package from PTRAN. In many applications one is using fixed materials, directional bins, energy ranges and number of energy bins. For these types of applications the cross sections would stay fixed, thus one could create a library of cross sections which could be used for many runs of the computational transport code. At the same time it would appear to be worthwhile to have cross section program re-written in complete double precision in order to gain cross sections with several digits of accuracy.

An additional concept to consider is the following. In the transport program it was assumed that the angular fluxes were constant on each angular bin. A better approximation would result by replacing the

constant angular fluxes with a linear approximation on each angular bin. There are several difficulties involved in this as well as requiring considerable programming.

Finally, one is led to the question of how to extend this computational transport code to include problems in X-Y geometry (two-dimensional geometry). This should be a problem of great interest, but again one which requires considerable effort in design, coding and testing.

## REFERENCES

### Textbooks:

1. Bell, G. I., S. Glasstone, Nuclear Reactor Theory, Van Nostrand Reinhold Co., 1970.
2. Evans, R. D., The Atomic Nucleus, McGraw Hill Book Co., 1955.
3. Lewis, E. E., W. F. Miller, Computational Methods of Neutron Transport, John Wiley & Sons, Inc., 1984.
4. Press, W. H., et. al., Numerical Recipes--The Art of Scientific Computing, Cambridge Press, 1986.
5. Shampine, L. F., R. C. Allen, Numerical Computing, W. B. Saunders Co., 1973.

### Journal Publications:

1. Morel, J. E., P. Nelson, "An Asymptotic Derivation of the Spencer-Lewis Equations," to be submitted.

1987 USAF-UES SUMMER FACULTY RESEARCH PROGRAM/

GRADUATE STUDENT SUMMER SUPPORT PROGRAM

Sponsored by the

AIR FORCE OFFICE OF SCIENTIFIC RESEARCH

Conducted by the

Universal Energy Systems, Inc.

FINAL REPORT

Database Processing in Real-Time Systems

Prepared by:	Ramez A. Elmasri, Ph.D.
Academic Rank:	Assistant Professor
Department and	Computer Science Department
University:	University of Houston
Research Location:	RADC/COTD
	Griffiss AFB
	Rome NY 13441
USAF Researcher:	Thomas F. Lawrence
Date:	14 August 1987
Contract No:	F49620-85-C-0013

## Database Processing in Real-Time Systems

by

Ramez A. Elmasri

### ABSTRACT

Real-time systems consist of a number of tasks, or processes. Whenever a task is invoked, it must be executed completely by a certain time deadline in a "hard" real-time system. In a "soft" real-time system, the value of a task to the overall system declines if it has not completed execution by a certain critical time. In most existing real-time systems, tasks are independent from one another and no access to shared databases by the tasks is considered.

In this work, we examine the issues that arise when shared databases are included in real-time systems. We identify research problems that must be resolved before shared databases can be successfully incorporated into real-time systems. These issues include specifying the timing characteristics of database operations; scheduling of database operations by real-time schedulers; using main memory for storage of "currently-in-use" portions of a database to improve performance; and issues that deal with the replication and distribution of the database.

### ACKNOWLEDGEMENTS

I would like to thank the Air Force Systems Command and the Air Force Office of Scientific Research for sponsoring this research, and UES for the administration of the program.

I also wish to thank Thomas F. Lawrence and Emilie J. Siarkiewicz of the Rome Air Development Center for providing the direction for this research, and for their help. Discussions with them clarified numerous issues, and they also provided me with many valuable technical references that helped the progress of this work. The support and help of other persons at RADC/COTD is also appreciated.

## I. INTRODUCTION:

Real-time systems are used in many applications such as computer based weapons systems, manufacturing control systems, robots, etc. Most real time systems are made up of a number of independent software tasks. These tasks are then assigned to hardware processors for execution. The main criterion for task allocation is that sufficient processing capacity exist on each hardware processor to allow each task to complete its processing within a specified time limit, called the task deadline. A task should meet its deadline every time it is invoked.

Recent applications of real-time systems have been identified at RADC/COTD that will require real-time tasks to access one or more shared databases. These applications are also expected to run in a distributed environment, so distributed databases will be needed. There is very little work reported in the database literature or real-time literature that discusses the use and incorporation of databases in real-time systems.

My area of reasearch has been mainly concerned with various aspects of database systems. I have worked on and published original research in distributed databases, database models, database languages, and database design and implementation. However, before this summer faculty research program fellowship at RADC, I was not very knowledgeable in the area of real-time systems. I suspect that few persons have conducted research in both database systems and real-time systems as indicated by the scarcity of research publications that address aspects of integrating the two types of systems together.

For this summer research program, I was assigned to research and study the general area



of using shared distributed databases in real-time systems, and to identify problems and issues that arise in such systems and need to be studied and resolved.

## II. OBJECTIVES OF THE RESEARCH EFFORT:

There were two main goals of the research conducted during this summer. The first goal was to conduct a search of the real-time literature to become knowledgeable in the concepts and techniques that have been used or suggested for use in real-time systems. The second goal was to identify the issues that need to be studied, and the problems that need to be solved so that databases can be incorporated into distributed real-time systems. As part of these goals, any research that reports on the use of databases in real-time systems would be identified and studied. However, as mentioned earlier, there were very few publications (practically none) that I could locate that report on the incorporation of shared databases into real-time systems.

## III. RESEARCHING THE REAL-TIME LITERATURE:

The first few weeks I spent at RADC were devoted to studying the real-time literature in order to understand the concepts and techniques used in these types of systems. A representative sample of the papers that were studied are listed in the section on references. In addition, during the same time period, several documents that discuss the specific applications at RADC that are expected to require the use of distributed databases in real-time systems were studied to get a feeling for the types of applications envisioned.

A partial classification of real-time systems research was then done. A seminar describing the results of this classification was given on August 3, 1987 at RADC. Also

presented at the seminar were the results that we discuss in Section IV of this report. Following is a summary of the real-time systems classification.

There are several models of real-time systems in the literature. One model, called the process model, is often used to study the fundamental properties of real-time systems. A real-time system is modeled as a set of processes. There are two main types of real-time processes--periodic processes and sporadic processes. Periodic processes are invoked every  $p$  time units on a regular basis, whereas sporadic processes are invoked on an irregular basis as needed. Each process  $T_i$  is a triple  $T_i = (c_i, d_i, p_i)$ , where  $c_i$  is the process computation time, and  $d_i$  is the deadline of the process (relative to its invocation time). For periodic processes,  $p_i$  is the period, whereas for sporadic processes  $p_i$  is the minimum time that must pass between successive invocations of the sporadic task (minimum period).

A fundamental problem in real-time systems is the scheduling of all invoked (ready) processes to meet their deadlines. A real-time scheduler examines the ready processes and schedules them to run on the available hardware processors so that none of the processes miss their deadlines. If this is not possible because the hardware processing capacity is insufficient, the scheduler must still attempt to schedule processes using criteria other than absolute deadline. For example, the scheduler could attempt to minimize the number of "late" processes that miss their deadline, or it could attempt to minimize the "average lateness" of all processes.

The problem of optimal scheduling [8]--that is, scheduling processes on processors so that all processes meet their deadlines whenever this is possible--is intractable (NP-complete) [4] in the general case of multiple hardware processors. This means that any such algorithm will take excessive time to determine the schedule. However, several simple algorithms are known to be optimal in the case of scheduling processes with deadlines to run on a single processor. Two of these algorithms are the closest deadline algorithm, which runs the process with the closest deadline, and the least slack time algorithm, which runs the process that has the least time left to start execution before it will miss its deadline for sure [10]. Both these algorithms use preemption if necessary.

Because optimal real-time scheduling is NP-complete in distributed systems, a technique that is often used is to use a simple scheduler (such as FCFS (First-Come-First-Serve)) at each hardware processor, or node. Processes (also called tasks or modules) are pre-analyzed for their computation times, deadlines, and invocation rates, and are allocated permanently to certain processors in the distributed system. Algorithms for task allocation attempt to ensure that there is sufficient processing capacity at each node to process the expected load of tasks allocated at that node. Every task should meet its deadline whenever the task is invoked. The problem with these static task allocation techniques [2, 3, 12] is that unexpected invocation rates may cause overloading of certain nodes while other nodes have surplus processing power. In addition, modifying the real-time system by adding new tasks may require running the task allocation algorithm to find a new task allocation. This is followed by retesting of the whole system, an expensive procedure.

Dynamic task scheduling algorithms [1, 11, 13] in a distributed real-time system have

been proposed. These algorithms use heuristics and attempt to dynamically balance system load at the various nodes. One algorithm works on the principle of "guaranteeing" a new task when it is submitted. A guarantee routine determines whether a newly submitted task can be guaranteed to meet its deadline based on the deadline and worst case execution time of the task and of all other "guaranteed ready tasks" at the node. If the new task cannot be guaranteed, an attempt to find another node in the system that can guarantee that the task will meet its deadline is made.

Another scheduling method proposes to treat tasks with hard and soft deadlines in a uniform way by assigning a value function  $v(t)$  to each task [5]. This function represents the value to the whole system of the task completing in time  $t$ . The scheduler attempts to maximize some measure of "total value" to the system as its scheduling philosophy.

All schedulers and task allocation schemes must be provided with estimates for the computation time of each task/process/module in the system. These can be worst-case times, or mean/variance, or even a distribution function and probability density function. Techniques to estimate the computation times of complex tasks from their component modules have been developed using probabilistic models and path analysis within the task [6, 7, 14].

Some issues that complicate scheduling and task allocation are the following: (a) when shared resources or devices exist in the real-time system [6], (b) when precedence constraints exist among the processes/tasks/modules [1], (c) when there is explicit synchronization among the processes/tasks/modules [10], and (d) when communication

costs are taken into account [3]. Research continues into incorporating all these factors into scheduling and task allocation algorithms.

#### IV. INCORPORATING DATABASES INTO DISTRIBUTED REAL-TIME SYSTEMS:

The second phase of the summer research was to identify the problems that arise and the issues that need to be resolved when databases are included in distributed real-time systems. The following issues were identified:

##### a. Storage Architectures for Real-Time Databases

This issue concerns the different types of storage architectures for real-time databases. Because deadlines exist in real-time systems, database access time will become critical. Most current database systems store the database on disk, which has a large storage capacity but is a relatively slow secondary storage device. Before data is processed, it is transferred from disk into fast main memory.

The main alternatives to be considered here are whether a database that is accessed by real-time tasks should be stored in main memory, on disk, or using a combination of both types of storage. Obviously, the size of the database will be an important factor. If a database application normally selects data from a subset of a large database for its current processing, then that subset could be "cached" into main memory and maintained as an in-memory database, while the part of the database that is not currently in use could be maintained on the disk. This is a form of the "memory caching" technique that is used by operating systems.

It is important to develop methods and algorithms to determine the portion of the database that is currently in use, and to dynamically adjust that portion by reading new portions from disk and writing old portions to disk. Methods based on the semantic properties of the data and the application could be used here rather than operating system-type methods such as LRU (Least Recently Used). For example, a system for controlling the firing of missiles on moving targets may have a certain limited target range at each node, and so that node only needs tracking information on the moving targets within this range area or near the boundary of the range area. This portion of a tracking database could then be kept in memory at that node while other tracking data is kept on disk.

In such cases of using main memory storage for the "currently in use" portion of a database, the database operations will take considerably less time than if the whole database was stored on disk. Hence, more tasks could be scheduled to meet their real-time deadlines. In addition, in-memory storage allows the true parallel execution of database operations if we assume that the "currently in use" database portion resides in a shared memory. If tasks are running on separate hardware processors, they can access the database at the same time. However, if the whole database is stored on a disk unit that has a single I/O channel, this would prohibit true parallelism in database access.

#### b. Scheduling and Performance Issues

##### b.1. Methods for accurately estimating database operation execution time

For real-time systems, all known scheduling and task allocation algorithms assume that the execution time of each real-time task is known in advance. Hence, we need to develop methods that accurately estimate the execution time of database operations that are

embedded in the real-time tasks. These methods should consider a variety of database access structures on files, and should determine for each access structure a formulation that gives an accurate estimate of the time it takes to access a record given the current size of the file. An operation that includes multiple record accesses can have its access time estimated by adding up the access times for individual record accesses in the operation. Both on-disk and in-core access structures should be analyzed. Specifically, at least the following access methods should be considered:

Disk-based files:

- (1) Multi-level indexing implemented as B-trees or B<sup>+</sup>-trees.
- (2) Static and dynamic hashing methods.
- (3) Clustering (hierarchical file) techniques.

Memory-based files:

- (1) Unordered files (linear search) and ordered files (binary search).
- (2) Indexing and hashing methods.

The performance characteristics of the above techniques is well known, and generally depends on the number of records in the file. However, we need to develop accurate absolute-time values for the different types of database access operations on specific hardware and software implementations. Operations to be considered include the selection operation to select records from a file based upon particular selection conditions, and the natural join operation which retrieves related records from two or more files. Also, techniques for estimating the time for operations on complex objects, which retrieve records from multiple files, are needed. In addition, accurate time estimates for operations that insert, delete, and update both single records and complex objects

consisting of multiple records should be developed.

Novel storage techniques should also be investigated, particularly for storage of complex objects. Time estimates for retrieval and update of complex objects for any new storage techniques must be developed along with the technique itself.

#### b.2. Scheduling of database operation within real-time transactions

Characteristics of database operations can be different from regular code that is used in a traditional real-time process. These characteristics will determine whether scheduling techniques that are similar to those used for process scheduling can be used for scheduling of database operations.

There are a number of possible alternatives for characterizing database operations. One possible model is to assume that database operations must be executed sequentially on the database system, with possible interleaving with other database operations but without "true parallelism". In this case, the database is considered as any other system resource that can be accessed by at most one process at a time. A second possibility is to allow database operations to execute in parallel without any constraints. A third possibility is to allow only non-conflicting operations to execute in true parallelism. Each of these cases implies certain assumptions on the database system. For example, the second possibility implies that no serializability or locking is enforced, and that the database is stored in some form of shared memory that allows true parallel access. The third possibility implies that certain operations can proceed in true parallelism, but that some form of a concurrency control mechanism ensures that conflicting operations are not executed in



parallel. An important area to be investigated in real-time database processing is to develop scheduling algorithms for the various types of characteristics exhibited by database operations.

We next examine some possible models for the structure of real-time processes that include database operations. One possible model is to assume that all database operations in a real-time process either occur at the beginning or at the end of the process. This corresponds to the case where each process has a data input phase, a processing phase, and a data output phase. The input phase, the output phase, or both may be absent from some processes. The process profile for this model is illustrated in Figure A.

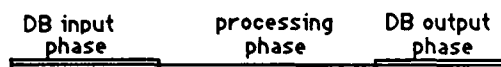


Figure A

A second model is more general and assumes that database operations can occur anywhere within the real-time process, as illustrated in Figure B.

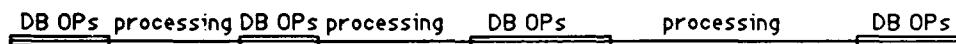


Figure B

Real-time scheduling algorithms for the models of transaction structure shown in Figures A and B need to be developed for the various characteristics of database operations discussed earlier. It is important to understand the characteristics of the various database operation execution models and process models, and to determine whether some of the assumptions made can lead to simple scheduling algorithms. Also, the above assumptions

must be studied to determine under what circumstances they are realistic for specific real-time database processing applications.

c. Replication and Distribution Issues

c.1. Replication Issues

One of the main advantages cited for distributed systems is increased reliability and availability. One technique for improving reliability and availability of distributed databases is the use of data replication. The main cost of such a technique--other than the increased storage costs--is the effort expended for maintaining copies of the same data consistent with one another whenever the database is updated. This effort can be quite costly in time, and hence is a problem in real-time systems.

There have recently been several proposals that question the need for up-to-the-minute consistency among replicas of the same database. This may lead to a consistency maintenance method that is feasible in a real-time environment. Current techniques for consistency maintenance among replicas include the following:

Primary node technique: All updates are submitted to a central node, which schedules the updates and then broadcasts their results to nodes containing other replicas of the database. This central node has the potential of becoming a bottleneck and its failure would be catastrophic.

Primary copy technique: Similar to primary node except that the primary copy can reside at any node. If the node with the primary copy fails, the remaining nodes can "elect" a new primary copy.

Majority consensus: Before an update is done, a majority of the nodes that contain copies

must be able to confirm that the update is possible. This technique may require excessive communication overhead and is susceptible to delays.

Hybrid techniques: Mixture of the above.

The above techniques may not have the performance characteristics required in a real-time system. In all of the above techniques, the assumption is that an update operation is executed at a single node, and then the result is broadcast to other nodes that contain database copies. A more recent suggestion is to broadcast the actual code of the database update operations to all nodes that contain copies, and execute the update operations at every such node. The update operations should be executed in the same order on every node.

If sufficient hardware capacity exists, this latter technique may be feasible. A read-only operations would then execute at any single node, whereas an update operation is broadcast and executed at every node. Some part of the system must be responsible for ordering the execution of update operations. This global ordering is necessary only if the operations can create an inconsistent database when they are not executed in the same order; that is, the operations are non-commutative.

#### c.2. Distribution Issues

In a distributed system, one of the potential advantages is load balancing. This is the capability to distribute the system processing load and database access load over the nodes of the distributed system.

In a real-time system where response time is of utmost importance, load balancing offers potential advantages. One of the issues to be determined here is whether static or dynamic load balancing techniques should be used, or whether a hybrid technique can be developed. In static load balancing, a priori assignment of particular database operations to particular nodes is made by a static assignment algorithm. This is analogous to task allocation techniques in real-time systems.

Dynamic load balancing means that the decision as to where a database operation or a process is to be executed is made depending upon the current system load. This approach usually assumes that all nodes have the same functionality, and is analogous to dynamic scheduling in real-time systems. Although this approach is more general, the problem is to design a good dynamic process scheduling and database operation scheduling algorithm that can run in real-time. Most simple dynamic scheduling algorithms such as earliest deadline are not optimal in a distributed or multi-processor environment. As mentioned earlier, the general scheduling problem is NP-complete (intractable), so that it is unlikely that an efficient optimal algorithm will be found. Hence, dynamic scheduling algorithms for a distributed environment use heuristic techniques.

The advantage of static scheduling is that the allocation algorithm is a pre-assignment algorithm that does not need to execute in real-time during system operation. The disadvantage is that it will not adapt to current system conditions and unexpected changes in system loads. Hybrid methods that do some static scheduling and some dynamic scheduling may need to be considered here.

Another aspect to examine is whether the characteristics of database operations may lead to "operation assignment" techniques that differ from the task/module/process allocation methods that have been proposed or are currently in use for distributed real-time systems. Also, new techniques or extensions to existing techniques may be needed for designing a real-time distributed system that includes both processes and database operations within these processes.

#### V. RECOMMENDATIONS:

The recommendations that came out of this research project are to further investigate each of the issues identified in the previous section (Section IV). In fact, RADDC already had started efforts to investigate some of these issues. A mini-grant proposal to investigate some of the issues identified in Section IV is being prepared. The mini-grant proposal concentrates on identifying the scheduling characteristics of database operations that are embedded in real-time processes. Additional efforts to study the effects of distribution and replication, and to develop techniques for analyzing the timing characteristics of database operations, will be conducted if time permits.

## REFERENCES

1. Cheng,S., J.Stankovic, and K.Ramamritham, Dynamic Scheduling of Groups of Tasks with Precedence Constraints in Distributed Hard Real-Time Systems, IEEE Real-Time Systems Symposium, December 1986, pp.166-174.
2. Chu,W., L.Holloway, M.Lan, and K.Efe, Task Allocation in Distributed Data Processing Systems, IEEE Computer, November 1980, pp.57-69.
3. Chu,W., and K.Leung, Module Replication and Assignment for Real-Time Distributed Processing Systems, Proceedings of the IEEE, May 1987, pp.547-562.
4. Garey,M., and D.Johnson, Complexity Results for Multiprocessor Scheduling Under Resource Constraints, SIAM Journal of Computing, Volume 4, 1975.
5. Jensen,E., C.Locke, and H.Tokuda, A Time-Driven Scheduling Model for Real-Time Operating Systems, IEEE Real-Time Systems Symposium, December 1985, pp.112-122.
6. Leinbaugh,D., Guaranteed Response Times in a Hard-Real-Time Environment, IEEE Transactions on Software Engineering, January 1980, pp.85-91.
7. Leinbaugh,D., and M.Yamini, Guaranteed Response Times in a Distributed Hard-Real-Time Environment, IEEE Transactions on Software Engineering.

December 1986, pp.1139-1144.

8. Liu,C., and J.Layland, Scheduling Algorithms for Multiprogramming in a Hard Real-Time Environment, Journal of the ACM, January 1973, pp.44-61.
9. Lui,S., J.Lehoczky, and R.Rajkumar, Solutions for Some Practical Problems in Prioritized Preemptive Scheduling, IEEE Real-Time Systems Symposium, December 1986, pp.181-191.
10. Mok,A., The Design of Real-Time Programming Systems Based on Process Models, IEEE Real-Time Systems Symposium, December 1984, pp.5-17.
11. Ramamritham,K., and J.Stankovic, Dynamic Task Scheduling in Hard Real-Time Distributed Systems, IEEE Software, July 1984, pp.65-75.
12. Rao,G., H.Stone, and T.Hu, Assignment of Tasks in a Distributed Processing System with Limited Memory, IEEE Transactions on Computers, April 1979, pp.291-299.
13. Stankovic,J., and K.Ramamritham, Evaluation of a Flexible Task Scheduling Algorithm for Distributed Hard Real-Time Systems, IEEE Transactions on Computers, December 1985, pp.1130-1143.
14. Woodbury,M., Analysis of the Execution Time of Real-Time Tasks, IEEE Real-Time Systems Symposium, December 1986, pp.89-96.

1987 USAF-UES SUMMER FACULTY RESEARCH PROGRAM  
GRADUATE STUDENT SUMMER SUPPORT PROGRAM

Sponsored by the  
AIR FORCE OFFICE OF SCIENTIFIC RESEARCH  
Conducted by the  
Universal Energy Systems, Inc.

FINAL REPORT

NON-UNIFORM SPATIAL SYSTEMS AND THE  
TRANSITION TO TURBULENCE

Prepared by:	John E. Erdei, Ph.D.
Academic Rank:	Assistant Professor
Department and	Department of Physics
University:	University of Dayton
Research Location:	Aero-Propulsion Laboratory Wright-Patterson AFB Dayton, Ohio
USAF Researcher:	W. M. Roquemore, Ph.D.
Date:	20-Aug-87
Contract No:	F49620-85-C-0013



NON-UNIFORM SPATIAL SYSTEMS AND THE  
TRANSITION TO TURBULENCE

by

John E. Erdei

ABSTRACT

The transition characteristics of a vertical Bénard Cell are studied through the use of slow amplitudes, or order parameters. In a previous study of the cell, it was assumed that the order parameters were spatially uniform, and an appropriate equation of motion was derived which described the temporal evolution of spatial states. The work given in this report extends the previous derivation by allowing non-uniformities in the spatial states. The final form suggests that if the conditions are favorable, the cell can become convectively unstable. Experiments on the cell appear to be in support of this contention.

During the course of the summer research period, other experiments which could be used to test the predictions of the order parameter models have been given serious consideration. In anticipation of a need for analysis of the experimental data, various computer routines have been written. For completeness, a brief description of each of the routines is also given in this report.

### Acknowledgements

I would like to thank the Air Force Systems Command and the Air Force Office of Scientific Research for their sponsorship of my research. I would also like to acknowledge the Aero-Propulsion Laboratory at The Wright-Patterson Air Force Base for providing the facilities and support for conducting my research. The personnel at the base have been instrumental in helping me through some of the details of the summer effort. In particular, Curtis Reeves, Jeff Stutrud, Lt. Alan Lesmerises, and Bill Lynn have all made contributions to the work associated with the analysis of experiment. And the suggestion of a direction for the theoretical analysis came from Dr. W. M. Roquemore of the APL.

I also would like to acknowledge the experimental work of Prof. R. S. Tankin and Ron Britton. Some preliminary studies have been carried out on data provided by their efforts. Finally, discussions with Prof. R. A. Piccirelli and Prof. K. R. Sreenivasan have been helpful in furthering the summer effort.

## I. INTRODUCTION:

It can be stated without too much argument that the understanding of turbulence is one of the major unsolved problems in science and engineering. Attacks which are based on the Navier-Stokes equation generally involve substantial (even non-existent) computer requirements. Although it cannot be denied that the use of new generation computers has increased the solving capabilities, there is no real intention to get at the nature of the issue of turbulence.

The difficulties associated with the solution to the Navier-Stokes equation have fostered an interest in a group at the Aero-Propulsion Laboratory in alternative approaches to the problem of turbulence. In particular, it has been noted that long standing problems in classical mechanics had been solved during the first quarter of the century by the introduction of a single concept, namely quantization in terms of Plank's constant,  $h$ . This concept was followed by the profound statement of particle-wave duality, which motivated Schrödinger to redefine the classical wave equation into a form applicable to particles (through the use of a wave-function). Essentially all of simple quantum mechanics could be described through the resulting equation, the Schrödinger equation. It is of value to note that the area of quantum mechanics grew from these two concepts.

It had been observed at APL that characteristics seen in quantum mechanics could also be observed in fluid systems. For example, vortex pairing might be thought of as obeying a type of selection rule, which governs the allowed resulting vortex. Thus, an examination of the role that quantum mechanical ideas might play in fluid mechanics was initiated at APL. My background is in a more modern form of quantum mechanics, namely field theory (or many-body theory). My

role in the Summer Faculty Research Program has been to address the possible use of quantum mechanical techniques in fluid mechanics.

## II. OBJECTIVES OF THE RESEARCH EFFORT:

The summer research has been a continuation of work started previously. The objectives of my work have been to examine the role that quantum mechanical techniques or concepts might play in a fluid system. This might involve the use of a wave-function, uncertainty principle, selection rules, or anything else which could be used in a non-traditional approach to fluid dynamics. It would then be required that some appropriate interpretation of the concept be given. By this it is meant that if a wave-function type entity is used, some physical interpretation must also be given. Finally, there is a wealth of experimental data available on flows of various configurations. Any predictions should in fact be in line with observation.

Throughout the effort, I have felt that the description must retain the classical features already known to be true for fluid mechanics. It was also believed that the formalism should be used strictly on a macroscopic level, rather than the microscopic scale at which quantum mechanics operates. Also, the inherent restrictions of the first formulation of quantum mechanics (namely, the lack of interactions, single particle characteristics,...) must be overcome by the use of the better suited formulation of second quantum mechanics, or many body theory. Finally, the characteristics of a given flow are intimately related to transition phenomena, and any ideas utilized must be general enough to allow for transition characteristics. With this in mind, a study of the classical analogues to wave-function has been considered. The use of

such entities is well known to the area of solid state physics and critical phenomena. These ideas are attractive in that the techniques of critical phenomena can be employed both statically and dynamically.

Initial stages of the research involved the applicability of the concepts; critical phenomena was originally introduced to study equilibrium phenomena, whereas interesting fluid flows are definitely not in equilibrium. However, critical steps have been taken by other researchers in many varied areas which allow for the association of macroscopic wavefunctions and critical phenomena with steady state phenomena out of equilibrium. In fluid mechanics, this idea has been used in great detail in the study of the convective instability in the Bénard cell.

The point made previously about the area of quantum mechanics must be emphasized again, that is, that there are really very few fundamental concepts from which most of the area is built. As stated earlier, in quantum mechanics one might suggest that the fundamental building blocks are the existence of Plank's constant (from which energy and angular momentum quantization can be determined) and particle-wave duality (upon which the Schrödinger equation is essentially based). One might point to the conjecture of Ruelle and Takens, that the turbulent state might be related to a strange attractor, as just such a fundamental building block. On a qualitative level, the features of the strange attractor hypothesis are so good that the idea demands consideration. Similarly, the hypothesis fits very nicely into the quantum mechanics ideas professed at APL.

The next question is one of construction. Many separate ingredients must be connected together in order to produce a sound theoretical model. Some of the issues which must be

investigated are as follows:

(a) Can one look to the strange attractor hypothesis as the crucial seed from which a theory can be based?

(b) How can a macroscopic theory based on a wavefunction-like entity be described? What is the appropriate function which characterizes the fluid mechanics? What are the relevant control parameters?

(c) What is the physical interpretation of the wavefunction?

(d) Is the resulting theory any simpler than simply solving the Navier-Stokes equation? Is there any new insight provided?

(e) Are there limits to the applicability of the theory?

(f) If the general direction is not good, then what exactly is wrong? Knowledge of failure is a step toward knowledge of success.

(g) Are there experimentally accessible predictions? If so, the measuring capabilities at APL might be used to test the predictions in flow configurations of interest to the lab.

(h) Can the concepts be used to enhance the theoretical treatment of important fluid mechanical quantities, such as fluxes?

(i) What is the relationship between the discrete iterative maps, ordinary differential equations, and partial differential equations to the macroscopic study of turbulence and attractors?

The above statements define a very large research program, and effort has been directed at the answer to these questions. Considerable progress has been made in the past efforts. An appropriate choice for the wavefunction-like entity is called an order parameter as used in equilibrium critical phenomena. The equation of motion for the order parameter in general governs the transition characteristics observed in a real flow. The macroscopic states are determined by the existence of attractors in the equation of motion, and in the case of non-equilibrium, non-linear models, the attractors can have the property of strangeness. As a result, it is hoped that one general model can account for the set of transitions through the formation of large scale structures (associated with point attractors) to the development of turbulence (associated with a strange attractor). However, in order to gain insight into the mechanisms involved, point (b) above must be addressed. To this end, an investigation of a particular experiment, the vertical Bénard cell, was initiated. Due to the fact that the system is closed and is similar to the horizontal case, it was expected that it was possible to directly attack point (b) above. An ordinary differential equation which determines the temporal evolution of the order parameter has been derived elsewhere<sup>1</sup>. In this report, we will discuss the extension of the previous work to a governing PDE for the order parameter. This extension was one of the main goals of the summer research.

As stated in point (g) above, it is also important to be able to produce experimental evidence in support of the theoretical aspects. In order to do so, a second goal of the summer has been to identify relevant laboratory experiments and to formulate an appropriate analysis. This has been aided greatly by discussions with Prof. Sreenivasan. In order to be able to analyze experimental information, a series of

computer routines have been written during the summer research period. Due to my familiarity with desk-top computers, the codes have all been written on a microcomputer for convenience. The proliferation of microcomputers in universities will allow the analysis to be carried out by students or collaborators without being tied to a large mainframe computer system. Disks of information can be transferred from one place to the other with ease, as long as there are compatible computers available. Programs have been written for any IBM PC compatible machine. Once routines are fully running, it may then be convenient to transfer them to a larger system.

### III. THE VERTICAL BENARD CELL

In previous work, the amplitude equations have been considered by allowing the order parameters to be functions of time only. This was a reasonable starting point, and is in line with general derivations of the Lorenz equations. It is expected that consideration of the uniform spatial characteristics can be handled by these temporal characteristics. We do not go into any detail, but one expects that in steady state, spatial variation is not strongly preferred. However, the experiments on the vertical slot by Elder<sup>2,3</sup>, and most recently Tankin and Heller<sup>3</sup>, show the tendency under the right conditions toward the irregular, or intermittent, production of wall waves. These waves are realized as clumps of (probably) turbulent material moving up the hot wall and down the cold. Clearly, spatial characteristics are not uniform in this situation, and a spatial dependence must be placed in the order parameters. One of the goals of the summer was to carry out this generalization. The work was also spurred on by the recent work of Deissler<sup>5</sup>, who has been examining intermittent characteristics of a specific form of the GTDLG equation.



His results could possibly be used in support of the derived model for the vertical slot. In this section, the results of the summer work on the slot will be summarized.

The relevant equations for the cell are the Navier-Stokes equation and the heat transport equation. These equations can be found elsewhere<sup>1</sup>, and will not be reproduced here. The procedure is initiated by attempting to identify a set of states which can be associated with stationary states. This is accomplished by linearizing the governing equations, so that they can be recast into the form

$$\frac{\partial}{\partial t} \Psi = L \Psi, \quad (1)$$

where  $\Psi$  is a vector composed of the velocity and temperature fields.  $L$  is a linear (matrix) operator. Separation of spatial and temporal variables is introduced through the choice

$$\Psi = \Phi e^{\Lambda t}, \quad (2)$$

and substitution into (1) produces an eigenvalue problem of the form

$$\Lambda \Phi = L \Phi. \quad (3)$$

The set of stationary states will be identified with the eigenvectors associated with zero eigenvalue ( $\Lambda = 0$ ); that is, the states given by the neutral stability curve. For the vertical Bénard cell,  $\Lambda$  is a function of Grashoff number, Prandtl number, and aspect ratio.

The next step is to take the set of eigenstates,  $\Phi_i$ , and form the general solution to the equations of motion through

the combination

$$\Psi = \sum_i \zeta_i \Psi_i, \quad (4)$$

where the amplitudes  $\zeta$  describe the probability of the system being observed in state  $i$ . The goal is to generate the equation of motion for the set  $\{\zeta_i\}$ , which will contain information regarding the possible evolution of the state  $i$ . The full non-linear nature of the system can be taken into account through the equations for the  $\zeta_i$ . The non-linearity allows for the interactions between individual states. In accordance with the comments at the beginning of this section, we will take

$$\zeta_i = \zeta_i(\mathbf{x}, t). \quad (5)$$

It is determined that the stationary states have an explicit dependence upon wavevector,  $k$ , and that each stationary state is characterized by a different value of  $k$ . The subscript  $i$  is then dropped in favor the more appropriate subscript  $k$ , and (4) and (5) are substituted into the original set of equations of motion (NSE and heat transport equation). The result is of the form

$$\begin{aligned}
\frac{\partial \zeta_k}{\partial t} = & \alpha_1 \frac{\partial^2 \zeta_k}{\partial x^2} + \alpha_2 \frac{\partial \zeta_k}{\partial x} + \Lambda_k \zeta_k \\
& - \sum_{k'} \beta_{k,k',[k-k']}^{(1)}(z) \zeta_{k'} \frac{\partial \zeta_{k-k'}}{\partial x} \\
& - \sum_{k'} \left\{ -i[k-k'] \right\} \beta_{k,k',[k-k']}^{(1)}(z) \zeta_{k'} \zeta_{k-k'} \\
& - \sum_{k'} \beta_{k,k',[k+k']}^{(1)}(z) \zeta_{k'}^* \frac{\partial \zeta_{k+k'}}{\partial x} \\
& - \sum_{k'} \left\{ -i[k+k'] \right\} \beta_{k,k',[k+k']}^{(1)}(z) \zeta_{k'}^* \zeta_{k+k'} \\
& - \sum_{k'} \beta_{k,k',[k-k']}^{(2)}(z) \zeta_{k'} \zeta_{k-k'} \\
& - \sum_{k'} \beta_{k,k',[k+k']}^{(2)}(z) \zeta_{k'}^* \zeta_{k+k'}, \tag{6}
\end{aligned}$$

where the coefficients in the above expression are determined by the original equations of motion.

The slaving concept<sup>6</sup> can now be employed by assuming that all amplitudes which are not critical are effectively constants. As a result, all derivative (spatial or temporal) terms are taken to be equal to zero unless the mode is a critical mode associated with wavevector  $k_0$ . For simplicity, we explicitly consider the interaction of the order parameter

mode with the most stable mode, associated with  $k = 0$ . Taking only the critical mode to have spatial and temporal dependence, we find

$$\frac{\partial \zeta_{k_c}}{\partial t} = \alpha_1 \frac{\partial^2 \zeta_{k_c}}{\partial x^2} + \alpha_2 \frac{\partial \zeta_{k_c}}{\partial x} + \Lambda_{k_c} \zeta_{k_c} - \beta_{k_c} \zeta_{k_c} \left| \zeta_{k_c} \right|^2, \quad (7)$$

where  $\beta_{k_c}$  is formed from the coefficients of the non-linear terms in (6). It should be noted that since the eigenvalues of the linearized problem are in general complex, the terms  $\Lambda_{k_c}$  and  $\beta_{k_c}$  can also be taken as complex.  $\alpha_1$  and  $\alpha_2$  are both real.

Extensive numerical work has been carried out by Deissler<sup>5</sup> on equations of the same form as (7). One of the major features of his work is the existence of an intermittent transition to chaotic behavior. It is to be expected that detailed experimental measurements should be able to verify this intermittent transition. As stated earlier in this report, it appears as though this intermittent transition has been observed in the work of various experimenters.

#### IV. COMPUTER ROUTINES

In support of the theoretical model described above and for the analysis of real experimental data, a series of programs have been written which have been designed specifically for the examination of raw data relevant to the discussion of attractors and chaos. The titles and application are listed in this section for reference. Files can then be transferred from one microcomputer to another as long as they are IBM PC compatible. This allows data to be generated at a given location (for example, APL) and then

analyzed in any convenient way at another location (someone's university). Many of the routines listed below are written in basic (extension .BAS), and for the most part basic is adequate for doing many of the calculations. The basic files listed below can handle data sets of up to 10,000 points (slowly), since this is the convenient limit of basic.

Routines which require a substantial amount of direct analysis of raw data have been written in Professional Fortran (extension .FOR). Some of the Fortran programs have been taken from reference 7 and will be noted in the listings below.

#### FFT2.FOR

This routine uses the Cooley-Tukey fast Fourier transform algorithm<sup>7</sup> to carry out the fourier transform of previously stored raw data. Transformed data can be stored in separate file for plotting with a graphics routine.

#### COVMTRX.BAS

This file takes raw data and computes the corresponding covariant matrix in the method of Broomhead and King<sup>8</sup>. Data is read from a previously generated data storage file of the raw data. Matrix elements can be stored in a file which can be generated within COVMTRX.BAS. This program runs acceptably fast for data sets up to a few thousand points, but can be used up to 10,000 data points. The output is an  $N \times N$  symmetric matrix, where  $N$  is the number of points chosen within the window used.

#### PSECTION.BAS

This file uses data which has been previously generated for a phase space trajectory and selects the data relevant for a Poincare section in a plane of the user's choice. The data is stored in a file generated by the user for plotting on a separate graphics routine.

#### EIGEN.BAS

This file computes the eigenvalues and eigenvectors of a previously generated symmetric matrix. Matrix elements are read into the routine. The Householder reduction method<sup>7</sup> can then be selected to reduce the matrix to tridiagonal form. The QL algorithm<sup>7</sup> can then be selected to generate the eigenvalues and eigenvectors of the reduced matrix. The user can then store the results in a separate file. This Basic file can be used with acceptable speed for virtually any relevant matrix generated in COVMTRX.BAS.

#### CMEPLOT.BAS

This file uses previously stored values of a set of eigenvalues and computes the quantity<sup>8</sup>

$$\alpha_i = \log \left[ \frac{\sigma_i}{\text{Tr } \Sigma} \right],$$

where  $\sigma_i \equiv i^{\text{th}}$  eigenvalue of the covariant matrix  $\Sigma$ , and

$$\text{Tr } \Sigma = \sum_{i=1}^N \sigma_i.$$

The  $\{\sigma_i\}$  can be stored in a separate file as an array  $(i, \sigma_i)$  for plotting with some graphics routine.

#### PSPROJ.BAS

Generates the elements of the trajectory matrix for the relevant subspace defined by the method of Broomhead and King. Eigenvectors and raw data from the corresponding window set are read into the routine. The elements of the trajectory matrix can be stored in a separate file.

#### DIGIPILOT.BAS

Program is used to draw surfaces in a given flow. Requires that information concerning flow (for example, intensities) have been digitized and stored on a floppy disk. Reads digitized data and allows user to draw a constant surface or fill in all points greater than some chosen value. Routine is used to make a copy of surface which is being analyzed by sending output to a plotter. The images can then be stored to a separate file for future use. DIGIPILOT.BAS will also redraw the stored image.

Along with the surface drawing capabilities, this routine uses a box counting algorithm to produce the required data for the computation of the fractal dimension of a digitized surface. Results are stored in a separate file for plotting with a graphics package.

## BOXCNT.FOR

Carries out the box counting algorithm from DIGILOT.BAS in fortran.

### V. RECOMMENDATIONS

The theoretical treatment of the vertical Bénard cell strongly suggest that the order parameter approach may be effectively used to treat stationary state situations, selection rule heirarchies, interations among modes, and transition characteristics seen in real fluid flows (at least on a qualitative level). What is called for now in more quantitative results. For example, predictions of TDLGT suggest that some signature of chaos be present in fluid systems. This could be through the presence of strange attractors, of real space fractal characteristics. These properties should have identifiable implications on the calculations of quantities such as fluxes. As such, these quantities should be examined through the use of the macroscopic models discussed above.

The characteristics should also be examined from a experimental point of view. Many of the predication have been studied by Sreenivasan<sup>9,10</sup>, but the existence of characteristics associated with fractal or chaos are still not firmly established. To this end, velocity measurements (or some equivalent quantity) should be used to generate phase space trajectories. Computation of relevant quantities can then be done using the routines produced during the summer effort. Similarly, the combination of the real space fractal concept with the ability to produce digitized images can be a powerful tool for the understanding of the mechanism which produces turbulence. The newly acquired digital camera at APL can and should be used to attack this issue.



## V. REFERENCES

1. Erdei, J. E., RISE Mini-Grant Final Report (1986).
2. Elder, J. W., J. Fluid Mech., 23, Part 1, 77 (1965).
3. Elder, J. W., J. Fluid Mech., 23, Part 1, 99 (1965).
4. Heller, J., Student Project Report, Northwestern University (1986).
5. Deissler, R. J., Physica 25D, 233 (1987).
6. Haken, H., "Synergetics", 3rd Ed. (Springer-Verlag, 1983).
7. Press, W. H., Flannery, B. P., Teukolsky, S. S., and Vetterling, W. T., "Numerical Recipes, the Art of Scientific Computing" (Cambridge University Press, 1986).
8. Broomhead, D. S., and King, G. P., Physica 20D, 217 (1986).
9. Sreenivasan, K. R., and Meneveau, C., J. Fluid Mech 173, 357 (1986).
10. Sreenivasan, K. R., "Fundamentals of Fluid Mechanics", (Springer-Verlag, 1985).

1987 USAF-UES SUMMER FACULTY RESEARCH PROGRAM/  
GRADUATE STUDENT SUMMER SUPPORT PROGRAM

Sponsored by the  
AIR FORCE OFFICE OF SCIENTIFIC RESEARCH

Conducted by  
Universal Energy Systems, Inc.

FINAL REPORT

BANK-TO-TURN CONTROL OF AIR-TO-AIR MISSILES

Prepared by: Dr. Joseph J. Feeley

Academic Rank: Associate Professor

Department and University: Department of Electrical Engineering  
University of Idaho

Research Location: Air Force Armament Laboratory  
Aeromechanics Division  
Guidance and Control Branch  
Advanced Guidance Concepts Group  
Eglin Air Force Base, Florida

USAF Researcher: Dr. James R. Cloutier

Date: September 15, 1987

Contract No: F49620-85-C-0013

# BANK-TO-TURN CONTROL OF AIR-TO-AIR MISSILES

by

Joseph J. Feeley

## ABSTRACT

Future Air Force missions will require air-to-air missiles with an asymmetrical cross section and a chin-inlet ramjet engine. These missiles will require advanced guidance and control systems to achieve necessary maneuverability and to avoid engine flame-out during lateral turns. The control strategy for these new missiles is termed bank-to-turn as opposed to the skid-to-turn strategy used in current missiles. This report summarizes the dynamics of the missile-target encounter, highlights the assumptions frequently made in missile autopilot design, and recommends further study of an integrated guidance and control system based on optimal differential game theory.

### Acknowledgements

I wish to thank the Air Force Systems Command and the Air Force Office of Scientific Research for their sponsorship of this research. I also wish to thank Universal Energy Systems for their help in the administration of this program.

The research effort itself was made considerably easier by the help of a number of people at AFATL. Specifically, I would like to thank Col. David LaBorde, Chief of the Aeromechanics Division, for his approval of my summer program at Eglin AFB; Dave Gardner, Manager of the Guidance and Control Branch, for providing a congenial and effective work environment; Jim Cloutier, Supervisor of the Advanced Guidance Concepts Section, for his technical direction and good-natured support; and to other members of the Guidance and Control Branch, especially Lt. Roger Smith, Johnny Evers, and Mike Vanden-Heuvel for their assistance, technical and otherwise, that made my work much easier and my stay more pleasant.

I. INTRODUCTION: Air-to-air missiles currently in use by the Air Force use a skid-to-turn (STT) steering control policy. These missiles are characterized by a cylindrical cross section, a cruciform tail fin, and an autopilot that makes no attempt to control roll angle. As a result, large side-slip angles often occur during lateral turns. In the future longer range, more maneuverable air-to-air missiles with wing-conformal asymmetrical cross sections will be required. The extended range requirement may well be met by the addition of a chin-inlet ramjet engine. To avoid engine flame-out and to take full advantage of the missile's aerodynamic shape, these advanced missiles will require advanced control systems capable of minimizing side-slip angle and accounting for cross-coupled aerodynamic forces.

II. OBJECTIVES OF THE RESEARCH EFFORT: The primary purpose of this research effort was to provide autopilot design support to Aeromechanics Division personnel engaged in the development of advanced air-to-air missile airframes. This task required a basic understanding of the dynamics of the missile-target engagement, knowledge of air-to-air missile mission requirements and the state-of-the-art of missile guidance and control systems, and familiarity with both modern and classical methods of control system design.

Accomplishment of this objective required an extensive review of the literature in the technical society journals

and in the in-house reports of AFATL and its contractors. The results of this review are summarized in this report. In addition, an integrated guidance and control system design approach based on optimal game theory is discussed, and will form the basis for a proposal for continued work. The proposal will be submitted to the Research Initiation Program of the Air Force Office of Scientific Research.

III. THE MISSILE-TARGET ENGAGEMENT: A representation of the missile-target engagement is pictured in Fig. 1. The principal axes of the missile at the time of launch ( $t=0$ ) is taken as an inertial coordinate system for the encounter. A vector along the line-of-sight (LOS) from the missile to the target has magnitude (range)  $R$  and orientation defined by azimuth and elevation angles  $\sigma_a$  and  $\sigma_e$ . The missile's seeker system provides measurements of  $R$ ,  $\sigma_a$ , and  $\sigma_e$  for use by other missile sub-systems. The purpose of the missile guidance and control system, in general terms, is to transform the seeker measurements into missile control surface positions in such a way that the missile hits the target. Fig. 1 shows the evolution of hypothetical missile and target trajectories over the course of an encounter from  $t = 0$  to the time of minimum range,  $t = t_f$ .

IV. BANK-TO-TURN MISSILE DYNAMICS: The missile control problem is complicated by two factors: the forces required to maneuver the missile are applied indirectly, through

positioning the aerodynamic control surfaces; and the missile is a rigid body whose motion is described by six, coupled, nonlinear, differential equations. Conventional control system design, using either modern or classical methods, requires a mathematical model relating the applied control effort to the resulting missile motion. This model is based on Newton's laws of motion which, in three dimensional inertial space are<sup>1</sup>

$$F = m \frac{dV}{dt} \quad (1)$$

$$G = \frac{dH}{dt} \quad (2)$$

where  $F$  is the resultant force acting on the missile,  $G$  is the resultant moment about the center of mass,  $m$  is the mass, and  $H$  is the angular momentum.

The scalar form of Eq. 2 is quite complex since it requires the time derivative of  $H$  which, in turn, contains time varying body rotational rates, moments of inertia, and products of inertia. Considerable simplification can be achieved if the equations of motion are written with respect to the principal axes of the missile. Fig. 2 shows a missile's principal axes coordinate system and its relationship to an inertial coordinate system. The missile, and its coordinate system  $\{x, y, z\}$ , move with translational velocity  $V$ , having velocity components  $u$ ,  $v$ , and  $w$  in the  $x$ ,

y, and z directions, and with angular velocity  $\omega$ , having rotational components p, q, and r representing roll, pitch, and yaw motion.

The equations of motion with respect to the principal axes of the missile become

$$F = m \left( \frac{\delta V}{\delta t} + \omega \times V \right) \quad (3)$$

$$G = \frac{\delta H}{\delta t} + \omega \times H \quad (4)$$

where the derivatives in Eqs. 3 and 4 assume the local coordinate system (x,y,z) is not rotating. In scalar form Eqs. 3 and 4 are known as the Euler six degree-of-freedom equations of motion

$$\dot{u} = \frac{F_{TH}}{m} + rv - qw + g_x + \frac{Q_0 S}{m} [C_x + C_{xT}] \quad (5)$$

$$\dot{v} = pw - ru + g_y + \frac{Q_0 S}{m} [C_{y\beta} \beta + C_{y\delta_R} \delta_R] \quad (6)$$

$$\dot{w} = qu - pv + g_z + \frac{Q_0 S}{m} [C_{z\alpha} \alpha + C_{z\delta_E} \delta_E] \quad (7)$$

$$\dot{p} = \frac{I_y - I_z}{I_x} q r + \frac{Q_0 S l}{I_x} \left[ C_{L\beta} \beta + C_{L\delta_A} \delta_A + C_{Lp} \frac{l p}{2|V|} \right] \quad (8)$$

$$\dot{q} = \frac{I_z - I_x}{I_y} r p + \frac{Q_0 S l}{I_y} \left[ C_M + C_{M\delta_E} \delta_E + C_{Mq} \frac{l q}{2|V|} \right] \quad (9)$$

$$\dot{r} = \frac{I_x - I_y}{I_z} q p + \frac{Q_0 S l}{I_z} \left[ C_{N\beta} \beta + C_{N\delta_R} \delta_R + C_{Nr} \frac{l r}{2|V|} \right] \quad (10)$$



where:

$C_i$  are the experimentally determined aerodynamic derivatives depending on Mach number,  $\alpha$ ,  $\beta$ , and  $\delta\epsilon$ ;

$\delta_A$ ,  $\delta_R$ ,  $\delta\epsilon$  are the aileron, rudder and elevator incremental positions;

$F_{TH}$  is the missile thrust;

$I_x$ ,  $I_y$ ,  $I_z$  are the moments of inertia;

$g_x$ ,  $g_y$ ,  $g_z$  are the accelerations due to gravity;

$S$  is the missile characteristic area;

$l$  is the missile characteristic length;

$Q_0$  is the dynamic pressure.

Fig. 2 also shows the missile's angle of attack  $\alpha$  and side-slip angle  $\beta$ , where

$$\alpha = \tan^{-1} \left( \frac{w}{u} \right) \quad (11)$$

$$\beta = \tan^{-1} \left( \frac{v}{\sqrt{u^2 + w^2}} \right) \quad (12)$$

The missile's Euler angles  $\psi$ ,  $\theta$ , and  $\phi$  are also shown in the figure. These angles determine the azimuth, elevation, and orientation (roll angle) of the missile (and its coordinate system) with respect to the given inertial system and are given by

$$\dot{\psi} = \sec \theta (r \cos \theta + q \sin \phi) \quad (13)$$

$$\dot{\theta} = q \cos \phi - r \sin \phi \quad (14)$$

$$\dot{\phi} = p + \tan \theta (r \cos \theta + q \sin \phi) \quad (15)$$

Finally, the position of the missile in inertial cartesian coordinates is related to the Euler angles and the missile velocity by

$$\begin{aligned} \dot{X} = & u \cos \psi \cos \theta + v(\cos \psi \sin \theta \sin \phi - \sin \psi \cos \phi) \\ & + w(\cos \psi \sin \theta \cos \phi + \sin \psi \sin \phi) \end{aligned} \quad (16)$$

$$\begin{aligned} \dot{Y} = & u \sin \psi \cos \theta + v(\sin \psi \sin \theta \sin \phi + \cos \psi \cos \phi) \\ & + w(\sin \psi \sin \theta \cos \phi - \cos \psi \sin \phi) \end{aligned} \quad (17)$$

$$\dot{Z} = -u \sin \theta + v \cos \theta \sin \phi + w \cos \theta \cos \phi \quad (18)$$

A complete description of the motion of the missile and target in inertial space, as required, for example, by a missile-target simulation program, requires simultaneous solution of Eqs. 5 through 18. Fortunately, the design of guidance and control systems for the missile-target intercept problem depends only on the relative positions of the missile and the target and can be described by a reduced set of equations. Furthermore, it is often useful to limit the engagement to two dimensions as an aid to understanding. This is considered further in the next section.

V. SIMPLIFIED DYNAMIC EQUATIONS OF A PLANAR ENGAGEMENT: A hypothetical missile-target engagement in a horizontal plane is shown in Fig. 3. A moving coordinate system is established with its center at the missile's center of mass and with its x axis aligned with the longitudinal axis of the missile. The position of the coordinate system at the beginning of the engagement is used to locate an inertial coordinate system for the problem. The Euler equations for this three degree-of-freedom system are

$$\dot{u} = \frac{F_{TH}}{m} + \kappa v + \frac{Q_0 S}{m} C_x \quad (19)$$

$$\dot{v} = -\kappa u + \frac{Q_0 S}{m} [C_{y\beta} \dot{\beta} + C_{y\delta_R} \dot{\delta}_R] \quad (20)$$

$$\dot{\kappa} = \frac{Q_0 S l}{I} \left[ C_{N\dot{\beta}} \dot{\beta} + C_{N\dot{\delta}_R} \dot{\delta}_R + C_{N\kappa} \frac{l \kappa}{2|V|} \right] \quad (21)$$

The side-slip angle  $\beta$ , the Euler angle  $\psi$ , and the LOS angle  $\sigma$  are given by

$$\beta = \tan^{-1} \frac{v}{u} \quad (22)$$

$$\dot{\psi} = \kappa \quad (23)$$

$$\sigma = \tan^{-1} \left[ \frac{Y_T - Y_M}{X_T - X_M} \right] \quad (24)$$

The position of the missile with respect to inertial coordinates is given by

$$\dot{x}_M = u \cos \psi - v \sin \psi \quad (25)$$

$$\dot{y}_M = u \cos \psi + v \sin \psi \quad (26)$$

Additional simplifications are possible if the missile is considered to be a point mass instead of a rigid body. In this case the need for a set of missile-fixed coordinates is avoided. Taking the x axis to be coincident with the initial line of sight (ILOS), and for further simplicity, restricting both missile and target acceleration to be perpendicular to the ILOS, the situation pictured in Fig. 4 is obtained. The major variables of interest are the net displacement of the target from the missile in the y direction, the net velocity in this direction v, the current LOS angle  $\psi$ , and the current distance to the target along the ILOS, R. The dynamics of this engagement are given by

$$\dot{v} = a_T - a_M \quad (27)$$

$$\dot{y} = v \quad (28)$$

While greatly simplified, these equations nevertheless are convenient to use and help in gaining insight into the problem.

## VI. CONTROL THEORETIC APPROACH TO CONTROL SYSTEM DESIGN:

Conventional missile autopilot design assumes that the missile guidance system presents commanded accelerations to the control system such that, if followed exactly by the missile, the target will be intercepted. The guidance systems inevitably use some variation of the proportional navigation law to generate the acceleration commands. Proceeding from this point control system design is straightforward and both classical and modern methods have been used successfully<sup>2,3</sup>. For example, if the target is assumed to move with constant velocity in the horizontal plane, the dynamic model equations become<sup>4</sup>

$$\dot{v} = a \quad (29)$$

$$\dot{y} = v \quad (30)$$

and the performance index is

$$J = \frac{1}{2} c y^2(t_f) + \frac{1}{2} \int_0^{t_f} a^2 dt \quad (31)$$

The linear-quadratic optimal control problem is, then, to find the feedback control that minimizes Eq. 31 subject to the constraints imposed by Eqs. 29 and 30. The solution is

$$a = - \frac{(t_f - t)^2}{\frac{1}{c} + \frac{1}{3}(t_f - t)^3} v - \frac{(t_f - t)}{\frac{1}{c} + \frac{1}{3}(t_f - t)^3} y \quad (32)$$

It is interesting to note that when the terminal miss distance is forced toward zero by weighting  $c$  very heavily,

and if the LOS angle is small, the control law becomes

$$a = -3 \left[ \frac{v}{t_f - t} + \frac{y}{(t_f - t)^2} \right] \quad (33)$$

If  $V_c$  is the closing velocity along the LOS then the LOS angle is

$$\sigma \cong \frac{y}{V_c (t_f - t)} \quad (34)$$

and the acceleration is given by

$$a = -3 V_c \dot{\sigma} \quad (35)$$

which is a mathematical statement of the proportional navigation law.

In actual system design, of course, the missile dynamic model is based on the more complete six degree-of-freedom equations, similar to Eqs. 5 through 10. Dealing with these equations as a coupled set is a formidable challenge, however, and a variety of simplifying, often decoupling, assumptions have been made by various authors<sup>2,3</sup>.

VII. GAME THEORETIC APPROACH TO CONTROL SYSTEM DESIGN: If the target is assumed to be capable of taking intelligent evasive action based on its sense of the missile's motion, a game theoretic approach may be more appropriate than the control theoretic approach. Mathematically, the problem is formulated by assuming that while the missile tries to

minimize a performance index based on miss distance, the target tries to maximize it. An appropriate performance index is

$$J = \frac{b}{2} y^2(t_f) + \frac{1}{2} \int_0^{t_f} \left[ \frac{a_M^2}{C_M} - \frac{a_T^2}{C_T} \right] dt \quad (36)$$

where  $b$  is the cost weighting factor on miss distance,  $C_M^{-1}$  weights the cost of accelerating the missile, and  $C_T^{-1}$  weights the cost of accelerating the target. The dynamic equations of constraint are

$$\dot{v}_M = a_M \quad \dot{v}_T = a_T \quad (37)$$

$$\dot{y}_M = v_M \quad \dot{y}_T = v_T \quad (38)$$

The control problem is to find a feedback control for the missile that will minimize the miss distance in spite of the target's optimal evasive maneuvers. The solution of this mini-max problem is<sup>4</sup>

$$a_M = \frac{-C_M(t_f - t) [y_M - y_T + (v_M - v_T)(t_f - t)]}{\frac{1}{b} + \frac{1}{3} (C_M - C_T)(t_f - t)^3} \quad (39)$$

$$a_T = \frac{C_T}{C_M} a_M \quad (40)$$

It is interesting to note that if the miss distance is heavily weighted and the LOS angle is small Eq. 39 becomes

$$a_M = -\frac{3}{\left(1 - \frac{C_T}{C_M}\right)} V \dot{\sigma} \quad (41)$$

which is again the law of proportional navigation with navigation constant

$$K_N = \frac{3}{1 - \frac{C_T}{C_M}} \quad (42)$$

In the case of a non-maneuvering target, the navigation constant becomes 3, while if the missile is assumed to be, say, twice as maneuverable as the target, the navigation constant becomes 6.

VIII. RECOMMENDATIONS: The missile-target engagement is clearly an example of a coupled dynamic system where motion of the missile influences motion of the target and vice versa. To make the problem more tractable it is usually assumed that the target's motion is completely known, a priori, throughout the encounter. More specifically, it is often assumed that the target has constant velocity. This allows decoupling of the missile-target equations and permits separate design of the guidance and control systems. The optimal solution then becomes a proportional navigation guidance system feeding commands to an acceleration-tracking autopilot.

A more general approach to the problem accounts for the



intelligent evasive action of the target and uses optimal differential game theory to design an integrated guidance-control system. Using this approach, Anderson<sup>5</sup> has shown, for several simple examples, that the game theoretic approach produces smaller miss distances than the optimal control approach. This topic should be explored further to more fully understand the relationships between the two methods and their relative advantages and disadvantages.

IX. REFERENCES:

1. B. Etkin, Dynamics of Flight - Stability and Control, Second Edition, Wiley & Sons, 1982.
2. A. Arrow, "Status and Concerns for Bank-to-Turn Control of Tactical Missiles," J. Guidance, Vol. 8, No. 2, March-April 1985.
3. D. E. Williams and B. Friedland, "Modern Control Theory for Design of Autopilots for Bank-to-Turn Missiles," J. Guidance, Vol. 10, No. 4, July-August 1987.
4. A. E. Bryson and Y. Ho, Applied Optimal Control, Wiley & Sons, 1975.
5. G. M. Anderson, "Comparison of Optimal Control and Differential Game Intercept Missile Guidance Laws," J. Guidance and Control, Vol. 4, No. 2, March-April 1981.

X. FIGURES:

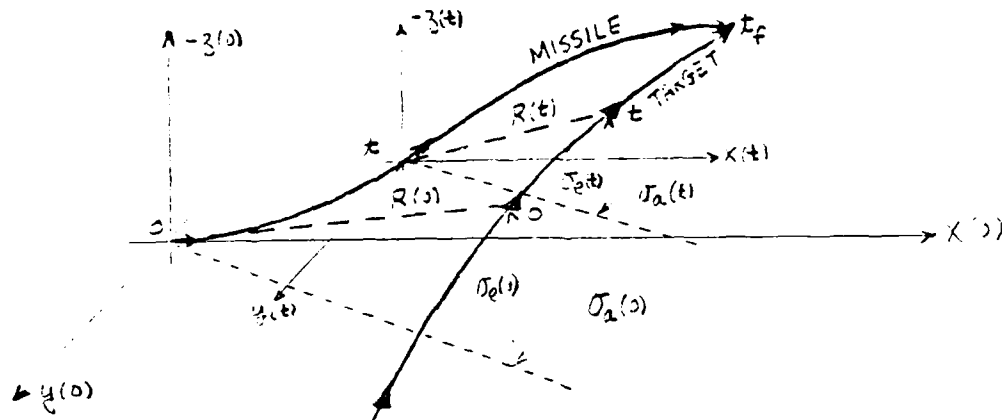


Fig. 1. Missile-target engagement in three dimensions.

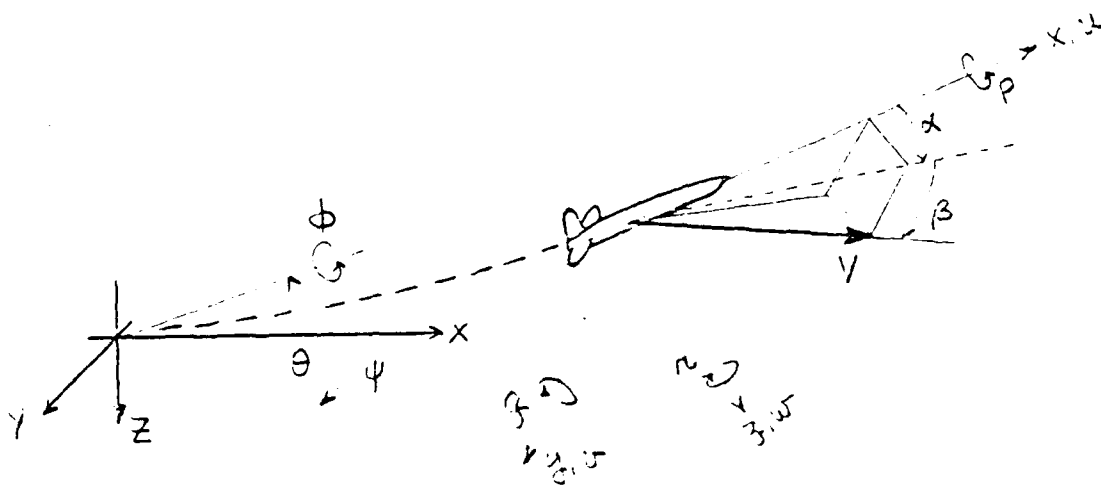
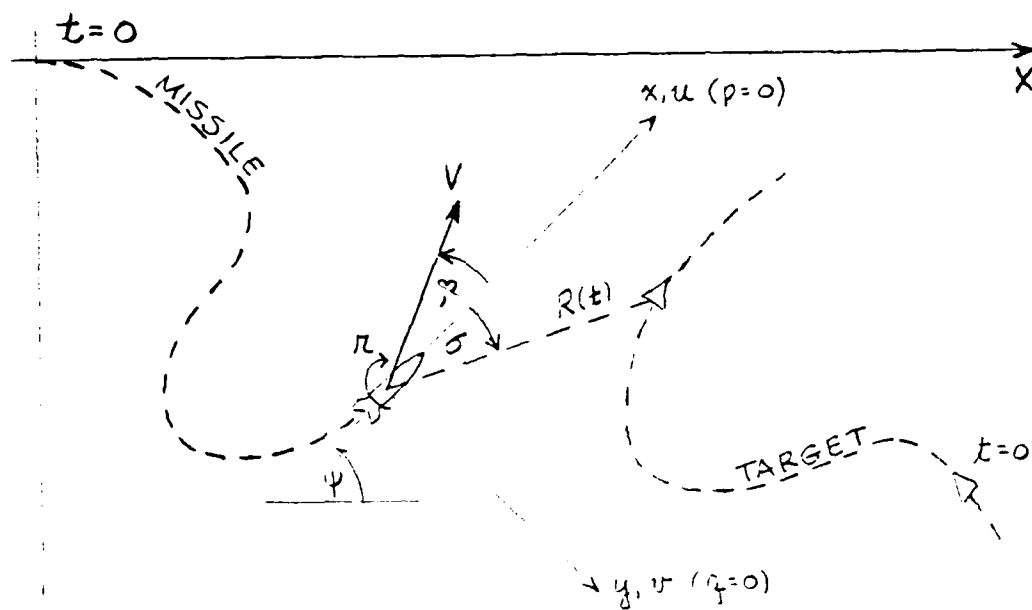


Fig. 2. Inertial and missile-principal-axes coordinate systems.



$y$

Fig. 3. Missile-target engagement on a horizontal plane.

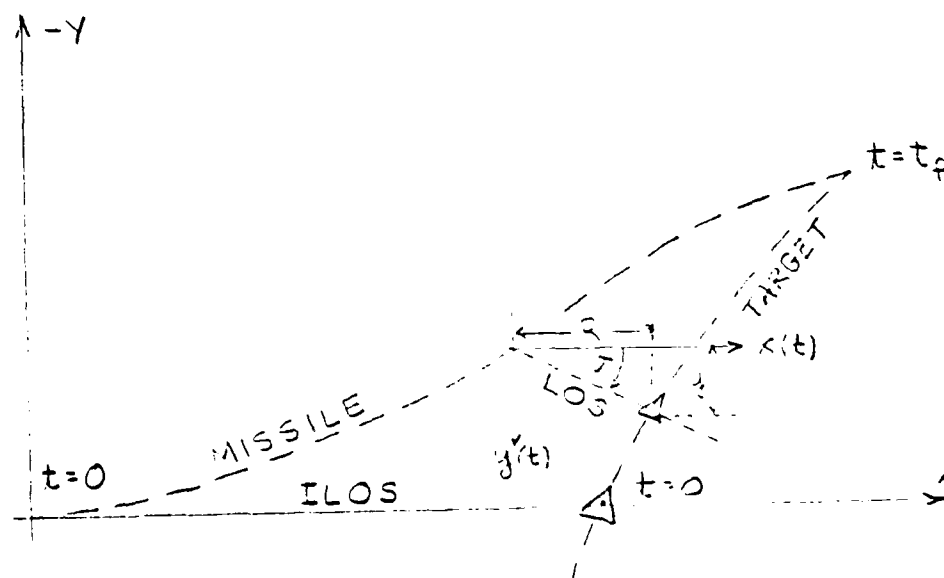


Fig. 4. Point-mass missile-target engagement on a horizontal plane.

1987 USAF-UES SUMMER FACULTY RESEARCH PROGRAM

GRADUATE STUDENT SUMMER SUPPORT PROGRAM

Sponsored by the  
AIR FORCE OFFICE OF SCIENTIFIC RESEARCH

Conducted by the  
Universal Energy Systems, Inc.

FINAL REPORT

Prepared by: Wilton Flemon, Ph.D.  
Academic Rank: Associate Professor  
Department and Chemistry Department  
University: Metropolitan State College  
Research Location: ASTRONAUTICS LABORATORY  
EDWARDS AFB CA 93523  
USAF Researcher: Robert D. Chapman  
Date: 27 Jul 87  
Contract No: F49620-85-C-0013

## BORAZINE REACTIONS

by

Wilton Flemon

### ABSTRACT

It has been known that certain covalently bonded cyclic compounds containing boron atoms linked to nitrogen atoms, externally bonded to nitro groups, amino substituents or polyintroaliphatic groups, were useful in the manufacture of chemicals that may be useful as propellants, explosives or other energetic related substances. The parent compound borazine (Stock, 1933) has been of especial interest in the preparation of these materials.

The direct or indirect preparation of these compounds by nitrolysis, aminolysis and/or polynitroalkylation of some N-tertiary aliphatic-B-haloborazines may be a route to the synthetic preparation of some of these compounds. Convenient methods to directly synthesize some N-aliphatic-or aryl-B-chloro or bromoborazine are known, however, direct synthesis of N-aliphatic-or aryl-B-fluoroborazine has been reported with difficulty (Steinberg, 1966 and Greenwood, 1954). Methods of dehydrofluorination of boron trifluoride amine adducts using metals (Kraus, 1930), metal hydrides (Lang, 1963) or organometallic compounds (Dornov, 1958) involves vigorous conditions, that are not suited to general laboratory application. B-Trifluoroborazine was reported to be indirectly synthesized (Niedenzu, 1962, 1963) and (Laubengayer, 1963). Other procedures using radical conditions (Wiberg, 1951) or difficultly obtainable reagents (Sujishi, 1957) gave unsatisfactory results.

Amine adducts using metals (Kraus, 1930), metal hydrides (Lang, 1963) or organometallic compounds (Dornov, 1958) involved vigorous conditions, that are not suited to general laboratory applications. B-trifluoroborazine was indirectly prepared (Niedenzu, 1962, 1963) and (Laubengayer, 1963) or difficultly obtained reagents (Sujishi, 1957) gave unsatisfactory results.

Harris, 1969, reported that N-tri-primary alkyl-B-trifluoroborazines were readily prepared by dehydrofluorinating primary amine adducts of boron trifluoride etherate or salts of fluoroboric with adducts of hindered, preferably tertiary amines with boron trifluoride.

This method was used to attempt to synthesize N-tri-tertiary butyl-B-trifluoroborazine, N-tri-acetyl-B-trimethylborazine and N-tri-tertiary butyl-B-trimethylborazine which would serve as precursors in the nitrolysis reactions. Attempts to synthesize the compounds failed.

Harris, 1969, reported that N-tri-alkyl-B-trifluoroborazines were readily prepared by dehydrofluorinating primary amine adducts of boron trifluoride etherate or salts of fluoroboric acid with adducts of hindered, preferably tertiary amine adducts with boron trifluoride.

The method of Harris, 1969, used to attempt to synthesize N-tri-tertiary butyl-trifluoroborazine, N-tri-acetyl-B-trimethylborazine and N-tri-tertiary butyl-B-trimethylborazine, compounds which serve as precursors in nitrolysis reactions. Attempts to synthesize these compounds were unsuccessful.

### ACKNOWLEDGEMENTS

I wish to thank the Air Force Systems Command and the Air Force Office of Scientific Research for sponsorship of this research. Universal Energy Systems must be mentioned for their concern and support.

Robert D. Chapman provided me with ideas, suggested synthesis schemes, encouragement, support that realized a rewarding, interesting, and enriching experience.

I would like to thank Louis A. Dee for running infrared spectra.

The Edwards Air Force Astronautics Laboratory provided me with a truly enjoyable work environment.

## I. INTRODUCTION:

Cyclic borazine of empirical formula,  $B_3N_3H_6$  (Stock, 1933 and Finch, 1969) and its derivatives containing compounds where amino substituents, polynitroaliphatic alkyl groups or nitro groups attached to boron and/or nitrogen ring atoms is of great interest to Edwards AFB Astronautics Laboratory.

It is belived that the introduction of such groups onto borazine would generate new compounds that may contain certain energetic properties that would be useful in explosives, propellants and other energetic type substances.

My research interests have been in the area of organic synthetic reactions in aprotic solvents; the preparation of alternative substances that may be useful as explosives and new techniques used in the synthesis of new energetic compounds.



## II. OBJECTIVES OF THE RESEARCH EFFORT:

Many synthetic routes to energetic compounds are derived at through analog of 2,4,6-trinitrotoluene (TNT). It is believed, however, that certain derivatives of borazine containing amino substituents, polynitroaliphatic alkyl groups or nitro group may be more effective energetic ingredients to modify the burn rates achievable in solid rocket propellants, explosives or other explosively energetic materials.

Dr Robert Chapman communicated with me, during the spring 1987, expressing interest in initiating new synthetic routes that possibly would lead to some energetic substances by the use of borazine derivatives.

During my pre-summer visit, I found chemicals and equipment available at the Astronautics Laboratory that were needed to attempt three borazine reactions. A library search (Harris, 1969) had indicated that a possible reaction scheme may be applicable in the synthesis of the compounds in mind.

It was decided to begin my Summer Faculty Research Program by attempting to synthesize N-tri-tertiary butyl-B-trifluoroborazine; followed by attempting to prepare, by analogy, N-tri-acetyl-B-trimethylborazine and N-tri-tertiary butyl-B-tri-methylborazine.

Synthetic routes to N-alkyl or aryl-B-trifluoroborazines received little attention during the years since Niedenzu, 1962, and Laubengayer, 1963, described their preparation employing the transhalogenation reaction between B-trichloroborazines and  $\text{TiF}_4$  or  $\text{SbF}_3$ . Noth, 1969, reported that the reactions of

$\text{BF}_3$  with either silylamines of the types  $(\text{CH}_3)_3\text{SiNHR}$  or  $(\text{CH}_3)_3\text{Si}_2\text{NCH}_3$  to give B-trifluoroborazines, along with  $(\text{CH}_3)_3\text{SiF}$  and in the former case,  $\text{RNH}_2 \cdot \text{BF}_3$  as well. Miller, 1968, indicated that B-tris(alkylamino-N-tri-alkylborazines and B-tris(arylamino-N-tri-arylborazines may be prepared almost quantitatively by employing the appropriate stoichiometry in the reaction between boron trichloride and an alkyl- or arylamine. The borazines so formed react with boron trifluoride or boron trifluoride etherate to give fair yields of B-trifluoro-N-trialkyl- and B-trifluoro-N-triarylborazines. These are indirect syntheses of B-trifluoroborazines.

However, Harris, 1969, reported that a convenient direct aminolysis of boron trifluoride or boron trifluoride etherate gives good yields of N-trialkyl-B-trifluoroborazines, when a suitable dehydrofluorinating reagent, usually a sterically hindered tertiary amine boron trifluoride adduct was employed, under selected stoichiometry. In general the procedure (Beachley, 1968, Turner, 1958, Butcher, 1965 and Muetteries, 1975) involved mixing of reagents at room temperature in an aprotic solvent such as benzene, ether, toluene or chlorobenzene. This is then heated to reflux, for several hours, where the borazine is formed, dissolved in the aprotic solution.

### III.

a. All reagents (except boron trifluoride etherate which had been previously distilled under house vacuum and refrigerated) were obtained from laboratory supply houses. The usual precautions necessary for moisture sensitive compounds were employed. Some drybox and vacuum line manipulation were used. Standard microlaboratory equipment was used.

Amines obtained from laboratory suppliers were refluxed and distilled before use. Methylboron dibromide was refluxed and distilled prior to use. Melting points were obtained using a Thomas Hoover Uni-melt Capillary Melting Point Apparatus. Proton nmr spectra were obtained using a JEOL FX-90Q FT-NMR Spectrometer (25°C). Infrared spectra were obtained using a Nicolet FT-IR Model 55XC Spectrometer.

b. In a typical reaction boron trifluoride etherate (0.016 mol) or methylboron dibromide (dissolved in benzene) was added in 10-25 minutes to a stirred solution of (0.01 mol) diisopropylethylamine or triethylamine (dissolved in benzene) and (0.06 mol) tertiary butylamine or acetamide (dissolved in benzene). The reaction mixture was stirred and heated (30-80°) to reflux for several hours (8 hours and sometimes overnight). The white, yellow to tan crystals and colorless solution originally formed being sometimes replaced by a rust colored slurry mixture containing a two layer system with solid crystals dispersed throughout both layers. After filtration, separation of layers and concentration of top layers, sublimation of both layers (100-210°/0.5mm-1.5mm Hg) produced yellow to rust to tan solids; melting points extended over wide temperature ranges.

c. Attempted synthesis of (1) N-tri-tertiary butyl-B-tri-fluoroborazine (2) N-tri-acetyl-B-trimethylborazine and (3) N-tri-tertiary butyl-B-trimethylborazine. The synthesis of these compounds were attempted as described above and as described by Harris, 1969. In all cases a two layer system formed with insoluble white to yellow to tan solid material dispersed throughout the layers. Filtration of the solids, concentration of the top benzene layer produced an oil; sublimation (100-210°C/0.5mm Hg-1.5mmHg) of both oily layers

#### IV. RECOMMENDATIONS

a. The attempted synthesis of N-tri-tertiary butyl-B-trifluoroborazine, N-tri-acetyl-B-trimethylborazine and N-tri-tertiary butyl-B-trimethyl by the method outlined by Harris, 1969, was not successful.

b. Attempts to communicate with Harris, 1969, will be made.

c. The amines used diisopropylethylamine and triethylamine, are of critical importance to the reaction. Their alkyl groups should be large enough to reduce the stability of the adducts. The chemistry is not well defined that describes the mechanism of effective dehydrofluorinating reagents (Curwell, 1967, Turner, 1965, and Pollock, 1962). More investigation into the chemistry of these adducts should be continued.

d. Further investigation should be undertaken in order to determine the influence of solvents toward the formation of these borazines. Benzene was the only solvent employed during this program. The effect of other solvents, particularly chlorobenzene, ether, toluene, and triethylamine should be further look at.

produced yellow to tanish solids. In all cases that solid produced melting points with wide temperature ranging; (1) 100-120°C, (2) 85-95°C (3) 60-65°C. Proton nmr spectra in all cases were complex including mixtures. IR spectra were suggesting salts.

## REFERENCE

- Beachley, O. T. Inorganic Chem. 7, 701 (1968).
- Butcher, M. I. and Gerraud, W. J. Inorg. Nucl. Chem. 8,411 (1967).
- Dornov, A. and Gehrt, H. H. Z. Anorg. Allgem. Chem. 294, 81 (1963).
- Finch, A., Leach, J. B. and Morris, J. H. Organometal. Chem. Rev. A4, 1 (1969).
- Greenwood, N. N. and Martin, R. L., Quart. Rev., London, 8, 1 (1954).
- Harris, J. J. and Rudner, B., Inorgan. Chem. 8, 1258 (1969).
- Kraus, C. A. and Brown, E. H. J. Amer. Chem. Soc., 52, 4414 (1930).
- Lang, K. and Schubert, F., U. S. Patent 3,090, 809 (1963).
- Laubengayer, A. W. and Beachley, O. T. Advan. Chem. Ser. 28, 281 (1963).
- Miller, J. J. and Johnson, F. A. J. Amer. Chem. Soc. 90, 218 (1968).
- Muetteries, E. L. "Boron Hydride Chemistry" Academic, New York (1975).
- Niedenzu, K. Inorg. Chem. 1, 963 (1962).
- Niedenzu, K., Beyer, H. and Jenne, H. Chem. Ber. 96, 2649 (1963).
- Noth, H. and Regnet, W. Chem. Ber. 102, 167 (1969).
- Pollock, J. M. U. S. Patent. 3,055,927 (1963)
- Sujishi, S. and Witz, S., J. Amer. Chem. Soc. 79, 2447 (1957).
- Steinberg, H. and Brotherton, R. J. Organoboron Chemistry, Vol 2.  
Boron-Nitrogen and Boron-Phosphorous Compounds. New York Interscience  
(1966).
- Stock, A. "Hydrides of Boron and Silicon" Cornell Univ Press, Ithaca, New York  
(1933).
- Turner, H. S. and Warne, R. J. Chem. Ind., London, 526 (1958)
- Turner, H. S. and Warne, R. J. Proc. Chem. Soc. 69 (1962).

1987 USAF-UES SUMMER FACULTY RESEARCH PROGRAM/

GRADUATE STUDENT SUMMER SUPPORT PROGRAM

Sponsored by the

AIR FORCE OFFICE OF SCIENTIFIC RESEARCH

Conducted by the

Universal Energy Systems, Inc.

FINAL REPORT

CHEMICAL AND SPECTROSCOPIC EVALUATION OF ANTIMONY SULFIDES

Prepared by:	Dennis R. Flentge, Ph. D.
Academic Rank:	Associate Professor
Department and University:	Science and Mathematics Cedarville College
Research Location:	Aero Propulsion Lab AFWAL/POSL Lubrication Lab Wright-Patterson AFB, OH
USAF Researcher:	Phillip W. Centers
Date:	September 11, 1987
Contract No:	F49620-85-C-0013

# CHEMICAL AND SPECTROSCOPIC EVALUATION OF ANTIMONY SULFIDES

by

Dennis R. Flentge

## ABSTRACT

Samples of  $\text{Sb}_2\text{S}_3$ ,  $\text{Sb}_2\text{S}_4$ , and  $\text{Sb}_2\text{S}_5$  were examined using infrared, Raman, and quantitative techniques to determine what factors contribute to the ability of  $\text{Sb}_2\text{S}_4$  to enhance the lubricating ability of  $\text{MoS}_2$ . The antimony sulfides were extracted using either isooctane or carbon disulfide and the extracted material was examined using infrared spectroscopy. No definite conclusions were reached concerning the source of the enhancing ability of the  $\text{Sb}_2\text{S}_4$ .



### Acknowledgments

I would like to thank the Air Force Systems Command and the Air Force Office of Scientific Research for sponsorship of my research. I would like to thank the Lubrication Lab of the Aero Propulsion Lab for the excellent facilities and the stimulating research atmosphere. I would like to thank Dr. Phillip W. Centers for special guidance in this research project, Chris Klenke and Lt. Charles Kelley, Ph. D., for helpful technical discussions, and Dr. Ken Kim for assistance in obtaining the infrared spectra.

## I. INTRODUCTION

Solid lubricants which could operate in the temperature range of 315-540°C and which could be used in roller bearings in small turbine engines have been the target of recent research.<sup>1, 2</sup> Centers<sup>2</sup> has studied the role of bulk additives in a series of mixtures which contained MoS<sub>2</sub> as the lubricant. He found that the essential mechanism for the enhancement of the lubricating ability of the MoS<sub>2</sub> was the ability of the additive to deform "...at asperity contact temperatures to permit and retain the tribologically preferred orientation of the solid lubricant."<sup>2</sup>

Performance of the additives generally followed a linear relationship that depended on the hardness of the additive. One substance, Sb<sub>2</sub>S<sub>4</sub>, showed better than normal behavior. It was of interest, therefore, to examine this compound in more detail to determine which of its structural or chemical properties contributed to its above average performance as an additive.

My research background includes a significant involvement in infrared and raman spectroscopy, two techniques that could be used to examine the antimony sulfides. My previous experience in the lubrication labs at Wright-Patterson AFB gave me a general understanding of the important properties of lubricants.

## II. OBJECTIVES OF THE RESEARCH EFFORT:

In order to study the structure and chemical properties of the antimony sulfides the following goals were set for this summer's work:

1. To use separation techniques to prepare a set of pure samples of the antimony sulfides.

2. To use infrared spectroscopy to study the bonding of the surface species in the antimony sulfides.
3. To apply a series of appropriate spectroscopic techniques to analyze the structure of the antimony sulfides.

### III. EXTRACTION TECHNIQUES

Samples of  $\text{Sb}_2\text{S}_3$ ,  $\text{Sb}_2\text{S}_4$ , and  $\text{Sb}_2\text{S}_5$  were treated with carbon disulfide and/or isooctane in a Soxhlet extraction apparatus in an attempt to remove any molecular sulfur from the solid samples. Sample weight loss during the extraction process ended after about 7 hours of extraction time. The extraction solvent was evaporated and the mass of residue was measured.  $\text{Sb}_2\text{S}_3$  showed no weight loss,  $\text{Sb}_2\text{S}_4$  showed a very small weight loss, and  $\text{Sb}_2\text{S}_5$  displayed a weight loss of about 15%. The mass of the residue matched the weight loss of the samples very well.

Quantitative analysis of the samples using a standard potassium permanganate solution<sup>3</sup> gave the results shown in Table 1. (The procedure described in reference 3 can be modified when pure antimony sulfide samples are used. The dissolution step in hot concentrated sulfuric acid can be eliminated and the sulfides can be dissolved directly in cold concentrated hydrochloric acid. The solution should be gently heated to drive off the hydrogen sulfide before the permanganate titration can be done.) Samples of the tetrasulfide and the pentasulfide seem to show an impurity present that was not removed with the extracting solvent. There is evidence that antimony exists in the +3 oxidation state in  $\text{Sb}_2\text{S}_5$ .<sup>4</sup> The amount of sulfur extracted from the  $\text{Sb}_2\text{S}_5$  sample leaves a stoichiometric ratio of Sb to S that is very close to that for  $\text{Sb}_2\text{S}_3$ .

Table 1. Percent Sb in Antimony Sulfide Samples

Sample	Unextracted	Extracted		Theoretical Value
		w/isooctane	w/CS <sub>2</sub>	
Sb <sub>2</sub> S <sub>3</sub>	71.70			71.69
Sb <sub>2</sub> S <sub>4</sub>	63.05	63.05		65.51
Sb <sub>2</sub> S <sub>5</sub>	57.59		69.46	60.30

#### IV. INFRARED STUDIES

Infrared studies were completed using the diffuse reflectance attachment of a Nicolet X60 Fourier Transform Infrared Spectrophotometer. Figures 1-7 contain the infrared spectra for the unextracted and extracted antimony sulfide samples, sulfur extracted from Sb<sub>2</sub>S<sub>5</sub>, and pure sulfur. Table 2 summarizes the peaks observed.

Sb<sub>2</sub>S<sub>3</sub> shows virtually no detail in its ir spectrum. Perhaps the dark surface does not reflect enough energy to provide adequate detail in the spectrum. Comparison of the spectra of extracted and unextracted Sb<sub>2</sub>S<sub>4</sub> shows only one significant change--the disappearance of the band at 1693 cm<sup>-1</sup>. There is a band at 1677 cm<sup>-1</sup> in the spectrum of the extracted sulfur from Sb<sub>2</sub>S<sub>5</sub> which may be associated with the same vibration as the band at 1693 cm<sup>-1</sup>. However, there is no evidence for this band in the spectrum of unextracted Sb<sub>2</sub>S<sub>5</sub> although it may be hidden under the band at 1624 cm<sup>-1</sup>. This band and the one centered around 3400 cm<sup>-1</sup> are most likely associated with water that is adsorbed on the sample.<sup>5</sup>

It is interesting to note that many of the bands seen in the spectra of the antimony sulfides are seen in the spectrum of the extracted sulfur and of pure sulfur. One could draw the conclusion that some of the detail in the antimony sulfide spectra is from sulfur which has been trapped within the sulfide structure. This would

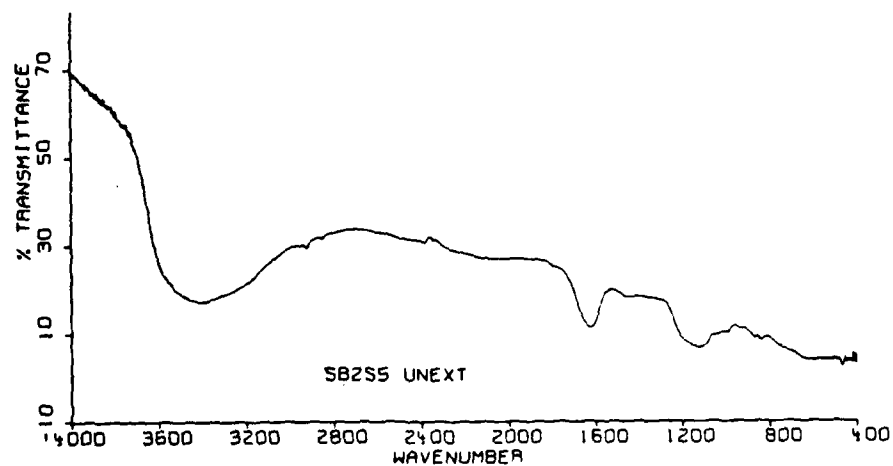
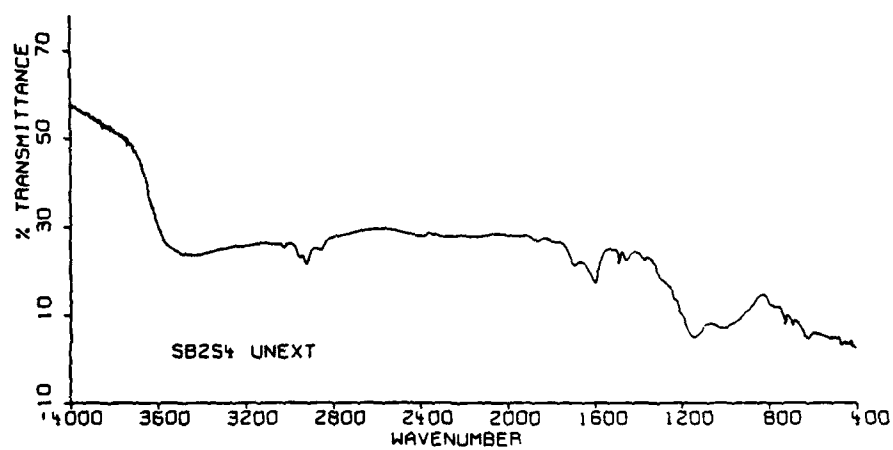
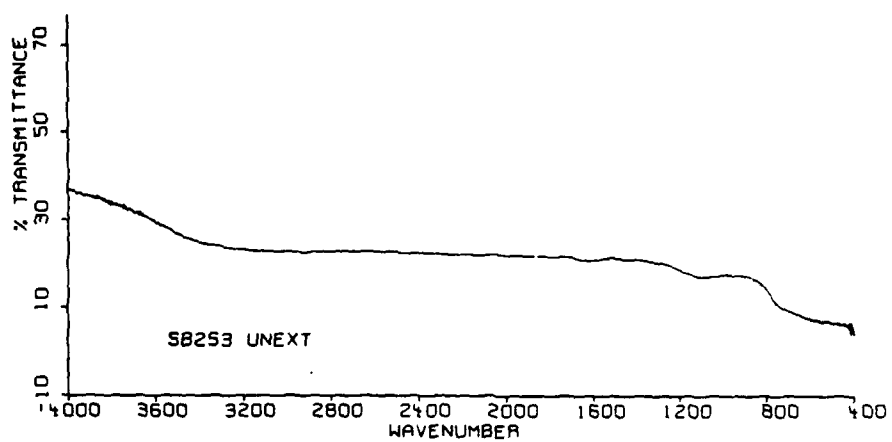


Figure 1

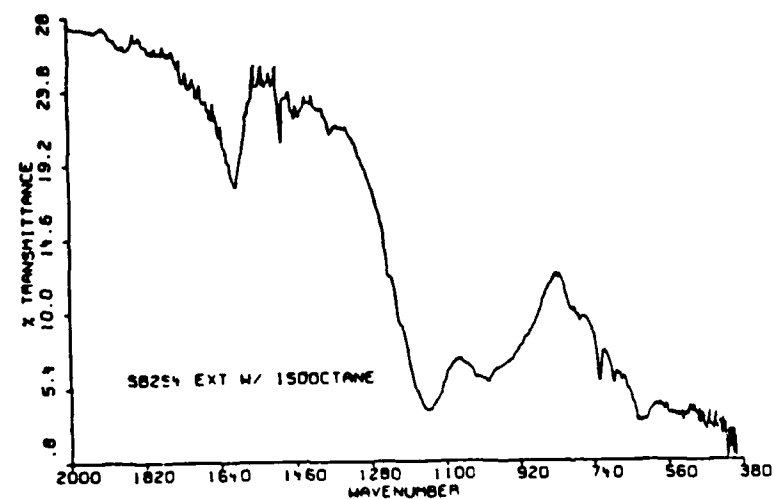
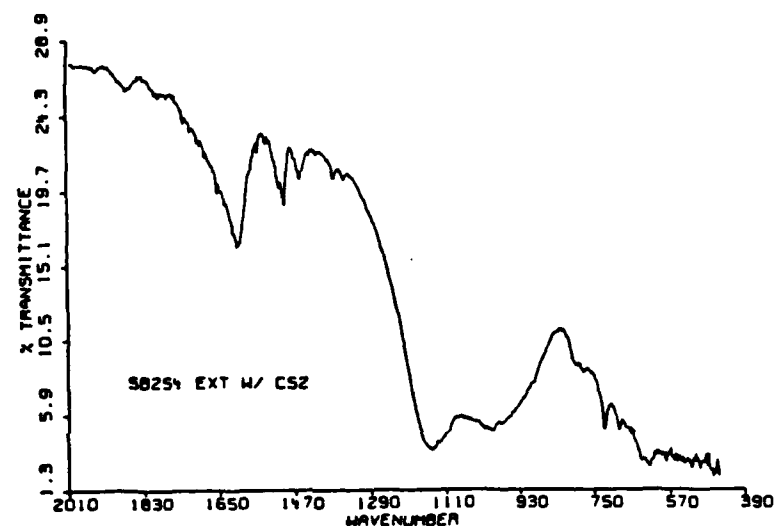
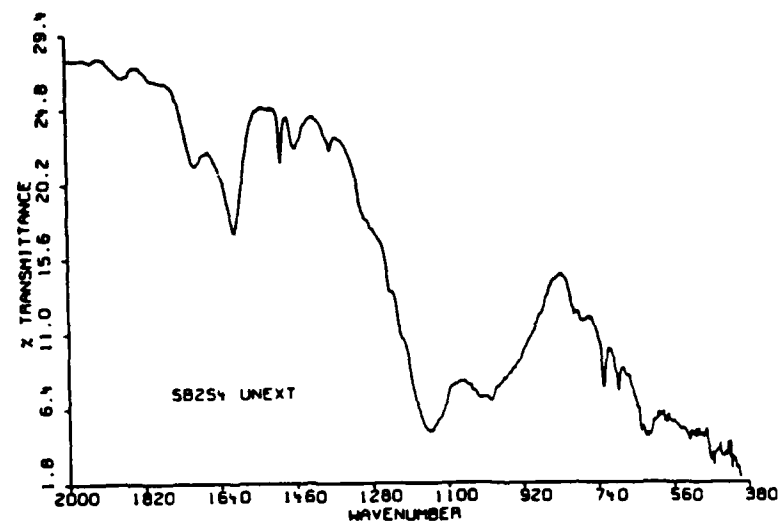


Figure 2

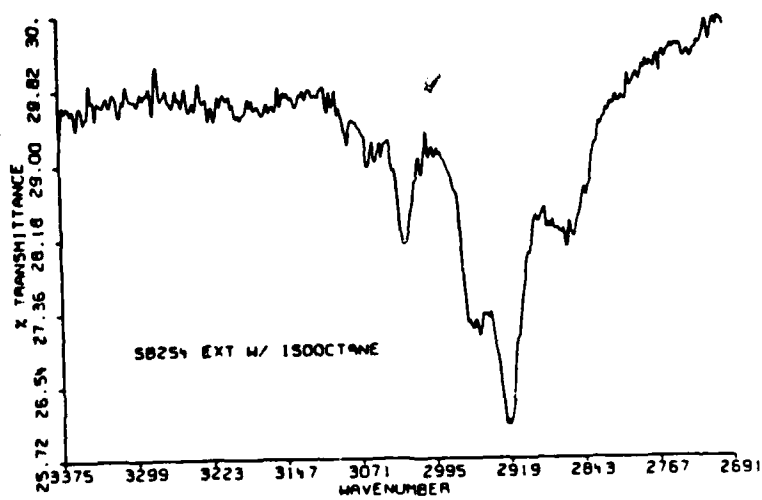
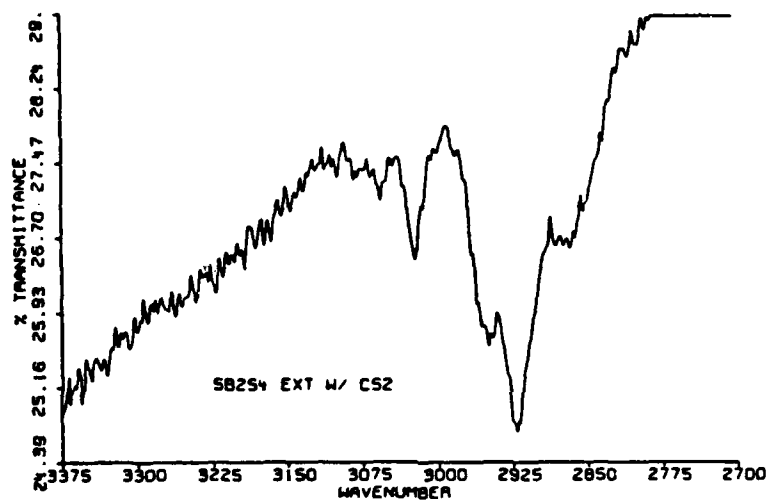
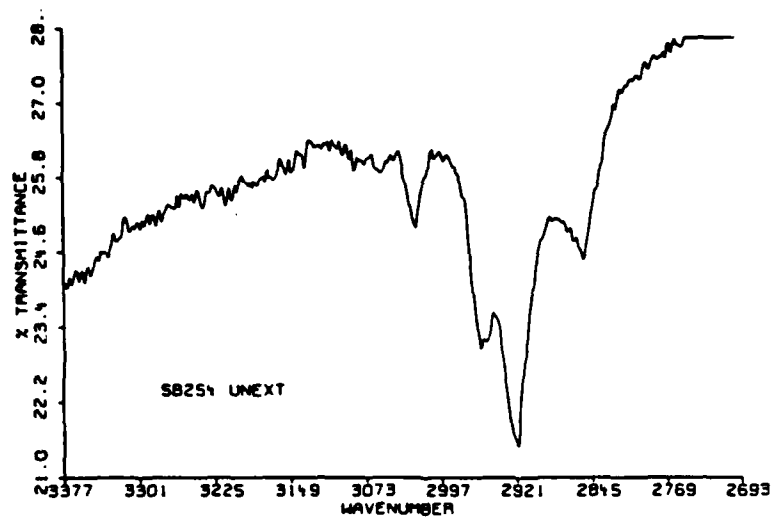


Figure 3

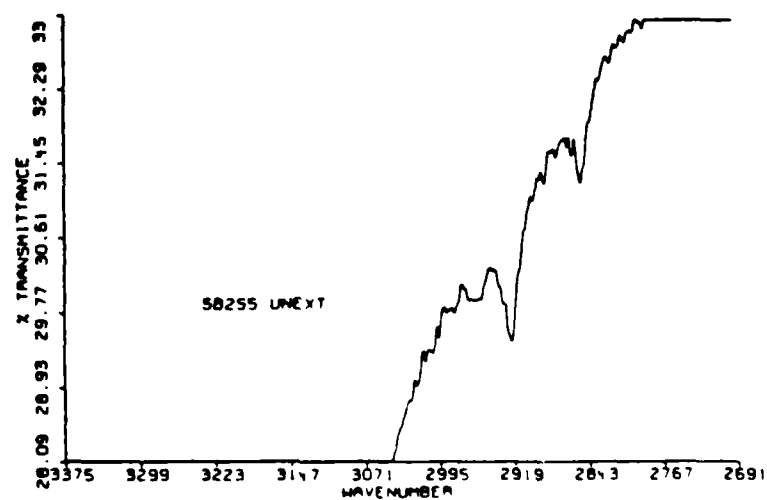
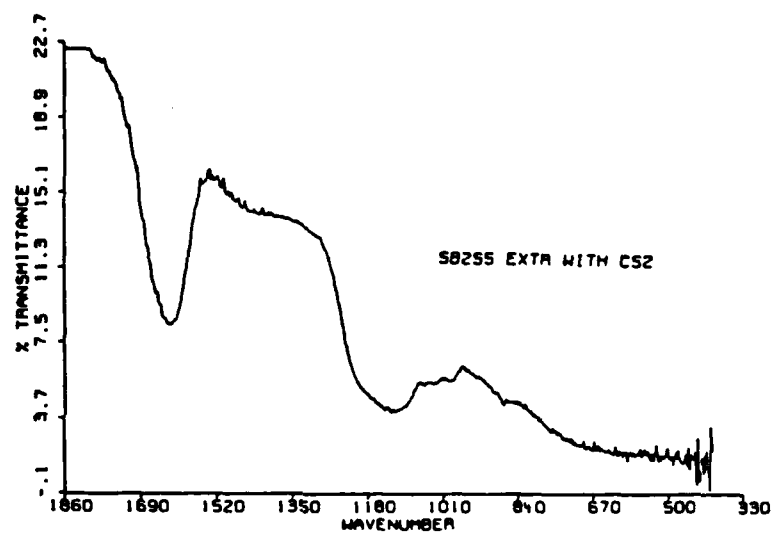
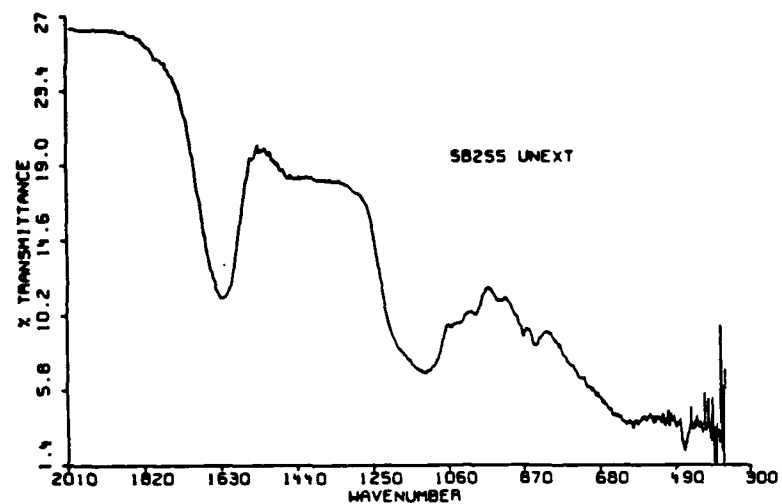


Figure 4



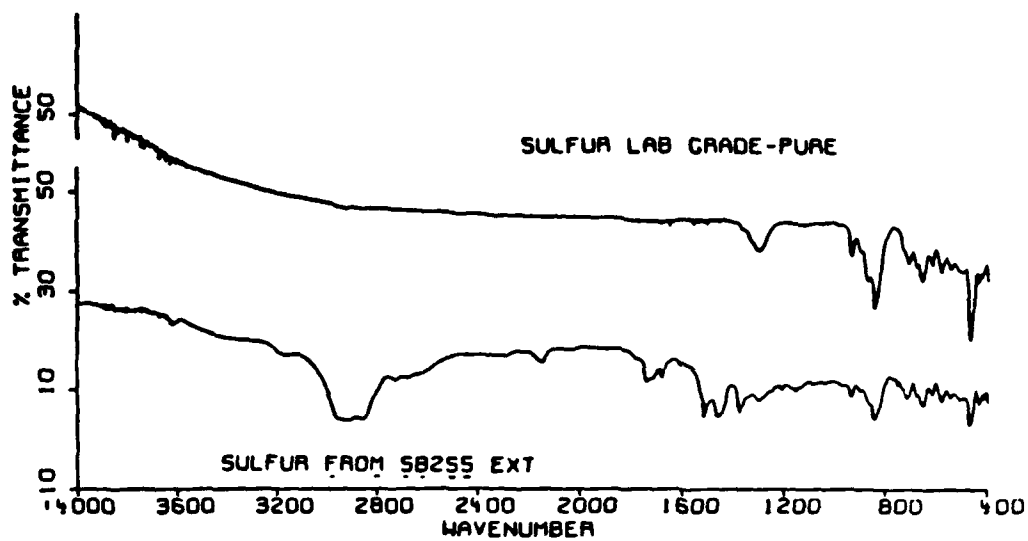


Figure 5.

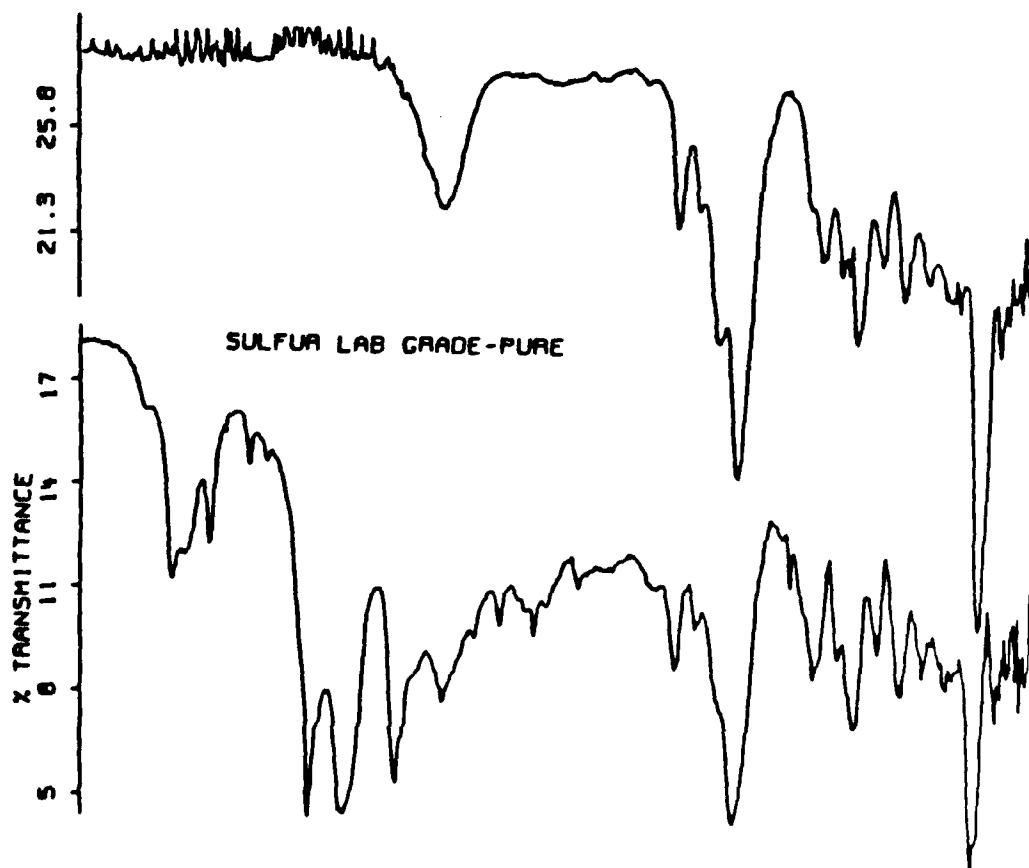


Figure 6. Sulfur spectra in the range below 1800 cm<sup>-1</sup>.

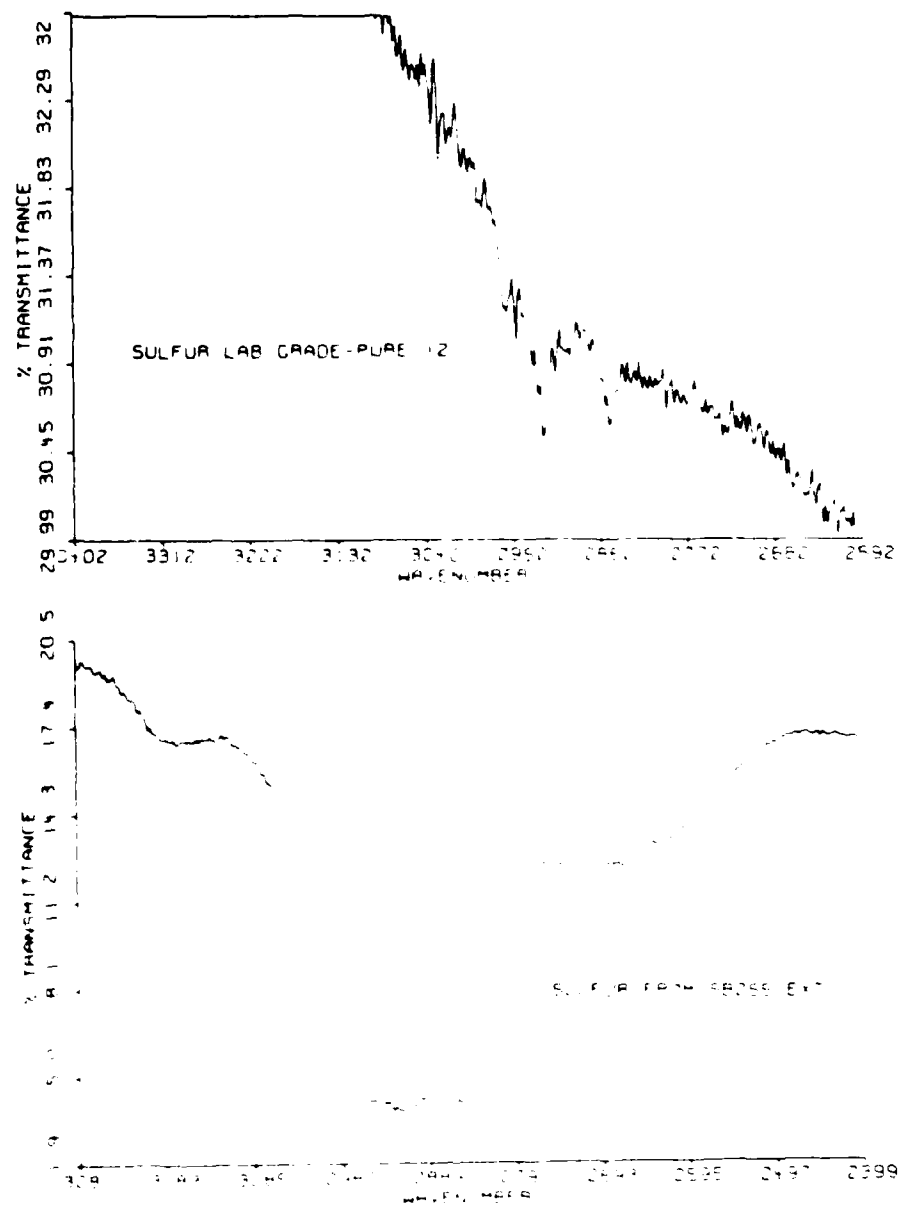


Figure 7

AO-A191 203

UNITED STATES AIR FORCE SUMMER FACULTY RESEARCH PROGRAM

11/11

(1987) PROGRAM TE. (U) UNIVERSAL ENERGY SYSTEMS INC

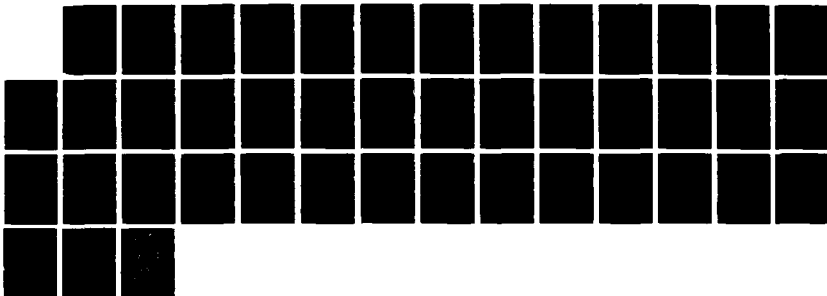
DAYTON OH R C DARRAN ET AL. DEC 87 AFOSR-TR-88-0212

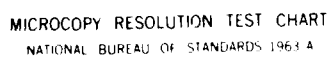
UNCLASSIFIED

F49620-85-C-0013

F/G 5/1

NL





MICROCOPY RESOLUTION TEST CHART  
NATIONAL BUREAU OF STANDARDS 1963 A

Table 2. Infrared Bands for Sb<sub>2</sub>S<sub>4</sub>, Sb<sub>2</sub>S<sub>5</sub>, and Sulfur

Sb <sub>2</sub> S <sub>4</sub> unext	Sb <sub>2</sub> S <sub>4</sub> ext w/ isooctane	Sb <sub>2</sub> S <sub>4</sub> ext w/ CS <sub>2</sub>	Sb <sub>2</sub> S <sub>5</sub> unext	Sb <sub>2</sub> S <sub>5</sub> ext w/ CS <sub>2</sub>	Sulfur ext. from Sb <sub>2</sub> S <sub>5</sub>	Sulfur pure
			3410	3400	3611 3160	
	3084vw					
3058	3055	3058				
3024	3026	3023	2984vw			
2954	2952	2949	2960		2958	2953vw
2918	2920	2921	2923		2917	2921vw
2853	2865	2872	2855		2851	2853vw
					2724	
					2669	
					2150	
					2032	
1866	1866	1862				
1778w		1779vw	1781w		1778	
					1738	
					1718	
1693	1680				1677	1690
1602	1303	1603	1624	1626	1611	
					1583	
					1515	
1458	1455	1457			1459	
1374	1374	1372	1394	1406	1376	
		1351vw				1358
					1300	1300
1283						
					1209	
1142	1148	1141	1122	1128	1153	1123vw
1019	1021		1044		1085	1046
994	994	999	989	994		984vw
			929		934	938
					901	899
			869			
			839		842	841
772	782				754vw	
728	727	728			717	708
694	692	698vw			680	679
					656	656
622	625	629vw			616	611
			591		581	582
					546	546
462w			469		470	467
					434	431

be consistent with the fact that Sb<sub>2</sub>S<sub>3</sub> shows virtually no ir bands and also gave up no sulfur to the extraction process.

The origin of bands above  $2800\text{ cm}^{-1}$  is not easily discerned. This is typically a region in which C-H stretching bands appear. Stretching vibrations from an S-H bond should be nearer  $2600\text{ cm}^{-1}$ . However, there should be no hydrogen present in the sample so the origin is even more puzzling. The bands could come from impurities introduced into the sample at some point in its preparation. It should be noted that very weak bands appear at 2853, 2921, and  $2953\text{ cm}^{-1}$  in the sublimed sample studied. These bands disappeared from the spectrum of  $\text{Sb}_2\text{S}_3$  upon extraction and appeared as reasonably strong bands in the sulfur that was extracted.

#### V. OTHER SPECTROSCOPIC TECHNIQUES

An unsuccessful attempt to record Raman spectra for the sulfides was made. The samples were poor scatterers of the laser light and only the plasma lines from the laser were observed.

Other individuals in the laboratory began differential scanning calorimetry and thermogravimetric analysis. Initial results have not produced definitive data.

Samples have been sent out to a lab which specializes in Mossbauer spectroscopy. Results have not been returned at this point.

#### VI. CONCLUSIONS AND RECOMMENDATIONS

Results from the extraction and quantitative analysis experiments indicate that most of the free sulfur is readily extractable using carbon disulfide or isooctane as the solvent. Quantitative analysis of extracted  $\text{Sb}_2\text{S}_4$  and  $\text{Sb}_2\text{S}_3$  samples indicates that a small percent of some substance, presumably sulfur, remains in the sulfide. Infrared spectra of  $\text{Sb}_2\text{S}_4$  support this observation.

The following experiments could add understanding to the data reported above.

1. Extraction of  $\text{Sb}_2\text{S}_4$  to get a sample of sulfur for infrared analysis.
2. Elemental analysis of the antimony sulfides and the extracted sulfur could determine if some impurities are present which are contributing to the infrared spectra.
3. Heating samples of pure  $\text{Sb}_2\text{S}_4$  and of a mixture of  $\text{MoS}_2$  and  $\text{Sb}_2\text{S}_4$  to temperatures used in the tribological studies and recording ir spectra (after cooling to room temperature).
4. DSC and TGA studies should be performed on the sulfides.
5. Extraction at lower temperature should be attempted to determine if the extraction procedure itself is contributing to the formation of free sulfur in the samples.

## REFERENCES

1. M. N. Gardos and B. D. McConnell, "Development of a High-Load, High-Temperature Self-Lubricating Composite--Part III: Additive Selection," ASLE-ASME Lubrication Conference, October 5-7, 1981, New Orleans, LA.
2. P. W. Centers, "The Role of Bulk Additions in Solid Lubricant Compacts," Ph. D. Dissertation, University of Dayton, December, 1986.
3. W. Pierce, E. Haenisch, and D. Sawyer, Quantitative Analysis, 4th Ed., 1958, John Wiley and Sons, New York, NY, pp. 283-4.
4. J. G. Stevens and L. H. Bowen, "Mossbauer Spectroscopy of Inorganic Antimony Compounds," Mossbauer Effect Methodology, Vol. 5, 1970, Plenum Press, pp. 27-43.
5. K. Nakamoto, Infrared Spectra of Inorganic and Coordination Compounds, 2nd Edition, 1970, Wiley-Interscience, New York, NY.



1987 USAF-UES SUMMER FACULTY RESEARCH PROGRAM/  
GRADUATE STUDENT SUMMER SUPPORT PROGRAM

Sponsored by the  
AIR FORCE OFFICE OF SCIENTIFIC RESEARCH

Conducted by the  
Universal Energy Systems, Inc.

FINAL REPORT

The Evaluation of a Thermal-Hydraulic Design  
of a Fixed Particle Bed Reactor and  
Suggested Model Revisions

Prepared by:	L. D. Flippen, Jr. Ph.D.
Academic Rank:	Assistant Professor
Department and	Department of Mechanical and Nuclear Engineering
University:	Mississippi State University
Research Location:	AFAL/LKCS Edwards AFB CA 93523
USAF Researcher:	George Allen Beale
Date:	17 August 1987
Contract No:	F49620-85-C-0013

The Evaluation of a Thermal-Hydraulic Design  
of a Fixed Particle Bed Reactor and  
Suggested Model Revisions

by

L. D. Flippen, Jr.

ABSTRACT

The thermal-hydraulic model used by the Brookhaven National Laboratory in their design of a fixed particle bed nuclear reactor for space propulsion applications has been evaluated. Possible areas of concern have been identified which suggest either further investigation or actual model revision. Considering the extremes between the simple Brookhaven model and a cumbersome all-inclusive model, it is suggested that an intermediate model be used which is easily expanded (if the need arises). Work has been initiated on the implementation of such an intermediate model.

### ACKNOWLEDGEMENTS

The author would like to thank the Air Force Systems Command, the Air Force Office of Scientific Research, and the Air Force Astronautics Laboratory (LKCS) for their sponsorship of this research. The help of Universal Energy Systems in connection with administrative matters is also appreciated.

The author would also like to thank the many individuals he worked with at LKCS for their generous help. In particular, thanks are due to George Allen Beale and Ryan Haaland, for whom this work has the most relevance.

## I. INTRODUCTION:

The Fixed Particle Bed Reactor (FPBR) appears to be a promising concept for nuclear propulsion in space. Because of its novelty, the design of a prototype FPBR should be given careful consideration. For this reason an FPBR design from Brookhaven National Laboratory (BNL) is currently being evaluated by the Air Force Astronautics Laboratory (AFAL) at Edwards Air Force Base. As part of this evaluation process, the remainder of this paper outlines some of the concerns of the author in connection with the BNL design. This document is not intended to be a comprehensive assessment of the design. The main effort centers on the core thermal-hydraulics, since this, (in combination with its structural consequences), had apparently provided the main limitations to past nuclear propulsion designs (Fraas, 1986). This design evaluation was based on the BNL design as presented by Botts et. al. (1983) and Powell et. al. (1987). The evaluation process ultimately lead the author to suggest ways to upgrade and expand the mathematical model used for the thermal-hydraulics design.

The author's background in nuclear engineering and mechanical engineering, with an emphasis in the thermal-fluid sciences, forms the fundamental basis of the author's qualifications to do the work carried out in this report. Though the author has not had prior experience specifically in porous media flow and heat transfer, nuclear propulsion, or particle bed reactors, this was not considered to be a serious handicap. In fact, a lack of prior bias in these areas may be perceived as being beneficial to an impartial evaluation of the design.

## II. OBJECTIVES OF THE RESEARCH EFFORT:

The Air Force Astronautics Laboratory is supporting the AFSC Forecast II initiative PT-02, Safe Compact Nuclear Propulsion. AFAL has solicited the National Laboratories for their conceptual nuclear reactor designs that may be applicable to space nuclear propulsion. Design considerations are: compactness, light weight, low nuclear fuel inventory, non-criticality potential during launch, high temperature operation (3000K), disposal after use, and economics. Three National Laboratories submitted designs or indicated their interest: Brookhaven National Laboratory (BNL) with their particle bed nuclear reactor, Idaho National Engineering Laboratory (INEL) with their Small Nuclear Reactor Engine (SNRE) design, and Los Alamos National Laboratory (LANL) with their version of the SNRE. AFAL is currently in the process of evaluating these conceptual designs to determine technology and safety issues. The plan is to downselect to two concepts by April 1988 for component evaluation. One concept is to be the particle bed reactor and the other design is to be based on the solid core design.

The particle bed nuclear reactor and the solid core nuclear reactor designs as submitted by the National Laboratories are being evaluated and assessed by AFAL as to their technological attainability and safety concerns. Initially, the author was asked to look over the submitted designs for the purpose of identifying key issues of concern with a subsequent narrowing of scope to the investigation of an area of one design in more detail. It was decided that the particle bed nuclear

reactor design of BNL, being the design with the greatest potential benefits but also the greatest uncertainty as to its feasibility, was the one to concentrate on. Little time was actually spent in the evaluation of the other two designs since the time allocated to the author was too limited to assess all three designs adequately. For similar reasons, the scope of the investigation was narrowed to the thermal-hydraulics aspects of the BNL design after an initial overview of the whole design by the author.

### III. MORE GENERAL THERMAL-HYDRAULICS MODELS:

Probably the best way to document the areas of possible concern in the thermal-hydraulics model used by BNL in their FPBR design is to first develop a more general model which relies upon fewer assumptions. This is carried out in great detail in the full report of this work (Flippen, 1987), of which this is a greatly condensed version (required because of the page limitation imposed on reports submitted to Universal Energy Systems for AFOSR). The more general model developed assumes: steady state, single phase flow, an effectively homogenized fuel bed, a Darcy's Law form for bed flow resistance, negligible external forces (such as gravity, etc.), and that the main density variations in the gas are due to heating. Limitations on the various correlations used are also discussed. The original (full) fuel bed gas flow model, derived in the full report, can be summarized as:

$$(D P_{,i})_{,i} = 0 \quad (1A)$$

for the fuel bed pressure  $P$  and

$$D = [ (4A |P_{,i}| + B^2)^{1/2} - B ] / (2A |P_{,i}| ) \quad (1B)$$

The mass flow rate per unit area is then found (for  $G_i = \rho U_i$ ) by

$$G_i = -D P_{,i} \quad (1C)$$

(which is a form of Darcy's Law). The results are analogous to sourceless heat conduction. (Cartesian tensor notation has been used, along with the usually associated summation convention.) One solves the elliptic system (1A) and (1B) subject to the boundary conditions

$$n_i G_i = -n_i D P_{,i} \text{ prescribed on all or part of } S$$

= prescribed normal mass flow rate per unit area

and

$$P \text{ prescribed on all or part of } S$$

where  $S$  is the surface boundary enclosing the bed and  $n_i$  is its outward unit normal vector at any given point. The energy equations are:

$$\begin{aligned} C_p G_i T_{,i} = & -(q_g)_{,i} + Q_g + \epsilon(\beta T/\rho) G_i P_{,i} \\ & + \rho \Phi + R + h_g (AV)_f (T_f - T) \end{aligned} \quad (2)$$

$$[K_{\text{eff}} (T_f)_{,i}]_{,i} - (q_{\text{rad}})_{,i} + Q - R - h_g (A/V)_f (T_f - T) = 0 \quad (3)$$

for the gas and the particle fuel bed, with the additional constitutive equations:

$$A = 1.75(1 - \epsilon)/[\epsilon^3 \rho_g d] \quad (4A)$$

$$B = 150(1 - \epsilon)^2 \mu / [\epsilon^3 \rho_g d^2] \quad (4B)$$

and

$$h_g = K_g \text{Nu}/d \quad (5A)$$

$$\text{Nu} = \text{Nu}(\epsilon, \text{Re}, \text{Pr}) \quad (5B)$$

$$\text{Pr} = C_p \mu / K_g \quad (5C)$$

$$\text{Re} = d |G_i| / \mu \quad (5D)$$

and also

$$Q = w F \quad (\text{within } V) \quad (6A)$$

where

$$w = P_{\text{th}} / \int_V F dV \quad (6B)$$

where the full explanation of the notation and symbols can be found in Flippen's report (1987).

The Brookhaven National Laboratory fuel bed model, which leaves



out many of the physical phenomena that is included in the above model, can be summarized as:

$$P(r) = P_0 + m^2/(4\pi^2) \int_{r_0}^r A(T(r',z))/r'^2 dr' + m/(2\pi) \int_{r_0}^r B(T(r',z))/r' dr' \quad (7A)$$

$$T(r) = T_0 - 2\pi/m \int_{r_0}^r [Q(r')/C_p] r' dr' \quad (7B)$$

$$G(r) = m/(2\pi r) = mH/(2\pi rH) = \dot{m}/A_r \quad (7C)$$

$$T_f = Q/[h_g (A/V)_f] + T \quad (7D)$$

where  $\dot{m}$  is the total mass flow rate through the fuel bed. This, along with equations (4), (5), and (6), is the model used by Botts et. al. (pg. A2-1 to A2-4, 1983). This is an extremely simple model of the thermal behavior of the bed and a number of unsupported assumptions have been made. Strictly speaking, each term neglected should be accompanied by at least an order-of-magnitude analysis to lend plausibility to its being neglected. The BNL design did not include such estimates.

Another potential problem with the BNL model was also found. The promotion of a uniform gas exit temperature from the hot frit is a BNL design goal. However, it is shown in the full report (Flippen, 1987) that a pure-radial-flow model and the control of axial flow distribution at the inlet to maintain uniform outlet temperature are not, in general, compatible. If one desires to approach the axial Q variation problem by varying the frit porosity then the author recommends the use of a model,

such as equations (8), which does not depend upon the pure-radial-flow assumption. The BNL design (Botts et. al., pg. 19, 1983, and Powell et. al., 1987) uses variation of frit porosity for flow control with a pure-radial-flow model.

A model which is intermediate between the above models, which was initially recommended above the other two for the initial modeling efforts, is:

$$(D P_{,i})_{,i} = 0 \quad (8A)$$

$$D = [ (4A |P_{,i}| + B^2)^{1/2} - B ] / (2A |P_{,i}|) \quad (8B)$$

in conjunction with

$$C_p G_i T_{,i} = Q \quad (8C)$$

and

$$G_i = -D P_{,i} \quad (8D)$$

where equations (4) determine temperature dependent A and B, (which requires T as input from (8C)). The source Q is input from (6). The  $T_f$  distribution may then be found via

$$T_f = Q/[h_g (A/V)_f] + T \quad (8E)$$

where  $h_g$  is obtained from equations (5).

A great deal of BNL's claims concerning the feasibility (and also expected superior performance) of their FPBR design are apparently based on calculations using the simple pure-radial-flow model given in this section. Because of this, the author regards the suggested modifications and questions raised in connection with the BNL model as being more than just refinements to their model. Finally, the stability of the flow through the fuel element is a consideration that needs to be addressed by BNL.

#### IV. POTENTIAL PROBLEMS WITH FRIT AND PLENUM DESIGN:

Botts et. al. (pg. 19, 1983) have advocated a pressure drop of 2/3 of the packed bed pressure drop for the two frits. The reason for this is "to maintain relatively uniform coolant flow in the presence of small local variations in bed voidage". Flow distribution control using frit porosity is very similar to distributor design in fluidized beds (Kunii and Levenspiel, pg. 86-90, 1969). Kunii and Levenspiel recommend the use of

Minimum  $\delta P_{\text{distributor}}$

$$= \text{Max} \{ 0.1 \delta P_{\text{bed}}, 100 \delta P_{\text{rr}}, 35 \text{ cm H}_2\text{O} \}$$

where one can interpret "distributor" as being analogous to frit. The  $\delta P_{\text{rr}}$  represents the pressure drop equivalent to the "resistance to rearrangement" of the incoming gas, which Kunii and Levenspiel say can be conservatively estimated as the pressure drop due to expansion into

the inlet plenum from the inlet connection in the case of distributor design. The Botts et. al. estimate of roughly  $1/3 \delta P_{bed}$  per frit is certainly larger than the  $0.1 \delta P_{bed}$  Kunii recommendation, but the Botts et. al. estimate apparently ignores the  $100 \delta P_{rr}$  estimate. Fraas (pg. 116, 1982) gives an estimate for distributor pressure drop as 20 to 30 per cent of bed pressure drop, but he also ignores the  $100 \delta P_{rr}$  contribution. The  $\delta P_{rr}$  for the FPBR design of BNL may possibly be significantly higher than that found in commercial fluidized bed applications. The reason the author suspects that this could be true is found in a comparison of inlet plenum flow conditions. In a commercial fluidized bed the inlet connection establishes a flow roughly in a line perpendicular to the bed distributor surface and the comparatively large plenum probably enhances uniformity of flow conditions into the distributor. In the FPBR design of BNL the flow into the cold frit plenum is largely axial and the plenum is relatively thin. This would seem to indicate that much of the cold frit plenum gas flow kinetic energy is inherently in opposition to entrance into the frit and the flow is likely to be highly non-uniform axially along the frit as well. The turning of flows in relatively short distances is not a trivial problem and it can often lead to such phenomena as local recirculation. Large  $\delta P_{rr}$  values for the FPBR design could require a very large pressure drop across the cold frit, which would greatly affect other aspects of the FPBR design. For example, higher required pressures may affect the propellant compressor design. Also, large frit pressure drops could potentially

cause large static and vibrational (gas flutter) stresses within the fuel element (Fraas, 1986). It is possible that the modern (carbon-carbon with ZrC coating) frit materials contemplated by BNL can withstand these stresses should they develop. This needs to be demonstrated.

The objection to the previous argument might be raised, initially, that commercial distributor design goals include the promotion of uniform gas flow through the distributor, whereas FPBR design tries to promote a non-uniform one for flow control. This argument seems to the author to be irrelevant however. The basic idea behind the use of the  $100 \delta P_{rr}$  contribution is that one is trying to "force" the gas to flow through the distributor (frit) with a desired distribution despite its inertial tendencies to the contrary in the inlet plenum. This is done by having the "forcing term"  $\delta P_{frit}$  dominate the "resistance term"  $\delta P_{rr}$  by one or more orders of magnitude. To the author, this line of reasoning holds whether one's goal is a uniform gas flow through the distributor (frit) or a specified (desirable) non-uniform flow distribution through the distributor (frit). The design of the cold frit plenum could be revised to reduce  $\delta P_{rr}$  if it is found to be needed. This may involve enlargening the plenum and the introduction of more radially inward flowing connections to the outer wall of the plenum along its axial length. This would surely affect the neutronics and the moderator heat transfer rates in a significant way, however, and may be impractical to manufacture.

An alternative approach, if  $\delta P_{rr}$  is sufficiently large to warrant it, would be to consider the detailed thermal-hydraulics of the cold plenum-cold frit-fuel bed-hot frit-hot plenum as an integral unit. One

would not try to maintain some pre-determined cold frit flow distribution via a cold frit porosity distribution and a large frit pressure drop. Instead, one would compromise with a lower frit pressure drop and vary the cold frit axial porosity distribution to obtain the best gas temperature distribution that one could get under the circumstances via calculations with the component-integrated model. The gas flow distribution through the cold frit would then be part of the results of the calculation. This approach could probably be enhanced by the use of axial fuel concentration variation in the bed. Obviously, cold frit plenum design will also involve moderator cooling concerns.

Whatever approach is ultimately taken to frit-plenum design, the analysis used in the design should take into account the literature on porous wall duct flow. Rohsenow et. al. (pg. 7-141 to 7-148 and 7-173 to 7-174, 1985) states that flow separation and reverse flow is possible for porous wall flows with suction, for example. Rohsenow et. al. also discusses turbulence in porous wall duct flows.

## V. RECOMMENDATIONS:

It is recommended that a more detailed, generalized model of the fuel element be developed which integrates at least the fuel bed, frits, cold frit inlet plenum, and hot frit outlet plenum. The model should address the issues raised in the full report and is certain to require more extensive computer coding for its implementation. It is the author's opinion that the model should be developed before large scale experiments are carried out. It is recommended that a computer code be

developed that has a very modular structure. The interaction between model-modification and experimental results should ultimately lead to enhanced insight as to how the fuel element realistically behaves and why. Ultimately, neutronics calculations, moderator cooling concerns, stress on structural components, etc. can be integrated into the model for actual FPBR design.

Originally, the model given by (8) was recommended for implementation, the details of carrying out this recommendation appearing in the full report (Flippen, 1987). The author originally proposed that the development of the sourceless heat conduction model (8A) for the pressure distribution with an arbitrary input  $D$  be the author's goal for the remainder of the time (about four weeks) available in the summer appointment. This was essentially accomplished. Other steps in implementing the rest of (8) (the fuel bed model) were to be carried out as time permitted, but it turned out that there was not sufficient time to do this. During the last week of the author's appointment, a superior approach to the problem occurred to the author. It involves significant modification of the above computer code but the author feels that it is worth the effort. The approach is summarized in the following paragraphs.

A better intermediate model than the one given previously, which covers the entire fuel element (not just the fuel bed), is summarized below:

$$G_i = \rho U_i \quad (9A)$$

The continuity (mass conservation) equation is:

$$(G_j)_{,j} = 0 \quad (9B)$$

The momentum conservation (Navier-Stokes) equation is:

$$G_j U_{i,j} = -P_{,i} + (\mu U_{i,j})_{,j} - F_{ij} G_j \quad (9C)$$

The energy conservation equation is still:

$$C_p G_i T_{,i} = Q \quad (9D)$$

and the fuel bed temperature is still found by:

$$T_f = Q/[h_g (A/V)_f] + T \quad (9E)$$

where equations (4), (5), and (6) are still required. The equations for the  $F_{ij}$  coefficients are:

$$\begin{aligned} F_{11} &= F_{xx} = A_x G + B_x \\ F_{12} &= F_{xy} = F_{yx} = F_{21} = 0 \\ F_{22} &= F_{yy} = A_y G + B_y \end{aligned} \quad (9F)$$

where  $G$  is the magnitude (Euclidean norm) of the vector  $G_i$ ; that is,  $G =$

$$|G_i| = (G_1^2 + G_2^2 + G_3^2)^{1/2} = (G_x^2 + G_y^2 + G_z^2)^{1/2}, \text{ and where } x$$



represents the radial direction and  $y$  the axial direction for this case. In the plenums the coefficients in (9F) take on the values:

$$A_x = A_y = 0$$

$$B_x = B_y = 0$$

whereas in the fuel bed they have the values:

$$A_x = A_y = A \text{ (of equation 4)}$$

$$B_x = B_y = B \text{ (of equation 4)}$$

and within the frits they are:

$$A_y = 0$$

$$B_y = \infty$$

above leads to  $U_y = G_y = 0$  and hence  $G = G_x$

$A_x$  and  $B_x$  are given functions for each frit

For the heat source, one has the restrictions:

$Q = 0$  in the plenums and frits

$Q$  is given by (6) in the fuel bed

The nice thing about the model just outlined is that, once it is

achieved, upgrade to a more general model is not conceptually difficult. This is because the input Q distribution can be replaced by the right-hand side of equation (2). Of course, one would then have to implement equation (3) into the model. It is recommended that the above model be implemented numerically on a digital computer via the methods of Patankar (1980). The development of the computer model may very well form the basis for a proposal for further support from the Air Force.

## REFERENCES

1. Botts, T. E., F. L. Horn, O. C. Jones, O. W. Lazareth, H. Ludewig, J. R. Powell, and J. L. Usher, "The Rotating and Fixed Bed Reactor Concepts", Final Report No. AFRPL TR-83-023, November 1983.
2. Flippen, L. D., "The Evaluation of a Thermal-Hydraulic Design of a Fixed Particle Bed Reactor and Suggested Model Revisions", Final Report to AFAL/LKCS, Edwards AFB, August 1987.
3. Fraas, A. P., Engineering Evaluation of Energy Systems, New York, McGraw-Hill, 1982.
4. Fraas, A. P., "Appraisal of the SMITE Concept", Memo to J. P. Nichols, February 1986.
5. Kunii, D., and O. Levenspiel, Fluidization Engineering, New York, John Wiley and Sons, 1969.
6. Patankar, S. V., Numerical Heat Transfer and Fluid Flow, New York, Hemisphere Publishing Corp., 1980.
7. Powell, J. R., et. al., "Nuclear Propelled Orbit Transfer Vehicle Project", Draft Final Report, AFAL, 1987.

8. Powell, J. R., et. al., "Nuclear Propulsion Systems for Orbit Transfer Based on the Particle Bed Reactor", Fourth Symposium on Space Nuclear Power Systems, Albuquerque, New Mexico, January 1987.
9. Rohsenow, W. M., J. P. Hartnett, and E. N. Ganic, Handbook of Heat Transfer Fundamentals, 2nd ed., New York, McGraw-Hill, 1985.

1987 USAF-UES SUMMER FACULTY RESEARCH PROGRAM/  
GRADUATE STUDENT SUMMER SUPPORT PROGRAM

Sponsored by the  
AIR FORCE OFFICE OF SCIENTIFIC RESEARCH  
Conducted by the  
Universal Energy Systems, Inc.

FINAL REPORT

SIFT STUDIES OF GAS PHASE ION-MOLECULE REACTIONS

Prepared by: Dr. Lee A. Flippin  
Academic Rank: Assistant Professor  
Department and Department of Chemistry and Biochemistry  
University: San Francisco State University  
Research Location: USAFGL-LID  
Hanscomb AFB  
Boston, Massachusetts  
USAF Researcher: Dr. John Paulson  
Date: September 20, 1987  
Contract No.: F49620-85-C-0013

## SIFT STUDIES OF GAS PHASE ION-MOLECULE REACTIONS

by

Dr. Lee A. Flippin

### ABSTRACT

The kinetics and product distributions of gas phase reactions of hydroxide ion,  $\text{OH}^-$ , with organic epoxides and episulfides were studied using the Selected Ion Flow Tube (SIFT) technique. Ethylene oxide and ethylene episulfide apparently undergo addition of  $\text{OH}^-$  followed by fast fragmentation to afford  $m/e = 59$  ( $\text{C}_2\text{H}_3\text{O}_2^-$ ) and  $m/e = 33$  ( $\text{HS}^-$ ), respectively. Propylene episulfides and epoxides with two or three C-H bonds adjacent to the three-membered ring undergo rapid proton transfer to  $\text{OH}^-$  to afford  $m/e = M-1$  products exclusively.

Selected perfluoroalkyl metal carbonyls were synthesized for SIFT studies of electron attachment reactions.

### ACKNOWLEDGMENTS

I gratefully acknowledge the Air Force Systems Command and the Air Force Office of Scientific Research for sponsorship of this research. I further acknowledge the gracious assistance afforded me by Rodney Darrah and Debbie Withers of Universal Energy Systems, Inc. in the administrative details of this program.

The research project would not have been possible without the guidance and support of Dr. John Paulson, Dr. Al Viggiano, and Dr. Bob Morris.

## I. INTRODUCTION:

Over the past decade-and-a-half a great deal of effort has been devoted to the gas phase study of ion-molecule reactions which have direct (and often extensively characterized) solution phase analogs. Among the important reasons for such research is the goal of isolating and properly defining the role of solvation vis-a-vis solution phase reaction dynamics. This perspective assumes that reactions between ionic and neutral species in the gas phase, unencumbered by solvent molecules, will lead to a picture of the intrinsic nature of ion-molecule interactions and that, by difference, the role of solvation in the solution phase analogs can be evaluated.

The AFGL-LID group at Hanscomb Air Force Base is primarily concerned with the chemistry and physics of ion-molecule reaction dynamics that have relevance to atmospheric processes, however, this group is also interested in the application of the SIFT technique to selected non-atmospheric reactions that may serve as useful models for evaluating ion-molecule reaction theory.

My research program at San Francisco State University is directed toward the development of new organic synthesis methods and the application of these methods to the construction of unusual molecules. We are also engaged in studies toward the elucidation of fundamental reaction mechanisms. Our group has recently become involved in the study of solution phase reactions of epoxides with nucleophiles, thus the opportunity to



complement these investigations with a parallel gas phase study led to my assignment to the AFGL-LID laboratory at Hanscomb AFB.

## II. OBJECTIVES OF THE RESEARCH EFFORT:

The central objectives of the research project were two-fold: (1) to compare and evaluate the kinetics of two divergent reaction pathways that are available within the epoxide/ $\text{OH}^-$  reactant system and to survey related reactions of hydroxide ion with the sulfur analogs of epoxides and, (2) to synthesize several perfluoroalkyl metal carbonyl compounds which show promise for their ability to capture thermalized electrons rapidly in the gas phase. The SIFT technique is uniquely suited to the fulfillment of the first objective and it is highly probable that the AFGL-LID SIFT can be successfully adapted to glean useful information concerning the rates and products of electron capture by the organometallic compounds that were prepared.

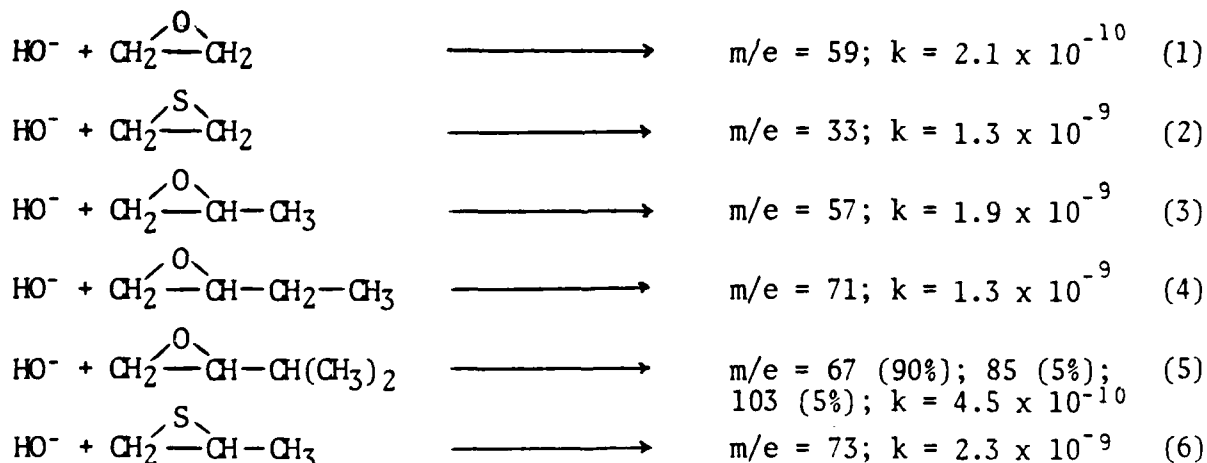
The SIFT experiment has been described in detail elsewhere<sup>1</sup>, however, a brief description of the general features of the technique is given here. In a typical experiment negative ions (as well as other reactive species) are created in the source region of the SIFT by electron bombardment of a suitable neutral precursor; the desired ion to be studied is then selected with a quadrupole mass filter and allowed to enter a flow tube in a stream of inert buffer gas (e.g., helium at ca.  $\frac{1}{2}$  torr). In the flow tube region a neutral reactant is added to the buffer stream and at the downstream end of the meter-long tube a second quadrupole mass filter is employed to

selectively monitor the reactant ion concentration as well as any product ions that may have been produced. The flow rates of neutral reactants, count rates of reactant and product ions, and the buffer stream flow rate are all measurable variables in the experiment and absolute rate constants can be determined over about four orders of magnitude.

### III. RESULTS:

(1) The product ions and bimolecular rate constants for the room temperature reactions of  $\text{OH}^-$  with selected epoxides and episulfides are shown in Scheme 1.

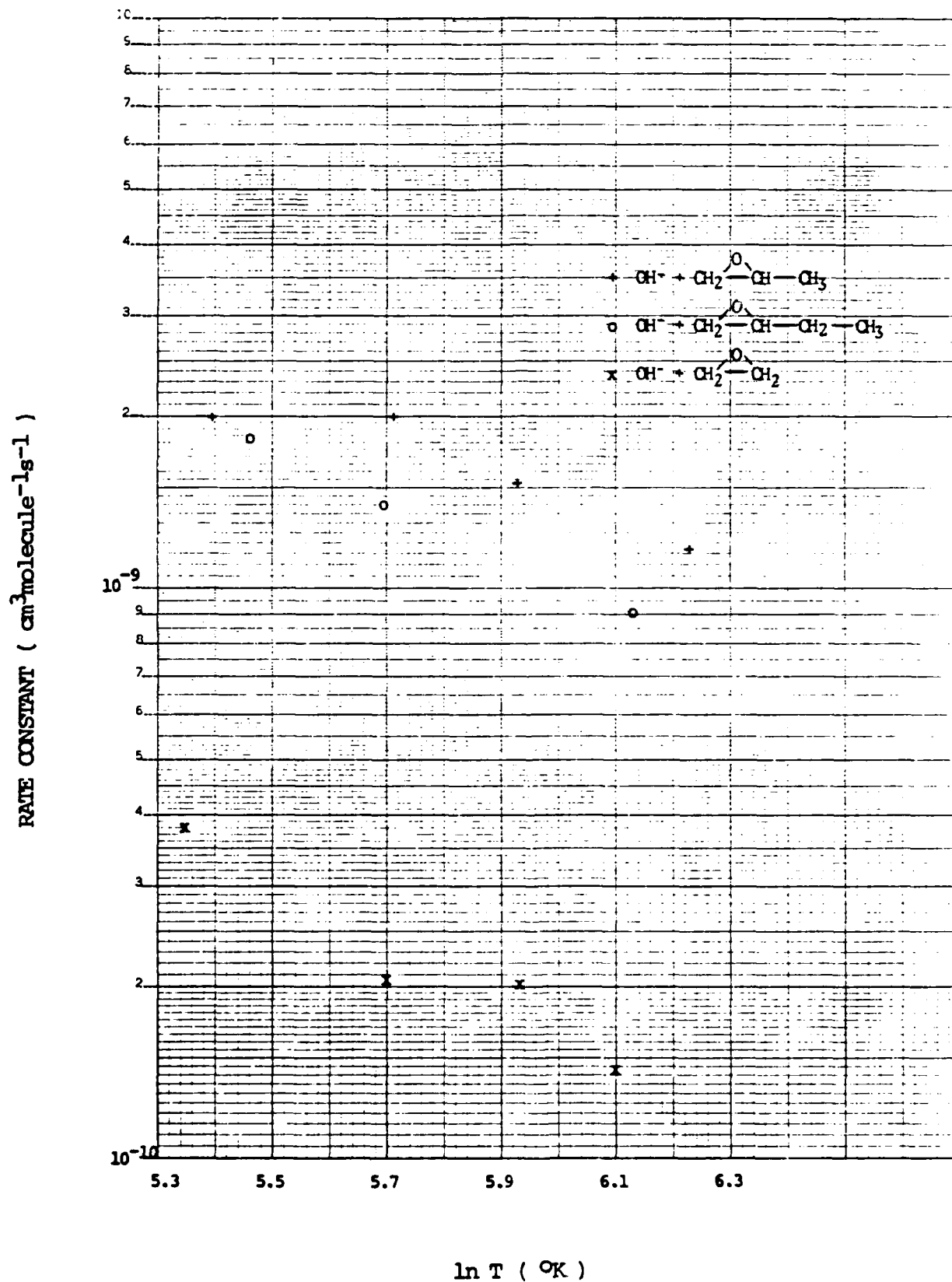
SCHEME 1



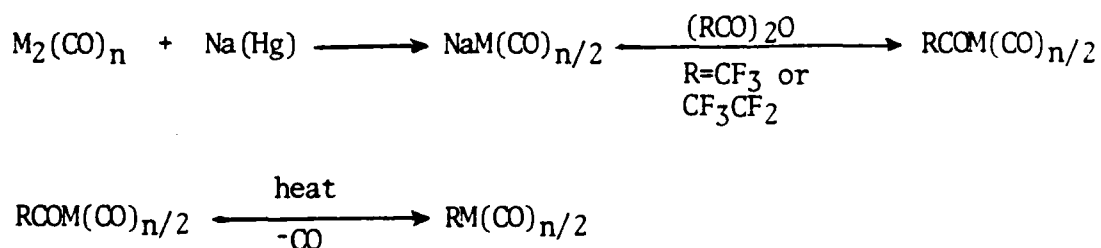
(Rate constant units are  $\text{cm}^3 \text{molecule}^{-1} \text{sec}^{-1}$ )

We also studied the temperature dependence of the rate constants for several of these reactions (Equations 1, 3, and 4 vide supra); these data are plotted in Figure 1.

FIGURE 1



(2) In other work supported by the USAF-UES Faculty Fellowship program I carried out synthetic work that led to the preparation of three organometallic compounds, (a) trifluoromethylmanganese pentacarbonyl, (b) trifluoromethylcobalt tetracarbonyl and, (c) pentafluoroethylcobalt tetracarbonyl. These compounds are of interest for SIFT studies because they exhibit reasonably high vapor pressures and they have the potential ability to attach thermalized electrons rapidly in the gas phase. Preliminary results obtained by an unrelated method indicate that trifluoromethylmanganese pentacarbonyl attaches electrons nearly as rapidly as  $\text{SF}_6^2$ . A schematic synthesis of the organometallic compounds is outlined below<sup>3</sup>:



The chemistry of these substances has not yet been explored via the SIFT technique.

#### IV. RECOMMENDATIONS:

(1) The SIFT technique represents an extraordinarily valuable method for the study of gas phase ion-molecule reaction kinetics. Based on our initial results from the epoxide/ $\text{OH}^-$  reactions, I believe that it would be useful to extend our studies in this area. For example, I wish to design a single epoxide substrate that will competitively react via both channels that have been observed separately in our study of substituted vs. unsub-

stituted epoxides with hydroxide ion. It would be quite useful to be able to measure the temperature dependence of the ratio of proton-transfer/addition in a single substrate because the absolute rate constants of separately measured reactions suffer from a rather large experimental uncertainty ( $\pm 30\%$ ); the relatively insensitive dependence of rate constants on temperature that we have observed in the epoxide series limits the interpretation of our results to qualitative terms. On the other hand, the inherent uncertainty associated with measuring a product ratio in the SIFT experiment depends mostly on mass discrimination effects in the detection-end quadrupole mass filter-- these effects can, in theory, be evaluated very accurately by calibration runs using well-defined reactant systems.

(2) Much work remains to be done in the area of electron attachment studies with the organometallic compounds that we prepared. If these compounds live up to their potential for rapid electron attachment it will be necessary to identify the ionic products of this process and to further study their subsequent ion chemistry; again, the SIFT technique is ideally suited for such investigations. In addition, there are many other organometallic compounds that may be of interest vis-a-vis their potential to rapidly attach electrons-- these include perfluoroalkyl derivatives of rhenium, iron, molybdenum, tungsten, and other transition metals.

#### REFERENCES

- 1.) The Selected Ion Flow Tube (SIFT); A Technique For Studying Ion-Neutral Reactions, N. G. Adams and D. M. Smith, International Journal of Mass Spectrometry and Ion Physics, 1976, 21, 349.
- 2.) Private communication from Professor David McFadden.
- 3.) Our scheme is a modification of the method of McClellan: Perfluoroalkyl and Perfluoroacyl Metal Carbonyls, W. R. McClellan, J. Am. Chem. Soc., 1961, 83, 1598.

1987 USAF-UES SUMMER FACULTY RESEARCH PROGRAM/

GRADUATE STUDENT SUMMER SUPPORT PROGRAM

Sponsored by the

AIR FORCE OFFICE OF SCIENTIFIC RESEARCH

Conducted by the

Universal Energy Systems, Inc.

FINAL REPORT

SILICON JUNCTION-DIFET ELECTROOPTIC MODULATOR

Prepared by: Lionel R. Friedman, Ph.D.  
Academic Rank: Professor  
Department and: Electrical Engineering  
University: Worcester Polytechnic Institute  
Research Location: RADC/ESO  
Hanscom AFB MA  
01731  
USAF Researcher: Richard A. Soref  
Date: 30 July 1987  
Contract No: F49620-85-C-0013

## Silicon Junction - DIFET Electrooptic Modulator

by

Lionel R. Friedman

### ABSTRACT

In-house work at RADC/ESO has established that crystalline silicon is an attractive waveguide medium for 1.3-1.55  $\mu\text{m}$  optical transmission. In an effort to provide active guided-wave components in silicon, we have considered a novel, double-injection transistor for the control of integrated-optical switches and modulators. It has been shown that large concentration of electrons and holes are possible due to double injection, and that this injected plasma substantially perturbs the refractive index. It has also been shown that the effective index change can be controlled by voltage-variable depletion widths adjacent to one or two gate electrodes. Numerical estimates of the injected densities and the effective index changes have been made for both of these cases. Limitations of the theory and the role of recombination are discussed.



### Acknowledgements

I wish to thank the Air Force Systems Command, RADC/ESO, the Air Force Office of Scientific Research, and Universal Engergy Systems for sponsorship of this research. I especially wish to thank my USAF colleague, Dr. Richard A. Soref, for his collaboration, and for the time which he devoted to this program. Thanks also are extended to Dr. Jerry Silverman and Capt. James Murguia for assistance on the SUN microsystem, to Drs Andrew Yang and Richard Payne for their support, and to Mary Murrin for typing assistance.

## I. INTRODUCTION:

There has been considerable interest at Rome Air Development Center in the use of crystalline silicon for guided-wave applications at the 1.3 and 1.55  $\mu\text{m}$  wavelengths. In-house research at RADC/ESO emphasized passive components, such as channel waveguides. Now, there is a need to develop active electrooptic switches and phase-shifting components. The linear electrooptic effect vanishes in crystalline silicon because of the centrosymmetry of the unit cell. Earlier work by myself and my present collaborator, Dr Richard A. Soref, on strained-layer  $\text{Ge}_x\text{Si}_{1-x}/\text{Si}$  superlattices showed that the centrosymmetry of the unit cell is removed in these ordered alloys, resulting in a nonvanishing electrooptic effect. This work resulted in two publications.

In our present work, we are studying the modification of the refractive index by the injection of charge. Earlier experimental work has been on the index modification due to the injection or depletion of charge of one sign (electrons or holes). Our present study concerns double-injection, the simultaneous injection of electrons and holes to yield a quasi-neutral plasma, and the concomitant larger change this produces in the optical index of refraction. We have made numerical estimates of the injected densities, index changes, and the means of electrically controlling the effective index change by voltage-variable depletion widths adjacent to single or double reverse-bias gate electrodes. Our numerical work show these transistor structures to be viable electrooptic phase modulators.

My research interests have been in the area of compositional superlattices.

In particular, I have studied electron-lattice scattering, thermoelectric power, and optical nonlinearities of these systems. My earlier cited collaborative work on  $\text{Ge}_x\text{Si}_{1-x}/\text{Si}$  strained layer superlattices, and subsequent interest in charge injection as a means of optical phase modulation, contributed to my assignment to this project.

## II. OBJECTIVES OF THE RESEARCH EFFORT:

The goals of this research program are to obtain an improvement in electrooptic modulation efficiency over a single injection p-n diode modulator, to obtain electrooptic switching speeds in the nanosecond to picosecond range, to utilize low power, and to accomplish this in  $2 \times 2$  and  $1 \times 1$  silicon channel-waveguide structures.

My specific objectives as a participant in the 1985 Summer Faculty Research Program (SFRP) were several-fold. First I was to obtain numerical estimates of the injected plasma densities and current densities due to double injection, for the cases of monomolecular (constant lifetime case) and bimolecular recombination. Secondly, in order to obtain the effective change in the optical index of refraction and hence the phase shift, it was necessary to compute the overlap integral of the index perturbation with the electric field intensity of the optical wave. We found it desirable to do this for two cases: two symmetrical depletion regions about the central conducting channel, and a single depletion region extending downward from an upper gate electrode. We wished to determine which configuration gave the larger electromodulation efficiency. Another objective was to access the constraints on device operation due to the

requirement that the injection current densities not be excessively large, and the requirement that the depletion widths provide adequate control of the effective index change for gate voltages sufficiently less than breakdown strength. Finally, it was our goal to propose prototype transistor structures, with specific dimensions and dopant densities, as the silicon junction DIFET electrooptic modulator.

### III.

A full report of this work can be obtained from Universal Energy Systems, Inc. The paper, which includes twenty-three pages of text and eleven illustrations, was submitted in August 1987 to the Journal of Applied Physics for publication. In addition, copies of the paper can be obtained from the authors:

Lionel Friedman  
Worcester Polytechnic Institute  
Department of Electrical Engineering  
Worcester, MA 01609

or

Richard A. Soref  
Rome Air Development Center  
Solid State Sciences Directorate  
Hanscom AFB, MA 01731

### IV. RECOMMENDATIONS:

a. The results of the present study have provided numerical estimates which support our original contention that the silicon junction DIFET can be used as an effective electrooptic modulator. It is recommended that some of the approximation of the present work be examined more carefully. The most important of these are the models of bulk and surface recombination, and

the incorporation of diffusion effects. The neglect of diffusion is common in most theories of double injection, but its inclusion becomes increasingly important as device dimensions shrink to micron or submicron values. Besides analytic work, this is best treated for arbitrary geometrics by a full two-dimensional simulation using the PISCES-II semiconductor device modeling program. Work on this program is suggested for follow-on research.

b. In this connection, it is recommended that the transverse configuration be studied in which the double injection currents are perpendicular to the direction of optical propagation. In the present study, they were taken to be colinear.

c. It is further recommended that future work be done on a DIFET in which the control of the effective index is by means of an insulated gate electrode, rather than by voltage-variable depletion widths. Again, it is anticipated that this will require two-dimensional simulation on PISCES-II.

d. Further investigation is suggested for future research on other ways in which charge injection can be used for phase modulation. In particular, n-i-p-i doping superlattices have the potential of injecting large amounts of charge electrically or by optical excitation, and then controlling this charge as a result of charge redistribution upon the application of an electric field.



END

DATE

FILMED

5-88

DTIC